Discovery of Antiprotozoal Compounds from Medicinal Plants

Inauguraldissertation

Zur

Erlangung der Würde eines Doktors der Philosphie

vorgelegt der

Philosophisch-Naturwissenschaftlichen Fakultät

der Universität Basel

von

Yoshie Adriana Hata-Uribe

aus Bogota

KOLUMBIEN

Basel, 2014

Genehmigt von der Philosophisch-Naturwissenschaftlichen Fakultät

auf Antrag von

Prof. Dr. Matthias Hamburger
Prof. Dr. Irmgard Merfort
Prof. Dr. Reto Brun

Basel, den 22.04.2014

Prof. Dr. Jörg Schibler
Dekan

Namensnennung-Keine kommerzielle Nutzung-Keine Bearbeitung 3.0 Schweiz
(CC BY-NC-ND 3.0 CH)

Sie dürfen: **Teilen** — den Inhalt kopieren, verbreiten und zugänglich machen

Unter den folgenden Bedingungen:

Namensnennung — Sie müssen den Namen des Autors/Rechteinhabers in der von ihm festgelegten Weise nennen.

Keine kommerzielle Nutzung — Sie dürfen diesen Inhalt nicht für kommerzielle Zwecke nutzen.

Keine Bearbeitung erlaubt — Sie dürfen diesen Inhalt nicht bearbeiten, abwandeln oder in anderer Weise verändern.

Wobei gilt:

- **Verzichtserklärung —** Jede der vorgenannten Bedingungen kann **aufgehoben** werden, sofern Sie die ausdrückliche Einwilligung des Rechteinhabers dazu erhalten.
- **Public Domain (gemeinfreie oder nicht-schützbare Inhalte) —** Soweit das Werk, der Inhalt oder irgendein Teil davon zur Public Domain der jeweiligen Rechtsordnung gehört, wird dieser Status von der Lizenz in keiner Weise berührt.
- **Sonstige Rechte —** Die Lizenz hat keinerlei Einfluss auf die folgenden Rechte:
    - Die Rechte, die jedermann wegen der Schranken des Urheberrechts oder aufgrund gesetzlicher Erlaubnisse zustehen (in einigen Ländern als grundsätzliche Doktrin des **fair use** bekannt);
    - Die **Persönlichkeitsrechte** des Urhebers;
    - Rechte anderer Personen, entweder am Lizenzgegenstand selber oder bezüglich seiner Verwendung, zum Beispiel für **Werbung** oder Privatsphärenschutz.
- **Hinweis —** Bei jeder Nutzung oder Verbreitung müssen Sie anderen alle Lizenzbedingungen mitteilen, die für diesen Inhalt gelten. Am einfachsten ist es, an entsprechender Stelle einen Link auf diese Seite einzubinden.

Quelle: http://creativecommons.org/licenses/by-nc-nd/3.0/ch/ Datum: 12.11.2013

"…What the eyes perceive in herbs or stones or trees is not yet a remedy;

the eyes see only the dross. But inside, under the dross,

there the remedy lies hidden.

First it must be cleaned from the dross, then it is there.

This is alchemy, and this is the office of Vulcan;

he is the apothecary and chemist of the medicine…"

Paracelsus (1493 – 1541)

TABLE OF CONTENTS

LIST OF ABBREVIATIONS

WHO	World Health Organization
DDT	Dichlorodiphenyltrichloroethane
NMR	Nuclear Magnetic Resonance
DHA	Dihydroartemisinin
TCTP	Malarial translationally controlled tumor protein
ACT	Artemisinin-based combinations treatment
DDD	Drug discovery and development
PK	Pharmacokinetics
SAR	Structure-activity relationship
ADME	Absorption, distribution, metabolism, and excretion
NPs	Natural products
NCES	New chemical entities
HTS	High throughput screening
NMR	Nuclear magnetic resonance
HPLC	High performance liquid chromatography
RP	Reverse Phase
UV	Ultraviolet
MS	Mass spectrometry
ESI	Electrospray ionization
APCI	Atmospheric pressure chemical ionization
API	Atmospheric pressure ionization
TOF	Time-of-flight
GABA	Gamma-aminobutyric acid
PDA	Photodiode array detector
ELSD	Evaporative light scattering detector
SPE	Solid phase extraction
COSY	Correlated spectroscopy
NOESY	Nuclear overhouser enhancement spectroscopy
HETCOR	Heteronuclear correlation
ROESY	Rotating frame overhauser enhancement spectroscopy
TOCSY	Total correlation spectroscopy
HSQC	Heteronuclear single quantum coherence
HMBC	Heteronuclear multiple bond correlation
AC	Absolute configuration
ECD	Electronic circular dichroism
PEGs	Pulsed-field gradients
NTD	Neglected tropical diseases
HAT	Human African Trypanosomiasis
DALYs	Disability-adjusted life years
BBB	blood-brain barrier
DNDi	Drugs for neglected diseases initiative
TDR	The special program for research and training in tropical diseases (WHO)
CNS	Central nervous system
PSA	Polar surface area
IC_{50}	Inhibitory Concentration 50
SI	Selectivity index

SUMMARY

Tropical parasitic diseases such as malaria, human African trypanosomiasis, chagas disease, and leishmaniasis affect hundreds of millions of people worldwide and have devastating consequences. Current drugs available to treat these diseases have serious drawbacks. New drugs are urgently needed.

Natural products (NPs) play a dominant role in drug discovery for the treatment of human diseases. Particularly, quinine and artemisinin have their origin in nature and have inspired successful drugs for malaria treatment.

In a medium throughput screening, a total of 507 extracts from South African plants were assayed for their antiprotozoal activity against *Plasmodium falciparum*, *Trypanosoma brucei rhodesiense*, *Trypanosoma cruzi* and *Leishmania donovani*. Extracts from *Abrus precatorius* L. ssp. *africanus* Verdc. (Fabaceae) and *Drypetes gerrardii* Hutch. var. *gerrardii* (Putranjivaceae) inhibited at least one of the parasites at a test concentration considered relevant. With the aim of identifying the compounds responsible for these activities, a HPLC-based activity profiling approach followed by dereplication was applied. Targeted isolation of promising compounds was achieved by a combination of chromatography techniques. Structure elucidation was achieved by HR-ESI-MS and NMR (^{1}H, ^{13}C, COSY, HMBC, HSQC, and NOESY spectroscopy). Absolute configuration was determined by comparison of electronic circular dichroism (ECD) spectra with calculated ECD data.

HPLC-based activity profiling of *A. precatorius* allowed the identification of abruquinones, a series of isoflavan quinones, as responsible for the trypanocidal activity of the crude extract. A total of ten abruquinones were isolated. Among these were five new compounds, and one compound was reported for the first time as natural product. Abruquinone B, I, A, D, K, and L showed remarkable inhibition (0.16 ± 0.060, 0.28 ± 0.051, 0.02 ± 0.003, 0.01 ± 0.001, 0.11 ± 0.053, and 0.02 ± 0.053, respectively) and notable selectivity, expressed as selectivity indices (SIs) which were calculated from cytotoxicity data in L-6 cells (51, 74, 1379, 668, 508, and 374, respectively). These results warrant *in vivo* assessment of abruquinones.

Abruquinones are promising hits due to their strong and selective *in vitro* inhibition of *T. b. rhodesiense*, their good compliance with Lipinski's "rule-of-5" and other molecular properties, as well as their predicted low/moderate toxic potential. Therefore, further studies are necessary to guarantee a botanical or chemical source, and to assess *in vivo* efficacy.

Two different extracts of *D. gerrardii* showed antiprotozoal activity, and the active constituents were tracked and isolated by HPLC-based activity profiling. The CH_2Cl_2/MeOH (1:1) stems extract inhibited *L. donovani* and *P. falciparum*. The major compound, a new phenanthrenone, showed good *in vitro* activity

(IC_{50} of 0.9 ± 0.3 μM) and selectivity (SI of 68) against *P. falciparum*. Based on these promising results, *in-vivo* studies were conducted. However, the compound was not able to reduce parasitemia in the *P. berghei* mouse model. A phenanthrenone heterodimer was also isolated and showed *in vitro* antiplasmodial activity (IC_{50} of 2.04 ± 0.15 μM and SI of 31). Furthermore, the CH_2Cl_2/MeOH (1:1) leaves extract displayed trypanocidal properties, and the known saponin putranoside A was isolated and tested against *T. b. rhodesiense*, (IC_{50} of 18.0 ± 3.8 μM and a SI of 4).

The phenanthrenone was the most active and selective *in vitro* inhibitor of *P. falciparum*, but showed no inhibition *in vivo* against *P. berghei*. However, the compound fulfilled Lipinski's "rule-of-5" and other molecular properties, which indicates a potential to meet requirements of an ideal antimalarial drug such as, oral bioavailability and blood-brain barrier permeability. According to Medicines for Malaria Venture compound progressing criteria, the phenanthrenone complies with some of the features of a validated hit such as sufficient activity against *P. falciparum in vitro* (< 1 μM). The assessment of *in vivo* activity in additional animal models, e.g. *Pf*-huMouse model could be considered for compound progression in the drug discovery pipeline.

Additionally, as part of a project aimed at investigating antiprotozoal European plants *Chrysanthemum cynerariifolium* (Trevir.) Vis. (Asteraceae), *Laurus nobilis* L. (Lauraceae), and *Eupatorium cannabinum* L. (Asteraceae) were studied. A hexane extract of *C. cynerariifolium* showed promising activity against *P. falciparum*. Pyrethrins (irregular monoterpenes) were the metabolites responsible for the antiplasmodial activities. Particularly, pyrethrin II and jasmolin II inhibited *P. falciparum* (IC_{50} 4.0 ± 1.1 μM and 5.0 ± 0.4 μM, respectively and SI of 24 and 6, respectively) *in vitro*. Synthetic pyrethroids were also tested, but they did not show activity. However, none of the two compounds fulfilled activity and selectivity requirements for *in vivo* evaluation.

Finally, as a contribution to the structure activity relationship study of sesquiterpene lactones showing activity against *T. b. rhodesiense*, costunolide and zaluzanin D were isolated from *Laurus nobilis* L. (Lauraceae) and eupatoriopicrin from *Eupatorium cannabinum* L. (Asteraceae). Germacrolides, i.e. costunolide and eupatoriopicrin, showed a higher inhibition (IC_{50} of 1.3 ± 0.4 μM and 1.2 ± 0.2 μM, respectively) on the protozoon, than the guaianolide zaluzanin D (IC_{50} of 10.8 μM). However, none of the sesquiterpene lactones showed sufficient activity and selectivity to warrant *in vivo* testing.

In brief, a total of 22 secondary metabolites were isolated from five species. Among them, seven new compounds were discovered. These compounds belong to the structural classes of isoflavonoids, phenanthrenones, and terpenes such as, sesquiterpene lactones, irregular monoterpenes and triterpenoid

saponins. Most of them (15 compounds) exhibited *in vitro* antiprotozoal activity, albeit at differing extent. The most promising compounds were the abruquinones and the phenanthrenone, which strongly and selectively inhibited *T. b. rhodesiense* and *P. falciparum*, respectively. Abruquinones and the phenanthrenone are drug-like compounds with a calculated toxic potential ranging from low to moderate.

ZUSAMMENFASSUNG

Tropische parasitäre Krankheiten wie Malaria, afrikanische Trypanosomiasis (Schlafkrankheit), Chagas-Krankheit und Leishmaniose betreffen Hunderte von Millionen Menschen weltweit und haben verheerenden Folgen. Aktuelle Medikamente, die zur Behandlung dieser Krankheiten zur Verfügung stehen, haben gravierende Nachteile. Neue Medikamente werden dringend benötigt.

Naturstoffe (NP) spielen eine dominierende Rolle in der Wirkstoffforschung für die Behandlung von menschlichen Erkrankungen. So haben Chinin und Artemisin ihren Ursprung in der Natur und führten zu erfolgreichen Medikamenten zur Malariabehandlung.

In einem mittleren Durchsatz-Screening wurden insgesamt 507 Extrakte von südafrikanischen Pflanzen auf ihre Aktivität gegen Protozoen - *Plasmodium falciparum*, *Trypanosoma brucei rhodesiense*, *Trypanosoma cruzi* und *Leishmania donovani* - getestet. Extrakte von *Abrus precatorius* L. ssp. *africanus* Verdc. (Fabaceae) und *Drypetes gerrardii* Hutch. var. *gerrardii* (Putranjivaceae) haben mindestens einen der Parasiten in einer als relevant bezeichneten Testkonzentration gehemmt.

Mit dem Ziel die für diese Aktivitäten verantwortlichen Verbindungen zu identifizieren wurde ein Ansatz bestehend aus HPLC-basiertes Aktivitäts-Profiling gefolgt von Dereplikation verwendet. Gezielte Isolierung der vielversprechenden Verbindungen erfolgte durch eine Kombination von Chromatographie-Techniken. Die Strukturaufklärung wurde durch HR-ESI-MS und NMR (^{1}H, ^{13}C, COSY, HMBC, HSQC, und NOESY Spektroskopie) durchgeführt. Die absolute Konfiguration wurde durch den Vergleich der elektronischen Zirkulardichroismus-(ECD)-Spektren mit berechneten ECD-Daten bestimmt.

HPLC-basiertes Aktivitäts-Profiling von *A. precatorius* ermöglichte die Identifizierung von Abruquinonen, einer Reihe von Isoflavan-Chinonen, als verantwortliche Substanzen für die trypanozide Aktivität des Rohextrakts. Es wurden insgesamt 10 Abruquinone isoliert, darunter fünf neue Verbindungen. Eine Verbindung wurde zum ersten Mal als Naturstoff beschrieben. Abruquinone B, I, A, D, K und L zeigten bemerkenswerte Hemmung (0.16 ± 0.060, 0.28 ± 0.051, 0.02 ± 0.003, 0.01 ± 0.001, 0.11 ± 0.053, und 0.02 ± 0.053) und beachtenswerte Selektivität, wiedergegeben als Selektivitätsindizes (SIs) die aus der Zytotoxizität in L-6 Zellen (51, 74, 1379, 668, 508, und 374) ermittelt wurden. Diese Ergebnisse rechtfertigen eine Prüfung der *in vivo*-Aktivität von Abruquinonen.

Wegen ihrer starken und selektiven *in vitro* Hemmung von *T. b. rhodesiense,* ihrer guten Übereinstimmung mit Lipinski's „5er Regel" und anderen molekularen Eigenschaften, sowie ihrem niederen/mässigen toxischen Potenzial sind Abruquinone vielversprechende Hits. Deshalb sind weitere

Studien notwendig um botanische oder chemische Quellen sicherzustellen und die *in-vivo* Wirksamkeit dieser Verbindungen zu bestimmen.

Zwei verschiedene Extrakte von *D. gerrardii* zeigten Aktivität gegen Protozoen. Die aktiven Bestandteile wurden mit Hilfe vom HPLC-basiertem Aktivitäts-Profiling identifiziert und isoliert. Der CH_2Cl_2/MeOH (1:1) Extrakt aus den Stängeln hemmte *L. donovani* und *P. falciparum*. Die Hauptverbindung, ein neues Phenanthrenon, zeigte gute *in vitro* Aktivität (IC_{50} von 0.9 ± 0.3 μM) und Selektivität (SI von 68) gegen *P. falciparum*. Basierend auf diesen vielversprechenden Resultaten wurden *in vivo* Studien durchgeführt. Allerdings war diese Verbindung nicht in der Lage die Parasitenbelastung im *P. berghei* Mausmodell zu reduzieren. Es wurde ebenfalls ein Phenanthrenon-Heterodimer isoliert, der *in vitro* Aktivität gegen Plasmodien (IC_{50} von 2.04 ± 0.15 μM und SI von 31) aufwies. Ausserdem zeigte der CH_2Cl_2/MeOH (1:1) Blattextrakt ausgewiesene trypanozidale Eigenschaften. Aus diesem Extrakt wurde das bekannte Saponin Putranoside A isoliert und gegen *T. b. rhodesiense,* (IC_{50} von 18.0 ± 3.8 μM und SI von 4) getestet.

Das Phenanthrenon war der aktivste und selektivste *in vitro* Inhibitor von *P. falciparum*, zeigte jedoch keine Hemmung *in vivo* gegen *P. berghei*. Die Verbindung erfüllte jedoch Lipinski's „5er Regel" und andere molekulare Eigenschaften, wie orale Bioverfügbarkeit und Durchlässigkeit der Blut-Hirn-Schranke, was ein mögliches Potenzial aufzeigt den Anforderungen eines idealen Antimalariawirkstoffs gerecht zu werden. Nach „Medicines for Malaria Venture"-Kriterien für die weitere Entwicklung eines Wirkstoffs erfüllt das Phenanthrenon einige der Merkmale eines validierten Hits wie ausreichende *in vitro* Aktivität gegen *P. falciparum* (< 1 μM). Die Bewertung der *in vivo* Aktivität in weiteren Tiermodellen, z.B. *Pf*-huMaus-Modell könnte für den weiteren Wirkstoffentwicklungsprozess in Betracht gezogen werden.

Als weiterer Teil des Projekts wurde die Wirkung von europäischen Heilpflanzen *Chrysanthemum cynerariifolium* (Trevir.) Vis. (Asteraceae), *Laurus nobilis* L. (Lauraceae), und *Eupatorium cannabinum* L. (Asteraceae) gegen Protozoen studiert. Ein Hexan-Extrakt von *C. cynerariifolium* zeigte vielversprechende Aktivität gegen *P. falciparum*. Phyrethrine (unregelmässige Monoterpene) waren die Inhaltsstoffe verantwortlich für die antiplasmodiale Aktivität. Besonders Pyrethrin II und Jasmolin II hemmten *P. falciparum* (IC_{50} 4.0 ± 1.1 μM und 5.0 ± 0.4 μM, und SI von 24 und 6) *in vitro*. Es wurden auch synthetische Pyrethroide getestet, sie zeigten aber keine Aktivität. Keiner der beiden Wirkstoffe erfüllte die Anforderungen an Aktivität und Selektivität für in vivo Evaluierung.

Schliesslich, als Beitrag zu den Struktur-Aktivitätsuntersuchungen von Sesquiterpenlactonen mit Aktivität gegen *T. b. rhodesiense*, wurden Costunolid und Zaluzanin D aus *Laurus nobilis* L. (Lauraceae) und Eupatoriopicrin aus *Eupatorium cannabinum* L. (Asteraceae) isoliert. Germacrolides, d.h. Costunolid und Eupatoriopicrin, zeigten eine höhere Hemmung (IC_{50} von 1.3 ± 0.4 μM und 1.2 ± 0.2 μM) auf Protozoen als das Guaianolid Zaluzanin D (IC_{50} von 10.8 μM). Keines der Sesquiterepenelactone zeigte ausreichende Aktivität und Selektivität für *in vivo* Tests.

Es wurden insgesamt 22 Sekundärmetaboliten aus fünf Arten isoliert, darunter sieben neue Verbindungen. Diese Substanzen gehören zu den Strukturklassen der Isoflavonoide, Phenanthrenone und Terpene einschliesslich Sesquiterpenelactone, unregelmässige Monoterpene und Triterpenoidsaponine. Die meisten von ihnen (15 Verbindungen) zeigten *in vitro* Aktivität gegen Protozoen wenn auch in unterschiedlichem Ausmass. Die vielversprechendsten Verbindungen waren die Abruquinone und das Phenanthrenon, die starke und selektive Hemmung gegen *T. b. rhodesiense* und *P. falciparum* zeigten. Abruquinone und das Phenanthrenon sind drug-like Verbindungen mit einem rechnerischen toxischen Potential von gering bis mässig.

1. AIM OF THE WORK

Tropical parasitic diseases blight the lives of hundreds of millions of people worldwide and result in significant mortality. The social and economic consequences are devastating [1, 2]. Malaria, human African trypanosomiasis (HAT), Chagas disease, and leishmaniasis accounted in 2011 for estimated 669.274 deaths and 61.012.393 disability-adjusted life years (DALYs) [3, 4]. Most of the drugs available to treat these diseases have serious drawbacks in efficacy, show severe side effects, poor patient compliance, and resistance [2, 5]. Hence, new drugs are urgently needed [6-8].

Natural products (NPs) play a dominant role in drug discovery for the treatment of human diseases [9, 10]. Particularly, several well-established antiprotozoal drugs such as quinine and artemisinin have their origins in nature [11]. In fact, the history of antimalarial drug discovery contributed fundamentally to the modern concept of chemotherapy [12].

The aim of this work was to find hit compounds from medicinal plants and to determine their potential for future optimization as a part of a drug discovery program attempting to develop drugs intended for the treatment of parasitic tropical diseases.

As a first step, 118 South African plant species, belonging to 69 botanical families were selected mainly based on their traditional use. The plants were recollected and three extracts were obtained by successive extraction with solvents of increasing polarity. The resulting 507 extracts were formatted into a focused extract library.

The extracts were screened in a medium throughput platform against *Plasmodium falciparum, Trypanosoma brucei rhodesiense, Trypanosoma cruzi*, and *Leishmania donovani*, causative agents of malaria, HAT, chagas disease, and leishmania, respectively. Every extract was assayed in two concentrations and the most active ones (>95% inhibition at 10 μg/mL) were subjected to IC_{50} determination. Extracts with an IC_{50} values ≤ 5 μg/mL were considered to be active. To select extracts for further investigation, activity, potential structural novelty of substances contained in the extract, and taxonomic criteria of the plant were considered.

Selected extracts had to be fractionated in microgram amounts and in parallel, on-line spectroscopic (PDA), spectrometric (ESI-MS), and ELSD data had to be recorded. Collected one-minute fractions had to be re-assayed against the corresponding parasites. Biological results, chromatograms, and analytical data are combined to obtain a HPLC-based activity profiling [13-15]. Dereplication is supported with natural product databases, SciFinder Scholar, and other bibliographic resources to prioritize the extracts [16].

Subsequently, constituents responsible for the activity had to be isolated in small amounts (1 - 5 mg) for structure elucidation and *in vitro* antiprotozoal assessment. Compounds which comply with acceptance criteria for activity, selectivity, and novelty, are classified for *in vivo* evaluation in primary rodent models.

References

[1] Organization, W.H., Working to overcome the global impact of neglected tropical diseases: First WHO report on neglected tropical diseases, World Health Organization, Geneva, 2010.

[2] Renslo, A.R., McKerrow, J.H., Drug discovery and development for neglected parasitic diseases, Nat Chem Biol. 2 (2006) 701-10.

[3] Organization, W.H., Global Health Estimates Summary Tables: Deaths by Cause, Age and Sex, in: GHE_DthGlobal2000_2001.xls (Ed.), World Health Organization, Geneva, 2013.

[4] Organization, W.H., Global Health Estimates Summary Tables:DALYs, by Cause, Age and Sex, in: GHE_DalyGlobal2000_2001.xls (Ed.), World Health Organization, Geneva, 2013.

[5] Maser, P., Wittlin, S., Rottmann, M., Wenzler, T., Kaiser, M., Brun, R., Antiparasitic agents: new drugs on the horizon, Curr. Opin. Pharmacol. 12 (2012) 562-6.

[6] Hopkins, A.L., Witty, M.J., Nwaka, S., Mission possible, Nature. 449 (2007) 166-9.

[7] Miller, L.H., Ackerman, H.C., Su, X.-z., Wellems, T.E., Malaria biology and disease pathogenesis: insights for new treatments, Nat. Med. 19 (2013) 156-67.

[8] Anon, Ask the Experts: Drug discovery for the treatment of leishmaniasis, African sleeping sickness and Chagas disease, Future Med. Chem. 5 (2013) 1709-18.

[9] Cragg, G.M., Grothaus, P.G., Newman, D.J., Natural products in drug discovery: recent advances, John Wiley & Sons, Inc., 2012, pp. 1-42.

[10] Harvey, A.L., Natural products in drug discovery, Drug Discovery Today. 13 (2008) 894-901.

[11] Hannaert, V., Sleeping sickness pathogen (*Trypanosoma brucei*) and natural products: therapeutic targets and screening systems, Planta Med. 77 (2011) 586-97.

[12] Renslo, A.R., Antimalarial Drug Discovery: From Quinine to the Dream of Eradication, Chem. Lett. Ahead of Print.

[13] Potterat, O., Hamburger, M., Concepts and technologies for tracking bioactive compounds in natural product extracts: generation of libraries, and hyphenation of analytical processes with bioassays, Nat. Prod. Rep. 30 (2013) 546-64.

[14] Bertrand, S., Petit, C., Marcourt, L., Ho, R., Gindro, K., Monod, M., et al., HPLC Profiling with At-line Microdilution Assay for the Early Identification of Anti-fungal Compounds in Plants from French Polynesia, Phytochem. Anal. 25 (2014) 106-12.

[15] Adams, M., Zimmermann, S., Kaiser, M., Brun, R., Hamburger, M., A protocol for HPLC-based activity profiling for natural products with activities against tropical parasites, Nat. Prod. Commun. 4 (2009) 1377-81.

[16] Cordell, G.A., Shin, Y.G., Finding the needle in the haystack. The dereplication of natural product extracts, Pure Appl. Chem. 71 (1999) 1089-94.

2. INTRODUCTION

2.1 Natural Products and Drug Discovery

2.1.1 Historical Background

Medicinal plants have been used since the dawn of mankind to alleviate and treat diseases [1-3]. Pre-helenic civilizations documented their knowledge in different kind of documents.

The Sumerian healers recorded the knowledge about medicinal agents, mostly plants, in more than 600 tablets of clay, written around 1700 BC [4]. The registers contain information regarding the used formulations, plant decoctions and other preparations [3, 4].

Ancient Egyptians listed in the Ebers Papyrus more than 800 prescriptions. This document dates back to around 1550 BC and describes remedies for skin, ocular, and gastrointestinal complaints. Most of the prescriptions include culinary plants, such as grapes, figs, wheat, and spices (coriander, caraway, fennel, peppermint, and thyme). Furthermore, fragrant resins of *Boswellia ssp*. (frankincense) and *Commiphora myrrh* (myrrh) were highly valued by Egyptian embalmers. In Egypt, the physicians were priests. At that time, elements of religion and magic were closely intertwined with use of herbal drugs [1, 3, 4].

In India, one of the most traditional systems of medicine is the Ayurveda. The word Ayurveda is derived from the Sanskrit word "*Ayus*" (all aspects of life from birth to death) and "*Veda*" (knowledge or science), meaning science of long life. In the Vedic time, treatment of diseases was done by specific persons called ascetic people. They transmitted their knowledge to the next generations in three books called "*Brihat Trayees*" (major three), written between 1000 BC to 7th AD. These books contain basic concepts of health, disease, herbal formulations, and the description of about 900 plant species. One of the best known plant in western culture is *serpaghanda*, *Rauwolfia serpentina*, which contains the antihypertensive and antipsychotic alkaloid reserpine [3-5].

Chinese knowledge in medicinal plants was collected in treatises called "*Bencao"*. The first one appeared during the late Han dynasty (206 BC - 200 AD). However, the most comprehensive and best known treatise is the "*Bencao" Gangmu* or "Systematic Materia Medica", compiled during the Ming dynasty (1518 - 1596 AD) [4, 6, 7]. One of the most valued Chinese medicinal plants is *Ginkgo biloba,* used to improve the memory and to sharpen mental alertness. The main constituents responsible for these effects are reported to be the ginkgolides and flavonoids. *Panax ginseng* is reported to maintain health. Its main constituents are saponins (ginsenosides). The number of medicinal plants currently used in China is larger than 5.000 [1, 3].

Most of the ancient civilizations explained illness as a supernatural phenomenon, and healing as an art related to magic and religion. However, the Greeks changed this, and supernatural beliefs were rejected in favor of rational concepts. They postulated that diseases were caused by an imbalance in body humors (blood, phlegm, yellow bile, and black bile). Consequently, finding drugs became based on the belief that they had to correct this imbalance. These ideas were mentioned for the first time in the "*Hippocratic Corpus",* a written work comprised of about 60 treatises, attributed to Hippocrates (born in Cos 460 or 450 BC). Moreover, from the Greek time the book "*Historia Plantarum"*, written by Theophrastus (ca. 370 - 287 BC), a former student of Aristotle (384 - 322 BC), classified and described more than 500 plants [3, 4].

In Rome, Dioscorides (ca. 40 - 90 AD) wrote "*De Materia Medica*", the major source of information about medicinal herbs used in the Hellenic world, in which he cited more than 600 plants. He provided a description of each herb and its habitat, discussed its humoral qualities and its characteristics so that adulteration could be recognized. Dioscorides also reported side effects. Amongst others, he described belladonna, cassia, cinnamon, cumin, fennel, ginger, liquorice, lavender, mint, mustard, olive oil, opium, rhubarb, rosemary, sage, and thyme. The "*De Materia Medica*" may be considered as the first compendium of pharmacy [3, 4].

Galen (129 - 199 AD), the most influential Roman physician, wrote the "*Opera Omnia*", a collection of 20 volumes in which he expressed his agreement with Hippocrates and Dioscorides [4]. Galen's approach to therapy involved polypharmacy. He prescribed medicines in simple or complex mixtures called "galenics" which were specifically devised for each therapy. He argued that for each disease, the body would be able to select the appropriate ingredient [3, 4].

After the fall of the Roman Empire, Europe entered the Medieval Age (5^{th} to 15^{th} centuries), and the cultural center was transferred to the East, to the Byzantine Empire and Arab world [3]. The Greco-Latin texts were translated into Arabic, and three important scientific figures emerged during that era.

Abu Bakr al-Razi, known in the West as Rhazes, was born in Iran (865 - 925). He was a physician and a philosopher and wrote about 200 books, including the two main works related to medicine "*Kitab al-Mansuri fi al-tibb*" ("The Book of Medicine for Mansur") and "*Kitab al-Hawi fi al-tibb*" ("The Comprehensive Book on Medicine"). Rhazes introduced sedative procedures with opium before performing surgery on his patients and also recommended to test the drugs in animals before administering them to humans. Later on, another physician from Persia surpassed his influence, *Abu Ali al-Hussain ibn Abdallah ibn Sina* (Avicenna in Latin) (980 - 1037). Avicenna merged Greek and Arab traditions, further developed Galen's complex ideas, and described the use and efficacy of 760 drugs

arranged alphabetically in his work "*al-Qanun fi at-tibb"* ("The Canon of Medicine"). In the 12th century this treatise was translated by Gerardo de Cremona into Latin (after the Arabs were driven out of Spain) and was adopted as a standard text for medical students throughout Europe until the 18th century [3, 4]. *Abu al-Qasim Al-Zahrawi* (Abulcasis in Latin) born in Cordoba, wrote the medical encyclopedia "*al-Tasrif"*. Volume 28 describes the correct manner of handling plant products for medicinal application, with an emphasis on the importance of drying and storage techniques. He included more than 1500 herbal drugs, such as liquorice root, opium, aloes, sandalwood, acacia, and cardamom, described the plants and their natural habitats, specified the selection of the plant organs as well as the season in which they should be collected. There is also information about the preparation of oils, vinegars, decoctions and other dosage forms. The work was translated into Latin by Simon of Genoa and printed in Venice in 1471, becoming known as "*Liber Servitoris"*. Many generations of European apothecaries relied on it as a first-hand source of information on pharmaceutical processes [3, 4].

With the development of the printing press by Johann Gutenberg in the mid-15th century, printed herbals and formularies listing drugs and their use became more widely accessible. In 1530, Otto Brunfels (Germany, 1488 - 1534), a Lutheran preacher, published the "*Herbarium Vivae Eicones*". The most influential herbal writer was Leonhart Fuchs (Germany, 1501 - 1566) whose "*De Historia Stirpium*" was published in 1542. He was a professor of medicine in Tübingen and described in his book more than 500 plants. Subsequently, Hieronymus Bock (1498 - 1554) published in 1546 his "*Kreuterbuch"* in German, in which he includes own observations on plants. Subsequently, Rembert Dodoens (Belgium, 1517 - 1585) wrote "*Cruydeboeck*" (1554) and "*Pemptades*" (1583). Later on, Valerius Cordus (Germany 1515 - 1544) collected the herbs described by Dioscorides in "*De Materia Medica*" and his observations and work were published by the Council of the city of Nuremberg under the name "*Dispensatorium*" in 1546 and 1561. It was edited and published as the herbal "*Historia Plantarum*" by the Swiss naturalist Conrad Gesner. In 1544, the Italian medical botanist Pietro Andrea Gregorio Mattioli (1501-1577) published "*Di Pedacio Dioscoride Anazarbeo Libri Cinque*", his translation of the work of Dioscorides [4]. Renaissance herbals contain a large collection of plants and combine information from Greek, Roman, and Arabic traditions. They were the predecessors of the pharmacopoeias [8].

In 1498, the first official pharmacopoeia was compiled and printed in Florence by the Guild of Apothecaries and the Medical Society, under the name "*Nuovo Receptario*". Other cities produced their own pharmacopoeias, including Barcelona and Zaragoza (1535), Nuremberg (1556), Basel (1561), Augsburg (1564), Cologne (1565), and London (1618) [9].

Amid the Renaissance, Philip Theophrastus Bombastus von Hohenheim - he called himself Paracelsus (1493 – 1541) - was born in Einsiedeln (Switzerland). His advanced ideas changed drug therapy, but were regarded as strongly controversial in his time. He used metals such as antimony and mercury to treat his patients. He knew that such substances were toxic, but he realized that the hazardous effects depended on the dose ("*sola dosis facit venenum*"). In this way, Paracelsus became the "Father of toxicology". He gave also great importance to the way the remedies were prepared. Separation was considered the fundamental process in his chemical philosophy: "what the eyes perceive in herbs or stones or trees is not yet a remedy; the eyes see only the dross. But inside, under the dross, there the remedy lies hidden" [4, 10-12].

The discovery of America in 1492 brought with it the incorporation of new plants used for medicinal purposes in Europe. Ipecacuanha root (*Cephaelis ipecacuanha*) and cinchona bark (*Cinchona ssp*.) were some of the best known [13-16].

- **History of Cinchona Bark**

The origin of the cinchona bark and how it first came to Europe lacks of precise information, and some legends and false statements have sprout around its history [17].

Allegedly, the cinchona bark was introduced in Europe in the early 17th century by Jesuit priests. They were doing missionary work among the new-world indigenous communities. During 1630, the Jesuit apothecary Agostino Salumbrino (1561-1642) learnt that Peruvian indigenous chewed the bark while working in cold airflows in Spanish-owned mines to stop shivering. He reasoned that the bark also might stop the shivering coming from attacks of the ague (British name for malaria[1]). The Jesuits brought this information together with the bark to southern Europe, where malaria was a serious problem. The bark became known as the Jesuit's powder, Peruvian bark, or quina-quina, amongst others [13-16].

Initially, cinchona bark was met with a lot of skepticism due to religious beliefs of that time. Some Protestants in England called it "the powder of the devil". Additionally, the evidence of efficacy was confusing. On the one hand, a number of European physicians had remarkable success in treating patients with cinchona bark, but there was also numerous failures. They could be attributed to a wide variety of cinchona species, which showed great differences in the active component (quinine) and due to lack of

[1] Malaria is the most important parasitic disease in human beings. It is a protozoan disease transmitted by *Anopheles* mosquitoes. Five species of the genus *Plasmodium* causes malarial infections in humans. The most characteristic symptom is fever that occurs in four-to-eight hour cycles. First, a feeling of coldness with shivering that lasts for up to an hour appears, then a fever that lasts for two to six hours develops, accompanied by severe sweating [23].

authenticity of the herbal samples. Usually, the merchants collected the bark only after the bitter taste [13, 14].

Later, the use of cinchona bark became firmly established throughout Europe thanks to the sustained therapeutic success of practitioners like Sir Robert Talbor (England, 1642 - 1681). The publication of books which favorably advocated cinchona for its antimalarial properties, namely "The English Remedy or Talbor's Wonderful Secret for Curing of Agues and Feavers" in 1686, and "Pyretologia, A Rational Account of the Causes and Cure of the Agues" in 1692, are both attributed to Talbor. Cinchona bark became one of the most valuable commodities shipped from America to Europe [13-17].

In 1741, Carl Linneus (Sweden, 1707-1778) established his system of botanical classification of plants and gave to the genus the name *Cinchona,* in honor of the Countess of Chinchón from Spain. Confusion over Spanish, Latin, and Italian orthography led to the accidental dropping of the first "h" [13, 16, 17].

By the late 18th century, formulations were standardized and prepared in pharmacies, which during this time started to grow to become into pharmaceutical companies. Cinchona was more widely accepted as a treatment for specific intermittent fevers. However, adulteration with other herbs, quality (content of active principles), and availability were still an issue. Several species of cinchona trees became almost extinct. The desire to overcome these problems together with the curiosity regarding biological activity prompted the isolation of the active principles [4, 13, 14, 18, 19].

In 1820, the French pharmacists Pierre Pelletier and Joseph Caventou isolated quinine from *Cinchona cordifolia* [2, 4] by repeating the experiments previously performed by the Portuguese surgeon Bernardino Gomez, who managed to isolate cinchonine in 1811 [4]. Quinine was not only more reliable, but also less bitter than the bark and soon became the norm in the treatment of malaria. Caventou established a factory for the production of quinine in the mid-1820s. This alkaloid became hence the first commercial pure drug substance [2, 13, 14]. The early 19th century became the first days of modern medicinal chemistry in which the focus was laid on the isolation of active principles from plants, mainly of alkaloids such as morphine, emetine, and atropine [2, 18, 19].

There was the need to establish cinchona tree plantations to obtain plant material to isolate quinine. Charles Ledger, an English entrepreneur, discovered together with his servant Manuel Incra Mamani a variety of cinchona species with high quinine content (*C. ledgeriana*). The seeds were sold to the Dutch government in 1865. Within a short time, the Dutch plantations established in Java were producing 97% of the world's supply of bark, in the 1930s about 10 million kilograms of bark per year. From the mid-19th century to the 1940s, quinine was the standard drug for malaria throughout the world [13, 16]. Cinchona

bark is one of the historically most successful herbal remedies and illustrates the value of folk medicine [6].

The total synthesis of quinine was achieved by Robert Woodward and Eggers Doering in 1944. However, the bark still remains the only economically practical source of quinine [13, 15].

By the end of the 19th century, the understanding of organic synthesis and chemical structures led to the structure elucidation and to the synthesis of first derivatives of isolated natural products. The chemical structure of quinine was elucidated in 1908 (Fig. 1) [2, 4, 13]. The course of structure determination in the early days of the natural product chemistry was a complex, indirect process combining evidence from many types of experiments [1].

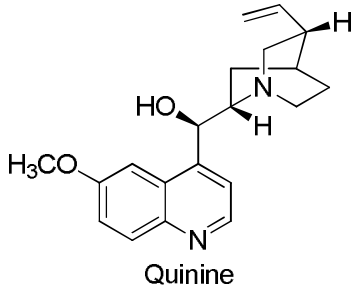

Figure 1. Chemical Structure of Quinine

The English chemist William Perkins failed in synthesizing quinine, but succeeded in synthesizing "mauveine", the first synthetic textile dye that did not wash off in water. This sparked the development of a German synthetic dye industry which had a profound influence on organic chemistry and medicine [4, 14, 20]. The German physician Paul Ehrlich (1854 - 1915) discovered the affinity of dyes for biological tissues. Based on these observations he postulated the existence of "chemoreceptors". Ehrlich later argued that certain chemoreceptors on parasites, microorganisms, and cancer cells would be different from analogous structures and claimed that these differences could be exploited therapeutically. This was the birth of chemotherapy. During his work with dyes, Ehrlich tested the effects of methylene blue on malaria parasites and trypan red on trypanosomes, and he became the first scientist searching for drugs against parasites [16, 20, 21].

Until the mid-20th century, most drug prototypes were derived from plants and once again, the fight against malaria became a good example of drug discovery during this era [4]. In World War I (1914 - 1918), German soldiers suffered from malaria, but Germany could not access quinine sources in Java. Bayer, one of the leading chemistry companies, was therefore commissioned during the 1920s to find a synthetic alternative based on quinine as prototype. Bayer developed plasmoquine (1925), mepacrine

(1932), resochin (1934), and sontochin (1936). The latter was considered as the most effective and toxic compound, and its production was initiated (Fig. 2) [13-15].

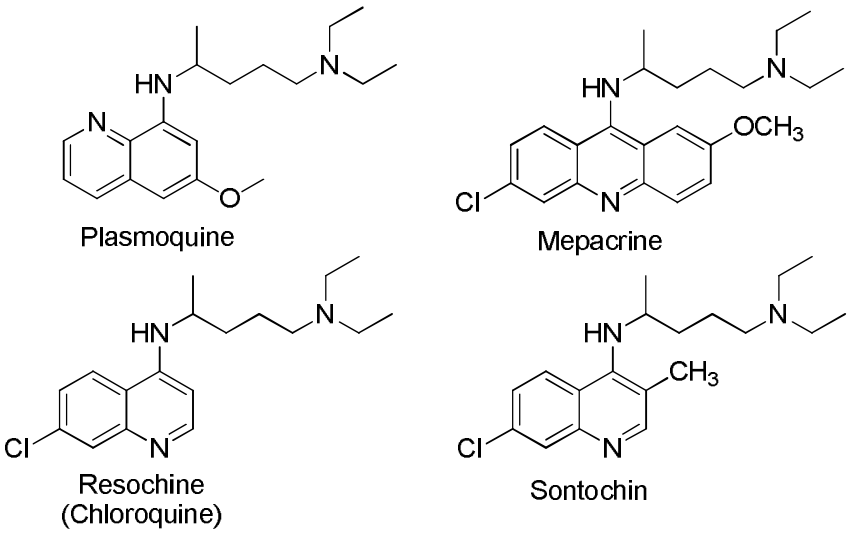

Figure 2. Some Antimalarial Derivatives Based on Quinine as a Prototype

In World War II the Allies neither had access to sontochin, since the trade with Germany had stopped, nor to quinine because of the Japanese occupation of Java. Thus, the Allies had to develop new synthetic antimalarials. British, Australian and American scientists synthesized and screened around 16.000 molecules. The most active and less toxic of these compounds was SN-7618. Subsequently, the assessment of its antimalarial properties in both animal models and humans was performed and its utility as a powerful antimalarial demonstrated. The compound was called chloroquine. This compound had previously been discovered and dropped by Germans (this became later on known as the "Resochin error") [13, 14, 16, 22].

In the 1950s and 1960s the World Health Organization (WHO) started a program for eradicating malaria. Chloroquine was selected as the WHO drug for a wide eradication campaign. In addition, DDT (dichloro-diphenyltrichloroethane) was recommended by the WHO as insecticide against the mosquito *Anopheles ssp*. which transmits the parasite. This action was very successful in areas such as Sri Lanka, where the cases of malaria fell from 3 million in 1946 to 29 cases in 1964. Yet, the resistance of *Plasmodium ssp*. to chloroquine (and *Anopheles ssp*. to DDT) gradually appeared in the 1960s and spread throughout the endemic areas. Therefore, new antimalarial drugs were needed [13, 14, 22, 23].

- **History of Artemisinin**

In 1960s, the government of the People's Republic of China embarked on a systematic examination of traditional remedies as sources for new drugs [7, 23]. One of the examined plants was *qing hao, Artemisia annua* L. (sweet worm-wood or annual wormwood), first mentioned in the "*bencao Gangmu"* nearly 2000 years ago and many times subsequently [6, 7, 15, 23].

In 1972, the female Chinese chemist Tu Youyou (1930-) isolated seven sesquiterpene compounds from an ethyl ether extract of *A. annua* obtained at low temperature. One of them, called *qinghaosu* (extract of *qing hao*), was found to bear the principal antimalarial activity. Its Western name is artemisinin [6, 7, 15].

The structure of artemisinin was determined in 1979 (Fig. 3). In the 1970s, there were already a number of physicochemical, spectroscopic, and spectrometric techniques available for structure elucidation. Still at that time, it was a major intellectual achievement. Its structure and absolute configuration was deduced with the aid of tehcniques as NMR, mass spectrometry, and X-ray diffraction analysis. Artemisinin is a sesquiterpene lactone with an unusual feature in its chemical structure, a 1,2,4-trioxane peroxide group [6, 7, 13].

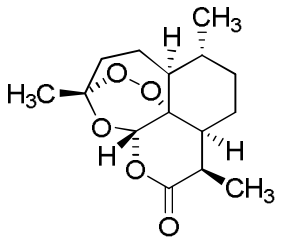

Figure 3. Chemical Structure of Artemisinin and Some Derivatives

The antimalarial activity of artemisinin *in vitro* was comparable with that of chloroquine. *In vivo* the compound was assessed in rodent, avian, and monkey malarial models with positive antimalarial activity, and total clearance of parasitemia was achieved [13, 23].

The toxicity of artemisinin was found to be low when tested in animal models, and no mutagenic or teratogenic effects were observed [7, 13].

In 1974, large-scale clinical trials started. During the first studies in China, more than 2099 cases of malaria (*P. vivax* and *P. falciparum* in a ratio of about 3:1) were treated with different dosage forms of artemisinin, leading to the clinical cure of all patients. Additionally, 143 cases of chloroquine-resistant falciparum malaria and 141 cases of cerebral malaria were successfully treated [7]. In summary,

artemisinin showed rapid action, low toxicity, and was effective against chloroquine-resistant *P. falciparum* [23].

Today, artemisinin is considered as one of the most potent and effective antimalarial drugs. Although it rapidly suppresses the parasitemia caused by of *P. falciparum* and *P. vivax,* the problems encountered with recrudescence and solubility, led to efforts to improve the natural product by modifying its chemical structure. The essentiality of the endoperoxide group became readily apparent when testing seven other sesquiterpenes isolated from *A. annua* which lacked this particular moiety [7, 24]. Dihydroartemisinin (DHA), which is obtained by reduction of artemisinin, showed better potency [7]. The two main types of DHA derivatives currently used in the treatment of malaria are ethers and esters (Fig. 4). The most active ether is artemether, and the most promising ester derivative is artesunate [7]. In general, artemisinin derivatives are more potent than the parent compound [23]. To avoid resistance and to overcome the recrudescence problem, artemisinin and its derivatives must be used in combination with other antimalarials [7, 13, 15, 25].

The mechanism of action of artemisinin is not fully understood, despite advances in the biology and biochemistry of the *Plasmodium* parasite. It is known that the integrity of the endoperoxide bridge is necessary, but not sufficient on its own, for antimalarial activity. The most likely mode of action is the ion-dependent alkylation of the heme group and the malarial translationally controlled tumour protein (TCTP). Nevertheless, it is clear and remarkable of that artemisinin has an entirely different mode of action than chloroquine [13, 24, 26].

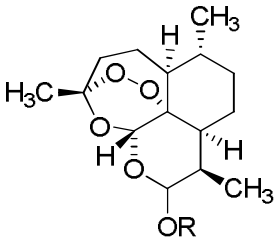

R = H	dehydroartemisinin (DHA)
R = CH_3	artemether
R = C_2H_5	arteether
R = $COCH_2CH_2CO_2Na$	sodium artesunate

Figure 4. Artemisinin Derivatives

As a result of the clinical and pharmacological research carried out during the last decades, standard therapy for uncomplicated falciparum malaria is an artemisinin derivative in combination with other antimalarial drugs (artemisinin combination therapy, ACT). In the case of severe malaria (caused by *P. falciparum, P. knowlesi,* or *P. vivax),* which constitutes a medical emergency, parenteral artesunate is the treatment of choice. ACT plays an important role in any program attempting to control malaria. The major problem today is to find a steady and inexpensive supply of artemisinin [13, 25, 27].

From a developing world perspective, plant-derived artemisinin remains expensive. The price ranges from US$ 150 to 1600 per Kg of compound. If the drug was made available at an affordable cost, it could be used not only for the treatment of malaria, but also of other parasitic tropical diseases such as schistosomiasis and leishmaniasis, for which artemisinin has also shown promising activity [28]. Even though different synthetic routes have been reported so far, *A. annua* still remains the best source of artemisinin worldwide [6, 7, 15]. The artemisinin content varies between 0.01 and 1% (w/w) of the dry leaves. Consequently, the production of artemisinin is struggling to keep up with the demand. To overcome this shortage, several strategies for the production of the drug have been developed as follow: i) semi-synthesis; ii) plant cell fermentation; iii) heterologous expression of the biosynthetic pathway in yeast or bacteria, frequently with modification of the genes to optimize production; iv) genetically modify *A. annua per se* to increase artemisinin yield by overexpression of the farnesyl diphosphate synthase. Yet these efforts have not resulted in dramatic improvements [7, 15, 29].

The discovery of artemisinin did not only contribute to a structurally novel and well-tolerated class of rapidly acting antimalarial agents, but also encouraged the investigation of folk medicine [7].

The history of malaria chemotherapy is a good example of how natural product-based drug discovery has evolved. The process can be summarized as follows: i) identification of medicinal plants (e.g. *Cinchona ssp*. and *Artemisia ssp.*) used by indigenous people to treat diseases; ii) early period of random isolation of active principles, and subsequent determination of structure and biological activity (e.g. quinine); iii) further isolation and structure elucidation of compounds (facilitated by the rapid advancement in chromatographic and spectroscopic techniques), semisynthesis of derivatives, and elucidation of biosynthetic pathways in the plants (e.g. artemisinin) [1, 4, 13-15, 18, 19, 30].

2.1.2 Current Drug Discovery Process

The process of drug discovery and development (DDD) requires between 12 – 15 years, 13.5 on average, and an estimated investment of US$ 1.5 billion for a single new drug [31-33]. Figure 5 provides a summary of the sequential steps that are necessary for a drug to progress through the DDD pipeline [34-36].

The initial phase of DDD is the drug discovery process, which typically involves three main stages: target identification and validation, hit generation, lead generation, and optimization. In the last 20 years, the incorporation of new technologies along these steps has evolved into a "new" concept in drug discovery. [35, 37].

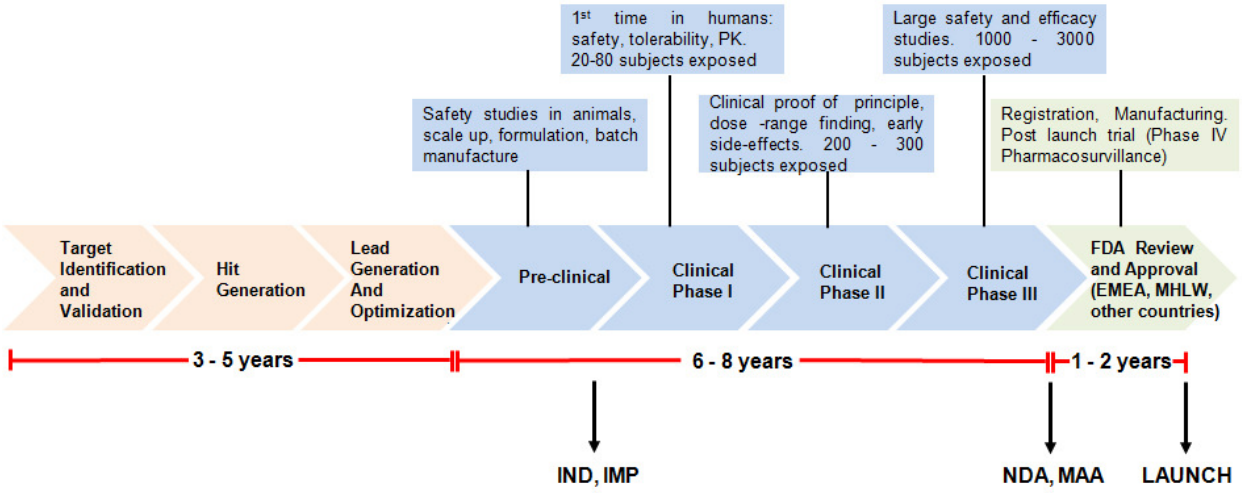

Figure 5. Drug Discovery and Development Pipeline. The figure shows an overview of the DDD course (arrows). Drug discovery comprises the first 3 phases (peach), while the drug development phase consists of the 4 following steps (blue). The rectangles (upper part) describe the objectives and major activities performed during each one of the development phases. The registration step (green) takes place in the different countries or regions where the drug is to be commercialized, i.d. USA (Food and Drug Administration, FDA), Europe (European Medicine Agency, EMA), and Japan (Ministry of Health, Labor, and Welfare of Japan, MHLW). At the bottom: average time span in each phase and required authorizations issued by regulatory agencies along the process. IND (Investigational New Drug application) to conduct clinical trials in the USA, IMP (Investigational Medicinal Product dossier) in Europe. NDA (New Drug Application) to approve a new pharmaceutical product in the USA, MAA (Marketing Authorization Application) in Europe. PK (pharmacokinetics). Adapted from [34, 36, 38, 39].

Identifying and validating disease-modifying targets is an essential early step in the drug discovery pipeline. The development of genomics, proteomics, and mouse gene knock-out models has opened the possibility to find a wide variety of molecular targets [33, 35, 37]. This has represented a major paradigm shift from older drug discovery strategies, which only utilized whole-animal physiology-based testings [33]. The target validation consists of confirmation of the role of the target prior to passing into the following drug discovery pipeline. It is accomplished by using either cellular or animal models for modulation of gene expression and/or protein function [40].

The next step is to perform a screening to find hits. A hit is an active compound which exceeds a certain activity threshold in a given assay [31, 41-43]. Currently there are several hit discovery techniques. Since approximately two decades one of the most commonly used approach is the high throughput screening (HTS). In the automated and miniaturized HTS formats, a large number of biochemical and cellular targets are exposed to a great number of small molecules [43].

The small molecules which should be tested can be derived from many sources. Theoretically the optimal strategy would be to screen as many molecules as possible. However, it is the resources required that indicate the optimal size of the compound collection. Therefore, assessing the chemical space and diversity of compound collections are essential components of the solution of this problem [32, 43].

Among this “new” drug discovery concept (HTS capability combined with a great number of molecular targets), it is possible to carry out a whole screening program within short time (typically around 3 months). This new approach is potentiated with the capability to synthesize a great number of new molecules through combinatorial chemistry, parallel synthesis, and other techniques. Consequently, a considerable amount of “hits” can be identified [19, 37, 41, 44-46]. Yet, the identified hits must be validated by demonstrating a desirable response in different biochemical and cellular assays [32, 43].

Once the hit has been validated, the hit-to-lead process starts. Not all biologically active compounds (hits) have the desired properties to become a drug. An optimized lead is a molecule with a good balance between potency, favorable pharmacokinetics (PK) properties, and and a good safety profile. Hence, during the hit-to-lead process, strategies such as bioisosteric replacement are applied to synthesize series of compounds with well established structure-activity relationship (SAR), wherein compounds with similar structures exhibit similar target binding affinities but with varying PK properties and safety profiles. Potency, PK, and safety of synthesized compounds are assessed in a set of *in silico*, *in vitro*, and *in vivo* tests which guide the compound selection [31, 35, 43, 47, 48].

Within the drug discovery process and particularly in the PK process where ADME (absorption, distribution, metabolism, and excretion) properties are assessed, the concept of drug-likeness is a key tool. This concept is associated with properties defined by Lipinski's "rule of five". Nineteen percent of the orally available drugs have fewer than 5 hydrogen-bond donors (expressed as the sum of OHs and NHs), less than 10 hydrogen-bond acceptors (expressed as the sum of Ns and Os), molecular masses of less than 500 Da, and logP values (a measurement of lipophilicity) of less than 5. Computational calculations predict "rule of five" properties for prospective compounds [31, 32, 41, 47, 49].

Figure 6 illustrates the optimization process from hit-to-lead of an imidazolepiperazine intended to be administered orally as antimalarial. After the lead optimization, the DDD course continues to the pre-clinical and further development phases (Fig. 5).

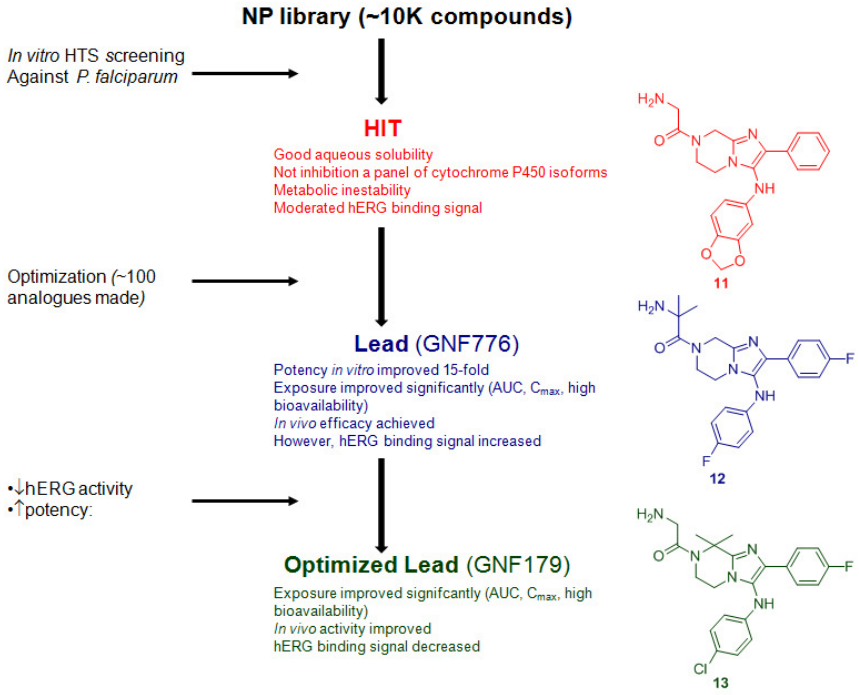

Figure 6. Optimization of an HTS Hit to Lead for an Orally Active Antimalarial. In this example the Novartis natural products (NP) and natural product-like synthetic compounds library was screened. Compound **11,** an imidazolepiperazine, was chosen as a hit due to its potency *in vitro* against *P. falciparum*and its favorable physicochemical and ADME properties. However, the compound showed some toxicity issues (hERG binding). After early optimization, a lead compound (**12**) was selected. Its *in vitro* potency, PK, and *in vivo* efficacy were improved in comparison to the hit, but the hERG binding was still a problem. After understanding the SAR of hERG binding and differentiation from potency, both safety and potency of the leadcould be improved alongside with its PK (the substitution of the benzylic carbon of the piperazine was a key point). As a result, an optimized lead compound was obtained (**13**) [50].

So far, the above described "new" concept of drug discovery has not been as productive as expected. Only very few leads and developed compounds can be attributed to the new drug discovery paradigm. From 2003 to 2009, a total of 12 compounds originated from HTS hits were introduced into the pharmaceutical market [19, 32, 41, 44-46].

- **Natural Products (NPs) and Their Role in Current Drug Discovery**

There is no doubt that NPs have been historically very valuable in the drug discovery process and that they still constitute a successful source for new drugs [1, 30, 41, 44, 46, 48, 51].

According to Newman and Cragg, a total of 1355 new chemical entities (NCEs) were approved between 1981 and 2010, including vaccines, biologicals, and "small molecules" [52]. In these 30 years, NPs were the source of 35% of all small molecules ranging from 12% in 1997 to 50% in 2010 [52-54].

Moreover, many semi-synthetic NPs analogs or synthetic compounds based on NPs pharmacophores have been obtained. Particularly, about 38 NPs-based drugs, 10 NPs, 15 semi-synthetic compounds, 12 NPs derivatives, and 1 synthetic congener were approved and launched in the market between 2000 and 2010. Fifteen were intended to treat infectious diseases, 7 to treat cancer, 7 against neurological disorders, 4 against metabolic and cardiovascular ailments, 1 to treat diabetes, and 4 intended for other areas (inflammation, immunomodulation, pain, etc.) [52-55].

Challenges

Despite of the NPs success, many large pharmaceutical companies have reduced and cut down the use of natural products in the drug discovery programs. The reasons for this decreased interest range from commercial to scientific, but one of the main explanations is that NPs are not amenable to the aggressive timelines of the HTS [30, 41, 44-46, 56, 57].

Additionally, NPs sources have some disadvantages compared to synthetic libraries concerning their incorporation into HTS programs: i) NPs show a higher number of false-positive results in the assays, due to the presence of compounds with non-specific activities, or interference with the assay read-out; ii) repeated isolation of the same compounds is challenging; iii) NPs may contain only very small quantities of a bioactive substance, often as a mixture with structurally related molecules, which requires labor-intensive and time-consuming purification procedures; sometimes the concentration of these small quantities of bioactive substances may even be too low to be effectively detected; iv) NPs are often structurally complex (a lot of functional groups and chiral centers); these factors delay the identification process and contribute to problems of supply and manufacture; v) increasing complications arise in the

handling of intellectual property and in the access of bio-materials as a result of the Rio Convention on Biological Diversity in 1992; vi) seasonal or environmental variations in the composition of living organisms can cause problems with initial detection of active compounds as well as subsequent repetition of assays or purification; the loss of source is also possible (extinction) and vii) NPs discovery has been perceived as old-fashioned compared to emerging technologies [30, 41, 44-46, 52, 58].

Opportunities

The pharmaceutical industry is currently facing high economic pressure due to product recalls, aggressive generic competition, and the looming patent cliff. Due to the lack of productivity of the "new" drug discovery concept, there is a steady decreased number of NCEs launched into the market. For instance, the number of small molecules introduced per year between 1981 and 1989 was 50, in the next decade the number lessened to 40, and between 2001 and 2010 it was around 20 (with the exception of the years 2002- 2005, when the figures climbed above 30). Moreover, not only less NCEs have been introduced in the market, but more money has been invested in discovery and development. As a result, the costs of bring a drug to market has increased [30, 33, 45, 52, 57, 59-61].

Owing to these factors, the industry has refocused efforts on strategies that are most likely to yield sustainable products. A critical part of this refocusing includes the re-evaluation of drug discovery processes. This is where the NPs may play an important role again in generating novel and structurally unique scaffolds [30, 41, 44-46, 61].

There is a number of characteristics that make NPs structures "privileged" to elicit a biological activity: i) higher chemical diversity and complexity. Even though, this is considered as an incompatibility factor with an HTS program, this is one of the noteworthy characteristics for both finding active compounds and new mechanisms of action; ii) biochemical specificity. NPs are produced by biosynthesis in living organisms as a result of evolutionary pressures to interact with a wide variety of proteins and other biological targets. This means that NPs have an imprint of biological space (protein fold topology) and preferentially bind to these folds. The fold space is the total repertoire of three-dimensional protein structures; iii) drug-like properties. NPs show compliance with Lipinski's type descriptors in approximately 90% [41, 45, 46, 51, 57, 58].

In addition to the priviledged structure of NPs, still much of the nature remains to be explored as source of novel active agents [52]. For instance, fewer than 1% of microbial species are culturable, and fewer than 12% of higher plants species have been examined for bioactivity [62]. Certain insects and other animals have been targeted for specific bioactivities, such as toxins, but are not generally subjected to

HTS efforts. Clearly, the biological resource is there, but access and examination is problematic, especially if there is pressure because of a short time frame for discovery of new compounds [57].

However, this renewed interest on NPs can only be sustained if NPs research can be competitive with other drug discovery techniques. Key factors to achieve this competitiveness include uninterrupted technological improvements in the NPs-based lead discovery, such as speed of dereplication, isolation, structure elucidation, and compound supply processes. Some of these approaches will be discussed in the next subchapter [30, 45].

2.1.3 Current State of NP Discovery

In the classical approach for NPs isolation, the process of "bioassay-guided fractionation" starts when a extract, obtained from terrestrial plants, marine organisms, microorganisms, and/or animals, shows a positive response in a screening. Then, it is necessary to isolate the pharmacologically active pure constituent from the total extract. However, extracts are complex matrices that require a long process, substantial material amount and financial resources [1, 42].

The original crude material (large amounts) is split into fractions which are tested in biological assays to track the active compounds. Typically, liquid-liquid partitioning between immiscible phases and consecutive chromatographic separations in open column chromatography (normal phase) are performed. Subsequent steps are generally of higher resolution by using RP-HPLC. The separation performance in these initial fractionation steps is poor and very often the activity is lost in the course of the isolation. Furthermore, the compounds' structures are disclosed only at the end of the whole elaborated and resource-consuming process. This can turn out in disappointment if the isolated compounds are already known structure. Therefore, the approach described above does not match the timelines and the workflow of modern drug discovery [30, 42, 58].

However, technological advances in instrumentation, robotics, and bioassay miniaturization have increased the speed of bioassay-guided isolation and structure elucidation of NPs considerably, and these improvements have allowed NPs research to be more competitive with synthetic compounds screening and HTS. Some of the most important advances in this field are discussed below [30, 45].

- **Libraries**

Ideally, NPs screening libraries would consist of pure compounds in order to obviate confounding responses derived from mixtures, and to avoid the lag time required to deconvolute a mixture for the identification of the active component [61]. Libraries of pure compounds, present in known amounts, are screen-friendly and accommodate the desire for short timelines in examination of a large number of molecules. These libraries combine one of the strengths of HTS with the concept of chemical diversity [32, 57].

Additionally, with a NPs compound library it is possible to create a target-oriented or focused-library approach which seeks to elaborate structural modifications onto an existing bioactive NP scaffold in a parallel, systematic fashion to improve the compound's inherent biological activity or drug-like properties. This can be performed either by semi-synthetic modification of the parent molecules, or by fully synthetic methods [41, 45].

However, assembling a highly diverse library of NPs for screening is a major endeavor because, the commercial availability of pure NPs remains quite limited. An alternative can be pre-fractionated NPs libraries, which combine the benefits of incorporating much greater chemical diversity with reasonable consistent biological readouts. Simplified mixtures resulting from pre-fractionation expedite the downstream processes of dereplication and of compound purification and therefore reduce the lag time. Pre-fractionation schemes aim to include the bulk of constituents, rather than only including major components or "peaks" hence the opportunity to discover novel compounds is preserved [30, 42, 61]. Some approaches go beyond and propose to create libraries of initial optimized extracts to lead-like and drug-like space with a particular emphasis on logP, one of the most important physicochemical parameters, followed by fractionation to afford a HTS-friendly NP screening library [51].

- **High performance liquid chromatography (HPLC)**

High performance liquid chromatography (HPLC) is one of the most powerful tools in chemistry, with the ability to separate, identify, and quantitate the compounds present in any sample that can be dissolved in a liquid. HPLC can separate water-soluble, thermally-labile, non-volatile compounds with speed, precision, and high resolution. HPLC is used routinely in phytochemistry both in analytical and preparative scale [63].

In recent years, a wide variety of stationary and mobile phases have been developed to give a large potential of different kinds of separations. Most common used stationary phases are reverse phase (RP), based on octadecyl (RP-18) and octyl (RP-8) materials with particle diameter around 5 μm. Current reverse-phases are highly selective, offer high separation power, robustness, stability, and efficiency. The introduction of spherical particles has led to a reduction in the size of the particles and the length of the columns, from 25 cm (8000-10000 plates/m) to around 10 cm, with the same number of plates/m. In ultra high-performance liquid chromatography (UHPLC), particle sizes of around 1.7 μm are used. Other modified phases such as cyano, phenyl, trimethylsilane, triazole, secondary and tertiary amines are available. Typically, the mobile phases are combinations of water and either methanol or acetonitrile [63, 64].

When HPLC is applied to analytical work, the goal is to get information about the sample. The most important parameters are resolution, sensitivity and fast analysis time. In preparative HPLC, larger columns and larger quantities of packing materials are needed. The aim here is to isolate and/or purify compounds, and the most important parameters in this kind of chromatography are the degree of solute purity, the throughput, measured as the amount of compound produced per unit time, and the load capacity [63].

The potential of HPLC has been boosted by coupling the LC part with different detectors such as UV/DAD (HPLC-UV), MS (HPLC-MS), MS/MS (HPLC-MS/MS), ELSD (HPLC-ELSD), NMR (HPLC-NMR) and circular dichroism (CD) (HPLC-CD). This hyphenation of HPLC with spectroscopic methods has led to new strategies that permit i) to authenticate botanical samples by creating fingerprints; ii) to obtain complete spectroscopic characterization of present compounds to differentiate between known and unknown compounds; iii) to determine the structure of unknown plant metabolites directly without previous isolation and minimum amounts of material iv) to establish the absolute configuration of the new compounds by measuring their CD spectra. Most of these applications are useful in analytical work, but also for preparative separations, the introduction of HPLC-MS has enhanced the range of application [58, 63-65].

- **LC-MS**

Mass spectrometry is one of the most sensitive analytical methods which provides information about the structure of analytes and about their molecular weight. This technique has had a dramatic and rapid advance in recent years. An LC-MS system includes the HPLC system, the ionization source (which interfaces the LC to the MS), and the mass spectrometer [1, 63, 66].

Their most common ionization sources are electrospray ionization (ESI) and atmospheric pressure chemical ionization (APCI). Both ESI and APCI ionization occurs at atmospheric presure, hence these sources are referred to as atmospheric pressure ionization (API) sources. In ESI, the high voltage field (3-5 kV) causes about nebulization of the column eluents resulting in charged droplets that are directed toward the mass analyzer. Ions are then released from the charged droplets by direct ion emission (a process called “ion-evaporation”), and are finally separated according to their mass/charge ratio in the mass spectrometer. In APCI, heat is applied to vaporize the column eluents, and then a corona discharge ionizes the solvent molecules, which results in the formation of analyte ions via chemical ionization [63, 66].

The most frequently used mass spectrometer for HPLC-MS is the single quadrupole, which provides a mass spectrum for each chromatographic peak that elutes from the LC column. Another type of spectrometer used in NPs research is the time-of-flight (TOF), which provides a high resolution spectrum for each analyzed component [66].

- **Dereplication**

Dereplication is the process of identifying known compounds that are responsible for the activity of an extract before bioassay-guided isolation begins. This process is used to eliminate, group, and/or prioritize

extracts for further studies, and it can save considerable research time. The chemical and biological characteristics of the unknown compounds are compared with the chemical and biological characteristics of known compounds from the data-bases to eliminate those that have been isolated previously [41, 45, 46, 58, 67].

The procedure involves separation of an extract using RP-HPLC and splitting of the eluent post column into a fraction collector using microtiter plates and in a mass spectrometer for analytical purposes. The collected fractions in the microtiter plates are dried, redisolved in an appropriate solvent, typically DMSO, and assayed. The retention times, UV spectra, MS data, and activity of the fractions are analysed, and commercial and in-house databases are used for comparison. Databases such as the Dictionary of Natural Products contain chemotaxonomic, pharmacological, and molecular weight information. This approach constitutes an off-line HPLC-based activity profiling. Other setups are fully integrated on-line approaches, where HPLC fractionation is coupled directly to biochemical assays, such as on-flow post-column bioassays and at-line settings. However, the off-line format is highly versatile because it can be applied to different kinds of bioassays after adaption of the fractionation protocol to the required sensitivity of the assay [30, 45, 58]. Some examples of the off-line approach include the HPLC-based activity profiling for the identification of NPs with $GABA_A$ receptor modulating activities [68] and for NPs with antiprotozoal activities [69]. The off-line approach has been used with numerous other targets, such as, for inhibitors of the DYRK1A kinase, a target implicated in neurodegenerative diseases [70], or for anti-HIV inhibitors [71].

Tracking bioactivity in extracts, which are complex matrices, remains a highly challenging task. But HPLC-based activity profiling allow not only to dereplicate known active compounds, but also to carry out a target preparative isolation of the active principles present in the active fraction [58, 67].

- **Structure Elucidation**

With the advances in X-ray crystallographic, NMR, chiroptical, and mass spectrometric techniques, structure determinations for NPs has become quite routine [1, 72].

NMR

Introduction of nuclear magnetic resonance (NMR) spectroscopy into organic chemistry has changed the way of structure determination. Fifty years ago, NPs structure elucidation was an extremely difficult and lengthy task which required carrying out several synthetic steps and degradation reactions. The thereby obtained data was combined to eventually allow the determination of the structure. However, even total chemical synthesis of compounds of interest was needed to corroborate the proposed structures. By the

1950s, the development of commercial IR and UV/VIS spectrometers allowed NPs chemists to use these techniques for functional group characterization. Following the discovery of the NMR phenomenon, its potential was early recognized and its application for the identification of organic compounds started. In 1950, NMR spectrometers required a skilled operator. However, with the introduction of user-friendly NMR spectrometers since the 1960s, the potential of this technique has become more accessible for the scientific community and over the time, the improvements in the commercial instrumentation have revolutionized NPs structure elucidation [1, 72, 73].

The NMR sensitivity has considerably improved. In 1960, a signal to noise (S/N) ratio of 10:1 on a 1.0% sample was obtained. With today's spectrometers, the S/N ratio is 10.000:1 on a 0.1% sample prepared in the same solvent. This improvement was achiveed by the introduction of: i) higher field spectrometers using superconducting solenoids; ii) progress in pulsed-field gradients (PEGs). Sensitivity itself is not the only determinant for spectral quality, the level of noise is another important factor. Any instability of the NMR system, fluctuations of the field-frequency-regulation circuit (the "lock") and fluctuations in room temperature or magnetic disturbances may introduce noise. When PEGs are used in experiments, only the desired coherences enter into the receiver, and the effects of short-term fluctuations interfere in a lesser extent; iii) probeheads with superior sensitivity. Cryogenically cooled probes (so-called "cryoprobes"): upon cooling the radio-frequency coil to a temperature of ca. 20 K, thermal noise is dramatically lowered, resulting in S/N ratios generally 3 or 4 times higher than for a conventional probe heads. All these advances provide sufficient sensitivity to record full sets of 2D data within a few hours and with sub-milligrams amounts of sample [72, 73].

Other important improvements were the introduction of Fourier-transformation, allowing more rapid acquisition of spectra and the development of multiple pulse sequences. Two-dimensional (2D) pulse sequences used for structure elucidation, including COSY (^{1}H-^{1}H correlation), HETCOR (1-bond ^{1}H-^{13}C correlations), and NOESY (^{1}H-^{1}H nuclear Overhouser enhancement spectroscopy), among others.

Another technological improvement for the application of NMR to NPs analysis is the hyphenation with HPLC. The objective is to create an interface able to deliver the HPLC fractions/pure compounds to the NMR coil. Flow NMR methods has been developed for this purpose. The HPLC fraction is transferred via capillaries into a flow NMR probe. A modification of this technique is the so-called "stopped –flow NMR", and the "loop storage". All these flow NMR methods have two main drawbacks. Firstly, due to the significantly lower sensitivity of NMR compared to MS, it is possible to obtain only a ^{1}H NMR spectrum in the limited time that the sample is present in the coil region of the flow cell. Secondly, deuterated solvents have to be used or alternative, multiple solvent peak suppression must be carried out.

The most successful approach, so far implemented, is the use of solid phase extraction (SPE) cartridges in combination with LC. By establishing such procedures, multiple injections can be done to build up amounts of isolated samples and the problem with the solvents is eliminated by evaporating the protonated solvents from the cartridges and eluting off the cartridges with deuterated solvents [72, 73].

The most widely used strategy, to determine the skeletal structures of NPs is combining ^{1}H-^{1}H correlations spectra (COSY or TOCSY) with one-bond ^{13}C-^{1}H correlations (HSQC and HMBC) to attach together the fragments. However, the actual pulse sequences used to obtain the data have been improved significantly, and additional methods to supplement these techniques has been developed [72, 73]. Previous determination of the molecular formula is very important to support the information deduced from the NMR analysis. Once the skeletal structure of the compound has been determined, the three-dimensional structure must be established. Again NMR information can be useful for doing this. The vicinal ^{1}H-^{1}H and germinal and vicinal ^{13}C-^{1}H coupling constants can be used to determine the dihedral angle, alongside with the 2D NOESY and/or ROESY, which constitute powerful methods for indentifying pairs of protons which are spatially close, even if separated by a large number of bonds [72, 73]. However, to assign the absolute configuration (AC) in an unequivocal way, chiroptical, X-ray christallographic, enzymatic or chiral derivatization methods must be applied [74].

Absolute Configuration

Most NPs and biologically active compounds are chiral and their biological functions are related to their chirality, i.e. their AC. Therefore, the determination of the AC of chiral compounds is critical for the studies of NPs. One of the most sensitive and versatile methods for this purpose is electronic circular dichroism (ECD) spectroscopy, because two enantiomers are unambiguously characterized by their fully opposite CD spectra. In the case of NPs, ECD is the most common approach for AC determination and nowadays, it is even possible to apply hyphenation of CD measurements with HPLC techniques. From the CD spectra, whether taken online or offline, the AC of the respective steroisomer can easily be determined by i) comparison of the CD spectrum with experimental data from structurally related compounds of known absolute configuration; ii) if the structure fits into semiempirical CD rules, e.g., the octant rule; iii) for novel-type structures, the most efficient alternative for the interpretation of CD spectra is the quantum chemical calculation simulation of the curve for both enantiomers, and their comparison with the experimental ones [65, 75].

References

[1] Nakanishi, K., A Brief History of Natural Products Chemistry, In: Meth-Cohn, O., Barton, D., Nakanishi, O. (Eds.), Comprehensive Natural Products Chemistry, Pergamon, Oxford, 1999, pp. 1-31.

[2] Potterat, O., Hamburger, M., Drug discovery and development with plant-derived compounds, Prog. Drug Res. 65 (2008) 45, 7-118.

[3] Ravina, E., Editor, Evolution of Drug Discovery: From Traditional Medicines to Modern Drugs, Wiley-VCH, 2011.

[4] Sneader, W., Drug Discovery: Past, Present and Future, John Wiley & Sons, 2005.

[5] Mukherjee, P.K., Nema, N.K., Venkatesh, P., Debnath, P.K., Changing scenario for promotion and development of Ayurveda-way forward, J Ethnopharmacol. 143 (2012) 424-34.

[6] Butler, A.R., Wu, Y., Artemisinin (qinghaosu): a new type of antimalarial drug, Chem. Soc. Rev. 21 (1992) 85-90.

[7] Klayman, D.L., Qinghaosu (artemisinin): an antimalarial drug from China, Science. 228 (1985) 1049-55.

[8] Adams, M., Alther, W., Kessler, M., Kluge, M., Hamburger, M., Malaria in the Renaissance: remedies from European herbals from the 16th and 17th century, J Ethnopharmacol. 133 (2011) 278-88.

[9] Urdang, G., Pharmacopoeias as witnesses of world history, J Hist Med Allied Sci. 1 (1946) 46-70.

[10] Ball, P., The Devil's Doctor: Paracelsus and the world of the Renaissance, Magic, and Science, Ferrar, Straus and Giroux New York, 2006.

[11] Waddell, W.J., History of dose response, J. Toxicol. Sci. 35 (2010) 1-8.

[12] Jacobi, J., Paracelsus: Selected Writings, Princeton University Press, Princeton, 1979, pp. 93, 95.

[13] Butler, A.R., Khan, S., Ferguson, E., A brief history of malaria chemotherapy, J R Coll Physicians Edinb. 40 (2010) 172-7.

[14] Meshnick, S.R., Dobson, M.J., The history of antimalarial drugs, in: Rosenthal, PJ (Ed.), Antimalarial chemotherapy: Mechanisms of action, resistance, and new directios in drug discovery., Humana Press Inc., Totowa, NJ, 2001, pp. 15-25.

[15] Fotie, J., Key Natural Products in Malaria Chemotherapy: From Quinine to Artemisinin and Beyond, In: Brahmachari, G. (Ed.), Natural products in drug discovery: impacts and opportunities - an assessment, World Scientific Publishing Co., Singapore, 2012, pp. 223-71.

[16] Hempelmann, E., Tesarowicz, I., Oleksyn, B.J., Short history of malaria chemotherapy, Pharm. Unserer Zeit. 38 (2009) 500-7.

[17] Keeble, T.W., A cure for the ague: the contribution of Robert Talbor (1642-81), J R Soc Med. 90 (1997) 285-90.

[18] Nakanishi, K., Berova, N., Lessons from nature, Chimia. 52 (1998) 3-9.

[19] Drews, J., Drug discovery: a historical perspective, Science. 287 (2000) 1960-4.

[20] Agueero, F., Al-Lazikani, B., Aslett, M., Berriman, M., Buckner, F.S., Campbell, R.K., et al., Genomic-scale prioritization of drug targets: the TDR Targets database, Nat. Rev. Drug Discovery. 7 (2008) 900-7.

[21] Kaufmann, S.H.E., Paul Ehrlich: founder of chemotherapy, Nat. Rev. Drug Discovery. 7 (2008) 373.

[22] Coatney, G.R., Pitfalls in a discovery: the chronicle of chloroquine, Am J Trop Med Hyg. 12 (1963) 121-8.

[23] Hien, T.T., White, N.J., Qinghaosu, Lancet. 341 (1993) 603-8.

[24] Meshnick, S.R., Artemisinin: mechanisms of action, resistance and toxicity, Int. J. Parasitol. 32 (2002) 1655-60.

[25] White, N.J., Pukrittayakamee, S., Hien, T.T., Faiz, M.A., Mokuolu, O.A., Dondorp, A.M., Malaria, Lancet. 383 (2014) 723-5.

[26] White, N.J., Qinghaosu (Artemisinin): The Price of Success, Science. 320 (2008) 330-4.

[27] Burchmore, R., Parasites in the brain? The search for sleeping sickness biomarkers, Expert Rev. Anti-Infect. Ther. 10 (2012) 1283-6.

[28] Weathers, P.J., Arsenault, P.R., Covello, P.S., McMickle, A., Teoh, K.H., Reed, D.W., Artemisinin production in Artemisia annua: studies in planta and results of a novel delivery method for treating malaria and other neglected diseases, Phytochem. Rev. 10 (2011) 173-83.

[29] Covello, P.S., Making artemisinin, Phytochemistry. 69 (2008) 2881-5.

[30] Potterat, O., Hamburger, M., Concepts and technologies for tracking bioactive compounds in natural product extracts: generation of libraries, and hyphenation of analytical processes with bioassays, Nat. Prod. Rep. 30 (2013) 546-64.

[31] Lombardino, J.G., Lowe, J.A., 3rd, The role of the medicinal chemist in drug discovery-then and now, Nat Rev Drug Discov. 3 (2004) 853-62.

[32] Macarron, R., Banks, M.N., Bojanic, D., Burns, D.J., Cirovic, D.A., Garyantes, T., et al., Impact of high-throughput screening in biomedical research, Nat. Rev. Drug Discovery. 10 (2011) 188-95.

[33] Caskey, C.T., The drug development crisis: efficiency and safety, Annu Rev Med. 58 (2007) 1-16.

[34] Roses, A.D., Pharmacogenetics in drug discovery and development: a translational perspective, Nat. Rev. Drug Discovery. 7 (2008) 807-17.

[35] Lennart, K.-L.P.a.B., Introduction to Drug Design and Discovery, in: Krogsgaard-Larsen Povl, SK, Madsen Ulf (Ed.), Text Book of Drug Design and Discovery, CRC Press, Boca Raton, 2010, pp. 1-14.

[36] Nwaka, S., Ridley, R.G., Virtual drug discovery and development for neglected diseases through public-private partnerships, Nat Rev Drug Discov. 2 (2003) 919-28.

[37] Alexander John C., S.D.E., Modern Drug Discovery and Development, in: Williams, DRaGH (Ed.), Clinical and Translational Science, San Diego, 2009, pp. 361-80.

[38] Ashburn, T.T., Thor, K.B., Drug repositioning: identifying and developing new uses for existing drugs, Nat. Rev. Drug Discovery. 3 (2004) 673-83.

[39] Royle, K.E., Jimenez, D.V.I., Kontoravdi, C., Integration of models and experimentation to optimise the production of potential biotherapeutics, Drug Discov Today. 18 (2013) 123-4.

[40] Lindsay, M.A., Target discovery, Nat Rev Drug Discov. 2 (2003) 831-8.

[41] Koehn, F.E., Carter, G.T., The evolving role of natural products in drug discovery, Nat. Rev. Drug Discovery. 4 (2005) 206-20.

[42] Carter, G.T., Natural products in drug discovery, CRC Press, 2010, pp. 89-105.

[43] Keseru, G.M., Makara, G.M., Hit discovery and hit-to-lead approaches, Drug Discov Today. 11 (2006) 741-8.

[44] Harvey, A.L., Natural products in drug discovery, Drug Discovery Today. 13 (2008) 894-901.

[45] Butler, M.S., The Role of Natural Product Chemistry in Drug Discovery, J. Nat. Prod. 67 (2004) 2141-53.

[46] Lam, K.S., New aspects of natural products in drug discovery, Trends Microbiol. 15 (2007) 279-89.

[47] Lipinski, C., Hopkins, A., Navigating chemical space for biology and medicine, Nature. 432 (2004) 855-61.

[48] Oprea, T.I., Davis, A.M., Teague, S.J., Leeson, P.D., Is There a Difference between Leads and Drugs? A Historical Perspective, J. Chem. Inf. Comput. Sci. 41 (2001) 1308-15.

[49] Lipinski, C.A., Lombardo, F., Dominy, B.W., Feeney, P.J., Experimental and computational approaches to estimate solubility and permeability in drug discovery and development settings, Adv. Drug Delivery Rev. 23 (1997) 3-25.

[50] Chatterjee, A.K., Cell-Based Medicinal Chemistry Optimization of High-Throughput Screening (HTS) Hits for Orally Active Antimalarials. Part 1: Challenges in Potency and Absorption, Distribution, Metabolism, Excretion/Pharmacokinetics (ADME/PK), J. Med. Chem. 56 (2013) 7741-9.

[51] Camp, D., Davis, R.A., Campitelli, M., Ebdon, J., Quinn, R.J., Drug-like Properties: Guiding Principles for the Design of Natural Product Libraries, J. Nat. Prod. 75 (2012) 72-81.

[52] Newman, D.J., Cragg, G.M., Natural Products As Sources of New Drugs over the 30 Years from 1981 to 2010, J. Nat. Prod. 75 (2012) 311-35.

[53] Newman, D.J., Cragg, G.M., Natural Products as Sources of New Drugs over the Last 25 Years, J. Nat. Prod. 70 (2007) 461-77.

[54] Newman, D.J., Cragg, G.M., Snader, K.M., Natural Products as Sources of New Drugs over the Period 1981-2002, J. Nat. Prod. 66 (2003) 1022-37.

[55] Brahmachari, G., Natural products in drug discovery: impacts and opportunities - an assessment, World Scientific Publishing Co., 2012, pp. 1-199.

[56] Extraction and purification of abruquinones from *Abrus precatorius* and their therapeutic uses, National Science Council, Taiwan. 1997, pp. 40.

[57] Li, J.W.H., Vederas, J.C., Drug discovery and natural products end of an era or an endless frontier?, Science. 325 (2009) 161-5.

[58] Potterat, O., Hamburger, M., Natural Products in Drug Discovery - Concepts and Approaches for Tracking Bioactivity, Current Organic Chemisty. 10 (2006) 899-920.

[59] Kong, D.-X., Li, X.-J., Zhang, H.-Y., Where is the hope for drug discovery? Let history tell the future, Drug Discov Today. 14 (2009) 115-9.

[60] Di, L., Kerns, E.H., Carter, G.T., Drug-like property concepts in pharmaceutical design, Curr. Pharm. Des. 15 (2009) 2184-94.

[61] Carter, G.T., Natural products and Pharma 2011: Strategic changes spur new opportunities, Nat. Prod. Rep. 28 (2011) 1783-9.

[62] Adams, M., Chammartin, M., Hamburger, M., Potterat, O., Case study of the Swiss flora for prior phytochemical and biological investigations, J. Nat. Prod. 76 (2013) 209-15.

[63] Marston, A., Role of advances in chromatographic techniques in phytochemistry, Phytochemistry. 68 (2007) 2786-98.

[64] Bucar, F., Wube, A., Schmid, M., Natural product isolation - how to get from biological material to pure compounds, Nat. Prod. Rep. 30 (2013) 525-45.

[65] Bringmann, G., Gulder, T.A.M., Reichert, M., Gulder, T., The online assignment of the absolute configuration of natural products: HPLC-CD in combination with quantum chemical CD calculations, Chirality. 20 (2008) 628-42.

[66] Korfmacher, W.A., Foundation review: Principles and applications of LC-MS in new drug discovery, Drug Discovery Today. 10 (2005) 1357-67.

[67] Cordell, G.A., Shin, Y.G., Finding the needle in the haystack. The dereplication of natural product extracts, Pure Appl. Chem. 71 (1999) 1089-94.

[68] Kim, H.J., Baburin, I., Khom, S., Hering, S., Hamburger, M., HPLC-based activity profiling approach for the discovery of GABAA receptor ligands using an automated two microelectrode voltage clamp assay on *Xenopus oocytes*, Planta Med. 74 (2008) 521-6.

[69] Adams, M., Zimmermann, S., Kaiser, M., Brun, R., Hamburger, M., A protocol for HPLC-based activity profiling for natural products with activities against tropical parasites, Nat. Prod. Commun. 4 (2009) 1377-81.

[70] Grabher, P., Durieu, E., Kouloura, E., Halabalaki, M., Skaltsounis, L.A., Meijer, L., et al., Library-based discovery of DYRK1A/CLK1 inhibitors from natural product extracts, Planta Med. 78 (2012) 951-6.

[71] Vidal, V., Potterat, O., Louvel, S., Hamy, F., Mojarrab, M., Sanglier, J.-J., et al., Library-Based Discovery and Characterization of Daphnane Diterpenes as Potent and Selective HIV Inhibitors in *Daphne gnidium*, J. Nat. Prod. 75 (2012) 414-9.

[72] Breton, R.C., Reynolds, W.F., Using NMR to identify and characterize natural products, Nat. Prod. Rep. 30 (2013) 501-24.

[73] Nadja, B.W., Kuehn, T., Moskau, D., Zerbe, O., Strategies and tools for structure determination of natural products using modern methods of NMR spectroscopy, Chem. Biodiversity. 2 (2005) 147-77.

[74] Allenmark, S., Gawronski, J., Determination of absolute configuration - an overview related to this special issue, Chirality. 20 (2008) 606-8.

[75] Berova, N., Ellestad, G.A., Harada, N., 9.04 - Characterization by Circular Dichroism Spectroscopy, in: Liu, H-W, Mander, L (Eds.), Comprehensive Natural Products II, Elsevier, Oxford, 2010, pp. 91-146.

2.2 Drug Discovery for Neglected Tropical Diseases (NTD)

2.2.1 Neglected Tropical Diseases

Today, there are 17 parasitic and bacterial infections classified by the WHO as neglected tropical diseases (NTD). These diseases are a substantial health and economic burden in Africa, Asia, and Latin America and cause about 534000 deaths every year. Among them we have Chagas disease, human African Trypanosomiasis (HAT), and leishmaniasis. NTD share common features such as: i) they constitute a proxy for poverty and disadvantage, ii) they affect populations with low visibility and little political voice, iii) their distribution is restricted to the tropics due to allocation of the vectors and their reservoirs, iv) they cause disfigurement and disability leading to social discrimination, v) they can be controlled, prevented, and potentially eliminated by using appropriate chemotherapy and preventive actions such as vector control, good hygiene practices, and personal preventive measures [1, 2].
Malaria was once considered as a NTD, but since 2000, a lot of progress has been made in fighting the disease. In doing so, a reduction of about 45% in mortality rates could be achieved. However, the political commitment and international community awareness must be sustained to avoid losing the progress so far obtained. The burden of malaria is still devastating and the need for drug discovery and development of new antimalarial drugs is urgent [3-7]. In the context of the present work, malaria will be addressed among the NTD. General information about the above mentioned NTD is shown in Table 1.

- **Malaria**

Malaria has caused greater suffering and mortality over the course of human history than perhaps any other disease. Nowadays, malaria is still the most important parasitic disease of humankind. In 2012, there was an estimated of 62700 deaths, mostly of children under 5 years of age in Africa. This implies that 1300 young lives are lost to malaria every day [3, 8].

The life cycle of *Plasmodium* parasites has two stages. The asexual stage develops in humans (or in tetrapod vertebrates, such as mammals, birds, reptiles), and the sexual stage evolves (or develops) in mosquito vectors (*Anopheles spp.*). The mosquito inoculates sporozoitos into the human body, while having a blood meal. Sporozoites are motile cells that target the human liver and invade hepatocytes, where they proliferate quickly [8].

After about one week, the developed schizonts burst in the liver, and thousands of merozoites are released into the human blood stream. The merozoites invade red blood cells, and the asexual reproduction begins. The intraerythrocytic cycle has three stages, ring, trophozoite, and schizont. Some parasites develop into gametocytes (the sexual forms), which can be transmitted back to anopheline mosquitos, where the sexual

reproduction starts. Firstly, an ookinete is formed, which develops into an oocyst and finally evolves into sporozoites [4, 8].

Table 1. Neglected Tropical Diseases [1, 8-13]

	Malaria	**HAT**	**Chagas disease**	**Leishmaniasis**
Causative agent	*Plasmodium falciparum, vivax, malarie, ovale, and knowlesi*	*Tripanosoma brucei rhodesiene, T. b. gambiense*	*Tripanosoma cruzi*	*Leishmania spp.* (~21 species)
Vector	*Anopheles spp.*	*Glossina spp.* (tsetse fly)	*Triatomine spp.* *Triatoma spp.* *Panstrongylus spp* (Kissing bug)	*Phlebotomus spp, Lutzomya spp.* (sandflies)
Geographic distribution	World-wide	Sub-saharan Africa (countries ~21)	South and Central America (18 countries)	South and Central America, Europe, Africa, Asia (88 endemic countries)
DALYs	55 413.529	1 345.594	499067	3 754.202
Deaths in 2011	589218	19026	7356	53675
Estimated cases	219 million cases	50000-70000 cases	7-8 million people infected	30000 cases of visceral form/ 5 million cases in total

DALYs: Disability-adjusted life years

In endemic areas, malaria is often the most common cause of fever. The first symptoms of malaria are nonspecific, and include a vague absence of wellbeing, headache, fatigue, and abdominal discomfort, among others. Most patients with uncomplicated malaria have fever, mild anemia, and after several days a palpable spleen. Manifestations of severe falciparum malaria are anemia, hypoglycemia, acute pulmonary edema, acute kidney injury, coma in the case of cerebral malaria, and acidosis [8].

Malaria was mainly treated with chloroquine until the 1960s (Fig. 2). But resistance of the parasites to this drug appeared and spread around the world. Currently, sodium artesunate (Fig. 4) is the treatment of choice for severe malaria worldwide (including *falciparum*, *vivax,* and *knowlesi* malaria), due to its effectiveness against cerebral malaria. In uncomplicated *falciparum* malaria cases, artemisinin combination treatment (ACT) (artemether-lumefantrine, artesunate-mefloquine, and dihydroartemisinin-piperaquine) is the recommended fist-line therapy in all endemic areas. This therapy is also highly effective against other human malarias. In the chloroquine-sensitive strains of *P. vivax, P. malariae, P.*

ovale, and *P. knowlesi*, chloroquine is still being used. But emerging resistance to ACT can make malaria resurge [14].

- **Human African Trypanosomiasis (HAT)/ sleeping sickness**

Human African Trypanosomiasis (HAT) is caused by the protozoa *Trypanosoma spp*. The life cycle of African trypanosomes begins in the disease vectors, which are the tsetse flies (*Glossina spp*.) and various mammals. HAT exists in two forms, depending on the subspecies of *Trypanosoma* involved. *T. b. gambiense* infection is characterized by a chronic progressive course of around 3 years and is endemic in 24 countries of western and central Africa. This infection is responsible for more than 98% of reported cases of HAT. In contrast, *T. b. rhodesiense* causes an acute form of the disease, and death can occur within weeks or months. This type of HAT is endemic in 13 countries of eastern and southern Africa and represents less than 2% of the cases. HAT is characterized by two stages. In the first stage, the parasites are in the blood and produce symptoms such as intermitent fever, headache, and pruritus. In the second stage, parasites are able to cross the blood-brain barrier (BBB), which causes clinical manifestations such as sleep disturbances and neuro-psychiatric disorders [1, 9, 15-17].

Currently there are five drugs used for the treatment of HAT, namely pentamidine, suramin, melarsoprol, nifurtimox, and eflornithine (Fig. 7). Pentamidine and suramin are used to treat first stage HAT caused by *T. b. gambiense* and *T. b. rhodesiense*, respectively. Eflornithine and melarsoprol are applied in the second stage of the disease. Regrettably, all used drugs show problems such as (i) lack of oral bioavailability (all compounds must be administered by parenteral route) and lack of chemical stability (suramin rapidly decomposes in air), (ii) complicated and long dose regimens (suramin administration can last up to 30 days) and short half-life (four infusions of eflornithine per day are necessary), and (iii) deadly adverse drug reactions (pentamidine is nephrotoxic, melarsoprol causes a fatal encephalopathy in 10% of the treated patients) [15, 18, 19]. In 2009, a new combination therapy including nifurtimox and eflornithine was released into the market for second stage treatment of HAT caused by *T. b. gambiense.* This treatment shows large advantages over the eflornithine monotherapy since it is easier to administer, reduces the amount of drug required to reach therapeutic effects and requires a significantly shorter hospital stay [13, 17, 19, 20].

- **Chagas disease (American trypanosomiasis)**

Chagas disease is a life-long infection caused by the protozoa parasite *Trypanosoma cruzi*. This pathogen was first described in 1909 by Carlos Chagas and has a life cycle with four developmental stages, two of them (epimastigotes and trypomastigotes) in the vector (kissing bug), and two of them in mammalian

hosts (amastigotes and bloodstream trypomastigotes). The kissing bug transmits the parasites to mammals, where the host cells are located in the heart, gut, CNS, smooth muscle, and adipose tissue. Clinically the disease is characterized by three phases: acute phase (4-8 weeks), indeterminate phase (10-20 years), and chronic phase. The severity of the disease depends on the parasite load, strain, and on patient immune responses. An estimated 30% of infected individuals develop the chronic form, which may be cardiac (arrhythmias, congestive heart failure, cardiac enlargement, thromboembolism, and sudden cardiac death), digestive (enlargement of esophagus and colon), or combined cardiac and digestive, which affects up to 10% of patients [1, 10].

Only two drugs are available for the therapeutic use against *T. cruzi* in humans: nifurtimox and benznidazole (Fig. 7). Both compounds are nitroheterocycles and act as prodrugs. The nitro group is responsible for the toxicity in the parasite, most likely via DNA damage [10]. Both drugs show variable efficacy in different *T. cruzi* strains and cause various side effects which result in treatment discontinuation. In general, benznidazole is the first-choice treatment because it is better tolerated. However, treatment failures are frequently reported [1, 10, 13, 21].

- **Leishmaniasis**

There are more than 21 species of *Leishmania spp.* The parasites' life cycle includes different stages and hosts. The promastigotes are present in sandflies (vector), the amastigotes are present in mammalian macrophages. There are three different types of manifestations of the disease: i) The cutaneous leishmaniasis (CL) is the most common form. Parasites are restricted to the skin and cause ulcers on the face, arms, and legs, which leads to disability and permanently disfiguring scars; ii) the mucocutaneous leishmaniasis (ML) is the most disfiguring form because the parasites destroy the soft tissues of nose, mouth, and throat; iii) the visceral leishmaniasis (VL), also called kala azar, is a systemic and the most severe form. If left untreated, the disease is fatal within 2 years. VL causes fever, weight loss, swelling of the spleen and liver, and pancytopenia. Additionally, some cases of VL may evolve to CL.

Pentavalent antimonials, sodium stibogluconate, and meglumine antimoniate have been used to treat the disease. But resistance has appeared in India, the treatments are long (28 days), and parenteral administration is required. In India, the first line of treatment of VL is amphotericin B. A recently developed liposomal formulation of amphotericin B (AmBisome®) is highly effective, but very expensive. Paromomycin (aminoglycoside) is also effective against VL and VC and shows less adverse effects than amphotericin B. Miltefosine, the first oral treatment of VL, has markedly improved leishmaniasis chemotherapy, but its use is limited due to teratogenicity and high costs (Fig. 7) [1, 9, 10, 13, 19].

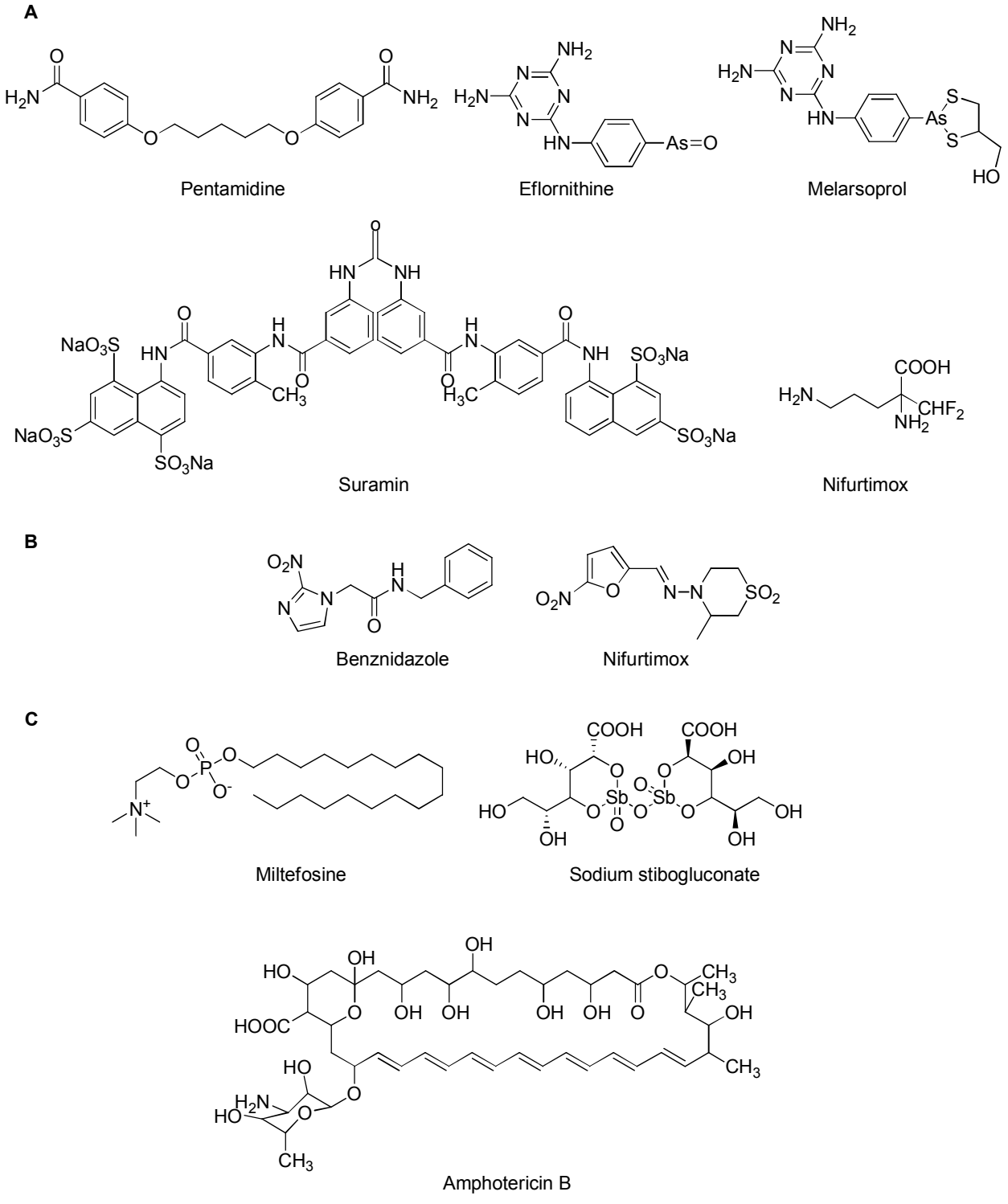

Figure 7. Drugs Currently Used for Treatment of HAT (A), Chagas Disease (B), and Leishmaniasis (C)

Available drugs for the treatment of NTD (Fig. 2, 4, and 7) are far from optimal, have shortcomings such as limited efficacy, severe side effects, poor patient compliance, and/or resistance [10, 22, 23]. Accordingly, new drugs are urgently needed. In general, requirements for an ideal drug intended to treat NTD are: sufficient effectiveness, safety, oral administration, short-course treatments, low-costs, stability of the drug in climatic zone IV for at least 3 years, suitability of the drug for children and for pregnant women. There are specific requirements depending on the disease such as activity against the different stages of the disease (HAT) or against a particular species (*P. vivax*) [4, 9, 13, 22, 24-26].

2.2.2 Drug Discovery for NTD

Drug discovery and development for parasitic diseases has little commercial incentives for the pharmaceutical industry. Sales are limited by the short duration of the treatment with antiparasitics compared to other drugs, which are consumed daily for prolonged periods (e.g. cholesterol-lowering and antihypertensive drugs). Nonetheless, development costs are similar for both antiparasitic and "long-term" drugs. Additionally, NTD are prevalent in the developing world and affect low-income people. Thus the deficit of new drugs entering development stage for tropical diseases results mainly from the gap between basic scientific research (early drug discovery), which is usually publicly funded, and clinical development, which is funded by pharmaceutical companies [1, 24, 27].

After this problem had been identified at the beginning of the last decade, a new collaborative mindset was created to produce a sustainable pipeline of new drug candidates to enter development. A new model for drug discovery based on networks and public-private partnerships was implemented. In this context, researchers, institutes, and pharmaceutical industry work in a coordinated effort using open innovation approach to discover and develop drugs to treat tropical neglected diseases. A number of non-profit organizations such as the Bill and Melinda Gates Foundation have supported this initiative. Examples of public-private partnerships and networks are "Medicines for Malaria Venture" (MMV) and "Drugs for Neglected Diseases initiative" (DNDi). Overall, the objective was to create a sustainable and scalable model of drug innovation for NTD with a collaborative work of industry, governments, and non-profit organizations. As a result of those joint efforts, it has been a renaissance of DDD in NTD during the last decade. Nevertheless, there are still major gaps and so far, these initiatives have brought to market only new formulations and combinations of already existing drugs. However, there is a series of compounds in the drug discovery pipeline [5, 7, 13, 23, 24, 28-30].

- **Compounds in Drug Discovery and Development Pipeline Against NTD**

Current projects of DNDi and MMV are listed in Table 2 and are shortly commented.

BCX4945

Plasmodium parasites are purine auxotrophs and require preformed purine bases for the synthesis of nucleotides, cofactors, and nucleic acids. Purine salvage in *P. falciparum* uses hypoxanthine, which is converted into inosine monophosphate, a precursor for all required purines. The purine nucleoside phosphorylase (PNP) is essential for the formation of hypoxanthine, making PNP a target for the purine salvage pathway. Blocking PNP kills parasites by purine starvation. BCX4945 (Fig. 8) causes depletion of hypoxanthine from *Aotus* blood (monkey model of falciparum malaria), demonstrating inhibition of

both hPNP and PfPNP *in vivo*. The efficacy, oral availability, chemical stability, unique mechanism of action, and low toxicity of BCX4945 demonstrate a potential for the development of combination therapies [31]. Currently this compound is undergoing preclinical studies [29].

Table 2. Some Projects of the Global Portafolio of DDD and MMV Pipeline [13, 32, 33]

Disease	Drug discovery	Development				Implementation
		Pre-clinical	Phase I	Phase IIa	Phase IIb/III	
Malaria	Oxaboroles Imidazol	BCX4945 SAR116242 PA1103/SAR116242	DHODH	OZ-439	OZ-277	Artesunate-amodiaquine
HAT	Nitroimidazole Oxaborole		SCYX-7158 (Oxaborale)		Fexinidazole	Nifurtimox-Elfornithine
Chagas	Nitroimidazole	Fenarimol series K777	Tak-187	Azoles (E1224)		Benznidazole Pediatric
Leishmania	Nitroimidazole	VL-2098 Fenarimol series		Fexinidazole (VL) Anfoleish (CL)		Sodium stibogluconate & paramomycin

OZ-277 and OZ-439

Artemisinin and its semi-synthetic derivatives are sesquiterpene lactones which bear an endoperoxide bridge. It is thought that the endoperoxide opens by reduction to alkylate the heme. However, artemisinin has a very short half-life. As a result, new fully synthetic peroxides with better pharmacokinetics have been synthesized. Arterolane (OZ-277) (Fig. 8) was assessed in clinical trials to treat uncomplicated falciparum malaria. Arterolane showed a rapid action, effectiveness, and safety in Phase II of clinical trials. These results prompted a phase III clinical trial to evaluate the drug in a combination therapy with piperaquine phosphate. As a result of these studies, arterolane was recently registered by Ranbaxy Laboratories Ltd. in India to treat acute uncomplicated malaria [28, 34, 35]. Another ozonide, OZ439 (Fig. 8), showed a remarkable efficacy, cured *P. berghei* infected mice with a single oral dose of 20 mg/Kg, and had a prolonged plasma exposure in animals and humans. It is currently in Phase II, showing good efficacy in the treatment of both *P. falciparum* and *P. vivax* patients. Due to its PK properties, this compound can potentially reach the goal of a single-dose oral cure [28].

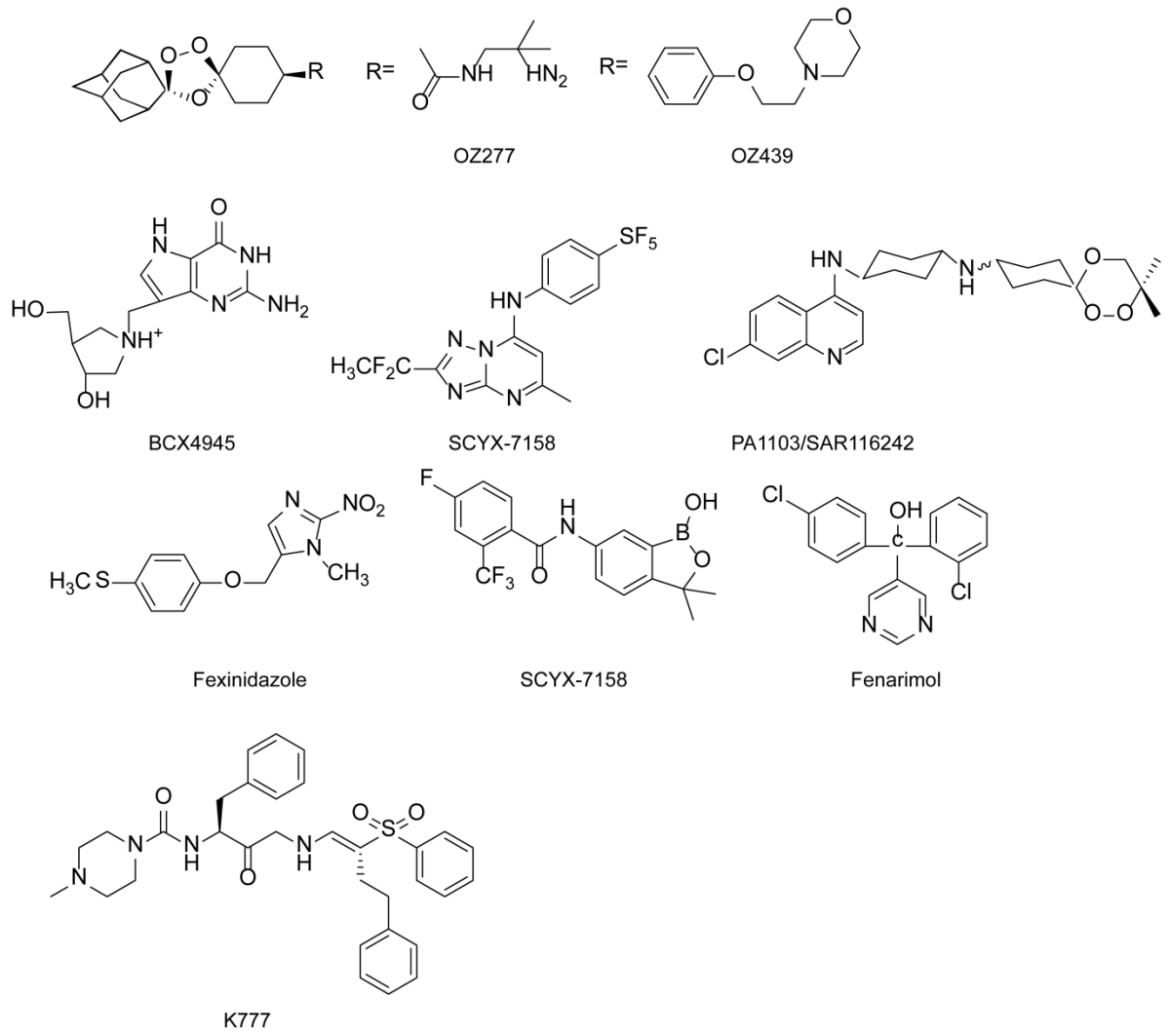

Figure 8. Some Compounds in the DDD Pipeline against Malaria, Trypanosomiasis, Leishmania, and Chagas disease

PA1103/SAR116242

Trioxaquines are hybrid (or chimeric) molecules which target the free heme. These molecules combine two active pharmacophores: a trioxane motif, thought to alkylate the heme and/or the proteins of the *Plasmodium* parasite, and an aminoquinoline moiety to facilitate accumulation in the parasite and interaction with free heme. PA1103/SAR116242 (Fig. 8) is highly active *in vitro* on *P. falciparum* strains at nanomolar concentrations, is also active on multidrug-resistant strains obtained from fresh patient isolates, and is active in the *Pf*-HuMouse models. These promising results combined with a good drug profile (preliminary absorption, metabolism, and safety) have led to further development. Currently, PA1103/SAR116242 is in preclinical stage [36, 37].

DSM265

DHODH has emerged as the best validated new target for the development of novel antimalarials. DHODH catalyzes the fourth step in the de novo pyrimidine biosynthetic pathway. The malaria parasite is uniquely vulnerable to inhibition of this pathway because it lacks the salvage enzymes that serve as an additional source of pyrimidine nucleosides in other organisms, including the human host. DSM265 (Fig. 8) is a potent and selective inhibitor of DHODH and is able to kill both drug-sensitive and drug-resistant strains of the parasite. The compound is currently in Phase I of clinical trials due to its good antimalarial activity, easy synthetic route, and good results in rodent PK studies [38].

Spiroindolones

Spiroindolones were found to inhibit *P. falciparum in vitro* with IC_{50} values around 1 nM. The optimized candidate NITD609 seems to have a different mechanism of action, cured mice infected with *P. berghei*, and showed PK profiles compatible with one-daily oral dosing. The compound has reached clinical Phase IIa [28, 39].

Fexinidazole

Fexinidazole (Fig. 8) is a nitroimidazole active against drug-resistant and drug-sensitive *T. brucei spp.* The compound also cured mice infected with *T. b. rhodesiense* and *T. b. gambiense,* and is able to cross the blood-brain barrier (BBB). Fexinidazole already went successfully through Phase I and currently is under clinical evaluation in Phase IIb/III [13, 28].

SCYX-7158

The oxaborol SCYX-7158 is a boro-containing molecule (Fig. 8) active *in vitro* against both *T. b. rhodesiense* and *T. b. gambiense.* The compound displays an excellent physicochemical profile, showed good efficacy in mice against stage 1 and 2 of the disease, is characterized by *in vitro* metabolic stability, low potential for CYP450 inhibition, lack of active efflux by the P-glycoprotein transporter, and high permeability. SCYX-7158 is currently in Phase I of clinical trials [13, 40].

K777

K777 is a vinyl sulfona (Fig. 8) compound which inhibits the cystein protease inhibitor cruzain in an irreversible way. Cruzain is a key protease required for the viability of *T. cruzi.* K777 was effective in

acute and chronic Chagas disease models. The compound is currently in pre-clinical phase and *in vivo* pharmacokinetic studies are in process, [13, 32, 41].

VL-2098

VL-2098 is a nitroimidazole with a very potent activity *in vitro* against a panel of *L. donovani* strains. *In vivo*, it is also active in rodent and hamster models with similar potency to miltefosine. Currently the compound is in pre-clinical stage of development [13].

Fenarimol

Fenarimol (Fig. 8) inhibited the proliferation of *Leishmania spp* promastigotes and amastigotes *in vitro* and ameliorated lesions caused by the parasites in mice. Biochemical studies demonstrated that fenarimol inhibited sterol biosynthesis by impairing the function of leishmania 14α-sterol demethylase, a key enzyme in the sterol biosynthetic pathway. Currently, this compound is in pre-clinical evaluation [13, 42].

- **Screening for Neglected Tropical Diseases (NTD)**

There are two opposing yet complementary screening strategies, namely the target-based and the phenotypic approach (whole organism screening). Both strategies have advantages and disadvantages. However, in the case of antiparasitic drugs, the whole organism screening has a successful historical base. The advantages of this approach are: i) initial chosen hits are cell-permeable and are devoid of efflux issues; ii) provide the opportunity to discover a new target and a potential new mechanism of action; iii) many of the antiprotozoal drugs used today exert their activity through the simultaneous inhibition of multiple targets within a host [4, 23, 43, 44, 45]. Furthermore, NPs are ideally suited for phenotypic screening because they are nature's fully developed small molecules effectors [45].

The target-based approaches have been extensively used in the pharmaceutical industry. However, there are relatively few validated drug targets across the infectious diseases. The target is the key to success in target-based drug discovery. The biology of the pathogens responsible for NTD is very complex and still a lot of research is needed. Nevertheless, the greatest advantage of this approach in NTD is that many proteins and enzymes in the parasite differ from their mammalian counterparts, which enhances the specificity of the drugs [4, 21, 43, 46]. In Table 3, some of the targets are listed.

Table 3. Examples of Molecular Targets for Drug Discovery

Disease	Molecular target	Examples	Ref.
Malaria	Dihydrofolate reductase Dihydropteroate synthase (DPR)	Pyrimetamine, DPR inhibitor	[43]
	Mitocondrial bc1 complex Dihydroorotate dehydrogenase (DHODH)	Atavaquone	[38, 43]
	Pathway from DOXP to IPP	-	[4]
	Nutrient channels (parasite-encoded nutrient uptake channels in erythrocyte membranes)		[4]
	AMA1 (apical membrane antigen 1)		[4]
HAT	N-Myristoyltransferase		[17, 43]
	Trypanothione synthetase (TryS)		[17, 18, 43, 47]
	Ornithine decarboxylase (ODC)	Eflornithine	[18, 48]
	6-phosphogluconate dehydrogenase		[18]
	Hexokinase, phosphofructokinase		[18]
	Protein farnesyl transferases (PFT)		[17, 18]
	Polyamide pathway enzymes (γ-glutamyl cysteine synthetase, spermidine synthetase)		[18]
	CRK3 (Cdc2-Related Kinase 3*)		[43]
Leishmania	Sterol 14-α-demethylase (CYP51)	Posaconazole, E1224 (prodrug of ravuconazole)	[43]
	Cystein proteinase (CP)	-	[49]
Chagas	TcCa (α-carbonic anhydrase)		[50]
	Cruzipain	K777	[32]

* This is a protein kinase potential for drug targets in kinetoplastid diseases.

- **Critical Pathway for Discovering Neglected Parasitic Diseases**

Establishing a standardized pathway for drug discovery of NTD speeds-up the process and optimizes resources of the international research community. Since the last decade, a standardized system for antimalarial drug screenings emerged, together with a compound progression criteria. In 2009, similar standards were developed for leishmaniasis and HAT (Table 4, Figures 9 and 10) [9, 25].

Table 4. MMV Compound Progression Criteria for Antimalarial Compounds [33]

Test	Consensus
	Screening Hits
Target assay	Biological activity at IC_{50} <3 μM
Cellular assay	Activity against *P. falciparum* 3D7, HB3, DD2 NF54 or W2 at IC_{50} <1 μM
	Validated Hits
Re-testing	Re-synthesis if necessary to validate results on compound > 90% pure
Activity	IC_{50} against biological target (if known) and whole parasites (strains as above) < 1 μM
Selectivity	Activity against mammalian enzyme and HepG2 cells show > 10-fold sensitivity
Chemistry	Looks drug-like and some initial SAR is established
ADMET	Good predicted computational ADMET properties
	Early Leads
Chemistry	Stable as solid and in test media with good solubility in PBS, initial SAR studies indicate opportunities for chemical targets with straightforward synthesis to yield Rule-of-5 compliant compounds
Biology	IC_{50} against biological target (if known) and whole cells < 1 μM, whole cell activity extends to key drug resistant strains, mode of action known or strategies to address it, depresses parasitemia in mouse model of malaria (oral administration)
ADMET	Stable in human and mouse plasma, reasonable stability with microsomes, CaCo-2 permeability > 2 x 10^{-6} cm/s, no known toxicophores/reactive groups, no preliminary mouse toxicity
	Late Leads
Chemistry	Structural identification of the compound is confirmed by H and C NMR, LC-MS, and elemental analysis, suitable physicochemical properties, easy, cheap, and environmentally friendly synthesis. Patentable
Biology	IC_{50} against biological target (if known) and whole cells < 1 μM, whole cell activity extends to key drug resistant strains and clinical isolates, ability to clear parasitemia in mouse model of malaria when administered by oral route daily for no more than 4 days with an ED_{50} < 10 mg/Kg and ED_{90} <30 mg/Kg, using a formulation acceptable for PK and toxicology studies
ADMET	Soluble in PBS at > 20 μg/mL, stability in human and murine plasma > 90% over 1h, extent of plasma protein binding known, fully PK in rat and dog after oral and iv dosing ok, including oral bioavailability > 20%, hERG and phototoxicity ok, no overt signs of toxicity in *in vivo* efficacy studies and MTD in mice at least x 10 curative dose

In a typical discovery program for antiprotozoal compounds, the first step is the selection of compounds which show *in vitro* activity against whole-cell assays and sufficient selectivity towards the parasite.

Compounds which match established cut-off values are ranked based on their *in silico/in vitro* ADMET and lead-like/drug-like properties. The best ranked compounds are tested *in vivo* in primary models to test efficacy. Further steps comprise evaluation of mechanisms of action, activity in *in vivo* secondary tests, together with medicinal chemistry and lead optimization efforts. Nowadays the drug-like properties are being screened in parallel with biological activity and constitute a selection criterion [6, 14 22, 23, 51].

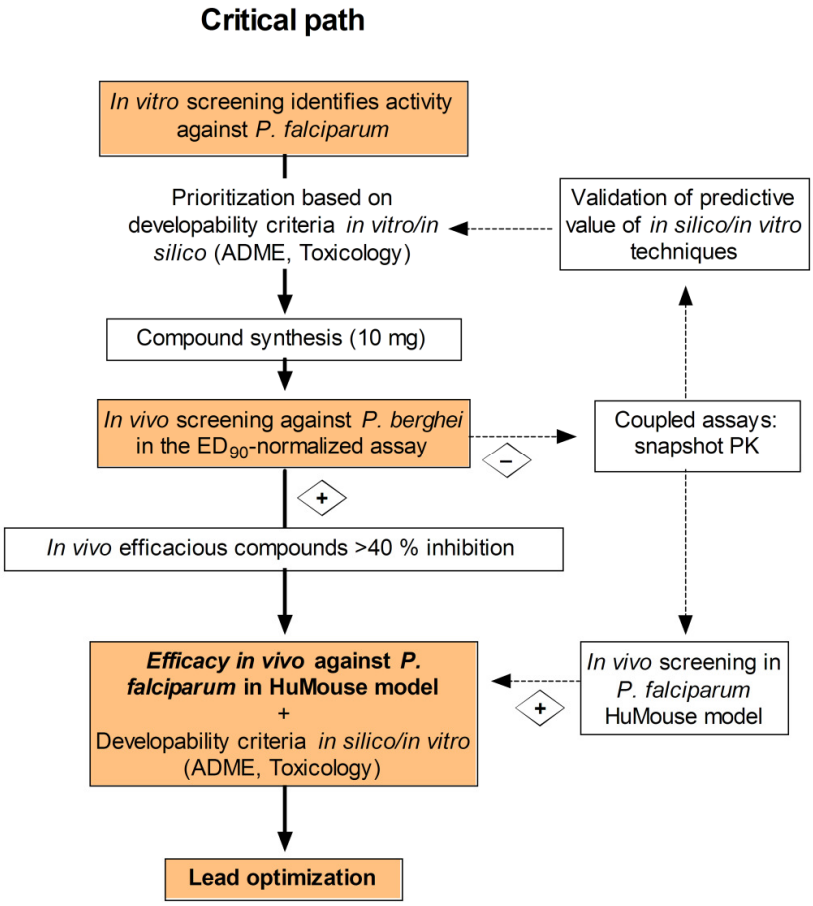

Fig 9. New Paradigm for Critical Path of Compound Progression in Antimalarial Drug Discovery from Jimenez-Diaz et al., 2013 [6]

Still, there is the need of more standardization to evaluate the potential of compounds active against trypanosomiasis, Chagas disease, and leishmaniasis. There is i) a lack of reference strains for compound screening, particularly for *T. b. gambiense*; ii) a lack of optimal animal models for testing compounds, particularly for studying some *in vivo* stages, e.g. the "late state" of Trypanosomiasis; iii) immense variability in the behavior among strains which makes it difficult to compare results of laboratories [17, 52, 53].

In this work, the activity of compounds (plant extracts/fractions) was tested in *in vitro* whole-cell assays (Table 5), alongside with testing the cytotoxicity in mammalian cells. The main purpose of the cytotoxicity test was to calculate the selectivity index (SI), which allows the discrimination of attractive compounds from poorly selective molecules.

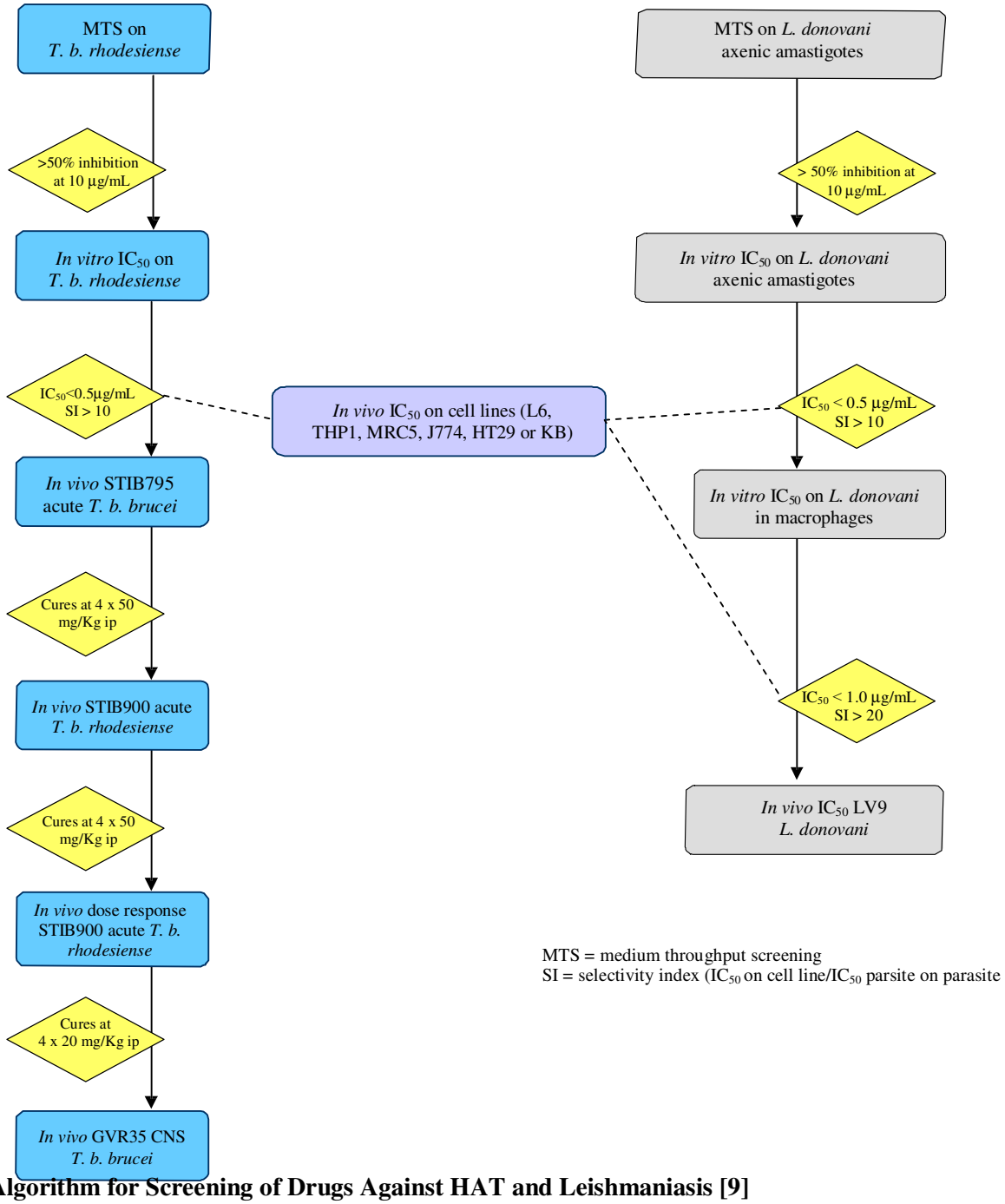

Fig 10. Algorithm for Screening of Drugs Against HAT and Leishmaniasis [9]

Compounds which complied with selection criteria of the Swiss TPH (Table 5) were challenged in primary *in vivo* models.

This approach was applied not only to malaria but also to HAT, Chagas disease, and leishmaniasis, resulting in an integrated screening approach for tropical diseases. This strategy is a more efficient tool for discovering high-quality hits with good efficiency compared to those which target pathogens individually [23].

Table 5. *In vitro* Activity Criteria [54]

Parasite (strain)	IC_{50} activity criteria		
	Active	**Mod. activity**	**Inactive**
Plasmodium falciparum (K1/NF54) (intraeritrocitic forms)	< 0.5 µg/mL SI>100	0.5 – 5 µg/mL	> 5 µg/mL
Trypanosoma brucei rhodesiense (STIB900) (blood stream forms)	< 0.5 µg/mL SI>20	0.2 – 3 µg/mL	> 3 µg/mL
Leishmania donovani (axenic amastigotes) (MHOM/ET/67/L82)	< 0.5 µg/mL SI>20	0.5 – 3 µg/mL	> 3 µg/mL
Trypanosoma cruzi (amastigotes in L6 cells) (Tulahuen C2C4 w/LacZ)	< 2 µg/mL SI>50	2 – 30 µg/mL	> 30 µg/mL
Cytotoxicity L6 cells (rat skeletal myoblast cell line)	-	-	-

SI (selectivity index): IC_{50} mammalian cell / IC_{50} parasite

- **Natural products and Drug Discovery for NTD**

The antiprotozoal activity of NPs derived from plants, bacteria, fungi, and marine organisms has been extensively studied. Published reviews retrieve this information and show that many secondary metabolites with a wide variety of scaffolds, namely diverse kind of alkaloids, terpenes, and phenolic compounds (e.g. lignans, tannins, coumarins, flavonoids) show potent inhibition on parasites responsible for NTD. Most of the compounds have been assayed in the whole-cell model and in some cases mechanistic studies have been conducted, mainly in the case of malaria and HAT. Despite the promising activity of some NPs, some of them showed limitations such as toxicity, low bioavailability, and/or poor solubility, which restrict their scope of use in humans. Nonetheless, these hits can be modified by semisynthetic approaches to overcome their drawbacks and to boost their benefits [17, 44, 49, 53, 55].

Networking among different areas such as biology, medical chemistry, and pharmacokinetics is required to move forward natural hits and leads through the drug discovery pipeline. The discovery of new validated drug targets and the recent technical progress in the field of NPS chemistry might facilitate this process [17].

Even tough, DDD focuses on pure chemical entities, the local and traditional knowledge remains an essential starting point. The observational knowledge about the effect of a plant, an animal, or a microorganism on other organisms offers ideal opportunities to limit the huge diversity of possible leads to more promising ones (knowledge-based drug discovery). Such observational knowledge is exemplified by the discovery of drugs used against parasitic diseases such as malaria [56].

References

[1] Organization, W.H., Working to overcome the global impact of neglected tropical diseases: First WHO report on neglected tropical diseases, World Health Organization, Geneva, 2010.

[2] Conteh, L., Engels, T., Molyneux, D.H., Socioeconomic aspects of neglected tropical diseases, Lancet. 375 (2010) 239-47.

[3] WHO, World Malaria Report 2013, Geneva, 2013, pp ix-xiv.

[4] Miller, L.H., Ackerman, H.C., Su, X.-z., Wellems, T.E., Malaria biology and disease pathogenesis: insights for new treatments, Nat. Med. 19 (2013) 156-67.

[5] Renslo, A.R., Antimalarial Drug Discovery: From Quinine to the Dream of Eradication, ACS Med. Chem. Lett. Ahead of Print. DOI:10.1021/ml4004414.

[6] Jimenez-Diaz, M.B., Viera, S., Ibanez, J., Mulet, T., Magan-Marchal, N., Garuti, H., et al., A new *in vivo* screening paradigm to accelerate antimalarial drug discovery, PLoS One. 8 (2013) e66967.

[7] Olliaro, P., Wells, T.N.C., The Global Portfolio of New Antimalarial Medicines Under Development, Clin. Pharmacol. Ther. 85 (2009) 584-95.

[8] White, N.J., Pukrittayakamee, S., Hien, T.T., Faiz, M.A., Mokuolu, O.A., Dondorp, A.M., Malaria, Lancet. 383 (2014) 723-35.

[9] Ioset, J.R., Brun, R., Wenzler, T., Kaiser, M., Yardley, V., Drug Screening for Kinetoplastids Diseases. A Training Manual for Screening in Neglected Diseases, The Pan-Asian Screening Network (2009).

[10] Stuart, K., Brun, R., Croft, S., Fairlamb, A., Gurtler, R.E., McKerrow, J., et al., Kinetoplastids: related protozoan pathogens, different diseases, J. Clin. Invest. 118 (2008) 1301-10.

[11]WHO, Global Health Estimates Summary Tables: DALYs, by Cause, Age and Sex, in: GHE_DalyGlobal2000_2001.xls, Geneva, 2013.

[12] Organization, W.H., Global Health Estimates Summary Tables: Deaths by Cause, Age and Sex, in: GHE_DthGlobal2000_2001.xls, Geneva, 2013.

[13] DNDi, R&D Portafolio Patients Needs-Driven Collaborative R&D Model for Neglected Diseases, DNDi, 2013. http://www.dndi.org/images/stories/pdf_portfolios/DNDi_Portfolio2013.pdf

[14] Fidock, D.A., Drug discovery: Priming the antimalarial pipeline, Nature. 465 (2010) 297-8.

[15] Brun, R., Blum, J., Chappuis, F., Burri, C., Human African trypanosomiasis, Lancet. 375 (2010) 148-59.

[16] WHO, Trypanosomiasis (sleeping sickness). Fact sheet N°259, June, 2013.

[17] Hannaert, V., Sleeping sickness pathogen (*Trypanosoma brucei*) and natural products: therapeutic targets and screening systems, Planta Med. 77 (2011) 586-97.

[18] Brun, R., Don, R., Jacobs, R.T., Wang, M.Z., Barrett, M.P., Development of novel drugs for human African trypanosomiasis, Future Microbiol. 6 (2011) 677-91.

[19] Croft, S.L., Barrett, M.P., Urbina, J.A., Chemotherapy of trypanosomiases and leishmaniasis, Trends Parasitol. 21 (2005) 508-12.

[20] Burri, C., Chemotherapy against human African trypanosomiasis: Is there a road to success?, Parasitology. 137 (2010) 1987-94.

[21] Lepesheva, G.I., Design or screening of drugs for the treatment of Chagas disease: what shows the most promise?, Expert Opin. Drug Discovery. 8 (2013) 1479-89.

[22] Renslo, A.R., McKerrow, J.H., Drug discovery and development for neglected parasitic diseases, Nat Chem Biol. 2 (2006) 701-10.

[23] Nwaka, S., Besson, D., Ramirez, B., Maes, L., Matheeussen, A., Bickle, Q., et al., Integrated dataset of screening hits against multiple neglected disease pathogens, PLoS Negl Trop Dis. 5 (2011) e1412.

[24] Hopkins, A.L., Witty, M.J., Nwaka, S., Mission possible, Nature. 449 (2007) 166-9.

[25] Fidock, D.A., Rosenthal, P.J., Croft, S.L., Brun, R., Nwaka, S., Antimalarial drug discovery: efficacy models for compound screening, Nat. Rev. Drug Discovery. 3 (2004) 509-20.

[26] Buckner, F.S., Experimental chemotherapy and approaches to drug discovery for Trypanosoma cruzi infection, Adv Parasitol. 75 (2011) 89-119.

[27] Li, J.W.H., Vederas, J.C., Drug discovery and natural products end of an era or an endless frontier?, Science. 325 (2009) 161-5.

[28] Maser, P., Wittlin, S., Rottmann, M., Wenzler, T., Kaiser, M., Brun, R., Antiparasitic agents: new drugs on the horizon, Curr. Opin. Pharmacol. 12 (2012) 562-6.

[29] Medicines for Malaria Venture (MMV), Global Malaria Portafolio, 4Q, 2013, MMV, Geneva, 2013. http://www.mmv.org/research-development/rd-portfolio

[30] Butera, J.A., Phenotypic Screening as a Strategic Component of Drug Discovery Programs Targeting Novel Antiparasitic and Antimycobacterial Agents: An Editorial, J. Med. Chem. 56 (2013) 7715-8.

[31] Cassera, M.B., Hazleton, K.Z., Merino, E.F., Obaldia, N., III, Ho, M.-C., Murkin, A.S., et al., Plasmodium falciparum parasites are killed by a transition state analogue of purine nucleoside phosphorylase in a primate animal model, PLoS One. 6 (2011) e26916.

[32] Clayton, J., Chagas disease: pushing through the pipeline, Nature. 465 (2010) S12-S5.

[33] Medicines for Malaria Venture (MMV), MMV Compound Progression Criteria, Geneva, 2008. http://www.mmv.org/sites/default/files/uploads/docs/essential_info_for_scientists/Compound_progression_criteria.pdf

[34] Valecha, N., Looareesuwan, S., Martensson, A., Abdulla, S.M., Krudsood, S., Tangpukdee, N., et al., Arterolane, a new synthetic trioxolane for treatment of uncomplicated Plasmodium falciparum malaria: a phase II, multicenter, randomized, dose-finding clinical trial, Clin Infect Dis. 51 (2010) 684-91.

[35] Valecha, N., Krudsood, S., Tangpukdee, N., Mohanty, S., Sharma, S.K., Tyagi, P.K., et al., Arterolane Maleate Plus Piperaquine Phosphate for Treatment of Uncomplicated Plasmodium falciparum Malaria: A Comparative, Multicenter, Randomized Clinical Trial, Clin. Infect. Dis. 55 (2012) 663-71.

[36] Cosledan, F., Fraisse, L., Pellet, A., Guillou, F., Mordmueller, B., Kremsner, P.G., et al., Selection of a trioxaquine as an antimalarial drug candidate, Proc. Natl. Acad. Sci. 105 (2008) 17579-84.

[37] Palumed, Palumed, Castanet-Tolosan 2013. http://www.palumed.fr/spip.php?article17

[38] Coteron, J.M., Marco, M., Esquivias, J., Deng, X., White, K.L., White, J., et al., Structure-Guided Lead Optimization of Triazolopyrimidine-Ring Substituents Identifies Potent *Plasmodium falciparum* Dihydroorotate Dehydrogenase Inhibitors with Clinical Candidate Potential, J. Med. Chem. 54 (2011) 5540-61.

[39] Rottmann, M., McNamara, C., Yeung, B.K.S., Lee, M.C.S., Zou, B., Russell, B., et al., Spiroindolones, a Potent Compound Class for the Treatment of Malaria, Science. 329 (2010) 1175-80.

[40] Nare, B., Wring, S., Bacchi, C., Beaudet, B., Bowling, T., Brun, R., et al., Discovery of novel orally bioavailable oxaborole 6-carboxamides that demonstrate cure in a murine model of late-stage central nervous system African trypanosomiasis, Antimicrob. Agents Chemother. 54 (2010) 4379-88.

[41] Rhee, S.-W., Bradford, W.W., Malerich, J.P., Tanga, M.J., Carbon-14 labeling of K777•HCl, a therapeutic agent for Chagas disease, J. Labelled Compd. Radiopharm. 56 (2013) 461-3.

[42] Zeiman, E., Greenblatt, C.L., Elgavish, S., Khozin-Goldberg, I., Golenser, J., Mode of action of fenarimol against Leishmania spp, J. Parasitol. 94 (2008) 280-6.

[43] Gilbert, I.H., Drug Discovery for Neglected Diseases: Molecular Target-Based and Phenotypic Approaches, J. Med. Chem. 56 (2013) 7719-26.

[44] Carter, G.T., Natural products in drug discovery, CRC Press, 2010, pp. 89-105.

[45] Carter, G.T., Natural products and Pharma 2011: Strategic changes spur new opportunities, Nat. Prod. Rep. 28 (2011) 1783-9.

[46] Singh, N., Mishra, B.B., Bajpai, S., Singh, R.K., Tiwari, V.K., Natural product based leads to fight against leishmaniasis, Bioorganic & Medicinal Chemistry. 22 (2014) 18-45.

[47] Zimmermann, S., Oufir, M., Leroux, A., Krauth-Siegel, R.L., Becker, K., Kaiser, M., et al., Cynaropicrin targets the trypanothione redox system in *Trypanosoma brucei*, Bioorg Med Chem. 21 (2013) 7202-9.

[48] Bacchi, C.J., Jacobs, R.T., Yarlett, N., New developments in the treatment of late-stage human African trypanosomiasis, Drug Discovery Infect. Dis. 4 (2013) 515-29.

[49] Singh, N., Mishra, B.B., Bajpai, S., Singh, R.K., Tiwari, V.K., Natural product based leads to fight against leishmaniasis, Bioorg. Med. Chem. 22 (2014) 18-45.

[50] Pan, P., Vermelho, A.B., Capaci Rodrigues, G., Scozzafava, A., Tolvanen, M.E.E., Parkkila, S., et al., Cloning, characterization, and sulfonamide and thiol inhibition studies of an α-carbonic anhydrase from *Trypanosoma cruzi*, the causative agent of Chagas disease, J. Med. Chem. 56 (2013) 1761-71.

[51] Di, L., Kerns E.H., Carter G.T. Drug-like properties in pharmaceutical design. Curr. Pharm. Des. 15 (2009) 2184-2194.

[52] Anon, Ask the Experts: Drug discovery for the treatment of leishmaniasis, African sleeping sickness and Chagas disease, Future Med. Chem. 5 (2013) 1709-18.

[53] Izumi, E., Ueda-Nakamura, T., Dias Filho, B.P., Veiga, V.F., Jr., Nakamura, C.V., Natural products and Chagas' disease: a review of plant compounds studied for activity against *Trypanosoma cruzi*, Nat. Prod. Rep. 28 (2011) 809-23.

[55] Brun, R., *In vitro* activity criteria for integrated screening approach for neglected tropical diseases. Personal Communication. 2010.

[55] Kaur, K., Jain, M., Kaur, T., Jain, R., Antimalarials from nature, Bioorg. Med. Chem. 17 (2009) 3229-56.

[56] Heinrich, M., Ethnopharmacology and Drug Discovery, in: Lew, M., Hung-Wen, L. (Eds.), Comprehensive Natural Products II, Elsevier, Oxford, 2010, pp. 351-81.

3. RESULTADOS

3.1 *In Vitro* Screening of Traditional South African Malaria Remedies Against *Trypanosoma brucei rhodesiense, Trypanosoma cruzi, Leishmania donovani,* and *Plasmodium falciparum*

Tsholofelo Mokoka, Stefanie Zimmermann, Tasqiah Julianti, **Yoshie Hata**, Nivan Moodley, Monica Cal, Michael Adams, Marcel Kaiser, Reto Brun, Neil Koorbanally, Matthias Hamburger

Planta Med., 2011, 77: 1663–1667. DOI: 10.1055/s-0030-1270932

Three hundred extracts from 107 South African plant species (42 botanical families) with antiparasitic traditional use were tested against a panel of 4 parasites (*Plasmodium falciparum, Trypanosoma brucei rhodesiense, Leishmania donovani,* and *Trypanosoma cruzi*). For the most active plants (24), an extensive bibliographic search was performed to select the most promising ones. Ten extracts, corresponding to 10 species, were prioritized to perform HPLC-activity profiles.

My contributions to this work were: (1) literature search for 24 of the active plants in the screening to select the most promising ones to follow up; (2) data interpretation for 34 HPLC-activity profiles performed for 10 selected extracts against P. falciparum, T. b. rhodesiense, and/or L. donovani.

Tasqiah Julianti performed the HPLC-activity profiling of the extracts and Tsholofelo Mokoka wrote the first draft of the paper. The antiprotozoal activity of the extracts and HPLC fractions was assessed at the Swiss TPH. Extracts were provided by the CSIRteam.

Yoshie Hata-Uribe

In vitro Screening of Traditional South African Malaria Remedies against *Trypanosoma brucei rhodesiense*, *Trypanosoma cruzi*, *Leishmania donovani*, and *Plasmodium falciparum*

Authors Tsholofelo A. Mokoka[1], Stefanie Zimmermann[2,3], Tasqiah Julianti[2,5], Yoshie Hata[2,6], Nivan Moodley[1], Monica Cal[3], Michael Adams[2], Marcel Kaiser[3], Reto Brun[3], Neil Koorbanally[4], Matthias Hamburger[2]

Affiliations The affiliations are listed at the end of the article

Key words
- South Africa
- antiprotozoal
- *Trypanosoma brucei rhodesiense*
- *Trypanosoma cruzi*
- *Leishmania donovani*
- *Plasmodium falciparum*

Abstract

Three hundred extracts were prepared from plants traditionally used in South Africa to treat malaria and screened *in vitro* for activity against *Trypanosoma brucei rhodesiense, Trypanosoma cruzi, Leishmania donovani*, and *Plasmodium falciparum*. For the 43 extracts which inhibited the growth of one or more parasites to more than 95% at 9.7 µg/mL, the IC_{50} values against all four protozoal parasites and cytotoxic IC_{50}s against rat myoblast L6 cells were determined. Amongst the most notable results are the activities of *Agathosma apiculata* (IC_{50} of 0.3 µg/mL) against *Plasmodium falciparum*, as well as *Salvia repens* and *Maytenus undata* against *Leishmania donovani* with IC_{50}s of 5.4 µg/mL and 5.6 µg/mL, respectively. This screening is the starting point for a HPLC-based activity profiling project in antiprotozoal lead discovery.

Supporting information available online at http://www.thieme-connect.de/ejournals/toc/plantamedica

received January 10, 2011
revised February 24, 2011
accepted February 26, 2011

Bibliography
DOI http://dx.doi.org/10.1055/s-0030-1270932
Published online March 16, 2011
Planta Med 2011; 77: 1663–1667 © Georg Thieme Verlag KG Stuttgart · New York · ISSN 0032-0943

Correspondence
Prof. Dr. Matthias Hamburger
Department of Pharmaceutical Sciences
Institute of Pharmaceutical Biology
University of Basel
Klingelbergstrasse 50
4056 Basel
Switzerland
Phone: + 41 6 12 67 15 55
Fax: + 41 6 12 67 14 74
matthias.hamburger@unibas.ch

Introduction

Half a billion people get infected with malaria every year, and 1–2 million die of the disease [1]. Up to thirty million people annually contract one of the so called "neglected tropical diseases", Chagas disease, human African trypanosomiasis, or leishmaniasis, and the three disorders lead to 120 000 deaths annually [2]. All these diseases are caused by protozoal parasites which are transmitted by insect vectors, and affect the poorest populations. Malaria drugs are reasonably affordable, available, and safe, yet few in number and increasingly compromised by resistances [3]. Only a few drugs are on the market to treat trypanosomatid infections (*Trypanosoma* and *Leishmania*), and their pharmacological profiles are insufficient by modern standards [1]. For decades, large pharmaceutical companies have been reluctant to invest in the development of new drugs for economic reasons. This may be changing though because there have been increasing drug discovery and development efforts in recent years from private initiatives and non-profit organizations. The Medicines for Malaria Venture (MMV), for instance, has initialized research networks [4], and philanthropist organizations like the Bill and Melinda Gates foundation and others have contributed substantial assets to such endeavors [5].

We report here on the outcome of a screen which is the starting point in the collaboration between the University of Basel, the Swiss Tropical and Public Health Institute, and the South African Council for Scientific and Industrial Research. The goal is to evaluate the antiprotozoal potential of plants used by traditional communities in South Africa to treat malaria. Extracts were screened against the most important protozoal parasites, *Plasmodium falciparum* (malaria), *Trypanosoma cruzi* (Chagas disease), *Trypanosoma brucei rhodesiense* (sleeping sickness), and *Leishmania donovani* (leishmaniasis). This screening study forms the base for an ongoing HPLC-based activity profiling project in antiprotozoal lead discovery. This library had been previously screened for antiplasmodial activity against chloroquine sensitive *Plasmodium falciparum* D10 strain [6].

Material and Methods

Plant species selection

Plants were collected from the wild at various locations in South Africa by different ethnobotanists based on their ethnomedicinal uses against

parasitic diseases, mainly malaria. A list of these uses can be found in an earlier publication [6]. Samples were identified at the South African National Biodiversity Institute (SANBI) by different botanists specializing in specific plant families, and voucher specimens deposited at the South African National Biodiversity Institute (SANBI). The plants project numbers are given in **Table 1S** as Supporting Information.

Preparation of plant extracts

The plant parts (roots, leaves, twigs, fruits, and stem bark) were dried in an oven at 30–60 °C. Dried plant material was ground to a coarse powder using a hammer mill and stored at ambient temperature prior to extraction. Of each sample, 100–500 g of powdered material was sequentially extracted, typically with 1 L of cold dichloromethane (DCM), DCM/methanol (MeOH) (1/1), MeOH, and purified water in 2-L glass jars with screw on lids. The extracts were filtered; the plant material was dried overnight in a fume hood and then extracted with the next more polar solvent. Organic extracts were concentrated using a rotary vacuum evaporator at a temperature below 45 °C and then further dried *in vacuo* at ambient temperature for 24 h. The aqueous extracts were concentrated by freeze-drying. The yields of the extracts, in terms of starting plant material, were recorded. All dried extracts were stored at − 20 °C. Analytical grade solvents for extraction were purchased from Romil Pure Chemistry. HPLC grade water was obtained from a TKA Ultra Pure water purification system.

Evaluation of *in vitro* antiprotozoal activity

Screening of the extract library against *Plasmodium falciparum* (K1 strain), *Trypanosoma brucei rhodesiense* (STIB 900 strain), *Trypanosoma cruzi* trypomastigote forms (Tulahuen strain), *and Leishmania donovani* (strain MHOM/ET/67/L82) was performed in 96-well plates at concentrations of 9.7 and 1.8 µg/mL. Tests were done in duplicate and repeated twice. IC_{50} values against the parasites as well as cytotoxic effects against rat myoblast (L6-cells) were determined by serial dilution and repeated twice. *Trypanosoma brucei rhodesiense* (STIB 900) were grown in axenic medium as described by Baltz et al. [7]. The samples were tested using the Alamar Blue assay protocol [8] to determine the 50 % inhibitory concentration (IC_{50}). A Spectramax Gemini XS micro plate fluorescence reader (Molecular Devices Cooperation) with an excitation wavelength of 536 nm and an emission wavelength of 588 nm was used to measure the plates. Melarsoprol (Arsobal®, purity > 95 %, Sanofi-Aventis) was used as a reference drug (IC_{50} = 0.03 ± 0.01 µM). The IC_{50} values were calculated by using Softmax Pro software (Molecular Devices Cooperation).

Trypanosoma cruzi trypomastigote forms [Tulahuen strain C2C4 containing *β*-galactosidase (Lac Z) gene] were cultured as described by Buckner et al. [9] in rat myoblast cells (L6-cells). Benznidazole (purity > 95 %, Sigma-Aldrich) was used as a standard drug (IC_{50} = 0.48 µg/mL). After incubation, the substrate chlorophenyl red *β*-D-galactopyranoside agent CPRG/Nonident was added to all wells, and a color change was developed within 2 to 6 h. The plates were read photometrically at 540 nm (Molecular Devices). Data were evaluated and IC_{50} values calculated using Softmax Pro software (Molecular Devices).

Axenically grown *L. donovani* amastigotes (strain MHOM/ET/67/L82) were cultured, and tests were done as previously described using the resazurin assay [10]. The plates were developed for 2–4 hours and read on a Spectramax Gemini XS micro plate fluorometer (Molecular Devices) using an excitation wavelength of 536 nm and emission wavelength of 588 nm. Fluorescence development was measured and expressed as a percentage of the negative control. Miltfosine (purity > 95 %, VWR) was used as a reference drug (IC_{50} = 0.241 µg/mL). Data were transferred to the graphics program Softmax Pro (Molecular Devices), with which IC_{50} values were calculated.

Screening of the extract library and determination of activity against *Plasmodium falciparum* K1 strain was done using a modified version of the ^{3}H-hypoxanthine incorporation assay by Trager and Jensen [11]. After incubation the plates were harvested using a Betaplate cell harvester (Wallac) onto glass-fiber filters and washed. The dried filters were inserted into plastic foils with 10 ml scintillation fluid. The radioactivity was counted with a Betaplate liquid scintillation counter (Wallac) as counts per minute per well at each drug concentration and compared to the untreated controls. Chloroquine (purity > 95 %, Sigma-Aldrich) was used as a positive control (IC_{50} = 0.05 ± 0.01 µM). IC_{50} values were calculated by linear interpolation. All assays were run in duplicate and repeated two times.

The cytotoxicity assay was performed by a similar protocol as the Alamar Blue assay whereby L6-cells were seeded in 100 µL RPMI 1640 supplemented in 96-well microtiter plates (4000 cells/well). Podophyllotoxin (purity > 95 %, Sigma-Aldrich) was used as the reference drug (IC_{50} = 0.05 ± 0.01 µM). After 68 h of incubation under humidified 5 % CO_2 atmosphere, 10 µL of the Alamar Blue marker was added to all wells. The plates were incubated for an additional 2 h. A Spectramax Gemini XS microplate fluorescence reader (Molecular Devices Cooperation) was used to measure the plates (Molecular Devices) using an excitation wavelength of 536 nm and an emission wavelength of 588 nm. The IC_{50}s were calculated by Softmax Pro software (Molecular Devices Cooperation).

Supporting information

A table (**Table 1S**) is provided containing the results of the initial antiprotozoal screen of 300 extracts tested at two concentrations against *Trypanosoma brucei rhodesiense*, *Trypanosoma cruzi*, *Leishmania donovani* and *Plasmodium falciparum*.

Results

One hundred and seven medicinal plants were selected because they had a reported tradition of being used as antiparasitic remedies. Dried plant parts were extracted using solvents of different polarity [DCM, DCM/MeOH (1 : 1), MeOH, and water] to give 300 extracts [6]. In a first step, the extracts were screened for their potential antiparasitic properties against *T. b. rhodesiense, T. cruzi, L. donovani*, and *P. falciparum* at the test concentrations 9.7 and 1.6 µg/mL (Supporting Information, **Table 1S**).

In a second stage, extracts which in the first step had shown more than 95 % inhibition of one or more parasites at a test concentration of 9.7 µg/ml were selected as potential "hits", and their IC_{50} values against all four parasites as well as their cytotoxicity against rat myoblast cells (**Table 1**) were determined. This enabled the direct comparison of activities, parasite specific actions and toxicities of each of our "hits" and served as a basis for the selection of the most promising extracts for HPLC-based activity profiling and identification of the active principles [10].

In general, *P. falciparum* was the most sensitive protozoal parasite towards the extract library. The most potent extract in the entire screen was the DCM/MeOH (1 : 1) extract of *Agathosma apiculata*

Table 1 Antiprotozoal *in vitro* activity (IC_{50}s in µg/mL) of 43 plant extracts against *Trypanosoma brucei rhodesiense, Trypanosoma cruzi, Leishmania donovani*, and *Plasmodium falciparum*. Extracts were considered "potential hits" when they inhibited one or more of the parasites at 9.7 µg/mL in a preliminary screen (Supporting Information see **Table 1S**). The positive controls melarsoprol, benznidazol, miltefosine, chloroquine, and podophyllotoxin were tested likewise. Tests were done twice in duplicate.

Plant name	Plant part	Bioprospecting no.	Extract type	*T. b. rhodesiense*	*T. cruzi*	*L. donovani*	*P. falciparum*	Cytotoxicity
Agathosma apiculata G. Mey.	whole plant	P09995b	DCM/MeOH (1 : 1)	11.1	41.5	16.0	0.209	42.9
Agathosma puberula (Steud.) Forc.	roots	P02011a	DCM	32.2	28.9	15.1	8.53	57.9
Alepidea amatymbica Eckl. & Zeyh.	whole plant	P02873b	DCM/MeOH (1 : 1)	20.3	73.1	12.1	3.7	52.7
Artabotrys monteiroae Oliv.	leaves	P18314b	DCM/MeOH (1 : 1)	10.3	41.3	16.6	8.79	40.9
Artemisia afra Jacq. ex Willd.	leaves	P00484b	DCM/MeOH (1 : 1)	21.9	54.5	8.8	7.5	15.8
Artemisia afra Jacq. ex Willd.	leaves	P00484a	DCM	9.6	27.6	5.68	6.22	21.5
Artemisia afra Jacq. ex Willd.	leaves	P00484c	MeOH	15.9	41.8	15.1	13.3	47.4
Asystasia gangetica T. Anderson	leaves	P05623b	DCM/MeOH (1 : 1)	13.2	74.7	12.4	4.2	15.9
Catha edulis (Vahl) Forssk. ex Endl.	roots	P00469a	DCM	14.2	19.1	7.65	4.91	17.8
Conyza albida Spreng.	whole plant	P12954b	DCM/MeOH (1 : 1)	18.8	38.3	16.2	5.79	40.8
Conyza podocephala DC.	whole plant	P03063b	DCM/MeOH (1 : 1)	13.9	47.2	15.8	5.45	51.6
Conyza scabrida DC.	leaves	P03170b	DCM/MeOH (1 : 1)	30.0	49.4	6.65	6.66	48.1
Croton menyhartii Pax	leaves	P12951b	DCM/MeOH (1 : 1)	11.7	33.3	15.8	2.63	46.4
Croton menyhartii Pax	twigs	P12952b	DCM/MeOH (1 : 1)	11.3	41.1	15.9	2.88	45.4
Croton menyhartii Pax	whole plant	P14867b	DCM/MeOH (1 : 1)	8.76	38.6	16.3	10.8	51.1
Cymbopogon validus (Stapf) Stapf ex Burtt Davy	whole plant	P12881b	DCM/MeOH (1 : 1)	11.9	47.1	17.9	6.67	48.7
Ekebergia capensis Sparrm.	fruits	P03111b	DCM/MeOH (1 : 1)	11.5	24.4	4.8	3.5	9.9
Ekebergia capensis Sparrm.	twigs	P03112b	DCM/MeOH (1 : 1)	15.6	46.4	15.9	13.3	55.4
Euclea natalensis A. DC.	roots	P08227b	DCM/MeOH (1 : 1)	28.1	43.7	14.8	7.59	57.9
Eucomis autumnalis (Mill.) Chitt.	flowers/buds	P01463a	DCM	37.1	29.7	7.62	22.1	51.3
Helichrysum nudifolium (L.) Less.	whole plant	P02847b	DCM/MeOH (1 : 1)	33.1	43.9	15.3	9.36	47.7
Hypericum aethiopicum Thunb.	leaves	P02817b	DCM/MeOH (1 : 1)	4.47	18.1	4.74	2.35	15.2
Leonotis leonurus (L.) R. Br.	leaves	P03269b	DCM/MeOH (1 : 1)	14.7	50.1	4.7	2.9	14.1
Leonotis ocymifolia var. ocymifolia (Burm. f.) Iwarsson	leaves	P00480a	DCM	9.1	63.5	18.5	2.7	22.1
Leonotis ocymifolia var. ocymifolia (Burm. f.) Iwarsson	leaves	P00480b	DCM/MeOH (1 : 1)	9.7	91.2	13.3	4.5	18.2
Maytenus undata (Thunb.) Blakelock	roots	P00153a	DCM	35.2	28.4	5.58	8.53	52.4
Pentzia globosa Less.	roots	P01516a	DCM	5.76	31.3	14.4	4.27	50.2
Pentzia globosa Less.	stem bark	P01517a	DCM	6.32	46.5	22.0	6.04	63.9
Pentzia globosa Less.	roots	P01516b	DCM/MeOH (1 : 1)	6.69	40.6	17.5	6.89	54.2
Pentzia globosa Less.	stem bark	P01517b	DCM/MeOH (1 : 1)	15.2	55.6	49.5	9.14	> 100
Plumbago zeylanica L.	leaves	P00631b	DCM/MeOH (1 : 1)	13.0	54.5	17.8	12.4	14.4
Ptaeroxylon obliquum (Thunb.) Radlk	leaves	P01870a	DCM	11.3	41.5	17.2	10.9	46.3
Rauvolfia caffra Sond.	roots	P00734a	DCM	17.9	41.1	15.5	8.44	46.6
Salvia repens Burch. ex Benth.	whole plant	P08214b	DCM/MeOH (1 : 1)	10.8	36.2	5.36	7.65	41.5
Schefflera umbellifera (Sond.) Baill.	roots	P00246a	DCM	20.9	57.6	5.03	2.7	13.9
Schefflera umbellifera (Sond.) Baill.	roots	P00246b	DCM/MeOH (1 : 1)	30.2	99.5	14.1	7.7	48.3
Setaria megaphylla (Steud.) T. Durand & Schinz	whole plant	P12880b	DCM/MeOH (1 : 1)	16.8	43.9	16.9	4.44	48.1
Tarchonanthus camphorates L.	roots	P01154b	DCM/MeOH (1 : 1)	13.4	42.9	16.3	17.7	31.9
Tarchonanthus camphorates L.	whole plant	P02554b	DCM/MeOH (1 : 1)	3.93	18.6	4.86	6.23	16.1
Vernonia hirsuta (DC.) Sch. Bip. ex Walp.	whole plant	P02834b	DCM/MeOH (1 : 1)	18.1	43.0	16.2	10.2	31.6
Vernonia natalensis Sch. Bip. ex Walp.	whole plant	P08212b	DCM/MeOH (1 : 1)	12.6	39.3	17.2	8.53	38.6
Vernonia oligocephala (DC.) Sch. Bip. ex Walp.	leaves	P01015a	DCM	4.67	14.3	16.1	7.69	6.54
Vernonia oligocephala (DC.) Sch. Bip. ex Walp.	leaves	P01015b	DCM/MeOH (1 : 1)	10.9	44.5	19.9	9.51	22.3
Melarsoprol				0.004				
Benznidazole					0.482			
Miltefosine						0.241		
Chloroquine							0.052	
Podophyllotoxin								0.003

(Rutaceae) with an IC_{50} of 0.21 µg/mL against *Plasmodium falciparum.* Seven more lipophilic (DCM/MeOH [1 : 1]) extracts showed antiplasmodial IC_{50}s of under 5 µg/mL: that of *Hypericum aethiopicum* leaves (IC_{50} = 2.4 µg/mL), *Leonotis leonurus* leaves (2.9 µg/mL), *Ekebergia capensis* fruits (3.5 µg/mL), *Alepidea amatymbica* whole plant (3.7 µg/mL), *Asystasia gangetica* leaves (4.2 µg/mL), *Setaria megaphylla* whole plant (4.4 µg/mL), and *Leonotis ocymifolia* var *ocymifolia* leaves (4.5 µg/mL). Also, the DCM extract of *Leonotis ocymifolia* var *ocymifolia* leaves was very active (2.7 µg/mL) (**Table 1**).

Against *Trypanosoma brucei rhodesiense*, the DCM/MeOH (1 : 1) extracts of *Tarchonardus camphorates* whole plant (3.9 µg/mL), *Hypericum aethiopicum* leaves (4.7 µg/mL), *Leonotis ocymifolia* var *ocymifolia* leaves (9.1 µg/mL), *Croton menyhartii* whole plant

(8.8 µg/mL), and the DCM extracts of *Pentzia globosa* roots (5.8 µg/mL), *Vernonia oligocephala* leaves (4.7 µg/mL), *Artemisia afra* leaves (9.6 µg/mL), and *Leonotis ocymifolia* var *ocymifolia* leaves (9.7 µg/mL) showed IC_{50}s lower than 10 µg/mL. Three further DCM, eighteen DCM/MeOH extracts, and one MeOH extract had IC_{50}s between 10 and 20 µg/mL against *Trypanosoma brucei* (**Table 1**). Despite the fact that most of the 43 "selected hits" showed relatively good activity against *T. brucei*, none showed selectivity towards this parasite, as it had been the case for the *Plasmodium falciparum* screen.

Trypanosoma cruzi was the least sensitive protozoal test organism. Three extracts, the DCM/MeOH extract of *Hypericum aethiopicum* leaves (18.1 µg/mL), the DCM extract of *Catha edulis* roots (19.1 µg/mL), and the DCM/MeOH extract of *Tarchonardus camphoratus* whole plant (18.6 µg/mL) inhibited *T. cruzi* with IC_{50}s under 20 µg/mL.

Seven extracts showed IC_{50} of less than 6 µg/mL against *Leishmania donovani*. These were the DCM/MeOH extract of *Hypericum aethiopicum* leaves (4.7 µg/mL), *Leonotis leonurus* leaves (4.7 µg/mL), *Ekebergia capensis* fruits (4.8 µg/mL), *Schefflera umbellifera* (5.0 µg/mL), *Salvia repens* (5.4 µg/mL), *Tachonanthus camphorates* (4.9 µg/mL), and the DCM extract of *Maytenus undata* (5.6 µg/mL).

Discussion

We screened an extract library generated from plants selected for their traditional antimalarial use against the most important human protozoal parasites. The goal was to identify extracts with potent and, ideally, selective activity against any one of the parasites. These hits are being followed up in an ongoing HPLC-based activity profiling project in antiprotozoal lead discovery.

The initial screening of this focused extract library delivered forty three "potential hits". These were defined as samples with almost complete (> 95 %) inhibition at 9.7 µg/mL. Twelve of them showed activity against *Plasmodium falciparum*, twenty-eight against *Trypanosoma brucei rhodesiense*. Six of these extracts were active against both parasites (Supporting Information, **Table 1S**). Against *Leishmania donovani* eleven extracts fulfilled the criteria for "potential hits". Five of these were also active against *T. brucei*. One extract, the DCM extract of *Catha edulis* roots, inhibited both *P. falciparum* and *Leishmania,* and the DCM/MeOH extract of *Hypericum aethiopicum* leaves inhibited the growth of all three parasites. No extract showed > 95% inhibition of *Trypanosoma cruzi* at 9.7 µg/mL. This parasite is generally less sensitive than *Trypanosoma brucei* because it is an intracellular test system.

In a second phase, the IC_{50}s of the 43 "potential hits" were determined against all the parasites and against L6 cells (**Table 1**). *Agathosma apiculata* (Rutaceae) was exceptional in the sense that it was by far the most active extract against *Plasmodium falciparum* and showed at the same time good selectivity. An IC_{50} of 0.3 µg/mL against *Plasmodium* compared to 43 µg/mL in L6 cells corresponded to a selectivity value of 143. The extract was also 140 times more active against *P. falciparum* than against *T. cruzi*, 53 times more active than against *Leishmania donovani*, and 37 times more active than against *T. brucei*.

Nine of the 43 selected active extracts showed IC_{50}s of < 10 µg/mL against *Trypanosoma brucei rhodesiense* (**Table 1**). Yet, despite the relatively high activity, none showed selectivity towards this parasite.

Salvia repens and *Maytenus undata* were shown to be preferentially active against *Leishmania donovani,* whilst showing only moderate cytotoxic effects (**Table 1**).

The most active extracts against *T. cruzi* showed nonspecific effects. The DCM/MeOH extracts of *Hypericum aethiopicum* leaves (18.1 µg/mL) and *Tarchonardus camphoratus* (18.6 µg/mL) and the DCM extract of *Catha edulis* roots (19.1 µg/mL) at the same time strongly inhibited L6 cells, which are *T. cruzi*'s host cells (**Table 1**). The DCM/MeOH and/or DCM extracts of *Hypericum aethiopicum, Leonotis leonurus, Ekebergia capensis, Catha edulis, Asystasia gangetica, Schefflera umbellifera*, and *Tarchonardus camphoratus* all showed relatively high cytotoxicity, with IC_{50}s < 20 µg/mL, and activities against most protozoal test organisms. Therefore, these extracts were not shortlisted for further follow-up.

In summary, screening of our focused library led to a shortlist of extracts with high activity against *Plasmodium falciparum, Trypanosoma brucei rhodesiense*, and *Leishmania donovani* in a primary screen. The percents of inhibition at the two initial test concentrations were roughly indicative of the half maximum inhibition concentration (IC_{50} values) to be expected in the second stage of the screening. Given the cellular test systems and their inherent variability, some extracts showed IC_{50}s slightly higher or lower than could have been predicted from the primary screen. For direct comparison of activities, it is therefore necessary to determine IC_{50}s by serial dilution (**Table 1**). This data, together with cytotoxicity data, helps to determine whether an activity is specific or just a generally toxic effect. Extracts with favorable activities are followed up by HPLC-based activity profiling [12]. We have recently developed and validated a microtiter-based protocol for the miniaturized and efficient identification of antiprotozoal compounds in extracts [10] and successfully applied this approach to the discovery of new antiprotozoal natural products in other library-based discovery projects [13–15]. Results from the profiling and identification of the active principles from the extracts in this screen will be reported in due course.

Conflict of interest

The authors have no conflict of interest.

Acknowledgements

The authors would like to thank the Council of Scientific and Industrial Research (CSIR) and the Swiss Confederation for financial support under the Swiss South African Joint Research Programme (grant JRP 03), and SANBI for the identification of plant species.

Affiliations

[1] Biosciences, CSIR, Pretoria, South Africa
[2] Institute of Pharmaceutical Biology, University of Basel, Basel, Switzerland
[3] Swiss Tropical and Public Health Institute, Basel, Switzerland
[4] School of Chemistry, University of KwaZulu-Natal, Durban, South Africa
[5] Faculty of Pharmacy, Pancasila University, Jakarta, Indonesia
[6] Departamento de Farmacia, Universidad Nacional de Colombia, Bogotá, Colombia

References

1 *Chirac P, Torreele E.* Global framework on essential health R&D. Lancet 2006; 367: 1560–1561
2 *Stuart K, Brun R, Croft S, Fairlamb A, Gürtler RE, McKerrow J, Reed S, Tarleton R.* Kinetoplastids: related protozoan pathogens, different diseases. J Clin Invest 2008; 118: 1301–1310
3 *World Health Organization.* Drug resistance: malaria. Available at http://www.who.int/drugresistance/malaria/en/. Accessed February 21, 2011
4 http://www.mmv.org/. Accessed February 21, 2011
5 http://www.gatesfoundation.org/Pages/home.aspx. Accessed February 21, 2011
6 *Clarkson C, Maharaj VJ, Crouch NR, Grace OM, Pillay P, Matsabisa MG, Bhagwandin N, Smith PJ, Folb PI. In vitro* antiplasmodial activity of medicinal plants native to or naturalised in South Africa. J Ethnopharmacol 2004; 92: 177–191
7 *Baltz T, Baltz D, Giroud C, Crockett J.* Cultivation in a semidefined medium of animal infective forms of *Trypanosoma brucei, T. equiperdum, T. evansi, T. rhodesiense, T. gamiense*. EMBO J 1985; 4: 1273–1277
8 *Räz B, Iten M, Grether-Bühler Y, Kaminsky R, Brun R.* The Alamar Blue assay to determine drug sensitivity of African trypanosomes (*T. b. rhodesiense* and *T. b. gambiense*) *in vitro*. Acta Trop 1997; 68: 139–147
9 *Buckner FS, Verlinde CL, La Flamme AC, Van Voorhis WC.* Efficient technique for screening drugs for activity against *Trypanosoma cruzi* using parasites expressing beta-galactosidase. Antimicrob Agents Chemother 1996; 40: 2592–2597
10 *Adams M, Zimmermann S, Kaiser M, Brun R, Hamburger M.* A protocol for HPLC-based activity profiling for natural products with activities against tropical parasites. Nat Prod Commun 2009; 4: 1377–1381
11 *Trager W, Jensen JB.* Human malaria parasites in continuous culture. Science 1976; 193: 673–675
12 *Potterat O, Hamburger M.* Natural products in drug discovery – concepts and approaches for tracking bioactivity. Curr Org Chem 2006; 8: 899–920
13 *Adams M, Christen M, Zimmermann S, Plitzko I, Kaiser M, Brun R, Hamburger M.* New antiplasmodial lanostanes from *Ganoderma lucidum* mushroom. J Nat Prod 2010; 73: 897–900
14 *Ślusarczyk S, Zimmermann S, Kaiser M, Matkowski A, Hamburger M, Adams M.* Antiplasmodial and antitrypanosomial activity of tanshinone-type diterpenoids from *Salvia miltiorrhiza*. Planta Med 2011; doi: 10.1055/s-0030-1270933
15 *Adams M, Plitzko I, Kaiser M, Brun R, Hamburger M.* 3-methoxy carpachromene – a new tetracyclic flavonol from *Pistacia atlantica* with anti plasmodial activity. Phytochem Lett 2009; 2: 159–162

Supporting information

In vitro screening of traditional South African malaria remedies against *Trypanosoma brucei rhodesiense*, *Trypanosoma cruzi*, *Leishmania donovani* and *Plasmodium falciparum*

Tsholofelo A. Mokoka[1], Stefanie Zimmermann[2, 3], Tasqiah Julianti[2], Nivan Moodley[1], Monica Cal[3], Michael Adams[2], Marcel Kaiser[3], Reto Brun[3], Neil Koorbanally[4], Matthias Hamburger[2]

[1]Biosciences, CSIR, Pretoria, South Africa

[2]Institute of Pharmaceutical Biology, University of Basel, Basel, Switzerland

[3]Swiss Tropical and Public Health Institute, Basel, Switzerland

[4]Department of Chemistry, University of KwaZulu-Natal, Durban, South Africa

Correspondence

Prof. Dr. Matthias Hamburger, Institute of Pharmaceutical Biology, Department of Pharmaceutical Sciences, University of Basel, Klingelbergstrasse 50, CH-4056 Basel, Switzerland. E-mail:matthias.hamburger@unibas.ch, Phone: +41 61 267 15 55 Fax: +41 61 267 14 74

Supporting information Table S1 Antiprotozoal *in vitro* activity (% inhibition at 9.7 and 1.8 µg/mL) of 300 plant extracts tested against *Trypanosoma brucei rhodesiense*, *Trypanosoma cruzi*, *Leishmania donovani* and *Plasmodium falciparum*. Plants were selected due to their reported traditional use against malaria in South Africa.

Plant species	Family	Project number	Plant part	Solvent	*T. brucei rhodesiense*		*T. cruzi*		*L. donovani*		*P. falciparum*	
					% inhibition (9.7 µg/mL)	% inhibition (1.8 µg/mL)	% inhibition (9.7 µg/mL)	% inhibition (1.8 µg/mL)	% inhibition (9.7 µg/mL)	% inhibition (1.8 µg/mL)	% inhibition (9.7 µg/mL)	% inhibition (1.8 µg/mL)
***Acacia nilotica* (L.) kraussianna**	Fabaceae	P12859b	Twigs	DCM/MeOH(1:1)	18	17	6	5	22	11	43	0
Acacia nilotica (L.) kraussianna	Fabaceae	P12859c	Twigs	Aqueous	6	9	10	1	18	2	0	0
***Acacia tortilis* (Forssk) Hayne**	Fabaceae	P12869b	Whole plant	DCM/MeOH(1:1)	17	4	12	3	28	7	59	4
***Achyranthes aspera* L.**	Amaranthaceae	P15190b	Whole plant	DCM/MeOH(1:1)	12	10	0	0	36	0	53	0
***Agathosma apiculata* G.Mey.**	Rutaceae	P09995b	Whole plant	DCM/MeOH(1:1)	99	0	0	0	73	14	80	21
***Agathosma puberula* (Steud.) Forc.**	Rutaceae	P02011a	Roots	DCM	98	7	0	0	68	8	58	1
***Agathosma puberula* (Steud.) Forc.**	Rutaceae	P02011b	Roots	DCM/MeOH (1:1)	0	1	0	0	29	1	34	1
***Agathosma puberula* (Steud.) Forc.**	Rutaceae	P02022a	Stem bark	DCM	3	8	10	2	53	5	95	9
***Agathosma puberula* (Steud.) Forc.**	Rutaceae	P02022b	Stem bark	DCM/MeOH (1:1)	5	0	4	0	17	4	25	14
***Ageratum conyzoides* L.**	Asphodelaceae	P12944b	Whole plant	DCM/MeOH (1:1)	4	1	9	3	27	17	36	0
***Ageratum conyzoides* L.**	Asphodelaceae	P12944c	whole plant	Aqueous	0	0	0	8	40	20	4	4
***Alepidea amatymbica* Eckl. & Zeyh.**	Apiaceae	P02873b	Whole plant	DCM/MeOH (1:1)	2	0	0	0	89	23	56	1
***Aloe ferox* Mill.**	Asphodelaceae	P01713a	Fruits	DCM	10	0	2	0	7	1	14	0
***Aloe ferox* Mill.**	Asphodelaceae	P01713b	Fruits	DCM/MeOH (1:1)	15	0	0	5	17	9	1	0
***Aloe ferox* Mill.**	Asphodelaceae	P01713c	Fruits	Aqueous	1	7	7	5	13	0	0	0
***Aloe ferox* Mill.**	Asphodelaceae	P03153b	Whole plant	DCM/MeOH (1:1)	9	4	0	0	42	11	59	5
***Aloe marlothii* A.Berger**	Asphodelaceae	P00054b	Leaves	DCM/MeOH (1:1)	13	10	0	0	5	0	0	4
***Aloe marlothii* A.Berger**	Asphodelaceae	P00054d	Leaves	Aqueous	15	8	0	0	21	9	3	0
***Aloe marlothii* A.Berger**	Asphodelaceae	P00770b	Whole plant	DCM/MeOH (1:1)	0	0	0	0	21	2	16	1
Annona senegalensis* Pers. subsp. *senegalensis	Annonaceae	P01034b	Leaves	DCM/MeOH (1:1)	0	3	0	0	11	0	93	0
***Anthocleista grandiflora* Gilg**	Gentianaceae	P01455c	Leaves	Aqueous	0	3	0	0	17	3	2	0
***Anthocleista grandiflora* Gilg**	Gentianaceae	P01455a	Leaves	DCM	43	24	0	0	32	5	26	0
***Anthocleista grandiflora* Gilg**	Gentianaceae	P01455b	Leaves	DCM/MeOH (1:1)	18	21	0	0	20	16	2	0
***Artabotrys brachypetalus* Benth.**	Annonaceae	P02239b	Twigs/Leaves	DCM/MeOH (1:1)	4	6	0	0	16	12	17	3
***Artabotrys brachypetalus* Benth.**	Annonaceae	P02239c	Twigs/Leaves	Aqueous	2	1	0	1	16	3	0	0
***Artabotrys monteiroae* Oliv.**	Annonaceae	P18314b	Leaves	DCM/MeOH (1:1)	99	0	9	8	25	5	40	0
Artabotrys monteiroae Oliv.	Annonaceae	P18314c	Leaves	Aqueous	0	0	15	5	18	10	0	0

Plant species	Family	Project number	Plant part	Solvent	*T. brucei rhodesiense*		*T. cruzi*		*L. donovani*		*P. falciparum*	
					% inhibition (9.7 µg/mL)	% inhibition (1.8 µg/mL)	% inhibition (9.7 µg/mL)	% inhibition (1.8 µg/mL)	% inhibition (9.7 µg/mL)	% inhibition (1.8 µg/mL)	% inhibition (9.7 µg/mL)	% inhibition (1.8 µg/mL)
***Artemisia afra* Jacq. ex Willd.**	Asteraceae	P00484a	Leaves	DCM	98	0	0	0	100	26	89	8
***Artemisia afra* Jacq. ex Willd.**	Asteraceae	P00484b	Leaves	DCM/MeOH (1:1)	97	0	0	0	100	43	77	3
***Artemisia afra* Jacq. ex Willd.**	Asteraceae	P00484c	Leaves	MeOH	96	5	0	0	81	0	35	0
***Asparagus virgatus* Baker**	Asparagaceae	P08216b	Whole plant	DCM/MeOH (1:1)	11	9	0	11	35	14	55	3
***Asystasia gangetica* T.Anderson**	Acanthaceae	P05622b	Twigs	DCM/MeOH (1:1)	6	0	0	0	28	0	40	3
***Asystasia gangetica* T.Anderson**	Acanthaceae	P05623b	Leaves	DCM/MeOH (1:1)	0	0	2	0	18	0	100	51
***Barringtonia racemosa* (L.) Roxb.**	Lecythidaceae	P15194c	Leaves	Aqueous	0	6	3	0	15	9	0	1
***Barringtonia racemosa* (L.) Roxb.**	Lecythidaceae	P15194b	Leaves	DCM/MeOH(1:1)	3	0	5	4	25	3	33	6
***Barringtonia racemosa* (L.) Roxb.**	Lecythidaceae	P15193b	Twigs	DCM/MeOH(1:1)	32	5	6	2	26	0	27	0
***Berula erecta* (Huds.) Coville**	Apiaceae	P05646b	Whole plant	DCM/MeOH(1:1)	17	9	0	0	36	5	44	6
***Bidens pilosa* L.**	Asteraceae	P00071b	Leaves	DCM/MeOH (1:1)	20	21	0	0	26	14	43	15
***Bidens pilosa* L.**	Asteraceae	P00071c	Leaves	MeOH	21	17	0	0	37	14	47	5
***Bidens pilosa* L.**	Asteraceae	P00071d	Leaves	Aqueous	19	15	0	0	23	14	13	0
***Bruguiera gymnorhiza* (L.) Lam.**	Rhizophoraceae	P18322b	Twigs	DCM/MeOH(1:1)	0	0	0	1	26	9	35	0
***Capparis tomentosa* Lam.**	Capparaceae	P00665a	Leaves	DCM	30	24	0	0	39	7	5	0
***Capparis tomentosa* Lam.**	Capparaceae	P00667a	Stem bark	DCM	8	6	0	0	30	0	15	0
***Capparis tomentosa* Lam.**	Capparaceae	P00669a	Roots	DCM	5	6	0	0	18	9	0	4
***Capparis tomentosa* Lam.**	Capparaceae	P00665b	Leaves	DCM/MeOH(1:1)	6	0	0	0	19	0	21	0
***Capparis tomentosa* Lam.**	Capparaceae	P00667b	Stem bark	DCM/MeOH(1:1)	4	17	0	0	10	0	1	0
Capparis tomentosa Lam.	Capparaceae	P00669b	Roots	DCM/MeOH(1:1)	22	3	0	0	32	4	0	0
***Carissa edulis* Vahl**	Apocynaceae	P00334a	Stem bark	DCM	0	6	0	0	36	12	28	3
***Carissa edulis* Vahl**	Apocynaceae	P00334b	Stem bark	DCM/MeOH (1:1)	9	7	0	0	33	7	14	0
***Carissa edulis* Vahl**	Apocynaceae	P00334c	Stem bark	MeOH	13	16	0	0	19	0	0	0
***Catha edulis* (Vahl) Forssk. ex Endl.**	Celastraceae	P00465a	Seed	DCM	0	0	0	0	33	10	37	0
***Catha edulis* (Vahl) Forssk. ex Endl.**	Celastraceae	P00465b	Seed	DCM/MeOH (1:1)	0	11	0	0	19	0	11	0
***Catha edulis* (Vahl) Forssk. ex Endl.**	Celastraceae	P00465c	Roots	MeOH	0	9	0	0	16	7	9	0
***Catha edulis* (Vahl) Forssk. ex Endl.**	Celastraceae	P00469a	Roots	DCM	57	10	0	0	100	23	99	9
***Catha edulis* (Vahl) Forssk. ex Endl.**	Celastraceae	P00469b	Roots	DCM/MeOH (1:1)	0	8	0	0	31	0	24	0

Plant species	Family	Project number	Plant part	Solvent	*T. brucei rhodesiense*		*T. cruzi*		*L. donovani*		*P. falciparum*	
					% inhibition (9.7 µg/mL)	% inhibition (1.8 µg/mL)	% inhibition (9.7 µg/mL)	% inhibition (1.8 µg/mL)	% inhibition (9.7 µg/mL)	% inhibition (1.8 µg/mL)	% inhibition (9.7 µg/mL)	% inhibition (1.8 µg/mL)
***Catha edulis* (Vahl) Forssk. ex Endl.**	Celastraceae	P00469c	Leaves	MeOH	3	3	0	0	9	3	18	0
***Catha edulis* (Vahl) Forssk. ex Endl.**	Celastraceae	P00470a	Leaves	DCM	5	0	0	0	21	0	29	0
***Catha edulis* (Vahl) Forssk. ex Endl.**	Celastraceae	P00470b	Leaves	DCM/MeOH (1:1)	0	8	0	0	14	0	42	8
***Catha edulis* (Vahl) Forssk. ex Endl.**	Celastraceae	P00465d	Seed	Aqueous	0	7	3	2	6	4	0	0
Catha edulis (Vahl) Forssk. ex Endl.	Celastraceae	P00469d	Roots	Aqueous	0	0	10	0	24	12	0	0
Catha edulis (Vahl) Forssk. ex Endl.	Celastraceae	P00470d	Leaves	Aqueous	0	4	2	6	24	9	92	0
***Centella asiatica* (L.) Urb.**	Apiaceae	P05632b	Leaves	DCM/MeOH (1:1)	0	0	0	3	43	2	39	7
Clausena anisata* (Willd.) Hook.f. ex *Benth var. anisata	Rutaceae	P09997b	Twigs	DCM/MeOH(1:1)	5	0	0	0	21	8	18	1
***Clausena anisata* (Willd.) Hook.f. e Benth var. anisata**	Rutaceae	P09998b	Leaves	DCM/MeOH(1:1)	5	0	4	0	31	3	25	0
***Clutia hirsuta* E.Mey. ex Sond.**	Euphorbiaceae	P11867b	Whole plant	DCM/MeOH(1:1)	8	4	0	1	40	12	69	10
Clutia hirsuta E.Mey. ex Sond.	Euphorbiaceae	P11867c	Whole plant	Aqueous	26	15	1	0	20	9	0	0
***Combretum zeyheri* Sond.**	Combretaceae	P13042b	Twigs	DCM/MeOH(1:1)	10	0	47	0	26	4	33	0
***Combretum zeyheri* Sond.**	Combretaceae	P13042c	Twigs	Aqueous	7	0	0	0	11	7	19	0
***Conyza albida* Spreng.**	Asteraceae	P12954b	Whole plant	DCM/MeOH(1:1)	100	0	0	3	63	10	97	6
***Conyza albida* Spreng.**	Asteraceae	P12954C	whole plant	Aqueous	0	3	0	1	21	11	1	0
***Conyza podocephala* DC.**	Asteraceae	P03063b	Whole plant	DCM/MeOH (1:1)	6	4	0	0	53	4	99	12
***Conyza scabrida* DC.**	Asteraceae	P03168b	Flowers/ Buds	DCM/MeOH (1:1)	2	6	0	0	93	12	60	0
Conyza scabrida DC.	Asteraceae	P03169b	Twigs	DCM/MeOH (1:1)	2	15	0	0	45	18	41	0
Conyza scabrida DC.	Asteraceae	P03170b	Leaves	DCM/MeOH (1:1)	0	3	0	0	100	5	53	7
***Crinum macowanii* Baker**	Amaryllidaceae	P05637b	Flowers/ Buds	DCM/MeOH (1:1)	52	26	1	3	36	5	47	0
***Crinum macowanii* Baker**	Amaryllidaceae	P05637c	Flowers/ Buds	Aqueous	0	0	0	0	2	0	2	0
***Crotalaria burkeana* Benth.**	Fabaceae	P00417b	Roots	DCM/MeOH (1:1)	25	9	0	0	22	5	21	0
***Crotalaria burkeana* Benth.**	Fabaceae	P00418b	Seed	DCM/MeOH (1:1)	18	8	0	0	63	10	66	5
***Crotalaria burkeana* Benth.**	Fabaceae	P00417c	Leaves	MeOH	6	5	0	0	29	9	5	0
***Crotalaria burkeana* Benth.**	Fabaceae	P00417d	Leaves	Aqueous	11	7	0	0	23	0	0	0
***Crotalaria burkeana* Benth.**	Fabaceae	P00418d	Roots	Aqueous	7	3	0	0	22	7	0	0
Croton gratissimus* Burch. var. *gratissimus	Euphorbiaceae	P00010c	Leaves	MeOH	14	13	0	0	31	5	24	13
Croton gratissimus* Burch. var. *gratissimus	Euphorbiaceae	P00010d	Leaves	Aqueous	4	17	0	0	10	3	0	0

Plant species	Family	Project number	Plant part	Solvent	*T. brucei rhodesiense*		*T. cruzi*		*L. donovani*		*P. falciparum*	
					% inhibition (9.7 µg/mL)	% inhibition (1.8 µg/mL)	% inhibition (9.7 µg/mL)	% inhibition (1.8 µg/mL)	% inhibition (9.7 µg/mL)	% inhibition (1.8 µg/mL)	% inhibition (9.7 µg/mL)	% inhibition (1.8 µg/mL)
***Croton menyhartii* Pax**	Euphorbiaceae	P12951b	Leaves	DCM/MeOH(1:1)	99	2	8	0	66	7	100	27
Croton menyhartii Pax	Euphorbiaceae	P12952b	Twigs	DCM/MeOH(1:1)	98	10	0	2	56	20	100	33
***Croton menyhartii* Pax**	Euphorbiaceae	P12951c	Leaves	Aqueous	16	7	0	12	28	17	4	0
Croton menyhartii Pax	Euphorbiaceae	P12952c	Twigs	Aqueous	4	5	0	3	28	26	1	0
***Cussonia spicata* Thunb.**	Araliaceae	P00042a	Roots	DCM	12	13	0	0	31	4	28	0
***Cussonia spicata* Thunb.**	Araliaceae	P00042c	Leaves	MeOH	15	7	0	0	92	16	17	2
***Cussonia spicata* Thunb.**	Araliaceae	P02612b	Leaves	DCM/MeOH (1:1)	2	6	11	3	68	6	71	12
***Cymbopogon validus* (Stapf) Stapf ex Burtt Davy**	Poaceae	P12881b	Whole plant	DCM/MeOH(1:1)	99	6	6	6	41	7	97	7
***Diosma* sp (exact species not identified)**	Rutaceae	P02051a	Roots	DCM	17	13	1	0	69	15	93	17
Diosma sp (exact species not identified)	Rutaceae	P02051b	Roots	DCM/MeOH (1:1)	10	3	0	0	18	0.0	13.8	0.0
***Diplorhynchus condylocarpon* (Müll.Arg.) Pichon**	Apocynaceae	P00940b	Roots	DCM/MeOH (1:1)	0	6	0	0	19	0	4	3
***Dodonaea viscosa* Jacq.**	Sapindaceae	P02291b	Leaves	DCM/MeOH (1:1)	1	1	5	5	65	14	32	0
***Ekebergia capensis* Sparrm.**	Meliaceace	P03111b	Fruits	DCM/MeOH (1:1)	99	12	0	0	96	20	81	17
Ekebergia capensis Sparrm.	Meliaceace	P03112b	Twigs	DCM/MeOH (1:1)	58	0	0	0	68	7	44	4
***Ekebergia capensis* Sparrm.**	Meliaceace	P03111c	Fruits	Aqueous	0	0	0	0	10	1	0	0
***Elephantorrhiza elephantina* (Burch.) Skeels**	Fabaceae	P08224b	Roots	DCM/MeOH(1:1)	0	3	0	0	32	3	23	0
***Elephantorrhiza elephantina* (Burch.) Skeels**	Fabaceae	P08224b	Leaves	DCM/MeOH(1:1)	2	0	0	3	27	6	35	0
***Elephantorrhiza elephantina* (Burch.) Skeels**	Fabaceae	P08224c	roots	Aqueous	41	20	18	0	29	20	6	0
Elephantorrhiza elephantina (Burch.) Skeels	Fabaceae	P08225c	Leaves	Aqueous	7	12	0	1	22	7	4	0
***Euclea natalensis* A.DC.**	Ebenaceae	P08226b	Stem bark	DCM/MeOH(1:1)	4	0	0	0	53	0	40	0
***Euclea natalensis* A.DC.**	Ebenaceae	P08227b	Roots	DCM/MeOH(1:1)	98	0	0	0	43	0	80	17
***Euclea undulata* Thunb.**	Ebenaceae	P09984b	Leaves	DCM/MeOH(1:1)	0	0	0	4	58	6	39	0
***Euclea undulata* Thunb.**	Ebenaceae	P09985b	Twigs	DCM/MeOH(1:1)	4	0	7	5	35	5	66	0
***Eucomis autumnalis* (Mill.) Chitt.**	Hyacinthaceae	P01463a	Flowers/Buds	DCM	2	0	0	0	96	33	23	2
***Eucomis autumnalis* (Mill.) Chitt.**	Hyacinthaceae	P01463b	Flowers/Buds	DCM/MeOH (1:1)	7	9	55	0	29	7	3	0
***Eucomis autumnalis* (Mill.) Chitt.**	Hyacinthaceae	P01463c	Flowers/Buds	Aqueous	18	19	0	0	16	8	0	0
***Euphorbia heterophylla* L.**	Euphorbiaceae	P12864b	Whole plant	DCM/MeOH(1:1)	7	7	0	1	30	6	41	7
***Euphorbia tirucalli* L.**	Euphorbiaceae	P00788a	Leaves	DCM	86	0	0	0	44	8	60	0

Plant species	Family	Project number	Plant part	Solvent	*T. brucei rhodesiense*		*T. cruzi*		*L. donovani*		*P. falciparum*	
					% inhibition (9.7 µg/mL)	% inhibition (1.8 µg/mL)	% inhibition (9.7 µg/mL)	% inhibition (1.8 µg/mL)	% inhibition (9.7 µg/mL)	% inhibition (1.8 µg/mL)	% inhibition (9.7 µg/mL)	% inhibition (1.8 µg/mL)
Euphorbia tirucalli L.	Euphorbiaceae	P00788b	Leaves	DCM/MeOH (1:1)	0	0	0	0	22	0	15	3
***Euphorbia tirucalli* L.**	Euphorbiaceae	P00788c	Leaves	MeOH	19	21	4	6	29	2	0	0
***Flacourtia indica* (Burm.f.) Merr.**	Flacourtiaceae	P00904a	Roots	DCM	0	1	0	0	11	2	9	0
***Flacourtia indica* (Burm.f.) Merr.**	Flacourtiaceae	P00904c	Roots	Aqueous	11	5	0	0	11	0	0	0
***Gloriosa superba* L.**	Colchicaceae	P08215b	Whole plant	DCM/MeOH(1:1)	7	9	27	0	25	13	44	11
***Gloriosa superba* L.**	Colchicaceae	P08215c	whole plant	Aqueous	0	17	23	0	12	4	0	0
***Gomphocarpus fruticosus* (L.) Aiton.f.**	Apocynaceae	P09988b	Fruits	DCM/MeOH(1:1)	1	0	7	0	22	14	5	0
***Gomphocarpus fruticosus* (L.) Aiton.f.**	Apocynaceae	P09989b	Leaves	DCM/MeOH(1:1)	9	1	3	3	21	11	23	0
***Helichrysum nudifolium* (L.) Less.**	Asteraceae	P02847b	Whole plant	DCM/MeOH (1:1)	0	11	0	0	100	14	63	3
***Hippobromus pauciflorus* (L.f.) Radlk.**	Sapindaceae	P12876b	Leaves	DCM/MeOH(1:1)	0	0	0	0	32	15	59	0
***Hippobromus pauciflorus* (L.f.) Radlk.**	Sapindaceae	P12876c	Leaves	Aqueous	14	1	1	0	15	4	0	0
***Hippobromus pauciflorus* (L.f.) Radlk.**	Sapindaceae	P12877b	Twigs	DCM/MeOH(1:1)	4	7	2	0	73	6	91	13
***Hypericum aethiopicum* Thunb.**	Clusiaceae	P02817b	Leaves	DCM/MeOH (1:1)	99	75	6	3	100	55	100	33
Hypericum aethiopicum Thunb.	Clusiaceae	P02817c	Leaves	Aqueous	0	5	0	0	15	2	0	5
***Hyptis pectinata* (L.) Poit.**	Lamiaceae	P02459b	Leaves	DCM/MeOH (1:1)	0	2	27	0	37	6	34	0
***Hyptis pectinata* (L.) Poit.**	Lamiaceae	P02459c	Twigs/Leaves	Aqueous	9	1	2	3	32	27	7	1
***Justicia flava* (Vahl) Vahl**	Acanthaceae	P05636b	Whole plant	DCM/MeOH (1:1)	0	12	0	0	12	0	21	0
***Kigelia africana* (Lam.) Benth.**	Bignoniaceae	P00692a	Leaves	DCM	12	12	0	0	33	3	6	0
***Kigelia africana* (Lam.) Benth.**	Bignoniaceae	P00692b	Leaves	DCM/MeOH (1:1)	15	4	0	0	10	9	6	0
***Kirkia wilmsii* Engl.**	Kirkiaceae	P13041c	Leaves	Aqueous	0	0	0	0	18	7	61	0
***Leonotis leonurus* (L.) R.Br.**	Lamiaceae	P03268b	Twigs	DCM/MeOH (1:1)	3	13	0	0	48	0	86	8
***Leonotis leonurus* (L.) R.Br.**	Lamiaceae	P03269b	Leaves	DCM/MeOH (1:1)	32	9	0	0	85	5	81	16
***Leonotis leonurus* (L.) R.Br.**	Lamiaceae	P02414c	roots	Aqueous	7	8	1	1	32	26	8	0
***Leonotis leonurus* (L.) R.Br.**	Lamiaceae	P03268c	Twigs	Aqueous	5	0	0	1	12	2	0	0
***Leonotis leonurus* (L.) R.Br.**	Lamiaceae	P03269c	Leaves	Aqueous	17	0	0	0	13	3	0	0
Leonotis ocymifolia* (Burm.f.) Iwarsson *var. raineriana (Vis.) Iwarsson	Lamiaceae	P14867b	Whole plant	DCM/MeOH(1:1)	98	14	0	0	36	5	39	0
***Leonotis ocymifolia* (Burm.f.) Iwarsson var. raineriana (Vis.) Iwarsson**	Lamiaceae	P00480d	Leaves	Aqueous	7	7	4	7	16	1	0	0

Plant species	Family	Project number	Plant part	Solvent	*T. brucei rhodesiense*		*T. cruzi*		*L. donovani*		*P. falciparum*	
					% inhibition (9.7 µg/mL)	% inhibition (1.8 µg/mL)	% inhibition (9.7 µg/mL)	% inhibition (1.8 µg/mL)	% inhibition (9.7 µg/mL)	% inhibition (1.8 µg/mL)	% inhibition (9.7 µg/mL)	% inhibition (1.8 µg/mL)
***Leonotis ocymifolia* (Burm.f.) Iwarsson var. raineriana (Vis.) Iwarsson**	Lamiaceae	P00481d	Fruits	Aqueous	0	3	0	0	26	10	0	0
***Leonotis ocymifolia* (Burm.f.) Iwarsson var. raineriana (Vis.) Iwarsson**	Lamiaceae	P00482c	Roots	MeOH	1	2	0	0	14	0	1	0
***Leonotis ocymifolia* (Burm.f.) Iwarsson var. raineriana (Vis.) Iwarsson**	Lamiaceae	P00482d	Roots	Aqueous	0	0	0	0	0	0	0	0
***Leonotis ocymifolia* var. *ocymifolia* (Burm.f.) Iwarsson**	Lamiaceae	P00480a	Leaves	DCM	100	13	0	0	54	10	74	9
***Leonotis ocymifolia* var. *ocymifolia* (Burm.f.) Iwarsson**	Lamiaceae	P00480b	Leaves	DCM/MeOH (1:1)	99	22	0	0	60	9	81	1
***Leonotis ocymifolia* var. *ocymifolia* (Burm.f.) Iwarsson**	Lamiaceae	P00480c	Leaves	MeOH	20	27	0	0	46	11	66	4
***Leonotis ocymifolia* var. *ocymifolia* (Burm.f.) Iwarsson**	Lamiaceae	P00481a	Fruits	DCM	13	13	0	0	49	8	36	3
***Leonotis ocymifolia* var. *ocymifolia* (Burm.f.) Iwarsson**	Lamiaceae	P00481b	Fruits	DCM/MeOH (1:1)	0	0	0	0	36	4	7	0
***Leonotis ocymifolia* var. *ocymifolia* (Burm.f.) Iwarsson**	Lamiaceae	P00481c	Fruits	MeOH	0	0	1	0	21	8	6	0
***Leonotis ocymifolia* var. *ocymifolia* (Burm.f.) Iwarsson**	Lamiaceae	P00482a	Roots	DCM	20	11	0	0	37	0	22	0
***Leonotis ocymifolia* var. *ocymifolia* (Burm.f.) Iwarsson**	Lamiaceae	P00482b	Roots	DCM/MeOH (1:1)	14	5	0	0	5	0	9	0
***Leucas martinicensis* (L.) R.Br.**	Lamiaceae	P12950b	Whole plant	DCM/MeOH(1:1)	91	19	4	12	53	12	84	10
***Leucas martinicensis* (L.) R.Br.**	Lamiaceae	P12950c	whole plant	Aqueous	9	6	6	8	30	20	2	0
***Macrostylis squarrosa* Bartl. & H.L. Wendl.**	Rutaceae	P02402b	Stem bark	DCM/MeOH (1:1)	8	7	0	0	41	0	79	13
***Maesa lanceolata* Forssk.**	Maesaceae	P12946c	Twigs	Aqueous	0	0	8	6	27	19	6	4
***Maytenus senegalensis* (Lam.) Exell.**	Celastraceae	P00690a	Roots	DCM	14	2	0	0	28	8	35	0
Maytenus senegalensis (Lam.) Exell.	Celastraceae	P00693a	Stem bark	DCM	0	6	0	0	24	0	25	1
Maytenus senegalensis (Lam.) Exell.	Celastraceae	P00693b	Stem bark	DCM/MeOH (1:1)	11	11	0	0	19	0	5	0
***Maytenus senegalensis* (Lam.) Exell.**	Celastraceae	P00693d	Stem bark	Aqueous	0	1	2	0	10	0	0	0
***Maytenus undata* (Thunb.) Blakelock**	Celastraceae	P00151b	Leaves	DCM/MeOH (1:1)	0	12	0	0	46	5	24	18
***Maytenus undata* (Thunb.) Blakelock**	Celastraceae	P00152a	Stem bark	DCM	18	13	3	0	83	17	26	5
***Maytenus undata* (Thunb.) Blakelock**	Celastraceae	P00152b	Stem bark	DCM/MeOH (1:1)	0	2	0	0	54	10	11	6
***Maytenus undata* (Thunb.) Blakelock**	Celastraceae	P00153a	Roots	DCM	1	6	0	0	99	30	42	0
***Maytenus undata* (Thunb.) Blakelock**	Celastraceae	P00153b	Roots	DCM/MeOH (1:1)	6	7	0	0	82	16	17	0
***Maytenus undata* (Thunb.) Blakelock**	Celastraceae	P00153c	Roots	MeOH	0	2	0	0	29	2	5	0
***Maytenus undata* (Thunb.) Blakelock**	Celastraceae	P00151c	Leaves	MeOH	4	7	0	0	19	4	14	9

Plant species	Family	Project number	Plant part	Solvent	*T. brucei rhodesiense*		*T. cruzi*		*L. donovani*		*P. falciparum*	
					% inhibition (9.7 µg/mL)	% inhibition (1.8 µg/mL)	% inhibition (9.7 µg/mL)	% inhibition (1.8 µg/mL)	% inhibition (9.7 µg/mL)	% inhibition (1.8 µg/mL)	% inhibition (9.7 µg/mL)	% inhibition (1.8 µg/mL)
***Maytenus undata* (Thunb.) Blakelock**	Celastraceae	P00152c	Stem bark	MeOH	0	2	4	3	39	14	6	0
***Maytenus undata* (Thunb.) Blakelock**	Celastraceae	P00151a	Leaves	DCM	3	9	0	0	41	0	8	0
***Maytenus undata* (Thunb.) Blakelock**	Celastraceae	P00151d	Leaves	Aqueous	3	0	9	9	17	0	0	0
***Maytenus undata* (Thunb.) Blakelock**	Celastraceae	P00152d	Stem bark	Aqueous	0	0	13	3	16	11	0	0
***Maytenus undata* (Thunb.) Blakelock**	Celastraceae	P00153d	Roots	Aqueous	9	0	14	4	20	13	0	0
***Momordica balsamina* L.**	Cucurbitaceae	P04038b	Stem bark	DCM/MeOH (1:1)	2	1	0	0	34	3	83	17
***Momordica balsamina* L.**	Cucurbitaceae	P04039b	Leaves	DCM/MeOH (1:1)	21	23	0	0	49	8	65	5
Ocimum americanum* L. var. *Americanum	Lamiaceae	P12866b	Whole plant	DCM/MeOH(1:1)	0	4	0	0	30	2	100	0
***Olea europaea* L. subsp. *africana* (Mill.) P.S.Green**	Oleaceae	P12848b	Leaves	DCM/MeOH(1:1)	55	0	15	6	52	8	46	0
***Olea europaea* L. subsp. *africana* (Mill.) P.S.Green**	Oleaceae	P12849b	Twigs	DCM/MeOH(1:1)	46	0	10	4	44	13	50	0
***Osteospermum imbricatum* L.**	Asteraceae	P02640b	Stem bark	DCM/MeOH (1:1)	7	13	3	2	51	3	93	3
***Parinari curatellifolia* Planch. ex Benth.**	Chrysobalanaceae	P00253a	Leaves	DCM	0	3	0	0	67	22	53	0
***Parinari curatellifolia* Planch. ex Benth.**	Chrysobalanaceae	P00253b	Leaves	DCM/MeOH (1:1)	19	5	0	0	26	0	9	0
***Parinari curatellifolia* Planch. ex Benth.**	Chrysobalanaceae	P00253c	Leaves	MeOH	0	1	0	0	11	0	0	0
***Parinari curatellifolia* Planch. ex Benth.**	Chrysobalanaceae	P00253d	Leaves	Aqueous	0	8	0	0	17	7	3	0
***Parinari curatellifolia* Planch. ex Benth.**	Chrysobalanaceae	P00254b	Roots	DCM/MeOH (1:1)	0	12	0	0	27	11	23	0
***Parinari curatellifolia* Planch. ex Benth.**	Chrysobalanaceae	P00254c	Roots	MeOH	14	8	0	0	23	14	12	0
***Parinari curatellifolia* Planch. ex Benth.**	Chrysobalanaceae	P00254d	Roots	Aqueous	9	7	0	0	14	2	0	2
***Parkinsonia aculeata* L.**	Fabaceae	P09990b	Twigs	DCM/MeOH(1:1)	6	2	0	3	26	3	32	0
***Pelargonium alchemilloides* (L.) L'Hér.**	Gentianaceae	P08205b	Whole plant	DCM/MeOH(1:1)	7	11	0	0	33	8	87	10
***Pentzia globosa* Less.**	Asteraceae	P01514a	Leaves	DCM	91	0	7	0	84	2	63	8
***Pentzia globosa* Less.**	Asteraceae	P01514b	Leaves	DCM/MeOH (1:1)	0	0	0	3	26	0	39	0
***Pentzia globosa* Less.**	Asteraceae	P01514c	Leaves	Aqueous	9	0	2	0	25	4	6	15
***Pentzia globosa* Less.**	Asteraceae	P01516a	Roots	DCM	99	7	10	9	63	18	96	21
***Pentzia globosa* Less.**	Asteraceae	P01516b	Roots	DCM/MeOH (1:1)	98	3	4	1	36	0	62	7
***Pentzia globosa* Less.**	Asteraceae	P01517a	Stem bark	DCM	99	0	8	0	34	12	76	5
***Pentzia globosa* Less.**	Asteraceae	P01517b	Stem bark	DCM/MeOH (1:1)	100	0	0	0	16	0	30	0
***Piliostigma thonningii* (Schumach.) Milne-Redh**	Fabaceae	P18548c	Fruits	Aqueous	17	3	1	0	20	5	0	0

Plant species	Family	Project number	Plant part	Solvent	*T. brucei rhodesiense*		*T. cruzi*		*L. donovani*		*P. falciparum*	
					% inhibition (9.7 µg/mL)	% inhibition (1.8 µg/mL)	% inhibition (9.7 µg/mL)	% inhibition (1.8 µg/mL)	% inhibition (9.7 µg/mL)	% inhibition (1.8 µg/mL)	% inhibition (9.7 µg/mL)	% inhibition (1.8 µg/mL)
***Piliostigma thonningii* (Schumach.) Milne-Redh**	Fabaceae	P18547c	Leaves	Aqueous	24	27	0	0	21	8	6	0
***Piliostigma thonningii* (Schumach.) Milne-Redh**	Fabaceae	P18549c	Twigs	Aqueous	19	6	4	0	22	3	0	0
***Pittosporum viridiflorum* Sims**	Pittosporaceae	P00213b	Whole plant	DCM/MeOH (1:1)	50	11	0	0	29	11	59	3
***Pittosporum viridiflorum* Sims**	Pittosporaceae	P00213c	Whole plant	MeOH	0	4	0	2	15	9	15	0
***Pittosporum viridiflorum* Sims**	Pittosporaceae	P00215a	Leaves	DCM	7	5	0	0	31	7	25	3
***Pittosporum viridiflorum* Sims**	Pittosporaceae	P00215b	Leaves	DCM/MeOH (1:1)	1	0	0	0	4	0	0	0
***Pittosporum viridiflorum* Sims**	Pittosporaceae	P00215c	Leaves	MeOH	0	5	0	0	23	9	0	0
***Plantago major* L.**	Plantaginaceae	P01571b	Whole plant	DCM/MeOH (1:1)	0	0	0	0	18	5	16	1
***Plumbago zeylanica* L.**	Plumbaginaceae	P00630a	Roots	DCM	20	19	0	0	20	0	16	0
***Plumbago zeylanica* L.**	Plumbaginaceae	P00630b	Roots	DCM/MeOH (1:1)	11	9	0	0	8	0	19	0
***Plumbago zeylanica* L.**	Plumbaginaceae	P00630c	Roots	MeOH	19	9	0	0	12	0	0	10
***Plumbago zeylanica* L.**	Plumbaginaceae	P00631b	Leaves	DCM/MeOH (1:1)	97	8	0	0	32	2	32	8
***Pollichia campestris* Aiton**	Illecebraceae	P00390b	Leaves	DCM/MeOH (1:1)	0	8	6	3	25	3	23	0
***Pollichia campestris* Aiton**	Illecebraceae	P00390c	Leaves	MeOH	18	9	0	0	18	6	0	0
***Pollichia campestris* Aiton**	Illecebraceae	P00391a	Fruits	DCM	4	0	0	0	42	6	58	0
***Pollichia campestris* Aiton**	Illecebraceae	P00391b	Fruits	DCM/MeOH (1:1)	4	8	0	0	22	6	7	0
***Pollichia campestris* Aiton**	Illecebraceae	P00391c	Leaves	MeOH	13	16	0	0	27	2	3	0
***Pollichia campestris* Aiton**	Illecebraceae	P03065b	Whole plant	DCM/MeOH (1:1)	9	10	0	0	51	0	84	8
***Pollichia campestris* Aiton**	Illecebraceae	P00390d	Leaves	Aqueous	0	0	0	0	16	6	0	0
***Pollichia campestris* Aiton**	Illecebraceae	P03065c	whole plant	Aqueous	0	0	0	0	15	0	0	0
***Pollichia campestris* Aiton**	Illecebraceae	P03318c	Twigs	Aqueous	19	0	0	1	17	2	0	0
***Psiadia punctulata* (DC.) Oliv. & Hiern ex Vatke**	Asteraceae	P00819b	Leaves	DCM/MeOH (1:1)	19	3	0	0	48	8	35	4
***Psiadia punctulata* (DC.) Oliv. & Hiern ex Vatke**	Asteraceae	P02527b	Whole plant	DCM/MeOH (1:1)	24	0	10	4	48	8	49	0
***Ptaeroxylon obliquum* (Thunb.) Radlk.**	Ptaeroxylaceae	P01842a	Roots	DCM	10	13	9	5	35	1	44	1
***Ptaeroxylon obliquum* (Thunb.) Radlk.**	Ptaeroxylaceae	P01842b	Roots	DCM/MeOH (1:1)	5	12	10	0	45	12	57	4
***Ptaeroxylon obliquum* (Thunb.) Radlk.**	Ptaeroxylaceae	P01870a	Leaves	DCM	100	0	0	0	55	5	41	5
***Ptaeroxylon obliquum* (Thunb.) Radlk.**	Ptaeroxylaceae	P01870b	Leaves	DCM/MeOH (1:1)	0	0	0	0	19	2	24	0
***Ptaeroxylon obliquum* (Thunb.) Radlk.**	Ptaeroxylaceae	P01890a	Stem bark	DCM	10	0	0	0	53	1	80	17

Plant species	Family	Project number	Plant part	Solvent	*T. brucei rhodesiense*		*T. cruzi*		*L. donovani*		*P. falciparum*	
					% inhibition (9.7 µg/mL)	% inhibition (1.8 µg/mL)	% inhibition (9.7 µg/mL)	% inhibition (1.8 µg/mL)	% inhibition (9.7 µg/mL)	% inhibition (1.8 µg/mL)	% inhibition (9.7 µg/mL)	% inhibition (1.8 µg/mL)
***Ptaeroxylon obliquum* (Thunb.) Radlk.**	Ptaeroxylaceae	P01890b	Stem bark	DCM/MeOH (1:1)	30	5	0	0	40	4	65	13
***Pterocarpus angolensis* DC.**	Fabaceae	P00304b	Stem bark	DCM/MeOH (1:1)	0	7	0	0	17	9	0	0
***Pterocarpus angolensis* DC.**	Fabaceae	P00304c	Stem bark	MeOH	7	6	0	0	16	6	1	1
***Pterocarpus angolensis* DC.**	Fabaceae	P00305b	Roots	DCM/MeOH (1:1)	18	0	0	0	21	5	17	0
***Pterocarpus angolensis* DC.**	Fabaceae	P00305c	Roots	MeOH	16	2	0	0	12	0	0	0
***Rauvolfia caffra* Sond.**	Apocynaceae	P00734a	Roots	DCM	100	8	0	3	3	0	45	0
***Rauvolfia caffra* Sond.**	Apocynaceae	P00734b	Fruits	DCM/MeOH (1:1)	5	9	0	0	24	1	20	4
***Rauvolfia caffra* Sond.**	Apocynaceae	P00735b	Roots	DCM/MeOH (1:1)	6	0	0	0	15	1	10	0
***Rauvolfia caffra* Sond.**	Apocynaceae	P00735d	Roots	Aqueous	6	7	0	0	13	0	0	0
***Rauvolfia caffra* Sond.**	Apocynaceae	P00735a	Fruits	DCM	13	16	0	1	20	8	15	0
Ricinus communis* L. var. *communis	Euphorbiaceae	P02300b	Leaves	DCM/MeOH (1:1)	0	4	0	0	63	1	56	10
Ricinus communis* L. var. *communis	Euphorbiaceae	P02311b	Fruits	DCM/MeOH (1:1)	5	1	0	0	7	0	13	0
***Ricinus communis* L. var. communis**	Euphorbiaceae	P02355b	Stem bark	DCM/MeOH (1:1)	0	0	0	0	46	0	79	14
Ricinus communis* L. var. *communis	Euphorbiaceae	P02300c	Leaves	Aqueous	7	2	11	1	35	22	2	7
Ricinus communis* L. var. *communis	Euphorbiaceae	P02311c	Fruits	Aqueous	8	5	10	0	40	27	7	0
Ricinus communis* L. var. *communis	Euphorbiaceae	P02355c	Stem bark	Aqueous	5	10	0	0	38	28	7	0
***Rumex crispus* L.**	Polygonaceae	P01689b	Roots	DCM/MeOH (1:1)	0	0	0	0	20	8	21	5
***Rumex crispus* L.**	Polygonaceae	P01634a	Leaves	DCM	2	0	0	0	12	4	10	2
***Rumex crispus* L.**	Polygonaceae	P01634b	Leaves	DCM/MeOH (1:1)	0	4	0	0	19	0	0	0
***Rumex crispus* L.**	Polygonaceae	P01689a	Roots	DCM	1	4	0	0	28	5	55	5
***Rumex sagittatus* Thunb.**	Polygonaceae	P12875b	Whole plant	DCM/MeOH(1:1)	7	0	4	0	19	4	38	0
***Salvia repens* Burch. ex Benth.**	Lamiaceae	P08214b	Whole plant	DCM/MeOH(1:1)	21	7	3	1	101	35	63	2
***Scaevola plumieri* (L.) Vahl**	Goodeniaceae	P08206b	Twigs	DCM/MeOH(1:1)	7	10	0	1	27	5	22	0
***Schefflera umbellifera* (Sond.) Baill.**	Araliaceae	P00245b	Leaves	DCM/MeOH (1:1)	23	8	0	0	69	16	64	16
***Schefflera umbellifera* (Sond.) Baill.**	Araliaceae	P00245c	Leaves	MeOH	8	11	0	0	39	11	24	5
***Schefflera umbellifera* (Sond.) Baill.**	Araliaceae	P00246a	Roots	DCM	0	11	0	0	80	16	26	9
***Schefflera umbellifera* (Sond.) Baill.**	Araliaceae	P00246b	Roots	DCM/MeOH (1:1)	0	16	0	0	71	15	39	6
***Schefflera umbellifera* (Sond.) Baill.**	Araliaceae	P00248a	Stem bark	DCM	5	0	9	0	57	9	46	5

Plant species	Family	Project number	Plant part	Solvent	*T. brucei rhodesiense*		*T. cruzi*		*L. donovani*		*P. falciparum*	
					% inhibition (9.7 µg/mL)	% inhibition (1.8 µg/mL)	% inhibition (9.7 µg/mL)	% inhibition (1.8 µg/mL)	% inhibition (9.7 µg/mL)	% inhibition (1.8 µg/mL)	% inhibition (9.7 µg/mL)	% inhibition (1.8 µg/mL)
***Schefflera umbellifera* (Sond.) Baill.**	Araliaceae	P00248b	Stem bark	DCM/MeOH (1:1)	0	0	0	0	49	12	28	0
***Schefflera umbellifera* (Sond.) Baill.**	Araliaceae	P00248c	Stem bark	MeOH	10	6	0	0	28	6	3	0
***Schefflera umbellifera* (Sond.) Baill.**	Araliaceae	P00248d	Stem bark	Aqueous	13	15	9	10	17	9	0	0
***Senecio oxyriifolius* DC.**	Asteraceae	P08209b	Whole plant	DCM/MeOH(1:1)	0	7	9	0	32	10	51	6
***Senna didymobotrya* (Fresen.) Irwin & Barneby**	Fabaceae	P08219b	Leaves	DCM/MeOH(1:1)	13	0	0	3	31	1	36	3
***Senna didymobotrya* (Fresen.) Irwin & Barneby**	Fabaceae	P08220b	Twigs	DCM/MeOH(1:1)	22	17	0	0	39	5	54	10
***Senna didymobotrya* (Fresen.) Irwin & Barneby**	Fabaceae	P08221b	Pods	DCM/MeOH(1:1)	10	2	0	0	29	8	34	3
***Senna didymobotrya* (Fresen.) Irwin & Barneby**	Fabaceae	P08220c	Twigs	Aqueous	11	8	11	2	30	15	0	0
***Senna didymobotrya* (Fresen.) Irwin & Barneby**	Fabaceae	P08219c	Leaves	Aqueous	3	3	0	0	13	3	0	0
***Senna petersiana* (Bolle) Lock**	Fabaceae	P18564c	Leaves	Aqueous	2	0	3	4	28	23	0	1
***Senna petersiana* (Bolle) Lock**	Fabaceae	P18565c	Twigs	Aqueous	0	2	15	8	31	21	0	0
***Setaria megaphylla* (Steud.) T.Durand & Schinz**	Poaceae	P12880b	Whole plant	DCM/MeOH(1:1)	18	2	4	7	34	4	100	19
***Spilanthes mauritiana* (Pers.) DC.**	Asteraceae	P00274a	Stem bark	DCM	11	10	0	0	60	9	71	1
***Spilanthes mauritiana* (Pers.) DC.**	Asteraceae	P00274b	Stem bark	DCM/MeOH (1:1)	2	11	0	0	35	9	30	1
***Spilanthes mauritiana* (Pers.) DC.**	Asteraceae	P00274c	Stem bark	MeOH	4	0	0	0	17	1	0	0
Syzigium cordatum* Hochst. ex Sond. var. *cordatum	Myrtaceae	P18315c	Twigs	Aqueous	13	16	2	8	15	6	17	0
***Syzigium cordatum* Hochst. ex Sond. var. cordatum**	Myrtaceae	P18315b	Twigs	DCM/MeOH(1:1)	0	1	0	0	51	16	54	11
***Syzigium cordatum* Hochst. ex Sond. var. cordatum**	Myrtaceae	P18316b	Leaves	DCM/MeOH(1:1)	0	5	0	0	57	12	42	0
***Syzigium cordatum* Hochst. ex Sond. var. cordatum**	Myrtaceae	P18316c	Leaves	Aqueous	0	0	0	0	9	0	84	0
***Tarchonanthus camphoratus* L.**	Asteraceae	P01089a	Leaves	DCM	86	0	7	1	75	16	76	2
***Tarchonanthus camphoratus* L.**	Asteraceae	P01089b	Leaves	DCM/MeOH (1:1)	14	0	0	0	62	8	42	0
***Tarchonanthus camphoratus* L.**	Asteraceae	P01154b	Roots	DCM/MeOH (1:1)	95	0	0	0	52	1	18	4
***Tarchonanthus camphoratus* L.**	Asteraceae	P02554b	Whole plant	DCM/MeOH (1:1)	99	64	6	1	100	25	49	0
***Tetradenia riparia* (Hochst.) Codd**	Lamiaceae	P00741a	Leaves	DCM	0	0	0	2	36	0	38	0
***Tetradenia riparia* (Hochst.) Codd**	Lamiaceae	P00741b	Leaves	DCM/MeOH(1:1)	6	0	2	2	16	0	7	7
***Tetradenia riparia* (Hochst.) Codd**	Lamiaceae	P00741d	Leaves	Aqueous	0	7	4	7	9	0	0	0
Trichilia emetica* Vahl subsp. *emetica	Meliaceace	P02470c	Twigs/Leaves	Aqueous	13	6	0	0	15	7	1	0
***Turraea floribunda* Hochst.**	Meliaceace	P15192c	Leaves	Aqueous	24	27	0	2	21	5	1	4

Plant species	Family	Project number	Plant part	Solvent	*T. brucei rhodesiense*		*T. cruzi*		*L. donovani*		*P. falciparum*	
					% inhibition (9.7 µg/mL)	% inhibition (1.8 µg/mL)	% inhibition (9.7 µg/mL)	% inhibition (1.8 µg/mL)	% inhibition (9.7 µg/mL)	% inhibition (1.8 µg/mL)	% inhibition (9.7 µg/mL)	% inhibition (1.8 µg/mL)
Vangueria infausta* Burch. subsp. *infausta	Rubiaceae	P02497b	Fruits	DCM/MeOH (1:1)	3	4	0	0	33	0	33	0
Vernonia colorata* (Willd.) Drake subsp. *colorata	Asteraceae	P18569c	Twigs	Aqueous	0	6	6	8	29	19	1	0
***Vernonia fastigiata* Oliv. & Hiern**	Asteraceae	P00393b	Leaves	DCM/MeOH (1:1)	58	4	0	0	29	0	30	0
***Vernonia fastigiata* Oliv. & Hiern**	Asteraceae	P00393c	Leaves	MeOH	10	11	0	0	24	8	21	0
***Vernonia hirsuta* (DC.) Sch.Bip. Ex Walp.**	Asteraceae	P02834b	Whole plant	DCM/MeOH (1:1)	99	5	0	0	81	6	46	0
***Vernonia myriantha* Hook.f.**	Asteraceae	P00170a	Roots	DCM	0	0	0	0	19	0	21	0
***Vernonia myriantha* Hook.f.**	Asteraceae	P00170b	Roots	DCM/MeOH (1:1)	6	15	0	0	31	10	16	5
***Vernonia myriantha* Hook.f.**	Asteraceae	P00170d	Roots	Aqueous	7	8	0	0	17	6	16	8
***Vernonia myriantha* Hook.f.**	Asteraceae	P00171a	Leaves	DCM	5	10	0	0	34	10	35	1
***Vernonia myriantha* Hook.f.**	Asteraceae	P00171b	Leaves	DCM/MeOH (1:1)	6	10	0	0	23	9	11	0
***Vernonia myriantha* Hook.f.**	Asteraceae	P00170c	Roots	MeOH	10	0	0	0	22	4	0	0
***Vernonia natalensis* Sch.Bip. ex Walp.**	Asteraceae	P08212b	Whole plant	DCM/MeOH(1:1)	100	5	1	2	46	8	57	10
***Vernonia oligocephala* (DC.) Sch.Bip. ex Walp.**	Asteraceae	P00989b	Roots	DCM/MeOH (1:1)	0	0	3	0	13	1	24	0
***Vernonia oligocephala* (DC.) Sch.Bip. ex Walp.**	Asteraceae	P01015a	Leaves	DCM	99	78	23	0	60	4	89	11
***Vernonia oligocephala* (DC.) Sch.Bip. ex Walp.**	Asteraceae	P01015b	Leaves	DCM/MeOH (1:1)	99	0	0	0	21	6	29	0
Ximenia caffra* Sond. var. *caffra	Olacaceae	P00351a	Leaves	DCM	0	7	0	0	31	6	12	0
Ximenia caffra* Sond. var. *caffra	Olacaceae	P00351b	Leaves	DCM/MeOH (1:1)	0	7	0	0	16	10	6	0
Ximenia caffra* Sond. var. *caffra	Olacaceae	P00351d	Leaves	Aqueous	8	11	5	4	17	0	0	0
***Ximenia caffra* Sond. var. caffra**	Olacaceae	P00352a	Roots	DCM	5	12	0	0	21	4	1	0
***Ximenia caffra* Sond. var. caffra**	Olacaceae	P00352b	Roots	DCM/MeOH(1:1)	1	2	0	0	16	8	0	0
***Ximenia caffra* Sond. var. caffra**	Olacaceae	P00352c	Roots	MeOH	1	7	0	0	19	4	0	0
***Xysmalobium undulatum* (L.) Aiton.f.**	Apocynaceae	P12869b	Whole plant	DCM/MeOH(1:1)	8	10	0	0	30	0	28	0
Zehneria scabra* (L.f.) Sond. subsp. *scabra	Cucurbitaceae	P08210b	Whole plant	DCM/MeOH(1:1)	5	8	9	6	22	0	21	5
Zehneria scabra* (L.f.) Sond. subsp. *scabra	Cucurbitaceae	P08210c	whole plant	Aqueous	28	0	0	4	17	13	0	4

3.2 Antiprotozoal Screening of 60 South African Plants, and the Identification of the Antitrypanosomal Germacranolides Schkuhrin I and II

Tsholofelo Mokoka, Peter K. Xolani, Stefanie Zimmermann, **Yoshie Hata**, Michael Adams, Marcel Kaiser, Nivan Moodley, Vinesh Maharaj, Neil A. Koorbanally, Matthias Hamburger, Reto Brun, Gerda Fouche

Planta Med., 2013, 79: 1380–1384. DOI: 10.1055/s-0033-1350691

Two hundred and seven extracts from 59 South African plant species (27 botanical families) with antiparasitic traditional use were tested against a panel of 4 parasites (*Plasmodium falciparum, Trypanosoma brucei rhodesiense, Leishmania donovani,* and *Trypanosoma cruzi*). The 10 most active plants were selected, among them *S. pinnata* and *V. mespilifolia*. The identification of the active compounds from these species was achieved with the aid of HPLC-based activity profiling.

My contributions to this work were: (1) HPLC microfractionation of 10 extract from 5 species; (2) recording and interpretation of analytical data for the 18 HPLC-activity profiles, obtained for the different parasites P. falciparum, T. b. rhodesiense, and/or L. donovani; (3) dereplication of the known constituents of the active fractions; (4) participation in drafting the paper.

Tsholofelo Mokoka performed the HPLC-activity profiling of additional 10 extracts, achieved the isolation of schkuhrin I, II, and cynaropicrin and wrote the first draft of the paper. The antiprotozoal activity of the extracts and HPLC fractions was assessed at the Swiss TPH. Extracts were provided by the CSIR team.

Yoshie Hata-Uribe

Antiprotozoal Screening of 60 South African Plants, and the Identification of the Antitrypanosomal Germacranolides Schkuhrin I and II

Authors Tsholofelo A. Mokoka[1], Peter. K. Xolani[1], Stefanie Zimmermann[2,3], Yoshie Hata[2,4], Michael Adams[2], Marcel Kaiser[3], Nivan Moodley[1,6], Vinesh Maharaj[1], Neil A. Koorbanally[5], Matthias Hamburger[2], Reto Brun[3], Gerda Fouche[1]

Affiliations The affiliations are listed at the end of the article

Key words
- screening
- plant extract library
- antiprotozoal activity
- sesquiterpene lactones
- *Trypansoma brucei rhodesiense*
- *Trypanosoma cruzi*
- *Leishmania donovani*
- *Plasmodium falciparum*
- *Psoralea pinnata* (Fabaceae)
- *Schkuhria pinnata* (Asteraceae)
- *Vernonia mespilifolia* (Asteraceae)

received June 3, 2013
revised June 18, 2013
accepted July 1, 2013

Bibliography
DOI http://dx.doi.org/10.1055/s-0033-1350691
Published online August 8, 2013
Planta Med 2013; 79: 1380–1384 © Georg Thieme Verlag KG Stuttgart · New York · ISSN 0032-0943

Correspondence
Dr. Gerda Fouche
Natural Product Chemistry, Biosciences
Council for Scientific and Industrial Research (CSIR)
PO Box 395
Pretoria 0001
South Africa
Phone: + 27 1 28 41 38 15
Fax: + 27 1 23 49 47 90
gfouche@csir.co.za

Correspondence
Prof. Matthias Hamburger
Department of Pharmaceutical Sciences
University of Basel, Basel
Klingelbergstrasse 50
4056 Basel
Switzerland
Phone: + 41 6 12 67 14 25

Abstract

Two hundred and seven extracts were prepared from sixty plants from South Africa and screened for *in vitro* activity against *Trypanosoma brucei rhodesiense, Trypanosoma cruzi, Leishmania donovani*, and *Plasmodium falciparum*. For the 21 extracts which inhibited the growth of one or more parasites with more than 95% at 10 µg/mL, the IC_{50} values against all four protozoal parasites and cytotoxic IC_{50} values against L6 myoblasts were determined. Amongst the most notable results are the activities of *Psoralea pinnata* (IC_{50} of 0.15 µg/mL), *Schkuhria pinnata* (2.04 µg/mL), and *Vernonia mespilifolia* (1.01 µg/mL) against *Trypansoma brucei rhodesiense.* HPLC-based activity profiling was used to identify the active constituents in the extracts, and the germacranolide sesquiterpene lactones schkuhrin I and II from *S. pinnata*, and cynaropicrin from *V. mespilifolia* were identified, with IC_{50} values of 0.9, 1.5, and 0.23 µM, respectively.

Supporting information available online at http://www.thieme-connect.de/ejournals/toc/plantamedica

Introduction

Neglected tropical diseases (NTDs) caused by *Leishmania* species (leishmaniasis), *Trypanosoma brucei* (sleeping sickness), and *Trypanosoma cruzi* (Chagas disease) are life-threatening and represent a risk to large parts of the populations in poor tropical countries. These diseases affect about 21 million people worldwide, mostly in economically challenged regions [1]. It is estimated that these three diseases are responsible for over 110 000 deaths every year [2]. In addition, malaria caused by *Plasmodium* species was responsible for approximately 216 million infections and over 655 000 deaths in 2010 [3]. The control of these parasitic infections relies on a few chemotherapeutic agents, most of which were discovered many decades ago [4] and pose many challenges due to adverse side effects, long treatment cycles, poor efficacy, high costs, the occurrence of drug resistances, and limited availability [1]. Therefore, the discovery of novel, safe, and effective antiprotozoal agents is an urgent need.

Natural products play a significant role in the discovery of new drug leads because of the unmatched availability of chemical diversity. We previously reported a screen of 300 extracts from plants traditionally used to treat malaria and their antiprotozoal effects against *L. donovani, T. b. rhodesiense, P. falciparum*, and *T. cruzi in vitro* [5]. This work is a continuation of the project, where 207 further extracts have been tested. Furthermore, we report the identification of three antitrypanosomal sesquiterpene lactones from the most active extracts, which were identified by HPLC-based activity profiling [6].

Results and Discussion

A total of 207 plants extracts from 60 plant species were assessed for antiprotozoal activity against four protozoan parasites at 10 and 2 µg/mL, respectively (**Table S1** in the Supporting Information). The most active extracts from the preliminary screening were subjected to IC_{50} value determination. Extracts which exhibited an IC_{50} value ≤ 5.0 µg/mL were considered active and were subjected to HPLC-based activity profiling to identify potential antiprotozoal compounds. The lipophilic extracts of *Psoralea pinnata* (Fabaceae) and *Drypetes gerrardii* (Euphorbiaceae) exhibited very good antiprotozoal activity

against *T. b. rhodesiense* (IC_{50}, 0.15 ± 0.02 and 0.31 ± 0.02 µg/mL) and *P. falciparum* (IC_{50}, 0.50 ± 0.23 µg/mL), respectively (**Table 1**). In addition, these extracts showed the best selectivity index values ranging between 97 and 139, indicating their selectivity towards killing the parasites with very little toxicity towards the myoblasts L-6 cells. *Vernonia mespilifolia* Less. (Asteraceae), *Oedera genistifolia* (Asteraceae), *Abrus precatorius africanus* (Fabaceae), and *Ekebergia capensis* (Meliaceae) also exhibited IC_{50} values ranging between 1.0 and 1.7 µg/mL against *T. b. rhodesiense* and *L. donovani*, however, with moderate selectivity indices ranging from 24 to 48.

The active extracts of *Psoralea pinnata, Schkuhria pinnata* (Asteraceae), and *Vernonia mespilifolia* (Asteraceae) were further studied to identify their active constituents. For the purpose of this study, we report the identification of active compounds from *S. pinnata* and *V. mespilifolia* with the aid of an HPLC-based activity profiling technique. However, the identification of active constituents from *P. pinnata* will be reported in a separate publication.

The one minute microfractions from the active DCM/MeOH extract from *Schkuhria pinnata* were tested against *T. b. rhodesiense,* and it was shown that the activity was concentrated in the active time windows of minutes 14 and 16 (**Fig. 1**), which showed 100% inhibition. These fractions both contained one main substance, which was isolated by semipreparative HPLC and structurally elucidated by NMR, high-resolution MS, and comparison of spectral data to the literature [7]. The compound from fraction 14 was shown to be schkuhrin I (**1**) and the one from fraction 16 was schkuhrin II (**2**) (**Fig. 3**). The two structurally similar germacranolides showed antiprotozoal activity against *T. b. rhodesiense* with IC_{50} values of 0.86 and 1.50 µM, respectively, and antiplasmodial activity with IC_{50} values of 2.05 and 1.67 µM, respectively (**Table 2**).

The HPLC activity profile of the DCM/MeOH extract of *V. mespilifolia* showed significant antiprotozoal activity in fractions 12 and 13 against *T. b. rhodesiense* (**Fig. 2**). The compound was isolated, and, by use of NMR, high-resolution MS, and comparison to literature data [8], identified as the known sesquiterpene lactone cynaropicrin (**3**) (**Fig. 3**). The IC_{50}s of **3** were 0.23 µM against *T. b. rhodesiense* and 1.56 µM against *P. falciparum. L. donovani* exhibited an IC_{50} value of 1.56 µM, whereas *T. cruzi* was the least susceptible parasite with an IC_{50} value of 5.14 µM.

This study is a continuation of our efforts of collecting and screening South African plants against protozoan parasites [5]. The results of a large screen of 207 extracts are shown (Supporting Information **Table S1**). Furthermore, by using HPLC-based activity profiling, the sesquiterpene lactones schkuhrin I (**1**) and II (**2**) from *Schkuhria pinnata*, and cynaropicrin (**3**) from *Vernonia mespilifolia*, were identified as potent antiprotozoal agents. The powdered leaf of *S. pinnata* has been used as a remedy for malaria, influenza, and colds [9]. Also, *S. pinnata* has been used as an insecticide, particularly to kill fleas [11]. Extracts from *S. pinnata* were shown to inhibit *Brucella abortus in vitro* [10], and have yielded several sesquiterpene lactones and the phenyl propanoids [11]. Both schkuhrin I (**1**) and II (**2**) have been isolated from the same species and other *Schkuhria* species, but their antiprotozoal activities have not been reported previously.

Some of the species belonging to the genus *Vernonia* have been used in folk medicine to treat malaria [12]. *V. mespilifolia* Less. is used traditionally by Zulus to treat malaria-related feverish conditions [13].

Sesquiterpenes are the largest known group of natural products [14] and are a chemical marker for the largest plant family, the Asteraceae [15]. Numerous sesquiterpene lactones have been tested for antiprotozoal activity *in vitro*. Schmidt et al. [16] showed in an antitrypanosomal-QSAR study of 40 STLs and, in 2012, supplied two excellent reviews of antiprotozoal *in vitro* effects of 883 plant-derived natural products including 83 sesquiterpene lactones [14, 16]. This study is the first report of the antiprotozoal effects of **1** and **2**, whereas the antitrypansomal effects of **3** have already been described by Zimmermann et al. [17]. In fact, **3** was the first and so far only plant-derived compound to inhibit *T. b. rhodesienese in vivo*. The mode of action of **3** was shown to be its ability to form stable bis-adducts with trypanothione via a Michael addition, thus depleting the parasites of their only means of redox control [18].

With this screening study we report recent *in vitro* results of a plant extract screen. This may provide a basis for selecting plants in the future for further phytochemical and bioactivity studies. Furthermore, we report the *in vitro* antiprotozoal effects of three compounds, which will contribute to a better understanding of sesquiterpene lactones antiprotozoal structure-activity relationships.

Materials and Methods

Plant collection and identification

Sixty plant species were collected between 1996 and 2002 at a variety of locations in South Africa. The selected plant species were based on their traditional uses against parasitic diseases (unpublished work). The species were identified by personnel of the South African National Biodiversity Institute (SANBI) where the voucher specimens were deposited (**Table S1** in the Supporting Information).

Plant extract preparations

The plant parts (roots, leaves, twigs, fruit, and stem bark) were dried in an oven at 30–60 °C, and extracts from finely ground plant parts were prepared as previously described [5]. Stock solutions were prepared at 10 mg/mL in DMSO and stored at − 80 °C until use. Dilutions for biological testing were freshly prepared in culture medium on the day of testing (< 1% DMSO).

Isolation and purification of active compounds 1, 2, and 3

For compounds **1, 2**, and **3**, semipreparative HPLC purification was performed using an Agilent HPLC 1200 series consisting of a low-pressure mixing pump with a degasser module, column oven, and PDA detector (Agilent). The extracts of the whole plant of *Schkuhria pinnata* (Lam.) Cabrera and *Vernonia mespilifolia* Less. (100 mg/mL in DMSO, respectively) were prepared by dissolving 1.0 g of DCM/MeOH (1 : 1) extract, filtered through 0.45 µm Millipore membrane filters. Several repetitions of 200 µL injections were made. The separation was performed on a Waters Sunfire RP-18 column (10 × 150 mm i. d.; 10 µm; Waters GmbH). The mobile system used was made up of water (A) and acetonitrile (B). The elution gradient was linear from A : B (90 : 10) to (0 : 100) in 30 min at a flow rate of 6.0 mL/min, followed by 5 min of acetonitrile washing, and returned to the initial elution conditions (90 : 10) over 5 min. The separation of all components was detected at a wavelength of 254 nm.

Table 1 The IC_{50} values ± standard deviation (µg/mL), selectivity index, and cytotoxicity of 18 South African plant species against *Trypanosoma brucei rhodesiense*, *Trypanosoma cruzi*, *Leishmania donovani*, *Plasmodium falciparum*, and myoblast L6 cells. The positive controls melarsoprol[a], benznidazole[b], miltefosine[c], chloroquine[d], and podophyllotoxin[e] were tested likewise. Tests were done twice in duplicate.

				T. b. rhodesiense		*T. cruzi*		*L. donovani*		*P. falciparum* (NF-54 strain)		Cytotoxicity (L6-cells)
Family	**Plant species**	**Plant part**	**Extract type**	**IC_{50}**	**SI**	**IC_{50}**	**SI**	**IC_{50}**	**SI**	**IC_{50}**	**SI**	**IC_{50}**
Sapindaceae	*Pappea capensis* Eckl. & Zeyh.	Roots	DCM	15.40 ± 1.84	2.43					10.10 ± 2.79	3.70	37.40 ± 22.42
Anacardiaceae	*Ozoroa sphaerocarpa* R. Fern. & A. Fern.	Whole plant	DCM	10.90 ± 7.09	4.76			5.78 ± 0.25	8.98	12.90 ± 7.42	4.02	51.90 ± 3.75
Fabaceae	*Acacia erioloba* E.Mey	Roots	DCM/MeOH (1 : 1)			18.50 ± 11.29	3.01			10.70 ± 2.74	5.21	55.70 ± 7.92
Fabaceae	*Psoralea pinnata* L.	Leaves	DCM	0.15 ± 0.02	97.32			5.08 ± 0.11	2.85	8.46 ± 5.03	1.71	14.50 ± 2.83
Fabaceae	*Psoralea pinnata* L.	Leaves	DCM/MeOH (1 : 1)	0.31 ± 0.02	139.61			6.73 ± 0.16	6.39	9.18 ± 1.61	4.68	43.00 ± 14.64
Asteraceae	*Oedera genistifolia* (L.) Anderb. & K.Bremer	Whole plant	DCM/MeOH (1 : 1)	4.38 ± 1.87	11.16	31.40 ± 12.10	1.56	1.71 ± 0.02	28.60	2.88 ± 1.37	16.98	48.90 ± 9.55
Fabaceae	*Abrus precatorius* L. subsp. *africanus* Verdc.	Whole plant	DCM/MeOH (1 : 1)	1.04 ± 0.45	48.17			8.84 ± 0.11	5.67	3.39 ± 0.07	14.78	50.10 ± 2.05
Euphorbiaceae	*Clutia pulchella* L. var. *pulchella*	Roots	DCM/MeOH (1 : 1)							3.19 ± 0.94	28.21	90.00 ± 14.21
Euphorbiaceae	*Clutia pulchella* L. var. *pulchella*	Leaves & stems	DCM/MeOH (1 : 1)							14.10 ± 5.73	3.74	52.70 ± 1.20
Asteraceae	*Schkuhria pinnata* (Lam.) Kuntze ex Thell	Whole plant	DCM/MeOH (1 : 1)	2.04 ± 0.02	8.63	17.90 ± 10.02	0.98	10.80 ± 4.05	1.63	2.19 ± 0.48	8.04	17.60 ± 0.99
Rutaceae	*Clausena anisata* (Willd.) Hook.f. ex Benth. var. *anisata*	Roots	DCM/MeOH (1 : 1)	7.19 ± 0.95	3.59			11.50 ± 5.21	2.24	3.61 ± 1.82	7.15	25.80 ± 5.73
Meliaceae	*Ekebergia capensis* Sparrm.	Roots	DCM/MeOH (1 : 1)	1.36 ± 0.85	24.26	17.40 ± 2.78	1.90	6.42 ± 2.59	5.14	6.81 ± 3.92	4.85	33.00 ± 23.41
Meliaceae	*Turraea floribunda* Hochst.	Bark	DCM/MeOH (1 : 1)	24.40 ± 12.16	2.28					4.52 ± 0.53	12.32	55.70 ± 16.26
Meliaceae	*Turraea floribunda* Hochst.	Leaves	DCM/MeOH (1 : 1)	17.10 ± 1.06	2.82					12.70 ± 5.24	3.80	48.30 ± 6.58
Meliaceae	*Turraea floribunda* Hochst.	Roots	DCM/MeOH (1 : 1)	22.40 ± 6.58	2.36			13.10 ± 4.17	4.03	5.56 ± 2.91	9.50	52.80 ± 7.00
Meliaceae	*Drypetes gerrardii* Hutch. var. *gerrardii*	Stems	DCM/MeOH (1 : 1)	8.39 ± 5.54	6.05			7.31 ± 0.85	6.95	0.50 ± 0.23	101.20	50.80 ± 1.77
Meliaceae	*Drypetes gerrardii* Hutch. var. *gerrardii*	Leaves	DCM/MeOH (1 : 1)	12.10 ± 0.28	4.49					21.60 ± 0.64	2.51	54.30 ± 2.90
Asteraceae	*Helichrysum pedunculatum* Hilliard & B. L.Burtt	Whole plant	DCM/MeOH (1 : 1)					13.50 ± 2.90	4.29	6.46 ± 3.44	8.96	57.90 ± 11.17
Sapindaceae	*Pappea capensis* Eckl. & Zeyh.	Roots	DCM/MeOH (1 : 1)							5.30 ± 1.75	16.00	84.80 ± 21.57
Sapindaceae	*Pappea capensis* Eckl. & Zeyh.	Leaves	DCM/MeOH (1 : 1)	14.10 ± 4.24	5.43					9.67 ± 0.38	7.91	76.50 ± 33.16
Asteraceae	*Vernonia mespilifolia* Less.	Leaves	DCM/MeOH (1 : 1)	1.01 ± 0.31	14.65	8.76 ± 12.01	1.69	2.48 ± 0.33	5.97	5.09 ± 1.86	2.91	14.80 ± 3.25
	Standard drug			0.002 ± 0.000[a]		0.36 ± 0.09[b]		0.18 ± 0.02[c]		0.003 ± 0.000[d]		0.008 ± 0.000[e]

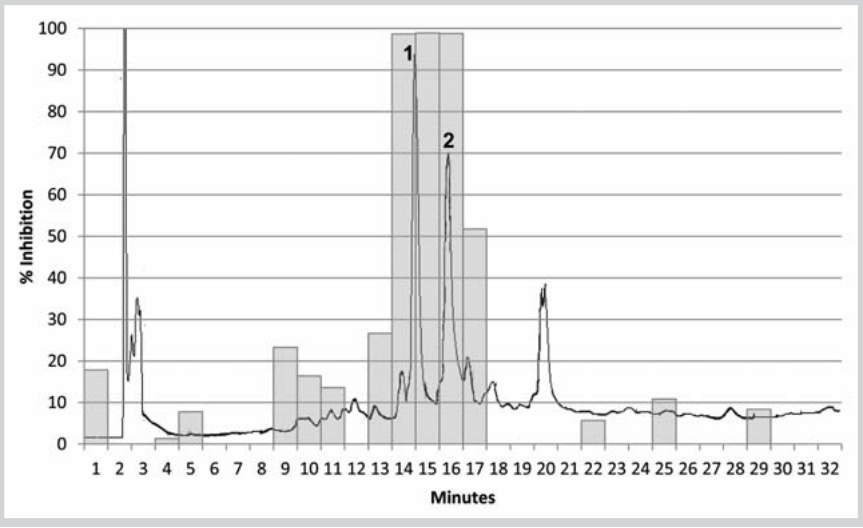

Fig. 1 HPLC-based activity profiling of *Schkuhria pinnata* organic extract against *T. b. rhodesiense*. The bar graphs show the inhibitory activity of individual HPLC fractions collected from a single separation of the crude extract. The HPLC chromatogram was measured at 254 nm.

Table 2 Antiprotozoal activity (IC_{50} values in μM) of schkuhrin I (**1**), schkuhrin II (**2**), and cynaropicrin (**3**) against *T. b. rhodesiense*, *T. cruzi*, *L. donovani*, and *P. falciparum*.

	T. b. rhodesiense		*T. cruzi*		*L. donovani*		*P. falciparum*		Cytotox. L6
	IC_{50}	SI	IC_{50}	SI	IC_{50}	SI	IC_{50}	SI	IC_{50}
Schkuhrin I (**1**)	0.86	6.12	16.40	0.32	39.00	0.13	2.05	2.57	5.26
Schkuhrin II (**2**)	1.50	6.02	26.96	0.33	65.00	0.14	1.67	5.41	9.03
Cynaropicrin (**3**)	0.23	5.61	5.14	0.25	1.56	0.83	1.56	0.83	1.29
Melarsoprol	0.01								
Benznidazole			2.25						
Miltefosine					0.47				
Chloroquine							0.015		
Podophyllotoxin									0.02

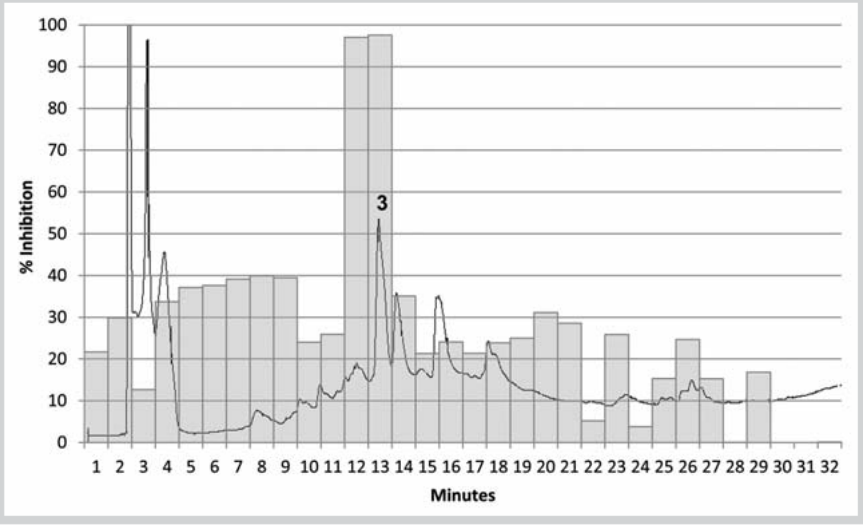

Fig. 2 HPLC-based activity profiling of *Vernonia mespilifolia* organic extract against *T. b. rhodesiense*. The bar graphs show the inhibitory activity of individual HPLC fractions collected from a single separation of the crude extract. The HPLC chromatogram was measured at 254 nm.

Biological assays

All extracts were screened as previously described [5] against *P. falciparum* (NF-54 strain), *T. b. rhodesiense* (STIB 900 strain), *T. cruzi* trypomastigote forms (Tulahuen strain), *and L. donovani* (strain MHOM/ET/67/L82) at 10 (high concentration) and 2 μg/mL (low concentration). Half maximal inhibition concentrations (IC_{50}s) were determined by serial dilution, and represent the mean of at least two independent experiments. HPLC-based activity profiling was done as previously described [7]. Positive controls, melarsoprol (Sanofi-Aventis) (*T. b. rhodesiense*), benznidazole (Sigma) (*T. cruzi*), miltefosine (VWR) (*L. donovani*), chloroquine (Sigma) (*P. falciparum*), and podophyllotoxin (Sigma) (L6 cells) were used. The purity of all controls was > 95 % according to the suppliers.

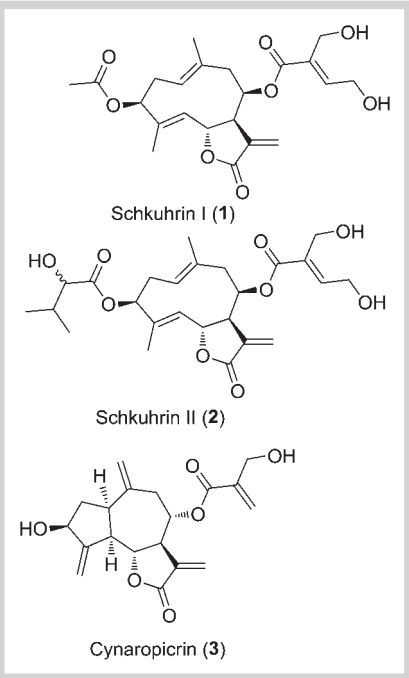

Fig. 3 Structures of the isolated compounds from *Schkuhria pinnata* and *Vernonia mespilifolia* crude extracts.

Supporting information

Data on the antiprotozoal activity of 60 South African medicinal plants, protocols for the purification and isolation of schkuhrin I, schkuhrin II, and cynaropicrin, as well as detailed protocols for the bioassays are available as Supporting Information.

Acknowledgements

The authors would like to thank the Council for Scientific and Industrial Research (CSIR), the Department of Science and Technology, and the Swiss Confederation for financial support under the Swiss South African Joint Research Programme (grant JRP 03), and the South African National Biodiversity Institute (SANBI) for the identification of plant species.

Conflict of Interest

The authors have no conflict of interest.

Affiliations

[1] Natural Product Chemistry, Biosciences, Council for Scientific and Industrial Research (CSIR), Pretoria, South Africa
[2] Department of Pharmaceutical Sciences, University of Basel, Switzerland
[3] Swiss Tropical and Public Health Institute, Basel, Switzerland
[4] Department of Pharmacy, Faculty of Sciences, National University of Colombia, Bogota D. C., Colombia
[5] School of Chemistry, University of KwaZulu-Natal, Durban, South Africa
[6] Present address: Defence Peace Safety and Security, Council for Scientific and Industrial Research (CSIR), Pretoria, South Africa

References

1 *Hotez PJ, Molyneuz DH, Fenwick A, Kumaresan J, Sachs SE, Sachs JD, Savioloi L.* Control of neglected tropical diseases. N Engl J Med 2007; 357: 1018–1027
2 *Stuart K, Brun R, Croft S, Fairlamb A, Gürtler RE, McKerrow J, Reed S, Tarleton R.* Kinetoplastids: related protozoan pathogens, different diseases. J Clin Invest 2008; 118: 1301–1310
3 *World Health Organization.* World malaria report 2011. Geneva: WHO; 2011: 1–278
4 *Orhan I, Şener B, Kaiser M, Brun R, Tasdemir D.* Inhibitory activity of marine sponge-derived natural products. Mar Drugs 2010; 8: 47–58
5 *Mokoka TA, Zimmerman S, Julianti T, Hata, Y, Moodley N, Cal M, Adams M, Kaiser M, Brun, R, Koorbanally N, Hamburger M. In vitro* screening of traditional South African malaria remedies against *Trypanosoma brucei rhodesiense, Trypanosoma cruzi, Leishmania donovani* and *Plasmodium falciparum.* Planta Med 2011; 77: 1663–1667
6 *Adams M, Zimmermann S, Kaiser M, Brun R, Hamburger M.* A protocol for HPLC-based activity profiling for natural products with activities against tropical parasites. Nat Prod Commun 2009; 4: 1377–1381
7 *Pettei MJ, Miura Y, Kubo Y, Nakanishi K.* Insect antifeedant sesquiterpene lactones from *Schkuhria pinnata*: the direct obtention of pure compounds using reverse-phase preparative liquid chromatography. Heterocycles 1978; 11: 471–480
8 *Yayli N, Baltaci C, Gök Y, Aydin E, Üçüncü O.* Sesquiterpene lactones from *Centaurea helenioides* Boiss. Turk J Chem 2006; 30: 229–233
9 *Watt JM, Breyer-Brandwijk MG.* The medicinal and poisonous plants of Southern and Eastern Africa, 2nd edition. London: E.&S. Livingstone Ltd.; 1962
10 *Luseba D.* The effects of extracts of some indigenous South African plants on *in vitro* cultures of *Brucella abortus.* Planta Med 2008; 74: PA336
11 *León A, Reyes BM, Delgado G.* Sesquiterpene lactones and other bioactive constituents from *Schkuhria pinnata* var. *wislizeni* (Asteraceae). Planta Med 2008; 74: 1034 (PB27)
12 *Clarkson C, Maharaj VJ, Crouch NR, Grace OM, Pillay P, Matsabisa MG, Bhagwandin N, Smith PJ, Folb PI. In vitro* antiplasmodial activity of medicinal plants native to or naturalised in South Africa. J Ethnopharmacol 2004; 92: 177–191
13 *Hutchings A, Scott AH, Lewis G, Cunningham A.* Zulu medicinal plants: an inventory. Pietermarizburg: Natal University Press; 1996
14 *Schmidt TJ, Khalid SA, Romanha, AJ, Alves TM, Biavatti, MW, Brun R, Da Costa FB, de Castro SL, Ferreira VF, de Lacerda MV, Lago JH, Leon LL, Lopes NP, das Neves Amorim RC, Niehues M, Ogungbe IV, Pohlit AM, Scotti MT, Setzer WN, de N C Soeiro M, Steindel M, Tempone AG.* The potential of secondary metabolites from plants as drugs or leads against protozoan neglected diseases – part I. Curr Med Chem 2012; 19: 2128–2175
15 http://www.mobot.org/MOBOT/research/APweb. Accessed October 10, 2012.
16 *Schmidt TJ, Nour AMM, Khalid SA, Kaiser M, Brun R.* Quantitative structure-antiprotozoal activity relationships of sesquiterpene lactones. Molecules 2009; 14: 2062–2076
17 *Zimmermann S, Kaiser M, Brun R, Hamburger M, Adams M.* Cynaropicrin: the first plant natural product with *in vivo* activity against *Trypanosoma brucei.* Planta Med 2012; 78: 553–556
18 *Zimmermann S, Oufir M, Leroux A, Krauth-Siegel RL, Becker K, Brun R, Hamburger M, Adams M.* Cynaropicrin targets the trypanothione redox system in *Trypanosoma brucei.* Int J Parasitol Drugs Drug Resist 2013; submitted

Supporting Information

Antiprotozoal Screening of 60 South African Plants, and the Identification of the Antitrypanosomal Germacranolides Schkuhrin I and II

Tsholofelo A. Mokoka[1], Xolani. K. Peter[1], Stefanie Zimmermann[2, 3], Yoshie Hata[2, 4], Michael Adams[2], Marcel Kaiser[3], Nivan Moodley[1, 6],Vinesh Maharaj[1], Neil A. Koorbanally[5], Matthias Hamburger[2*], Reto Brun[3], Gerda Fouche[1]*

[1]*Natural Product Chemistry, Biosciences, Council for Scientific and Industrial Research (CSIR), Pretoria, South Africa*

[2]*Department of Pharmaceutical Sciences, University of Basel, Basel, Switzerland*

[3]*Swiss Tropical and Public Health Institute, Basel, Switzerland*

[4]*Department of Pharmacy, Faculty of Sciences, National University of Colombia, Bogota D.C., Colombia*

[5]*School of Chemistry, University of KwaZulu-Natal, Private Bag X54001, Durban 4000, South Africa*

[6]*Present address: Defence Peace Safety and Security, Council for Scientific and Industrial Research (CSIR), Pretoria, South Africa*

Correspondence Dr. Gerda Fouche[1], Natural Product Chemistry, Biosciences, Council for Scientific and Industrial Research (CSIR), PO Box 395, Pretoria, South Africa. E-mail:gfouche@csir.co.za, Phone: +27 12 8413815 Fax: +27 12 3494790 and Prof. Matthias Hamburger, Department of Pharmaceutical Sciences, University of Basel, Basel, Klingelbergstrasse 50, 4056 Basel, Switzerland. E-mail:matthias.hamburger@unibas.ch, Phone: +41 61 267 1425 Fax: +41 61 267 1474

Table 1S. Antiprotozoal activity of 60 South African medicinal plants species against *Trypanosoma brucei rhodesiense*, *Trypanosoma cruzi*, *Leishmania donovani*, and *P. falciparum*. The activity is expressed as percentage (%) growth inhibition. Plants extracts showing more than 95% growth inhibition at 10 µg/mL were considered potential "hits". The tests were done twice and in duplicate.

					Percentage (%) growth inhibition							
					T. b. rhodesiense		***T. cruzi***		***L. donovani***		***P. falciparum***	
Family	**Species**	**Plant part**	**Extract type**	**Extract no.**	**10 µg/mL**	**2 µg/mL**	**10 µg/mL**	**2 µg/mL**	**10 µg/mL**	**2 µg/mL**	**10 µg/mL**	**2 µg/mL**
Fabaceae	***Abrus precatorius* L. subsp. *africanus* Verdc**.	Whole plant	DCM/MeOH (1:1)	P06218B	100.0	100.0	44.0	16.7	75.5	16.1	97.8	37.0
Fabaceae	***Acacia caffra* (Thunb.) Willd.**	Leaves	DCM/MeOH (1:1)	P00855B	3.0	0.0	42.3	17.6	33.5	8.3	19.9	0.3
Fabaceae	***Acacia caffra* (Thunb.) Willd.**	Roots	DCM/MeOH (1:1)	P00866B	93.9	0.0	46.1	25.7	34.7	8.9	55.0	7.0
Fabaceae	***Acacia erioloba* E.Mey.**	Roots	DCM/MeOH (1:1)	P08470B	18.6	6.4	48.9	18.8	50.2	26.3	61.4	72.6
Euphorbiaceae	***Acalypha peduncularis* E.Mey. ex Meisn.**	Leaves	DCM/MeOH (1:1)	P02855B	98.8	0.0	37.2	8.5	60.2	0.0	77.7	19.2

					Percentage (%) growth inhibition							
					T. b. rhodesiense		*T. cruzi*		*L. donovani*		*P. falciparum*	
Family	**Species**	**Plant part**	**Extract type**	**Extract no.**	**10 µg/mL**	**2 µg/mL**	**10 µg/mL**	**2 µg/mL**	**10 µg/mL**	**2 µg/mL**	**10 µg/mL**	**2 µg/mL**
Asparagaceae	***Asparagus virgatus* Baker**	Leaves	DCM/MeOH (1:1)	P00558B	10.3	0.0	47.6	15.7	0.0	0.0	36.5	0.0
Lamiaceae	***Becium obovatum* (E.Mey. ex Benth.) N.E.Br. subsp. *obovatum* var. *obovatum***	Roots	DCM/MeOH (1:1)	P04123B	49.4	11.9	37.5	3.9	97.5	5.7	99.3	38.2
Scrophulariaceae	***Bowkeria cymosa* MacOwan**	Leaves	DCM/MeOH (1:1)	P11785B	46.1	17.6	59.8	26.2	94.1	31.2	87.0	27.8
Scrophulariaceae	***Bowkeria cymosa* MacOwan**	Twigs	DCM/MeOH (1:1)	P11786B	14.0	4.6	36.9	8.4	47.5	24.3	60.1	7.6
Scrophulariaceae	***Bowkeria cymosa* MacOwan**	Roots	DCM/MeOH (1:1)	P11787B	17.1	0.0	53.0	15.2	39.9	17.0	80.7	14.6
Scrophulariaceae	***Bowkeria cymosa* MacOwan**	Stems	DCM/MeOH (1:1)	P11788B	5.6	0.0	54.0	22.3	31.7	17.1	45.2	3.5

					Percentage (%) growth inhibition							
					T. b. rhodesiense		*T. cruzi*		*L. donovani*		*P. falciparum*	
Family	**Species**	**Plant part**	**Extract type**	**Extract no.**	**10 µg/mL**	**2 µg/mL**	**10 µg/mL**	**2 µg/mL**	**10 µg/mL**	**2 µg/mL**	**10 µg/mL**	**2 µg/mL**
Asteraceae	***Brachylaena discolor* DC.**	Roots	DCM/MeOH (1:1)	P04199B	20.9	10.3	35.0	7.4	28.9	14.5	38.2	4.8
Asteraceae	***Brachylaena discolor* DC.**	Lleaves	DCM/MeOH (1:1)	P04321B	50.0	12.6	34.2	15.3	30.4	19.0	71.5	10.3
Asteraceae	***Brachylaena discolor* DC.**	Roots	DCM/MeOH (1:1)	P04459B	37.0	16.0	37.4	15.4	36.4	18.8	60.2	15.9
Euphorbiaceae	***Bridelia micrantha* (Hochst.) Baill.**	Leaves	DCM/MeOH (1:1)	P04722B	98.0	0.0	38.2	11.6	30.7	0.0	84.3	12.8
Euphorbiaceae	***Bridelia micrantha* (Hochst.) Baill.**	Stems	DCM/MeOH (1:1)	P04806B	58.4	24.3	37.5	13.7	54.0	20.0	92.5	23.3
Euphorbiaceae	***Bridelia micrantha* (Hochst.) Baill.**	Roots	DCM/MeOH (1:1)	P04815B	42.0	0.0	30.6	14.3	15.8	0.0	80.7	34.6
Rubiaceae	***Canthium mundianum* (Cham.**	Leaves	DCM/MeOH (1:1)	P00413B	12.8	0.0	48.9	20.2	30.7	23.0	24.1	0.0

					Percentage (%) growth inhibition							
					T. b. rhodesiense		*T. cruzi*		*L. donovani*		*P. falciparum*	
Family	**Species**	**Plant part**	**Extract type**	**Extract no.**	**10 µg/mL**	**2 µg/mL**	**10 µg/mL**	**2 µg/mL**	**10 µg/mL**	**2 µg/mL**	**10 µg/mL**	**2 µg/mL**
	& Schltdl.) Lantz											
Rubiaceae	***Canthium mundianum* (Cham. & Schltdl.) Lantz**	Leaves	MeOH	P00413C	10.1	0.0	45.0	16.3	30.8	28.3	22.6	0.0
Rubiaceae	***Canthium mundianum* (Cham. & Schltdl.) Lantz**	Roots	DCM	P00414A	23.1	0.0	49.9	22.3	65.7	22.4	87.1	15.5
Rubiaceae	***Canthium mundianum* (Cham. & Schltdl.) Lantz**	Roots	DCM/MeOH (1:1)	P00414B	14.5	0.0	49.9	18.5	31.8	21.4	29.6	0.0
Rubiaceae	***Canthium mundianum* (Cham. & Schltdl.) Lantz**	Roots	MeOH	P00414C	12.8	0.0	43.0	24.7	29.4	19.8	30.1	0.0
Rubiaceae	***Canthium mundianum* (Cham. & Schltdl.) Lantz**	Fruits	DCM/MeOH (1:1)	P00415B	10.6	0.0	46.7	20.3	20.5	19.0	26.3	0.0
Rubiaceae	***Canthium mundianum* (Cham.)**	Fruits	MeOH	P00415C	0.7	0.0	38.1	9.7	0.0	0.0	25.2	0.1

					Percentage (%) growth inhibition							
					T. b. rhodesiense		*T. cruzi*		*L. donovani*		*P. falciparum*	
Family	**Species**	**Plant part**	**Extract type**	**Extract no.**	**10 µg/mL**	**2 µg/mL**	**10 µg/mL**	**2 µg/mL**	**10 µg/mL**	**2 µg/mL**	**10 µg/mL**	**2 µg/mL**
	& Schltdl.) Lantz											
Capparaceae	***Capparis tomentosa* Lam.**	Roots	DCM/MeOH (1:1)	P06167B	31.2	30.2	30.5	13.1	35.1	23.8	76.3	26.4
	***Capparis tomentosa* Lam.**	Fruits	DCM/MeOH (1:1)	P06168B	17.7	0.0	24.8	15.7	17.6	19.6	37.8	3.7
	***Capparis tomentosa* Lam.**	Stems	DCM/MeOH (1:1)	P06169B	34.0	3.4	67.1	17.2	86.5	32.7	93.5	30.9
Asteraceae	***Cirsium vulgare* (Savi) Ten.**	Whole plant	DCM	P02112A	10.2	0.0	49.1	30.2	33.1	24.9	46.3	0.0
	***Cirsium vulgare* (Savi) Ten.**	Whole plant	DCM/MeOH (1:1)	P02112B	23.2	5.3	42.9	29.3	30.7	27.6	49.1	0.0
	***Cirsium vulgare* (Savi) Ten.**	Leaves	DCM/MeOH (1:1)	P06377B	11.3	1.4	42.2	10.2	39.7	18.4	81.0	20.6
		Roots	DCM/MeOH (1:1)	P06381B	28.7	1.8	8.3	5.3	38.2	16.7	51.9	11.8
Asteraceae	***Cirsium vulgare* (Savi) Ten.**	Stems	DCM/MeOH (1:1)	P06384B	5.9	0.0	46.8	20.6	35.3	15.2	70.6	16.5
Rutaceae	***Clausena anisata* (Willd.) Hook.f. ex Benth. var. *anisata***	Leaves	DCM/MeOH (1:1)	P04413B	98.8	13.6	28.8	8.7	53.3	4.5	77.8	15.4

					Percentage (%) growth inhibition							
					T. b. rhodesiense		*T. cruzi*		*L. donovani*		*P. falciparum*	
Family	**Species**	**Plant part**	**Extract type**	**Extract no.**	**10 µg/mL**	**2 µg/mL**	**10 µg/mL**	**2 µg/mL**	**10 µg/mL**	**2 µg/mL**	**10 µg/mL**	**2 µg/mL**
Rutaceae	***Clausena anisata* (Willd.) Hook.f. ex Benth. var. *anisata***	Roots	DCM/MeOH (1:1)	P04411B	82.5	6.3	25.0	7.1	71.4	1.4	100.0	51.5
Lamiaceae	***Clerodendrum glabrum* E.Mey.**	Stems	DCM/MeOH (1:1)	P09466B	5.5	0.0	42.3	15.3	42.8	18.7	82.5	19.1
Lamiaceae	***Clerodendrum glabrum* E.Mey.**	Roots	DCM/MeOH (1:1)	P09467B	19.7	0.0	50.0	17.7	69.8	31.5	58.6	4.5
Euphorbiaceae	***Clutia pulchella* L. var. *pulchella***	Twigs	DCM	P00020A	18.2	6.8	28.8	16.7	38.2	21.3	69.4	2.4
Euphorbiaceae	***Clutia pulchella* L. var. *pulchella***	Twigs	DCM/MeOH (1:1)	P00020B	20.0	10.8	37.6	23.1	33.3	20.9	38.0	2.7
Euphorbiaceae	***Clutia pulchella* L. var. *pulchella***	Twigs	MeOH	P00020C	18.3	9.9	38.1	16.5	31.9	19.3	36.0	0.0
Euphorbiaceae	***Clutia pulchella* L. var. *pulchella***	Leaves	DCM/MeOH (1:1)	P00476B	11.8	4.7	48.2	24.6	34.3	24.9	59.9	1.1
Euphorbiaceae	***Clutia pulchella* L. var. *pulchella***	Leaves	MeOH	P00476C	3.8	0.0	48.5	22.6	31.2	20.6	53.1	8.3
Euphorbiaceae	***Clutia pulchella* L. var. *pulchella***	Roots	DCM/MeOH (1:1)	P10738B	12.5	1.9	47.6	16.6	14.2	0.0	97.7	75.0
Euphorbiaceae	***Clutia pulchella* L.**	Leaves &	DCM/MeOH	P10739B	42.3	8.3	34.7	19.9	40.1	14.1	74.0	12.5

					Percentage (%) growth inhibition							
					T. b. rhodesiense		*T. cruzi*		*L. donovani*		*P. falciparum*	
Family	**Species**	**Plant part**	**Extract type**	**Extract no.**	**10 µg/mL**	**2 µg/mL**	**10 µg/mL**	**2 µg/mL**	**10 µg/mL**	**2 µg/mL**	**10 µg/mL**	**2 µg/mL**
	var. *pulchella*	stems	(1:1)									
Euphorbiaceae	***Clutia pulchella* L. var. *pulchella***	Stems	DCM/MeOH (1:1)	P10740B	19.2	5.0	40.2	24.3	48.3	17.1	76.8	19.1
Euphorbiaceae	***Croton gratissimus* Burch. var. *gratissimus***	Leaves	DCM/MeOH (1:1)	P07086B	40.1	3.2	38.0	15.6	96.4	26.1	71.8	27.1
Euphorbiaceae	***Croton gratissimus* Burch. var. *gratissimus***	Stems	DCM/MeOH (1:1)	P07087B	38.9	6.4	25.3	12.7	60.6	0.0	83.2	42.9
Euphorbiaceae	***Croton gratissimus* Burch. var. *gratissimus***	Bark	DCM/MeOH (1:1)	P07089B	100.0	1.9	13.3	16.0	67.2	29.6	79.6	31.0
Iridaceae	***Dietes iridioides* (L.) Sweet ex Klatt**	Leaves	DCM/MeOH (1:1)	P08597B	98.8	0.0	43.5	22.9	30.4	18.1	69.4	8.4
Iridaceae	***Dietes iridioides* (L.) Sweet ex Klatt**	Roots	DCM/MeOH (1:1)	P08598B	97.9	0.0	35.0	0.0	0.0	0.0	77.7	24.0
Iridaceae	***Dietes iridioides* (L.) Sweet ex Klatt**	Flowers	DCM/MeOH (1:1)	P08599B	99.9	0.0	41.8	13.1	55.8	17.1	69.9	24.8
Iridaceae	***Dietes iridioides* (L.) Sweet ex Klatt**	Fruits	DCM/MeOH (1:1)	P08600B	100.0	4.7	31.3	12.2	42.8	19.3	76.9	12.1

					Percentage (%) growth inhibition							
					T. b. rhodesiense		*T. cruzi*		*L. donovani*		*P. falciparum*	
Family	**Species**	**Plant part**	**Extract type**	**Extract no.**	**10 µg/mL**	**2 µg/mL**	**10 µg/mL**	**2 µg/mL**	**10 µg/mL**	**2 µg/mL**	**10 µg/mL**	**2 µg/mL**
Apocynaceae	***Diplorhynchus condylocarpon* (Müll.Arg.) Pichon**	Leaves	DCM	P00933A	20.6	0.0	49.0	26.5	80.4	28.2	78.2	9.9
Apocynaceae	***Diplorhynchus condylocarpon* (Müll.Arg.) Pichon**	Leaves	DCM/MeOH (1:1)	P00933B	6.0	0.0	46.0	16.1	35.5	25.2	37.9	0.0
Apocynaceae	***Diplorhynchus condylocarpon* (Müll.Arg.) Pichon**	Roots	DCM	P00940A	12.7	0.0	38.9	18.2	57.3	27.2	43.8	0.0
Apocynaceae	***Diplorhynchus condylocarpon* (Müll.Arg.) Pichon**	Roots	DCM/MeOH (1:1)	P00940B	18.6	0.0	58.7	13.9	35.3	26.5	61.7	0.0
Apocynaceae	***Diplorhynchus condylocarpon* (Müll.Arg.) Pichon**	Twigs	DCM/MeOH (1:1)	P03406B	14.7	0.0	50.0	17.8	54.6	15.7	73.0	10.0
Apocynaceae	***Diplorhynchus condylocarpon* (Müll.Arg.) Pichon**	Leaves & Twigs	DCM/MeOH (1:1)	P03407B	40.0	3.0	34.5	5.3	86.2	18.9	97.4	19.5
Apocynaceae	***Diplorhynchus condylocarpon* (Müll.Arg.) Pichon**	Stems	DCM/MeOH (1:1)	P07108B	21.1	1.9	40.2	10.3	47.1	24.9	93.3	28.2
Euphorbiaceae	***Drypetes gerrardii***	Stems	DCM/MeOH	P05778B	60.7	28.5	30.9	0.0	80.5	24.9	100.0	99.5

					Percentage (%) growth inhibition							
					T. b. rhodesiense		*T. cruzi*		*L. donovani*		*P. falciparum*	
Family	**Species**	**Plant part**	**Extract type**	**Extract no.**	**10 µg/mL**	**2 µg/mL**	**10 µg/mL**	**2 µg/mL**	**10 µg/mL**	**2 µg/mL**	**10 µg/mL**	**2 µg/mL**
	Hutch. var. *gerrardii*		(1:1)									
Euphorbiaceae	***Drypetes gerrardii* Hutch. var. *gerrardii***	Leaves	DCM/MeOH (1:1)	P05800B	96.5	37.3	32.0	6.9	28.1	23.6	69.9	21.6
Meliaceae	***Ekebergia capensis* Sparrm.**	Leaves	DCM/MeOH (1:1)	P04616B	98.8	0.9	39.3	13.3	50.6	0.0	71.9	13.8
Meliaceae	***Ekebergia capensis* Sparrm.**	Roots	DCM/MeOH (1:1)	P04929B	100.0	100.0	102.4	95.3	100.0	56.9	98.6	57.0
Euphorbiaceae	***Euphorbia clavarioides* Boiss. var. *truncata* (N.E.Br.) A.C.White, R.A.Dyer & B.Sloane**	Leaves	DCM/MeOH (1:1)	P01559B	7.6	0.0	37.8	32.4	42.5	12.5	59.9	12.7
Euphorbiaceae	***Euphorbia clavarioides* Boiss. var. *truncata* (N.E.Br.) A.C.White, R.A.Dyer & B.Sloane**	Roots	DCM/MeOH (1:1)	P01568B	17.2	0.0	46.8	25.5	45.9	17.4	63.9	5.4
Euphorbiaceae	***Euphorbia pulcherrima* Willd. ex Klotzsch**	Leaves	DCM/MeOH (1:1)	P10453B	11.8	0.0	30.7	21.1	42.8	20.4	63.4	6.3
Euphorbiaceae	***Euphorbia pulcherrima* Willd.**	Stems	DCM/MeOH (1:1)	P10454B	17.8	0.0	45.6	15.4	55.2	22.9	86.5	16.4

					Percentage (%) growth inhibition							
					T. b. rhodesiense		*T. cruzi*		*L. donovani*		*P. falciparum*	
Family	**Species**	**Plant part**	**Extract type**	**Extract no.**	**10 µg/mL**	**2 µg/mL**	**10 µg/mL**	**2 µg/mL**	**10 µg/mL**	**2 µg/mL**	**10 µg/mL**	**2 µg/mL**
	ex Klotzsch											
Euphorbiaceae	***Euphorbia pulcherrima* Willd. ex Klotzsch**	Roots	DCM/MeOH (1:1)	P10455B	13.5	0.0	45.4	17.4	42.7	18.5	81.7	23.2
Asteraceae	***Felicia filifolia* (Vent.) Burtt Davy *subsp. filifolia***	Leaves	DCM/MeOH (1:1)	P10676B	7.3	1.1	45.2	11.5	0.0	14.9	88.2	19.3
Asteraceae	***Helichrysum mundtii* Harv.**	Stems	DCM	P00464A	19.3	0.0	79.0	34.9	64.7	31.0	84.3	20.7
Asteraceae	***Helichrysum mundtii* Harv.**	Stems	DCM/MeOH (1:1)	P00464B	9.9	4.4	75.4	33.2	61.5	28.0	81.1	14.2
Asteraceae	***Helichrysum mundtii* Harv.**	Stems	MeOH	P00464C	2.0	0.0	59.2	26.7	38.4	29.5	34.9	0.0
Asteraceae	***Helichrysum mundtii* Harv.**	Roots	DCM	P00466A	38.8	0.0	89.9	44.2	80.7	35.1	89.7	19.9
Asteraceae	***Helichrysum mundtii* Harv.**	Roots	DCM/MeOH (1:1)	P00466B	15.2	0.7	73.7	32.8	47.8	27.4	71.5	3.2
Asteraceae	***Helichrysum mundtii* Harv.**	Roots	MeOH	P00466C	17.3	0.0	58.9	28.0	36.9	23.9	55.2	0.0
Asteraceae	***Helichrysum***	Leaves	DCM/MeOH	P00467B	7.7	0.0	52.2	19.0	32.3	21.2	46.5	0.3

					Percentage (%) growth inhibition							
					T. b. rhodesiense		*T. cruzi*		*L. donovani*		*P. falciparum*	
Family	**Species**	**Plant part**	**Extract type**	**Extract no.**	**10 µg/mL**	**2 µg/mL**	**10 µg/mL**	**2 µg/mL**	**10 µg/mL**	**2 µg/mL**	**10 µg/mL**	**2 µg/mL**
	***mundtii* Harv.**		(1:1)									
Asteraceae	***Helichrysum mundtii* Harv.**	Leaves	MeOH	P00467C	5.5	0.0	46.1	15.2	0.0	0.0	37.1	3.5
Asteraceae	***Helichrysum pedunculatum* Hilliard & B.L.Burtt**	Whole plants	DCM/MeOH (1:1)	P08309B	9.2	0.0	40.0	8.1	36.3	31.8	61.9	24.0
Apiaceae	***Heteromorpha arborescens* (Spreng.) Cham. & Schltdl. var. *abyssinica* (A.Rich.) H.Wolff**	Roots	DCM/MeOH (1:1)	P12488B	17.3	0.0	40.2	26.8	38.0	32.0	66.2	27.7
Apiaceae	***Heteromorpha arborescens* (Spreng.) Cham. & Schltdl. var. *abyssinica* (A.Rich.) H.Wolff**	Bark	DCM/MeOH (1:1)	P12489B	19.0	0.0	33.4	14.9	44.8	28.2	84.0	26.5
Lamiaceae	***Hyptis pectinata* (L.) Poit.**	Leaves, stems, fruits	DCM/MeOH (1:1)	P02459B	32.2	0.0	53.4	17.4	53.5	18.2	85.0	19.9
Proteaceae	***Leucospermum cuneiforme* (Burm.f.) Rourke**	Leaves	DCM/MeOH (1:1)	P02599B	21.8	6.4	44.0	23.1	50.6	10.5	99.4	21.3

					Percentage (%) growth inhibition							
					T. b. rhodesiense		*T. cruzi*		*L. donovani*		*P. falciparum*	
Family	**Species**	**Plant part**	**Extract type**	**Extract no.**	**10 µg/mL**	**2 µg/mL**	**10 µg/mL**	**2 µg/mL**	**10 µg/mL**	**2 µg/mL**	**10 µg/mL**	**2 µg/mL**
Proteaceae	***Leucospermum cuneiforme* (Burm.f.) Rourke**	Roots	DCM/MeOH (1:1)	P02606B	18.5	3.3	49.0	19.7	11.1	3.5	41.2	9.9
Euphorbiaceae	***Macaranga capensis* (Baill.) Benth. ex Sim**	Leaves	DCM/MeOH (1:1)	P04676B	83.4	7.9	55.0	17.2	49.6	0.0	91.7	22.0
Sapotaceae	***Mimusops zeyheri* Sond.**	Leaves	DCM	P00488A	18.1	0.0	49.2	25.9	42.5	22.9	71.1	3.4
Sapotaceae	***Mimusops zeyheri* Sond.**	Leaves	MeOH	P00488C	99.3	0.0	50.8	24.2	28.5	23.3	30.1	0.0
Sapotaceae	***Mimusops zeyheri* Sond.**	Fruits	DCM	P00489A	18.6	0.0	48.0	27.0	40.6	26.8	53.2	0.0
Sapotaceae	***Mimusops zeyheri* Sond.**	Fruits	MeOH	P00489C	6.7	0.0	45.2	27.9	48.5	26.2	26.2	0.0
Sapotaceae	***Mimusops zeyheri* Sond.**	Roots	DCM	P00490A	10.3	0.0	46.7	22.1	45.9	27.9	83.4	9.3
Sapotaceae	***Mimusops zeyheri* Sond.**	Roots	MeOH	P00490C	9.4	0.0	41.6	23.3	35.0	22.9	27.3	0.0
Sapotaceae	***Mimusops zeyheri* Sond.**	Stems	DCM	P00491A	12.8	0.0	40.9	29.0	56.0	27.2	88.7	14.8

					Percentage (%) growth inhibition							
					T. b. rhodesiense		*T. cruzi*		*L. donovani*		*P. falciparum*	
Family	**Species**	**Plant part**	**Extract type**	**Extract no.**	**10 µg/mL**	**2 µg/mL**	**10 µg/mL**	**2 µg/mL**	**10 µg/mL**	**2 µg/mL**	**10 µg/mL**	**2 µg/mL**
Sapotaceae	***Mimusops zeyheri* Sond.**	Stems	MeOH	P00491C	17.6	0.0	48.1	27.8	27.7	21.9	23.8	0.0
Sapotaceae	***Mimusops zeyheri* Sond.**	Leaves & twigs	DCM	P02237A	34.0	0.0	48.0	25.3	61.6	27.9	98.5	16.6
Sapotaceae	***Mimusops zeyheri* Sond.**	Leaves & twigs	DCM/MeOH (1:1)	P02237B	99.5	0.0	42.5	24.9	27.4	23.0	26.4	0.0
Euphorbiaceae	***Monadenium lugardiae* N.E.Br.**	Whole plants	DCM/MeOH (1:1)	P02587B	97.8	2.3	40.6	15.8	69.5	16.1	97.7	27.7
Lamiaceae	***Ocimum gratissimum* L. *subsp. gratissimum* var. *gratissimum***	Leaves	DCM	P00766A	12.3	0.0	47.9	29.2	55.5	14.6	88.7	25.7
Lamiaceae	***Ocimum gratissimum* L. *subsp. gratissimum* var. *gratissimum***	Leaves	DCM/MeOH (1:1)	P00766B	0.3	0.0	43.2	21.3	0.0	0.0	51.9	21.0
Lamiaceae	***Ocimum gratissimum* L. *subsp. gratissimum* var. *gratissimum***	Roots	DCM/MeOH (1:1)	P00775B	6.7	4.8	45.6	11.8	30.5	11.6	22.0	10.8
Lamiaceae	***Ocimum gratissimum* L. *subsp. gratissimum***	Stems	DCM	P00777A	26.5	3.7	39.0	22.9	52.9	17.9	90.5	29.2

					Percentage (%) growth inhibition							
					T. b. rhodesiense		*T. cruzi*		*L. donovani*		*P. falciparum*	
Family	**Species**	**Plant part**	**Extract type**	**Extract no.**	**10 µg/mL**	**2 µg/mL**	**10 µg/mL**	**2 µg/mL**	**10 µg/mL**	**2 µg/mL**	**10 µg/mL**	**2 µg/mL**
	var. *gratissimum*											
Lamiaceae	***Ocimum gratissimum* L. *subsp. gratissimum* var. *gratissimum***	Stems	DCM/MeOH (1:1)	P00777B	0.5	0.0	44.3	22.0	33.6	11.5	28.4	0.0
Asteraceae	***Oedera genistifolia* (L.) Anderb. & K.Bremer**	Whole plant	DCM/MeOH (1:1)	P03206B	100.0	100.0	50.8	18.6	100.0	69.8	100.0	99.3
Asteraceae	***Othonna carnosa* Less. var. *carnosa***	Stems	DCM/MeOH (1:1)	P02700B	100.0	2.3	43.9	17.1	29.0	3.8	98.5	37.8
Anacardiaceae	***Ozoroa sphaerocarpa* R.Fern. & A.Fern.**	Whole plant	DCM	P00437A	100.0	67.1	41.9	23.2	87.1	22.8	74.7	15.7
Anacardiaceae	***Ozoroa sphaerocarpa* R.Fern. & A.Fern.**	Whole plant	DCM/MeOH (1:1)	P00437B	100.0	0.0	51.1	24.0	82.7	26.1	81.5	18.1
Anacardiaceae	***Ozoroa sphaerocarpa* R.Fern. & A.Fern.**	Whole plant	MeOH	P00437C	99.6	0.0	40.2	10.9	33.3	24.1	39.1	0.0
Anacardiaceae	***Ozoroa sphaerocarpa* R.Fern. & A.Fern.**	Stems	DCM	P00439A	3.6	0.0	42.7	15.8	97.4	23.7	85.9	25.1

					Percentage (%) growth inhibition							
					T. b. rhodesiense		*T. cruzi*		*L. donovani*		*P. falciparum*	
Family	**Species**	**Plant part**	**Extract type**	**Extract no.**	**10 µg/mL**	**2 µg/mL**	**10 µg/mL**	**2 µg/mL**	**10 µg/mL**	**2 µg/mL**	**10 µg/mL**	**2 µg/mL**
Anacardiaceae	***Ozoroa sphaerocarpa* R.Fern. & A.Fern.**	Stems	DCM/MeOH (1:1)	P00439B	99.1	0.0	40.3	29.5	39.9	23.3	54.9	0.0
Anacardiaceae	***Ozoroa sphaerocarpa* R.Fern. & A.Fern.**	Stems	MeOH	P00439C	99.6	0.0	35.1	21.9	30.1	25.3	31.2	1.4
Anacardiaceae	***Ozoroa sphaerocarpa* R.Fern. & A.Fern.**	Leaves	DCM/MeOH (1:1)	P00440B	100.0	0.0	34.2	24.3	43.7	22.6	47.7	0.0
Anacardiaceae	***Ozoroa sphaerocarpa* R.Fern. & A.Fern.**	Leaves	DCM	P00440A	98.3	0.0	42.2	20.4	80.2	25.2	82.0	13.4
Anacardiaceae	***Ozoroa sphaerocarpa* R.Fern. & A.Fern.**	Leaves	MeOH	P00440C	100.0	0.0	42.3	26.7	32.0	20.8	22.8	0.0
Sapindaceae	***Pappea capensis* Eckl. & Zeyh.**	Roots	DCM	P00397A	100.0	9.7	34.0	17.6	40.5	14.8	76.0	100.0
Sapindaceae	***Pappea capensis* Eckl. & Zeyh.**	Roots	DCM/MeOH (1:1)	P00397B	0.1	0.0	40.0	14.7	0.0	0.0	37.4	4.5
Sapindaceae	***Pappea capensis* Eckl. & Zeyh.**	Roots	MeOH	P00397C	19.5	0.0	46.0	26.6	30.7	25.3	36.7	1.1

					Percentage (%) growth inhibition							
					T. b. rhodesiense		*T. cruzi*		*L. donovani*		*P. falciparum*	
Family	**Species**	**Plant part**	**Extract type**	**Extract no.**	**10 µg/mL**	**2 µg/mL**	**10 µg/mL**	**2 µg/mL**	**10 µg/mL**	**2 µg/mL**	**10 µg/mL**	**2 µg/mL**
Sapindaceae	***Pappea capensis* Eckl. & Zeyh.**	Leaves	DCM/MeOH (1:1)	P10670B	99.7	0.0	17.6	15.5	15.5	0.0	79.2	35.9
Sapindaceae	***Pappea capensis* Eckl. & Zeyh.**	Bark	DCM/MeOH (1:1)	P10671B	14.5	0.0	29.7	22.4	30.6	22.2	78.3	25.8
Sapindaceae	***Pappea capensis* Eckl. & Zeyh.**	Roots	DCM/MeOH (1:1)	P10673B	15.2	0.0	29.5	25.7	44.5	25.4	95.9	54.1
Geraniaceae	***Pelargonium zonale* (L.) L'Hér.**	Stems	DCM	P01688A	1.7	0.0	43.4	5.1	26.0	23.6	30.9	0.0
Geraniaceae	***Pelargonium zonale* (L.) L'Hér.**	Stems	DCM/MeOH (1:1)	P01688B	99.4	0.0	40.0	21.8	28.7	24.1	33.5	0.0
Geraniaceae	***Pelargonium zonale* (L.) L'Hér.**	Twigs	DCM/MeOH (1:1)	P03391B	15.7	4.1	44.4	19.9	26.9	17.2	52.1	5.1
Geraniaceae	***Pelargonium zonale* (L.) L'Hér.**	Leaves	DCM/MeOH (1:1)	P03392B	16.4	2.8	43.4	11.2	24.0	10.1	88.2	3.9
Fabaceae	***Peltophorum africanum* Sond.**	Roots	DCM	P00394A	99.9	26.0	34.2	18.6	44.9	21.0	84.3	17.4
Fabaceae	***Peltophorum africanum* Sond.**	Roots	DCM/MeOH (1:1)	P00394B	100.0	8.2	34.9	18.0	26.2	20.6	54.0	2.0
Fabaceae	***Peltophorum africanum* Sond.**	Roots	MeOH	P00394C	100.0	6.1	32.1	12.2	23.9	21.7	34.8	0.0

					Percentage (%) growth inhibition							
					T. b. rhodesiense		*T. cruzi*		*L. donovani*		*P. falciparum*	
Family	**Species**	**Plant part**	**Extract type**	**Extract no.**	**10 µg/mL**	**2 µg/mL**	**10 µg/mL**	**2 µg/mL**	**10 µg/mL**	**2 µg/mL**	**10 µg/mL**	**2 µg/mL**
Fabaceae	***Peltophorum africanum* Sond.**	Stems	DCM	P00401A	99.6	49.3	60.7	29.0	31.5	22.4	90.2	31.6
Fabaceae	***Peltophorum africanum* Sond.**	Stems	DCM/MeOH (1:1)	P00401B	100.0	10.6	52.4	25.2	28.8	21.6	63.8	11.4
Fabaceae	***Peltophorum africanum* Sond.**	Stems	MeOH	P00401C	100.0	11.6	51.6	15.2	29.8	22.0	66.5	9.2
Fabaceae	***Peltophorum africanum* Sond.**	Leaves & twigs	DCM	P02244A	100.0	0.0	56.5	23.9	78.3	28.5	98.8	29.6
Fabaceae	***Peltophorum africanum* Sond.**	Leaves & twigs	DCM/MeOH (1:1)	P02244B	57.6	0.0	40.6	22.1	28.2	22.8	49.7	3.7
Fabaceae	***Peltophorum africanum* Sond.**	leaves & twigs	MeOH	P02244C	95.4	0.0	40.5	6.7	0.0	0.0	30.3	0.0
Asteraceae	***Phymaspermum acerosum* (DC.) Källersjö**	Whole plant	DCM/MeOH (1:1)	P03661B	100.0	13.1	44.5	13.1	67.7	17.8	98.6	37.8
Lamiaceae	***Plectranthus laxiflorus* Benth.**	Whole plants	DCM/MeOH (1:1)	P12870B	92.1	9.9	40.0	14.4	51.5	29.0	59.9	14.6
Polygalaceae	***Polygala fruticosa* P.J. Bergius**	Leaves	DCM/MeOH (1:1)	P03756B	37.3	14.4	68.9	34.7	65.6	0.0	98.6	35.6
Polygalaceae	***Polygala fruticosa***	Twigs	DCM/MeOH	P03757B	24.7	11.7	46.8	17.8	35.3	0.0	82.5	23.2

					Percentage (%) growth inhibition							
					T. b. rhodesiense		*T. cruzi*		*L. donovani*		*P. falciparum*	
Family	**Species**	**Plant part**	**Extract type**	**Extract no.**	**10 µg/mL**	**2 µg/mL**	**10 µg/mL**	**2 µg/mL**	**10 µg/mL**	**2 µg/mL**	**10 µg/mL**	**2 µg/mL**
	P.J. Bergius		(1:1)									
Fabaceae	***Psoralea pinnata* L. var. *pinnata***	Leaves	DCM	P01617A	98.7	100.0	36.6	30.0	91.9	26.9	98.8	19.0
Fabaceae	***Psoralea pinnata* L. var. *pinnata***	Leaves	DCM/MeOH (1:1)	P01617B	99.7	99.2	32.1	19.8	73.3	22.7	83.9	0.6
Fabaceae	***Psoralea pinnata* L. var. *pinnata***	Stems	DCM	P01676A	7.5	0.0	52.8	20.5	32.4	15.9	52.4	1.9
Fabaceae	***Psoralea pinnata* L. var. *pinnata***	Stems	DCM/MeOH (1:1)	P01676B	4.3	0.0	47.3	16.4	0.0	0.0	38.5	7.1
Fabaceae	***Psoralea pinnata* L. var. *pinnata***	Roots	DCM	P01679A	8.6	0.0	44.7	24.1	35.5	23.2	41.0	0.0
Fabaceae	***Psoralea pinnata* L. var. *pinnata***	Roots	MeOH	P01679C /B	8.2	0.0	44.9	12.4	24.5	21.2	39.3	0.0
Rubiaceae	***Psychotria capensis* (Eckl.) Vatke *subsp. capensis* var. *capensis***	Roots	DCM/MeOH (1:1)	P09181B	17.4	0.0	31.1	13.0	39.0	21.4	28.9	5.5
Rubiaceae	***Psychotria capensis* (Eckl.) Vatke *subsp. capensis* var. *capensis***	Leaves	DCM/MeOH (1:1)	P09182B	18.4	0.0	30.6	14.8	37.4	20.4	36.7	10.3

					Percentage (%) growth inhibition							
					T. b. rhodesiense		*T. cruzi*		*L. donovani*		*P. falciparum*	
Family	**Species**	**Plant part**	**Extract type**	**Extract no.**	**10 µg/mL**	**2 µg/mL**	**10 µg/mL**	**2 µg/mL**	**10 µg/mL**	**2 µg/mL**	**10 µg/mL**	**2 µg/mL**
Rubiaceae	***Psychotria capensis* (Eckl.) Vatke *subsp. capensis* var. *capensis***	Stems	DCM/MeOH (1:1)	P09183B	99.9	0.0	36.7	3.1	39.4	19.1	30.1	0.0
Lamiaceae	***Rabdosiella calycina* (Benth.) Codd**	Stems	DCM	P00451A	98.4	0.0	45.3	8.6	103.4	40.6	77.5	11.3
Lamiaceae	***Rabdosiella calycina* (Benth.) Codd**	Stems	DCM/MeOH (1:1)	P00451B	38.1	0.0	48.8	23.2	14.1	0.0	49.2	2.8
Lamiaceae	***Rabdosiella calycina* (Benth.) Codd**	Stems	MeOH	P00451C	99.9	0.0	44.4	18.3	59.7	24.6	51.2	9.6
Lamiaceae	***Rabdosiella calycina* (Benth.) Codd**	Leaves	DCM/MeOH (1:1)	P00453B	5.4	0.0	52.0	16.0	33.3	21.1	33.0	0.0
Lamiaceae	***Rabdosiella calycina* (Benth.) Codd**	Leaves	MeOH	P00453C	0.0	0.0	44.4	26.5	32.5	21.9	27.9	0.0
Lamiaceae	***Rabdosiella calycina* (Benth.) Codd**	Whole plant	DCM/MeOH (1:1)	P08318B	99.6	0.0	44.1	12.1	80.4	22.6	76.9	20.6

					Percentage (%) growth inhibition							
					T. b. rhodesiense		*T. cruzi*		*L. donovani*		*P. falciparum*	
Family	**Species**	**Plant part**	**Extract type**	**Extract no.**	**10 µg/mL**	**2 µg/mL**	**10 µg/mL**	**2 µg/mL**	**10 µg/mL**	**2 µg/mL**	**10 µg/mL**	**2 µg/mL**
Myrsinaceae	***Rapanea melanophloeos* (L.) Mez**	Leaves	DCM/MeOH (1:1)	P08222B	19.9	34.7	37.3	14.8	60.6	30.8	44.7	5.1
Myrsinaceae	***Rapanea melanophloeos* (L.) Mez**	Twigs	DCM/MeOH (1:1)	P08223B	95.8	0.0	41.3	15.5	100.0	28.5	43.1	10.8
Myrsinaceae	***Rapanea melanophloeos* (L.) Mez**	Stems	DCM/MeOH (1:1)	P09405B	33.3	0.0	32.1	8.7	38.7	17.8	16.6	0.6
Myrsinaceae	***Rapanea melanophloeos* (L.) Mez**	Roots	DCM/MeOH (1:1)	P09406B	99.0	0.0	38.3	18.6	67.0	20.6	17.8	13.0
Vitaceae	***Rhoicissus tridentata* (L.f.) Wild & R.B.Drumm. *subsp. cuneifolia* (Eckl. & Zeyh.) Urton**	Leaves	DCM/MeOH (1:1)	P09322B	82.2	0.0	46.0	16.8	39.5	18.5	37.0	4.1
Vitaceae	***Rhoicissus tridentata* (L.f.) Wild & R.B.Drumm. *subsp. cuneifolia* (Eckl. & Zeyh.)**	Fruits	DCM/MeOH (1:1)	P09323B	99.7	0.0	41.1	17.6	47.0	25.7	54.3	11.7

					Percentage (%) growth inhibition							
					T. b. rhodesiense		*T. cruzi*		*L. donovani*		*P. falciparum*	
Family	**Species**	**Plant part**	**Extract type**	**Extract no.**	**10 µg/mL**	**2 µg/mL**	**10 µg/mL**	**2 µg/mL**	**10 µg/mL**	**2 µg/mL**	**10 µg/mL**	**2 µg/mL**
	Urton											
Vitaceae	***Rhoicissus tridentata* (L.f.) Wild & R.B.Drumm. *subsp. cuneifolia* (Eckl. & Zeyh.) Urton**	Roots	DCM/MeOH (1:1)	P09324B	0.0	0.0	46.7	24.6	38.5	20.8	30.4	9.9
Vitaceae	***Rhoicissus tridentata* (L.f.) Wild & R.B.Drumm. *subsp. cuneifolia* (Eckl. & Zeyh.) Urton**	Bark	DCM/MeOH (1:1)	P09325B	97.9	0.0	44.4	19.8	29.9	17.7	32.1	1.0
Vitaceae	***Rhoicissus tridentata* (L.f.) Wild & R.B.Drumm. *subsp. cuneifolia* (Eckl. & Zeyh.) Urton**	Stems	DCM/MeOH (1:1)	P09326B	13.5	0.0	45.2	22.1	26.5	14.8	50.9	2.3
Apocynaceae	***Sarcostemma viminale* (L.) R.Br.**	Leaves	MeOH	P00363C	18.1	2.2	33.4	15.3	36.4	20.4	49.6	7.4
Apocynaceae	***Sarcostemma viminale* (L.) R.Br.**	Stems	DCM	P01381A	12.1	0.0	40.1	27.4	38.4	23.8	70.0	2.7

					Percentage (%) growth inhibition							
					T. b. rhodesiense		*T. cruzi*		*L. donovani*		*P. falciparum*	
Family	**Species**	**Plant part**	**Extract type**	**Extract no.**	**10 µg/mL**	**2 µg/mL**	**10 µg/mL**	**2 µg/mL**	**10 µg/mL**	**2 µg/mL**	**10 µg/mL**	**2 µg/mL**
Apocynaceae	***Sarcostemma viminale* (L.) R.Br.**	Whole plant	DCM/MeOH (1:1)	P02503B	33.8	7.1	46.4	21.7	18.3	4.3	74.9	12.9
Apocynaceae	***Sarcostemma viminale* (L.) R.Br.**	Roots	DCM/MeOH (1:1)	P06980B	99.5	7.0	46.3	20.0	57.6	24.3	99.3	31.8
Asclepiadaceae	***Sarcostemma viminale* (L.) R.Br.**	Stems	DCM/MeOH (1:1)	P01381B	6.5	0.0	46.0	17.3	29.7	22.2	35.5	0.0
Asteraceae	***Schkuhria pinnata* (Lam.) Kuntze ex Thell.**	Whole plants	DCM/MeOH (1:1)	P03491B	99.4	97.1	67.4	16.9	69.7	0.0	100.0	73.8
Fabaceae	***Senna septemtrionalis* (Viv.) H.S.Irwin & Barneby**	Roots	DCM/MeOH (1:1)	P06145B	43.0	5.9	33.8	17.2	24.9	22.0	45.6	14.4
Fabaceae	***Senna septemtrionalis* (Viv.) H.S.Irwin & Barneby**	Stems	DCM/MeOH (1:1)	P06146B	98.5	11.4	37.5	10.7	23.8	15.0	45.4	15.3
Fabaceae	***Senna septemtrionalis* (Viv.) H.S.Irwin & Barneby**	Leaves	DCM/MeOH (1:1)	P06147B	39.7	9.7	40.2	18.7	33.9	13.4	83.7	18.5
Fabaceae	***Senna septemtrionalis***	Seeds	DCM/MeOH	P06148B	0.0	0.0	34.7	12.7	0.5	0.0	33.6	11.4

					Percentage (%) growth inhibition							
					T. b. rhodesiense		*T. cruzi*		*L. donovani*		*P. falciparum*	
Family	**Species**	**Plant part**	**Extract type**	**Extract no.**	**10 µg/mL**	**2 µg/mL**	**10 µg/mL**	**2 µg/mL**	**10 µg/mL**	**2 µg/mL**	**10 µg/mL**	**2 µg/mL**
	(Viv.) H.S.Irwin & Barneby		(1:1)									
Apiaceae	***Steganotaenia araliacea* Hochst. var. *araliacea***	Roots	DCM	P00758A	20.6	0.0	52.5	44.4	35.1	24.3	64.9	11.0
Malvaceae	***Sterculia rogersii* N.E.Br.**	Leaves	DCM/MeOH (1:1)	P03870B	100.0	13.0	32.8	8.6	44.7	18.4	61.6	18.6
Malvaceae	***Sterculia rogersii* N.E.Br.**	Roots	DCM/MeOH (1:1)	P03872B	14.1	5.9	35.8	13.8	39.9	14.7	42.4	15.6
Malvaceae	***Sterculia rogersii* N.E.Br.**	Bark	DCM/MeOH (1:1)	P03873B	32.9	33.7	25.1	12.5	62.0	18.4	91.9	30.2
Rutaceae	***Toddalia asiatica* (L.) Lam.**	Roots	DCM/MeOH (1:1)	P00599B	98.1	0.0	45.4	17.4	36.0	20.8	94.2	25.6
Rutaceae	***Toddalia asiatica* (L.) Lam**	Leaves & twigs	DCM/MeOH (1:1)	P02460B	16.7	0.0	40.3	14.2	53.5	20.2	68.5	14.3
Ulmaceae	***Trema orientalis (L.)* Blume**	Leaves	DCM/MeOH (1:1)	P11527B	98.3	0.0	82.3	10.9	100.0	27.6	94.5	24.3
Ulmaceae	***Trema orientalis (L.)* Blume**	Flowers	DCM/MeOH (1:1)	P11528B	3.6	0.0	36.2	14.3	41.7	23.0	85.0	21.2
Ulmaceae	***Trema orientalis (L.)***	Roots	DCM/MeOH	P11529B	14.4	2.2	49.7	27.3	34.0	17.1	74.5	13.2

					Percentage (%) growth inhibition							
					T. b. rhodesiense		*T. cruzi*		*L. donovani*		*P. falciparum*	
Family	**Species**	**Plant part**	**Extract type**	**Extract no.**	**10 µg/mL**	**2 µg/mL**	**10 µg/mL**	**2 µg/mL**	**10 µg/mL**	**2 µg/mL**	**10 µg/mL**	**2 µg/mL**
	Blume		(1:1)									
Ulmaceae	***Trema orientalis (L.)* Blume**	Stems	DCM/MeOH (1:1)	P11530B	11.7	3.1	46.9	18.3	0.0	19.2	88.8	27.1
Meliaceae	***Turraea floribunda* Hochst.**	Bark	DCM/MeOH (1:1)	P05214B	93.5	12.8	28.3	15.6	28.4	20.4	89.9	39.9
Meliaceae	***Turraea floribunda* Hochst.**	Leaves	DCM/MeOH (1:1)	P05294B	100.0	14.2	38.1	22.3	39.7	22.2	78.3	27.4
Meliaceae	***Turraea floribunda* Hochst.**	Roots	DCM/MeOH (1:1)	P05329B	64.4	10.0	18.3	18.8	53.6	21.3	98.9	58.6
Rubiaceae	***Vangueria infausta* Burch. *subsp. infausta***	Fruits	DCM	P00008A	29.5	18.9	31.2	7.4	0.0	0.0	35.7	3.1
Rubiaceae	***Vangueria infausta* Burch. *subsp. infausta***	Fruits	DCM/MeOH (1:1)	P00008B	21.6	13.3	43.1	14.1	23.1	20.0	33.6	2.6
Rubiaceae	***Vangueria infausta* Burch. *subsp. infausta***	Fruits	MeOH	P00008C	17.3	7.6	45.0	16.0	31.5	21.4	30.4	0.0
Rubiaceae	***Vangueria infausta* Burch. *subsp. infausta***	Roots	DCM/MeOH (1:1)	P09344B	17.4	5.2	37.4	14.6	16.8	0.0	44.6	14.1

					Percentage (%) growth inhibition							
					T. b. rhodesiense		*T. cruzi*		*L. donovani*		*P. falciparum*	
Family	**Species**	**Plant part**	**Extract type**	**Extract no.**	**10 µg/mL**	**2 µg/mL**	**10 µg/mL**	**2 µg/mL**	**10 µg/mL**	**2 µg/mL**	**10 µg/mL**	**2 µg/mL**
Rubiaceae	***Vangueria infausta* Burch. *subsp. infausta***	Stems	DCM/MeOH (1:1)	P09345B	22.2	10.2	38.1	14.9	38.1	17.3	43.9	11.6
Rubiaceae	***Vangueria infausta* Burch. *subsp. infausta***	Leaves	DCM/MeOH (1:1)	P09346B	99.2	0.0	36.9	10.5	45.5	19.8	52.9	15.2
Asteraceae	***Vernonia mespilifolia* Less**	Leaves	DCM/MeOH (1:1)	P11137B	100.0	100.0	90.1	34.5	100.0	29.5	96.6	32.5
Asteraceae	***Vernonia mespilifolia* Less**	Stems	DCM/MeOH (1:1)	P11138B	95.1	0.0	35.1	25.9	84.5	29.8	55.8	8.4
Asteraceae	***Vernonia mespilifolia* Less**	Roots	DCM/MeOH (1:1)	P11139B	16.8	0.0	38.9	21.5	36.4	26.1	48.4	9.6
Asteraceae	***Vernonia myriantha* Hook.f.**	Roots	DCM	P00170A	7.7	0.0	37.4	14.5	0.0	0.0	36.9	15.8
Asteraceae	***Vernonia myriantha* Hook.f.**	Roots	DCM/MeOH (1:1)	P00170B	13.6	4.3	46.0	24.6	32.5	17.0	37.0	12.2
Asteraceae	***Vernonia myriantha* Hook.f.**	Leaves	DCM	P00171A	8.6	0.0	36.5	19.3	39.0	16.6	59.5	7.5
Asteraceae	***Vernonia myriantha* Hook.f.**	Leaves	DCM/MeOH (1:1)	P00171B	1.5	0.0	30.5	22.1	36.0	21.5	29.2	1.9

					Percentage (%) growth inhibition							
					T. b. rhodesiense		*T. cruzi*		*L. donovani*		*P. falciparum*	
Family	**Species**	**Plant part**	**Extract type**	**Extract no.**	**10 µg/mL**	**2 µg/mL**	**10 µg/mL**	**2 µg/mL**	**10 µg/mL**	**2 µg/mL**	**10 µg/mL**	**2 µg/mL**
Asteraceae	***Vernonia myriantha* Hook.f.**	Leaves	MeOH	P00171C	0.2	0.0	39.1	23.5	36.4	26.5	26.3	6.2
Asteraceae	***Vernonia myriantha* Hook.f.**	Stems	DCM	P00172A	5.3	0.0	40.0	17.0	37.4	25.6	32.6	14.9
Asteraceae	***Vernonia myriantha* Hook.f.**	Stems	MeOH	P00172C	0.0	0.0	43.2	14.8	32.6	21.1	17.0	0.0
Asteraceae	***Vernonia myriantha* Hook.f.**	Seeds	DCM	P00173A	0.0	0.0	39.6	20.0	35.7	19.0	32.9	0.4
Asteraceae	***Vernonia myriantha* Hook.f.**	Seeds	DCM/MeOH (1:1)	P00173B	0.0	0.0	35.8	18.1	38.0	22.1	36.9	0.1
Olacaceae	***Ximenia caffra* Sond. var. *caffra***	Leaves	DCM/MeOH (1:1)	P03508B	25.3	15.2	42.7	17.3	33.9	26.7	51.9	0.0
Olacaceae	***Ximenia caffra* Sond. var. *caffra***	Twigs	DCM/MeOH (1:1)	P03509B	40.7	0.0	32.7	10.8	0.0	0.0	50.1	9.2
Rutaceae	***Zanthoxylum capense* (Thunb.) Harv.**	Leaves	DCM/MeOH (1:1)	P07947B	34.0	0.0	39.5	16.6	46.1	30.1	99.7	38.8
Rutaceae	***Zanthoxylum capense* (Thunb.) Harv.**	Stems	DCM/MeOH (1:1)	P07948B	27.5	5.7	39.0	18.8	51.7	27.0	95.4	40.0

					Percentage (%) growth inhibition							
					T. b. rhodesiense		*T. cruzi*		*L. donovani*		*P. falciparum*	
Family	**Species**	**Plant part**	**Extract type**	**Extract no.**	**10 µg/mL**	**2 µg/mL**	**10 µg/mL**	**2 µg/mL**	**10 µg/mL**	**2 µg/mL**	**10 µg/mL**	**2 µg/mL**
Rutaceae	***Zanthoxylum capense* (Thunb.) Harv.**	Roots	DCM/MeOH (1:1)	P07949B	11.6	34.3	44.2	7.2	47.5	29.3	86.1	32.5
Rutaceae	***Zanthoxylum capense* (Thunb.) Harv.**	Fruits	DCM/MeOH (1:1)	P07950B	7.2	0.0	37.1	19.8	36.2	27.9	70.0	14.3
Rutaceae	***Zanthoxylum davyi* (I.Verd.) P.G.Waterman**	Leaves	DCM/MeOH (1:1)	P10430B	49.3	2.2	35.7	12.7	88.9	30.3	82.2	25.4
Rutaceae	***Zanthoxylum davyi* (I.Verd.) P.G.Waterman**	Fruits	DCM/MeOH (1:1)	P10431B	5.2	0.0	32.0	7.9	30.4	26.1	44.3	8.5
Rutaceae	***Zanthoxylum davyi* (I.Verd.) P.G.Waterman**	Stems	DCM/MeOH (1:1)	P10432B	23.7	14.8	39.0	18.4	34.3	16.9	84.0	30.1

Purification and isolation of schkuhrin I and schkuhrin II

The (DCM/MeOH; 1:1) extract of *Schkuhria pinnata* (8.0 g) was suspended in a mixture of methanol and dichloromethane and chromatographed on silica gel 60 (80 g). The column was initially eluted with a mixture of hexane (Hex) and ethyl acetate (EtOAc) (1:1). Twenty fractions of 50 mL each were collected and thereafter the polarity was increased to Hex:

EtOAc (4:6) and a further twenty-six fractions collected. Finally, the polarity was increased to 100% EtOAc and 30% methanol (MeOH), respectively. The collected fractions were analysed using thin-layer chromatography (TLC) plates and similar fractions were combined resulting in twelve (A-L) fractions. Semipreparative RP-HPLC purification was employed using a SunFire™ C18 column (3.5 µm, 10 × 150 mm; Waters) with H_2O (solvent A) and MeCN (solvent B) to give fraction I (950 mg) and fraction J (300 mg) which were further purified to yield schkuhrin I (**1**) (250 mg) and schkuhrin II (**2**) (120 mg), respectively. The structures and stereochemistry of **1** [6] and **2** [6] were compared to that of published data and the purity of the compounds was > 95% as determined by the NMR data.

Purification and isolation of cynaropicrin (3)

The (DCM/MeOH; 1:1) extract of *Vernonia mespilifolia* (1.0 g) was suspended in chloroform and chromatographed on silica gel 60 (10 g). The column was eluted with a mixture of hexane (Hex) and ethylacetate (EtOAc) (6:4). Finally, the polarity was increased to 30% methanol (MeOH). The collected fractions (50 mL) were monitored by TLC and similar fractions were combined. Fraction J (30 mg) was further purified by semipreparative RP-HPLC using a SunFire™ C18 column (3.5 µm, 10 × 150 mm; Waters) with H_2O (solvent A) and MeCN (solvent B), resulting in the isolation of cynaropicrin (**3**) (11.0 mg). The structure of **3** [7] was compared to that of published data and the purity of cynaropicrin (**3**) was > 95% as determined by NMR.

Bioassays

a. In vitro* test against *Trypanosoma brucei rhodesiense

Trypanosoma brucei rhodesiense (STIB 900) were grown in axenic medium as previously described [3].The compounds were tested using a modified Alamar Blue assay protocol [4] to determine the 50% inhibitory concentration (IC_{50}). Serial threefold drug dilutions were prepared in 96-well microtitre plates and 50 µL of *T. b. rhodesiense* STIB 900 bloodstream

forms were added to each well except for the negative controls. Melarsoprol (Arsobal®; Sanofi-Aventis) was used as a reference drug. After 70 h of incubation, the Alamar Blue marker (12.5 mg resazurin dissolved in 100 mL distilled water) was added. The plates were then incubated for an additional 2 to 5 h. A Spectramax Gemini XS microplate fluorescence reader (Molecular Devices Cooperation) with an excitation wavelength of 536 nm and an emission wavelength of 588 nm was used to read the plates. The IC_{50} values were calculated from the sigmoidal growth inhibition curves using Softmax Pro software (Molecular Devices).

b. In vitro testing against *Plasmodium falciparum*

A modification of the [^{3}H]-hypoxanthine incorporation assay was used to determine the intra-erythrocyticantiplasmodial activity (Desjardins 1979) of the extract library and purified compounds in 96-well plates. Chloroquine (Sigma-Aldrich) and artesunate (Mepha) were used as standard drugs. Briefly, infected human red blood cells in RPMI 1640 medium (100 µL per well with 2.5% haematocrit and 0.3% parasitaemia) were exposed to twofold serial drug dilutions in 96-well microtitre plates. After 48 h incubation, 0.5 µCi [^{3}H]-hypoxanthine was added to each well. The plates were incubated for a further 24 h before being harvested using a Betaplate cell harvester (Wallac) The radioactivity was counted with a Betaplate liquid scintillation counter (Wallac) as counts per minute per well at each drug concentration and compared to the untreated controls. IC_{50} values were calculated from sigmoidal inhibition curves using Microsoft Excel. All assays were run in duplicate and repeated three times [5].

c. In vitro cytotoxicity testing

Cytotoxicity was assessed using a similar Alamar Blue assay protocol [3] whereby 4000 rat myoblast cells/well were seeded in RPMI 1640 medium. All following steps were according to the *T.b. rhodesiense* protocol. Podophyllotoxin (Sigma-Aldrich) was used as the reference drug.

References

[1] *Wagner H, Bladt S*. Plant Drug Analysis. A thin layer Chromatography Atlas, 2nd edition. Berlin: Springer-Verlag, 1996: 359

[2] *Adams M, Plitzko I, Kaiser M, Brun R, Hamburger M*. HPLC-profiling for antiplasmodial compounds – 3-methoxy carpachromene from *Pistacia atlantica*. Phytochem Lett. 2009; 2: 159-162

[3] *Baltz T, Baltz D, Giroud C, Crockett J*. Cultivation in a semidefined medium of animal infective forms of *Trypanosoma brucei*, *T. equiperdum, T. evansi*, *T. rhodesiense*, *T. gamiense.* EMBO J 1985; 4: 1273- 1277

[4] *Räz B, Hen M, Grether-Bühler Y, Kaminsky R, Brun R*. The Alamar Blue assay to determine drug sensivity of African trypanosomes *in vitro*. Acta Trop 1997; 68: 139-147

[5] *Desjardins RE, Canfield CJ, Haynes JD, Chulay JD*. Quantitative assessment of antimalarial activity *in vitro* by a semiautomated microdilution technique. Antimicrob Agents Chemother 1979; 16: 710-718

[6] *Pacciaroni ADV, Sosa VE, Espinar LA, Oberti JC*. Sesquiterpene lactones from *Schkuhria pinnata.* Phytochemistry 1995; 39: 127-131

[7] *Bernhard HO*. Quantitative determination of bitter sesquiterpenes from *Cynara scolymus* L. and *Cynara cardunculus* L. Pharm Acta Helv 1982; 57: 179–180

3.3 Antiprotozoal Isoflavan Quinones from *Abrus precatorius* ssp. *africanus*

Yoshie Hata, Melanie Raith, Samad Nejad Ebrahimi, Stefanie Zimmermann, Tsholofelo Mokoka, Dashnie Naidoo, Gerda Fouche, Vinesh Maharaj, Marcel Kaiser, Reto Brun, Matthias Hamburger

Planta Med., 2013, 79: 492–498. DOI: 10.1055/s-0032-1328298

HPLC-based activity profiling allowed the identification of 5 isoflavanquinones from *Abrus precatorius*. Two of them were new compounds and one was a new natural product. Abruquinones I and B showed strong *in vitro* activity against *Trypanosoma brucei rhodesiense* and remarkable selectivity. These results classified abruquinones I and B for *in vivo* evaluation of their trypanocidal activity.

My contributions to this work were: (1) HPLC microfractionation; (2) isolation of isoflavanquinones; (3) recording and interpretation of analytical data for structure elucidation (HPLC-PDA-ESI-MS, TOF-MS, 1D and 2D NMR, CD measurements) and other measurements such as optical rotation; (4) writing of the first draft of the manuscript, preparation of figures, tables, and supporting information.

Samad Ebrahimi did the quantum-chemical calculation of ECD spectra, and under his supervision I participated in the respective data analysis. Melanie Raith supervised structure elucidation. In vitro tests were performed by Stefanie Zimmermann and the team of the Swiss TPH. The crude extract was provided by the CSIR team.

Yoshie Hata-Uribe

Antiprotozoal Isoflavan Quinones from *Abrus precatorius* ssp. *africanus*

Authors Yoshie Hata[1,4], Melanie Raith[1], Samad Nejad Ebrahimi[1,5], Stefanie Zimmermann[1,2], Tsholofelo Mokoka[3], Dashnie Naidoo[3], Gerda Fouche[3], Vinesh Maharaj[3], Marcel Kaiser[2], Reto Brun[2], Matthias Hamburger[1]

Affiliations The affiliations are listed at the end of the article

Key words
- antiprotozoal
- *Trypanosoma brucei rhodesiense*
- isoflavan quinone
- *Abrus precatorius*
- Fabaceae
- electronic circular dichroism

Abstract

A library of 206 extracts from selected South African plants was screened *in vitro* against a panel of protozoan parasites, *Plasmodium falciparum, Trypanosoma brucei rhodesiense*, and *Leishmania donovani*. A CH_2Cl_2/MeOH (1 : 1) extract of *Abrus precatorius* L. ssp. *africanus* strongly inhibited *P. falciparum* (98%), *T. b. rhodesiense* (100%), and *L. donovani* (76%) when tested at a concentration of 10.0 µg/mL. The active constituents were tracked by HPLC-based activity profiling and isolated by preparative and semipreparative RP-HPLC chromatography. Structures were established by HR-ESIMS, and 1D and 2D NMR (^{1}H, ^{13}C, COSY, HMBC, HSQC, and NOE difference spectroscopy). Five compounds were obtained and identified as two isoflavan hydroquinones, abruquinone H (**1**) and abruquinone G (**2**), and three isoflavan quinones, abruquinone I (**3**), abruquinone B (**4**), and 7,8,3′,5′-tetramethoxyisoflavan-1′,4′-quinone (**5**). Compounds **1** and **3** were new natural products. The absolute configuration of compounds was determined by comparison of electronic circular dichroism spectra with calculated ECD data. Compounds **3** and **4** showed strong activity against *T. b. rhodesiense* (IC_{50} values of 0.30 and 0.16 µM, respectively) and good selectivity (selectivity indices of 73.7 and 50.5, respectively).

Abbreviations

NTDs:	neglected tropical diseases
HAT:	human African trypanosomiasis
DALYS:	disability-adjusted life years
ELSD:	evaporative light scattering detector
HR-ESIMS:	high-resolution electrospray ionization mass spectrometry
AC:	absolute configuration
ECD:	electronic circular dichroism
CE:	Cotton effect
DTF:	density functional theory
TD-DFT:	time-dependent density functional theory
CPCM:	conductor polarized continuum model
SCRF:	self-consistent reaction field
OPLS:	optimized potential for liquid simulations
B3LYP:	Becke, 3-parameter, Lee-Yang-Parr

Supporting information available online at http://www.thieme-connect.de/ejournals/toc/plantamedica

received July 18, 2012
revised January 9, 2013
accepted February 7, 2013

Bibliography
DOI http://dx.doi.org/10.1055/s-0032-1328298
Published online March 19, 2013
Planta Med 2013; 79: 492–498

ISSN 0032-0943

Correspondence
Prof. Matthias Hamburger
Division of Pharmaceutical Biology
University of Basel
Klingelbergstrasse 50
4056 Basel
Switzerland
Phone: + 41/61/2671425
Fax: + 41/61/2671474
matthias.hamburger@unibas.ch

Introduction

NTDs affect the lives of a billion people worldwide, in particular in developing countries. Some of these are caused by protozoan parasites, such as HAT, leishmaniasis, malaria, and Chagas disease. The responsible parasites are *Trypanosoma brucei rhodesiense* and *T. b. gambiense* (HAT), *Leishmania sp., Plasmodium spp.* (*P. falciparum, P. vivax, P. ovale, P. malariae,* and *P. knowlesi*), and *Trypanosoma cruzi*, respectively [1,2]. These diseases cause an enormous burden, and according to the WHO, HAT is accountable for 1 673 000, leishmaniasis for 1 974 000, malaria for 33 976 000 and Chagas for 430 000 DALYs [1,3]. Drugs currently available to treat these illnesses are old, limited in efficacy, and cause severe side effects [4,5]. Hence, new drugs with better therapeutic profiles are urgently needed.

Natural products such as quinine and artemisinin have significantly contributed to the development of modern antiprotozoal drugs. We have recently embarked on a library-based discovery of natural product leads with antiprotozoal activity [6–9]. In

a library of 206 extracts prepared from ethnobotanically preselected medicinal plants from South Africa, a CH_2Cl_2/MeOH (1 : 1) extract from aerial parts of *Abrus precatorius* L. ssp. *africanus* Verdc. (Fabaceae) strongly inhibited *P. falciparum* (98%), *T. b. rhodesiense* (100%), and *L. donovani* (76%) when tested at a concentration of 10.0 µg/mL. In contrast, it did not show inhibition against *T. cruzi*.

A. precatorius is a climber shrub native from India but now also grows in other regions of the world [10–12]. The seeds are highly toxic due to abrin, a ribosome-inactivating lectin [10]. However, leaves and roots are used in folk medicine to treat different conditions like skin diseases, hepatitis, bronchitis, laryngitis, and malaria [13–15]. Antiplatelet, anti-inflammatory, antiallergic [13], antimalarial [14, 15], and antitubercular activities [16] have been reported. A spectrum of secondary metabolites have been identified from *A. precatorius*, including triterpenoids [12, 17, 18], alkaloids [19], flavonoids [12, 20], and isoflavanquinones [11, 13, 16, 21]. We report here on the localization and identification of active isoflavan quinones from the extract with the aid of HPLC-based activity profiling [6, 22], determination of absolute configuration by ECD, and *in vitro* testing of pure compounds.

Materials and Methods

General experimental procedures

HPLC-grade methanol (MeOH), acetonitrile (MeCN) (Scharlau Chemie S.A.), and water (obtained by an EASY-pure II from Barnstead water purification system) were used for HPLC separations. HPLC solvents contained 0.1% HCOOH (Sigma) for analytical separations. Chloroform-*d* (100 atom% D) and methanol-d_4 (100 atom% D) for NMR were purchased from Armar Chemicals. Solvents used for extraction were of analytical grade (Romil Pure Chemistry). Reference drugs for bioassays were artesunate (purity > 95%; Mepha), melarsoprol (purity > 95%; Sanofi-Aventis), benznidazole (purity > 95%; Sigma-Aldrich), miltefosine (purity > 95%; VWR), and podophyllotoxin (purity > 95%; Sigma-Aldrich). HPLC-PDA-MS analyses were performed with an Agilent 1100 system consisting of a degasser, a quaternary pump, a column oven, a PDA detector connected to a Gilson 215 injector and to an Esquire 3000 plus ion trap mass spectrometer (Bruker Daltonics). Data acquisition and processing were performed using HyStar 3.0 software (Bruker Daltonics). Preparative HPLC was carried out on a Shimadzu LC-8A instrument equipped with a SCL-10A VP system controller, an LC-8A pump, an SPD-M10A VP PDA detector, and VP 6.14 SP2A control software. Semipreparative HPLC was performed with an Agilent 1100 series instrument equipped with a PDA detector. Data acquisition and processing were performed using HyStar 3.2 software (Bruker Daltonics). Chromatographic purity of the isolated compounds was assessed on an Alliance 2695 HPLC system (Waters) equipped with 996 PDA (Waters) and Alltech 2000ES ELSD detectors. For HR-ESIMS, a micrOTOF ESI-MS system (Bruker Daltonics) was used. Mass calibration was performed with a solution of formic acid 0.1% in 2-propanol/water (1 : 1) containing 5 mM NaOH. Mass spectra were recorded in the range of *m/z* 150–1500 in the positive ion mode with the aid of micrOTOF control software 1.1 (Bruker Daltonics). NMR spectra were recorded on a Bruker AVANCE III™ 500 MHz spectrometer equipped with a 1-mm TXI microprobe (^{1}H and 2D NMR) or a 5-mm BBO probe (^{13}C NMR) (Bruker BioSpin) operating at 500 (^{1}H) and 125 MHz (^{13}C). Chemical shifts are reported as δ values (ppm) with the residual solvent signal as the internal reference, *J* in Hz. Standard pulse sequences from Topspin 2.1 software package were used. Further spectroscopic data were acquired on a Hewlett Packard 8453 photometer (UV), an AVIV CD spectrometer Model 62ADS (CD), and a Perkin Elmer polarimeter (model 341) equipped with a 1-dm microcell (OR).

Plant material

Samples of the whole plant of *A. precatorius* were collected at Jozini, KwaZulu Natal Province in South Africa during November 2001 by a botanist, Mr. Hans Vahrmeijer. A plant specimen was deposited at the South African National Biodiversity Institute (SANBI), and the plant was identified as *Abrus precatorius* L. ssp. *africanus* Verdc. (Fabaceae) (voucher specimen number PRE 442421).

Extraction

The whole plant was dried in an oven at 30–60 °C. Dried plant material was ground to a coarse powder using a hammer mill and stored at ambient temperature prior to extraction. 200 g of dried, ground material was extracted with 1 L of a mixture of CH_2Cl_2 and MeOH (1 : 1) at room temperature for 1 h with occasional stirring. The solvent was filtered, and the residual plant material was further extracted overnight with 500 mL CH_2Cl_2/MeOH (1 : 1) followed by filtration. Finally, a third extraction of the pulp was done with 500 mL solvent for 1 h with filtration. The pulp was discarded, and the filtrates combined and concentrated using a rotary vacuum evaporator at a temperature below 45 °C and then further dried *in vacuo* at room temperature for 24 h. The dried extract of 15.4 g (7.7%, w/w) was stored at − 20 °C.

Microfractionation and activity profiling

Microfractionation for HPLC-activity profiling was performed as previously described [6], on a SunFire™ C18 column (3.5 µm, 3.0 × 150 mm; Waters) with H_2O (solvent A) and MeCN (solvent B) using the following gradient profile: 10% → 100% B (0–30 min), 100% B (31–32 min). The flow rate was 0.5 mL/min. 35 µL of a solution of the extract (10 mg/mL in DMSO) was injected. 32 one-minute fractions were collected by the aid of a F204 fraction collector (Gilson) into a 96-deep-well plate (Eppendorf). After solvent removal in an Evaporex 96 channel N_2-evaporator (Apricot Designs), the dried fractions were redissolved in methanol (100 µL) and transferred to 96-v-well plates (Thermo Scientific), dried again, and stored in a refrigerator (2–8 °C) until assayed.

Preparative isolation of abruquinones

For isolation of compounds, 850 mg of a CH_2Cl_2/MeOH (1 : 1) extract of the whole plant was separated in a SunFire™ RP-C18 column (5 µm, 30 mm × 150 mm; Waters) with a gradient consisting of H_2O (solvent A) and MeOH (solvent B) as follows: 10% → 100% B (0–30 min), 100% B (31–35 min). The flow rate was 20 mL/min. The extract was dissolved in DMSO at a concentration of 100 mg/mL, and aliquots of 380 µL were injected. Fraction 1 (28.1 mg, t_R 21.0 min), fraction 2 (33.2 mg, t_R 22.8 min), fraction 3 (29.8 mg, t_R 23.8 min), and fraction 4 (47.6 mg, t_R 25.3 min) were collected and purified by semipreparative RP-HPLC using a SunFire™ C18 column (3.5 µm, 10 × 150 mm; Waters) with H_2O (solvent A) and MeCN (solvent B) and the following gradient: 10% → 100% B (0–30 min), 100% B (31–35 min). The flow rate was 5 mL/min. The fractions were dissolved in DMSO (10 and 20 mg/mL, depending on their solubility) and injected in aliquots of 250 µL. Compound

Table 1 ^{1}H and ^{13}C NMR spectroscopic data for compounds **1** and **3** (500 MHz for δ_H, 125 MHz for δ_C).

Position	1[a]		1[b]		3[a]	
	δ_H	δ_C[c]	δ_H	δ_C	δ_H	δ_C
2α	4.30 (dd, 10.7, 5.1)	66.6	4.50 (dd, 10.7, 4.7)	67.7	4.21 (ddd, 10.7, 3.4, 2.1)	68.2
2β	3.66 (dd, 10.7, 11.1)		3.86 (dd, 10.7,10.7)		4.43 (dd, 10.7,10.4)	
3	3.51 (1H, m)	40.9	3.77 (1H, m)	42.4	3.60 (1H, m)	31.3
4	5.43 (d, 7.0)	78.1	5.68 (d, 7.0)	80.8	Hα 3.12 (dd, 15.5, 12.3) Hβ 2.65 (ddd, 15.5, 4.7, 1.8)	29.3
5	6.62 (1H, s)	103.9	6.85 (1H, s)	104.8	6.49 (d, 8.9)	119.2
6	–	147.7	–	149.4	6.44 (d, 8.5)	104.5
7	–	137.5	–	139.0	–	134.2
8	–	nd[d]	–	140.6	–	145.7
9	–	138.3	–	140.7	–	142.3
10	–	114.8	–	116.8	–	115.8
1′	–	143.6	–	145.0	–	186.8
2′	–	136.9	–	141.4	5.82 (1H, s)	107.6
3′	–	139.0	–	139.6	–	157.4
4′	–	nd[d]	–	146.1	–	178.3
5′	6.58 (1H, s)	105.0	6.79 (1H, s)	107.4	–	155.9
6′	–	122.4	–	124.6	–	131.3
2′- OCH_3	3.89 (3H, s)	60.9	4.04 (3H, s)	61.7	–	–
3′- OCH_3	3.96 (3H, s)	60.9	4.13 (3H, s)	61.0	3.77 (3H, s)	56.6
5′- OCH_3	–	–	–	–	3.93 (3H, s)	61.7
6- OCH_3	3.85 (3H, s)	56.3	4.02 (3H, s)	56.8	–	–
7- OCH_3	3.90 (3H, s)	60.3	4.05 (3H, s)	61.3	3.83 (3H, s)	56.7
8-OH	–	–	–	–	5.43 (br s)	

[a] In $CDCl_3$; [b] in CD_3OD; [c] ^{13}C NMR signals reported here were obtained indirectly from HSQC and HMBC spectra; [d] not detected

1 (1.7 mg, t_R 12.0 min) was obtained from fraction 1. Compounds **2** (3.9 mg, t_R 14.6 min) and **3** (5.8 mg, t_R 14.3 min) were isolated from fraction 2. Compounds **4** (14.7 mg, t_R 16.2 min) and **5** (2.4 mg, t_R 16.8 min) were purified from fractions 3 and 4, respectively. Purity of compounds **1** and **3**-**5** was > 95% as determined by ^{1}H-NMR and HPLC-ELSD analyses. Compound **2** showed a single peak in HPLC analysis, but the ^{1}H NMR spectrum revealed the presence of about 15% of an unidentified related metabolite (**Fig. 5S**, Supporting Information).

(3S-4R)-4,8,1′,4′-tetrahydroxy-6,7,2′,3′-tetramethoxyisoflavan (*abruquinone H*, **1**): Colorless amorphous substance; UV (MeOH): λ_{max} (log ε) = 206 (4.59), 295 (3.67) nm; $[\alpha]_D^{18}$: − 192 (*c* = 0.1, MeOH); CD (MeOH): $\Delta\varepsilon_{212\,nm} = -31.5$, $\Delta\varepsilon_{238\,nm} = -6.89$ (sh), $\Delta\varepsilon_{285\,nm} = -1.02$, $\Delta\varepsilon_{302\,nm} = +1.43$; ^{1}H and ^{13}C NMR data in $CDCl_3$ and CD_3OD, see ◉ **Table 1**; HR-ESIMS: *m/z* = 399.1023 [M − H_2O + Na]$^+$ (calcd. for $C_{19}H_{22}NaO_9$: 399.1050).

(3S-4R)-4,1′,4′-trihydroxy-6,7,8,2′,3′-pentamethoxyisoflavan (*abruquinone G,* **2**) [16]: For physicochemical characterization, see Supporting Information. $[\alpha]_D^{18}$: − 59.9 (*c* = 0.1, MeOH); CD (MeOH): $\Delta\varepsilon_{215\,nm} = -49.0$; $\Delta\varepsilon_{232\,nm} = -12.2$; $\Delta\varepsilon_{285\,nm} = -2.24$; $\Delta\varepsilon_{304\,nm} = +4.35$.

(3R)-8-hydroxy-7,3′,5′-trimethoxyisoflavan-1′,4′-quinone (*abruquinone I,* **3**): Yellow amorphous substance; UV (MeOH): λ_{max} (log ε) = 205 (4.58), 286 (4.07) nm; $[\alpha]_D^{19}$: + 21.0 (*c* = 0.1, MeOH); CD (MeOH): $\Delta\varepsilon_{212\,nm} = +8.40$, $\Delta\varepsilon_{215\,nm} = +4.84$, $\Delta\varepsilon_{233\,nm} = -0.62$, $\Delta\varepsilon_{256\,nm} = +0.20$, $\Delta\varepsilon_{283} = -0.20$, $\Delta\varepsilon_{305\,nm} = +0.06$; ^{1}H and ^{13}C NMR data in $CDCl_3$, see ◉ **Table 1**; HR-ESIMS: *m/z* = 369.0908 [M + Na]$^+$ (calcd. for $C_{18}H_{18}NaO_7$: 369.0945).

(3R)-6,7,8,2′,3′-pentamethoxyisoflavan-1′,4′-quinone (*abruquinone B,* **4**) [11,13,16,21]: For physicochemical characterization, see Supporting Information. $[\alpha]_D^{20}$: − 9.0 (*c* = 0.1, $CHCl_3$); $[\alpha]_D^{19}$: − 65.0 (*c* = 0.1, MeOH); CD (MeOH): $\Delta\varepsilon_{212\,nm} = -7.46$; $\Delta\varepsilon_{258\,nm} = -4.45$; $\Delta\varepsilon_{293\,nm} = +1.92$; $\Delta\varepsilon_{312\,nm} = -0.22$; $\Delta\varepsilon_{393\,nm} = +0.55$.

(3S)-7,8,3′,5′-tetramethoxyisoflavan-1′,4′-quinone (**5**) [23]: For physicochemical characterization, see Supporting Information. $[\alpha]_D^{20}$: − 1.3 (*c* = 0.1, $CHCl_3$); $[\alpha]_D^{19}$: − 19 (*c* = 0.1, MeOH); CD (MeOH): $\Delta\varepsilon_{216\,nm} = -6.74$; $\Delta\varepsilon_{238\,nm} = -3.62$; $\Delta\varepsilon_{274\,nm} = -0.37$; $\Delta\varepsilon_{294\,nm} = +0.39$.

Conformational analysis, geometrical optimization, and ECD calculation

Conformational analysis of **2, 3, 4**, and **5** was accomplished with Schrödinger MacroModel 9.1 software employing the OPLS 2005 (optimized potential for liquid simulations) force field in H_2O. Conformers within a 1 Kcal/mol energy window from the global minimum were picked for geometrical optimization and energy calculation applying DFT with the Becke's nonlocal three parameter exchange and correlation functional, and the Lee-Yang-Parr correlation functional level (B3LYP) using the 6–31 G** basis set in the gas phase with the Gaussian 09 program package [24]. Vibrational evaluation was done at the same level to confirm minima. Excitation energy (denoted by wavelength in nm), rotator strength dipole velocity (R_{vel}), and dipole length (R_{len}) were calculated in MeOH by TD-DFT/B3LYP/6–31 G**, using the SCRF method, with the CPCM model. ECD curves were obtained on the basis of rotator strengths with a half-band of 0.2 eV using SpecDis v1.51 [25]. The spectra were combined after Boltzmann weighting according to their population contribution.

Bioassays

The antiprotozoal activity of the CH_2Cl_2/MeOH (1 : 1) extract of *A. precatorius* was tested *in vitro* against *Plasmodium falciparum* (K1 strain), *Trypanosoma brucei rhodesiense* (STIB 900 strain), *Trypanosoma cruzi* (Tulahuen strain C2C4 w/LacZ), and *Leishmania donovani* (strain MHOM/ET/67/L82), in 96-well microtiter plates at concentrations of 10.0 µg/mL and 2.0 µg/mL. HPLC mi-

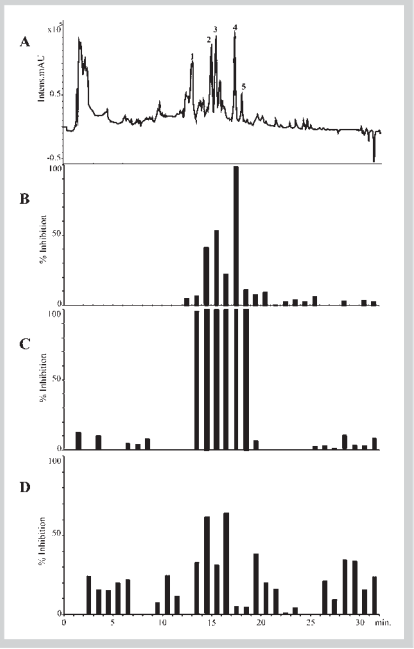

Fig. 1 HPLC-based activity profiling of *A. precatorius* extract for antiprotozoal properties. HPLC chromatogram (190–700 nm) for 32 one-minute fractions from 350 µg of extract (**A**) and inhibition (in %) of three different parasites *P. falciparum* (**B**), *T. b. rhodesiense* (**C**), and *L. donovani* (**D**) by the time-based collected fractions.

crofractionations were assayed against *P. falciparum, T. b. rhodesiense*, and *L. donovani*. Isolated compounds were evaluated for their antiprotozoal activity using the parasites as described above. Additionally, cytotoxicity was determined using the rat skeletal myoblast cell line (L-6 cells). For the assays, DMSO stock solutions (10 mg/mL) of extracts and purified compounds were each time freshly diluted in medium (final DMSO concentration in assay < 1%). Assays were performed with three independent repetitions, except for *L. donovani*. Details on culturing of parasites and assay protocols are provided as Supporting Information.

Supporting information

Detailed protocols of biological activity, NMR spectra (1D and 2D) of compounds **1** and **3**, ^{1}H NMR spectra of all compounds, physicochemical and spectroscopic data of compounds **2, 4**, and **5**, as well as experimental and calculated ECD spectra of all compounds are provided.

Results and Discussion

The CH_2Cl_2/MeOH (1 : 1) extract of *A. precatorius* inhibited *P. falciparum* (98%) and *L. donovani* (76%) at a concentration of 10.0 µg/mL. Additionally, it completely inhibited *T. b. rhodesiense* (100%) at 2.0 µg/mL. In contrast, the extract did not show any activity against *T. cruzi* at these concentrations. The extract was submitted to HPLC-based activity profiling using a previously validated protocol [6]. An aliquot (350 µg) of the extract was separated by analytical HPLC, and 32 one-minute microfractions were collected into a 96-deep-well plate. After drying, they were tested against *P. falciparum, L. donovani*, and *T. b. rhodesiense*. The HPLC chromatogram and the corresponding activity profiles are shown in **Fig. 1**. The chromatogram showed strong UV-absorbing peaks at t_{rs} = 12.9, 14.8, 15.3, 15.8, 17.3, and 18.0 min. In this time window (minutes 13–18), inhibition of *P. falciparum, L. donovani*, and *T. b. rhodesiense* was observed, corresponding to fractions 15 and 17 (*P. falciparum* by 54% and 99%, respectively), fractions 14 to 16 (*L. donovani* by 62% and 64%, respectively), and fractions 13 and 14 to 18 (*T. b. rhodesiense* by 99% to 100%).

Isolation of compounds **1**–**5** (**Fig. 2**) in the active time window was achieved by preparative RP-HPLC followed by final purification on semipreparative RP-HPLC. Structures were established by NMR spectroscopy (^{1}H, ^{13}C, COSY, HSQC, and HMBC), HR-ESIMS, and ECD. Compounds **2** [(3*S*-4*R*)-4,1′,4′-trihydroxy-6,7,8,2′,3′-pentamethoxyisoflavan] and **4** [(3*R*)-6,7,8,2′,3′-pentamethoxyisoflavan-1′,4′-quinone] have been reported as abruquinones G and B, respectively [11, 13, 16, 21]. Compound **5** [(3*S*)-7,8,3′,5′-tetramethoxyisoflavan-1′,4′-quinone] has been previously described as a synthetic derivative but not as a natural product [23]. Compounds **1** [(3*S*-4*R*)-4,8,1′,4′-tetrahydroxy-6,7,2′,3′-tetramethoxyisoflavan] and **3** [(3*R*)-8-hydroxy-7,3′,5′-trimethoxyisoflavan-1′,4′-quinone] are new and have been designated as abruquinone H and abruquinone I, respectively.

A molecular formula of $C_{19}H_{22}O_9$ for compound **1** was deduced from HR-ESIMS (*m/z* 399.1023 [M – H_2O + Na]$^+$; calcd.: 399.1050). The formula accounted for 9 degrees of unsaturation. The ^{1}H and ^{13}C NMR spectra (**Table 1**) showed 18 proton and 19 carbon signals, respectively. Twelve of the carbon signals were in the region between δ_C 103.9 and 147.7, and were indicative of a highly substituted aromatic ring system. The ^{1}H NMR spectrum in $CDCl_3$ (**Table 1**) displayed four singlets of aromatic methoxy groups (δ_H 3.96, 3.90, 3.89, and 3.85), in accordance with four carbon signals at δ_C 60.9, 60.9, 60.3, and 56.3. Additionally, the ^{1}H NMR spectrum showed four aliphatic signals at δ_H 5.43 (d, J = 7.0 Hz), 4.30 (dd, J = 10.7, 5.1 Hz), 3.66 (dd, J = 10.7, 11.1 Hz), and 3.51 (m), suggesting an isoflavan scaffold with a hydroxyl group at C-4. Unambiguous assignment of ^{1}H and ^{13}C NMR data was achieved by a combination of COSY, HMBC, HSQC, and NOE difference experiments, together with the comparison with reported data of abruquinones and -hydroquinones [11, 13, 16, 21]. The connectivity of the rings as well as the positions of the methoxy groups were determined with the aid of HMBC correlations (**Fig. 3**). The connectivity of rings A and C was confirmed by $^3J_{C-H}$ coupling between C-9 (δ_c 138.3) and H-5 (δ_H 6.62, ring A) and H-4 (δ_H 5.43, ring C). An HMBC correlation between H-3 (δ_H 3.51, ring C) and C-6′ (δ_c 122.4, ring B) corroborated the connectivity between rings B and C and the presence of an isoflavan scaffold. The vicinal coupling constants H-2α/H-3 (J = 5.1 Hz) and H-2β/H-3 (J = 11.1 Hz) corresponded to dihedral angles of 60° and 180°, respectively, indicating an axial orientation of H-3. The coupling constant H-4/H-3 (J = 7.0 Hz) agreed with a dihedral angle of 30 to 50° or 130 to 150°, indicating two possible orientations for H-4 in a half-chair. Both possible orientations – pseudo-axial or pseudo-equatorial – of H-4 are in accordance with the NOE effect observed between H-4 (δ_H 5.43) and H-3 (δ_H 3.51). The pseudo-axial orientation of H-4 was finally derived from the ECD spectrum in comparison with the calculated spectrum of compound **2** (see below).

The NMR spectra of compounds **1** and **2** were similar (**Table 1**; **Table 1S**, Supporting Information), the only major difference being in the substituent at C-8 (hydroxyl in **1** and methoxyl in **2**) [16].

The absolute configuration of **2** was established by comparing its experimental ECD spectrum with calculated data of the (3*S*,4*R*)- and (3*S*,4*S*)-diastereomers (**Fig. 4A**). Conformational analysis revealed 68 and 51 conformers, respectively, within a 1 Kcal/mol energy window from the particular global minimum. The conformers were subjected to geometrical optimization DTF and B3LYP level using the 6–31 G** basis set in the gas phase. Vibra-

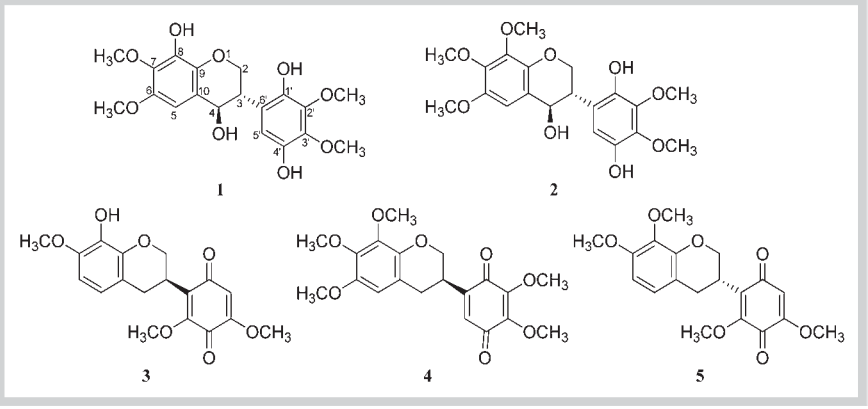

Fig. 2 Structures of compounds **1**–**5**.

tional analysis was performed to confirm minima. No imaginary frequencies were found. In total, 49 and 30 stable conformers, respectively, were obtained (**Fig. 4B**; **Fig. 14S A**, Supporting Information). ECD spectra of the conformers were calculated by TDDFT-B3LYP using 6–31 G** as basis set in MeOH as the solvent and the SCRF method with the CPCM model. For the (3*S*,4*R*)-stereoisomer, the calculated ECD spectrum showed one positive CE around 290 nm along with three negative CEs around 220, 250, and 285 nm (**Fig. 4A**). For the (3*S*,4*S*)-stereoisomer, the averaged ECD spectrum showed two positive CEs at 290 and 250 nm, and two negative CEs around 220 and 240 nm (**Fig. 4A**). Even though both spectra were relatively similar, the pattern for the (3*S*,4*R*)-stereoisomer matched well with the experimental ECD spectrum. In particular, the negative CEs at 220, 250, and 285 nm were in very good agreement with the experimental data. We thus concluded that **2** was (3*S*,4*R*)-abruquinone G. The experimental ECD spectrum of **1** was comparable to that of **2**, and we therefore conclude that abruquinone H also has the (3*S*,4*R*)-configuration.

Compound **3** had a molecular formula of $C_{18}H_{18}O_7$, as derived from HR-ESI-MS (*m/z* 369.0908 $[M + Na]^+$; calcd.: 369.0945). The ^1H and ^{13}C NMR spectra (**Table 1**) showed the presence of 18 proton and 18 carbon signals, respectively. Ten carbon signals in the region between δ_C 104.5 and 155.9 were indicative of a highly substituted aromatic ring system. Two resonances at δ_C 178.3 and 186.8 were indicative of conjugated carbonyl groups. The ^1H NMR spectrum (**Table 1**) showed three singlets for three methoxy groups (δ_H 3.93, 3.83, and 3.77), in agreement with the respective carbon signals at δ_C 61.7, 56.7, and 56.6. Five signals at δ_H 4.43 (dd, J = 10.7 and 10.4 Hz), 4.21 (ddd, J = 10.7, 3.4, 2.1 Hz), 3.60 (m), 3.12 (dd, J = 15.5, 12.3 Hz), and 2.65 (ddd, J = 15.5, 4.7, 1.8 Hz) were indicative of an isoflavan scaffold. A comparison of the ^{13}C NMR data of ring A with those of laurentiquinone [26] suggested a methoxy group at C-7 and a hydroxy residue at C-8. ^{13}C NMR data of ring C were comparable to those of compound **5** (**Table 1** and **Table 1S**). Connectivity of the rings and positions of the methoxy groups were corroborated by HMBC correlations (**Fig. 3**). $^3J_{C-H}$ correlation between C-9 (δ_c 142.3) and H-5 (δ_H 6.49, ring A) and H-4*α* and H-4*β* (δ_H 3.12 and 2.65, ring C) confirmed the connectivity of rings A and C. A correlation between H-3 (δ_H 3.60, ring C) and C-6′ (δ_c 131.3, ring B) confirmed the presence of an isoflavan scaffold. Vicinal coupling constants in ring C and NOE difference measurements were used to establish the relative configuration. The vicinal coupling constants H-2*α*/H-3 (J = 3.4 Hz) and H-2*β*/H-3 (J = 10.4 Hz) corresponded to dihedral angles of 60° and 180°, respectively, indicating an axial orientation of H-3. The coupling constants H-4*α*/H-3 (J = 12.3 Hz) and H-4*β*/H-3 (J = 4.7 Hz) were in accordance with dihedral angles of 140 to 160° and 40 to 60°, respectively, indicating that H-4*α* was in a pseudo-axial orientation, and H-4*β* in a pseudo-equatorial position, respectively [27].

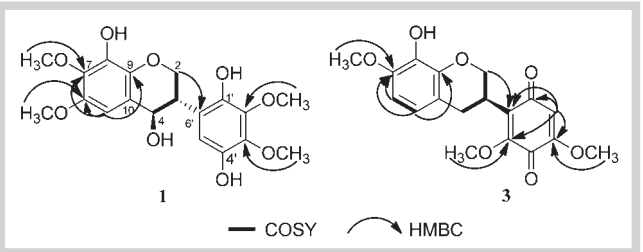

Fig. 3 Key HMBC and COSY correlations for compounds **1** and **3**.

Conformational analysis of **3** displayed 10 conformers within a 1 Kcal/mol energy window from the particular global minimum. Geometrical optimization and energy calculation followed by calculation of ECD spectra were performed as described above. We obtained 9 stable conformers (**Fig. 5B**; **Fig. 14S B**, Supporting Information). The calculated ECD spectrum of the (3*R*)-enantiomer showed one positive CE at 206 nm along with two negative CEs around 260 and 320 nm (**Fig. 5A**). The experimental ECD spectrum showed a positive CE at 212 and a negative CE at 233. The pattern of the calculated ECD spectrum for the (3*R*)-configuration was in good agreement with the experimental ECD spectrum, while the calculated ECD spectra of the (3*S*)-enantiomer (**Fig. 5A**) showed CEs with opposite signs around 206 and 260 nm. As a result, we concluded that abruquinone I (**3**) had the (3*R*)-configuration.

The absolute configuration of compounds **4** (**Figs. 13S A** and **14S C**, Supporting Information) and **5** (see **Figs. 13S B** and **14S D**, Supporting Information) has been established by comparison of the experimental and calculated ECD spectra as 3*R* and 3*S*, respectively. The absolute configuration of abruquinone B (**4**) had been previously determined by different methods, but reports were contradictory and suggest that both enantiomers may have been isolated from this plant. On the basis of ORD data, a compound was described as (3*S*)-abruquinone [11], and a positive optical rotation was reported [16]. On the other hand, an ECD study assigned the (3*R*)-configuration to the enantiomer exhibiting negative optical rotation [21]. Our ECD data and the sign of optical rotation were in good agreement with [21], which corroborates the

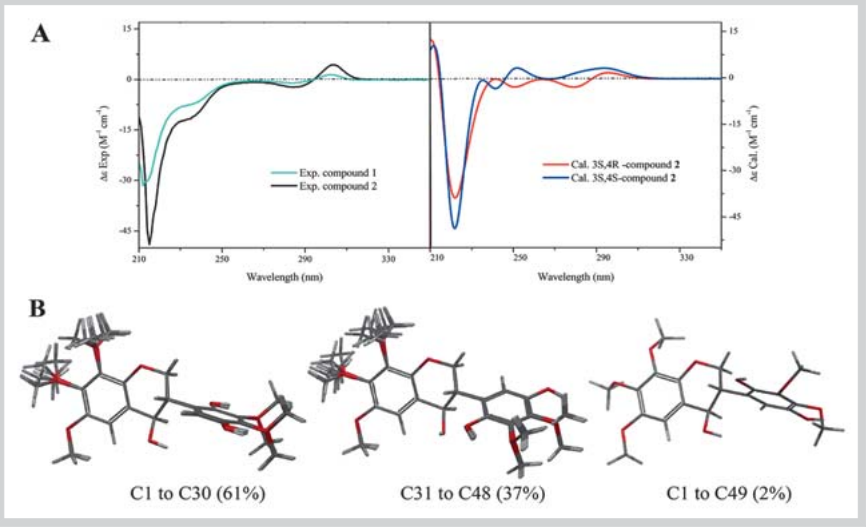

Fig. 4 Comparison of the experimental ECD of **1** and **2** with calculated spectra for the (3*S*,4*R*)- and (3*S*,4*S*)-diastereomers of **2** (**A**). DFT optimized conformers at the B3LYP/6–31 G** level in the gas phase (within 1 kcal/moL range from the global minimum) of the (3*S*,4*R*)-stereoisomer. Fifty-two conformers grouped in three different core conformers which differed in the alignment of the B ring (**B**). (Color figure available online only.)

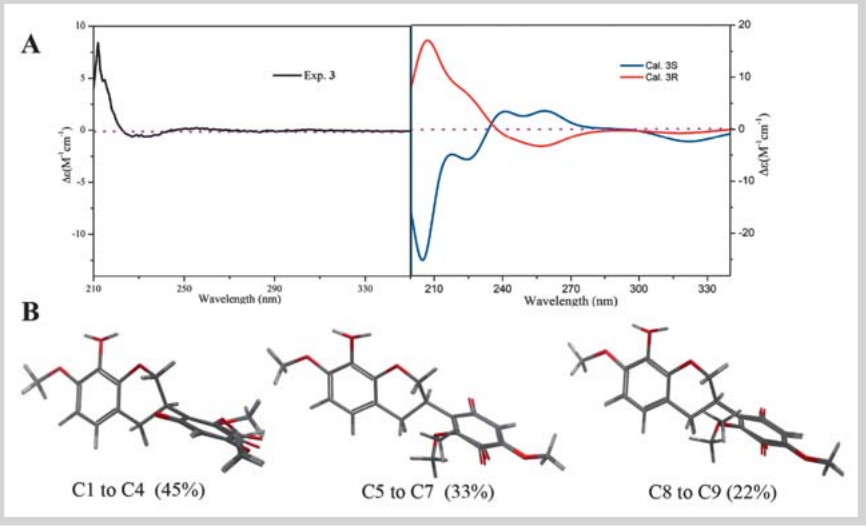

Fig. 5 Comparison of the experimental ECD of **3**, with calculated spectra for the (3*S*)- and (3*R*)-enantiomers (**A**). DFT optimized conformers at the B3LYP/6–31 G** level in the gas phase (within 1 kcal/moL range from the global minimum) of the (3*R*)-enantiomer. Nine conformers were grouped in three core conformers differing in the alignment of the B ring (**B**). (Color figure available online only.)

Table 2 *In vitro* antiprotozoal activities of **1**–**5** against *P. falciparum*, *T. b. rhodesiense*, and *L. donovani*, as well as cytotoxic activity against L-6 cells.

Compound	*P. falciparum*		*T. b. rhodesiense*		*L. donovani*		Cytotoxicity
	IC_{50} (μM)[a]	SI	IC_{50} (μM)[a]	SI	IC_{50} (μM)	SI	IC_{50} (μM)[a]
1	8.0 ± 1.1	15.4	12.0 ± 3.8	0.2	inactive[b]	–	122.8 ± 21.3
2[d]	inactive[c]	–	17.0 ± 4.2	3.0	35.3	1.5	51.8 ± 11.1
3	20.4 ± 1.3	1.1	0.3 ± 0.1	73.7	3.4	6.5	22.1 ± 3.5
4	4.1 ± 0.4	2.5	0.2 ± 0.1	50.5	2.9	3.5	10.1 ± 1.3
5	8.9 ± 4.2	0.4	0.9 ± 0.1	4.3	5.0	0.9	3.9 ± 0.4
Artesunate[e]	0.002 ± 0.001	–	–	–	–	–	–
Melarsoprol[e]	–	–	0.007 ± 0.002	–	–	–	–
Miltefosine[e]	–	–	–	–	0.285 ± 0.059	–	–
Podophyllotoxin[e]	–	–	–	–	–	–	0.014 ± 0.006

[a] Values are expressed as mean ± standard error of the mean; [b] No activity observed at the highest test concentration of 10 μg/mL, which corresponds to molar test concentrations of 24.5 to 28.9 μM; [c] No activity observed at the highest test concentration of 90 μg/mL, which corresponds to molar test concentrations of 260.0 to 220.5 μM; [d] Compound **2** contains about 15% of an unidentified related metabolite; [e] Reference drugs. SI (Selectivity index): Quotient of IC_{50} in L-6 cells and IC_{50} against parasite

(3*R*)-configuration of **4**. As to compound **5** the negative sign of optical rotation agrees with the data reported before for the (3*S*)-enantiomer prepared by semisynthesis starting from (3*S*)-duartin [23].

Isoflavonoid hydroquinones **1** and **2** exhibited low activity in both antiprotozoal and cytotoxicity tests (**Table 2**). In contrast, quinone-type isoflavonoids **3, 4**, and **5** showed strong activity against *T. b. rhodesiense* (IC_{50}s of 0.3, 0.2, and 0.9 μM, respectively). Compounds **3** and **4** showed low cytotoxicity in the L-6 cell

line (IC_{50} values of 22.1 and 10.1 µM, respectively). A selectivity index (SI) of 73.7 and 50.5 qualifies the compounds as good candidates for assessment of *in vivo* activity in a murine model [28]. Cytotoxicity of compound **5**, in contrast, was considerably higher (IC_{50} of 3.9 µM) and resulted in a low SI. We are currently isolating compounds **3** and **4** at a larger scale for an *in vivo* study. There has been so far only one plant-derived natural product, cynaropicrin [8], for which *in vivo* activity against *T. brucei* has been demonstrated. Given that abruquinones **3** and **4** possess a tenfold higher SI than cynaropicrin, these compounds are of considerable interest.

Acknowledgements

The authors would like to thank the Council for Scientific and Industrial Research (CSIR), the Swiss Confederation, and the Department of Science and Technology for financial support under the Swiss South African Joint Research Programme (grant JRP 03), and SANBI for the identification of the plant species. Y. Hata gratefully acknowledges a PhD stipend from the Administrative Department of Science and Technology from Colombia (Colciencias) managed by LASPAU. We thank Dr. O. Potterat for helpful comments and Mrs. M. Rogalski for proofreading the manuscript.

Conflict of Interest

The authors declare no conflict of interest.

Affiliations

[1] Department of Pharmaceutical Sciences, University of Basel, Basel, Switzerland
[2] Swiss Tropical and Public Health Institute and University of Basel, Basel, Switzerland
[3] Biosciences, Council for Scientific and Industrial Research (CSIR), Pretoria, South Africa
[4] Departament of Pharmacy, Faculty of Sciences, National University of Colombia, Bogota D. C., Colombia
[5] Department of Phytochemistry, Medicinal Plant and Drugs Research Institute, Shahid Beheshti University, G. C., Tehran, Iran

References

1 *World Health Organization (WHO).* Working to overcome the global impact of neglected tropical diseases: First WHO report on neglected tropical diseases. Geneva: WHO; 2010 (iii): 13, 14, 75, 82–84, 91–92
2 *World Health Organization (WHO).* Global malaria report. Geneva: WHO; 2011: 1
3 *World Health Organization (WHO).* The global burden of diseases: 2004 update. Geneva: WHO; 2008: 60
4 *Rensol AR, McKerrow JH.* Drug discovery and development for neglected diseases. Nat Chem Biol 2006; 2: 701–710
5 *Hannaert V.* Sleeping sickness pathogen (*Trypanosoma brucei*) and natural products: therapeutic targets and screening systems. Planta Med 2011; 77: 586–597
6 *Adams M, Zimmermann S, Kaiser M, Brun R, Hamburger M.* A protocol for HPLC-based activity profiling for natural products with activities against tropical diseases. Nat Prod Commun 2009; 4: 1377–1381
7 *Mokoka TA, Zimmermann S, Julianti T, Hata Y, Moodley N, Cal M, Adams M, Kaiser M, Brun R, Koorbanally N, Hamburger M. In vitro* screening of traditional South African malaria remedies against *Trypanosoma brucei rhodesiense, Trypanosoma cruzi, Leishmania donovani*, and *Plasmodium falciparum*. Planta Med 2011; 77: 1663–1667
8 *Zimmermann S, Kaiser M, Brun R, Hamburger M, Adams M.* Cynaropicrin: the first natural product with *in vivo* activity against *Trypanosoma brucei rhodesiense*. Planta Med 2012; 78: 553–556
9 *Hata Y, Zimmermann S, Quitschau M, Kaiser M, Brun R, Hamburger M, Adams M.* Antiplasmodial and antitrypanosomal activity of pyrethrins and pyrethroids. J Agric Food Chem 2011; 59: 9172–9176
10 *Olsnes S.* The history of ricin, abrin and related toxins. Toxicon 2004; 44: 361–370
11 *Lupi A, Monache FD, Marini-Bettolo GB.* Abruquinones: new natural isoflavanquinones. Gazz Chim Ital 1979; 109: 9–12
12 *Ma C, Nakamura N, Hattori M.* Saponins and *C*-glycosyl flavones from the seeds of *Abrus precatorius*. Chem Pharm Bull 1998; 46: 982–987
13 *Kuo SC, Chen SC, Chen LH, Wu JB, Wang JP, Teng CM.* Potent antiplatelet, anti-inflammatory and antiallergic isoflavanquiones from the roots of *Abrus precatorius*. Planta Med 1995; 61: 307–312
14 *Gathirwa JW, Rukunga GM, Mwitari PG, Mwikwabe NM, Kimani CW, Muthaura CN, Kiboi DM, Nyangacha RM, Omar SA.* Traditional herbal antimalarial therapy in Kilifi district, Kenya. J Ethnopharmacol 2011; 134: 434–442
15 *Ménan H, Banzouzi JT, Hocquette A, Pélissier Y, Blache Y, Koné M, Mallié M, Assi LA, Valentin A.* Antiplasmodial activity and cytotoxicity of plants used in West Africa traditional medicine for the treatment of malaria. J Ethnopharmacol 2006; 105: 131–136
16 *Limmatvapirat C, Sirisopanaporn S, Kittakoop P.* Antitubercular and antiplasmodial constituents of *Abrus precatorus*. Planta Med 2004; 70: 276–278
17 *Choi YH, Hussain RA, Pezzuto JM, Kinghorn AD, Morton JF.* Abrusosides A–D, four novel sweet-tasting triterpene glycosides from the leaves of *Abrus precatorius*. J Nat Prod 1989; 52: 1118–1127
18 *Xiao ZH, Wang FZ, Sun AJ, Li CR, Huang CG, Zhang S.* A new triterpenoid saponin from *Abrus precatorius* Linn. Molecules 2012; 17: 295–302
19 *Ghosal S, Dutta SK.* Alkaloids of *Abrus precatorius*. Phytochemistry; 1971; 10: 195–198
20 *Bhardwaj DK, Bisht MS, Mehta CK.* Flavonoids from *Abrus precatorius*. Phytochemistry 1980; 19: 2040–2041
21 *Song CQ, Hu ZB.* Abruquinone A, B, D, E, F, and G from the root of *Abrus precatorius*. Acta Bot Sin 1998; 40: 734–739
22 *Potterat O, Hamburger M.* Natural products in drug discovery – concepts and approaches for tracking bioactivity. Curr Org Chem 2006; 10: 899–920
23 *Kurosawa K, Ollist WD, Redman BT, Sutherland IO, Alves HM, Gottlieb OR.* Absolute configuration of isoflavans. Phytochemistry 1978; 17: 1423–1426
24 *Frisch MJ, Trucks GW, Schlegel HB, Scuseria GE, Robb MA, Cheeseman JR, Scalmani G, Barone V, Mennucci B, Petersson GA, Nakatsuji H, Caricato M, Li X, Hratchian HP, Izmaylov AF, Bloino J, Zheng G, Sonnenberg JL, Hada M, Ehara M, Toyota K, Fukuda R, Hasegawa J, Ishida M, Nakajima T, Honda Y, Kitao O, Nakai H, Vreven T, Montgomery JA, Peralta JE, Ogliaro F, Bearpark M, Heyd JJ, Brothers E, Kudin KN, Staroverov VN, Kobayashi R, Normand J, Raghavachari K, Rendell A, Burant JC, Iyengar SS, Tomasi J, Cossi M, Rega N, Millam JM, Klene M, Knox JE, Cross JB, Bakken V, Adamo C, Jaramillo J, Gomperts R, Stratmann RE, Yazyev O, Austin AJ, Cammi R, Pomelli C, Ochterski JW, Martin RL, Morokuma K, Zakrzewski VG, Voth GA, Salvador P, Dannenberg JJ, Dapprich S, Daniels AD, Farkas O, Foresman JB, Ortiz JV, Cioslowski J, Fox DJ.* Gaussian 09, Revision A02. Wallingford: Gaussian, Inc; 2009
25 *Bruhn T, Hemberger Y, Schaumlöffel A, Bringmann G.* SpecDis, Version 1.51. Würzburg: University of Würzburg; 2011
26 *Kamnaing P, Fanso Free SNY, Nkengfack AE, Folefoc G, Forum ZT.* An isoflavan-quinone and a flavonol from *Millettia laurentii*. Phytochemistry 1999; 51: 829–832
27 *Slade D, Ferreira D, Marais JPJ.* Circular dichroism, a powerful tool for the assessment of absolute configuration of flavonoids. Phytochemistry 2005; 66: 2177–2215
28 *Gichuki C, Brun R.* Animal models of CNS (second-stage) sleeping sickness. In: Zak O, Sande MA, editors. Animal models of infection. Bath: Academic Press; 1999: 795–801

Supporting Information

Antiprotozoal isoflavan quinones from *Abrus precatorius ssp. africanus*

Yoshie Hata[1,4], Melanie Raith[1], Samad Nejad Ebrahimi[1,5], Stefanie Zimmermann[1,2], Tsholofelo Mokoka[3], Dashnie Naidoo[3], Gerda Fouche[3], Vinesh Maharaj[3], Marcel Kaiser[2], Reto Brun[2], and Matthias Hamburger[1]

Affiliations

[1] Division of Pharmaceutical Biology, University of Basel, Klingelbergstrasse 50, 4056 Basel, Switzerland

[2] Swiss Tropical and Public Health Institute, and University of Basel, Basel, Switzerland

[3] Biosciences, Council for Scientific and Industrial Research (CSIR), Pretoria, South Africa

[4] Departamento de Farmacia, Facultad de Ciencias, Universidad Nacional de Colombia, Bogotá D.C., Colombia

[5] Department of Phytochemistry, Medicinal Plant and Drugs Research Institute, Shahid Beheshti University, G. C., Tehran, Iran

Correspondence:

Prof. Matthias Hamburger, Division of Pharmaceutical Biology, University of Basel, Klingelbergstrasse 50, CH-4056 Basel, Switzerland.

e-mail: matthias.hamburger@unibas.ch, Phone: +41 61 267 14 25 Fax: +41 61 267 14 74

Assays for *in vitro* antiprotozoal activity

Antiplasmodial activity was determined by a modification of the ^{3}[H]-hypoxanthine incorporation assay [1] with the *P. falciparum* K1 strain (resistant to chloroquine and pyrimethamine), growth according to the method described by Trager and Jensen [2]. Artesunate (purity >95%, Sigma-Aldrich) was used as positive control.

Briefly, a suspension of infected red blood cells (final parasitemia 0.3% and hematocrit 1.25%) in RPMI 1640 medium supplemented with 2 μM $_{L}$-glutamine, 5.95 g/L Hepes, 2 g/L $NaHCO_3$, and 5% of Albumax II was exposed to serial drug dilutions covering a range from 10 μg/mL to 0.156 μg/mL.in 96-well microtiter plates. After 48 h of incubation (4% CO_2, 3% O_2, and 93% N_2 at 37°C), 50 μL of ^{3}[H]-hypoxanthine (0.25 μM) were added to each well (Costar). The plates were incubated for further 24 h before being harvested by using a Betaplate cell harvester (Wallac) onto glass-fiber filters and then washed with distilled water. The dried filters were inserted into plastic foils with 10 mL scintillation fluid. The radioactivity was counted with a Betaplate liquid scintillation counter (Wallac) as counts per minute per well at each drug concentration and compared to the untreated controls. Counts were expressed as percentages of the control and presented as sigmoidal inhibition curves. IC_{50} values were calculated by linear interpolation.

Antitrypanosomal activity against *T. brucei rhodesiense* STIB 900 was determined according to [3]. Melarsoprol (Arsorbal, purity >95%, Sanofi-Aventis) was used as positive control. Minimum essential medium (MEM) with Earle's salts supplemented with 2-mercaptoethanol, as described by Baltz *et al*. [4], 1 mM sodium pyruvate, 0.5 mM hypoxanthine, and 15% heat-inactivated horse serum was added (50 μL) to each well of a 96-well microtiter plate (Costar) except of the negative control. Serial drugs dilutions were prepared covering range from 90 to 0.123 μg/mL followed by the parasite suspension of 2000 *T. brucei rhodesiense* STIB 900 bloodstream forms/well. After 70 hours of incubation (humidified 5% CO_2 atmosphere at 37°C), 10 μL resazurin solution (12.5 mg resazurin (Sigma-Aldrich) dissolved in 100 mL of distilled water) were added and incubation was continued for further 2 to 6 h. The plate was read with a Spectramax Gemini XS microplate fluorescence reader (Molecular Devices) with an excitation wavelength of 536 nm and an emission wavelength of 588 nm. Fluorescence development was expressed as percentage of the control and the IC_{50} values were determined from the sigmoid curves using Softmax Pro Software (Molecular Devices).

The assay with *T. cruzi* was performed according to [5], with some modifications. Rat skeletal myoblast cells (L6-cells) were seeded in 96-well microtiter plates (Costar) at 2000 cell/well/100 μL in RPMI 1640 medium supplemented with10% fetal bovine serum (FBS) and 2 mM $_{L}$-glutamine). After 24 h of incubation (humidified 5% CO_2 atmosphere at 37°C, the medium was replaced by 100 μL of fresh medium containing 5000 trypomastigote forms of *T. cruzi*/well (Tulahuen strain C2C4 containing the β-galactosidase (Lac Z) gene). After 48 h, the medium was removed from the wells and replaced by 100 μL of fresh medium with the serial drug dilution, covering a range from 90 μg/mL to 0.123 μg/mL. After 96 h ofincubation 50 μL chlorophenyl red β-D-galactopyranoside agent (CPRG)/Nonident (Sigma - Aldrich) was added to all wells. The plates were read photometrically at 540 nm [5]. Optical density values were expressed as percentages of control, and IC_{50} values were calculated from the sigmoid inhibition curve. Benzinidazole (purity >95%, Sigma-Aldrich) was used as positive control.

Leishmanicidal activity was determined with *L. donovani* (axenic amastigotes) MHOM-ET/67/L82 strain according to [6], with some modifications. Fifty microlitres of SM medium at pH 5.4 supplemented with 10% heat-inactivated FBS was added to each well of 96-well microtiter plate (Costar). Serial drug dilutions were prepared covering a range from 90 to 0.123 μg/mL. Then, 10^5 axenically growth *L. donovani* amastigotes in 50 μL medium, were added to each well and the plate was incubated for 72 h (humidified 5% CO_2 atmosphere at 37°C). Ten microlitres resazurin solution (12.5 mg resazurin (Sigma-Aldrich) dissolved in 100 mL of distilled water) were added to each well and incubated for further 2 to 4 h. The plate was read with a Spectramax Gemini XS microplate fluorescence reader (Molecular Devices) with an excitation wavelength of 536 nm and an emission wavelength of 588 nm. Fluorescence development was expressed as percentage of the control and the IC_{50} values were determined from the sigmoid curves using Softmax Pro Software (Molecular Devices). Miltefosine (purity >95%, VWR) was used as positive control.

***In vitro* cytotoxicity assay**

The cytotoxicity assay was performed using a protocol based on the Alamar Blue assay [7], whereby rat skeletal myoblast cells (L-6 cells) were seeded in 96-well microtiter plates using MEM supplemented with 10% heat inactivated FBS (4000 cells/well). Serial threefold drug dilutions ranging from 90 to 0.123 mg/mL were prepared. After 72 h, 10 μL resazurin

solution was added (12.5 mg resazurin (Sigma-Aldrich) dissolved in 100 mL of distilled water) and the plates were incubated for further 2 to 4 h. A Spectramax Gemini XS micro plate fluorescence reader (Molecular Devices) was used to measure the plates at an excitation wavelength of 536 nm and an emission wavelength of 588 nm. Fluorescence development was expressed as percentage of the control and the IC_{50} values were determined from the sigmoid curves using Softmax Pro Software (Molecular Devices). Podophyllotoxin (purity >95%, Sigma-Aldrich) was used as a reference drug.

Physicochemical data of 2, 4 and 5

(3*S*-4*R*)-4,1',4'-trihydroxy-6,7,8,2',3'-pentamethoxyisoflavan (Abruquinone G, **2**) [8]: White amorphous substance; UV (MeOH): λ_{max} (log ε) = 205 (4.66), 296 (3.88) nm; ^{1}H and ^{13}C NMR data, see Table 1S; HRESI-MS: *m/z* = 413.1178 $[M\text{-}H_2O+Na]^+$ (calcd. for $C_{20}H_{24}NaO_9$: 413.1027).

(3*R*)-6,7,8,2',3'-pentamethoxyisoflavan-1',4'-quinone (Abruquinone B, **4**) [8, 9, 10, 11]: Red-brown amorphous substance; UV (MeOH): λ_{max} nm (log ε) = 203 (4.61), 268 (4.06) nm; ^{1}H NMR data, see Table 1; ^{13}C NMR data, see Table 1; HRESI-MS: *m/z* = 413.1182 $[M+Na]^+$ (calcd. for $C_{20}H_{22}NaO_8$: 413.1207).

(3*S*)-7,8,3',5'-tetramethoxyisoflavan-1',4'-quinone (**5**) [12]: Orange amorphous substance; UV (MeOH): λ_{max} (log ε) = 205 (4.59) nm, 286 (3.91) nm; ^{1}H NMR data, see Table 1; ^{13}C NMR data, see Table 1; HRESI-MS: *m/z* = 383.1143 $[M+Na]^+$ (calcd. for $C_{19}H_{20}NaO_7$: 383.1101).

Table 1S. ^{1}H and ^{13}C NMR data (CD_3OD, 500 MHz for ^{1}H, 125 MHz for ^{13}C) for compounds **2, 4,** and **5**.

	2		**4**		**5**	
position	δ_H	δ_C[a]	δ_H	δ_C	δ_H	δ_C[a]
2a 2b	3.60 (dd, 11.1, 4.8) 2.91 (dd, 11.1, 10.7)	66.3	4.23 (dd, 10.7, 3.2) 4.21 (dd, 10.7, 6.3)	68.2	4.43 (dd,10.7, 10.4) 4.23 (ddd,10.7, 3.8, 1.6)	67.8
3	2.79 (1H, m)	40.7	3.42 (1H, m)	31.0	3.60 (1H, m)	31.0
4a 4b	4.71 (1H, d, 6.9)	78.1	Ha 3.02 (dd, 16.3, 6.3) Hb 2.69 (dd, 16.3, 6.4)	29.5	Ha 3.15 (dd, 15.5, 12.4) Hb 2.66 (ddd, 15.5, 5.1, 1.6)	29.3
5	6.81 (1H, s)	108.1	6.31 (1H, s)	107.1	6.69 (1H, d, 8.5)	123.3
6	-	148.1	-	147.7	6.47 (1H, d, 8.5)	105.0
7	-	143.7	-	141.9*	-	151.2
8	-	142.5	-	142.5	-	137.6
9	-	143.7	-	146.5	-	148.3
10	-	114.9	-	115.1	-	115.9
1'	-	143.6	-	183.7	-	186.7
2'	-	137.7	-	145.3*	5.84 (1H, s)	107.3
3'	-	139.2	-	144.9	-	156.9
4'	-	nd[b]	-	184.2	-	178.7
5'	5.87 (1H, s)	104.6	6.32 (1H, br d, 1.1)	131.2	-	155.4
6'	-	122.9	-	141.9	-	131.0
2'- OCH_3	3.98 (3H, s)	60.1	3.99 (3H, s)	61.5	-	-
3'- OCH_3	3.99 (3H, s)	61.1	3.98 (3H, s)	61.5	3.79 (3H, s)	56.2
5'- OCH_3	-	-	-	-	3.95 (3H, s)	61.2
6- OCH_3	3.77 (3H, s)	56.4	3.77 (3H, s)	56.5	-	-
7- OCH_3	3.85 (3H, s)	61.1	3.85 (3H, s)	61.5	3.83 (3H, s)	56.2
8- OCH_3	3.85 (3H, s)	61.0	3.85 (3H, s)	61.5	3.85 (3H, s)	60.7

[a] ^{13}C NMR signals were extracted from HSQC and HMBC spectra, [b] not detected. *interchangable

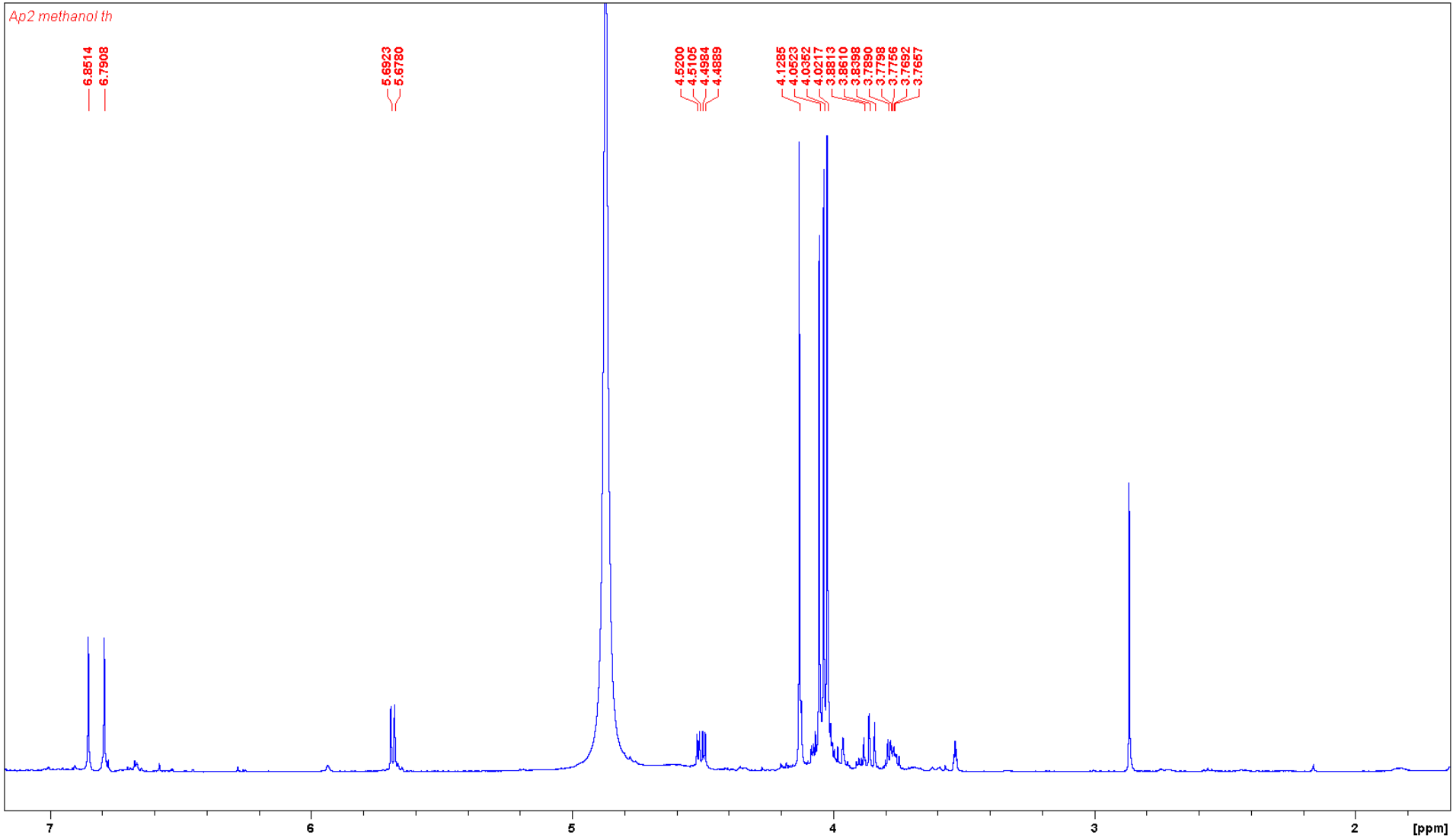

Fig. 1S. ^{1}H NMR spectrum of Abruquinone H (**1**) in CD_3OD.

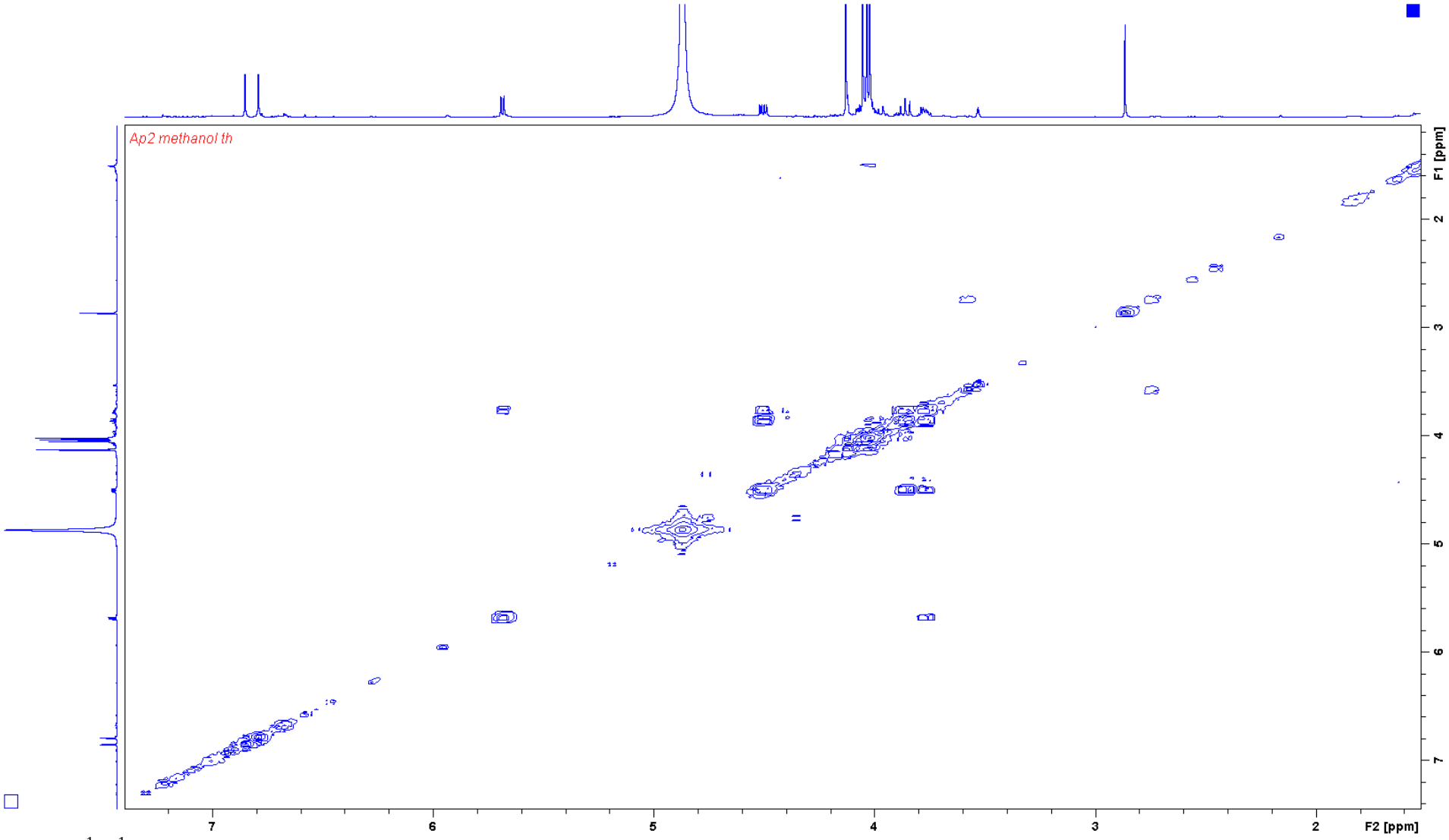

Fig. 2S. ^{1}H ^{1}H COSY spectrum of Abruquinone H (**1**) in CD_3OD.

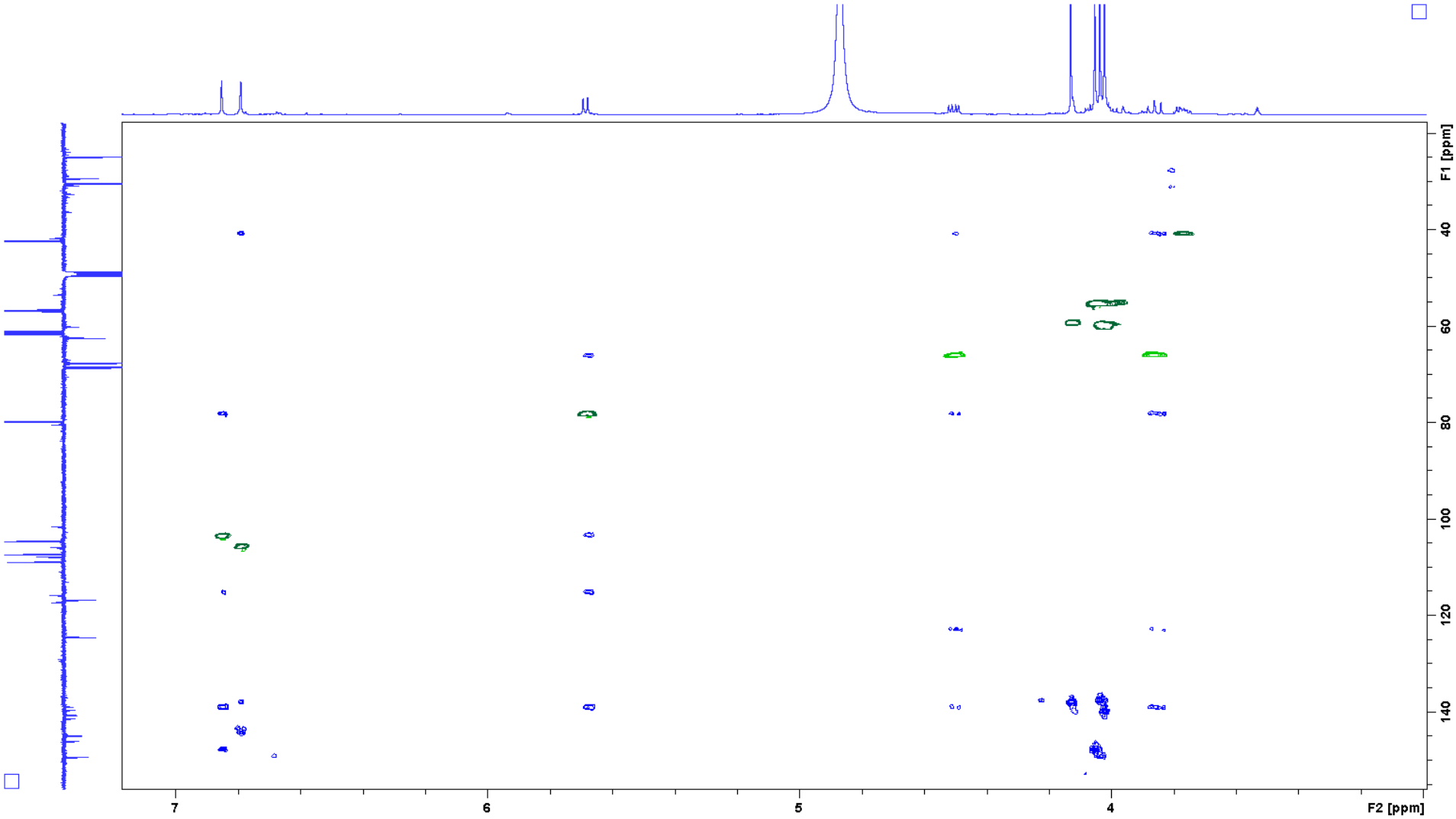

Fig. 3S. HSQC and HMBC overlaid spectra of Abruquinone H (**1**) in CD_3OD.

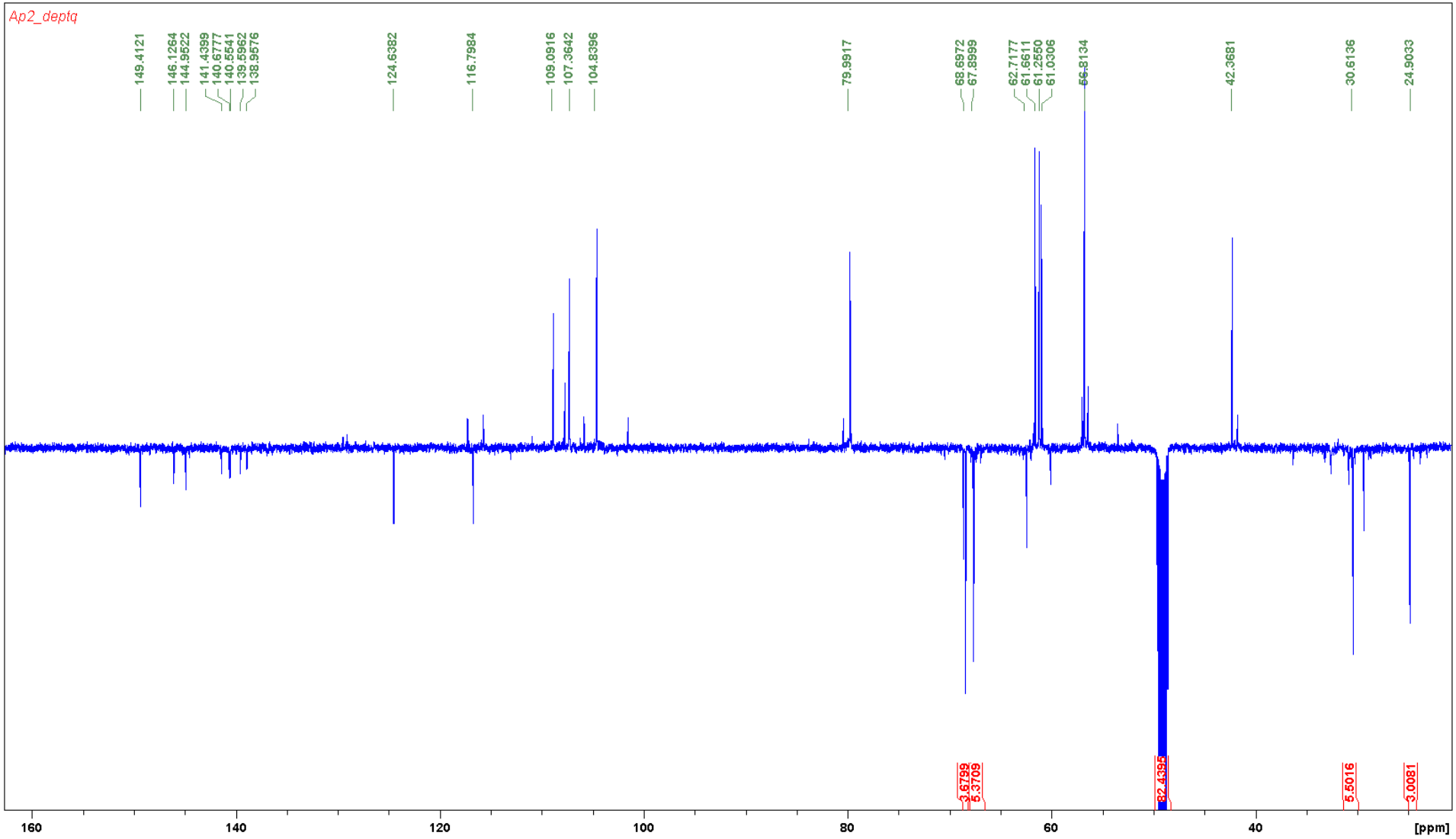

Fig. 4S. DEPTQ spectrum of Abruquinone H (**1**) in CD_3OD.

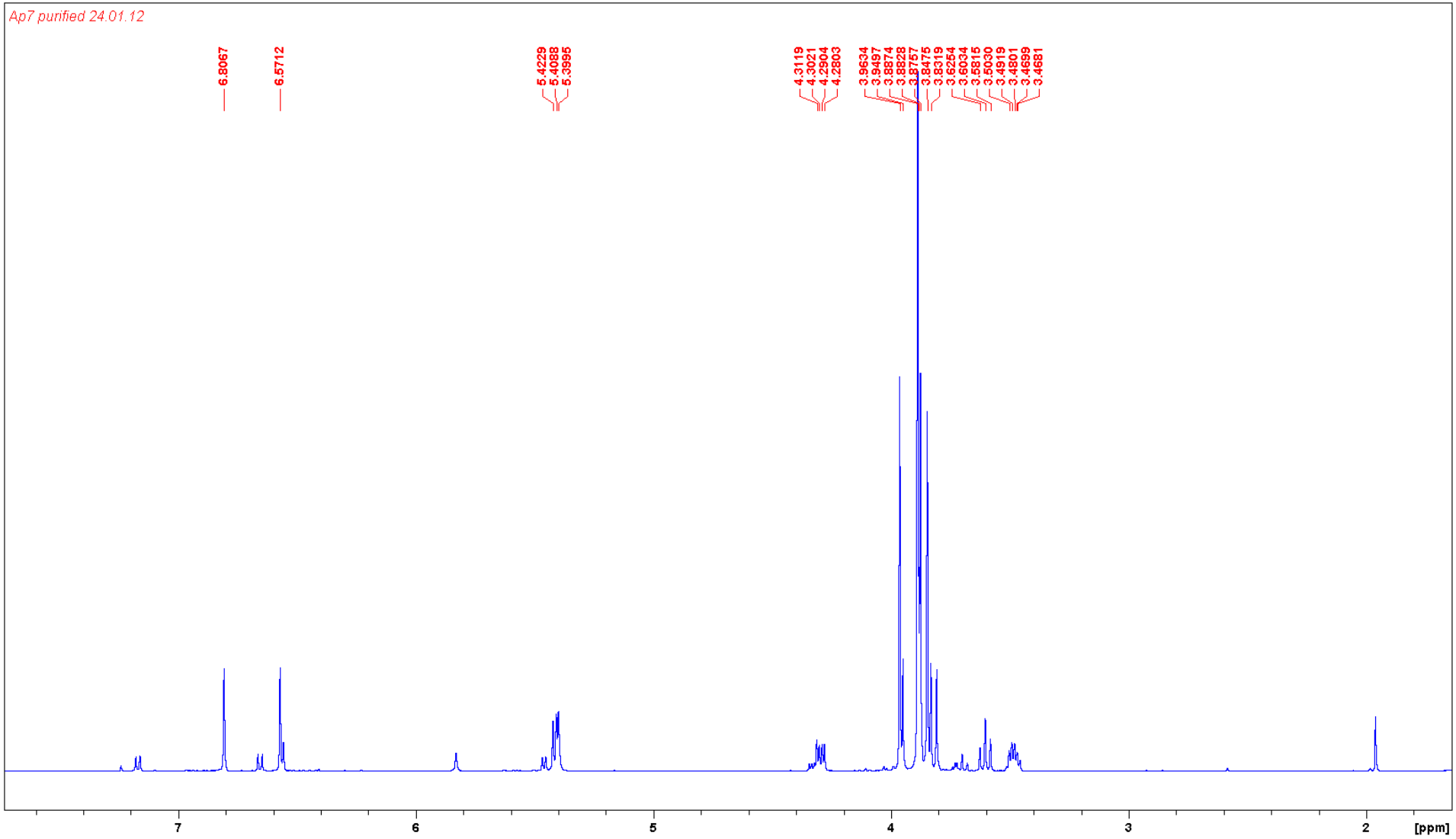

Fig. 5S. ^{1}H NMR spectrum of Abruquinone G (**2**) in $CDCl_3$.

10

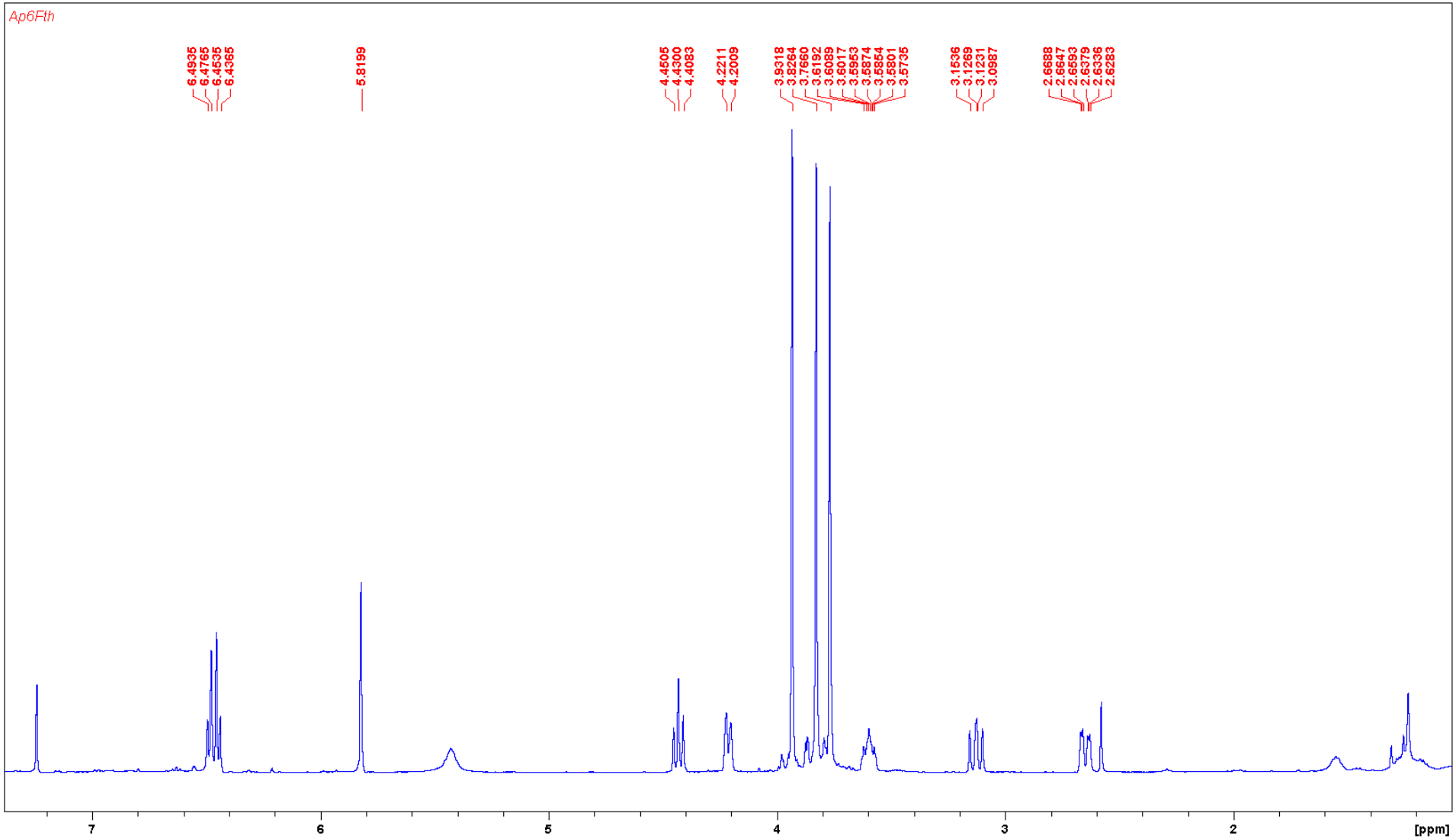

Fig. 6S. ^{1}H NMR spectrum of Abruquinone I (**3**) in $CDCl_3$.

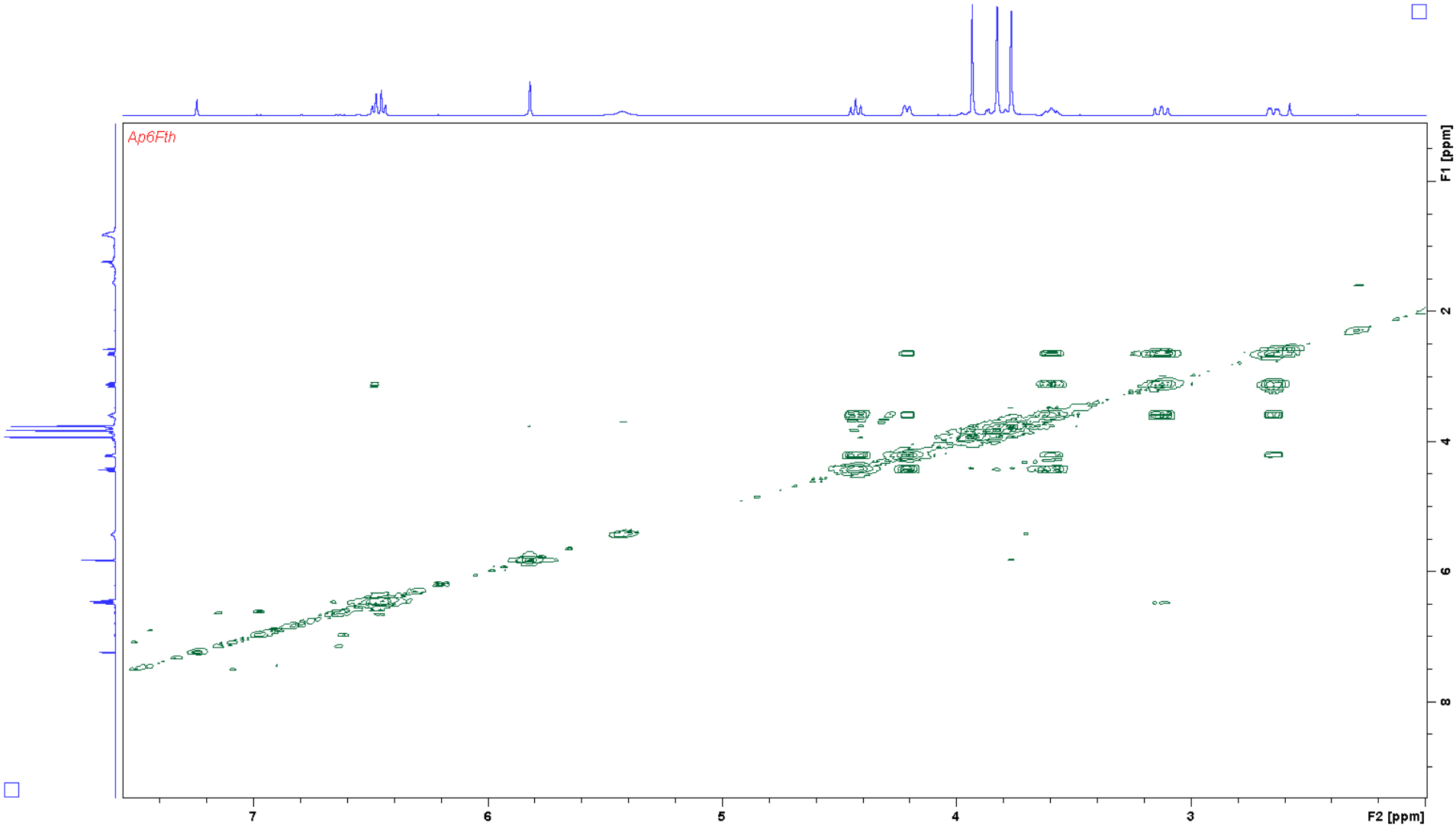

Fig. 7S. ^{1}H ^{1}H COSY spectrum of Abruquinone I (**3**) in $CDCl_3$.

12

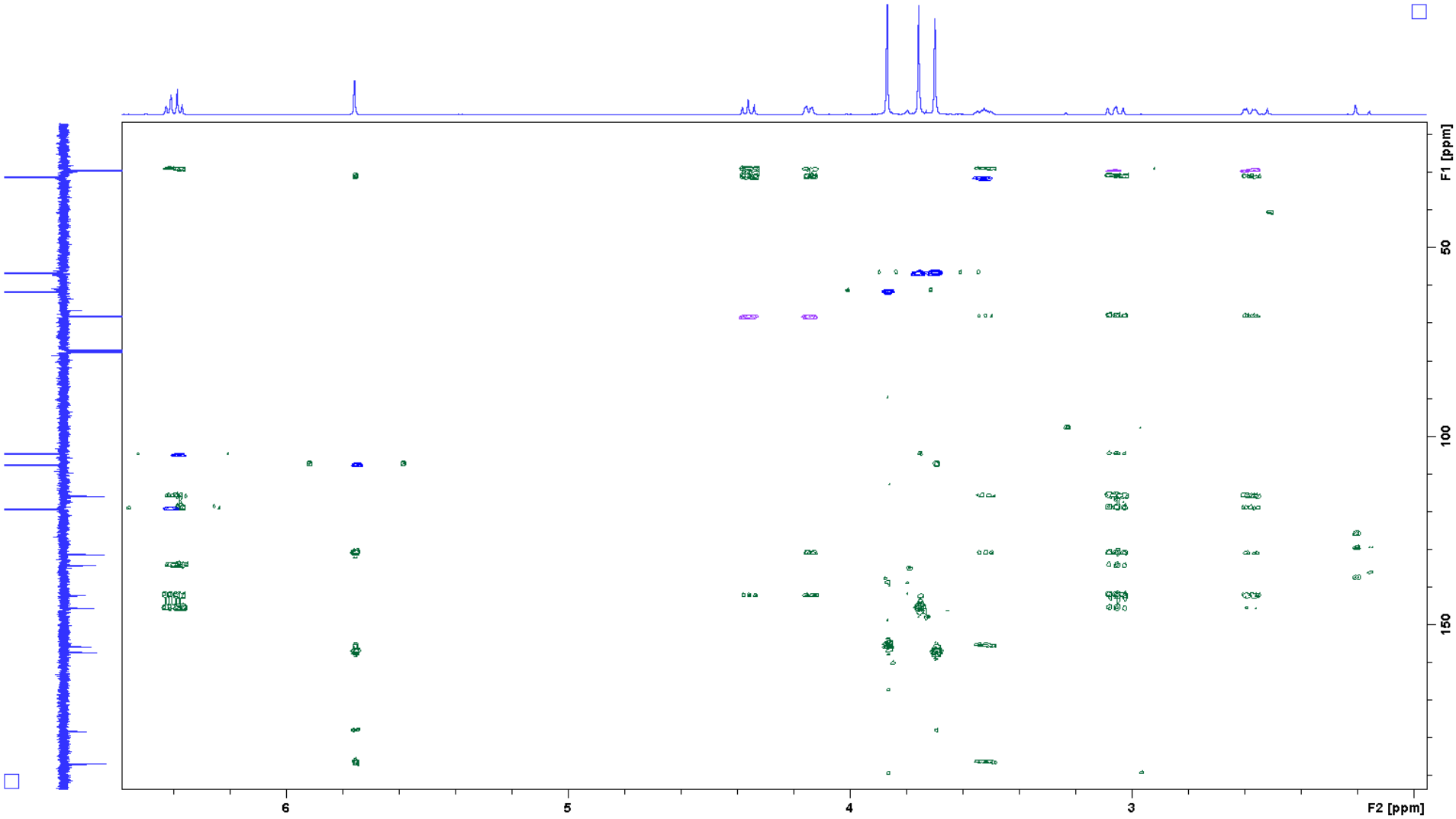

Fig. 8S. HMQC and HMBC overlaid spectra of Abruquinone I (**3**) in $CDCl_3$.

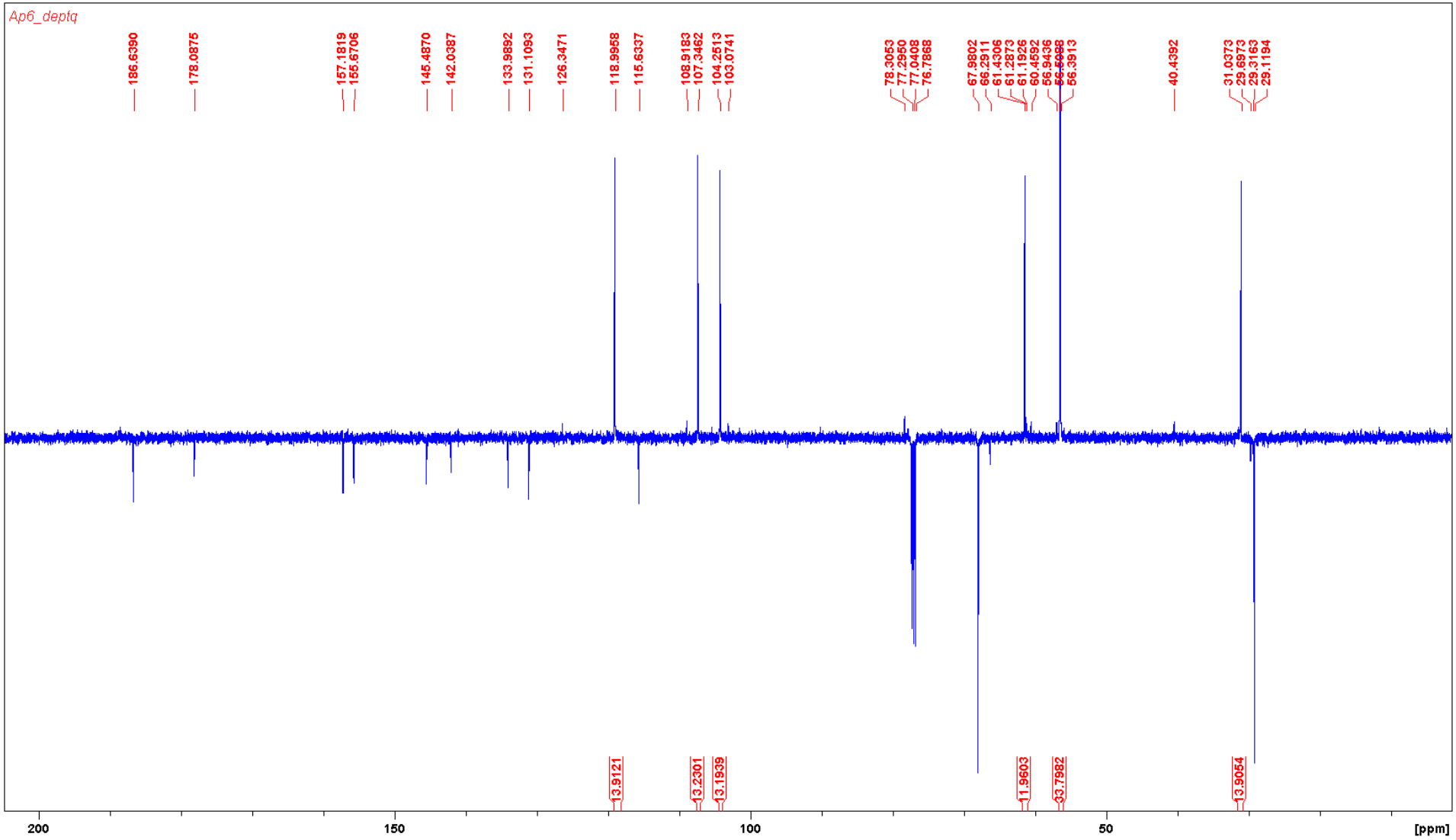

Fig. 9S. DEPTQ spectrum of Abruquinone I (**3**) in $CDCl_3$.

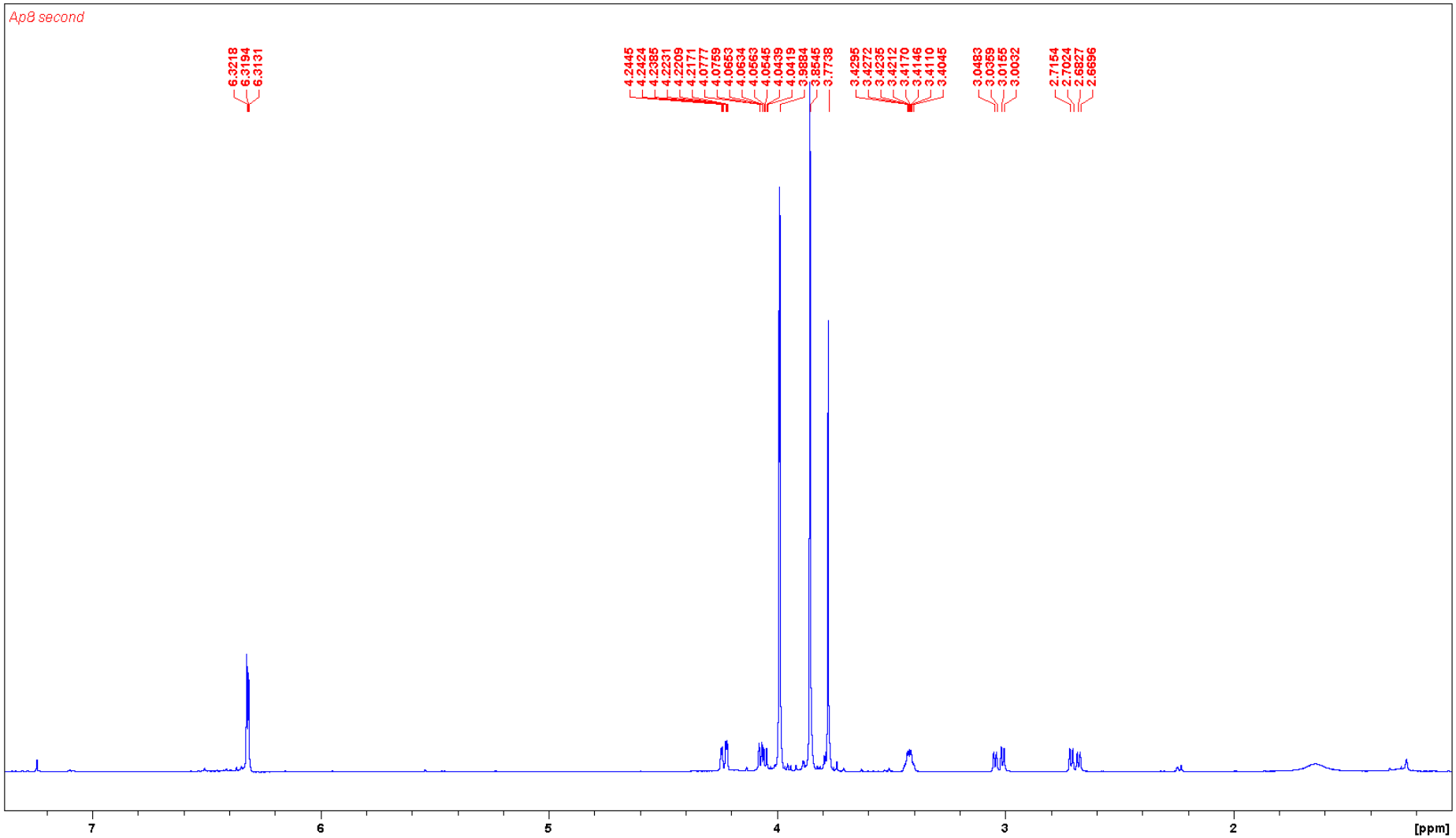

Fig. 10S. ^{1}H NMR spectrum of Abruquinone B (**4**) in $CDCl_3$.

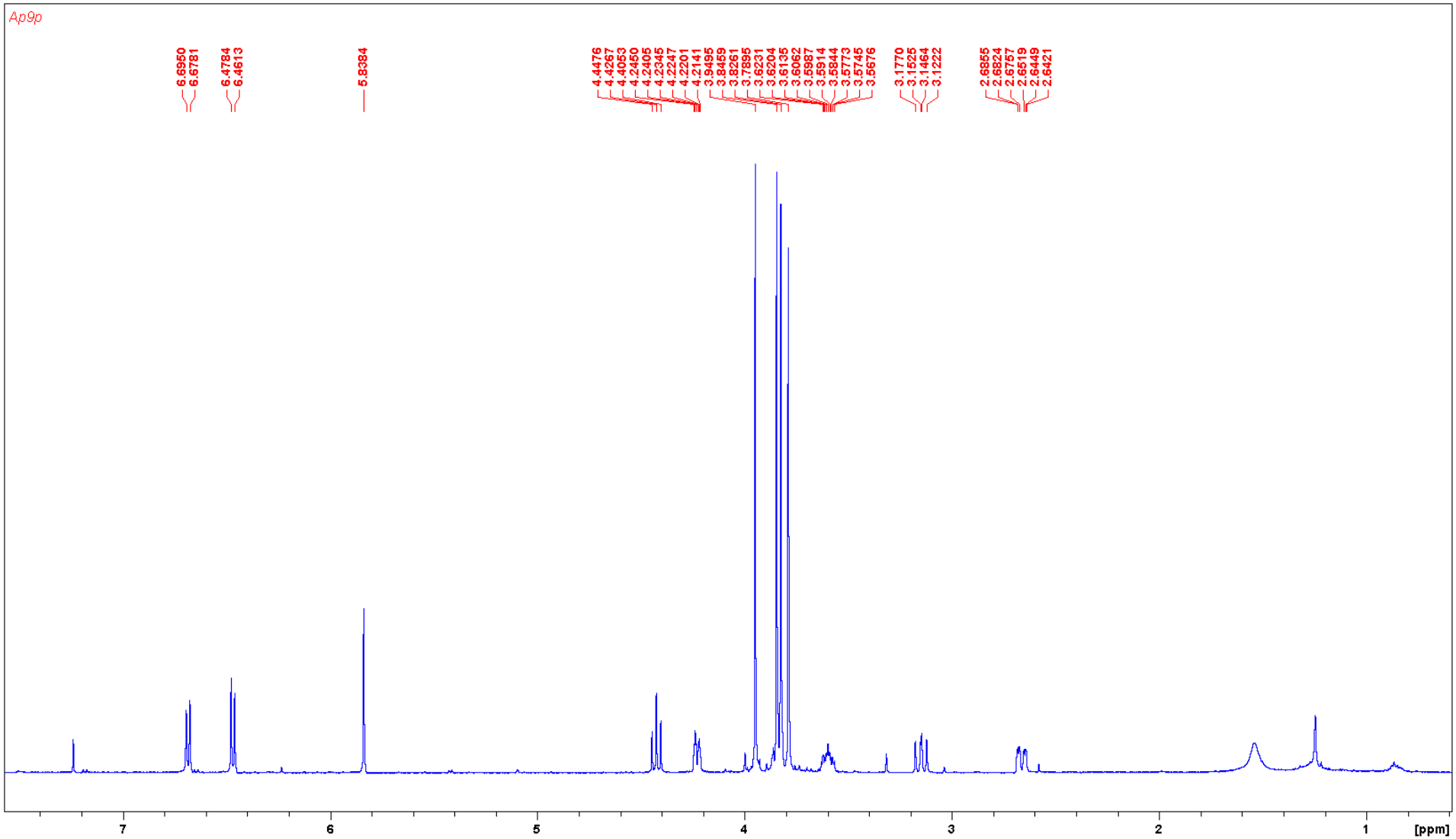

Fig. 11S. ^{1}H NMR spectrum of compound **5** in $CDCl_3$.

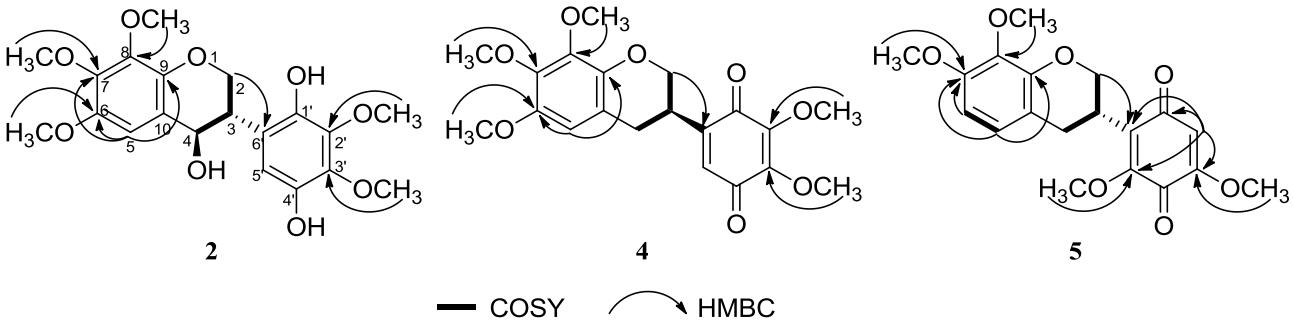

2 **4** **5**

Fig. 12S Key HMBC and COSY correlations for **2, 4** and **5**.

Table 2S. Conformers resulting of the conformational analysis for compounds **2**, **3**, **4**, and **5**

Compound	Isomer	Conformation analysis	Optimized conformers
2	3*S*,4*R*	68	49
	3*S*,4*S*	51	30
3	3*R*	10	9
	3*S*	17	9
4	3*R*	96	72
5	3*R*	29	11

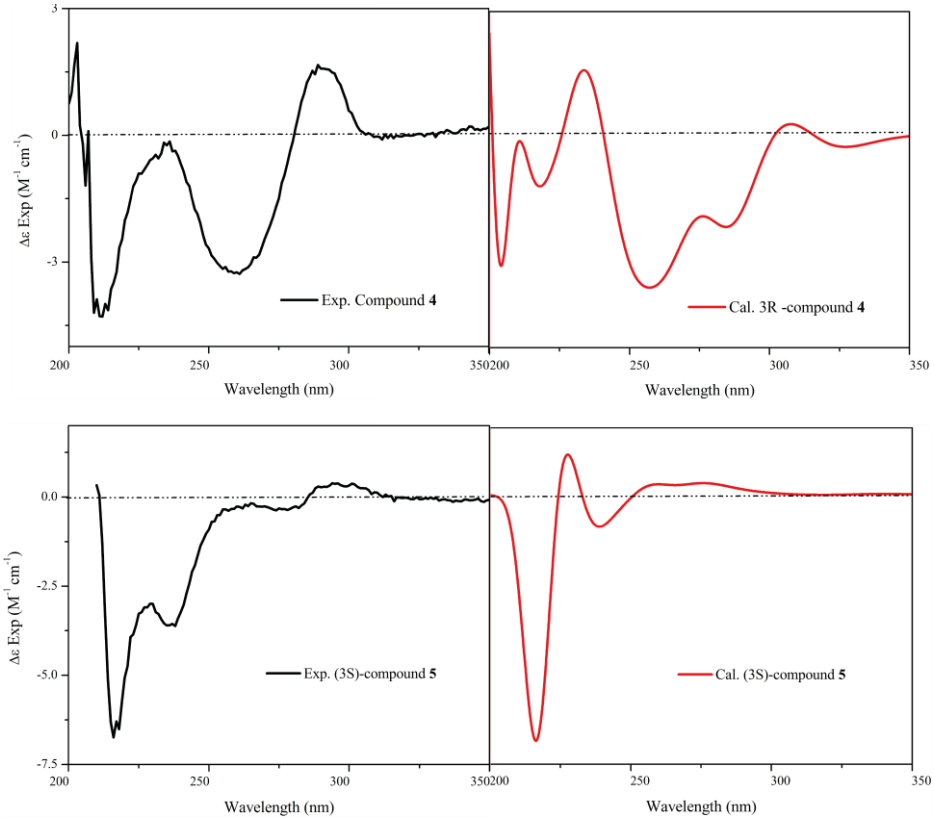

Fig. 13S Comparison of the experimental ECD of **4** and calculated spectra for the (3*R*)-enantiomer (**A**). Comparison of the experimental ECD of **5** and calculated spectra for (3*S*)-enantiomer (**B**).

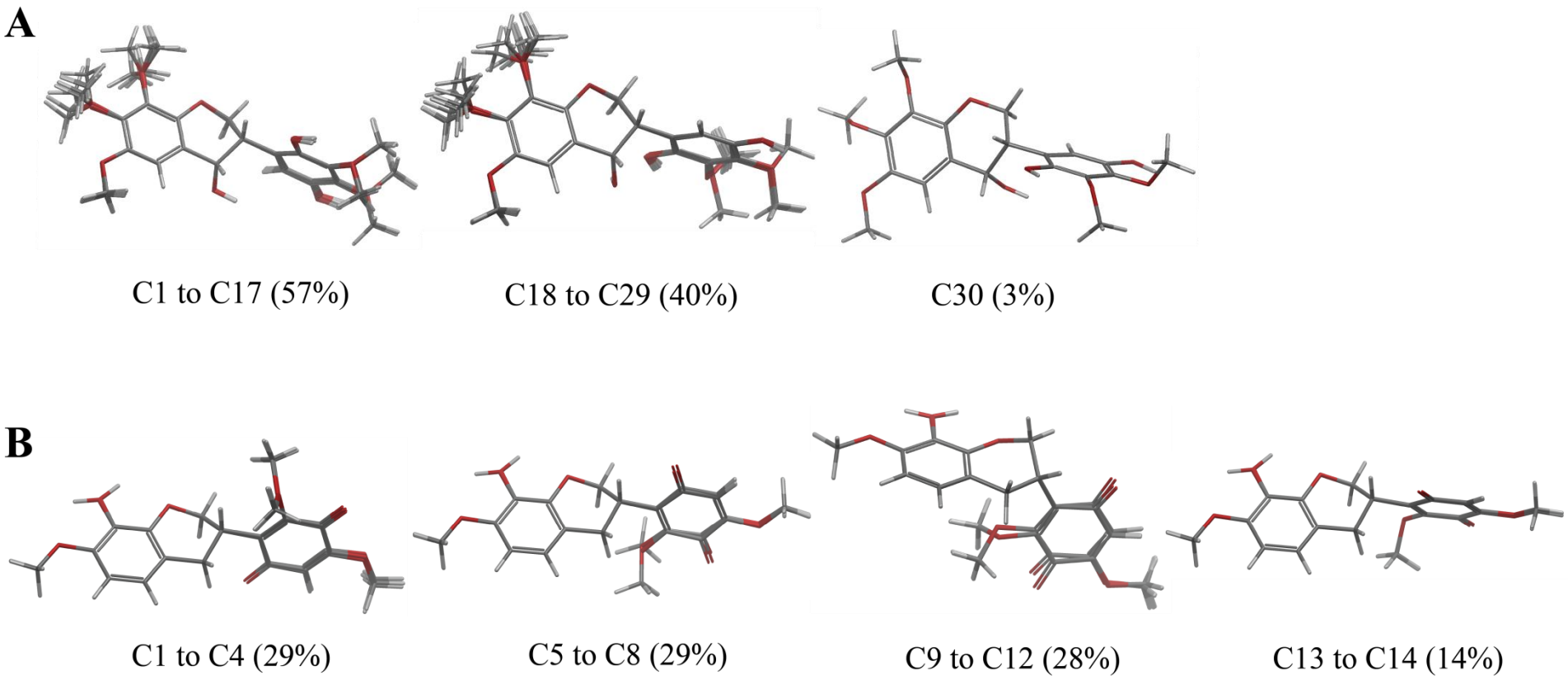

Fig. 14S. Superimposed lowest energy conformers (within 1 kcal/moL range from the global minimum) obtained from the conformational search were re-calculated using DFT at the B3LYP/6-31G** level in the gas phase. Thirty conformers obtained for the (3*S*,4*S*)-stereoisomer of **2** were grouped in three distinct core conformers (**A**). Fourteen conformers of (3*S*)**-3** corresponded to four different core conformers (**B**).

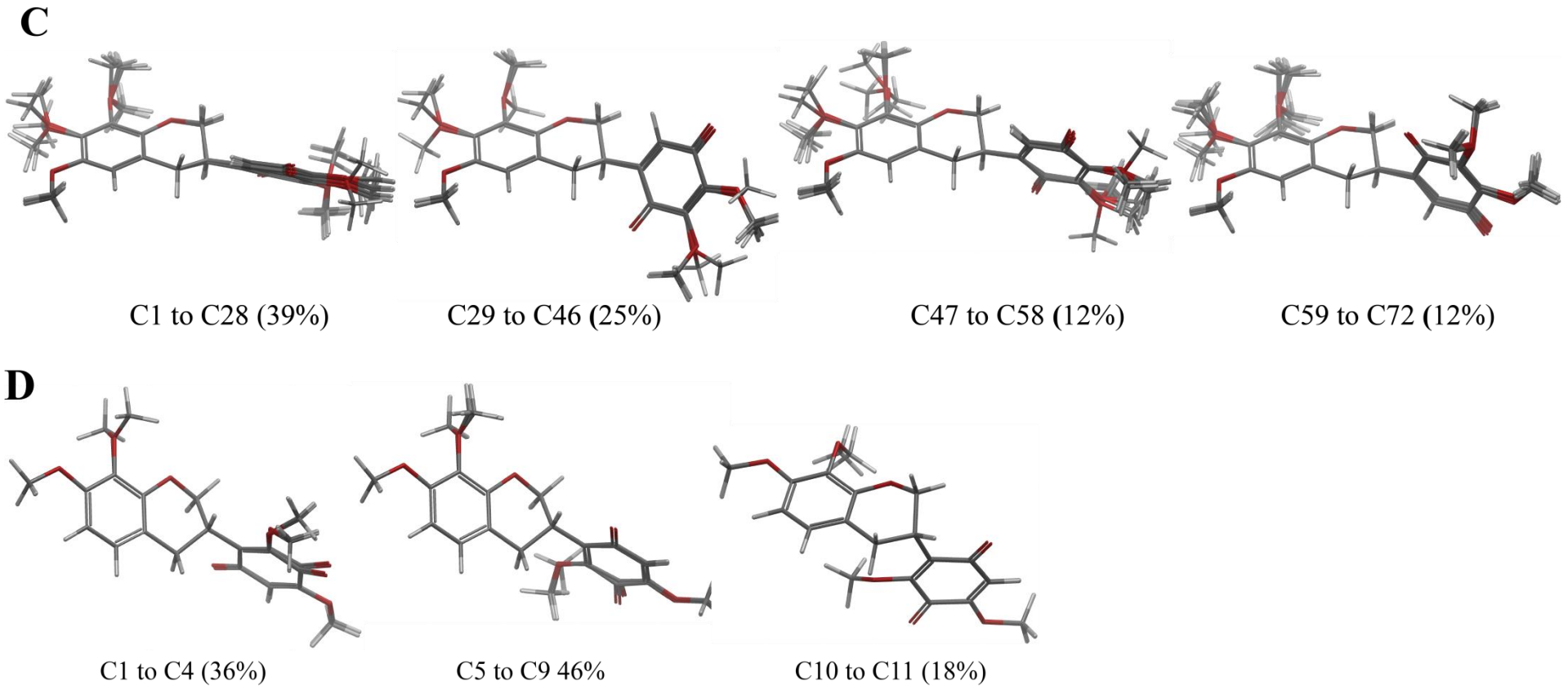

Fig. 14S Seventy two conformers of (3*R*)-**4** were grouped in four distinct core conformers (**C**). Eleven conformers of (3*S*)-**5** were grouped in three different core conformers (**D**).

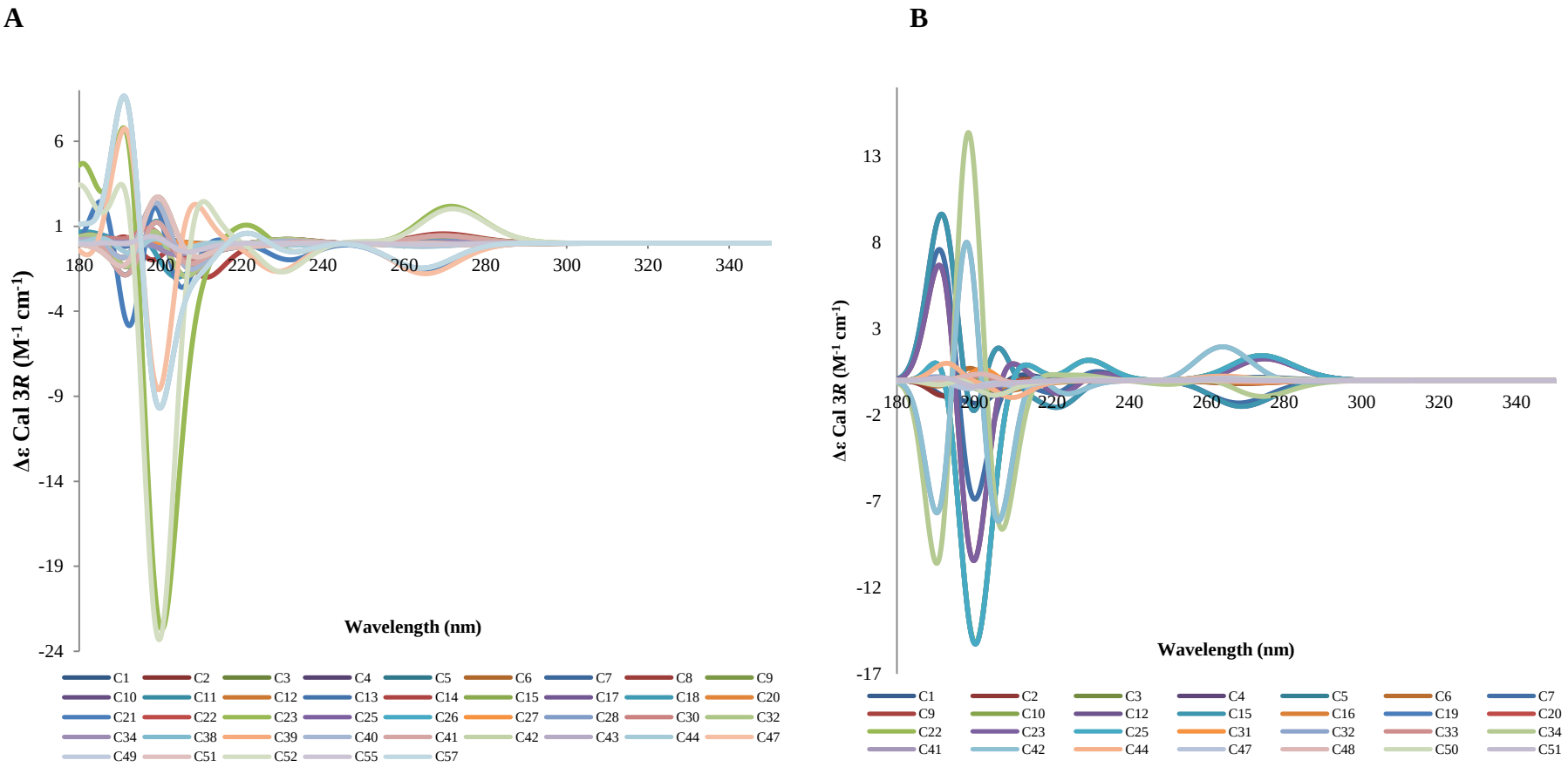

Fig. **15S** Calculated ECD spectra in MeOH (CPCM) for the minimized conformers (DTF/B3LYP/6-31G**) of compound **2**. Spectra of individual conformers (within an energy range of 1 Kcal/mol) for the (3*S*,4*R*)-stereoisomer (**A**); for individual conformers (within an energy range of 1 Kcal/mol) for the (3*S*,4*S*)-stereoisomer (**B**).

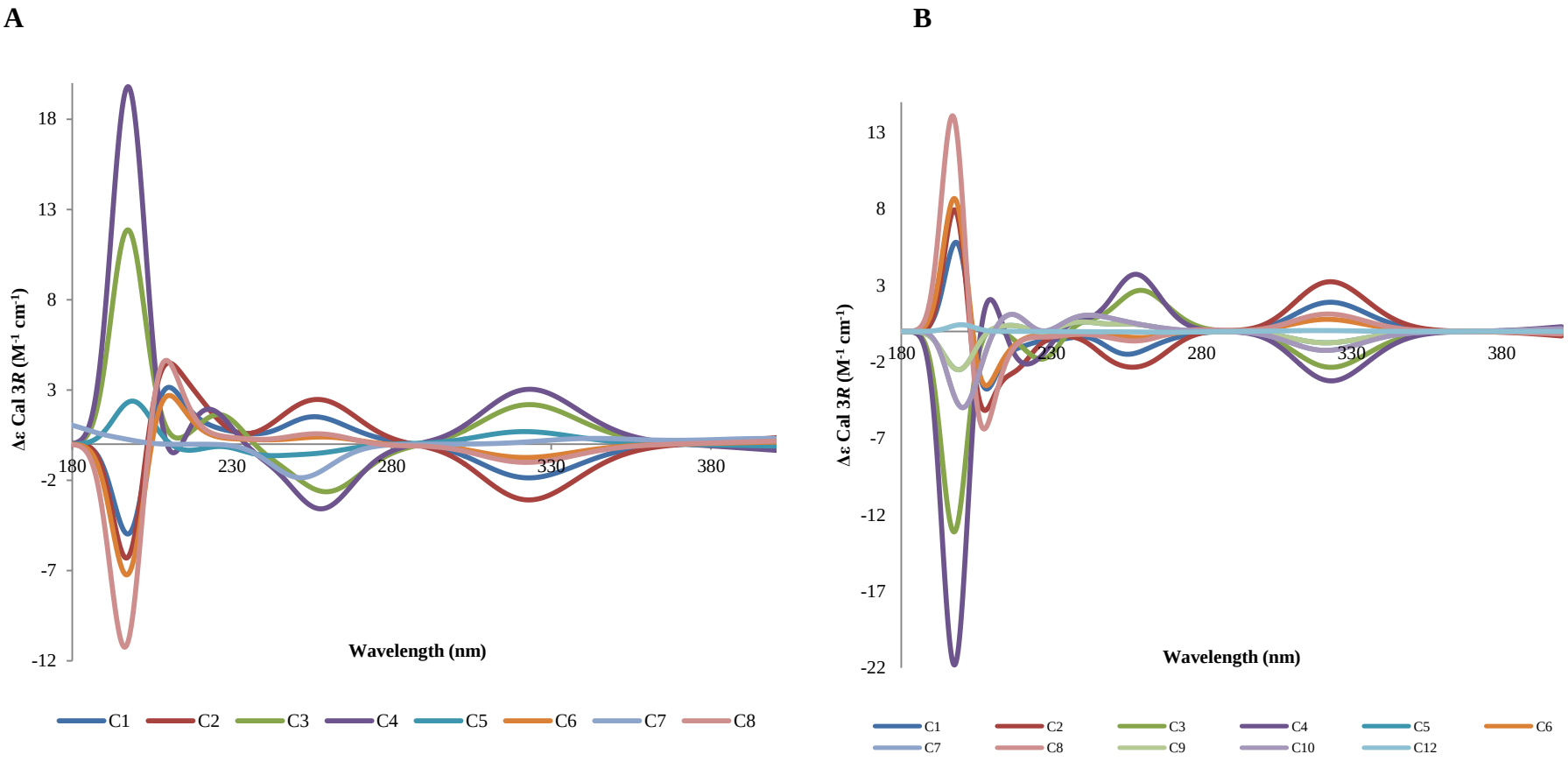

Fig. **16S** Calculated ECD spectra in MeOH (CPCM) for the minimized conformers (DTF/B3LYP/6-31G**) of compound **3**. Spectra of individual conformers (within an energy range of 1 Kcal/mol) for the (3*S*)-enantiomer (**A**); spectra of individual conformers (within an energy range of 1 Kcal/mol) for the (3*R*)-enantiomer(**B**).

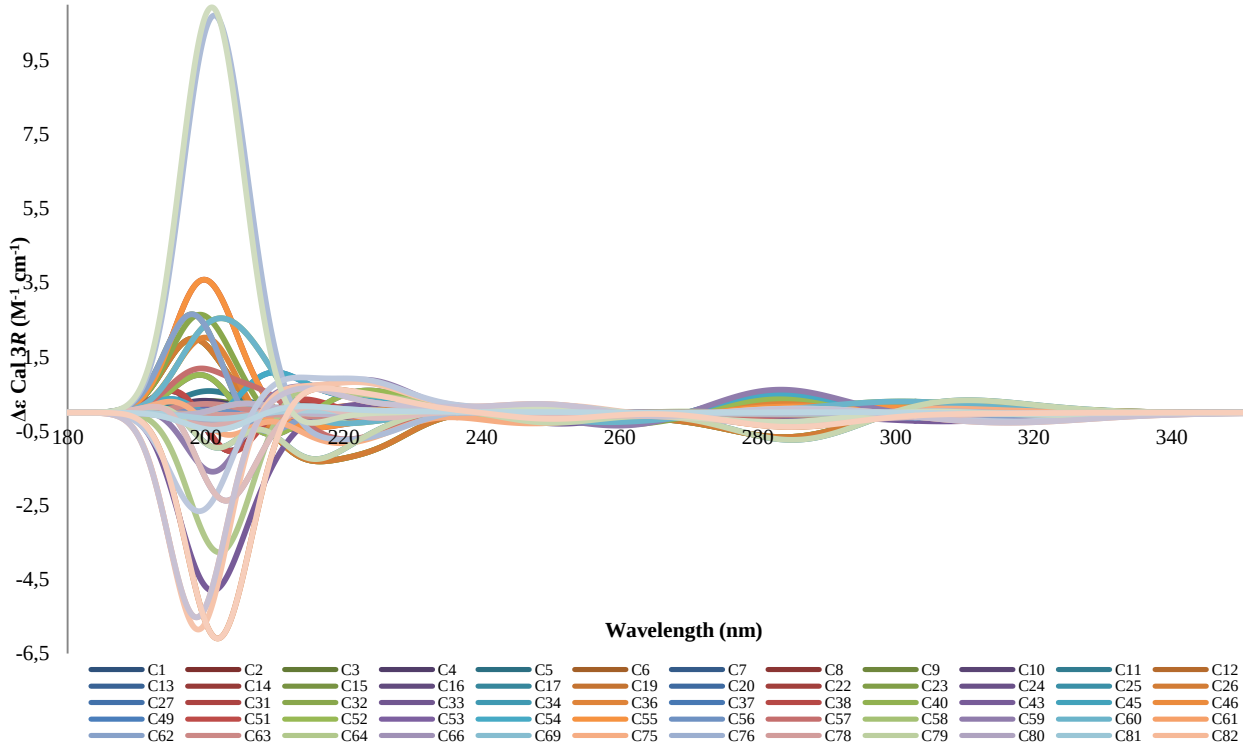

Fig. **17S** Calculated ECD spectra in MeOH (CPCM) for the minimized conformers (DTF/B3LYP/6-31G**) of compound **4**. Spectra of individual conformers (within an energy range of 1 Kcal/mol) for the (3*R*)-enantiomer are shown.

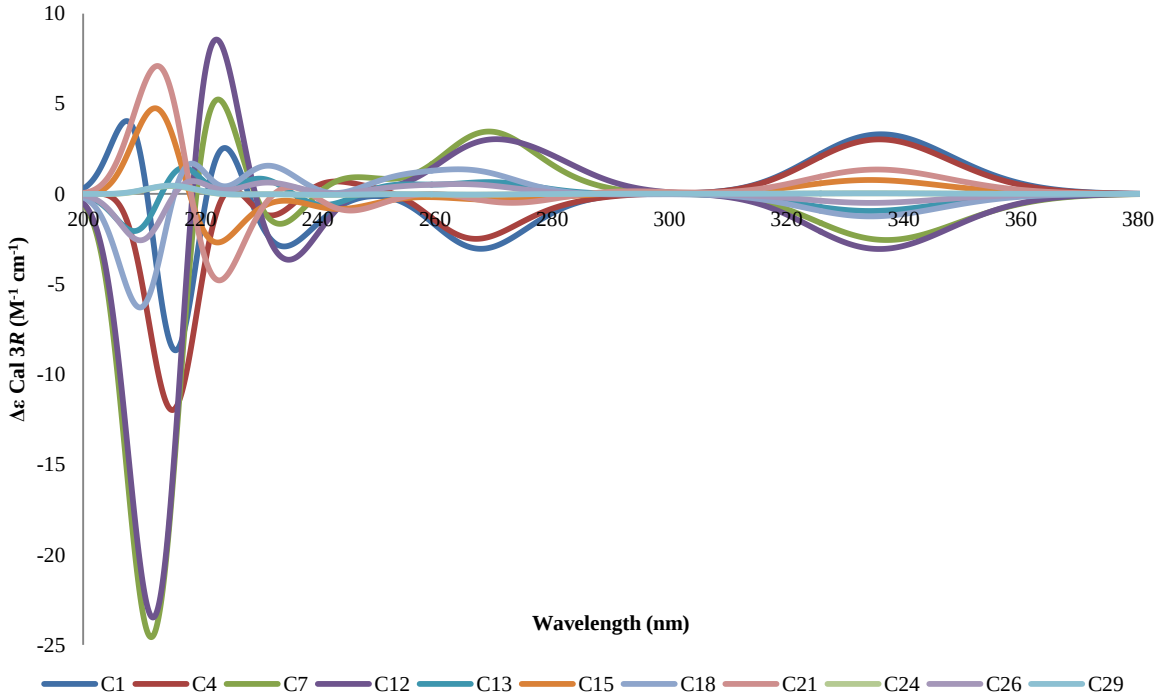

Fig. 18S Calculated ECD spectra in MeOH (CPCM) of the minimized conformers (DTF/B3LYP/6-31G**) of compound **5**. Spectra of individual conformers (within an energy range of 1 Kcal/mol) for the (3*R*)-enantiomer are shown.

References

1. *Desjardins RE, Canfield CJ, Haynes D, Chulay JD*. Quantitative assessment of antimalarial activity *in vitro* by a semiautomated microdilution technique. Antimicrob Agents Chemother 1979; 16: 710-718
2. *Trager W, Jensen JB*. Human Malaria Parasites in Continuous Culture. Science 1979; 109: 673-675
3. *Räz B, Iten M, Grether-Bühler Y, Kaminsky R, Brun R*. The Alamar Blue assay to determine drug sensitivity of African trypanosomes (*T. b. rhodesiens* and *T. b. gambiense*) *in vitro*. Acta Trop 1997; 68: 139–147
4. *Baltz T, Baltz D, Giroud C, Crockett J*. Cultivation in a semidefined medium of animal infective forms of *Trypanosoma brucei, T. equiperdum, T. evansi, T. rhodesiense, T. gambiense*. EMBO J 1985; 4: 1273-1277
5. *Buckner FS, Verlinde CL, LaFlamme AC, Van Voorhis WC*. Efficient technique for screening drugs for activity against *Trypanosma cruzi* using parasites expressing β-galactosidase. Antimicrob. Agents Chemother 1996; 40: 2592 – 2597
6. *Cunningham I*. New culture medium for maintenance of tstse tissues and growth of trypanosomatids. J Protozool 1977; 24: 325-329
7. *Page B, Page M, Noël C*. A new fluorometric assay for cytotoxicity measurements *in vitro*. Int J Oncol1993; 9: 473-476
8. *Limmatvapirat C, Sirisopanaporn S, Kittakoop P*. Antitubercular and antiplasmodial constituents of *Abrus precatorus*. Planta Med 2004; 70:276-278
9. *Lupi A, Monache FD, Marini-Bettolo GB*. Abruquinones: New natural isoflavanquinones. Gazz Chim Ital 1976; 193 :9-12
10. *Kuo SC, Chen SC, Chen LH, Wu JB, Wang JP, Teng CM*. Potent antiplatelet, anti-inflammatory and antiallergic isoflavanquiones from the roots of *Abrus precatorius*. Planta Med 1995; 61: 307-312
11. *Song CQ, Hu ZB*. Abruquinone A, B, D, E, F, and G from the root of *Abrus precatorius*. Acta Bot Sin1998; 40: 374-379
12. *Kurosawa K, Ollist WD, Redman BT, Sutherland IO, Alvest HM, Gottlieb OR*. Phytochemistry 1978; 17: 1423-1426

3.4 Antitrypanosomal Activity of Isoflavan Quinones from *Abrus precatorius*

Yoshie Hata, Samad Nejad Ebrahimi, Maria de Mieri, Stefanie Zimmermann, Tsholofelo Mokoka, Dashnie Naidoo, Gerda Fouche, Vinesh Maharaj, Marcel Kaiser, Reto Brun, Olivier Potterat, Matthias Hamburger

Fitoterapia 93 (2014) 91-87. DOI: 10.1016/j.fitote.2013.12.015

In an attempt to isolate sufficient amounts of abruquinone B and I (at least 30 mg of each one) to perform *in vivo* trypanocidal assays in mice, a second batch of *Abrus precatorius* was recollected. The chemical profiles of batch I and II were compared, and major differences were found. Five abruquinones were isolated as minor compounds, 3 of them resulted to be new compounds. Four of the substances showed high *in vitro* activity against *Trypanosoma brucei rhodesiense* and remarkable selectivity. Even though the initial goal of isolating abruquinones B and I in large amounds could not be accomplished, we isolated new antiprotozoal abruquinones, confirming our findings that these compounds are promising for further *in vivo* evaluation.

My contributions to this work were: (1) large scale separation of the CH_2Cl_2/MeOH (1:1) extract of A. precatorius; (2) isolation of abruquinones; (3) recording and interpretation of analytical data for structure elucidation (HPLC-PDA-ESI-MS, TOF-MS, 1D and 2D NMR, CD measurements) and other measurements such us optical rotation; (4) writing of the draft manuscript, preparation of figures, tables, and supporting information.

Samad Ebrahimi did the quantum-chemical calculation of ECD spectra and, under his supervision I participated in the respective analysis. Maria De Mieri supervised structure elucidation. In vitro antiprotozoal and cytotoxicity tests were performed in the Swiss TPH. The crude extract was provided by the CSIR team.

Yoshie Hata-Uribe

Fitoterapia 93 (2014) 81–87

Contents lists available at ScienceDirect

Fitoterapia

journal homepage: www.elsevier.com/locate/fitote

Antitrypanosomal isoflavan quinones from *Abrus precatorius*

Yoshie Hata [a,d], Samad Nejad Ebrahimi [a,e], Maria De Mieri [a], Stefanie Zimmermann [a], Tsholofelo Mokoka [c], Dashnie Naidoo [c], Gerda Fouche [c], Vinesh Maharaj [c], Marcel Kaiser [b], Reto Brun [b], Olivier Potterat [a], Matthias Hamburger [a,*]

[a] Department of Pharmaceutical Sciences, University of Basel, Klingelbergstrasse 50, CH-4056 Basel, Switzerland
[b] Swiss Tropical and Public Health Institute and University of Basel, Socinstrasse 57, CH-4002 Basel, Switzerland
[c] Biosciences, Council for Scientific and Industrial Research (CSIR), PO Box 395, Pretoria 0001, South Africa
[d] Department of Pharmacy, Faculty of Sciences, National University of Colombia, Carrera 30 No. 45-03, Bogota D.C. 111321, Colombia
[e] Department of Phytochemistry, Medicinal Plant and Drugs Research Institute, Shahid Beheshti University, G. C., Tehran, Iran

ARTICLE INFO

Article history:
Received 1 November 2013
Accepted in revised form 16 December 2013
Available online 29 December 2013

Keywords:
Trypanosoma brucei rhodesiense
Isoflavan quinone
Abrus precatorius
Fabaceae
ECD

ABSTRACT

Human African trypanosomiasis is a neglected tropical disease in sub Saharan Africa that is fatal if left untreated. In a search for new natural products with antitrypanosomal activity, we recently identified abruquinones B and I from *Abrus precatorius* as potent *in vitro* trypanocidal compounds with high selectivity indices. To obtain sufficient compound for *in vivo* efficacy tests in mice, a second batch of plant material was re-collected and extracted. However, the chemical profiles of the two batches differed, and additional abruquinones were isolated and identified by HR-ESI-MS, and 1D and 2D NMR (^{1}H, ^{13}C, COSY, HMBC, HSQC, and NOESY) spectroscopy. Abruquinones J (**1**), K (**2**), and L (**3**) were new, while abruquinones A (**4**) and D (**5**) were known from the first batch of plant material. The absolute configuration of compounds **1** to **3** was determined by comparison of electronic circular dichroism (ECD) spectra with calculated ECD data. Compounds **2** to **5** showed high *in vitro* activity against *T. b. rhodesiense* (IC_{50} of 0.01, 0.02, 0.02 and 0.01 μM, respectively), and remarkable SIs of 508, 374, 1379, and 668, respectively.

1. Introduction

Human African trypanosomiasis (HAT) is a neglected tropical disease caused by two subspecies of *Trypanosoma brucei*. *T. b. gambiense* is endemic in 24 countries of western and central Africa and causes more than 95% of the reported cases of HAT, while *T. b. rhodesiense* is endemic in 13 countries of eastern and southern Africa. Trypanosomiasis mainly affects population located in poor and remote rural regions. The number of infected individuals reported annually is decreasing since the turn of the millennium reaching 7200 reported cases in 2012 while the estimated number of cases is 20,000 to 30,000 [1,2].

Four drugs are currently used for the treatment of HAT, namely pentamidine, suramin, melarsoprol, and eflornithine. However, these drugs suffer from severe limitations, such as (i) lack of oral bioavailability (all of them must be administered parenterally) and chemical stability (suramin rapidly decomposes in air), (ii) complicated and long dose regimens (suramin administration can last up to 30 days) and short half-life (four infusions of eflornithine per day are necessary), and (iii) severe adverse drug reactions (pentamidine is nephrotoxic, and melarsoprol causes a fatal encephalopathy in up to 10% of the treated patients) [2–4]. The need for better drugs is urgent [3,5,6].

Natural products have been a promising source for drugs, especially for treatment of infectious and neglected diseases [4,7,8]. In a medium throughput screening of an extract library of South African medicinal plants with traditional use in protozoan diseases [8–12] the CH_2Cl_2/MeOH (1:1) extract of *Abrus precatorius* L. *ssp. africanus* Verdc had shown *in vitro*

* Corresponding author at: Division of Pharmaceutical Biology, University of Basel, Klingelbergstrasse 50, CH-4056 Basel, Switzerland. Tel.: +41 61 267 14 25; fax: +41 61 267 14 74.
E-mail address: matthias.hamburger@unibas.ch (M. Hamburger).

0367-326X/$ – see front matter © 2013 Elsevier B.V. All rights reserved.
http://dx.doi.org/10.1016/j.fitote.2013.12.015

activity against *T. b. rhodesiense*. With the aid of HPLC-based activity profiling we then identified two isoflavan quinones with potent *in vitro* activity and promising selectivity [11]. The two compounds, abruquinones B and I, fulfilled the criteria for progressing to an *in vivo* assessment of their trypanocidal activity. However, the amounts of pure compound available at that time were not sufficient for a preliminary study in mice. Therefore, a second batch of plant material was collected for the purpose of a large scale isolation of abruquinones B and I. This second collection was carried out at the same location as the first one, albeit at a different time of the year (November for the first, and April for the second collection). When comparing the phytochemical profiles of extracts from the first and second collection of *A. precatorius* (batch I and II, respectively) by TLC and HPLC-PDA-MS, we found substantial differences in their chemical composition. Most important, no peaks corresponding to abruquinones B and I were detected in batch II (Fig. 1). Isoflavonoids were found only after enrichment by flash chromatography. Given that the HPLC-PDA-MS data suggested the presence of new isoflavan quinones in these fractions, we proceeded to a targeted isolation of these compounds.

2. Materials and methods

2.1. General experimental procedures

HPLC-grade acetonitrile (MeCN) (Scharlau Chemie S.A.), and water (obtained by an EASY-pure II from Barnstead water purification system, Dubuque) were used for HPLC separations. HPLC solvents contained 0.1% HCOOH (Sigma) for analytical separations. Chloroform-*d* (100 atom% D) and benzene-d_6 (100 atom% D) for NMR were purchased from Armar Chemicals. Solvents used for extraction were of analytical grade (Romil Pure Chemistry). Reference drugs for bioassays were chloroquine (>98%, Sigma-Aldrich), melarsoprol (>95%, Sanofi-Aventis), miltefosine (>95%, VWR), and podophyllotoxin (>95%, Sigma-Aldrich). HPLC-PDA-MS analyses were performed with an Agilent 1100 system consisting of a degasser, a quaternary pump, a column oven, and a PDA detector connected to a Gilson 215 injector and to an Esquire 3000 plus ion trap mass spectrometer (Bruker Daltonics). Data acquisition and processing were done by using HyStar 3.0 software (Bruker Daltonics).

Flash chromatography was carried out with a PuriFlash® 4100 chromatography system (Interchim) controlled by InterSoft V5.0 software. Semi-preparative HPLC was performed with an Agilent 1100 series instrument equipped with a PDA detector. Data acquisition and processing were performed using HyStar 3.2 software (Bruker Daltonics). For HR-ESI-MS a micrOTOF ESI-MS system (Bruker Daltonics) was used. Mass calibration was performed with a solution of formic acid 0.1% in 2-propanol/water (1:1) containing 5 mM NaOH. Mass spectra were recorded in the range of *m/z* 150–1500 in positive ion mode with the aid of micrOTOF control software 1.1 (Bruker Daltonics). NMR spectra were recorded on a Bruker AVANCE III™ 500 MHz spectrometer equipped

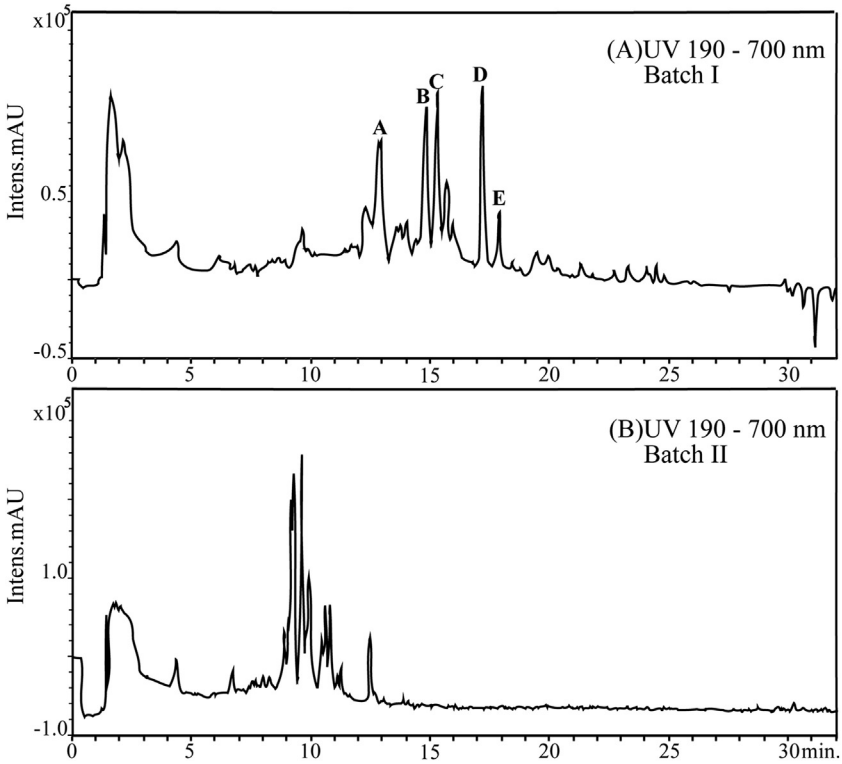

Fig. 1. HPLC-PDA analysis of batch I and II of *A. precatorius*. For separation conditions, see Section 2.3. Peak letters, in batch I between minutes 13 and 18, refer to the abruquinones isolated from batch I [11]. Abruquinone H (**A**), abruquinone G (**B**), abruquinone I (**C**), abruquinone B (**D**), and 7,8,3′,5′-tetramethoxyisoflavan-1′,4′-quinone (**E**). No peaks are present, in the same time window, in batch II.

with a 1 mm TXI microprobe (^{1}H and 2D NMR) or a 5 mm BBO probe (^{13}C NMR) (Bruker BioSpin) operating at 500 (^{1}H) and 125 MHz (^{13}C). Chemical shifts are reported as δ values (ppm) with the residual solvent signal as internal reference, *J* in Hz. Standard pulse sequences from Topspin 3.0 software package were used. CD spectra were recorded with a Chirascan™ CD Spectrometer, Pro-Data Software V2.4.2 and optical rotation with a Jasco P-2000 polarimeter, equipped with a 1 dm microcell and software Spectra Manager version 2.

2.2. Plant material

Samples of the whole plant of *A. precatorius* (batch II) were collected at Jozini, KwaZulu Natal Province in South Africa during April 2012 by a botanist, Mr. Hans Vahrmeijer. The plant was identified as *Abrus precatorius* L. *ssp. africanus* Verdc, and a herbarium specimen was deposited at the South African National Biodiversity Institute (SANBI) (voucher specimen number PRE 782945).

The whole plant was dried in an oven at 30–60 °C. Dried plant material was ground to a coarse powder using a hammer mill and stored at ambient temperature prior to extraction. One kilogram of dried, ground material was extracted with 5 L of a mixture of CH_2Cl_2 and MeOH (1:1) at room temperature for 1 h with occasional stirring. The solvent was filtered and the residual plant material further extracted overnight with 2.5 L CH_2Cl_2/MeOH (1:1) followed by filtration. Finally, a third extraction of the pulp was done with 2.5 L solvent for 1 h with filtration. The pulp was discarded and the filtrates combined and concentrated using a rotary vacuum evaporator at a temperature below 45 °C and then further dried *in vacuo* at room temperature for 24 h. The dried extract of 55.0 g (5.5%, w/w) was stored at −20 °C.

2.3. Fractionation and isolation

The CH_2Cl_2/MeOH (1:1) extract of the whole plant (15 g) was separated by flash chromatography on a silica gel (15–40 μm) column (50 × 3500 mm, 300 g) by a gradient elution with ethyl acetate (B) in *n*-hexane (A) as follows 0% → 40% B (0–3 h), 40% B (1 h), and 40% → 100% B (1 h) at a flow rate of 22 mL/min. Fractions (22 mL each) were combined based on TLC analysis. Twenty two fractions were obtained and analyzed by HPLC-PDA-MS on a SunFire™ C18 column (3.5 μm, 3.0 × 150 mm; Waters) with H_2O (solvent A) and MeCN (solvent B) using the flowing gradient profile: 10% → 100% B (0–30 min) and 100% B (31–32 min). The flow rate was 0.5 mL/min. Fractions F12 (19.1 mg), F13 (36.0 mg), F16 (23.4 mg), and F17 (31.1 mg) were found to contain abruquinones (Fig. A1 of Appendix A). These fractions were purified by semi-preparative RP-HPLC using a SunFire™ C18 column (3.5 μm, 10 × 150 mm, Waters) with H_2O (solvent A) and MeCN (solvent B) and the following gradient 25% → 42% B (0–11.1 min), 42% → 48% B (11.1–20.9 min), 48% → 100% B (20.9–27.2 min), and 100% B (27.2–34.8 min). The flow rate was 4 mL/min. Fractions were dissolved in DMSO (10 or 20 mg/mL, depending on their solubility) and injected in aliquots of 300 μL. Eight compounds were obtained. Compounds **1** to **5** were obtained only from batch II. Compound **1** (5.1 mg, t_R 13.7 min) was isolated from F16 and F17, compound **2** (6.1 mg, t_R 15.2 min) from F17, compound **3** (1.3 mg, t_R 12.6 min) from F13, compound **4** (3.4 mg, t_R 17.9 min) from F13 and compound **5** (3.2 mg, t_R 12.4 min) from F16 and F17. In addition, previously reported [11] abruquinone H (**A**) (2.3 mg, t_R 12.9 min) was obtained from F16 and F17, abruquinone I (**C**) (3.1 mg, t_R 14.9 min) from F13, and 7,8,3′,5′-tetramethoxyisoflavan-1′,4′-quinone

Table 1
^{1}H and ^{13}C NMR spectroscopic data for compounds **1**, **2**, and **3** ($CDCl_3$, 500 MHz for δ_H, 125 MHz for δ_C).

Position	1		2		3	
	δ_H	δ_C	δ_H	δ_C	δ_H	δ_C
2α	4.19 (dd, 10.8, 5.0)	66.9	4.19 (dd, 10.9, 5.0)	66.5	4.25 (ddd, 10.5, 3.1, 1.6)	69.6
2β	3.62 (dd, 10.8, 10.8)		3.61 (dd, 10.9, 10.8)		3.97 (dd, 10.0, 9.8)	
3	3.52 (ddd, 10.8, 6.9, 5.0)	40.6	3.45 (ddd, 10.8, 6.9, 5.0)	40.8	3.52 (dddd, 11.0, 9.0, 5.5, 3.5)	32.3
4	5.49 (d, 6.9)	79.6	5.42 (d, 6.9)	78.9	Hα 2.87[a] Hβ 2.87[a]	30.5
5	7.09 (s)	115.7	6.96 (s)	112.2	6.52 (s)	112.0
6	–	140.8	–	142.3	–	141.3
7	–	148.2	–	147.5	–	145.1
8	6.43 (s)[a]	100.2	6.51 (s)	103.7	6.45 (s)	103.5
9	–	149.4	–	150.5	–	148.8
10	–	112.0	–	110.9	–	112.7
1′	–	146.4	–	143.8	–	140.7
2′	–	130.98	–	139.2	5.82 (s)	138.6
3′	–	148.3	–	137.9	–	139.7
4′	6.42 (d, 8.0)[a]	104.0	–	144.2	–	142.5
5′	6.70 (dd, 8.0, 1.0)	114.9	6.57 (s)	104.7	6.46 (s)	108.6
6′	–	121.8	–	123.4	–	122.9
2′-OCH_3	–	–	3.89 (s)	61.6	3.87 (s)	61.0
3′-OCH_3	3.84 (s)	56.7	3.96 (s)	60.8	3.90 (s)	61.1
6-OCH_3	–	–	3.87 (s)	56.5	3.79 (s)	56.8
7-OCH_3	3.82 (s)	56.2	–	–	–	–
–OH	–	–	–		5.44 (br s)	–
–OH	–	–	–		5.66 (br s)	–

[a] Overlapping signals within the same column.

(E) (3.7 mg, t_R 17.0 min) from F12 and F13 (Fig. 1). Purity of compounds **1**–**5** was >95% as determined by ^{1}H-NMR (Fig. A2, A11, A16, A20, and A21 of Appendix A).

(3*S*,4*S*)-4,6,1′,2′-tetrahydroxy-7,3′-dimethoxyisoflavan (abruquinone J, 1): colorless amorphous compound; $[\alpha]_D^{20}$-173 (*c* 0.1, $CHCl_3$); UV (MeOH) λ_{max} (log ε) 208 (4.92), 295 (3.88) nm; CD (MeOH): $\Delta\varepsilon_{201\ nm} = +48.8$, $\Delta\varepsilon_{213\ nm} = -71.4$, $\Delta\varepsilon_{236\ nm} = -10.1$ (sh), $\Delta\varepsilon_{293\ nm} = +3.55$; ^{1}H and ^{13}C NMR data in $CDCl_3$ and C_6D_6, see Table 1 and Table A1 of Appendix A; HR-ESI-MS: *m/z* = 339.0848 $[M\text{-}H_2O + Na]^+$ (calculated for $C_{17}H_{18}O_7$: 334.1053).

(3*S*,4*R*)-4,7,1′,4′-tetrahydroxy-6,2′,3′-trimethoxyisoflavan (abruquinone K, **2**): colorless amorphous substance; $[\alpha]_D^{20}$-153 (*c* 0.1, $CHCl_3$); UV (MeOH) λ_{max} (log ε) 205 (4.69), 295 (3.81) nm; CD (MeOH): $\Delta\varepsilon_{200\ nm} = +25.9$, $\Delta\varepsilon_{210\ nm} = -45.1$, $\Delta\varepsilon_{235\ nm} = -7.82$ (sh), $\Delta\varepsilon_{284\ nm} = -1.28$, $\Delta\varepsilon_{304\ nm} = +2.97$; ^{1}H and ^{13}C NMR data in $CDCl_3$, see Table 1; HR-ESI-MS: *m/z* = 369.1000 $[M\text{-}H_2O + Na]^+$ (calculated for $C_{18}H_{20}O_8$: 364.1158).

(3*R*)-7,1′,4′-trihydroxy-6,2′,3′-trimethoxyisoflavan (abruquinone L, **3**): orange amorphous substance; $[\alpha]_D^{20}$-45.5 (*c* 0.1, $CHCl_3$); UV (MeOH) λ_{max} (log ε) 201 (4.77), 293 (3.90) nm; CD (MeOH): $\Delta\varepsilon_{202\ nm} = +10.5$, $\Delta\varepsilon_{212\ nm} = -7.26$, $\Delta\varepsilon_{228\ nm} = -3.29$ (sh), $\Delta\varepsilon_{272\ nm} = -0.33$, $\Delta\varepsilon_{301} = +0.60$; ^{1}H and ^{13}C NMR data in $CDCl_3$ see Table 1; HR-ESI-MS: *m/z* = 371.1155 $[M + Na]^+$ (calculated for $C_{18}H_{20}O_7$: 348.1209).

(3*R*)-6,7,2′,3′-tetramethoxyisoflavan-1′,4′-quinone (abruquinone A, **4**) [13]: For physico-chemical characterization, see Appendix A. CD (MeOH) $\Delta\varepsilon_{199\ nm} = +4.19$; $\Delta\varepsilon_{210\ nm} = -3.28$; $\Delta\varepsilon_{236\ nm} = +0.99$; $\Delta\varepsilon_{254\ nm} = -2.71$; $\Delta\varepsilon_{293\ nm} = +1.45$; ^{1}H and ^{13}C NMR data in $CDCl_3$; see Table A1.

(3*R*)-7-hydroxy-6,2′,3′-trimethoxyisoflavan-1′,4′-quinone (abruquinone D, **5**) [14]: for physico-chemical characterization, see Appendix A. CD (MeOH) $\Delta\varepsilon_{198\ nm} = +0.77$; $\Delta\varepsilon_{209\ nm} = -2.85$; $\Delta\varepsilon_{236\ nm} = +0.18$; $\Delta\varepsilon_{258\ nm} = -1.46$, $\Delta\varepsilon_{291\ nm} = +0.60$; ^{1}H and ^{13}C NMR data in $CDCl_3$; see Table A1.

2.4. Electronic circular dichroism

The absolute configuration (AC) of compounds **1** and **3** was established by electronic circular dichroism (ECD). Experimental ECD spectra were compared with calculated data, as previously described [11,15,16]. A detailed procedure is given in Appendix A.

2.5. Antiprotozoal and cytotoxicity tests

The *in vitro* antiprotozoal activity of compounds was tested against *Plasmodium falciparum* (K1 strain), *Trypanosoma brucei rhodesiense* (STIB 900 strain), *Trypanosoma cruzi* (Tulahuen strain C2C4 w/LacZ), and *Leishmania donovani* (strain MHOM/ET/67/L82). Cytotoxicity was determined with the rat skeletal myoblast cell line (L-6 cells). For the assays DMSO stock solutions (10 mg/mL) of extracts and purified compounds were freshly diluted in medium prior to testing (final DMSO concentration in assay <1%). Assays were performed in three independent repetitions. Details on culturing of parasites and assay protocols are provided as Appendix A.

3. Results and discussion

The phytochemical profiles of batches I and II were compared by HPLC-PDA-MS (Fig. 1). In the CH_2Cl_2/MeOH (1:1) extract of batch II no abruquinones were detected. After an enrichment by silica gel flash chromatography, isoflavan quinones could be detected, albeit in much lower concentrations than in batch I. Purification of isoflavonoids was achieved by semi-preparative RP-HPLC of selected fractions, and a total of eight compounds were obtained in milligram amounts. Structures were established by NMR spectroscopy (^{1}H, ^{13}C, COSY, HSQC, and HMBC), HR-ESI-MS and ECD. Compounds **1** [(3*S*,4*S*)-4,6,1′,2′-tetrahydroxy-7,3′-dimethoxyisoflavan], **2** [(3*S*,4*R*)-4,7,1′,4′-tetrahydroxy-6,2′,3′-trimethoxyisoflavan], and **3** [(3*R*)-7,1′,4′-trihydroxy-6,2′,3′-trimethoxyisoflavan] are new natural products and have been designated as abruquinones J, K, and L, respectively (Fig. 2).

For compound **1**, a molecular formula of $C_{17}H_{18}O_7$ was deduced from HR-ESI-MS (*m/z* 339.0848 $[M\text{-}H_2O + Na]^+$; calculated: 334.1053). The ^{13}C NMR spectrum (Table 1) showed 17 signals, twelve of which were found in the region between δ_C 100.2 and 149.4. This was indicative of a highly substituted aromatic ring system. The remaining carbon resonances were attributed to an oxygenated methine (δ_C 79.6), an oxygenated methylene (δ_C 66.9), two methoxy (δ_C 56.7 and 56.2), and one methine group (δ_C 40.6). The ^{1}H NMR spectrum (Table 1) displayed signals indicative of four aromatic protons (δ_H 7.09 (s), 6.70 (dd, J = 8.0, 1.0 Hz), 6.43 (s) and 6.42 (d, J = 8.0 Hz)), and two aromatic methoxy

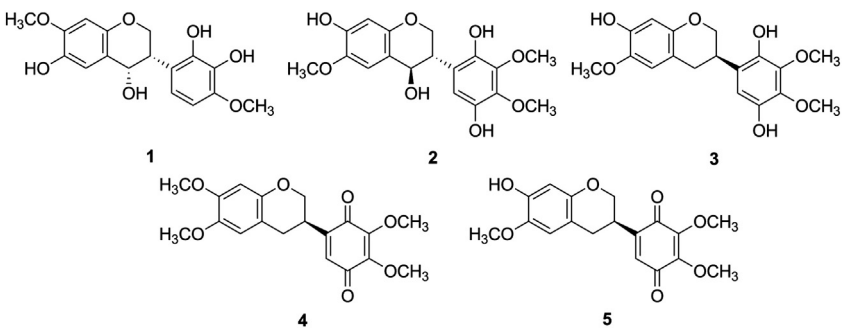

Fig. 2. Structure of compounds **1**–**5**.

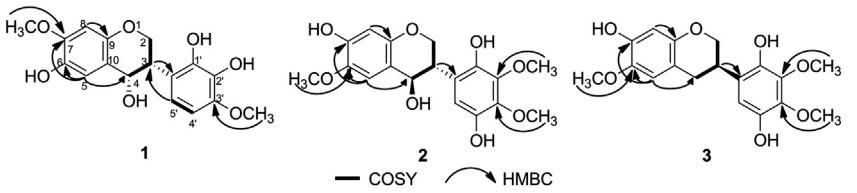

Fig. 3. Key HMBC and COSY correlations for compounds **1** and **3**.

groups (δ_H 3.84 and 3.82). Four aliphatic protons were observed at δ_H 5.49 (d, J = 6.9 Hz), 3.52 (ddd, J = 10.8, 6.8, 5.0 Hz), 3.62 (t, J = 10.7 Hz), and 4.19 (dd, J = 10.8, 4.9 Hz), suggesting an isoflavan scaffold with a hydroxy group at C-4. Unambiguous assignment of ^{1}H and ^{13}C NMR data was achieved by a combination of COSY, HMBC, HSQC, and NOESY experiments, and by comparison with reported data of isoflavan quinones and -hydroquinones [11,13,14,17,18]. The connectivity of rings A and C was confirmed by $^3J_{C\text{-}H}$ coupling between H-5 (δ_H 7.09, ring A) and C-4 (δ_c 79.6, ring C), and HMBC correlations between H-3 (δ_H 3.52, ring C) and C-6′ (δ_c 121.8, ring B), and H-5′ (δ_H 6.70, ring B) and C-3 (δ_C 40.6, ring C) corroborated the connectivity between rings B and C (Fig. 3). The vicinal coupling constants H-2α/H-3 (J = 5.0 Hz) and H-2β/H-3 (J = 10.8 Hz) corresponded to dihedral angles of 60° and 180°, respectively, and indicated an axial orientation of H-3. The coupling constant H-4/H-3 (J = 6.9 Hz) agreed with a dihedral angle of 30° to 50°, or 130° to 150°, indicating two possible orientations for H-4 in a half-chair [19]. The NOESY contact observed between H-4 (δ_H 5.49) and H-3 (δ_H 3.52) did not allow for the unambiguous differentiation between a pseudo-axial or pseudo-equatorial orientation of H-4. The pseudo-equatorial orientation of H-4 was finally deduced from a conformational analysis performed for the calculation of the ECD spectrum of compound **1**. The absolute configuration was established by comparing the experimental ECD spectrum with data calculated for the (3*S*,4*R*) and (3*S*,4*S*) diastereomers (Fig. 4). A total of 8 and 6 conformers, respectively, were found within a 1 Kcal/mol energy window from the particular global minimum (Fig. A24 of Appendix A). The conformers were subjected to geometrical optimization in the gas phase [20,21], ECD spectra were calculated for each one of them (Fig. A26 of Appendix A), and a final ECD spectrum was obtained after combination of the individuals spectra, according to their population contribution. The calculated ECD spectrum for the (3*S*,4*R*)-stereoisomer showed three negative CEs around 200, 213, and 280 nm, and two positive CEs at 230 and 263 nm (Fig. 4), while the ECD spectrum for the (3*S*,4*S*)-stereoisomer showed a positive CE around 200 nm. Hence, the strong positive CE around 200 nm and the general appearance of the experimental ECD spectrum matched well with the calculated spectrum of the (3*S*,4*S*)-stereoisomer, and compound **1** was thus established as (3*S*,4*S*)-4,6,1′,2′-tetrahydroxy-7,3′-dimethoxyisoflavan.

Compound **2** had a molecular formula of $C_{18}H_{20}O_8$, as derived from HR-ESI-MS (m/z 369.1000 $[M\text{-}H_2O + Na]^+$; calculated: 364.1158). The ^{13}C NMR and ^{1}H NMR spectra (Table 1) showed an additional methoxy group when compared to **1**. Like compound **1**, the ^{1}H NMR spectrum of **2** showed four aliphatic protons. The COSY and HMBC correlations (Fig. 3) confirmed the presence of an isoflavan scaffold with a hydroxyl group at C-4. A pseudo-axial orientation of H-4 was finally derived from a conformational analysis performed for calculation of the ECD spectrum [11]. Compound **2** showed a strong negative CE around 210 nm, and a weak negative CE at 290 nm (Fig. A23A of Appendix A), similar to (3*S*,4*R*)-abruquinone G [11]. Therefore, the absolute configuration was established as (3*S*,4*R*). Compound **3** had a molecular formula of $C_{18}H_{20}O_7$, as indicated by its HR-ESI-MS (m/z 371.1155 $[M\text{-}H_2O + Na]^+$; calculated: 348.1209). Analysis of the ^{13}C NMR and ^{1}H NMR spectra (Table 1) showed that **3** was closely related to isoflavonoid **2**,

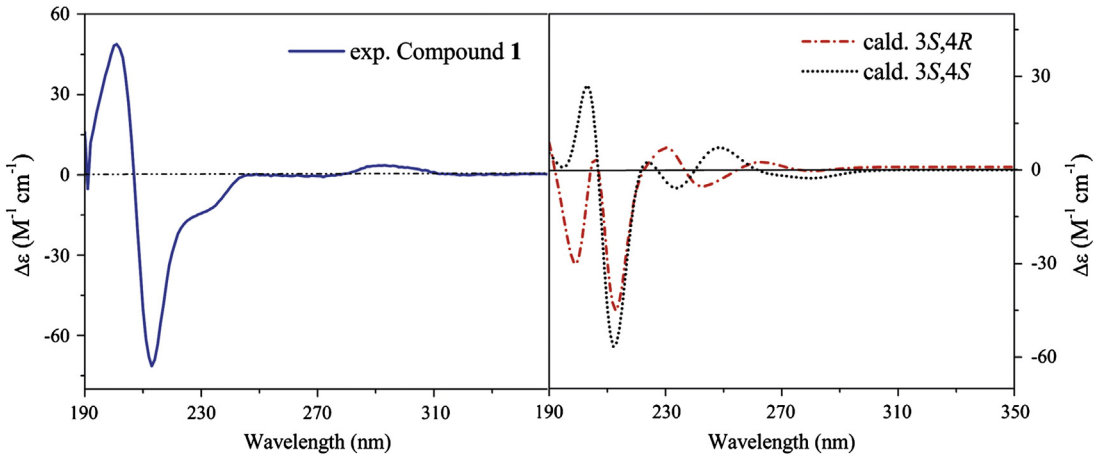

Fig. 4. Comparison of the experimental ECD of **1** with calculated spectra for the (3*S*,4*R*) and (3*S*,4*S*)-diastereomers.

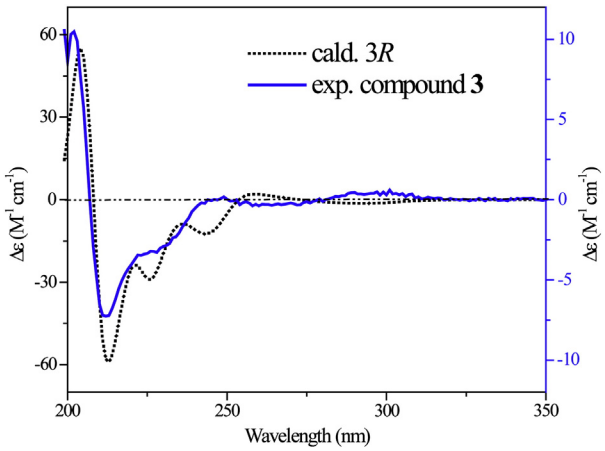

Fig. 5. Comparison of the experimental ECD of **3**, with calculated spectra for the (3*R*)-enantiomer.

the main difference being the presence of a methylene group (m, δ_H 2.87, δ_C 30.5) instead of an oxygenated methine. The COSY and HMBC correlations (Fig. 3) were in agreement with those observed for **2** and confirmed the presence of an isoflavan scaffold. The equatorial orientation of the B-ring was deduced from the vicinal coupling pattern of 3-H (δ_H 3.52, *dddd* J = 11.0, 9.0, 5.5, 3.5) that indicated a *trans*-diaxial orientation of H-2_{axial}/H-3 (J = 11.0 Hz), and H-3/H-$4_{pseudoaxial}$ (J = 9.0 Hz). A conformational analysis of **3** revealed 11 conformers within a 1 Kcal/mol energy window from the particular global minimum (Fig. A25 of Appendix A). The calculated ECD spectrum of the (3*R*)-enantiomer showed a positive CE around 204 nm, and two negative CEs at 212 and 235 nm. This pattern fitted well with the experimental spectrum of **3** (Fig. 5) which showed a strong positive CE at 202 nm and two negative CEs at 212 and 233 nm. Compound **3** was thus (3*R*)-7,1′,4′-trihydroxy-6,2′,3′-trimethoxyisoflavan.

Isoflavonoids **4** and **5** were identified from their HR-ESI-MS, 1D and 2D NMR data, as abruquinones A [13,14] and D [14], respectively. The AC of both compounds was assessed by ECD (Fig. A23B and A23C of Appendix A). Their experimental spectra were very similar and fitted well with the spectrum of (3*R*)-abruquinone B [11]. Accordingly, **4** and **5** were thus [(3*R*)-6,7,2′,3′-tetramethoxyisoflavan-1′,4′-quinone] and [(3*R*)-7-hydroxy-6,2′,3′-trimethoxyisoflavan-1′,4′-quinone], respectively. The AC of **4** had been reported earlier, but reports were contradictory and suggested that both enantiomers had been found in *A. precatorius* [11,13,14]. In contrast, our findings for **5** were in agreement with the literature [14]. Abruquinone H, I and 7,8,3′,5′-tetramethoxyisoflavan-1′,4′-quinone had been previously isolated from batch I of *A. precatorius* [11].

Compounds **2** to **5** showed strong *in vitro* activity against *T. b. rhodesiense* (IC_{50} values of 0.11, 0.02, 0.02, and 0.01 μM, respectively) and low cytotoxicity in L-6 cells (IC_{50} values of 57.3, 7.5, 34.5, and 4.8 μM, respectively). The selectivity indices (SIs of 508, 374, 1379, and 668) are high enough to warrant *in vivo* tests in mice. In addition, *in vitro* activity against *P. falciparum* and *L. donovani* was assessed (Table 2). However, all compounds showed low or no inhibitory effect at the concentrations tested.

Even though the initial goal of isolating abruquinones B and I for *in vivo* testing was not achieved, we were able to identify a series of new isoflavan quinones with promising *in vitro* activity. This corroborates our earlier findings that these compounds warrant an *in vivo* evaluation in the acute rodent model of *T. b. rhodesiense* [22]. The qualitative and quantitative differences in isoflavonoids between the two batches appear to be a seasonal effect given that the material was collected in the same location, but at different times of the

Table 2
In vitro antiprotozoal activities of **1**–**5** against *P. falciparum*, *T. b. rhodesiense*, and cytotoxic activity in L-6 cells.

Compound	*P. falciparum*		*T. b. rhodesiense*		*L. donovani*		Cytotoxicity
	IC_{50} (μM)[a]	SI	IC_{50} (μM)[a]	SI	IC_{50} (μM)	SI	IC_{50} (μM)[a]
1	83.7 ± 4.0	1.8	11.2 ± 3.337	13.6	Inactive[b]	–	152.1 ± 7.8
2	14.1 ± 0.4	4.1	0.11 ± 0.053	508.5	Inactive[b]	–	57.3 ± 4.3
3	13.4 ± 0.6	0.6	0.02 ± 0.003	374.3	Inactive[b]	–	7.5 ± 1.2
4	9.2 ± 1.5	3.7	0.02 ± 0.003	1379.4	Inactive[b]	–	34.5 ± 16.3
5	3.5 ± 0.16	1.4	0.01 ± 0.001	668.0	Inactive[b]	–	4.8 ± 1.6
Chloroquine[c]	0.004 ± 0.001	–	–	–	–	–	–
Melarsoprol[c]	–	–	0.003 ± 0.002	–	–	–	–
Miltefosine[c]	–	–	–	–	1.536 ± 0.051	–	–
Podophyllotoxin[c]	–	–	–	–	–	–	0.019 ± 0.006

[a] Values are expressed as mean ± standard error of the mean.
[b] No activity observed at the highest test concentration of 90 μg/mL (247.2 to 269.4 μM).
[c] Reference drugs. SI (selectivity index): quotient of IC_{50} value for L-6 cells and IC_{50} for parasite.

year (November (summer) for batch I, April (autumn) for batch II). From soybeans it is known that isoflavonoid accumulation is affected by environmental factors such as temperature and water regimen [23].

Conflict of interest

The authors declare no conflict of interest.

Acknowledgments

The authors thank the Council for Scientific and Industrial Research (CSIR), the Swiss Confederation, and the Department of Science and Technology for financial support under the Swiss South African Joint Research Program (grant JRP 03), and the South African Biodiversity Institute (SANBI) for the identification of the plant species. Y. Hata gratefully acknowledges a PhD stipend from the Administrative Department of Science and Technology from Colombia (Colciencias) managed by LASPAU. We thank Mrs. M. Rogalski for proofreading the manuscript.

Appendix A. Supplementary data

Detailed protocols of biological activity, NMR spectra (1D and 2D) of compounds **1** to **5**, physicochemical, spectroscopic data of compounds **4** and **5**, and additional ECD data are provided as Supplementary data. Supplementary data associated with this article can be found, in the online version, at http://dx.doi.org/10.1016/j.fitote.2013.12.015.

References

[1] World Health Organization (WHO). Trypanosomiasis, human African (sleeping sickness). Fact sheet no. 259. http://www.who.int/mediacentre/factsheets/fs259/en/.
[2] Brun R, Blum J, Chappuis F, Burri C. Human African trypanosomiasis. Lancet 2010;375:148–59.
[3] Renslo AR, McKerrow JH. Drug discovery and development for neglected parasitic diseases. Nat Chem Biol 2006;2:701–10.
[4] Hannaert V. Sleeping sickness pathogen (*Trypanosoma brucei*) and natural products: therapeutic targets and screening systems. Planta Med 2011;77:586–97.
[5] Hopkins AL, Witty MJ, Nwaka S. Mission possible. Nature 2007;449:166–9.
[6] Maser P, Wittlin S, Rottmann M, Wenzler T, Kaiser M, Brun R. Antiparasitic agents: new drugs on the horizon. Curr Opin Pharmacol 2012;12:562–6.
[7] Butler MS. Natural products to drugs: natural product-derived compounds in clinical trials. Nat Prod Rep 2008;25:475–516.
[8] Zimmermann S, Kaiser M, Brun R, Hamburger M, Adams M. Cynaropicrin: the first plant natural product with *in vivo* activity against *Trypanosoma brucei*. Planta Med 2012;78:553–6.
[9] Mokoka TA, Zimmermann S, Julianti T, Hata Y, Moodley N, Cal M, et al. *In vitro* screening of traditional South African malaria remedies against *Trypanosoma brucei rhodesiense*, *Trypanosoma cruzi*, *Leishmania donovani*, and *Plasmodium falciparum*. Planta Med 2011;77:1663–7.
[10] Adams M, Zimmermann S, Kaiser M, Brun R, Hamburger M. A protocol for HPLC-based activity profiling for natural products with activities against tropical parasites. Nat Prod Commun 2009;4:1377–81.
[11] Hata Y, Raith M, Ebrahimi SN, Zimmermann S, Mokoka T, Naidoo D, et al. Antiprotozoal isoflavan quinones from *Abrus precatorius ssp. africanus*. Planta Med 2013;79:492–8.
[12] Mokoka T, Xolani P, Zimmermann S, Hata Y, Adams M, Kaiser M, et al. Antiprotozoal screening of 60 South African plants, and the identification of the antitrypanosomal eudesmanolides schkurin I and II. Planta Med 2013;79:1380.
[13] Lupi A, Delle MF, Marini-Bettolo GB, Costa DLB, D'Albuquerque IL. Abruquinones: new natural isoflavanquinones. Gazz Chim Ital 1979;109:9–12.
[14] Song CQ, Hu ZB. Abruquinone A, B, D, E, F, and G from the root of *Abrus precatorius*. Zhiwu Xuebao (Acta Bot Sin) 1998;40:734–9.
[15] Bringmann G, Gulder TAM, Reichert M, Gulder T. The online assignment of the absolute configuration of natural products: HPLC-CD in combination with quantum chemical CD calculations. Chirality 2008;20:628–42.
[16] Moradi-Afrapoli F, Ebrahimi SN, Smiesko M, Raith M, Zimmermann S, Nadjafi F, et al. Bisabololoxide derivatives from *Artemisia persica*, and determination of their absolute configurations by ECD. Phytochemistry 2013;85:143–52.
[17] Kuo SC, Chen SC, Chen LH, Wu JB, Wang JP, Teng CM. Potent antiplatelet, anti-inflammatory and antiallergic isoflavanquinones from the roots of *Abrus precatorius*. Planta Med 1995;61:307–12.
[18] Limmatvapirat C, Sirisopanaporn S, Kittakoop P. Antitubercular and antiplasmodial constituents of *Abrus precatorius*. Planta Med 2004;70:276–8.
[19] Slade D, Ferreira D, Marais JPJ. Circular dichroism, a powerful tool for the assessment of absolute configuration of flavonoids. Phytochemistry 2005;66:2177–215.
[20] Frisch M, Trucks GW, Schlegel HB, Scuseria GE, Robb MA, Cheeseman JR, et al. Gaussian 09, Revision A02 ed. Wallingford CT: Gaussian Inc.; 2009.
[21] Bruhn THY, Schaumlöffel A, Bringmann G. SpecDis, 1.51 ed. Germany, Wuerzburg: University of Wuerzburg; 2011.
[22] Gichuki C, Brun R. Animal models of CNS (second-stage) sleeping sickness. In: Zak OSM, editor. Animal models of infection. Bath: Academic Press; 1999. p. 795–801.
[23] Gutierrez-Gonzalez JJ, Guttikonda SK, Tran L-SP, Aldrich DL, Zhong R, Yu O, et al. Differential expression of isoflavone biosynthetic genes in soybean during water deficits. Plant Cell Physiol 2010;51:936–48.

Appendix A. Supplementary data

Antitrypanosomal isoflavan quinones from *Abrus precatorius*

Yoshie Hata[a,d], Samad Nejad Ebrahimi[a,e], Maria de Mieri[a], Stefanie Zimmermann[a],Tsholofelo Mokoka[c], Dashnie Naidoo[c], Gerda Fouche[c], Vinesh Maharaj[c], Marcel Kaiser[b], Reto Brun[b], Olivier Potterat[a], and Matthias Hamburger[a]

Affiliations

[a]Department of Pharmaceutical Sciences, University of Basel, Klingelbergstrasse 50, CH-4056 Basel, Switzerland

[b]Swiss Tropical and Public Health Institute and University of Basel, Socinstrasse 57, CH-4002 Basel, Switzerland

[c]Biosciences, Council for Scientific and Industrial Research (CSIR), PO Box 395, Pretoria 0001, South Africa

[d]Department of Pharmacy, Faculty of Sciences, National University of Colombia, Carrera 30 No. 45-03, Bogota D.C. 111321, Colombia

[e]Department of Phytochemistry, Medicinal Plant and Drugs Research Institute, Shahid Beheshti University, G. C., Tehran, Iran

Corresponding author:

Prof. Matthias Hamburger, Division of Pharmaceutical Biology, University of Basel, Klingelbergstrasse 50, CH-4056 Basel, Switzerland.

e-mail: matthias.hamburger@unibas.ch, Phone: +41 61 267 14 25 Fax: +41 61 267 14 74

Assays for *in vitro* antiprotozoal activity

Antiplasmodial activity was determined by a modification of the ^{3}[H]-hypoxanthine incorporation assay [1] with the *P. falciparum* K1 strain (resistant to chloroquine and pyrimethamine), growth according to the method described by Trager and Jensen [2]. Artesunate (purity >95%, Sigma-Aldrich) was used as positive control.

Briefly, a suspension of infected red blood cells (final parasitemia 0.3% and hematocrit 1.25%) in RPMI 1640 medium supplemented with 2 μM L-glutamine, 5.95 g/L Hepes, 2 g/L $NaHCO_3$, and 5% of Albumax II was exposed to serial drug dilutions covering a range from 10 μg/mL to 0.156 μg/mL in 96-well microtiter plates. After 48 h of incubation (4% CO_2, 3% O_2, and 93% N_2 at 37°C), 50 μL of ^{3}[H]-hypoxanthine (0.25 μM) were added to each well (Costar). The plates were incubated for further 24 h before being harvested by using a Betaplate cell harvester (Wallac) onto glass-fiber filters and then washed with distilled water. The dried filters were inserted into plastic foils with 10 mL scintillation fluid. The radioactivity was counted with a Betaplate liquid scintillation counter (Wallac) as counts per minute per well at each drug concentration and compared to the untreated controls. Counts were expressed as percentages of the control and presented as sigmoidal inhibition curves. IC_{50} values were calculated by linear interpolation.

Antitrypanosomal activity against *Trypanosoma brucei rhodesiense* STIB 900 was determined according to [3]. Melarsoprol (Arsorbal, purity >95%, Sanofi-Aventis) was used as positive control. Minimum essential medium (MEM) with Earle's salts supplemented with 2-mercaptoethanol, as described by Baltz *et al.* [4], 1 mM sodium pyruvate, 0.5 mM hypoxanthine, and 15% heat-inactivated horse serum was added (50 μL) to each well of a 96-well microtiter plate (Costar) except of the negative control. Serial drugs dilutions were prepared covering a range from 90 to 0.123 μg/mL followed by the addition of 2000 *T. brucei rhodesiense* STIB 900 bloodstream forms/well. After 70 hours of incubation (humidified 5% CO_2 atmosphere at 37°C), 10 μL resazurin solution (12.5 mg resazurin (Sigma-Aldrich) dissolved in 100 mL of distilled water) were added and incubation was continued for further 2 to 6 h. The plate was read with a Spectramax Gemini XS microplate fluorescence reader (Molecular Devices) with an excitation wavelength of 536 nm and an emission wavelength of 588 nm. Fluorescence development was expressed as percentage of the control and the IC_{50} values were determined from the sigmoid curves using Softmax Pro Software (Molecular Devices).

Leishmanicidal activity was determined with *L. donovani* (axenic amastigotes) MHOM-ET/67/L82 strain according to [6], with some modifications. Fifty microlitres of SM medium at pH 5.4 supplemented with 10% heat-inactivated FBS was added to each well of 96-well microtiter plate (Costar). Serial drug dilutions were prepared covering a range from 90 to 0.123 μg/mL. Then, 10^5 axenically grown *L. donovani* amastigotes in 50 μL medium were added to each well and the plate was incubated for 72 h (humidified 5% CO_2 atmosphere at 37°C). Ten microlitres resazurin solution (12.5 mg resazurin (Sigma-Aldrich) dissolved in 100 mL of distilled water) were added to each well and incubated for further 2 to 4 h. The plate was read with a Spectramax Gemini XS microplate fluorescence reader (Molecular Devices) with an excitation wavelength of 536 nm and an emission wavelength of 588 nm. Fluorescence development was expressed as percentage of the control and the IC_{50} values were determined from the sigmoid curves using Softmax Pro Software (Molecular Devices). Miltefosine (purity >95%, VWR) was used as positive control.

In vitro cytotoxicity assay

The cytotoxicity assay was performed using a protocol based on the Alamar Blue assay [7], whereby rat skeletal myoblast cells (L-6 cells) were seeded in 96-well microtiter plates using MEM supplemented with 10% heat inactivated FBS (4000 cells/well). Serial threefold drug dilutions ranging from 90 to 0.123 mg/mL were prepared. After 72 h, 10 μL resazurin solution was added (12.5 mg resazurin (Sigma-Aldrich) dissolved in 100 mL of distilled water) and the plates were incubated for further 2 to 4 h. A Spectramax Gemini XS micro plate fluorescence reader (Molecular Devices) was used to measure the plates at an excitation wavelength of 536 nm and an emission wavelength of 588 nm. Fluorescence development was expressed as percentage of the control and the IC_{50} values were determined from the sigmoid inhibition curves using Softmax Pro Software (Molecular Devices). Podophyllotoxin (purity >95%, Sigma-Aldrich) was used as a reference drug.

Calculation of electronic circular dichroism (ECD) spectra

Conformational analysis of **1**, **2**, and **3** was accomplished with Schrödinger MacroModel 9.1 software employing the OPLS 2005 (optimized potential for liquid simulations) force field in H_2O. Conformers within a 1 Kcal/mol energy window from the global minimum were picked for geometrical optimization and energy calculation applying density functional theory (DFT)

with the Becke's nonlocal three parameter exchange and correlation functional, and the Lee-Yang-Parr correlation functional level (B3LYP, Becke, 3-paramiter, Lee-Yang-Parr) using the 6-31G** basis set in the gas phase with the Gaussian 09 program package [8]. Vibrational evaluation was done at the same level to confirm minima. Excitation energy (denoted by wavelength in nm), rotator strength dipole velocity (Rvel), and dipole length (Rlen) were calculated in MeOH by TD-DFT/B3LYP/6-31G**, using self-consistent reaction field (SCRF) method, with the conductor polarized continuum model (CPCM) model. ECD curves were obtained on the basis of rotator strengths using a half-band of 0.2 eV using SpecDis v1.51 [9]. The spectra were combined after Boltzmann weighting according to their population contribution.

Physicochemical data of 4 and 5

(3*R*)-6,7,2',3'-Tetramethoxyisoflavan-1',4'-quinone (Abruquinone A, **4**) [10]: Orange amorphous substance; UV (MeOH): λ_{max} (log ε) = 200 (4.57), 268 (3.91) nm; ^{1}H and ^{13}C NMR data, see Table 1S; HRESI-MS: *m/z* = 383.1135 $[M+Na]^+$ (calcd. for $C_{19}H_{20}O_7$: 360.1209).

(3*R*)-7-Hydroxy-6,2',3'-trimethoxyisoflavan-1',4'-quinone (Abruquinone D', **5**) [11]: Orange amorphous substance; UV (MeOH): λ_{max} nm (log ε) = 198 (4.33), 268 (3.68) nm; ^{1}H NMR data, see Table 1; ^{13}C NMR data, see Table 1; HRESI-MS: *m/z* = 369.0963 $[M+Na]^+$ (calcd. for $C_{18}H_{18}O_7$: 346.1053).

Table A.1. ^{1}H and ^{13}C NMR data (500 MHz for ^{1}H, 125 MHz for ^{13}C) for compounds **1**, **4,** and **5**.

	1[a]		**4**[b]		**5**[b]	
position	δ_H	δ_C[c]	δ_H	δ_C[c]	δ_H	δ_C[c]
2a	3.97 (dd, 10.8, 5.1)	66.5	4.17	68.0	4.16 (dd,10.7, 2.5)	67.9
2b	3.54 (dd, 10.8, 10.7)		3.97 (dd, 10.9, 2.9)[d]		3.98[d]	
3	3.09 (m)[d]	40.6	3.39 (m)	30.8	3.39 (m)	30.8
4a	5.18 (d, 7.1)	79.0	Ha 3.39 (dd, 15.9, 6.3)	29.1	Ha 3.00 (dd, 16.0, 6.1)	29.3
4b			Hb 2.99 (dd, 15.9, 6.3)		Hb 2.65 (dd, 16.0, 6.1)	
5	7.26 (s)	115.8	6.49 (s)	112.5	6.48 (s)	111.3
6	-	140.8	-	143.8	-	141.4
7	-	147.9	-	148.3	-	145.0
8	6.33 (s)	100.0	-	147.7	6.40 (s)	103.2
9	-	149.0	-	146.5	-	148.2
10	-	112.5	-	110.4	-	110.4
1'	-	147.5	-	183.2	-	183.4
2'	-	131.5	-	144.8	5.84 (s)	149.4
3'	-	148.4	-	144.8	-	144.9
4'	6.15 (d, 8.2)	104.0	-	174.6	-	nd[f]
5'	6.42 (dd, 8.2, 0.6)	114.1	6.33 (s)	130.8	6.33 (d 1.1)	130.8
6'	-	121.9	-	146.7	-	146.3
2'- OCH_3	-	-	3.97 (s)[d,e]	61.1	3.98 (s)[d]	61.1
3'- OCH_3	3.26	55.9	3.97 (s)[d,e]	61.1	3.98 (s)[d]	61.1
5'- OCH_3	-	-	-	-	6.33 (s)	130.8
6- OCH_3	-	-	3.77 (s)	56.0	3.80 (s)	56.4
7- OCH_3	3.08 (s)[d]	55.0	3.78 (s)	55.9	3.83 (s)	56.2
8- OCH_3	-	-	3.85 (s)	61.5	3.85 (s)	60.7

[a]measured in C_6D_6, [b]measured in $CDCl_3$, [c]^{13}C NMR signals were extracted from HSQC and HMBC spectra, [d]overlapping signals within the same column, [e]interchangeable data, [f]not detected

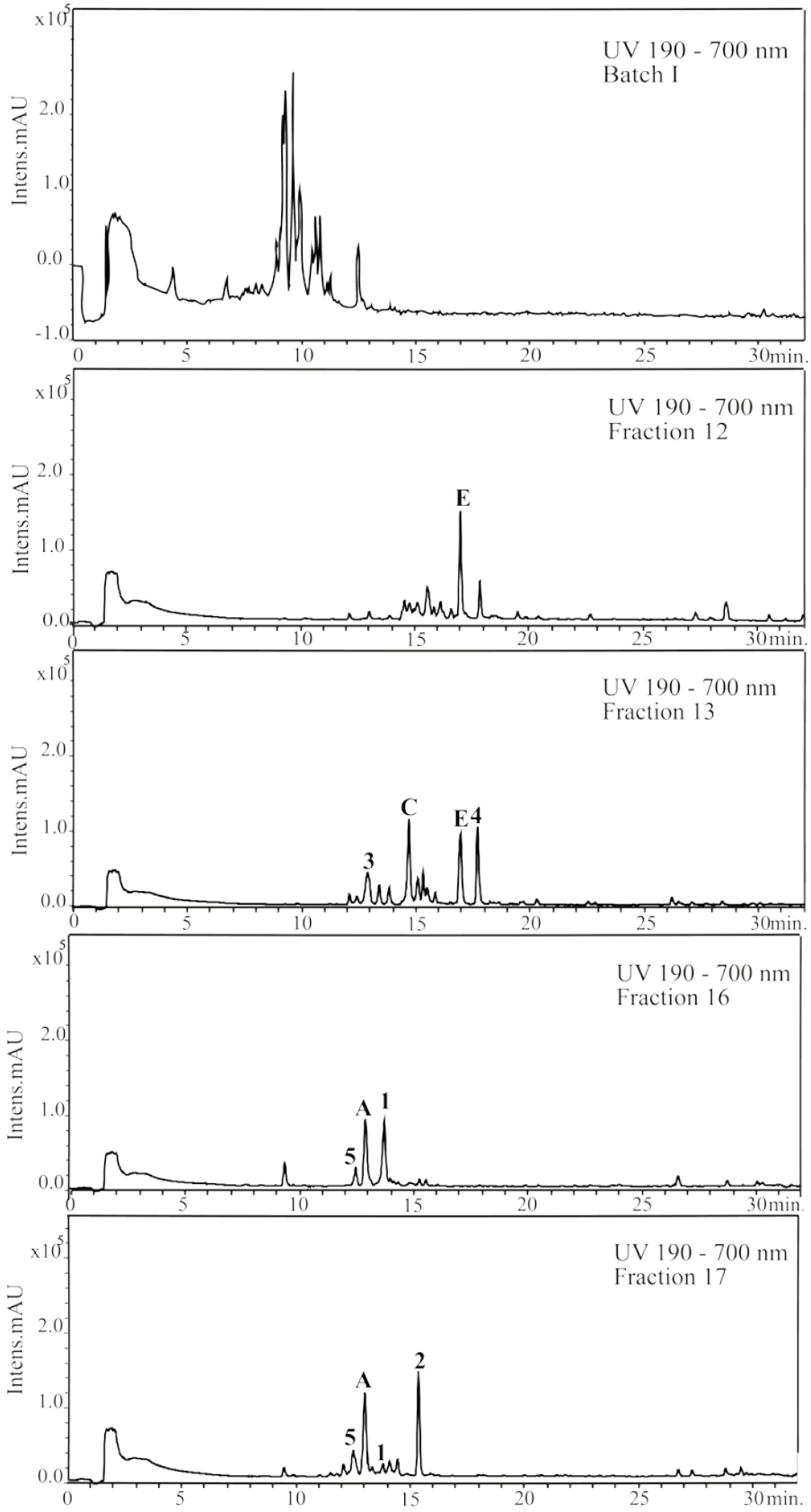

Fig. A.1. HPLC-PDA analysis of whole extract of *A. precatorius* batch II (top) and selected fractions after flash chromatography. Peak numbering refers to compounds **1-5** isolated from batch II, and peaks labelled with A, C, and E refer to compounds previously found in batch I.

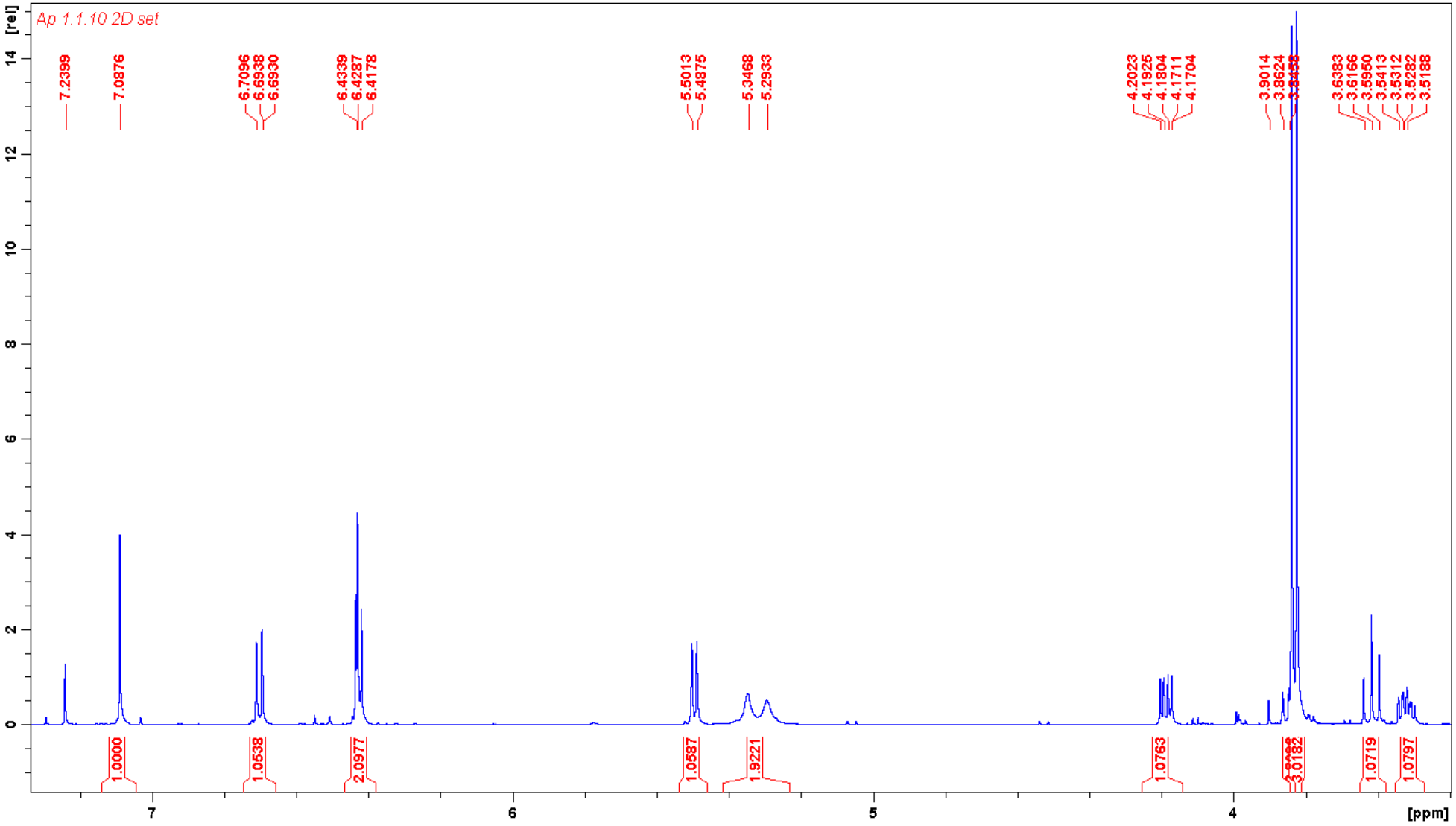

Fig. A.2. ^{1}H NMR spectrum of abruquinone J (**1**) in $CDCl_3$

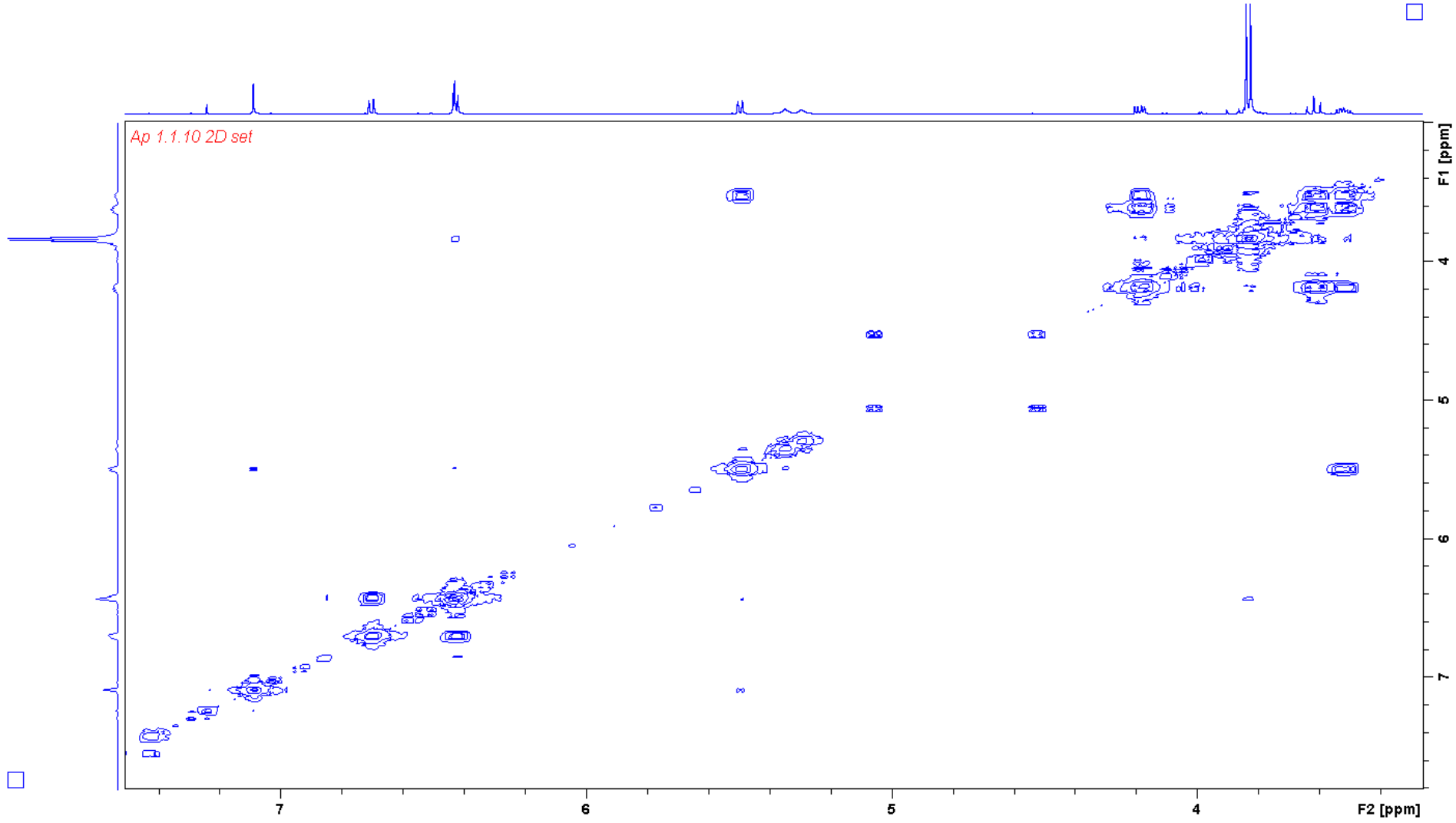

Fig. A.3. ^{1}H ^{1}H COSY spectrum of abruquinone J (**1**) in $CDCl_3$.

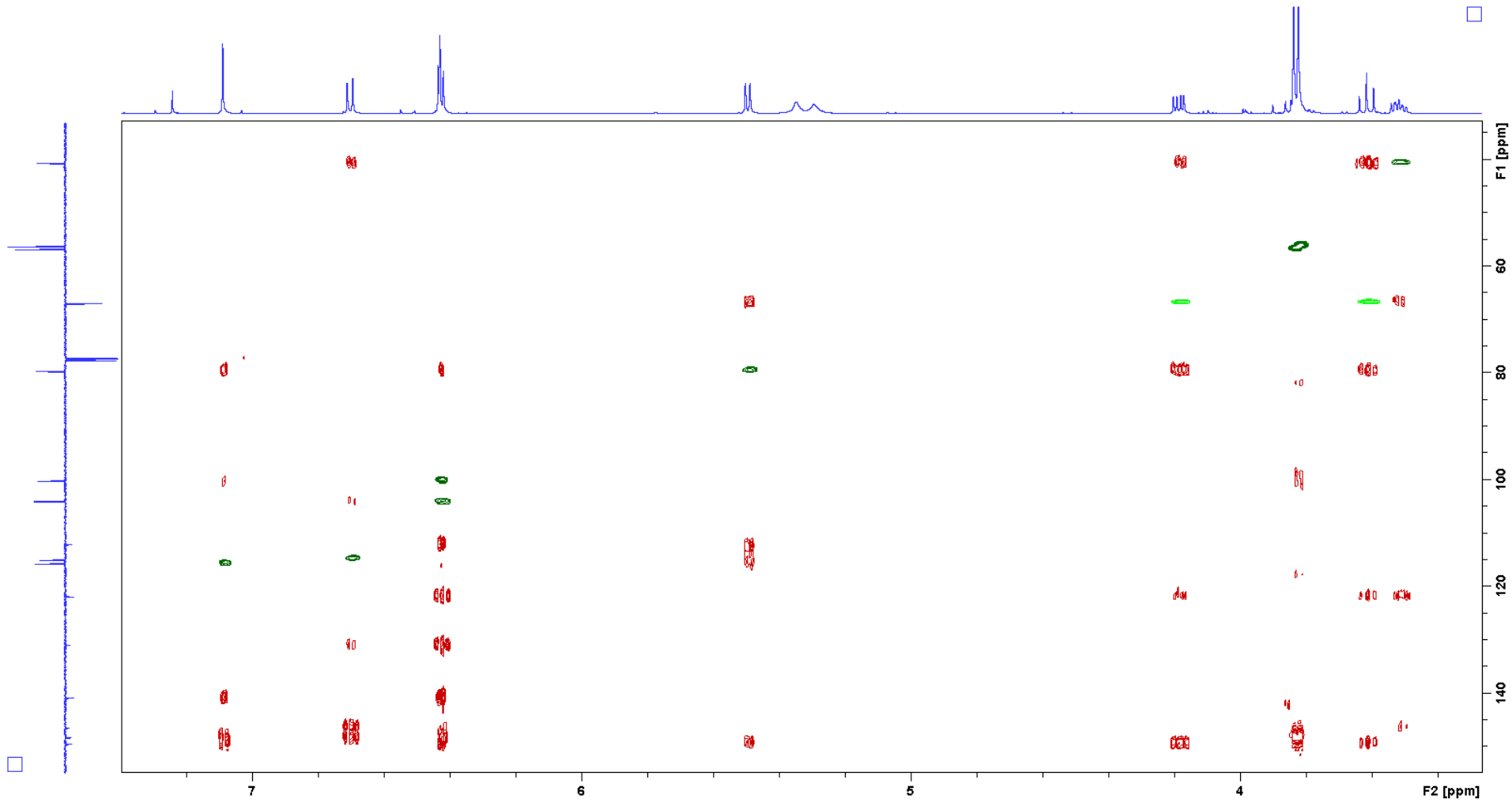

Fig. A.4. HSQC and HMBC overlaid spectra of abruquinone J (**1**) in $CDCl_3$.

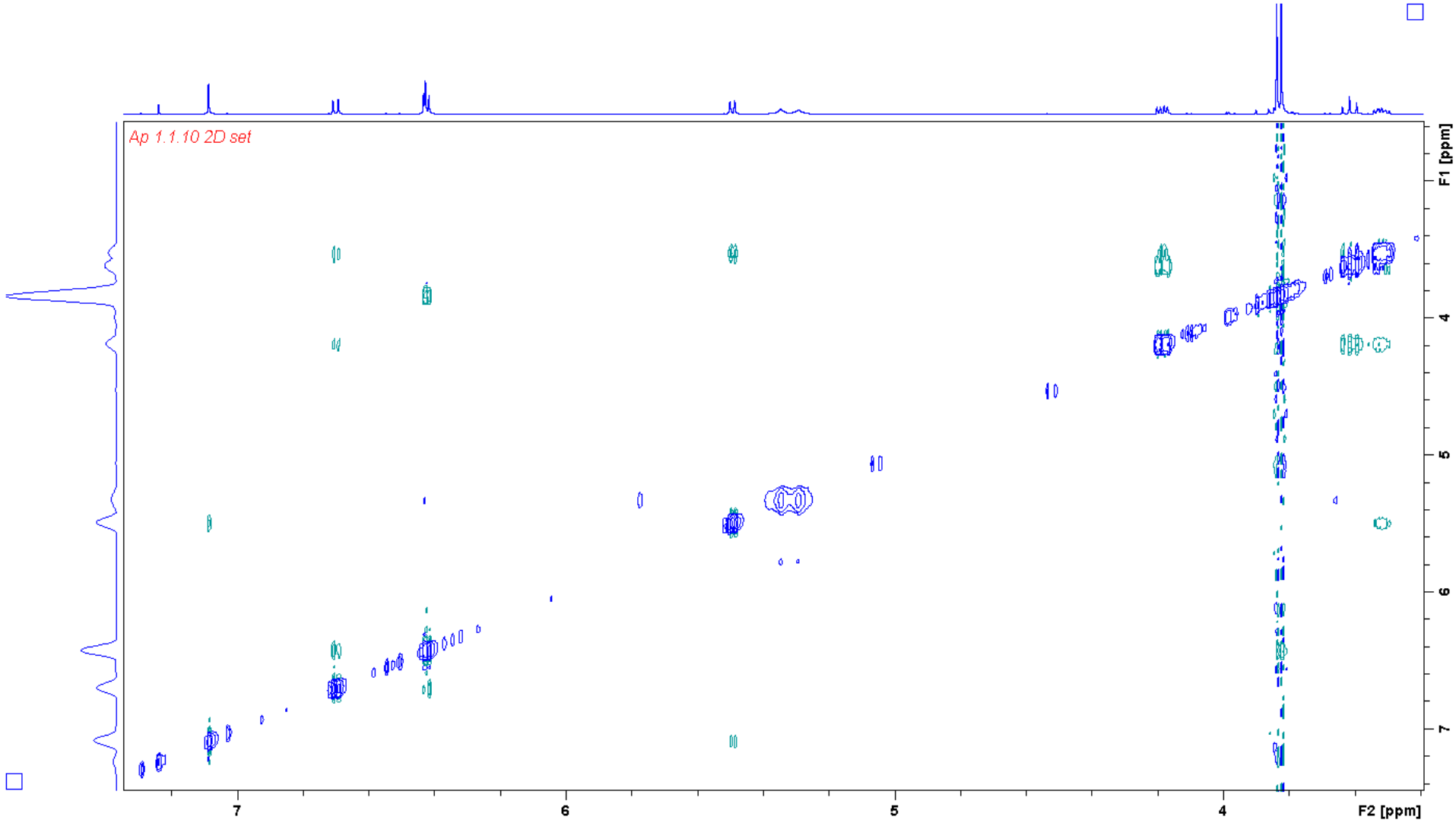

Fig. A.5. ^{1}H ^{1}H NOESY spectrum of abruquinone J (**1**) in $CDCl_3$.

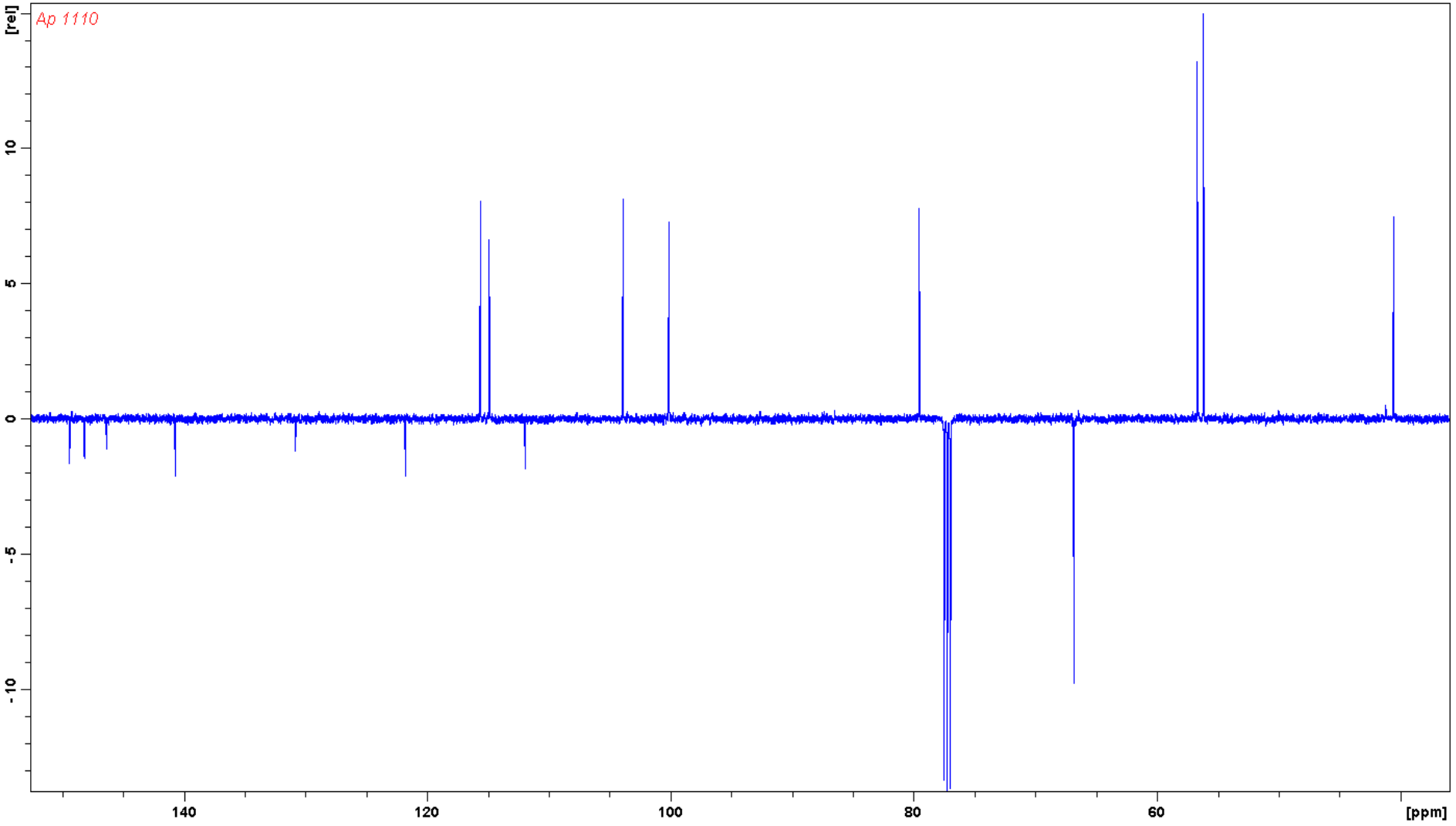

Fig. A.6. DEPTQ spectrum of abruquinone J (**1**) in $CDCl_3$.

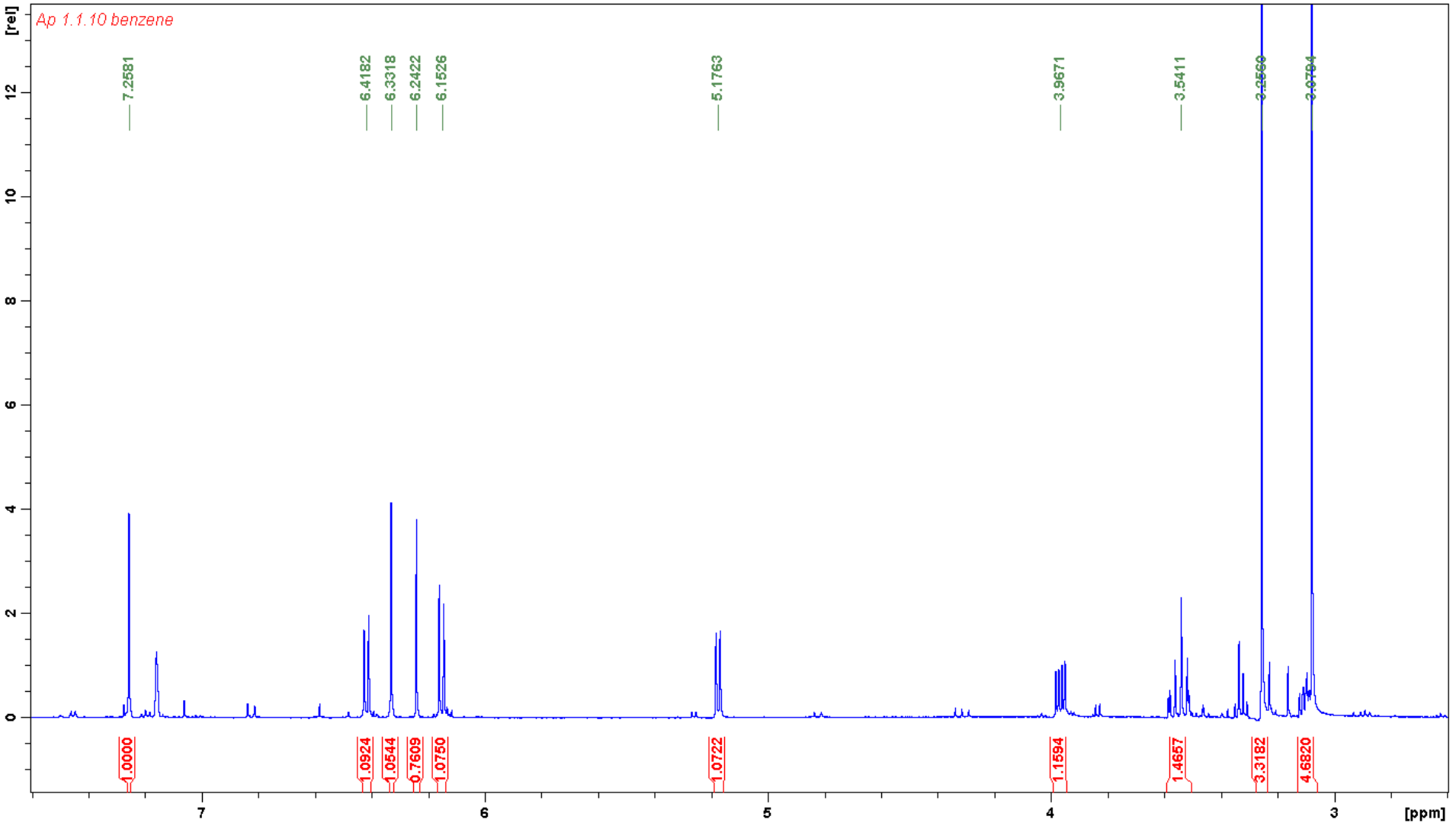

Fig. A.7. ^{1}H NMR spectrum of abruquinone J (**1**) in C_6D_6.

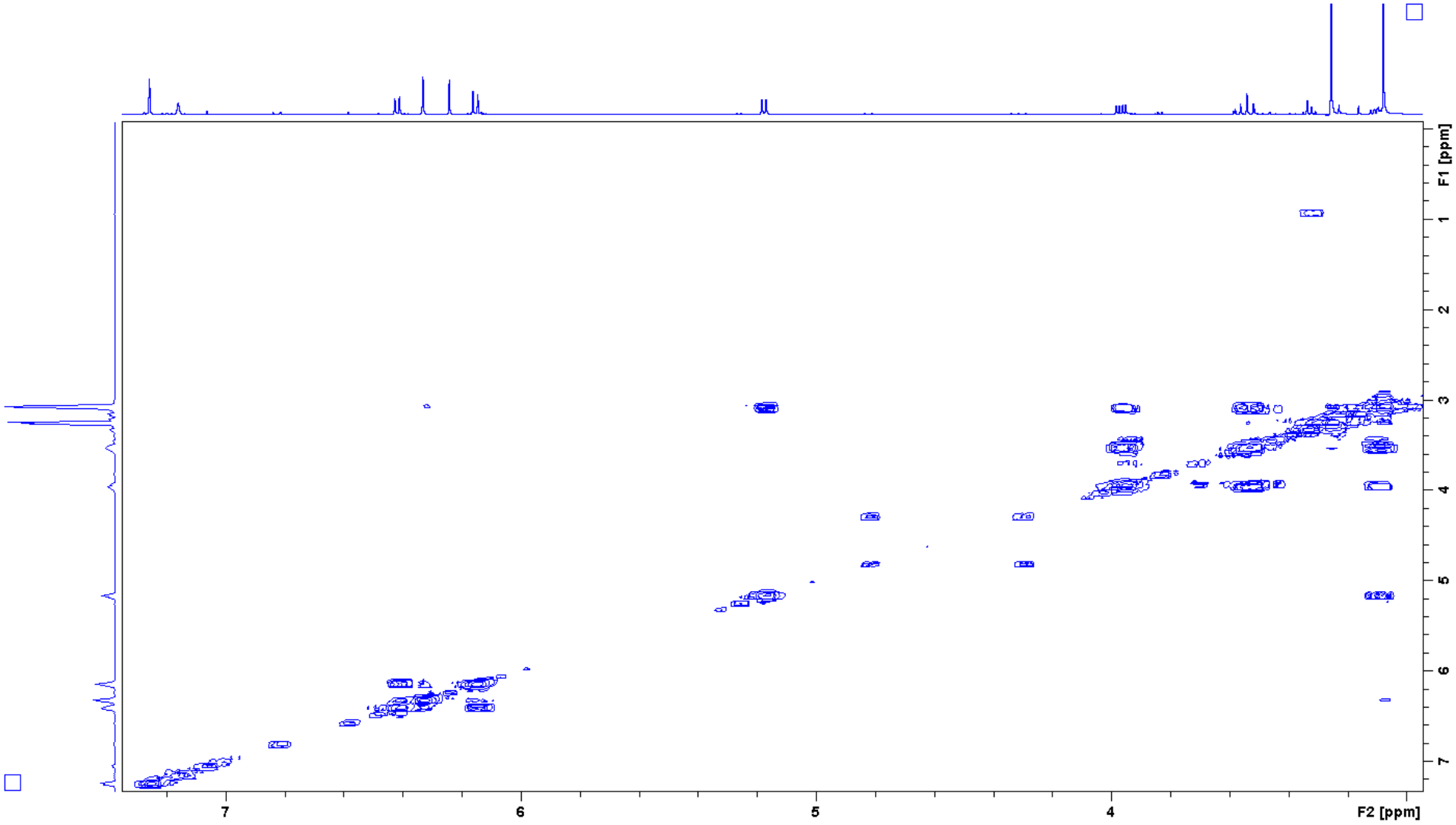

Fig. A.8. ^{1}H ^{1}H COSY spectrum of abruquinone J (**1**) in C_6D_6.

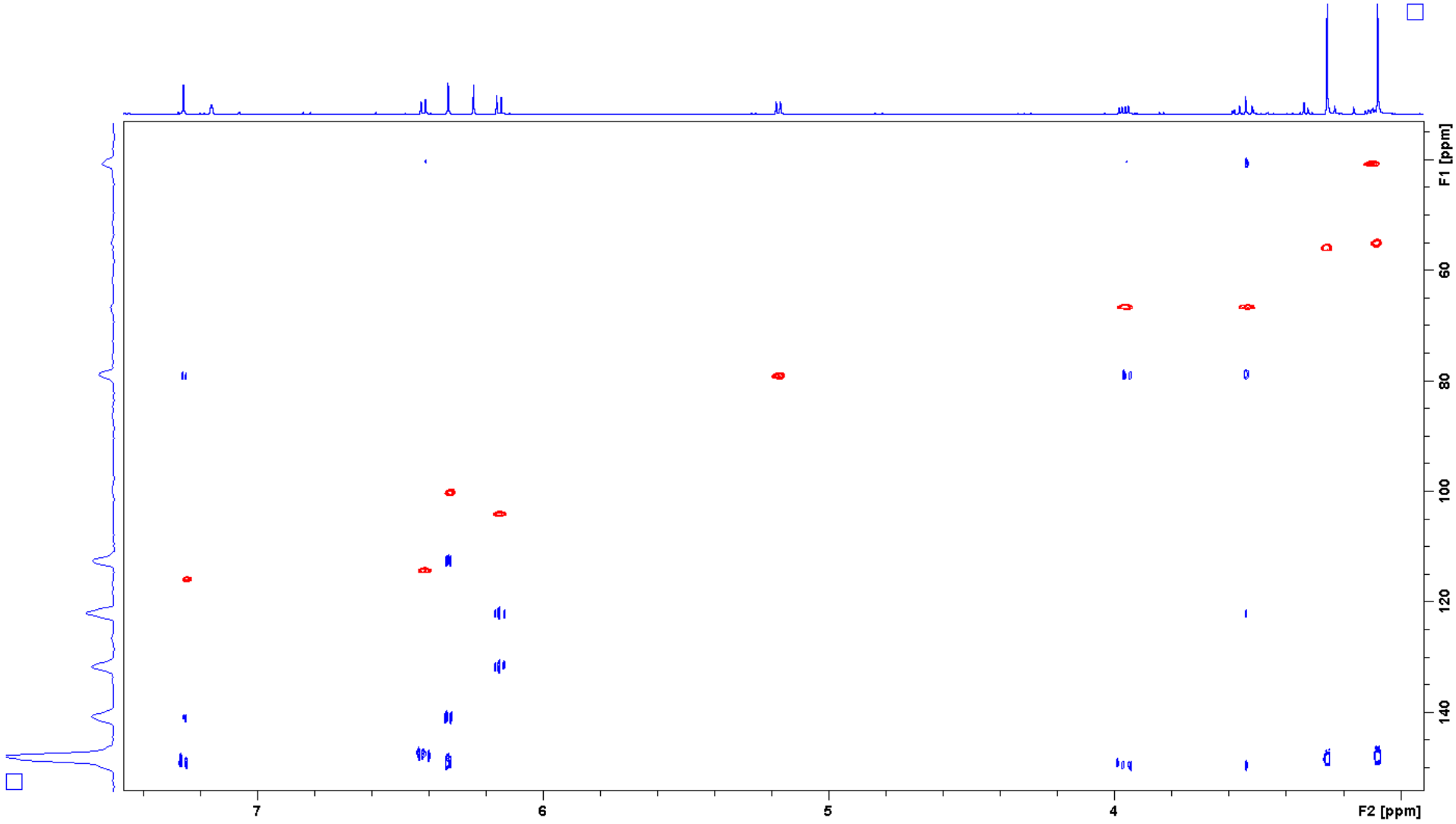

Fig. A.9. HSQC and HMBC overlaid spectra of abruquinone J (**1**) in C_6D_6.

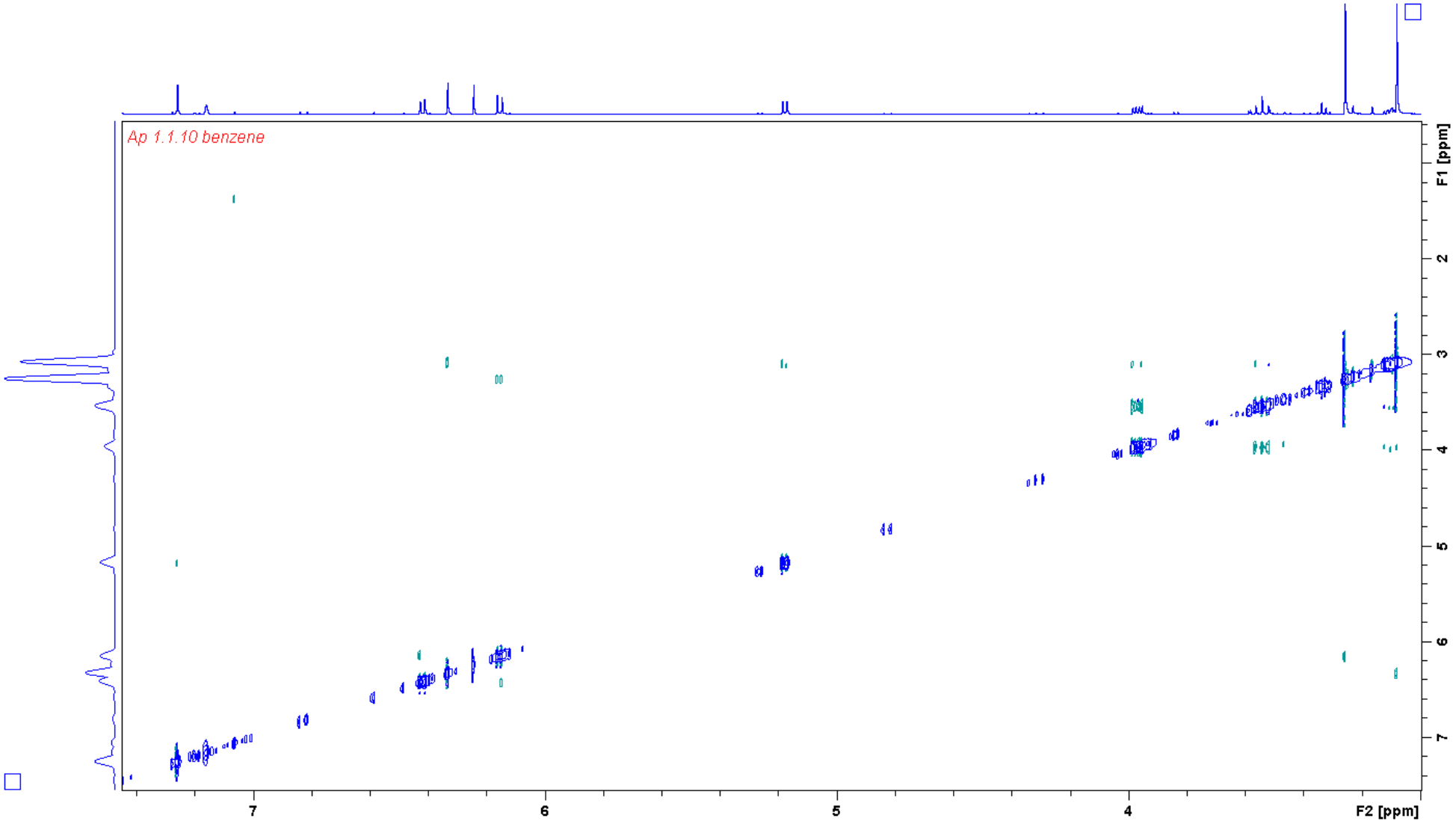

Fig. A.10. ^{1}H ^{1}H NOESY spectrum of abruquinone J (**1**) in C_6D_6.

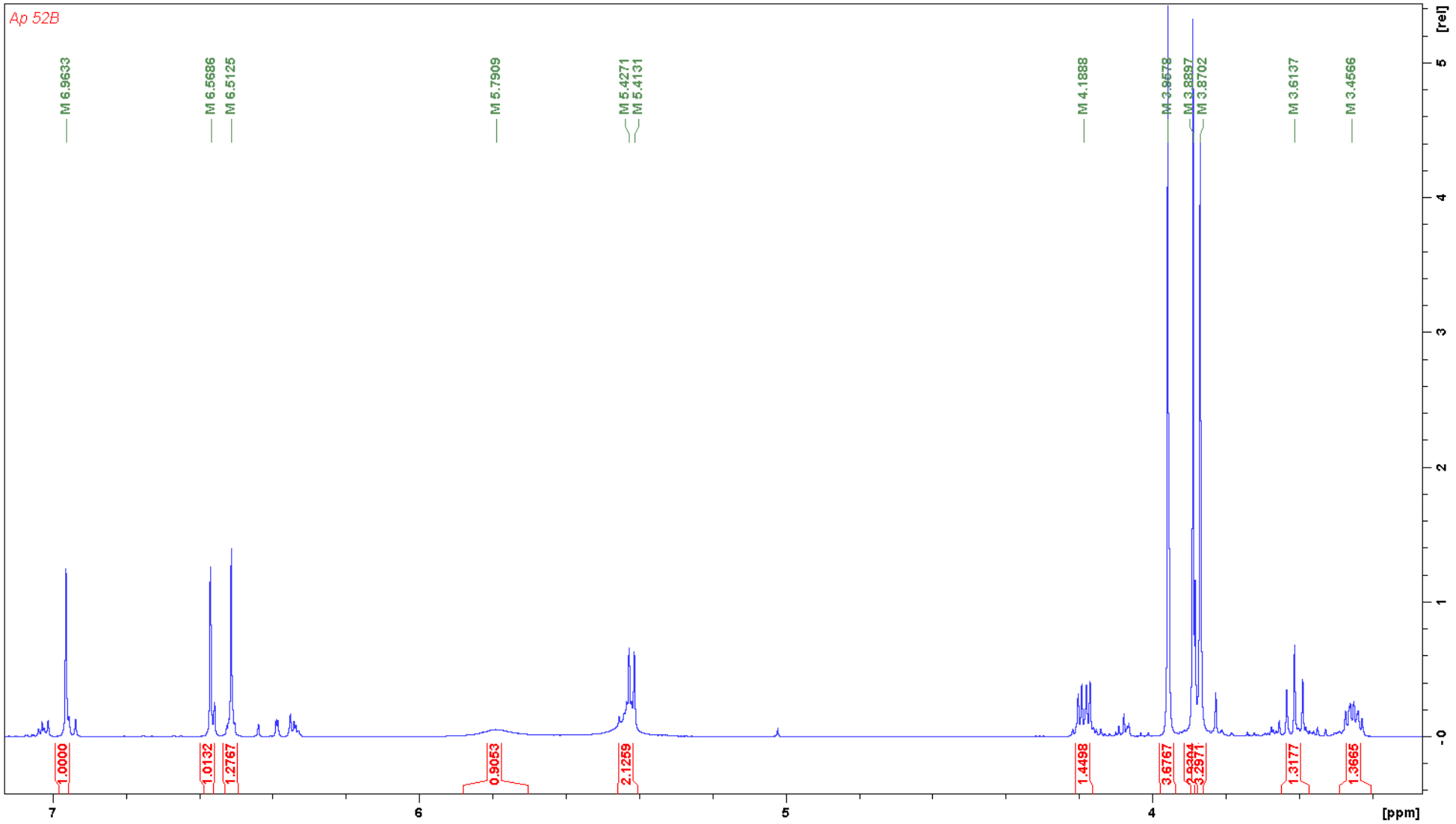

Fig. A.11. ^{1}H NMR spectrum of abruquinone K (**2**) in $CDCl_3$.

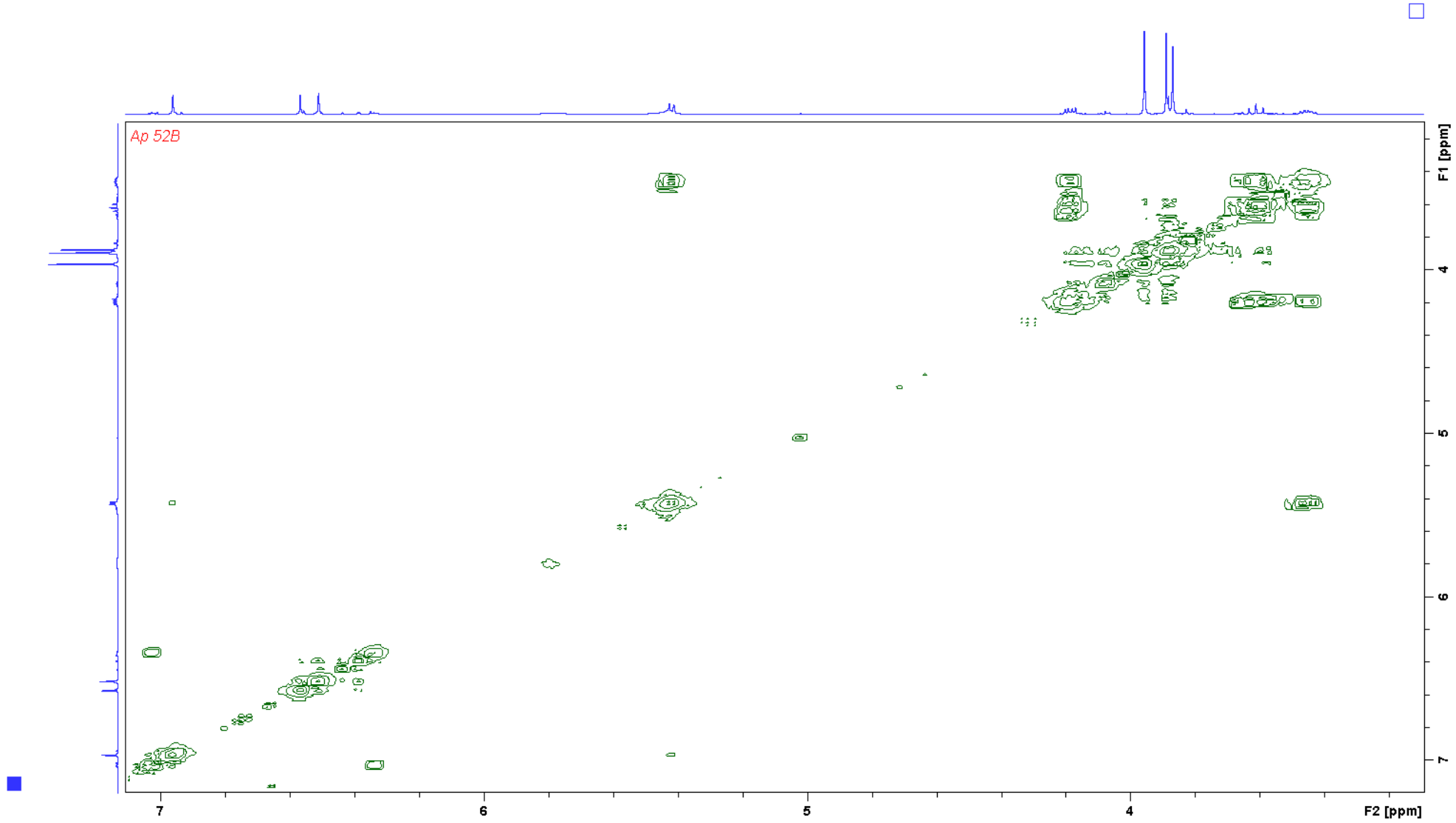

Fig. A.12. ^{1}H ^{1}H COSY spectrum of abruquinone K (**2**) in $CDCl_3$.

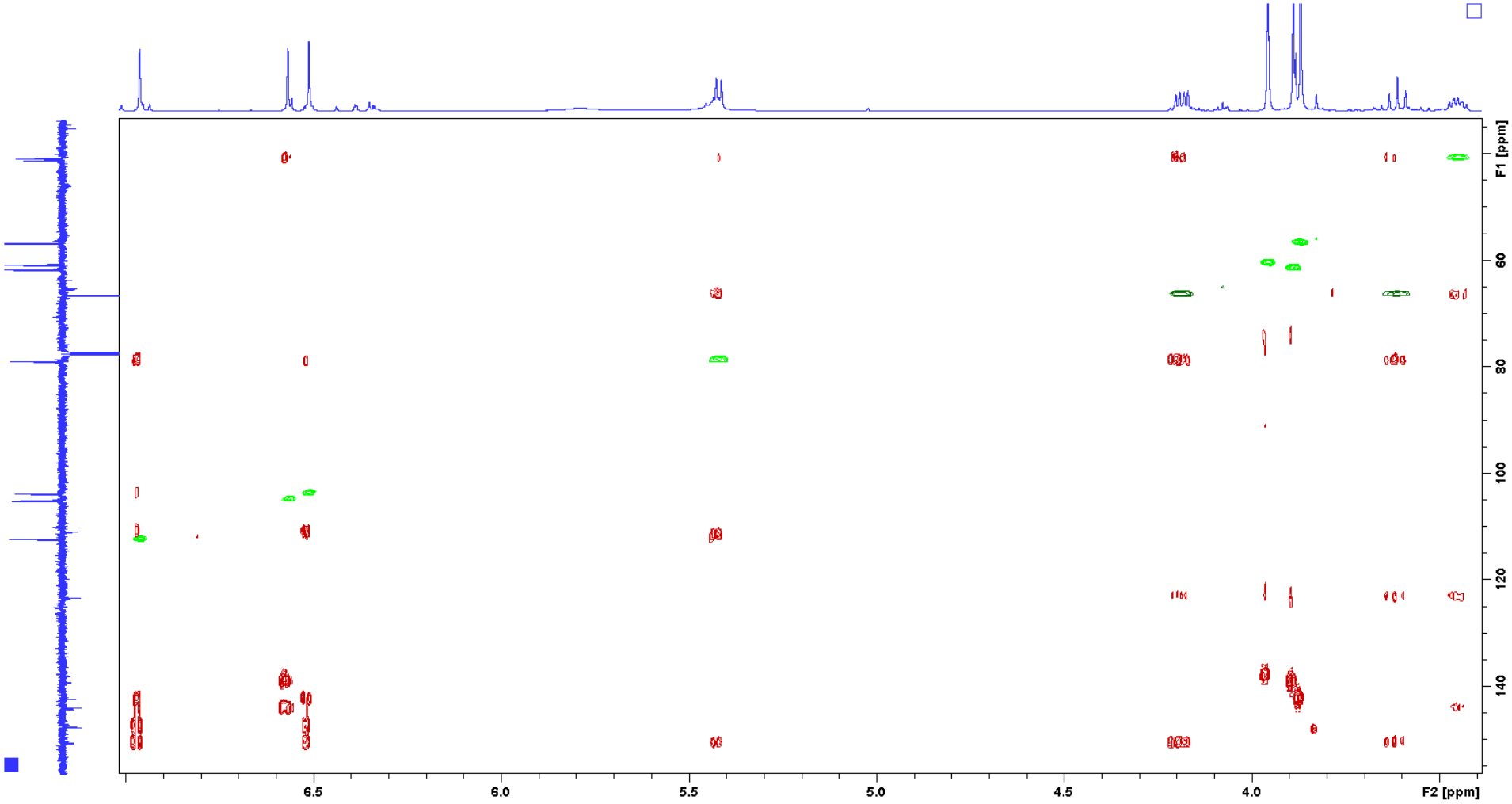

Fig. A.13. HMQC and HMBC overlaid spectra of abruquinone K (**2**) in $CDCl_3$.

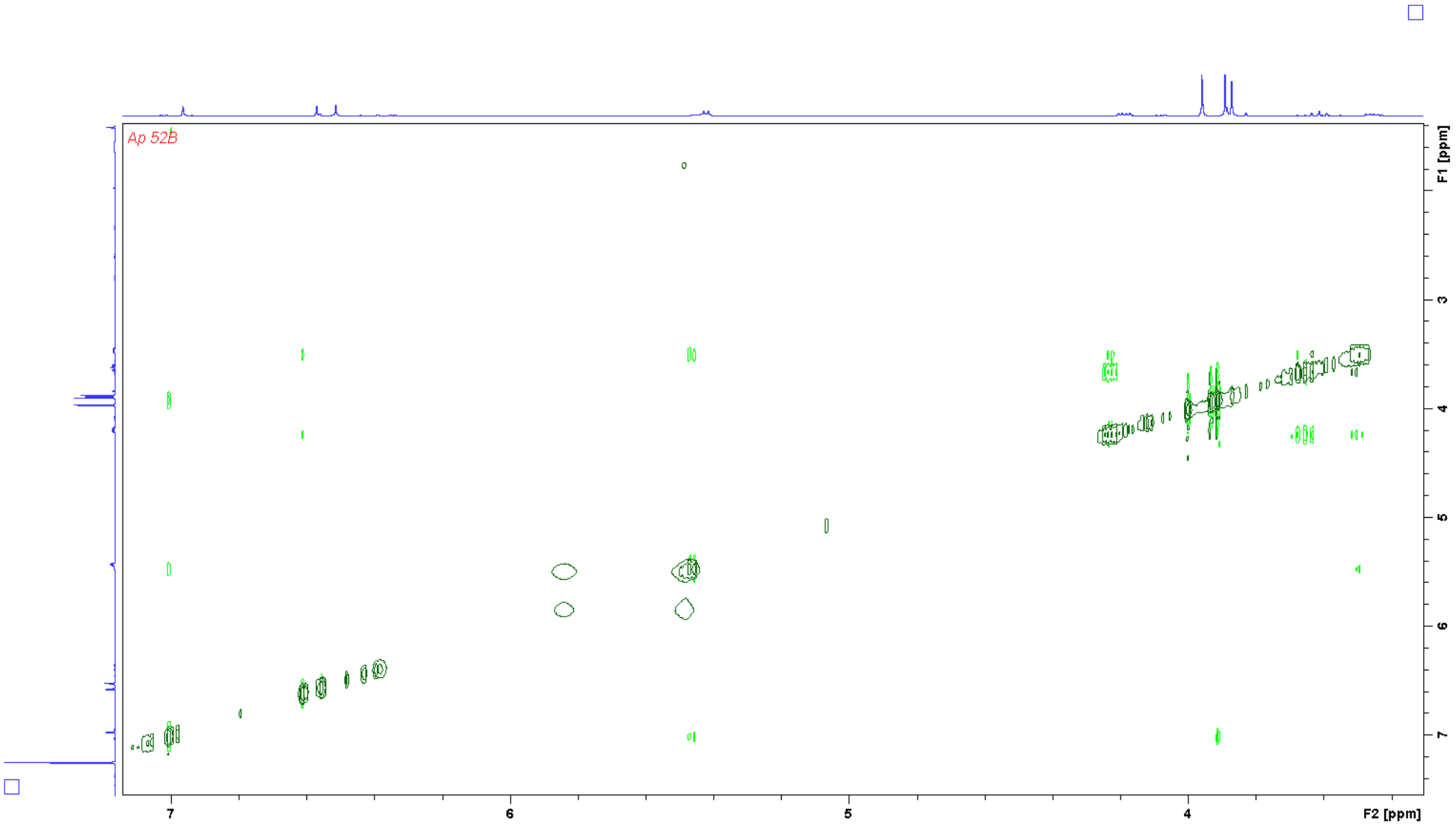

Fig. A.14. ^{1}H ^{1}H NOESY NMR spectrum of abruquinone K (**2**) in $CDCl_3$.

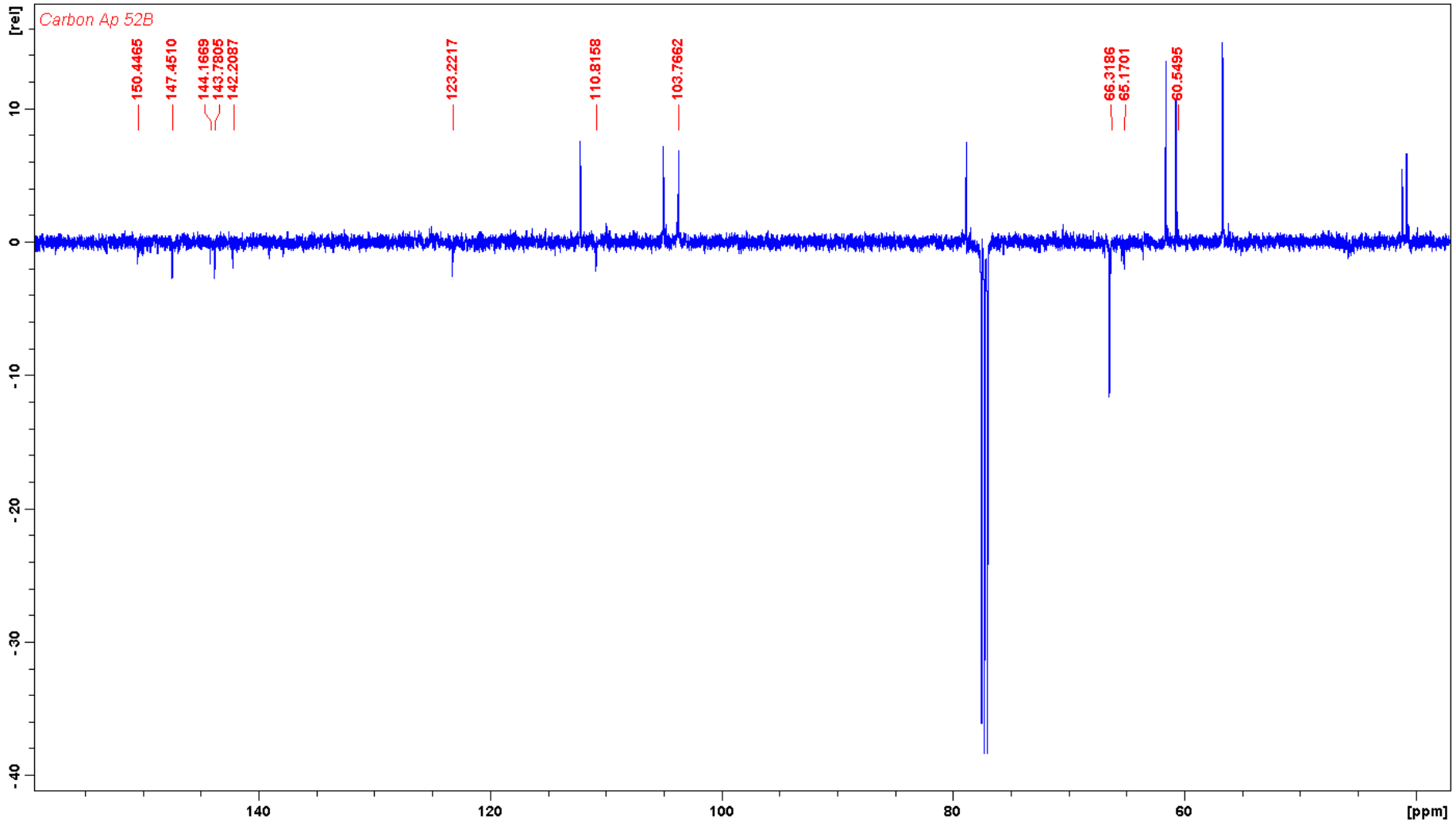

Fig. A.15. DEPTQ spectrum of abruquinone K (**2**) in $CDCl_3$.

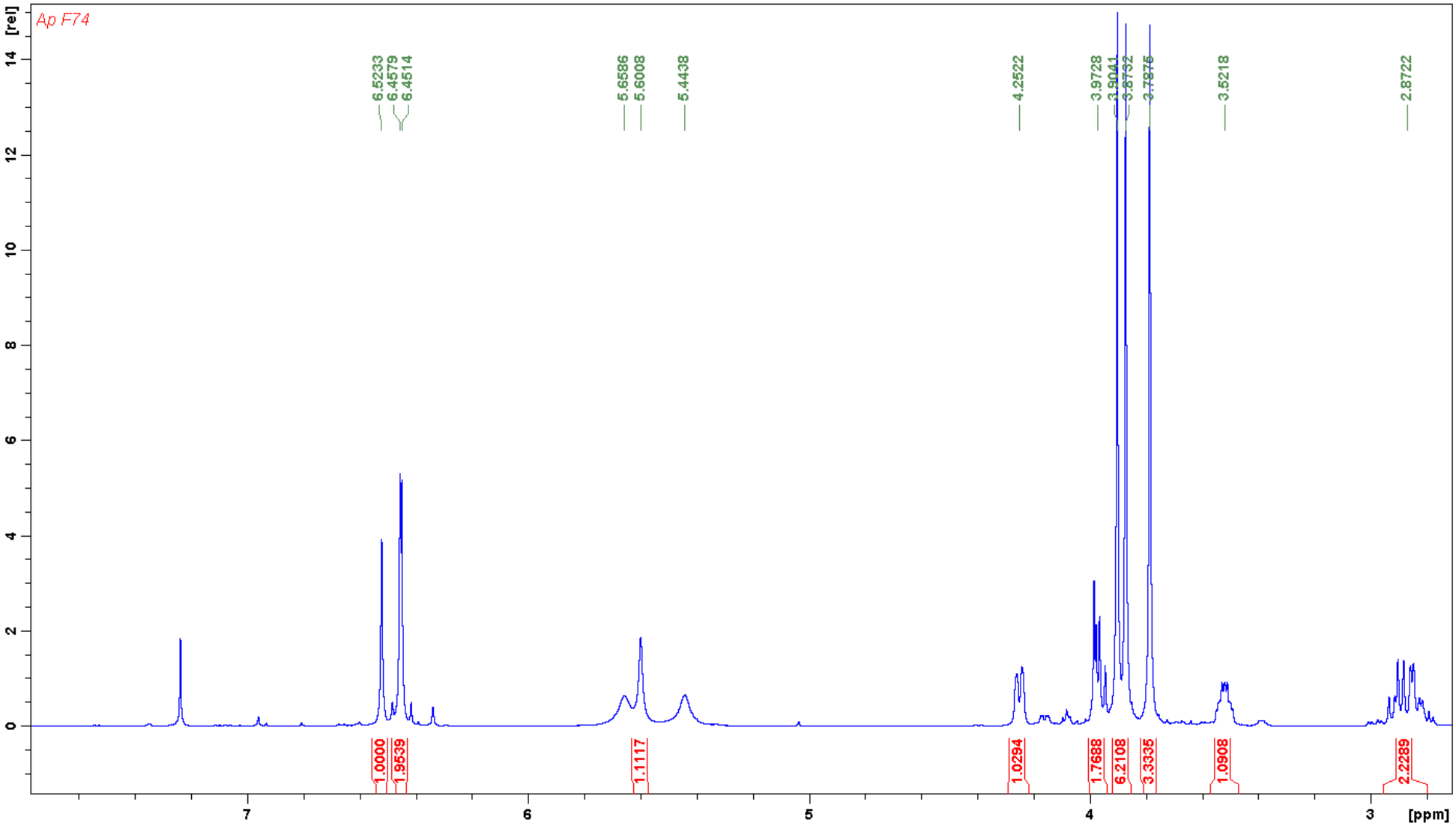

Fig. A.16. ^{1}H NMR spectrum of abruquinone L (**3**) in $CDCl_3$.

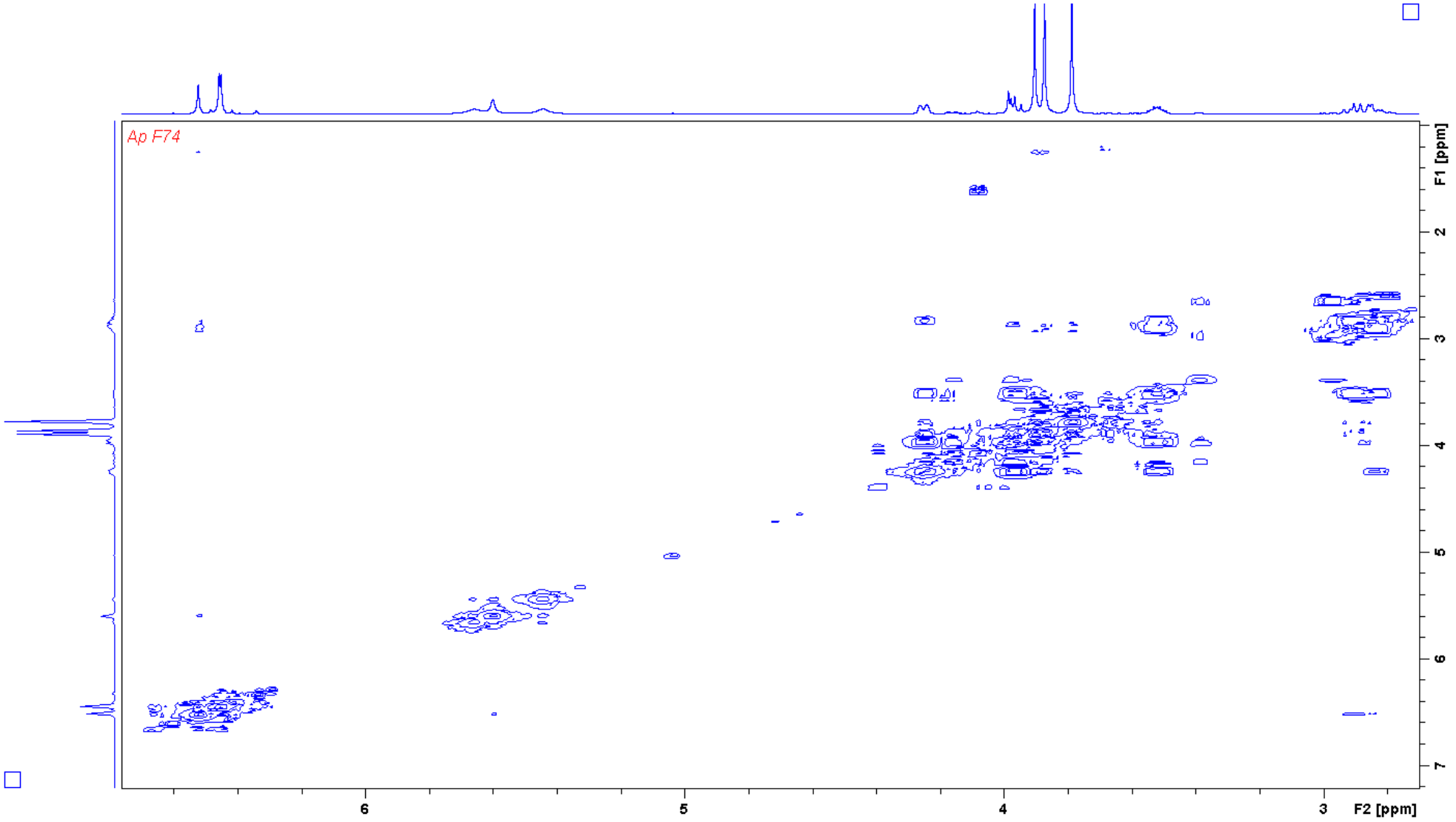

Fig. A.17. ^{1}H ^{1}H COSY spectrum of abruquinone L (**3**) in $CDCl_3$.

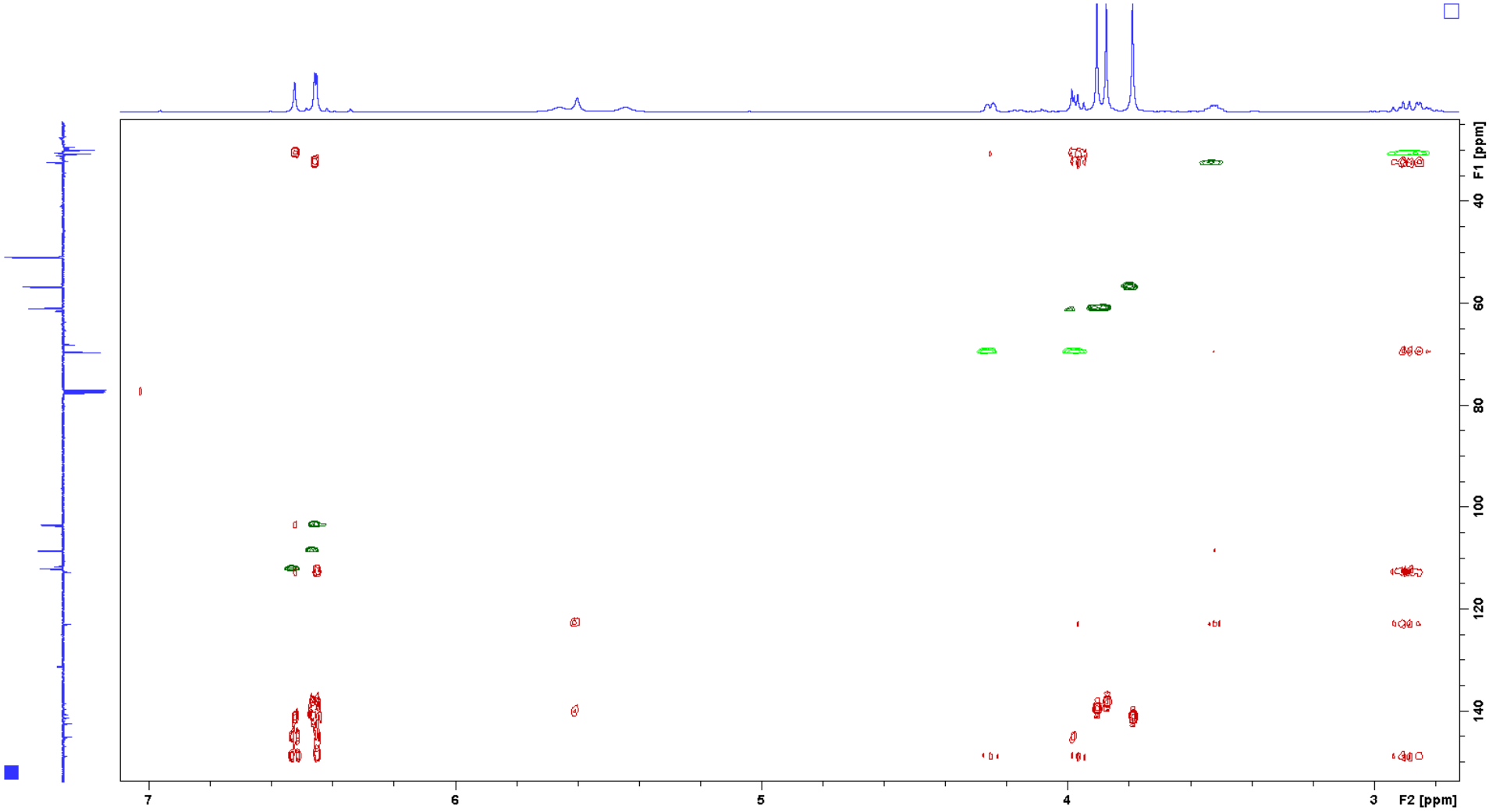

Fig. A.18. HMQC and HMBC overlaid spectra of abruquinone L (**3**) in $CDCl_3$.

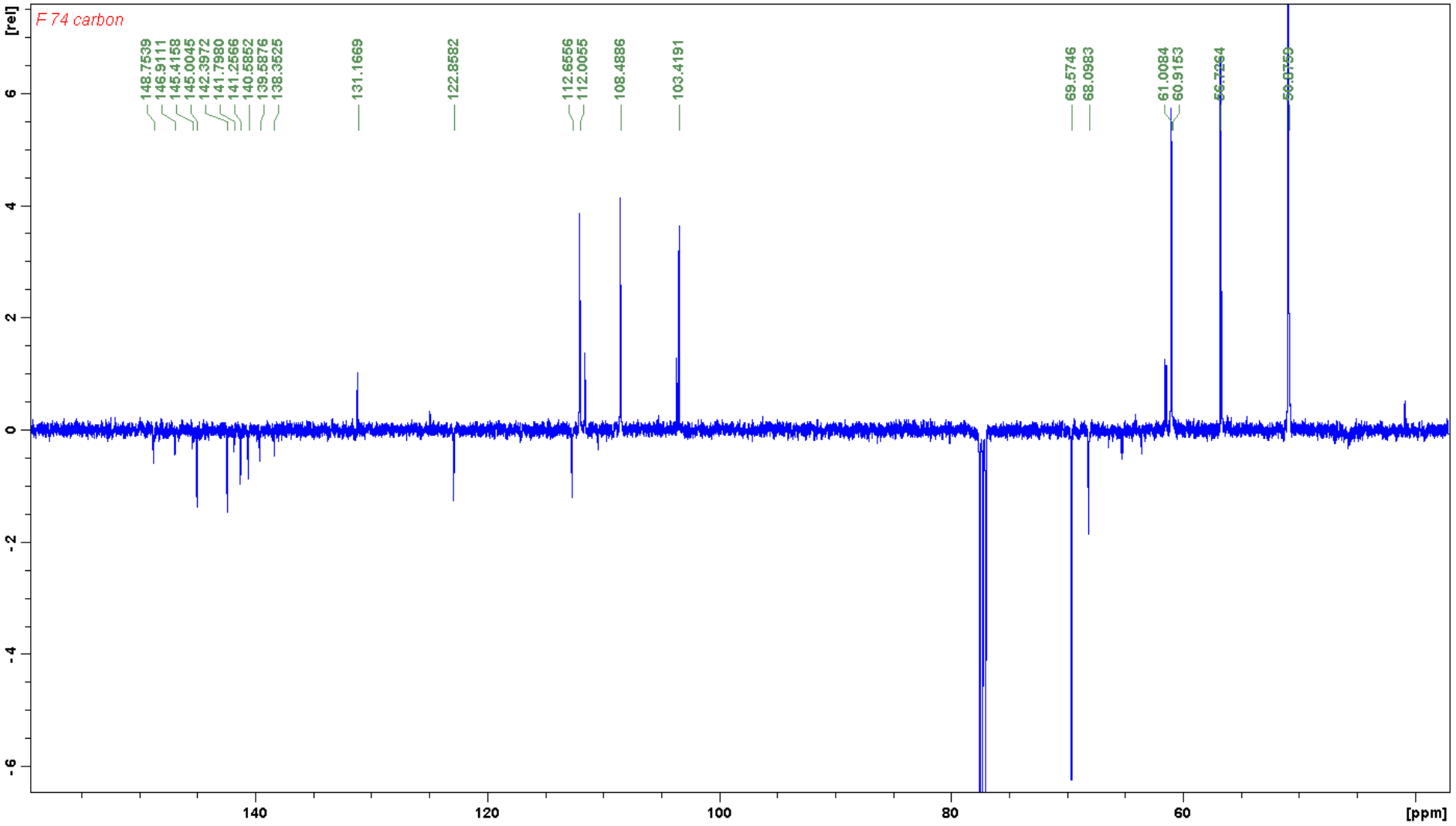

Fig. A.19. DEPTQ spectrum of abruquinone L (**3**) in $CDCl_3$.

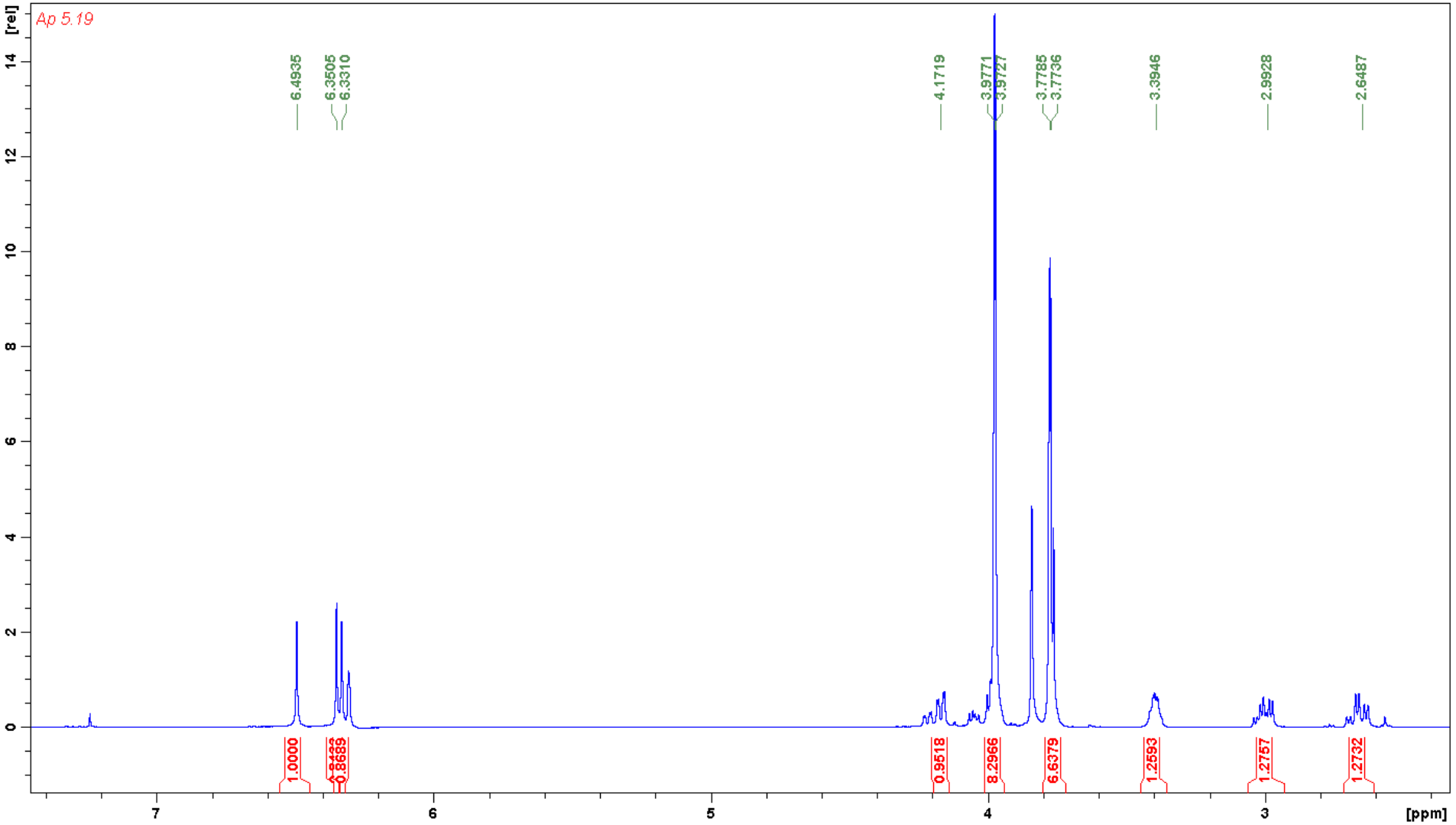

Fig. A.20. ^{1}H NMR spectrum of abruquinone A (**4**) in $CDCl_3$.

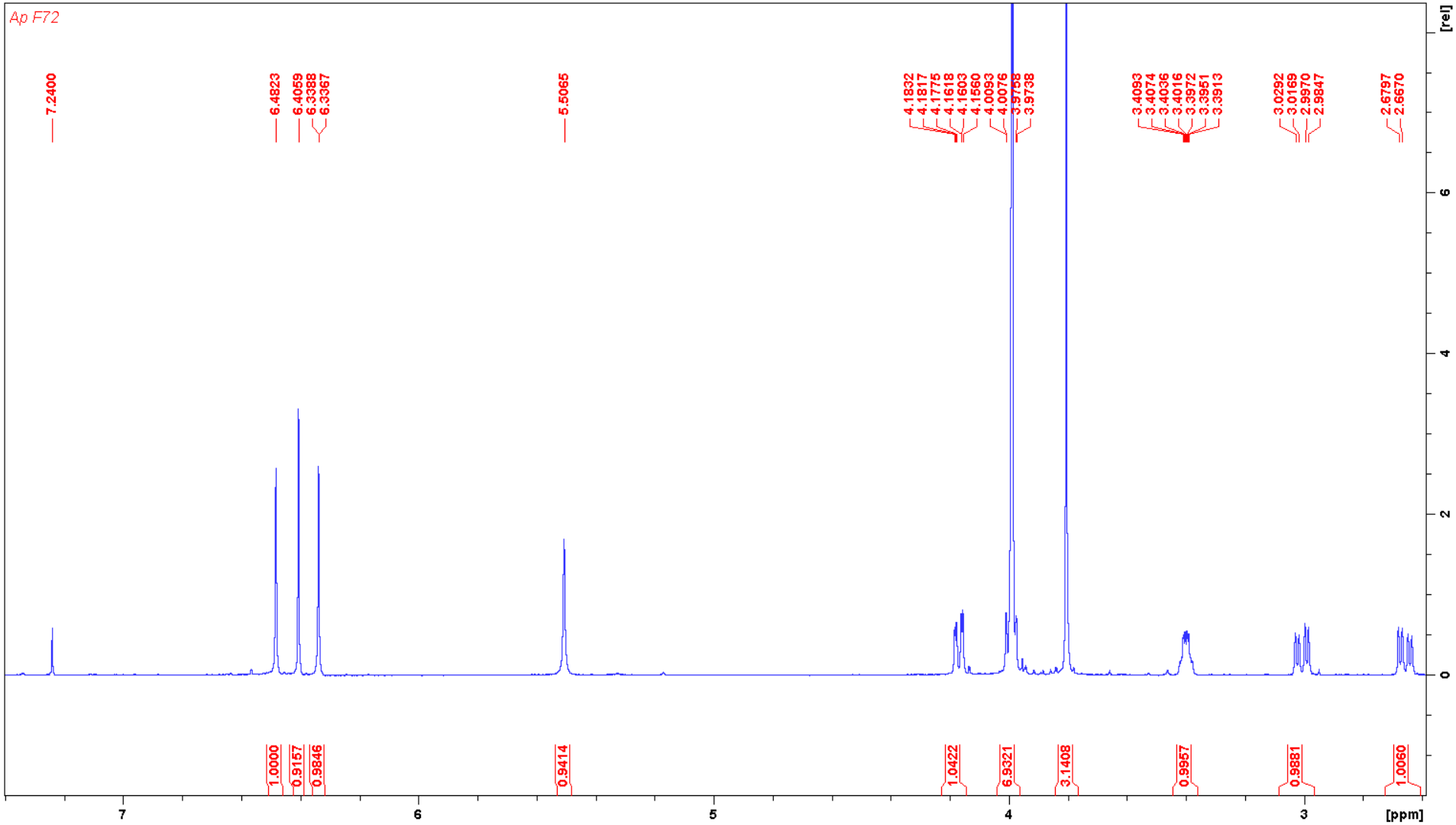

Fig. A.21. ^{1}H NMR spectrum of abruquinone D (**5**) in $CDCl_3$

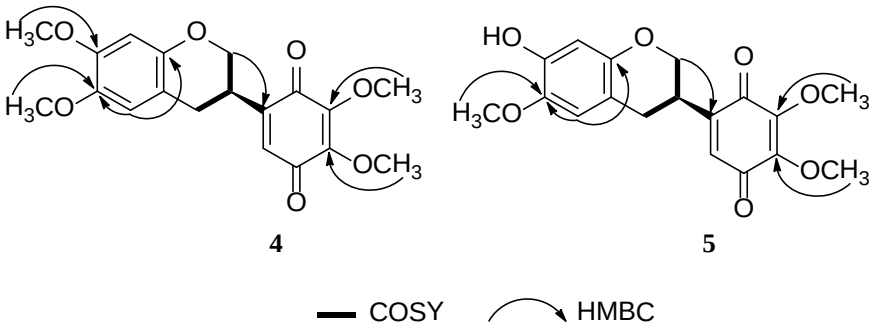

Fig. A.22 Key HMBC and COSY correlations for **4** and **5**.

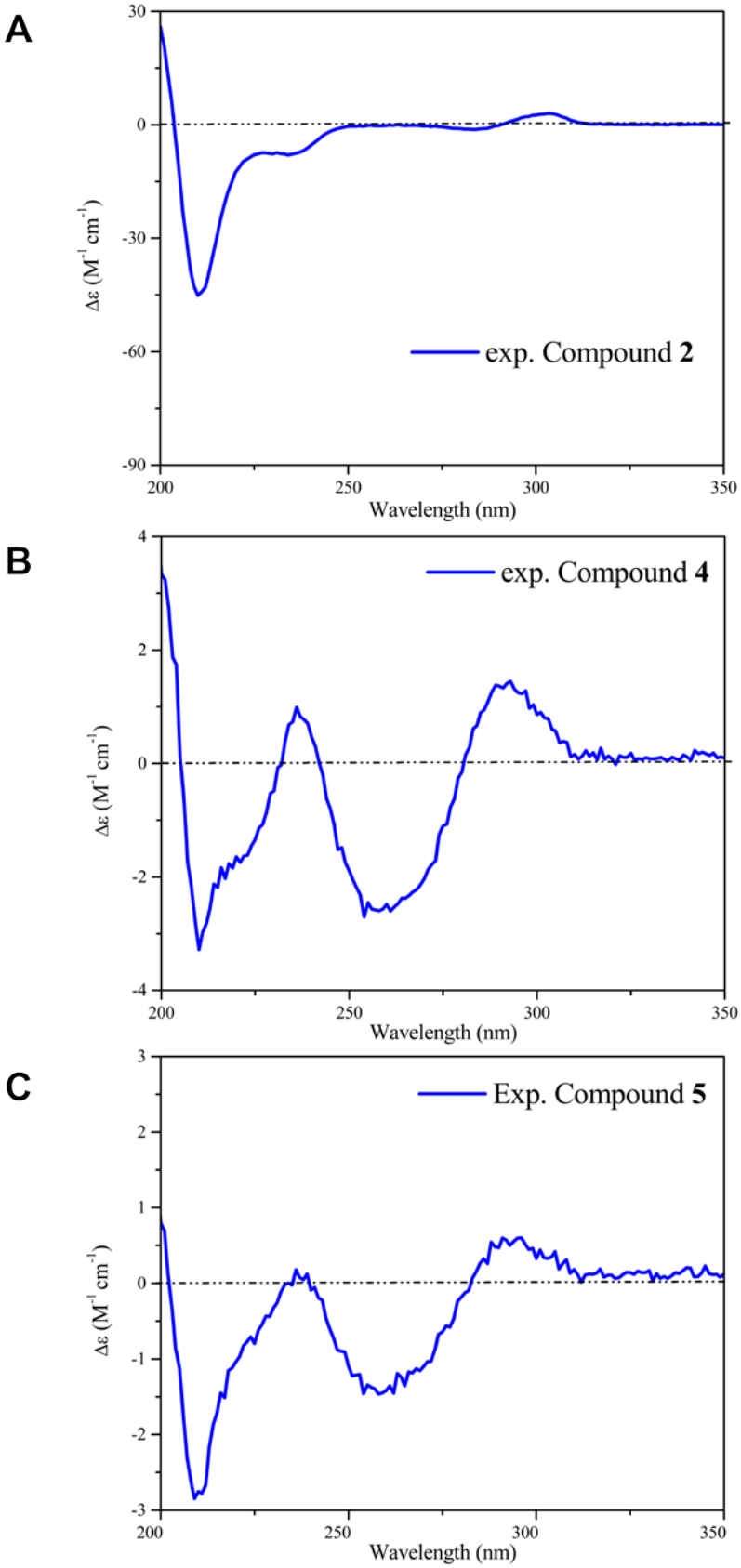

Fig. A.23 Experimental ECD spectra of compounds **2 (A)**, **4 (B)**, and **5 (C)**.

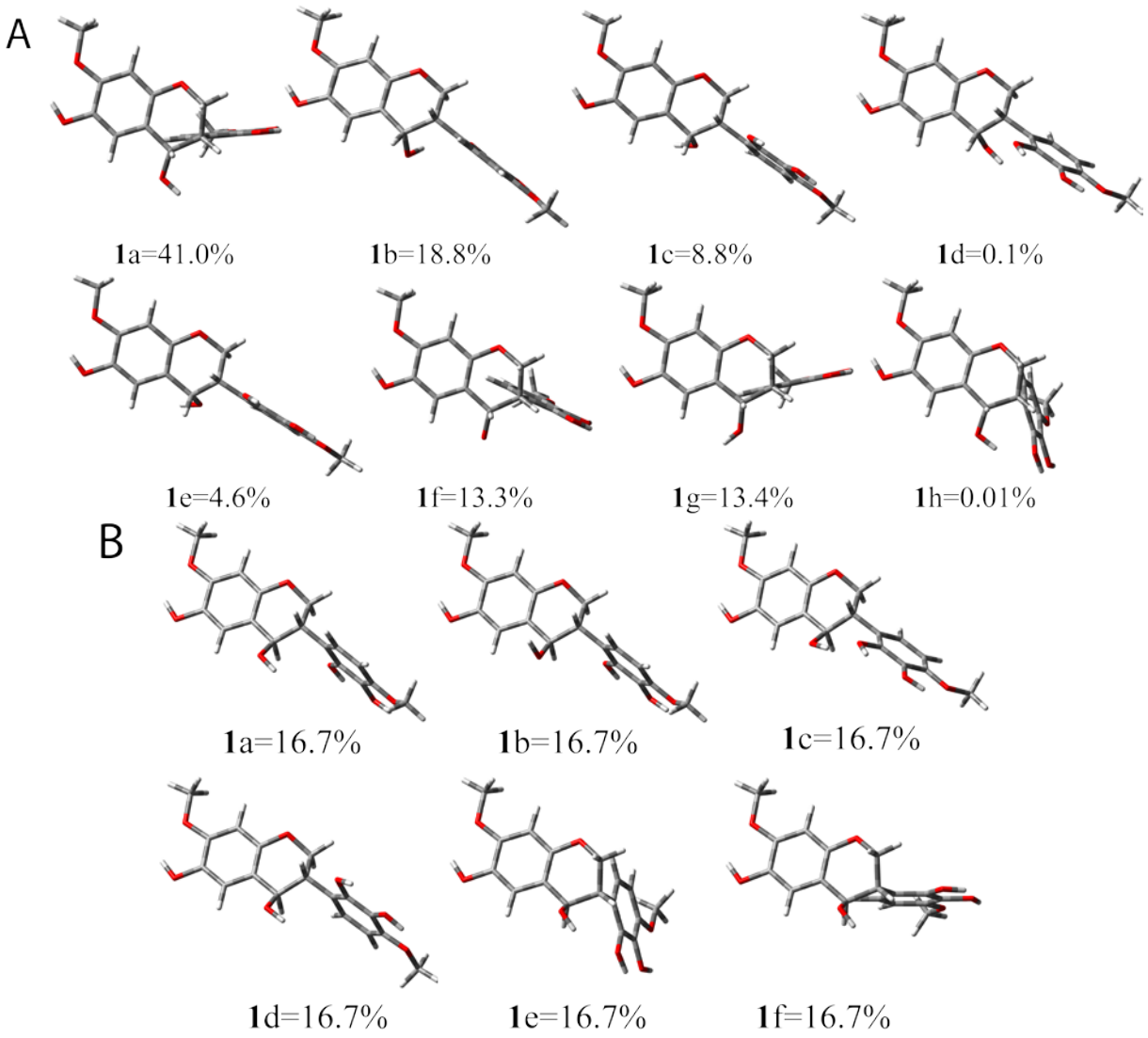

Fig. A.24. Lowest energy conformers (within 1 kcal/moL range from the global minimum) for (3*S*,4*S*)-**1** (**A**) and (3*S*,4*R*)-**1** (**B**). They were calculated using DFT at the B3LYP/6-31G** level in the gas phase. Eight conformers were obtained for the (3*S*,4*S*)-**1** (**A**), and six for (3*S*,4*R*)-**1** stereoisomer (**B**).

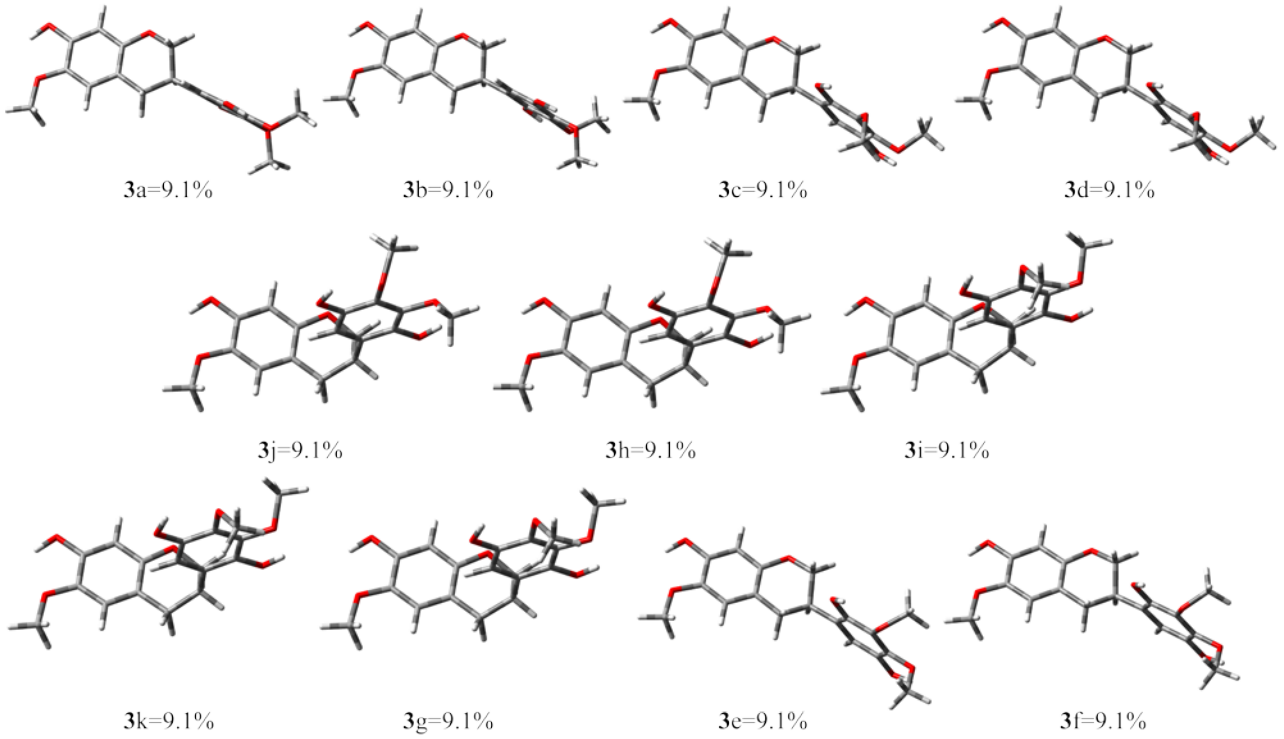

Fig. A.25. Lowest energy conformers (within 1 kcal/moL range from the global minimum) for (3*R*)-**3.** Data obtained from the conformational search were re-calculated using DFT at the B3LYP/6-31G** level in the gas phase. Eleven conformers were obtained for the (3*R*)-**3** enantiomer.

A

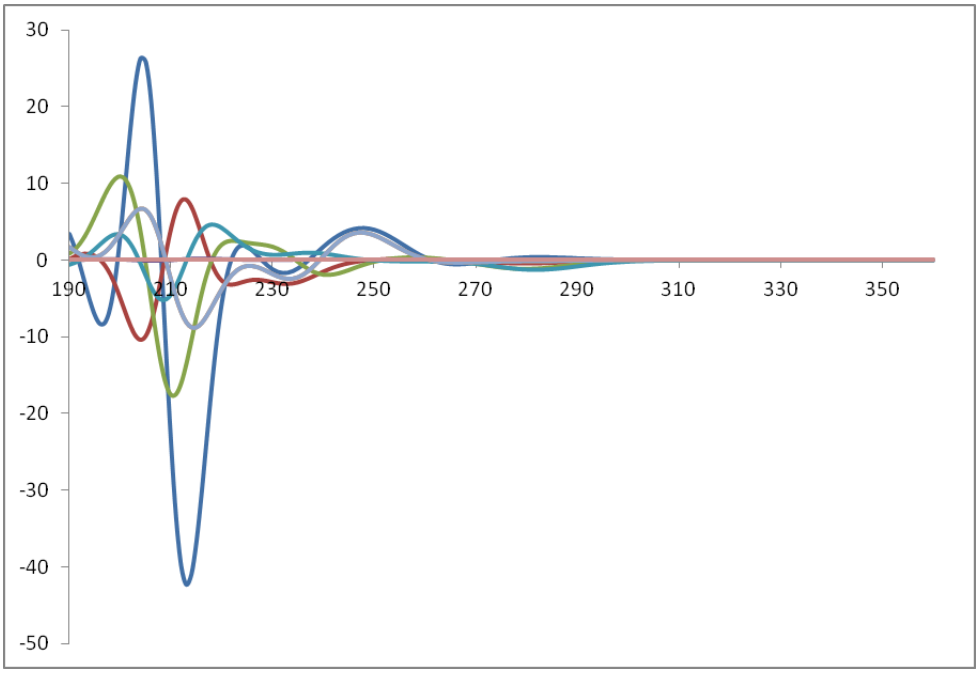

B

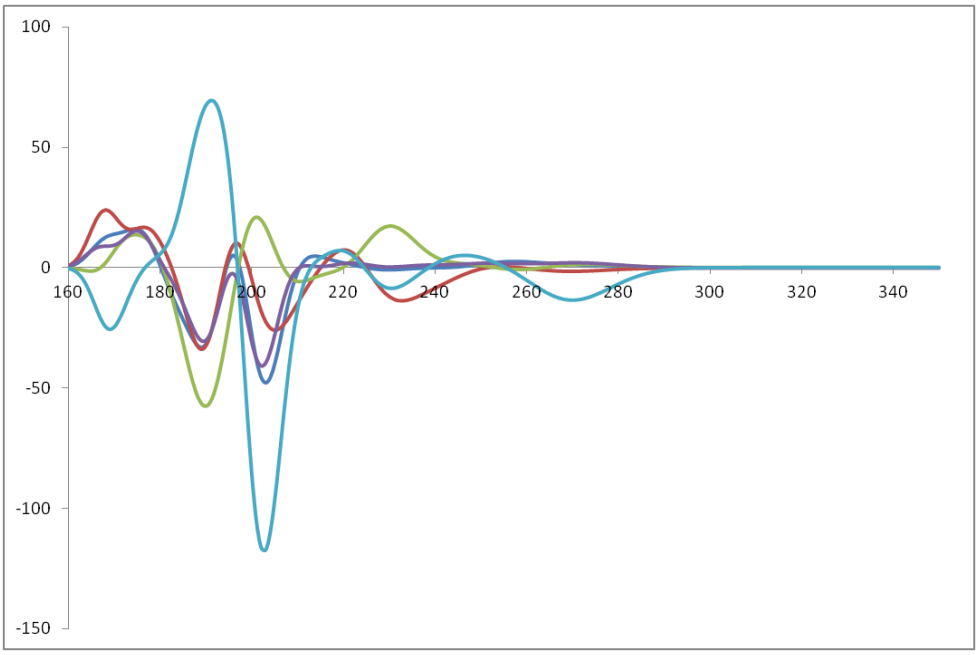

Fig. A.26. Calculated ECD spectra in MeOH (CPCM) of the minimized conformers DTF/B3LYP/6-31G**) of compound **1**. Spectra of individual conformers (within an energy range of 1 Kcal/mol) for the (3*S*,4*S*)-(**A**) and (3*S*,4*R*)-stereoisomers (**B**) are shown.

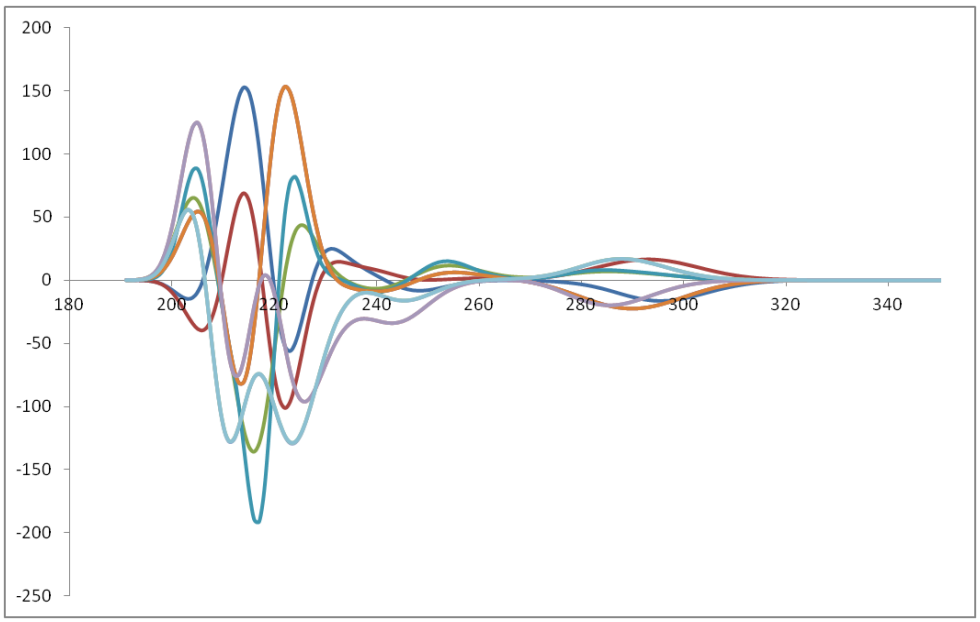

Fig. A.27. Calculated ECD spectra in MeOH (CPCM) of the minimized conformers DTF/B3LYP/6-31G**) of compound **3**. Spectra of individual conformers (within an energy range of 1 Kcal/mol) for the (3*R*)-enantiomer are shown.

References

1. *Desjardins RE, Canfield CJ, Haynes D, Chulay JD.* Quantitative assessment of antimalarial activity *in vitro* by a semiautomated microdilution technique. Antimicrob Agents Chemother 1979; 16: 710-718
2. *Trager W, Jensen JB.* Human Malaria Parasites in Continuous Culture. Science 1979; 109: 673-675
3. *Räz B, Iten M, Grether-Bühler Y, Kaminsky R, Brun R.* The Alamar Blue assay to determine drug sensitivity of African trypanosomes (*T. b. rhodesiens* and *T. b. gambiense*) *in vitro*. Acta Trop 1997; 68: 139–147
4. *Baltz T, Baltz D, Giroud C, Crockett J.* Cultivation in a semidefined medium of animal infective forms of *Trypanosoma brucei, T. equiperdum, T. evansi, T. rhodesiense, T. gambiense*. EMBO J 1985; 4: 1273-1277
5. *Buckner FS, Verlinde CL, LaFlamme AC, Van Voorhis WC.* Efficient technique for screening drugs for activity against *Trypanosma cruzi* using parasites expressing β-galactosidase. Antimicrob. Agents Chemother 1996; 40: 2592 – 2597
6. *Cunningham I.* New culture medium for maintenance of tstse tissues and growth of trypanosomatids. J Protozool 1977; 24: 325-329
7. *Page B, Page M, Noël C.* A new fluorometric assay for cytotoxicity measurements *in vitro*. Int J Oncol1993; 9: 473-476
8. *Bruhn T., H.Y., Schaumlöffel A., Bringmann G.* , SpecDis, 1.51 ed., University of Wuerzburg, Germany, Wuerzburg, 2011.
9. *Frisch, M., Trucks, GW, Schlegel, HB, Scuseria, GE, Robb, MA, Cheeseman, JR, Scalmani, G, Barone, V, Mennucci, B, Petersson, GA, Nakatsuji, H, Caricato, M, Li, X, Hratchian, HP, Izmaylov, AF, Bloino, J, Zheng, G, Sonnenberg, JL, Hada, M, Ehara, M, Toyota, K, Fukuda, R, Hasegawa, J, Ishida, M, Nakajima, T, Honda, Y, Kitao, O, Nakai, H, Vreven, T, Montgomery, JA, Peralta, JE, Ogliaro, F, Bearpark, M, Heyd, JJ, Brothers, E, Kudin, KN, Staroverov, VN, Kobayashi, R, Normand, J, Raghavachari, K, Rendell, A, Burant, JC, Iyengar, S.S., Tomasi, J., Cossi, M., Rega, N., Millam, J.M., Klene, M., Knox, J.E., Cross, JB, Bakken, V, Adamo, C, Jaramillo, J, Gomperts, R, Stratmann, RE, Yazyev, O, Austin, AJ, Cammi, R, Pomelli, C, Ochterski, JW, Martin, RL, Morokuma, K, Zakrzewski, VG, Voth, GA, Salvador, P, Dannenberg, JJ, Dapprich, S, Daniels, AD, Farkas, O, Foresman, JB, Ortiz, JV, Cioslowski, J, Fox, DJ,* Gaussian 09, Revision A02 ed., Gaussian Inc, Wallingford CT, 2009.
10. *Lupi A, Monache FD, Marini-Bettolo GB.* Abruquinones: New natural isoflavanquinones. Gazz Chim Ital 1976; 193 :9-12
11. *Song CQ, Hu ZB.* Abruquinone A, B, D, E, F, and G from the root of *Abrus precatorius*. Acta Bot Sin1998; 40: 374-379.

3.5 Identification of two new phenathrenones and a saponin as antiprotozoal constituents of *Drypetes gerrardii*

Yoshie Hata[1,4*], Maria De Mieri[1*], Samad Nejad Ebrahimi[1,5], Tsholofelo Mokoka[3], .Gerda Fouche[3], Marcel Kaiser[2], Reto Brun[2], Olivier Potterat[1], and Matthias Hamburger[1]

Phytochemistry letters. Accepted.

HPLC-based activity profiling allowed the identification of a new phenanthrenone from the stems extract of *Drypetes gerrardii.* Alongside, its dimer could be isolated. Both compounds showed activity against *Plasmodium falciparum*. However, the phenanthrenone exhibited more potency and selectivity than the dimer. As a result, the phenanthrenone was isolation in large scale for *in vivo* assessment. Interestingly, the compound turned out to be inactive. Furthermore, a saponin with weak trypanocidal activity, putranoside A, could be isolated from the leaves extract after being localized by the aid of a HPLC-based activity profiling.

My contributions to this work were: (1) HPLC microfractionation of the CH_2Cl_2/MeOH (1:1) extract of Drypetes gerrardii (stems); (2) isolation of a phenanthrenone and its dimer, (3) recording and interpretation of analytical data for structure elucidation (HPLC-PDA-ESI-MS, TOF-MS, 1D and 2D NMR); (4) large scale isolation of the phenanthrenone for in vivo antimalarial test; (5) HPLC microfractionation of the CH_2Cl_2/MeOH (1:1) extract of D. gerrardii (leaves); (6) isolation of a saponin, hydrolysis, recording and interpretation of analytical data for structure elucidation (HPLC-PDA-ESI-MS, TOF-MS, 1D and 2D NMR), data analysis, (7) writing of the manuscript draft, preparation of figures, tables, and supporting information.

Maria de Mieri supported the structure elucidation of the phenanthrenones and wrote the corresponding results section in the paper. Melanie Raith supervised the saponin structure elucidation. In vitro antiprotozoal and cytotoxicity tests were performed at the Swiss TPH. The crude extracts were provided by the CSIR team.

Yoshie Hata-Uribe

Identification of two new phenathrenones and a saponin as antiprotozoal constituents of *Drypetes gerrardii*

Yoshie Hata[a,d*], Maria De Mieri[a*], Samad Nejad Ebrahimi[a,e], Tsholofelo Mokoka[c], Gerda Fouche[c], Marcel Kaiser[b], Reto Brun[b], Olivier Potterat[a], and Matthias Hamburger[a]

Affiliations

[a]Department of Pharmaceutical Sciences, University of Basel, Klingelbergstrasse 50, CH-4056 Basel, Switzerland

[b]Swiss Tropical and Public Health Institute and University of Basel, Socinstrasse 57, CH-4002 Basel, Switzerland

[c]Biosciences, Council for Scientific and Industrial Research (CSIR), PO Box 395, Pretoria 0001, South Africa

[d]Department of Pharmacy, Faculty of Sciences, National University of Colombia, Carrera 30 No. 45-03, Bogota D.C. 111321, Colombia

[e]Department of Phytochemistry, Medicinal Plant and Drugs Research Institute, Shahid Beheshti University, G. C., Tehran, Iran

Corresponding author:

Prof. Dr. Matthias Hamburger, Division of Pharmaceutical Biology, University of Basel, Klingelbergstrasse 50, CH-4056 Basel, Switzerland.

e-mail: matthias.hamburger@unibas.ch, Phone: +41 61 267 14 25 Fax: +41 61 267 14 74

*These two authors contributed equally to this work.

Abstract

In an *in vitro* screen of 206 extracts from South African plants, the CH_2Cl_2/MeOH (1:1) stem extract of *Drypetes gerrardii* Hutch. var *gerrardii* (Putranjivaceae) inhibited *Plasmodium falciparum* and *Leishmania donovani* (IC_{50}s of 0.50 and 7.31 µg/ml, respectively). In addition, the CH_2Cl_2/MeOH (1:1) extract of the leaves showed activity against *Trypanosoma brucei rhodesiense* (IC_{50} of 12.1 µg/ml). The active constituents were tracked by HPLC-based activity profiling, and isolated by preparative and semi-preparative RP-HPLC chromatography. Their structures were established by HRESIMS, and 1D and 2D NMR (^{1}H, ^{13}C, COSY, HMBC, HSQC, and NOESY). From the stem extract, a new phenanthrenone derivative, drypetenone D (**1**), and a phenanthrenone heterodimer, drypetenone E (**2**), were isolated. Compound **1** showed potent *in vitro* activity against *P. falciparum* (IC_{50} of 0.9 µM) with a selectivity index (SI) of 71, as calculated from cytotoxicity data for L-6 cells. These data qualified **1** for *in vivo* assessment in the *Plasmodium berghei* mouse model, but the compound turned out to be inactive. Compound **2** also exhibited good *in vitro* antiplasmodial activity (IC_{50} of 2.0 µM) and selectivity (SI 31). From the leaf extract, the saponin putranoside A (**3**) was isolated and identified. Compound **3** showed weak *in vitro* trypanocidal activity, with an IC_{50} of 18.0 µM, and a SI of 4.

Keywords: Antiprotozoal, *Drypetes gerrardii*, Putranjivaceae, phenanthrenones, HPLC-based activity profiling.

1. Introduction

Tropical parasitic diseases have devastating social and economic effects for Third World countries (Renslo and McKerrow, 2006). According to WHO estimations, 207 million cases of malaria infections and 627000 malaria deaths occurred worldwide in 2012. Malaria is transmitted by mosquitoes of the genus *Anopheles* and caused by five *Plasmodium* species. Artemisinin derivatives are the most recent drugs, but artemisinin-resistant *P. falciparum* strains have already emerged in Asia (Miller et al., 2013; WHO, 2013). Human African trypanosomiasis (HAT) is confined to sub-Saharan African countries where tsetse flies (genus *Glossina*) transmit the disease. The number of reported cases was 7197 in 2012. *Trypanosoma brucei gambiense* accounts for more than 98% of the reported cases of HAT and *T. b. rhodesiense* for the rest. Drugs in current use show varying degrees of toxicity and efficacy, and all require parenteral administration (WHO, June, 2013; Brun et al., 2011). There are more than 21 species of *Leishmania* sp. that cause various forms of leishmaniasis ranging from the cutaneous form to the lethal, if untreated, visceral form (VL). VL has an estimated global incidence of 200000 – 500000 cases and a prevalence of 5 million cases worldwide. Antileishmanial drugs are available, but suffer from limited efficacy, long treatments, or high costs (Stuart et al., 2008; WHO, 2010). In view of the unsatisfactory therapeutic options currently available, there is an urgent need for new drugs to treat these diseases (Renslo and McKerrow, 2006; Stuart et al., 2008).

Natural products constitute an invaluable source of new drug scaffolds, particularly in the area of infectious diseases (Hannaert, 2011; Renslo, 2013). In the search for new antiprotozoal compounds, we screened a library of South African medicinal plants for antiprotozoal activity (Hata et al., 2013; Hata et al., 2011; Mokoka et al., 2011; Mokoka et al., 2013). A stem extract from *Drypetes gerrardii* Hutch. var. *gerrardii* (Putranjivaceae) showed pronounced antiplasmodial and antileishmanial activities. In addition, a leaf extract of the same plant

exhibited trypanocidal properties (Mokoka et al., 2013). There are few reports about the phytochemistry of *D. gerrardii*. So far, triterpenes belonging to the friedelane, hopane and lupane series, and flavone dimers, amentoflavone and drypetdimer A, have been isolated (Ng'ang'a et al., 2008; Ng'ang'a et al., 2011). The antiplasmodial activity of the dimeric flavonoids was evaluated against the K1 strain of *P. falciparum* (Ng'ang'a et al., 2012). We report here on the identification of the antiprotozoal constituents from stem and leaf extracts, and on the biological assessment of the isolated compounds.

2. Results and discussion

The CH_2Cl_2/MeOH 1:1 extract of the stems of *D. gerrardii* inhibited *P. falciparum* and *L. donovani* with IC_{50} values of 0.50 µg/ml and 7.31 µg/ml, respectively. Activity in the extract was tracked by HPLC-based activity profiling (**Fig**. **1**). The chromatogram exhibited a strong UV-absorbing peak at t_r = 19.0 min which correlated with 71% inhibition of *L. donovani*, and 95% inhibition of *P. falciparum.* The compound was isolated by flash chromatography of the CH_2Cl_2/MeOH (1:1) extract, followed by semi-preparative RP-HPLC. In addition, a structurally related compound **2** was obtained. The structures of **1** and **2** were determined by HRESIMS and NMR analyses (^{1}H NMR, ^{13}C NMR, HMBC, HSQC, and NOESY). Compound **1** had a molecular formula of $C_{17}H_{16}O_2$ (HRESIMS *m/z* = 275.1067 [M+Na]+ (calcd. for $C_{17}H_{16}NaO_2$, 275.1043), thus requiring 10 degrees of indices of hydrogen deficiency. The ^{1}H and ^{13}C NMR spectra displayed resonances in the low field region of the spectrum and were indicative of a highly substituted aromatic ring system. The ^{1}H NMR spectrum in $CDCl_3$ displayed an AX olefinic spin system at δ_H 8.20 (d, *J* = 10.1 Hz) and 6.29 (d, *J* = 10.1 Hz), two *ortho* coupled aromatic protons at δ_H 7.75 (d, *J* = 8.5 Hz) and 7.39 (d, *J* = 8.5 Hz), two aromatic protons as singlets at δ_H 7.59 and 7.53, an aliphatic geminal dimethyl group δ_H 1.51 (6H, s), and an aromatic methyl group at δ_H 2.42. The ^{13}C NMR spectrum

displayed seventeen signals consistent with three methyls, six methines, eight quaternary carbons including a carbonyl (δ_C 205.5), one oxygenated aromatic carbon (δ_C 154.7) and a quaternary carbon bearing the *gem*-dimethyl group (δ_C 48.1). A careful analysis of HMBC and NOESY correlations (**Fig. 4**) suggested that **1** possessed a phenanthrenone skeleton similar to trigohowilol A (**4**) (Tang et al., 2012) except for the absence of the hydroxyl group at C-9 and of the *O*-methyl substituent at C-6 in **1**. The location of the scalar coupled doublets (δ_H 7.75 and 7.39, J = 8.5 Hz) at positions C-9 and C-10, respectively, was inferred from HMBC correlations from H-9 to C-8, C-4b and C-10a, and from H-10 to C-4a and C-8a. This structural assignment was corroborated by a NOESY correlation between H-9 and H-8, and between H-10 and the *gem*-dimethyl group at C-1. Thus, the structure of **1** was established as shown in **Fig. 3** and the compound was named drypetenone D.

The molecular formula of compound **2** was determined as $C_{34}H_{30}O_4$ (HRESIMS *m/z* = 525.2063 [M+Na]+ (calcd. for $C_{34}H_{30}NaO_4$, 525.2036), with 20 indices of hydrogen deficiency. The ^{1}H and ^{13}C spectra showed the presence of two sets of signals resembling those found for compound **1**, thus suggesting a heterodimeric structure for **2**. The ^{1}H NMR spectrum displayed the resonances of: (1) two *gem*-dimethyl groups, Me-1 (δ_H 1.43, s) and Me-1' (δ_H 1.45, s); (2) two aromatic methyl groups CH_3-7 (δ_H 2.76, s), CH_3-7' (δ_H 2.51, s); (3) two sets of AX olefinic doublets H-3 (δ_H 6.03) and H-3' (δ_H 5.96), H-4 (δ_H 7.40) and H-4' (δ_H 8.70); (4) two sets of *ortho* coupled aromatic protons H-9 (δ_H 7.78) and H-9' (δ_H 7.88), H-10 (δ_H 7.43) and H-10' (δ_H 7.49); (5) three uncoupled aromatic protons H-5 (δ_H 6.93), H-8 (δ_H 7.77) and H-8' (δ_H 7.66).

The ^{13}C NMR spectrum showed the signals for the aforementioned protonated carbons (see **Table 1**) and additionally: (1) two carbonyl C-atoms resonating at δ_C 204.5 (C-2) and δ_C 203.9 (C-2'); (2) three oxygen bearing aromatic carbons δ_C 154.6 (C-6), δ_C 147.7 (C-6') and δ_C 134.2 (C-5'); (3) two aliphatic quaternary carbons δ_C 48.0 (C-1), δ_C 48.6 (C-1'); (4) ten

aromatic quaternary carbons δ_C 122.2 (C-4a) and δ_C 121.7 (C-4a'), 130.3 (C-4b) and δ_C 123.5 (C-4b'), 127.0 (C-7) and δ_C 127.6 (C-7'), 129.0 (C-8a) and δ_C 128.7 (C-8a'), 147.5 (C-10a) and δ_C 149.2 (C-10a'). Based on HMBC and NOESY correlations the two substructures A and B (**Fig. 5**) were identified. Substructure A corresponded to compound **1**, while in substructure B position C-5' was hydroxylated. In substructure B, the substitution of the aromatic C ring unit was established on the basis of the NOESY correlations between H-8' and H-9' and between H-8' and CH_3-7'. The positions C-6' (δ_C 147.7) and C-5' (134.2) of ring C were oxygenated; C-6' chemical shift was assigned to be δ_C 147.7 by the $^3J_{H\text{-}C}$ HMBC correlation from 7'-CH_3 while the remaining upfield shifted ^{13}C resonance was assigned to position C-5'. Considering the substituents of the substructures A and B it became obvious that they were connected through an ether linkage between position C-6 of substructure A and positions C-5' or C-6' of substructure B. Unfortunately, no cross peaks were detected in the HMBC spectrum from H-5 to substructure B. In a further effort to discriminate between the two possible regioisomers, a long-range optimized (4 Hz) HMBC spectrum was measured. No correlations between the C rings of the two substructures were detected. However, position C-5' could be unequivocally assigned by the $^4J_{H\text{-}C}$ HMBC observed with H-9' and H-8'. It was identified as the point of attachment of the ether linkage on substructure B considering the diagnostic upfield shift of δ_C C-5' (δ_C 134.2), with respect to C-6' (δ_C 147.7). A further support to this structure assignment came from the NOESY spectrum that showed a strong dipolar coupling between CH_3-7 (δ_H 2.76) and H-4' (δ_H 8.70). On the basis of these data the structure of **2** was assigned as reported in **Fig. 3** and the new compound named drypetenone E.

A conformational analysis of **2** was performed, followed by geometrical optimization for the conformers found within 1 Kcal/mol from the corresponding global minimum energy. Two iso-energetic conformers were found (**Fig. 6**). DFT-optimized structures showed that the two substructures A and B were almost perpendicular and the distance between CH_3-7 and H-4'

was 3.45 Å for both conformers, thus matching the observed dipolar coupling. The tridimensional rearrangement of drypetenone E (**2**) could also provide an explanation of the significant differences in the ^{1}H chemical shift between drypetenone D (**1**) and substructure A of **2**.

There are few reports of naturally occurring phenanthrenones. Such compounds have been isolated from a marine bacterium, *Pseudomonas stutzeri* (Uzair et al., 2008), and from terrestrial plants of the genera *Strophioblachia* (Seephonkai et al., 2013a, b; Seephonkai et al., 2009) and *Trigonostemon* (Hu et al., 2009; Kokpol et al., 1990; Tang et al., 2012; Zhu et al., 2010), which belong to the Euphorbiaceae family. Interestingly, the genus *Drypetes* was formerly included in this family.

Compound **1** showed low *in vitro* activity against *L. donovani* (**Table 2**). In contrast, **1** remarkably inhibited *P. falciparum* (IC_{50} of 0.96 µM) and displayed low cytotoxicity for the L-6 cell line (IC_{50} of 68 µM). The selectivity index (SI) calculated as the quotient of IC_{50} for L-6 cells and IC_{50} against parasites gave a value of 71. Compound **2** displayed good *in vitro* activity against *P. falciparum* (IC_{50} of 2.0 µM), even though the selectivity (SI = 31) was not as high as the one of **1**. The low yield of the compound probably explains that its activity was not detected in the HPLC-based activity profiling. These results granted *in vivo* assessment of the antimalarial efficacy of **1** in a mouse model. The full suppressive four-day test was performed on female NMRI mice infected with a GFP-transfected *P. berghei* strain ANKA. Animals treated with compound **1** showed no parasitemia reduction on day 4 compared to untreated control mice. The absence of activity in this model can be due either to absorption problems or unfavourable PK.

Molecular properties associated with drug-likeness and toxicity are essential in early compound selection. Descriptors, such us Lipinski's "rule of 5" (molecular weight, log P, sum of H-donors/acceptors), rotatable bonds, and polar surface area (PSA) can predict drug-

likeness. Compound **1** had a molecular weight of 252 Da, log P of 3.96, sum of H-donors/acceptors of 2, 0 rotatable bonds and a PSA of 37.3 $Å^2$, as calculated by Molinspiration Cheminformatics software (Cheminformatics, 2014). All these values fulfil established drug-likeness criteria (Lipinski and Hopkins, 2004; Pajouhesh and Lenz, 2005). Accordingly, oral absorption and blood-brain barrier permeability can be expected for compound **1**. Oral availability is a desired characteristic for an ideal antimalarial drug (Fidock et al., 2004) while blood-brain barrier permeability is prerequisite for an advanced HAT infection (Brun et al., 2011).

An early *in silico* toxicity prediction can help to anticipate potential "off-target" activity. There are a series of proteins involved in development of adverse effects. When the ability of a compound to bind to these proteins is simulated and quantified *in silico,* it is possible to obtain an estimated toxic potential (TP). By using the virtual technology "Virtual ToxLab" we estimated a TP of endocrine and/or metabolic disruption, carcinogenicity, and cardiotoxicity (Vedani et al., 2012). Binding affinities of **1** toward 16 target proteins, were calculated to obtain a TP of 0.52. This TP value categorizes **1** as a class I compound (in a scale of 0 to IV, being IV the most toxic). The binding affinity to critical proteins such as hERG, a potassium ion channel related with cardiotoxicity (IC_{50} of 40.2 μM), was low. Nevertheless, **1** bound the progesterone receptor with high affinity (IC_{50} of 46.8 nM). In case the compound progresses through the drug discovery pipeline, this aspect would require further attention since this receptor has a fundamental role during pregnancy and antimalarial drugs are expected to be administered also to pregnant women (Fidock et al., 2004).

The second active extract, the CH_2Cl_2/MeOH 1:1 leaf extract, showed inhibition against *T. b. rhodesiense* with an IC_{50} of 12.1 μg/ml. HPLC-based activity profiling revealed strong inhibition in the time window of 19 – 20 min which matched with an intense peak in the HPLC-ELSD chromatogram (**Fig. 2**). Targeted isolation of this compound by a combination

of flash chromatography and open column chromatography afforded **3.** Acid hydrolysis afforded two sugar moieties which were identified by GC-MS analysis after derivatization with cysteine methyl ester and silylation (Severi et al., 2010) as L-rhamnose and D-glucuronic acid. The compound was identified by means of HRESIMS, extensive NMR analyses (^{1}H NMR, ^{13}C NMR, HMBC, HSQC, and NOESY) and comparison with literature data as 3-*O*-[α-L-rhamnopyranosyl-(1→3)-β-D-glucuropyranosyl] oleanolic acid, known as putranoside A (**Fig. 3**) (Borel and Hostettmann, 1987; Hariharan, 1973, 1974; Melek et al., 2003). Compound **3** showed weak *in vitro* trypanocidal (IC_{50} of 18.0 µM) and antileishmanial activities (IC_{50} of 7.8 µM).

It is noteworthy that the antiplasmodial triterpenoids which were previously reported from the leaves and stems of *D. gerradii*, including the most active lupane-type derivative resinone (IC_{50} of 0.09 mg/ml, SI 942) (Ng'ang'a et al., 2012; Ng'ang'a et al., 2011), were not detected by HPLC-MS analysis in the course of our study.

3. Materials and Methods

3.1 General experimental procedures

HPLC-grade methanol (MeOH), acetonitrile (MeCN) (Scharlau Chemie S.A.), and water (obtained by an EASY-pure II from Barnstead water purification system, Dubuque) were used for HPLC separations. HPLC solvents contained 0.1% HCO_2H (Sigma) for analytical separations. $CDCl_3$ (100 atom% D), DMSO-d_6 (100 atom% D), and pyridine-d_5 (100 atom% D) for NMR were purchased from Armar Chemicals (Switzerland). Solvents used for extraction were of analytical grade (Romil Pure Chemistry). Reference drugs for bioassays

were chloroquine (>98%, Sigma-Aldrich), melarsoprol (purity >95%, Sanofi-Aventis), miltefosine (purity >95%, VWR), and podophyllotoxin (purity >95%, Sigma-Aldrich). HPLC-PDA-MS analyses were performed on an Agilent 1100 system consisting of a degasser, a quaternary pump, a column oven, a PDA detector and to an Esquire 3000 plus ion trap mass spectrometer (Bruker Daltonics). Data acquisition and processing were performed using HyStar 3.0 software (Bruker Daltonics). HPLC-PDA-ELSD analyses were carried out on an Alliance 2695 HPLC system (Waters) equipped with a 996 PDA (Waters) and an Alltech 2000ES ELSD. ELSD parameters were set as follows: N_2 flow = 3.2 l/min, temp. = 115ºC, gain = 8, impactor = off. Empower Pro software (Waters) was used to acquire and process data. Sugar analysis of compound **3** was performed with a HP 5890 Series II gas chromatograph equipped with a HP 5971 mass detector. He was used as a carrier gas. Flash chromatography was carried out on a chromatography system PuriFlash® 4100 (Interchim), controlled with InterSoft V5.0 software. Semi-preparative HPLC was performed on an Agilent 1100 series instrument equipped with a PDA detector. Data acquisition and processing were carried out using HyStar 3.2 software (Bruker Daltonics). For HRESIMS a micrOTOF ESI-MS system (Bruker Daltonics) was used. Mass calibration was performed with a solution of formic acid 0.1% in 2-PrOH/H_2O (1:1) containing 5mM NaOH. Mass spectra were recorded in the range of *m/z* 150 – 1500 in positive ion mode with the aid of micrOTOF control software 1.1 (Bruker Daltonics). NMR spectra were recorded at 18 °C on a Bruker AVANCE III™ 500 MHz spectrometer operating at 500.13 (^{1}H) and 125.77 MHz equipped with a 1 mm TXI microprobe (^{1}H and 2D NMR) or a 5 mm BBO probe (^{13}C NMR) (Bruker BioSpin). The ^{13}C spectrum of **2** was recorded on a Bruker Ascend™ III 600 MHz spectrometer equipped with a QCI cryoprobe. Chemical shifts are reported as δ values (ppm) with the residual solvent signal as internal reference, *J* in Hz. Standard pulse sequences from Topspin 3.0 software package were used.

3.2 Plant material

Samples of the stems of *D. gerrardii* were collected at Hlatikulu Forest on top of the Lebombo mountains in Gwalewemi, KwaZulu Natal Province in South Africa in April 2012 by a botanist, Mr. Hans Vahrmeijer. A plant specimen was deposited at the South African National Biodiversity Institute (SANBI), and the plant identified as *Drypetes gerrardii* Hutch. var. *gerrardii (*Putranjivaceae) (voucher specimen number PRE 45954).

3.3 Extraction

Stems and leaves were collected, separated and dried separately in an oven at 30-60°C. Dried plant material was ground to a coarse powder using a hammer mill, and stored at ambient temp. prior to extraction. 800 g of dried, ground stems were extracted with 4 l of a mixture of CH_2Cl_2 and MeOH (1:1) at room temp. for 1h with occasional stirring. The extract was filtered, and the residual plant material further extracted overnight with 2 l CH_2Cl_2/MeOH (1:1), followed by filtration. Finally, a third extraction of the pulp was carried out with 2 l solvent for 1h with filtration. The filtrates were combined and concentrated using a rotary vacuum evaporator at a temp. below 45°C, and the residue dried *in vacuo* at room temp. for 24 h. The dried extract of 35.0 g (4.4%, w/w) was stored at –20°C.

The dried, ground leaves (115 g) of the plant were extracted in a similar way as described above to yield 6.31 g (5.5%, w/w) of extract.

3.4 Microfractionation and activity profiling

HPLC-based activity profiling was performed on a SunFire™ C18 column (3.5 µm, 3.0 × 150 mm, Waters) equipped with a precolumn (3 x 10 mm) as previously described (Adams et al., 2009). H_2O (solvent A) and MeCN (solvent B) were used as solvents, and the following gradient was applied: 10% → 100% B in 30 min, then 100% B for 1 min. The flow rate was 0.5 ml/min. Aliquots (35 µl) of extracts (10 mg/ml in DMSO) were injected, and 32

one-minute fractions collected into a 96 deep well plate (Eppendorf) with the aid of a F204 fraction collector (Gilson). After solvent removal in an Evaporex 96 channel N_2-evaporator (Apricot Designs), the dried fractions were re-dissolved in methanol (100 µl) and transferred to 96 v-well plates (Thermo Scientific), dried again, and stored in a refrigerator (2 – 8ºC) until use for bioassay.

3.5 Preparative isolation

The CH_2Cl_2/MeOH (1:1) stem extract of *D. gerrardii* (3.4 g) was fractionated by flash chromatography on a silica gel 60 column (15 – 40 µM, 35 x 430 mm, 180 g) with a gradient of 100-0% hexane in EtOAc in 3 h, using a flow rate of 40 ml/min. Fractions (22 ml each) were collected and compared by TLC analysis [silica gel; hexane/EtOAc (9:1 and 7:3); anisaldehyde/sulphuric acid spraying reagent, heated at 110ºC]. Fractions 10 (121.4 mg) and 11 (34.8 mg) were found to contain phenanthrenones. They were purified by semi-preparative RP-HPLC using a SunFire™ C18 column (3.5 µM, 10 x 150 mm; Waters) equipped with a precolumn (10 x 10 mm). H_2O (Solvent A) and MeCN (Solvent B) were used as solvents and the following gradient was applied: 40% → 60% B in 5 min, then 60% → 70% B in 25 min. The flow rate was 4 ml/min. The fractions were dissolved in DMSO (Fr.10: 10 mg/ml; Fr. 11: 20 mg/ml) and injected in aliquots of 300 µl. Compound **1** (24.8 mg, t_R 7.7 min) was isolated from Fr. 10 and Fr. 11. Compound **2** (1.4 mg, t_R 24.0 min) was obtained from Fr. 10.

The CH_2Cl_2/MeOH (1:1) leaf extract (355 mg) was separated by flash chromatography on a Sepacore® system system (Büchi) by using a pre-packed silica gel 60 cartridge (40 - 63 µm, 40 x 150 mm) with a gradient of 0 - 60% EtOAc in MeOH, over 2 h. The flow rate was 15 ml/min. Fractions (20 ml; each) were combined based on TLC analysis [silica gel; $CHCl_3$/MeOH/H_2O (65:30:5); vanillin/sulphuric acid reagent, heated at 110ºC]. Similar fractions were pooled into four fractions (Fr. A - D). Fr. B (148.7 mg) was further purified by

CC on silica gel (40 - 63 μm, 8 x 160 mm, 12.1 g) using a step gradient of $CHCl_3$ and MeOH (100:0, 95:5, 92.5:7.5, 90:10 87.5:12.5, 85:15, 80:20, 70:30, 60:40, 50:50; 50 ml each) to yield 9 sub-fractions (Fr. B_1 - B_9). Subfraction Fr. B_4 eluted with $CHCl_3$/MeOH (80:20) afforded pure compound **3** (31.3 mg).

Purity of compounds **1** and **3** was > 95%, and that of **2** > 90%, as determined by ^{1}H NMR (Figs. 1S, 5S, 9S, and 15S of Supplementary content).

6-Hydroxy-1,1,7-trimethylphenanthren-2(1*H*)-one (drypetenone D, **1**): Yellow amorphous substance; ^{1}H and ^{13}C NMR data in $CDCl_3$ and DMSO-d_6, see **Table 1**; HRESIMS: *m/z* = 275.1067 [M+Na]+ (calcd. for $C_{17}H_{16}Na\ O_2$, 275.1043).

6-Hydroxy-1,1,7-trimethyl-5-((2,8,8-trimethyl-7-oxo-7,8-dihydrophenanthren-3-yl)oxy)phenanthren-2(1*H*)-one (drypetenone E, **2**): Yellow amorphous substance; ^{1}H and ^{13}C NMR data in $CDCl_3$, see **Table 1**; HRESIMS: *m/z* = 525.2063 [M+Na]+ (calcd. for $C_{34}H_{30}NaO_4$, 525.2036).

3-*O*-[α-L-rhamnopyranosyl-(1→3)-β-D-glucuropyranosyl] oleanolic acid (putranoside A, **3**) [37-40]: White amorphous substance; ^{1}H and ^{13}C NMR data see **Table 1S** Supplementary content; HRESIMS: *m/z* = 801.4396 [M+Na]+ (calcd. for $C_{42}H_{66}NaO_{13}$, 801.4396).

3.6 Conformational analysis and geometrical optimization

Conformational analysis of compound **2** was accomplished with Schrödinger MacroModel 9.1 software employing the OPLS 2005 (optimized potential for liquid simulations) force field in H_2O. Conformers within a 1 Kcal/mol energy window from the global minimum were picked for geometrical optimization and energy calculation applying DFT with the B3LYP functional using the 6-31G (d,p) basis set in the gas phase with the Gaussian 09 program package (Frisch, 2009). Vibrational evaluation was done at the same level to confirm minima.

3.7 Bioassays

Extracts were tested *in vitro* against *Plasmodium falciparum* (NF54 strain), *Trypanosoma brucei rhodesiense* (STIB 900 strain), and *Leishmania donovani* (strain MHOM/ET/67/L82), in 96-well microtiter plates at concentrations of 10.0 μg/ml and 2.0 μg/ml. IC_{50}s were subsequently determined for active extracts. HPLC microfractions from the CH_2Cl_2/MeOH (1:1) stem extract of *D. gerrardii* were assayed against *P. falciparum* and *L. donovani.* Those from the CH_2Cl_2/MeOH (1:1) leaf extract were tested on *T. b. rhodesiense*. Compounds **1**and **3** were evaluated for their antiprotozoal activity against the three parasites. Due to the scarcity of isolated material, compound **2** was tested only against *P. falciparum*. Additionally, for pure compounds, cytotoxicity was determined by using a rat skeletal myoblast cell line (L-6 cells). For the assays DMSO stock solutions (10 mg/ml) of extracts and purified compounds were freshly diluted in medium (final DMSO concentration in assay <1%). Assays were performed in two independent replicates. *In vivo* antimalarial activity was assessed as previously described (Peters, 1987) and conducted according to the rules and regulations for the protection of animal rights ('Tierschutzverordnung') of the Swiss 'Bundesamt für Veterinärwesen'. They were approved by the veterinary office of the Canton Basel-Stadt, Switzerland. The animal experiment approval number for *in vivo* testing against *P. berghei* is 1731. Details on assay protocols are provided as Supplementary content.

Appendix A. Supplementary data

Supplementary data associated with this article can be found, in the online version, at

Acknowledgments

The authors thank the Council for Scientific and Industrial Research (CSIR), and the Swiss Confederation for financial support under the Swiss South African Joint Research Programme (grant JRP 03). Y. Hata gratefully acknowledges a PhD stipend from Administrative Department of Science and Technology from Colombia (Colciencias) managed by LASPAU. We thank Dr. D. Haussinger (Department of Chemistry, University of Basel) for recording the ^{13}C NMR spectrum of **2**, O. Fertig for GC-MS analysis, and Dr. M. Raith for her support in the structure elucidation. Thanks are also due to Mrs. M. Rogalski for proof-reading the manuscript.

Conflicts of Interest

The authors declare no conflict of interest.

References

Adams, M., Zimmermann, S., Kaiser, M., Brun, R., Hamburger, M., 2009. A protocol for HPLC-based activity profiling for natural products with activities against tropical parasites. Nat. Prod. Commun. 4, 1377-1381.

Borel, C., Hostettmann, K., 1987. Molluscicidal saponins from *Swartzia madagascariensis* Desvaux. Helv. Chim. Acta 70, 570-576.

Brun, R., Don, R., Jacobs, R.T., Wang, M.Z., Barrett, M.P., 2011. Development of novel drugs for human African trypanosomiasis. Future Microbiol. 6, 677-691.

Cheminformatics, M., 2014. Molinspiration. http://molinspiration.com/, Slovak Republic. Last accessed: January 2014.

Fidock, D.A., Rosenthal, P.J., Croft, S.L., Brun, R., Nwaka, S., 2004. Antimalarial drug discovery: efficacy models for compound screening. Nat. Rev. Drug Discovery 3, 509-520.

Frisch, M., Trucks, GW, Schlegel, HB, Scuseria, GE, Robb, MA, Cheeseman, JR, Scalmani, G, Barone, V, Mennucci, B, Petersson, GA, Nakatsuji, H, Caricato, M, Li, X, Hratchian, HP, Izmaylov, AF, Bloino, J, Zheng, G, Sonnenberg, JL, Hada, M, Ehara, M, Toyota, K, Fukuda, R, Hasegawa, J, Ishida, M, Nakajima, T, Honda, Y, Kitao, O, Nakai, H, Vreven, T, Montgomery, JA, Peralta, JE, Ogliaro, F, Bearpark, M, Heyd, JJ, Brothers, E, Kudin, KN, Staroverov, VN, Kobayashi, R, Normand, J, Raghavachari, K, Rendell, A, Burant, JC, Iyengar, S.S., Tomasi, J., Cossi, M., Rega, N., Millam, J.M., Klene, M., Knox, J.E., Cross, JB, Bakken, V, Adamo, C, Jaramillo, J, Gomperts, R, Stratmann, RE, Yazyev, O, Austin, AJ, Cammi, R, Pomelli, C, Ochterski, JW, Martin, RL, Morokuma, K, Zakrzewski, VG, Voth, GA, Salvador, P, Dannenberg, JJ, Dapprich, S, Daniels, AD, Farkas, O, Foresman, JB, Ortiz, JV, Cioslowski, J, Fox, DJ, 2009. Gaussian 09, Revision A02 ed. Gaussian Inc, Wallingford CT.

Hannaert, V., 2011. Sleeping sickness pathogen (*Trypanosoma brucei*) and natural products: therapeutic targets and screening systems. Planta Med. 77, 586-597.

Hariharan, V., 1973. Saponins of seed-coats of *Putranjiva roxburghii*. Indian J. Chem. 11, 830-831.

Hariharan, V., 1974. Structures of putranosides from the seed coats of *Putranjiva roxburghii*. Indian J. Chem. 12, 447-449.

Hata, Y., Raith, M., Ebrahimi, S.N., Zimmermann, S., Mokoka, T., Naidoo, D., Fouche, G., Maharaj, V., Kaiser, M., Brun, R., Hamburger, M., 2013. Antiprotozoal Isoflavan Quinones from *Abrus precatorius* ssp. *africanus*. Planta Med 79, 492-498.

Hata, Y., Zimmermann, S., Quitschau, M., Kaiser, M., Hamburger, M., Adams, M., 2011. Antiplasmodial and Antitrypanosomal Activity of Pyrethrins and Pyrethroids. Journal of Agricultural and Food Chemistry 59, 9172-9176.

Hu, X.-J., Wang, Y.-H., Kong, L.-Y., He, H.-P., Gao, S., Liu, H.-Y., Ding, J., Xie, H., Di, Y.-T., Hao, X.-J., 2009. New phenanthrenes from *Trigonostemon lii* Y.T. Chang. Tetrahedron Lett. 50, 2917-2919.

Kokpol, U., Thebpatiphat, S., Boonyaratavej, S., Chedchuskulcai, V., Ni, C.Z., Clardy, J., Chaichantipyuth, C., Chittawong, V., Miles, D.H., 1990. Structure of trigonostemone, a new phenanthrenone from the Thai plant *Trigonostemon reidioides*. J. Nat. Prod. 53, 1148-1151.

Lipinski, C., Hopkins, A., 2004. Navigating chemical space for biology and medicine. Nature 432, 855-861.

Melek, F.R., Miyase, T., Khalik, S.M.A., El-Gindi, M.R., 2003. Triterpenoid saponins from *Schefflera arboricola*. Phytochemistry 63, 401-407.

Miller, L.H., Ackerman, H.C., Su, X.-z., Wellems, T.E., 2013. Malaria biology and disease pathogenesis: insights for new treatments. Nat. Med. 19, 156-167.

Mokoka, T.A., Zimmermann, S., Julianti, T., Hata, Y., Moodley, N., Cal, M., Adams, M., Kaiser, M., Brun, R., Koorbanally, N., Hamburger, M., 2011. In vitro screening of traditional

South African malaria remedies against *Trypanosoma brucei rhodesiense*, *Trypanosoma cruzi*, *Leishmania donovani*, and *Plasmodium falciparum*. Planta Med. 77, 1663-1667.

Mokoka, T.X., Peter; Zimmermann, Stefanie; Hata, Yoshie; Adams, Michael; Kaiser, Marcel; Moodley, Nivan; Maharaj, Vinesh; Koorbanally, Neil A.; Hamburger, Matthias; Brun, Reto; Fouche, Gerda 2013. Antiprotozoal screening of 60 South African plants, and the identification of the antitrypanosomal eudesmanolides schkurin I and II. Planta Med 79, 1380.

Ng'ang'a, M.M., Chhabra, S., Langat-Thoruwa, C., Hussain, H., Krohn, K., 2008. Chemical constituents from the leaves of *Drypetes gerrardii*. Biochem. Syst. Ecol. 36, 320-322.

Ng'ang'a, M.M., Hussain, H., Chhabra, S., Langat-Thoruwa, C., Irungu, B.N., Al-Harrasi, A., Riaz, M., Krohn, K., 2012. Antiplasmodial activity of compounds from *Drypetes gerrardii*. Chem. Nat. Compd. 48, 339-340.

Ng'ang'a, M.M., Hussain, H., Chhabra, S., Langat-Thoruwa, C., Riaz, M., Krohn, K., 2011. Drypetdimer A: a new flavone dimer from *Drypetes gerrardii*. Nat. Prod. Commun. 6, 1115-1116.

Pajouhesh, H., Lenz, G.R., 2005. Medicinal chemical properties of successful central nervous system drugs. NeuroRx 2, 541-553.

Peters, W., 1987. Chemotherapy and Drug Resistance in Malaria. Academic Press, Inc., New York, pp. 145-273.

Renslo, A.R., 2013. Antimalarial Drug Discovery: From Quinine to the Dream of Eradication. Chem. Lett. 4, 1126-1128.

Renslo, A.R., McKerrow, J.H., 2006. Drug discovery and development for neglected parasitic diseases. Nat Chem Biol 2, 701-710.

Seephonkai, P., Pyne, S.G., Willis, A.C., Lie, W., 2013a. Bioactive compounds from the roots of *Strophioblachia fimbricalyx*. J. Nat. Prod. 76, 1358-1364.

Seephonkai, P., Pyne, S.G., Willis, A.C., Lie, W., 2013b. Fimbricalyx A, a novel phenanthrenone derivative having a rare 2H-benz[e]inden-2-one substructure. Tetrahedron Lett. 54, 2085-2088.

Seephonkai, P., Sangdee, A., Bunchalee, P., Pyne, S.G., 2009. Cytotoxic and Antiplasmodial Compounds from the Roots of *Strophioblachia fimbricalyx*. J. Nat. Prod. 72, 1892-1894.

Severi, J.A., Fertig, O., Plitzko, I., Vilegas, W., Hamburger, M., Potterat, O., 2010. Oleanane Saponins and Glycerogalactolipids from the Leaves of *Guapira graciliflora*. Helv. Chim. Acta 93, 1058-1066.

Stuart, K., Brun, R., Croft, S., Fairlamb, A., Gurtler, R.E., McKerrow, J., Reed, S., Tarleton, R., 2008. Kinetoplastids: related protozoan pathogens, different diseases. J. Clin. Invest. 118, 1301-1310.

Tang, G.-H., Zhang, Y., Yuan, C.-M., Li, Y., Gu, Y.-C., Di, Y.-T., Wang, Y.-H., Zuo, G.-Y., Li, S.-F., Li, S.-L., He, H.-P., Hao, X.-J., 2012. Trigohowilols A-G, degraded diterpenoids from the stems of *Trigonostemon howii*. J. Nat. Prod. 75, 1962-1966.

Uzair, B., Ahmed, N., Ahmad, V.U., Mohammad, F.V., Edwards, D.H., 2008. The isolation, purification and biological activity of a novel antibacterial compound produced by *Pseudomonas stutzeri*. FEMS Microbiol. Lett. 279, 243-250.

Vedani, A., Dobler, M., Smiesko, M., 2012. VirtualToxLab - a platform for estimating the toxic potential of drugs, chemicals and natural products. Toxicol Appl Pharmacol 261, 142-153.

WHO, 2010. Working to overcome the global impact of neglected tropical diseases: First WHO report on neglected tropical diseases. World Health Organization, Geneva. pp. 91-95.

WHO, 2013. World Malaria Report 2013. World Health Organization, Geneva. pp. v-xiv.

WHO, June 2013. Trypanosomiasis, Human African (sleeping sickness). Fact sheet N°259. World Health Organization, Geneva.

Zhu, Q., Tang, C.-P., Ke, C.-Q., Li, X.-Q., Liu, J., Gan, L.-S., Weiss, H.-C., Gesing, E.-R., Ye, Y., 2010. Constituents of *Trigonostemon chinensis*. J Nat Prod 73, 40-44.

Table 1. ^{1}H and ^{13}C NMR spectroscopic data of compounds **1** and **2** in $CDCl_3$

position	**1**		**2**[a]		
	δ_H (*J* in Hz)	δ_C[b]	δ_H (*J* in Hz)	δ_C[c]	HMBC (H → C)
1	-	48.1	-	48.0	
2	-	205.5	-	204.5	
3	6.29 (d, 10.1)	123.6	6.03 (d, 10.4 Hz)	124.0	C-1,C-4a,
4	8.20 (d, 10.1)	139.9	7.40 (d, 10.4 Hz)	138.8	C-2,C-4b,C-10a
5	7.53 (s)	104.2	6.93 (s)	103.0	C-6,C-7,C-4a,C-8a
6	-	154.7	-	154.6	
7	-	126.8	-	127.0	
8	7.59 (s)	130.2	7.77 (s)	131.3	C-6
9	7.75 (d, 8.5)	130.2	7.78 (d, 8.7 Hz)	130.0	C-4b,C-10a
10	7.39 (d, 8.5)	121.8	7.43 (d, 8.7 Hz)	123.0	C-1,C-4a,C-8a
4a	-	121.6	-	122.2	
4b	-	131.0	-	130.3	
8a	-	127.9	-	129.0	
10a	-	147.1	-	147.5	
1-Me x 2	1.51 (s)	28.0	1.43	27.8	C-1,C-2,C-10a
7-Me	2.42 (s)	16.4	2.76	17.2	C-6,C-7,C-8
1'			-	48.6	
2'			-	203.9	
3'			5.96 (d, 10.6 Hz)	123.0	C-1',C-4a'
4'			8.70 (d, 10.6 Hz)	141.8	C-2',C-4b',C-10a'
5'			-	134.2	
6'			-	147.7	
7'			-	127.6	
8'			7.66 (s)	128.0	C-6',C-9',C-4b'
9'			7.88 (d, 8.6 Hz)	131.0	C-4b',C-10a'
10'			7.49 (d, 8.6 Hz)	122.9	C-1,C4a',C-8a'
4a'			-	121.7	
4b'			-	123.5	
8a'			-	128.7	
10a'			-	149.2	
1'-Me x 2			1.45	27.8	C-1', C-2', C-10a'
7'-Me			2.51	16.5	C-6', C-7', C-8'

[a]The numbering does not follow the IUPAC nomenclature [b]125.77 MHz, [c]150.95 MHz

Table 2 *In vitro* antiprotozoal activities of **1** – **3** against *P. falciparum, T. b. rhodesiense*, *L. donovani*, and cytotoxic activity against L-6 cells

Compound	*P. falciparum*		*T. b. rhodesiense*		*L. donovani*		Cytotoxicity
	IC_{50} (µM)[a]	SI	IC_{50} (µM)[a]	SI	IC_{50} (µM)[a]	SI	IC_{50} (µM)[a]
1	0.96 ± 0.25	71.4	6.0 ± 2.7	11.5	14.0	4.9	68.4 ± 4.6
2	2.04 ± 0.15	31.4	-	-	-	-	64.0 ± 22.4
3	inactive[b]		18.0 ± 2.6	3.8	7.8	8.8	68.2 ± 3.9
Chloroquine[c]	0.004 ± 0.001	-	-	-	-	-	-
Melarsoprol[c]	-	-	0.003 ± 0.001	-	-	-	-
Miltefosine[c]	-	-	-	-	0.552 ± 0.051	-	-
Podophyllotoxin[c]	-	-	-	-	-	-	0.019 ± 0.006

[a] Values are expressed as mean ± standard error of the mean.

[b] No activity observed at the highest test concentration of 90 µg/ml, which corresponds to a molar test concentration of 115.7 µM.

[c] Reference drugs.

SI (Selectivity index): Quotient of IC_{50} for L-6 cells and IC_{50} against parasite.

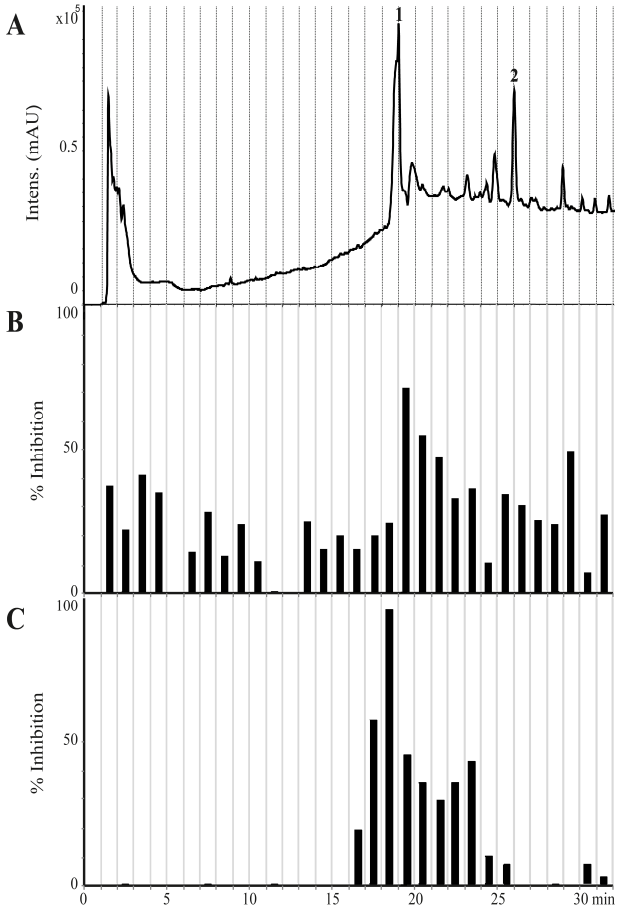

Fig. 1 HPLC-based activity profiling of the CH_2Cl_2/MeOH (1:1) stem extract of *D. gerrardii* for antiprotozoal activity. HPLC-UV chromatogram (210-700 nm) (**A**), and inhibition (in %) of *L. donovani* (**B**) and *P. falciparum* (**C**) by microfractions.

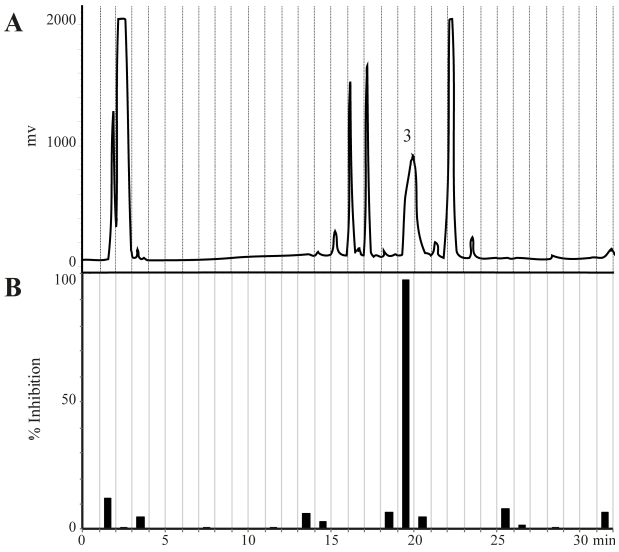

Fig. 2 HPLC-based activity profiling of the CH_2Cl_2/MeOH (1:1) leaf extract of *D. gerrardii* for antitrypanosomal activity. HPLC-ELSD chromatogram (A) and inhibition (in %) of *T. b. rhodesiense* (B) by microfractions.

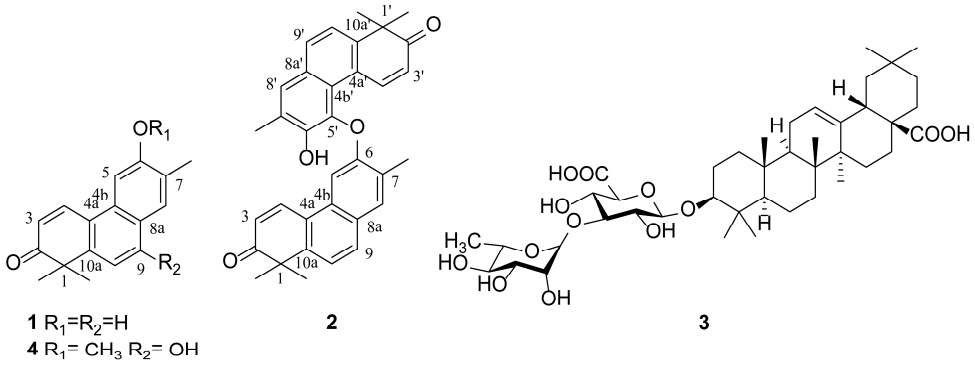

Fig. 3 Structures of compounds **1 - 4**.

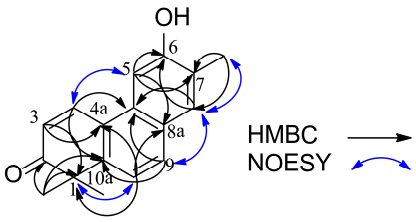

Fig. 4 Key HMBC and NOESY correlations of compound **1**.

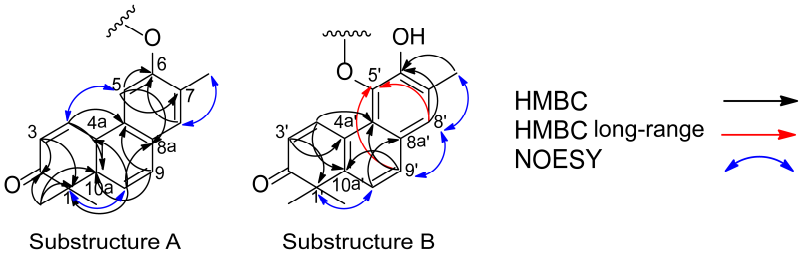

Fig. 5 Key HMBC and NOESY correlations for substructures **A** and **B** of compound **2**.

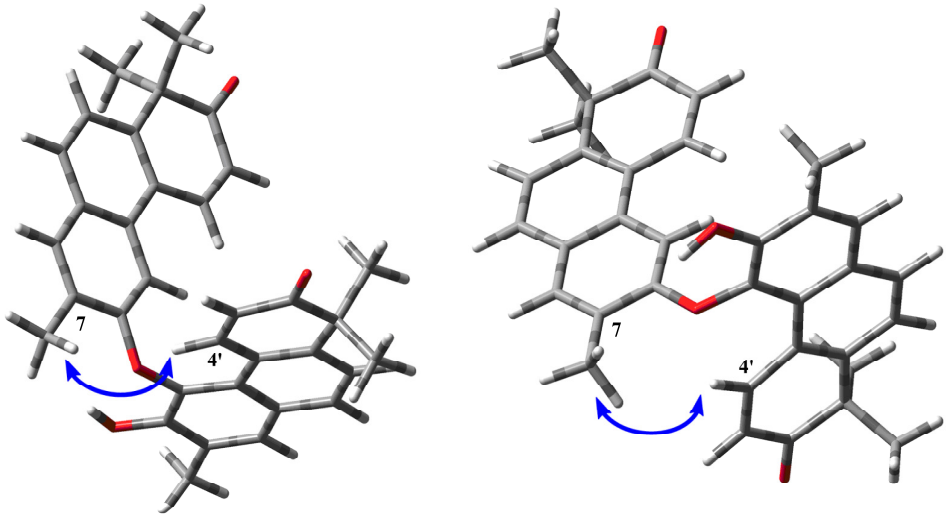

Fig. 6 DFT optimized conformers of compound **2**. Atoms CH_3-7 and H-4' showing a key NOESY correlation between the 2 substructures. Intramolecular distance between CH_3-7 and H-4' was 3.45 Å in both conformers.

Highlights

- HPLC-based activity profiling led us to identify the antiprotozoal compounds.
- A new phenanthrenone (**1**) with high antiplasmodial *in vitro* activity was discovered.
- A new heterodimer (**2**) with antiplasmodial *in vitro* activity was isolated.
- A saponin (**3**) was isolated and showed weak trypanocidal activity.

Appendix A

Supplementary data

Identification of two new phenathrenones and a saponin as antiprotozoal constituents of *Drypetes gerrardii*

Yoshie Hata[1,4*], Maria De Mieri[1*], Samad Nejad Ebrahimi[1,5], Tsholofelo Mokoka[3], Dashnie Naidoo[3], Gerda Fouche[3], Vinesh Maharaj[3], Marcel Kaiser[2], Reto Brun[2], Olivier Potterat[1], and Matthias Hamburger[1]

Affiliations

[1] Division of Pharmaceutical Biology, University of Basel, Klingelbergstrasse 50, 4056 Basel, Switzerland

[2] Swiss Tropical and Public Health Institute, and University of Basel, Basel, Switzerland

[3] Biosciences, Council for Scientific and Industrial Research (CSIR), Pretoria, South Africa

[4] Department of Pharmacy, Faculty of Sciences, National University of Colombia, Bogota D.C., Colombia

[5] Department of Phytochemistry, Medicinal Plant and Drugs Research Institute, Shahid Beheshti University, G. C., Tehran, Iran

Correspondence:

Prof. Matthias Hamburger, Division of Pharmaceutical Biology, University of Basel, Klingelbergstrasse 50, CH-4056 Basel, Switzerland.

e-mail: matthias.hamburger@unibas.ch, Phone: +41 61 267 14 25 Fax: +41 61 267 14 74

*These two authors contributed equally to this work.

Assays for *in vitro* Antiprotozoal Activity

Antiplasmodial activity was determined by a modification of the ^{3}[H]-hypoxanthine incorporation assay [1] with the *P. falciparum* NF54 strain, growth according to the method described by Trager and Jensen [2]. Chloroquine (purity >95%, Sigma-Aldrich) was used as positive control.

Briefly, a suspension of infected red blood cells (final parasitemia 0.3% and hematocrit 1.25%) in RPMI 1640 medium supplemented with 2 µM $_L$-glutamine, 5.95 g/l Hepes, 2 g/l $NaHCO_3$, and 5% of Albumax II was exposed to serial drug dilutions covering a range from 10 µg/mL to 0.156 µg/ml in 96-well microtiter plates. After 48 h of incubation (4% CO_2, 3% O_2, and 93% N_2 at 37°C), 50 µl of ^{3}[H]-hypoxanthine (0.25 µM) were added to each well (Costar). The plates were incubated for further 24 h before being harvested by using a Betaplate cell harvester (Wallac) onto glass-fiber filters and then washed with distilled water. The dried filters were inserted into plastic foils with 10 ml scintillation fluid. The radioactivity was counted with a Betaplate liquid scintillation counter (Wallac) as counts per minute per well at each drug concentration and compared to the untreated controls. Counts were expressed as percentages of the control and presented as sigmoidal inhibition curves. IC_{50} values were calculated by linear interpolation.

Antitrypanosomal activity against *T. brucei rhodesiense* STIB 900 was determined according to [3]. Melarsoprol (Arsorbal, purity >95%, Sanofi-Aventis) was used as positive control. Minimum essential medium (MEM) with Earle's salts supplemented with 2-mercaptoethanol, as described by Baltz *et al*. [4], 1 mM sodium pyruvate, 0.5 mM hypoxanthine, and 15% heat-inactivated horse serum was added (50 µl) to each well of a 96-well microtiter plate (Costar) except of the negative control. Serial drugs dilutions were prepared covering range from 90 to 0.123 µg/ml followed by the parasite suspension of 2000 *T. brucei rhodesiense* STIB 900 bloodstream forms/well. After 70 hours of incubation (humidified 5% CO_2 atmosphere at 37°C), 10 µl resazurin solution (12.5 mg resazurin (Sigma-Aldrich) dissolved in 100 ml of distilled water) were added and incubation was continued for further 2 to 6 h. The plate was read with a Spectramax Gemini XS microplate fluorescence reader (Molecular Devices) with an excitation wavelength of 536 nm and an emission wavelength of 588 nm. Fluorescence development was expressed as percentage of the control and the IC_{50} values were determined from the sigmoid curves using Softmax Pro Software (Molecular Devices).

Leishmanicidal activity was determined with *L. donovani* (axenic amastigotes) MHOM-ET/67/L82 strain according to [5], with some modifications. Fifty microlitres of SM medium at pH 5.4 supplemented with 10% heat-inactivated FBS was added to each well of 96-well microtiter plate (Costar). Serial drug dilutions were prepared covering a range from 90 to 0.123 µg/ml. Then, 10^5 axenically growth *L. donovani* amastigotes in 50 µl medium, were added to each well and the plate was incubated for 72 h (humidified 5% CO_2 atmosphere at 37°C). Ten microlitres resazurin solution (12.5 mg resazurin (Sigma-Aldrich) dissolved in 100 ml of distilled water) were added to each well and incubated for further 2 to 4 h. The plate was read with a Spectramax Gemini XS microplate fluorescence reader (Molecular Devices) with an excitation wavelength of 536 nm and an emission wavelength of 588 nm. Fluorescence development was expressed as percentage of the control and the IC_{50} values were determined from the sigmoid curves using Softmax Pro Software (Molecular Devices). Miltefosine (purity >95%, VWR) was used as positive control.

In vitro Cytotoxicity Assay

The cytotoxicity assay was performed using a protocol based on the Alamar Blue assay [6], whereby rat skeletal myoblast cells (L-6 cells) were seeded in 96-well microtiter plates using MEM supplemented with 10% heat inactivated FBS (4000 cells/well). Serial threefold drug dilutions ranging from 90 to 0.123 mg/ml were prepared. After 72 h, 10 µl resazurin solution was added (12.5 mg resazurin (Sigma-Aldrich) dissolved in 100 ml of distilled water) and the plates were incubated for further 2 to 4 h. A Spectramax Gemini XS micro plate fluorescence reader (Molecular Devices) was used to measure the plates at an excitation wavelength of 536 nm and an emission wavelength of 588 nm. Fluorescence development was expressed as percentage of the control and the IC_{50} values were determined from the sigmoid curves using Softmax Pro Software (Molecular Devices). Podophyllotoxin (purity >95%, Sigma-Aldrich) was used as a reference drug.

Assays for *in vivo* Antimalarial Activity

In vivo antimalarial activity was assessed basically as previously described [7]. Groups of three female NMRI mice (20–22 g) were intravenously infected with 2 $x10^7$ with GFP-transfected *P. berghei* strain ANKA [8] parasitized erythrocytes on day 0. Compounds were dissolved in 100% DMSO, diluted 10-fold in distilled water and administered intraperitoneally in a volume of 10 ml/kg (dose of 50 mg/Kg) on four consecutive days (4, 24,

48 and 72 h post infection). Parasitemia was determined on day 4 post infection (24 h after last treatment) by FACS analysis. Activity was calculated as the difference between the mean per cent parasitemia for the control (n=5 mice) and treated groups expressed as a per cent relative to the control group. The survival time in days was also recorded up to 30 days after infection. A compound was considered curative if the animal survived to day 30 after infection with no detectable parasites. Mice were euthanized by carbon dioxide inhalation.

Protocol for Acid Hydrolysis of Compound 3

Compound **3** (2.0 mg) was dissolved in 4 ml of a mixture 1:1 of dioxane/TFA 2N and heated at 105°C for 2 h. The solvent was evaporated and the remaining solution was extracted three times with 1 ml of $CHCl_3$. TLC analysis of the organic phase revealed decomposition of the aglycone. The aqueous phase was dried and the residue re-dissolved in anhydrous pyridine. The sugars were derivatized with L-cysteine methyl ester hydrochloride (200 µl, 60°C, 1 h) and subsequently silylated with hexamethyldisilzane and chlorotrimethylsilane (Fluka) in pyridine (2:1:10, 300 µl; 60°C, 30 min). GC analysis on a capillary DB-225MS column (30 m x 0,25 mm i.d., 0,25 m; Agilent; column temp. 150°C for 2 min, then 5°C/min. to 210°C, then 10°C/min to 240°C).

Table 1S. ^{1}H and ^{13}C NMR spectroscopic data for compound **1** (DMSO-d_6, 500 MHz)

position	**1**	
	δ_H (J in Hz)	**δ_C[a]**
1	-	47.2
2	-	203.1
3	6.25 (d, 10.2)	122.8
4	8.27 (d, 10.2)	139.2
5	7.62 (s)	103.1
6	-	156.1
7	-	126.9
8	7.64 (s)	129.0
9	7.80 (d, 8.6)	129.4
10	7.45 (d, 8.6)	120.6
4a	-	120.3
4b	-	130.3
8a	-	126.4
10a	-	145.9
1-Me x 2	1.41 (s)	27.0
7-Me	2.31 (s)	15.9

[a] ^{13}C NMR signals reported here were obtained indirectly from HSQC and HMBC spectra

Table 2S. ^{1}H and ^{13}C NMR data (pyridine-d_5, 500 MHz for ^{1}H, 125 MHz for ^{13}C) for compound **3**.

Position	δ_H (J in Hz)	δ_C
Triterpene moiety		
1	1.38[a] 0.84[a]	38.8
2	2.16(m)[a] 1.77 (m)[a]	26.8
3	3.27 (m)	89.4
4	-	39.7
5	0.77 [a]	55.9
6	1.30[a] 1.50(m)[a]	18.7
7	1.20 (m)[a] 1.46[a]	33.5
8	n.d.	40.0
9	1.64 (dd, 8.9, 8.7)	48.2
10	-	37.2
11	1.87 (m)[a] 2.13	24.0
12	5.44 (br m)	122.8
13	-	145.1
14	-	42.4
15	1.18 (m)[a] 2.13[a]	28.6
16	1.93 (m)[a] 1.93 (m)[a]	23.9
17	-	46.9
18	3.27 (m)	42.2
19	1.27 (m)[a] 1.80[a]	46.7
20	-	31.2
21	1.20 (m)[a] 1.44[a]	34.5
22	1.78 (m) 2.00 (dt, 13.7, 4.0)	33.4
23	1.23 (s)	28.4
24	0.93 (s)	17.2
25	0.80 (s)	15.7
26	0.95 (s)	17.6
27	1.31 (s)	26.5
28	-	180.4
29	0.96 (s)	33.5
30	1.00 (s)	24.0

position	δ_H (*J* in Hz)	δ_C
3-O-Sugar Glc A		
1	4.81 (d, 6.5)	107.2
2	3.98 (dd, 7.6, 7.4)	76.0
3	4.34 (m) [a]	82.0
4	4.34 (m) [a]	72.0
5	4.45 (m) [a]	77.9
6	-	n.d.
Rham		
1	6.19 (br s)	103.1
2	4.67 (br s)	72.7
3	4.50 (dd, 9.0, 3.0)	72.9
4	4.23 (dd, 9.5, 9.4)	74.3
5	4.95 (m)	70.0
6	1.64 (d, 5.9)	18.9

[a]Overlapping signals. n.d. not detected.

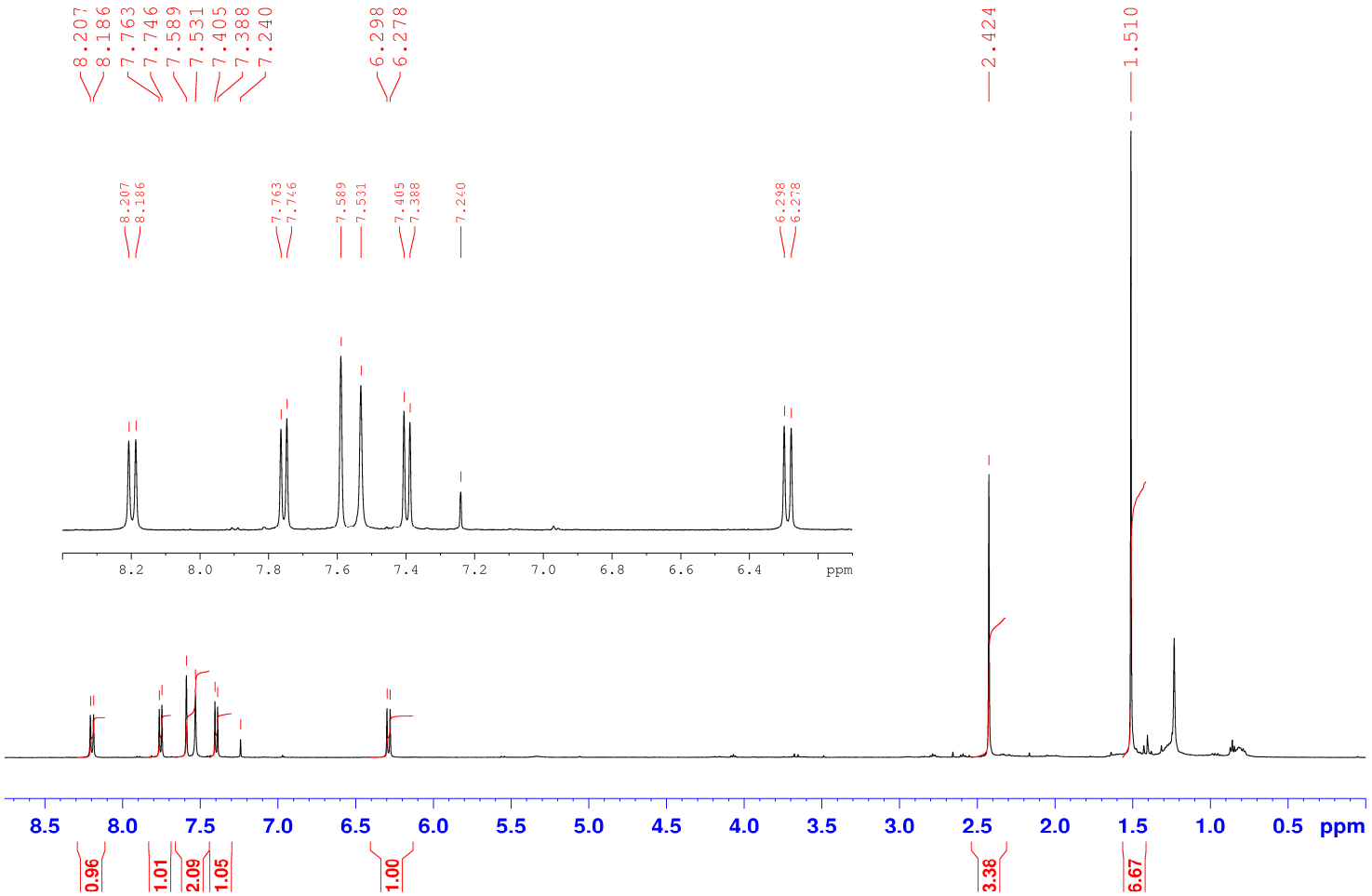

Fig. 1S. ^{1}H NMR spectrum of **1** in $CDCl_3$.

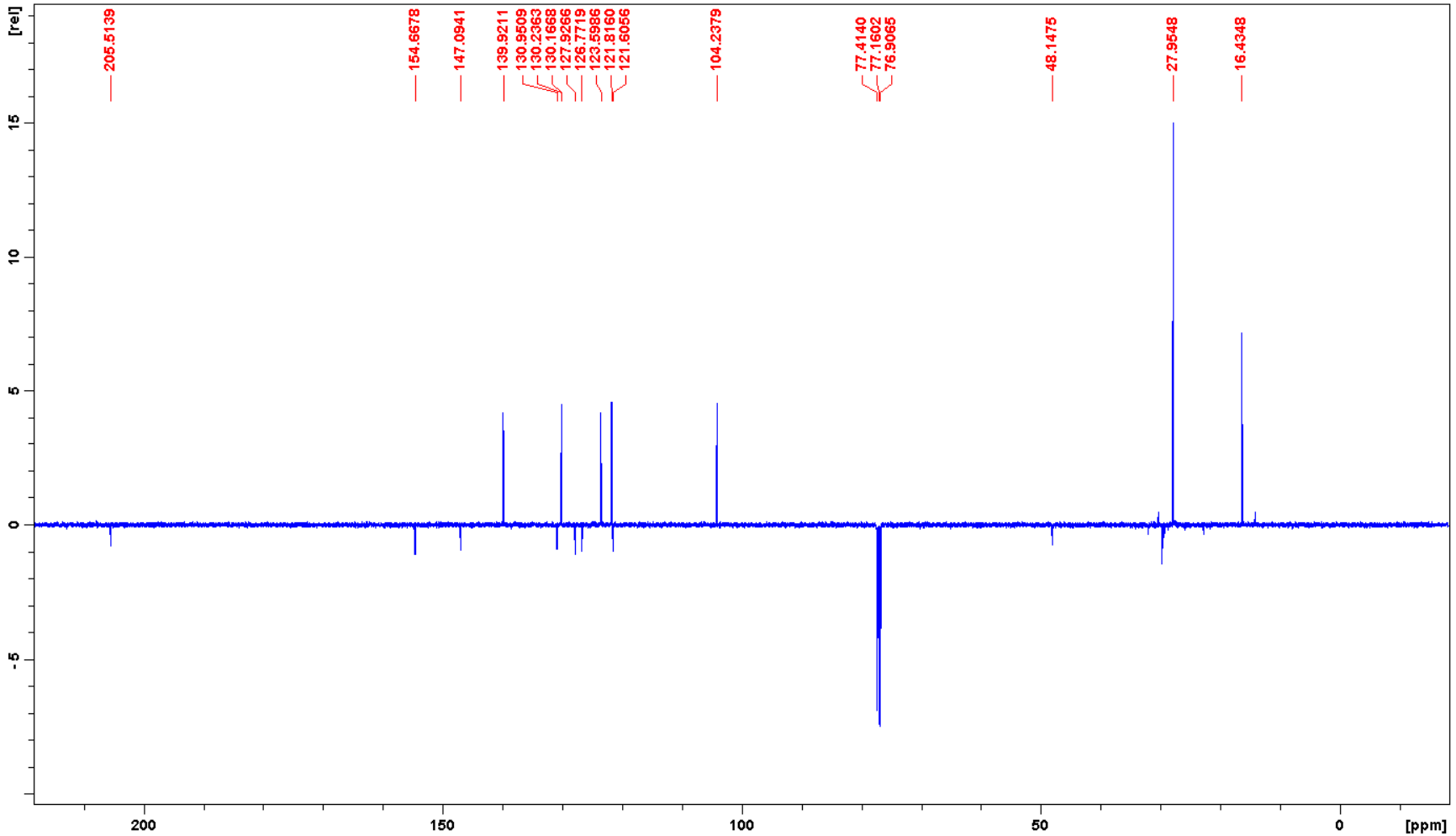

Fig. 2S. DEPTQ spectrum of **1** in $CDCl_3$.

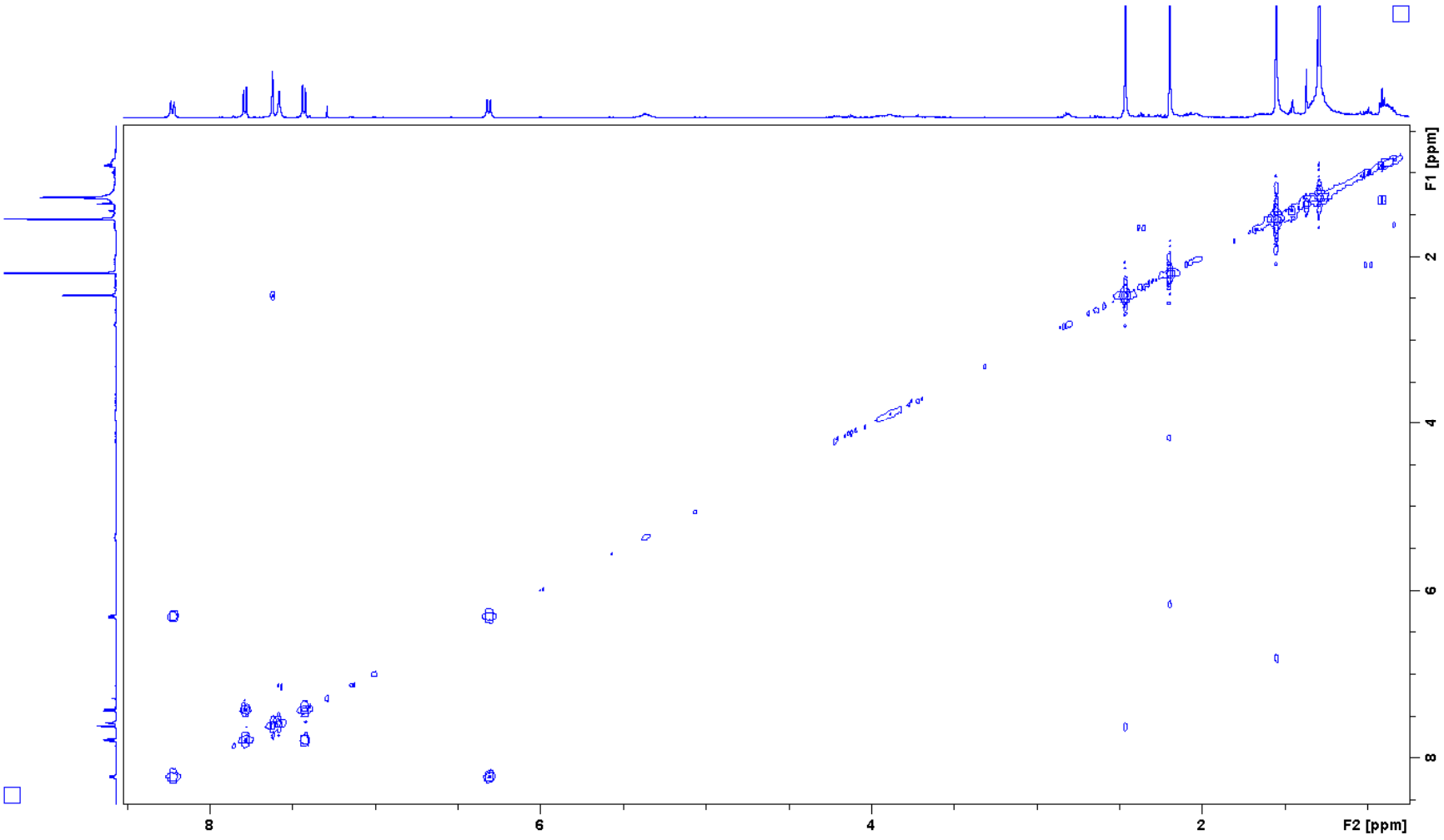

Fig. 3S. ^{1}H ^{1}H COSY spectrum of **1** in $CDCl_3$

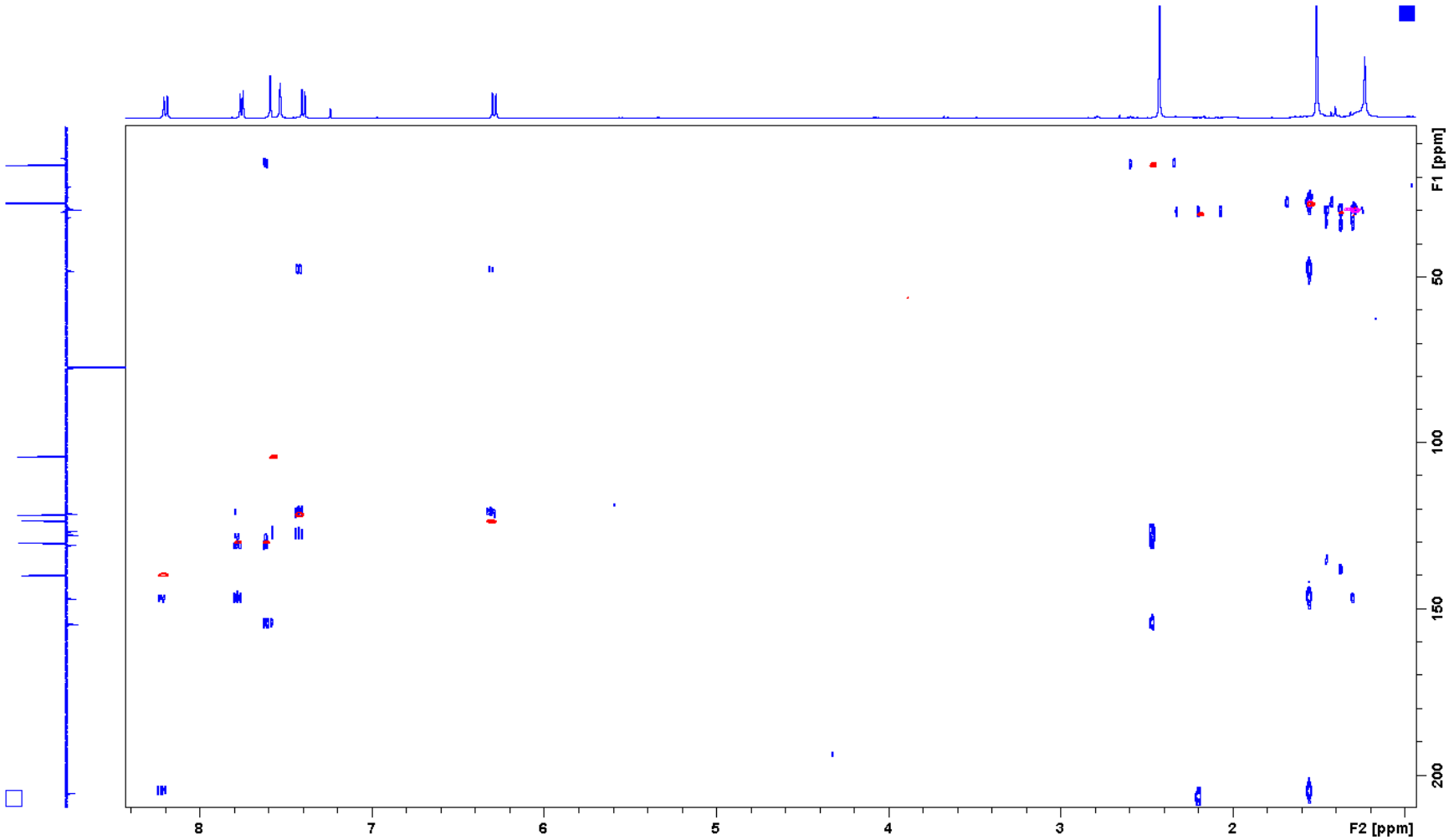

Fig. 4S. HSQC and HMBC overlaid spectra of **1** in $CDCl_3$.

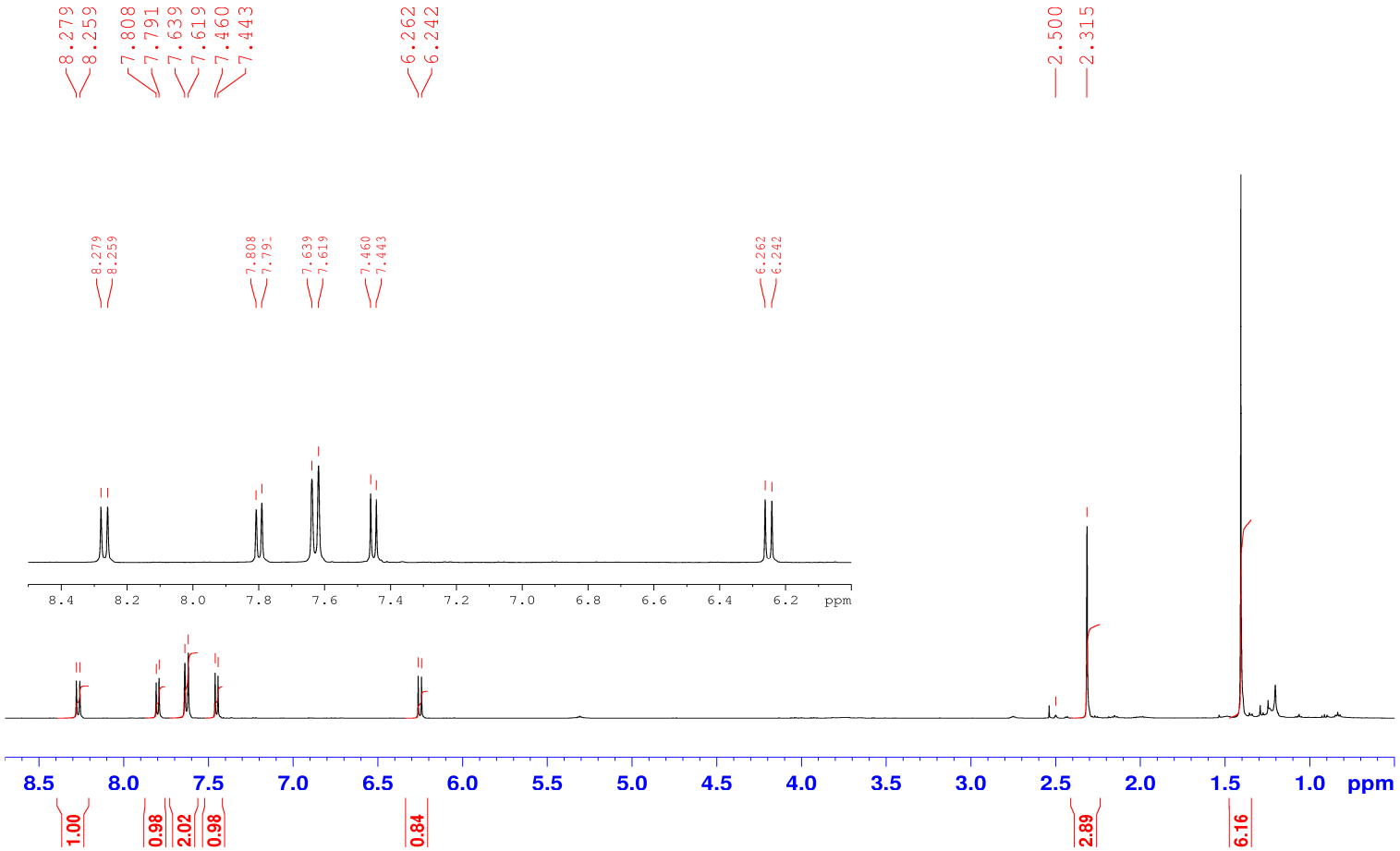

Fig. 5S. ^{1}H NMR spectrum of **1** in DMSO-d_6.

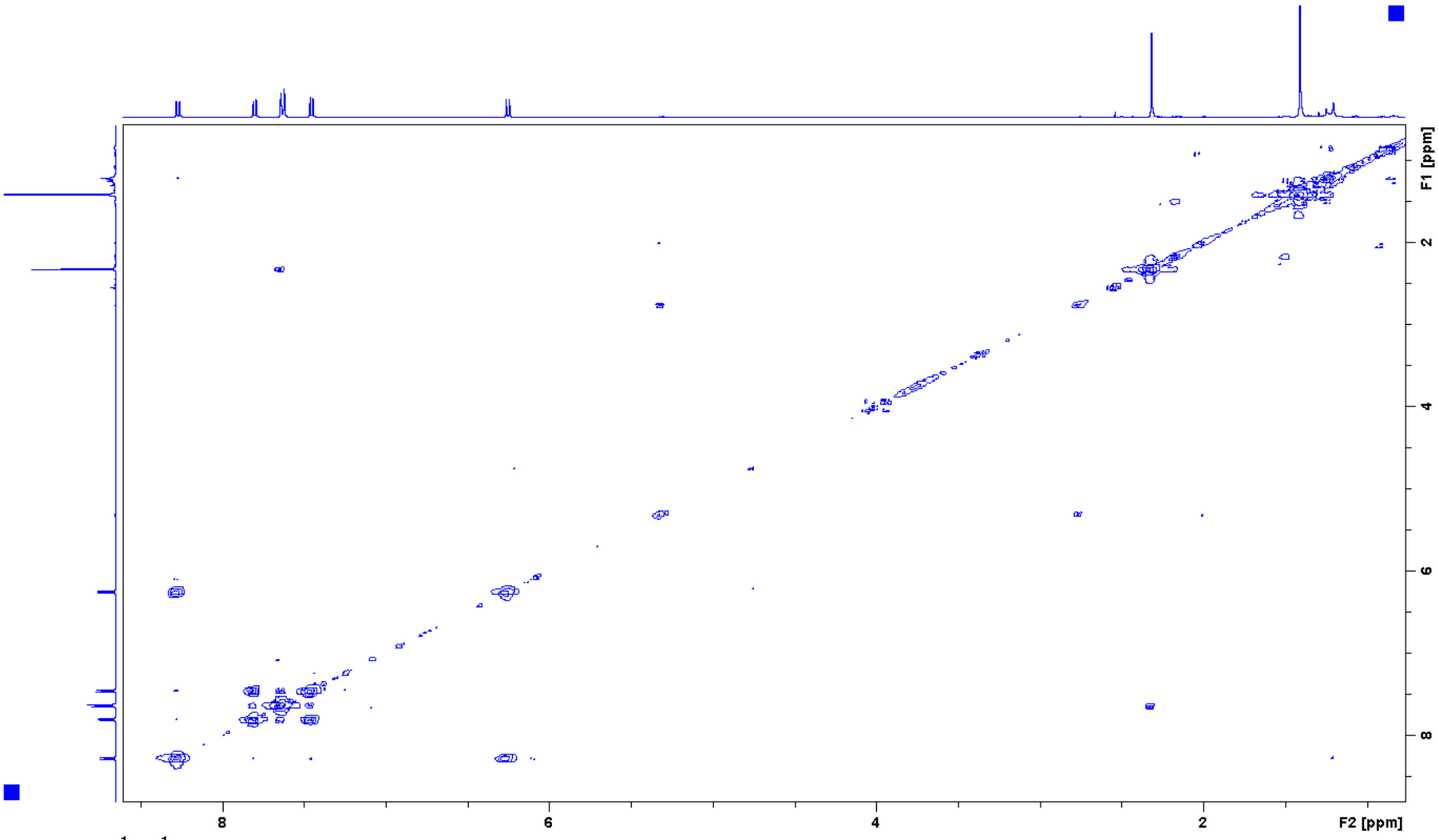

Fig. 6S. ^{1}H ^{1}H COSY spectrum of **1** in DMSO-d_6

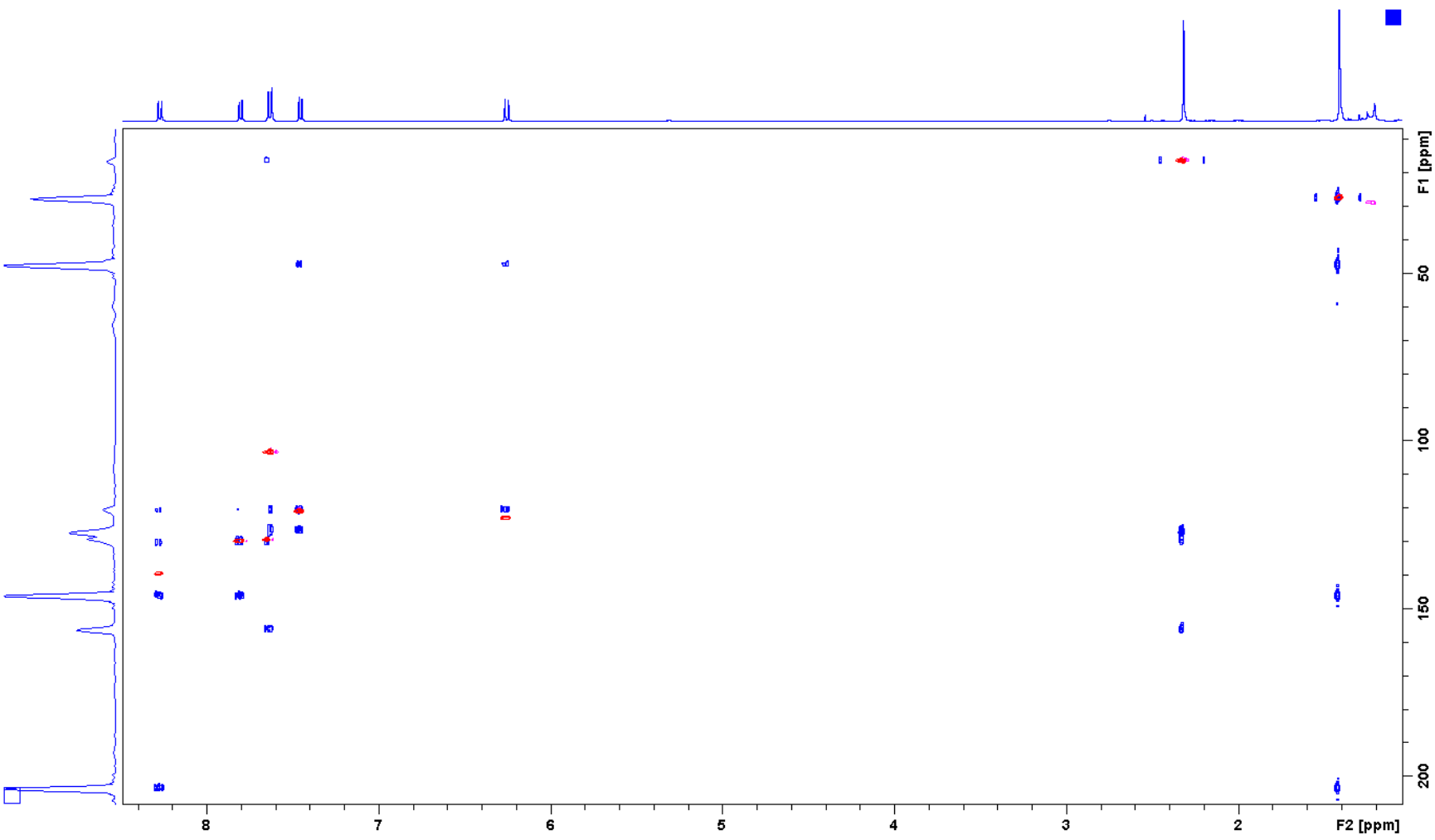

Fig. 7S. HSQC and HMBC overlaid spectra of **1** in DMSO-d_6.

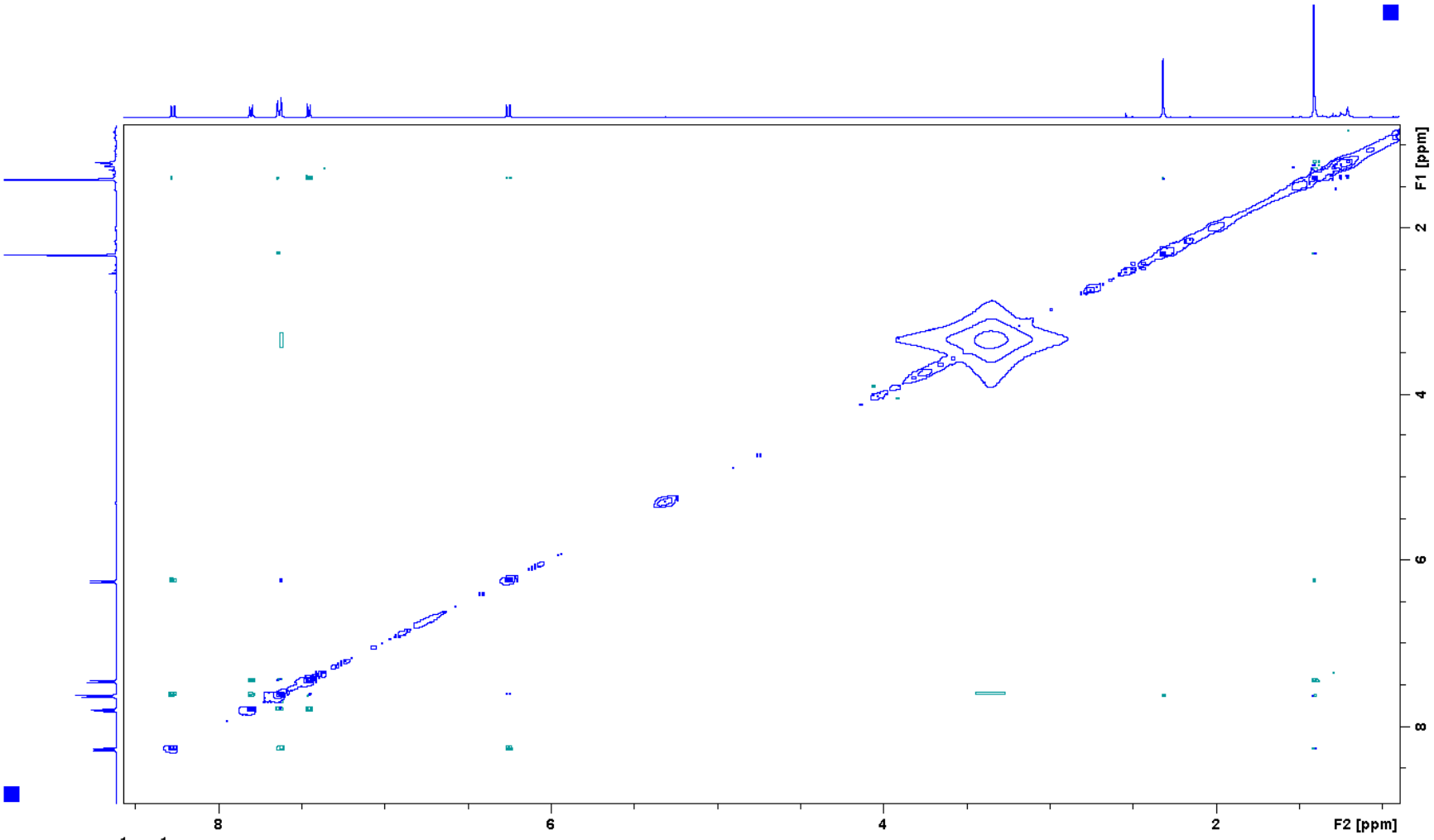

Fig. 8S. ^{1}H ^{1}H NOESY spectrum of **1** in DMSO-*d6*.

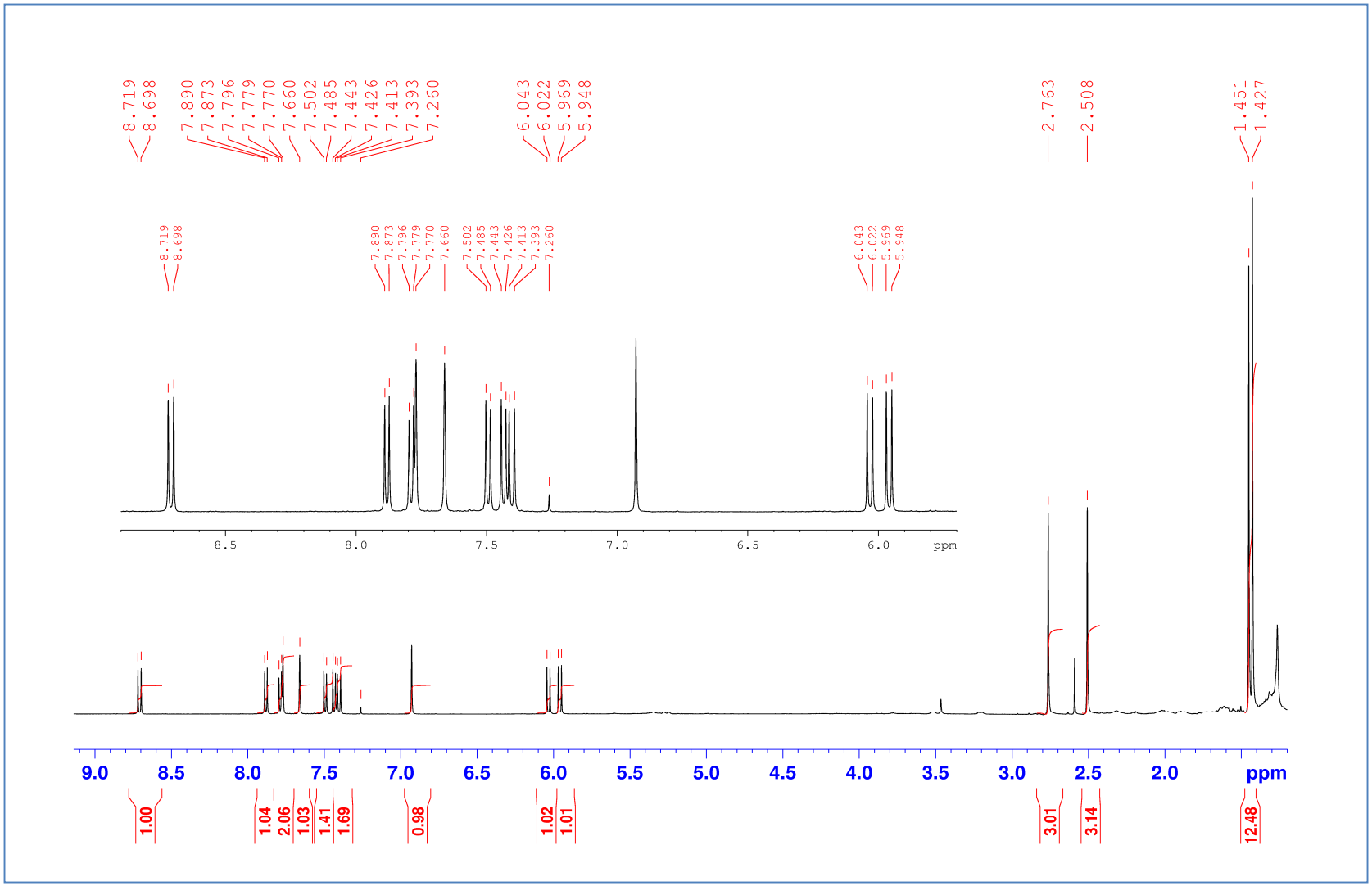

Fig. 9S. ^{1}H NMR spectrum of **2** in $CDCl_3$.

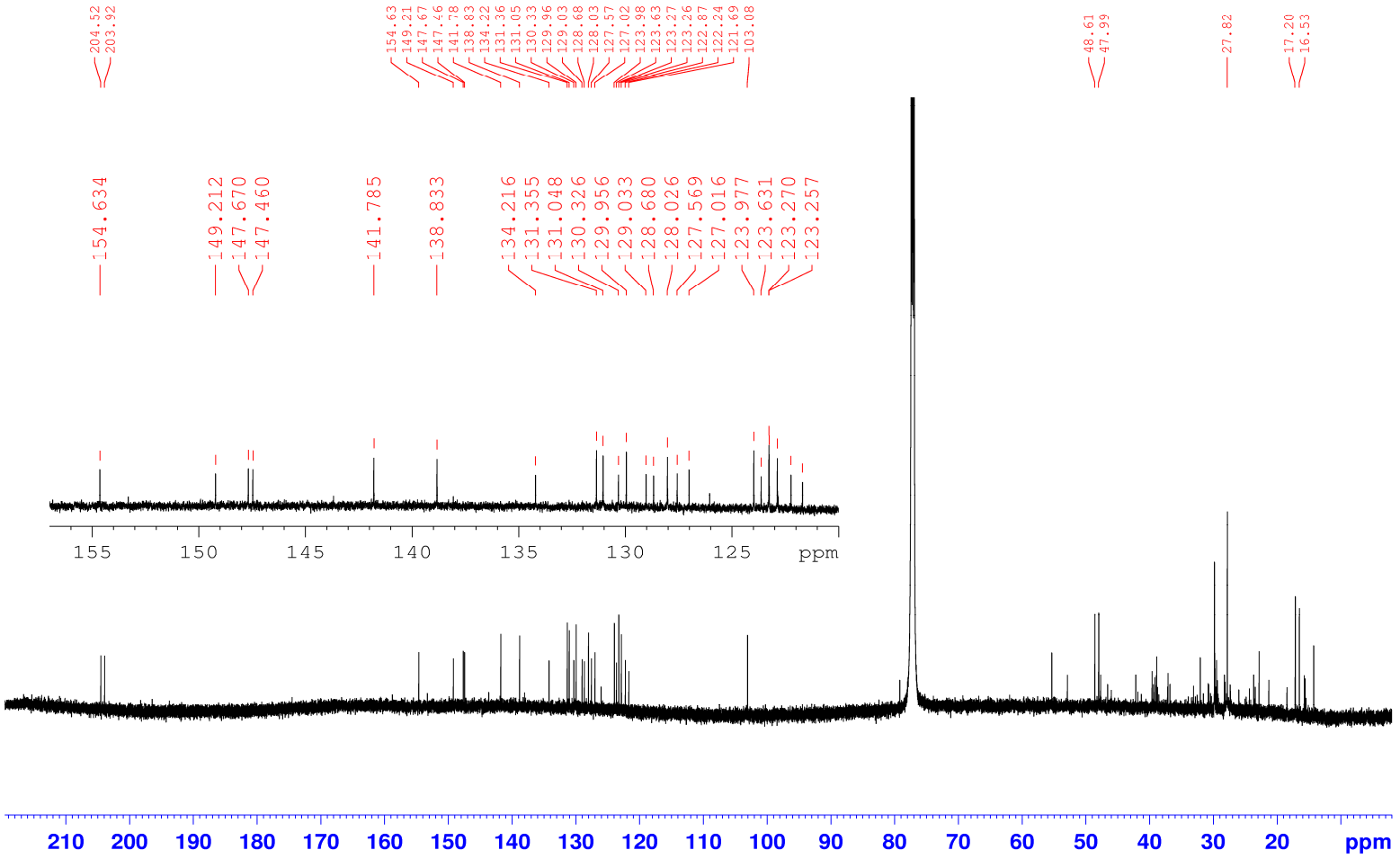

Fig. 10S. ^{13}C spectrum of **2** in $CDCl_3$.

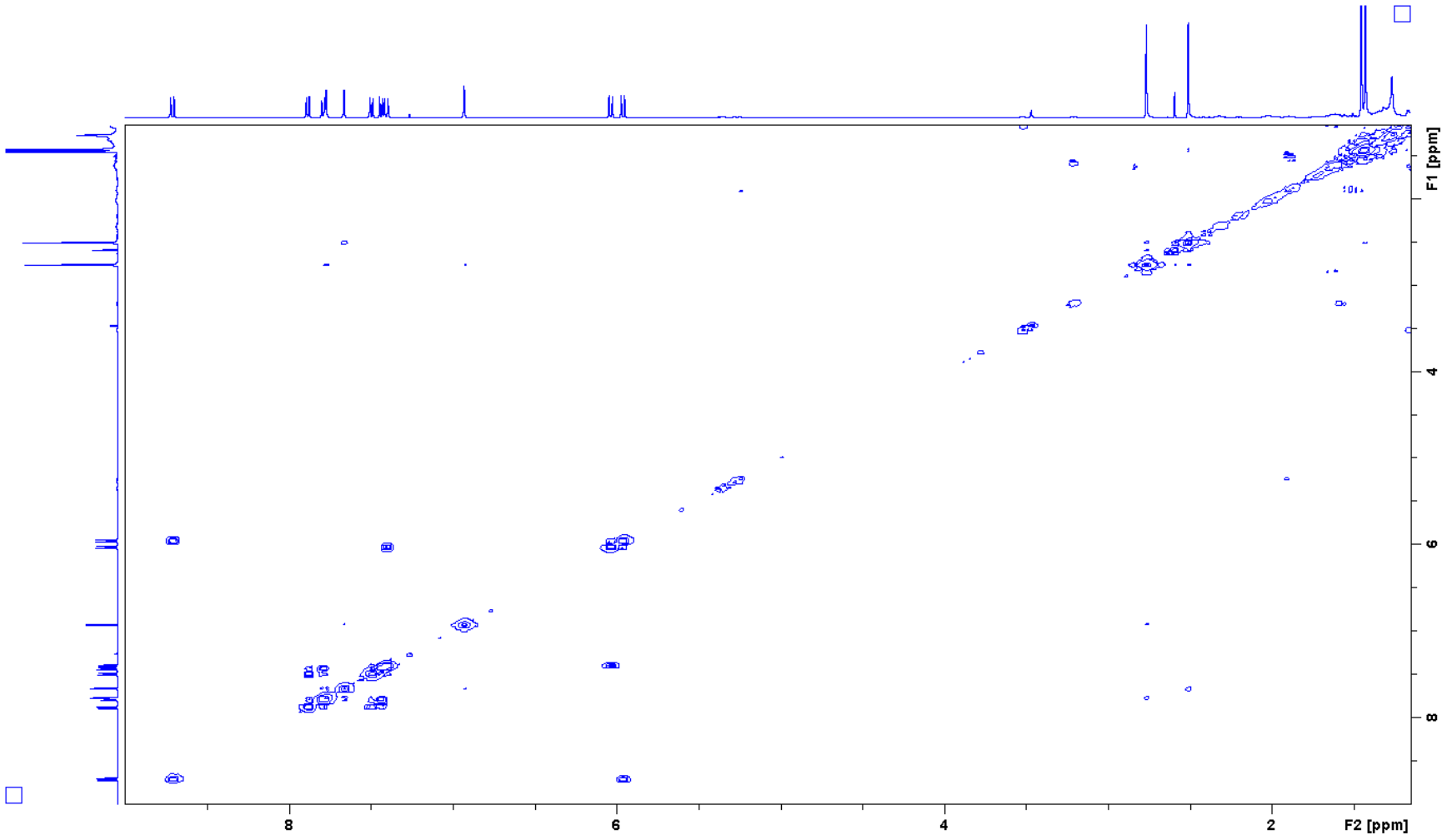

Fig. 11S. ^{1}H ^{1}H COSY spectrum of **2** in $CDCl_3$

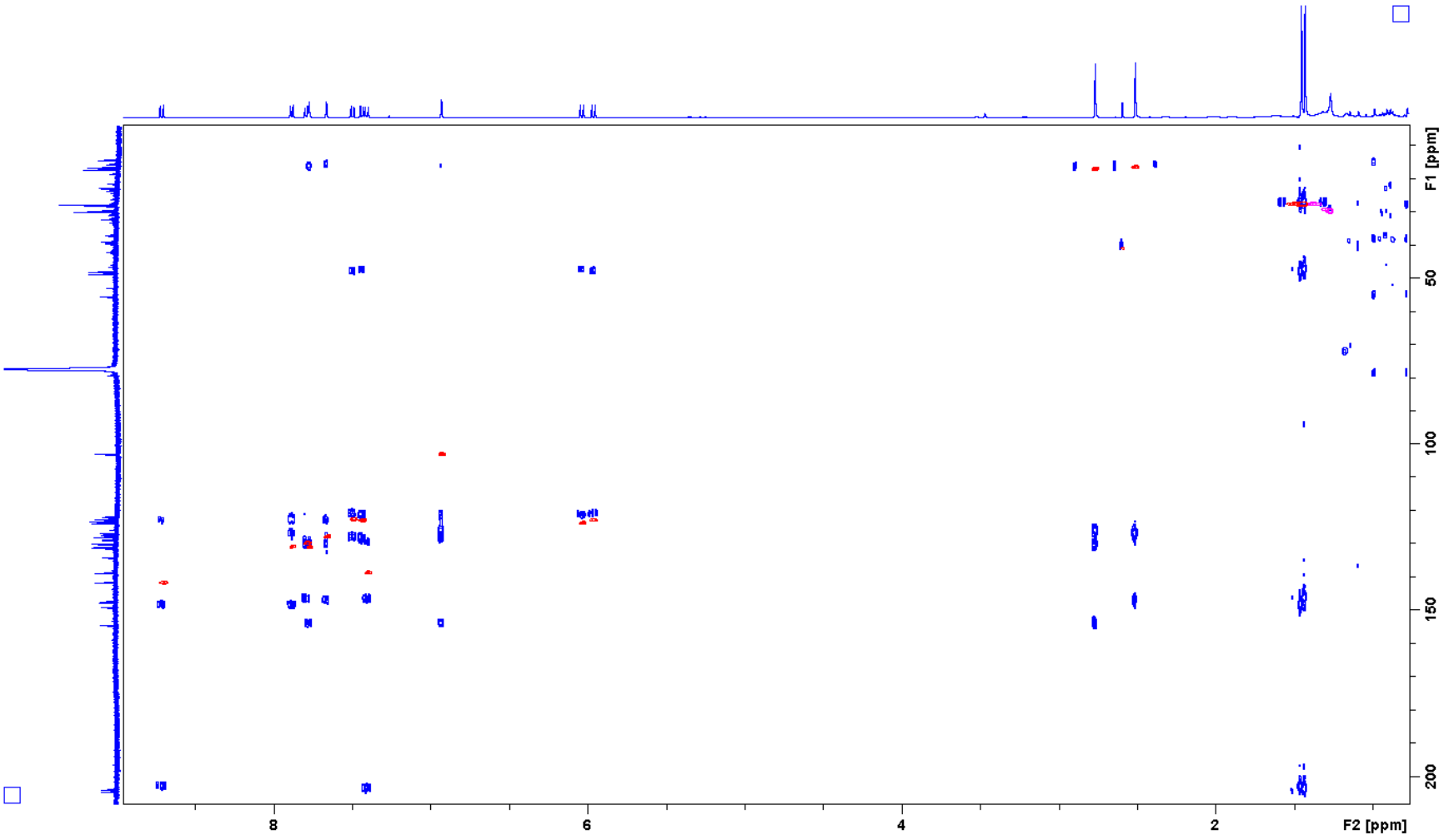

Fig. 12S. HSQC and HMBC overlaid spectra of **2** in $CDCl_3$.

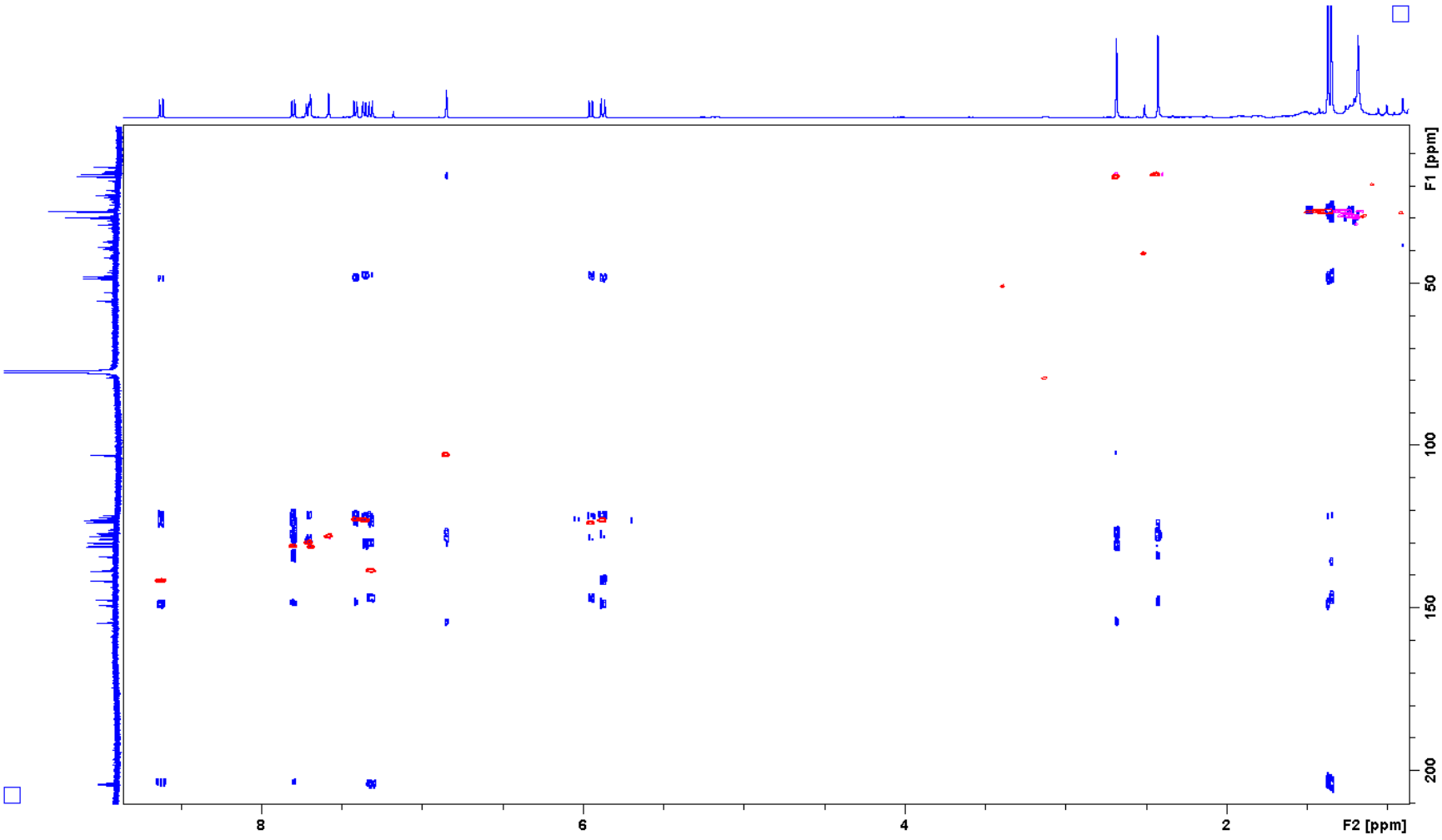

Fig. 13S. HSQC and long range HMBC overlaid spectra of **2** in $CDCl_3$.

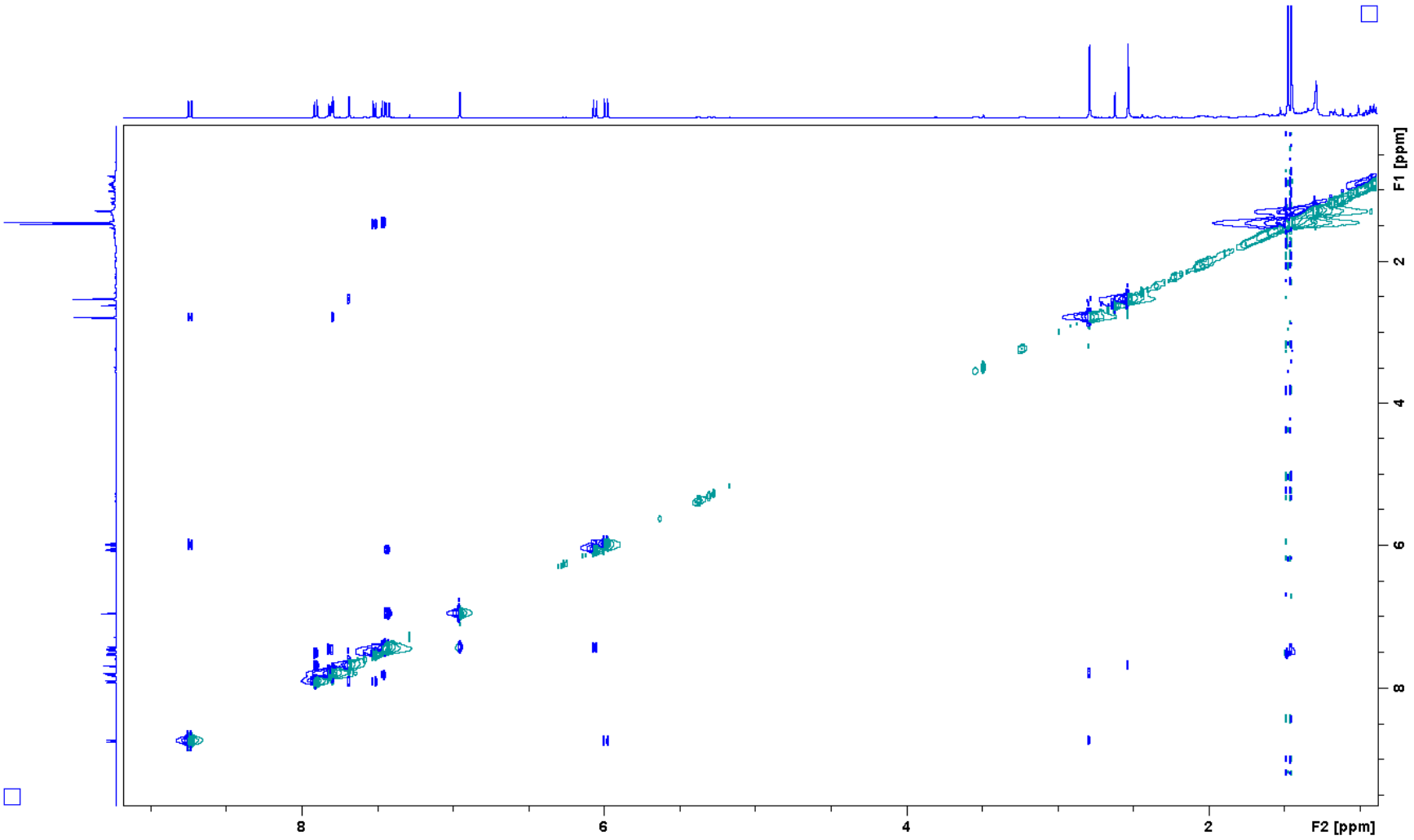

Fig. 14S. ^{1}H ^{1}H NOESY spectrum of **2** in $CDCl_3$.

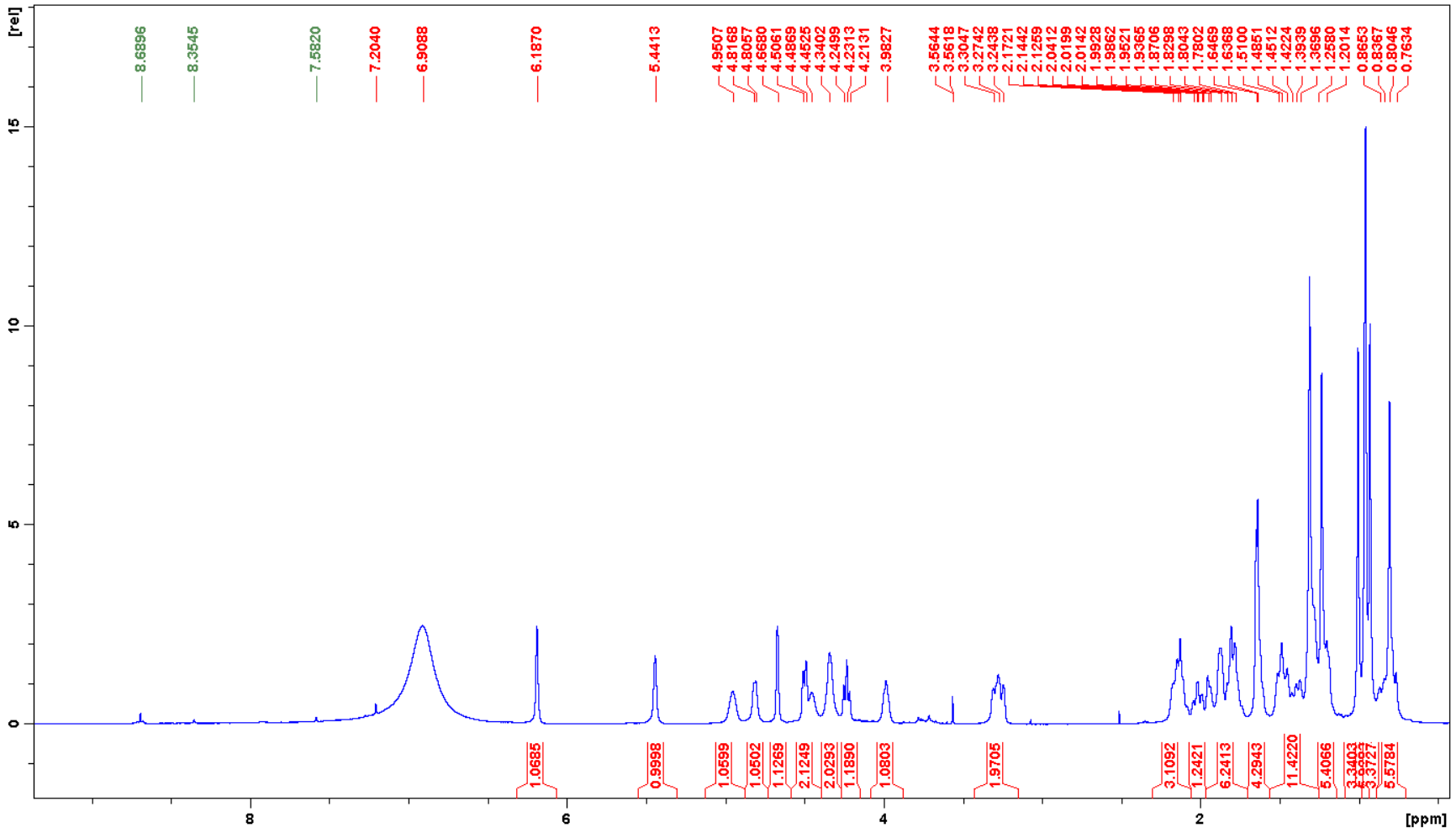

Fig. 15S. ^{1}H NMR spectrum of **3** in pyridine-d_5.

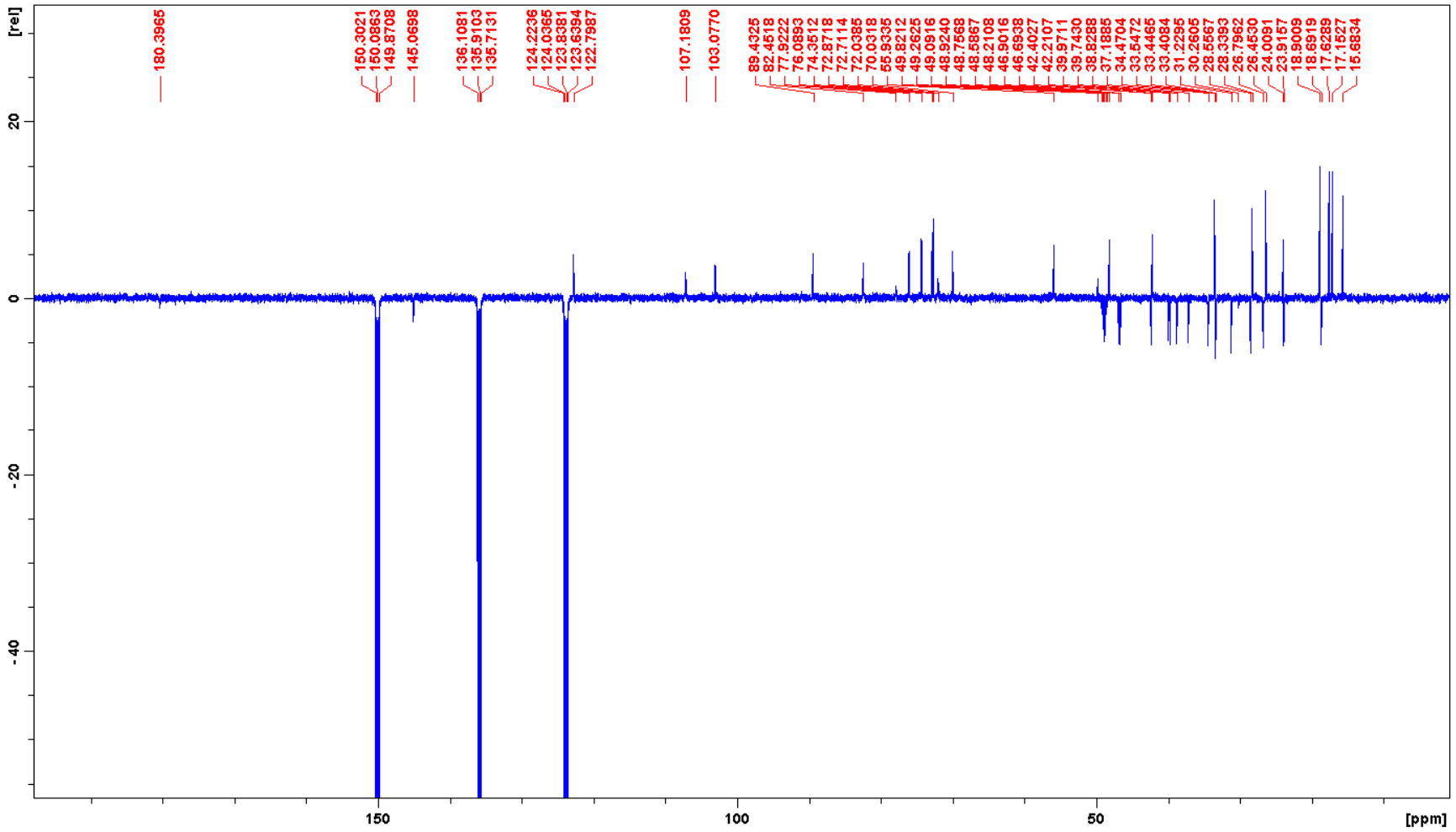

Fig. 16S. DEPTQ spectrum of **3** in pyridine-d_5.

References

1. *Desjardins RE, Canfield CJ, Haynes D, Chulay JD*. Quantitative assessment of antimalarial activity *in vitro* by a semiautomated microdilution technique. Antimicrob Agents Chemother 1979; 16: 710-718
2. *Trager W, Jensen JB*. Human Malaria Parasites in Continuous Culture. Science 1979; 109: 673-675
3. *Räz B, Iten M, Grether-Bühler Y, Kaminsky R, Brun R*. The Alamar Blue assay to determine drug sensitivity of African trypanosomes (*T. b. rhodesiense* and *T. b. gambiense*) *in vitro*. Acta Trop 1997; 68: 139–147
4. *Baltz T, Baltz D, Giroud C, Crockett J.* Cultivation in a semidefined medium of animal infective forms of *Trypanosoma brucei, T. equiperdum, T. evansi, T. rhodesiense, T. gambiense*. EMBO J 1985; 4: 1273-1277
5. *Cunningham I.* New culture medium for maintenance of tstse tissues and growth of trypanosomatids. J Protozool 1977; 24: 325-329
6. *Page B, Page M, Noël C.* A new fluorometric assay for cytotoxicity measurements *in vitro*. Int J Oncol1993; 9: 473-476
7. *Peters W*. Chemotherapy and Drug Resistance in Malaria. New York: Academic Press; 1987: 145-273
8. *Franke-Fayard B, Trueman H, Ramesar J, Mendoza J, van der Keur M, van der Linden R., Sinden RE, Waters AP, Janse CJ*. A *Plasmodium berghei* reference line that constitutively expresses GFP at a high level throughout the complete life cycle. Mol Biochem Parasitol 2004; 137: 23-33

3.6 Antiplasmodial and Antitrypanosomal Activity of Pyrethrins and Pyrethroids

Yoshie Hata, Stefanie Zimmermann, Melanie Quitschau, Marcel Kaiser, Matthias Hamburger, and Michael Adams

J. Agric. Food Chem., 2011, 59: 9172–9176. **DOI:** 10.1021/jf201776z

Five pyrethrins were isolated from *Chrysantemum cinerariifolium*. Their antiprotozoal activity was evaluated against *Plasmodium falciparum* and *Trypanosoma brucei rhodesiense* and compared with synthetic pyrethroids. Pyrethrin II and Jasmolin II inhibited *P. falciparum.* Natural pyrethrins were more active than pyrethroids.

My contributions to this work were: (1) extraction of plant material; (2) isolation of pyrethrins; (3) recording and interpretation of analytical data for structure elucidation (HPLC-PDA-ESI-MS and 1D and 2D NMR), data analysis; (4) writing of the manuscript draft, preparation of figure, table, and supporting information.

In vitro antiplasmodial and cytotoxicity tests were performed by Stefanie Zimmermann in the Swiss TPH. Melanie Quitschau supervised structure elucidation.

Yoshie Hata-Uribe

JOURNAL OF AGRICULTURAL AND FOOD CHEMISTRY

ARTICLE

pubs.acs.org/JAFC

Antiplasmodial and Antitrypanosomal Activity of Pyrethrins and Pyrethroids

Yoshie Hata,[†,‡] Stefanie Zimmermann,[†,§] Melanie Quitschau,[†] Marcel Kaiser,[§,∥] Matthias Hamburger,[†] and Michael Adams*[,†]

[†]Department of Pharmaceutical Sciences, University of Basel, Klingelbergstrasse 50, 4056 Basel, Switzerland

[‡]Departamento de Farmacia, Universidad Nacional de Colombia, Carrera 30 45-03, Bogotá, Colombia

[§]Swiss Tropical and Public Health Institute, Socinstrasse 57, CH-4002 Basel, Switzerland

[∥]University of Basel, 4056 Basel, Switzerland

Supporting Information

ABSTRACT: In a screen of 1800 plant and fungal extracts for antiplasmodial, antitrypanosomal, and leishmanicidal activity, the *n*-hexane extract of *Chrysanthemum cinerariifolium* (Trevir.) Vis. flowers showed strong activity against *Plasmodium falciparum*. We isolated the five pyrethrins [i.e., pyrethrin II (**1**), jasmolin II (**2**), cinerin II (**3**), pyrethrin I (**4**), and jasmolin I (**5**)] from this extract. These were tested together with 15 synthetic pyrethroids for their activity against *P. falciparum* and *Trypanosoma brucei rhodesiense* and for cytotoxicity in rat myoblast L6 cells. The natural pyrethrins showed antiplasmodial activity with IC_{50}s between 4 and 12 μM, and antitrypanosomal activity with IC_{50}s from 7 to 31 μM. The pyrethroids exhibited weaker antiplasmodial and antitrypanosomal activity than the pyrethrins. Both pyrethrins and pyrethroids showed moderate cytotoxicity against L6 cells. Pyrethrin II (**1**) was the most selective antiplasmodial compound, with a selectivity index of 24.

KEYWORDS: *Chrysanthemum cinerariifolium*, Asteraceae, pyrethrins, pyrethroids, antiplasmodial, antitrypanosomal, malaria, trypanosomiasis

INTRODUCTION

Pyrethrum (*Chrysanthemum cinerariifolium* (Trevir.) Vis. (synonyms *Tanacetum cinerariifolium* (Trevir.) Schultz Bip. and *Pyrethrum cinerariifolium* (Trevir.)), a herbaceous perennial of the Asteraceae family, is the most widely used botanical insecticide. Currently, it is cultivated in Kenya, Australia, and United States of America, among other countries.[1−3] The secondary metabolites responsible for the insecticidal activity of pyrethrum are six closely related esters of the pyrethric and chrysanthemic acids and the pyrethrolone, cinerolone, or jasomolone alcohols.[1,3,4] Pyrethrins are very potent and selective natural insecticides. However, these compounds are quickly degraded when they are exposed to air and sunlight, which limits their efficacy.[1,5]

To overcome instability issues, pyrethrin-inspired synthetic insecticides, the pyrethroids, were developed. They have increased photostability while maintaining the potent, rapid insecticidal activity, and relatively low acute mammalian toxicity of the pyrethrins.[1,5] Currently, pyrethroids are used in agriculture and as active ingredients of household insecticidal products. They have been applied to control vectors of human diseases such as *Anopheles gambiae*, an important carrier for malaria transmission. As a result, pyrethrins occupy an important place in the world's insecticide market, representing 18% of the U.S. dollar value.[5,6]

Pyrethroids can be classified into the classes type I and type II, the main structural difference being the presence of an α-cyano-3-phenoxybenzylalcohol moiety in type II pyrethroids.[7−9] Pyrethrins and pyrethroids exert their insecticidal activity by modification of the insect's voltage-gated sodium channels by slowing the kinetics of channel gate activation and inactivation. This results in increased anion permeability leading to membrane depolarization and a subsequent rise of neuronal action potential.[5,10,11] Besides sodium channels, pyrethrins and pyrethroids can interact with voltage-gated calcium, potassium, and chloride channels, as well as GABA, glutamate, and acetylcholine receptors.[5,8,10]

Pyrethrins and type I pyrethroids have quantitatively and qualitatively different effects than the type II pyrethroids on ion channels and different visible effects on insects.[7−11]

The biological activity of pyrethrins beyond their insecticidal properties has not been extensively investigated. However, some data on antimycobacterial (*M. avium* and *M. tuberculosis* H37Rv) and antiviral properties (Herpes Simplex Virus, HSV-1, MacIntyre strain ATCC No. VR-539 and HSV-2, MS strain)[4,12] have been reported.

Our interest in pyrethrum was raised when, in a project for natural product based lead discovery, we performed an antiprotozoal screen of 1800 plant and fungal extracts for effects against the parasites *Trypanosoma brucei rhodesiense*, *Trypanosoma cruzi*, *Plasmodium falciparum*, and *Leishmania donovani*. These protozoal parasites are the causal agents of human African trypanosomiasis, Chagas disease, malaria, and leishmaniasis, respectively. The extract library included an *n*-hexane extract of pyrethrum flowers that exhibited potent activity against *P. falciparum* and *T. brucei rhodesiense* at a test concentration of 4.8 μg/mL; the inhibition was 87% and 99%, respectively. To identify the compounds responsible for the activity, a series of pyrethrins

Received: May 12, 2011
Accepted: July 25, 2011
Revised: July 19, 2011
Published: July 25, 2011

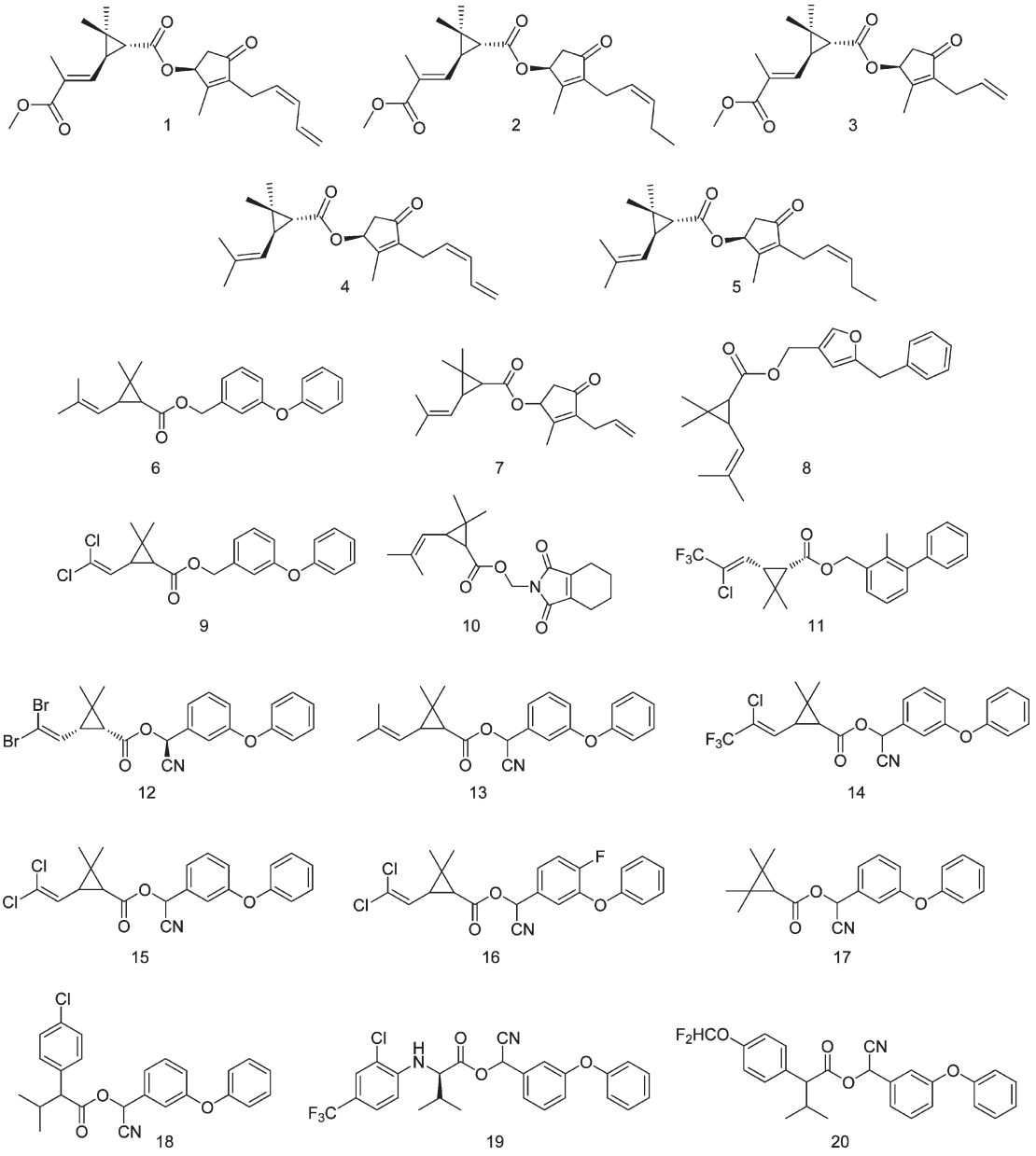

Figure 1. Structures of the pyrethrins **1**−**5**, type I pyrethroids **6**−**11**, and type II pyrethroids **12**−**20**. The comercial pyrethroids (**6**−**20**) are diasteromeric mixtures, with the exception of **11** (*Z*)-(1*S*,3*S*) and **12** (*S*)-(1*R*,3*R*).

(Figure 1) were isolated from the *n*-hexane extract and evaluated for their in vitro antiprotozoal activity. Since the natural products showed activity against the two protozoan parasites, we included six type I pyrethroids and nine type II pyrethroids (Figure 1) to evaluate their effects on the parasites too. The idea was that these commercial compounds, if exerting their antiprotozoal activity possibly on the same targets as the active natural products, might be good leads due to their favorable physicochemical properties, potency, and stability. Besides the antiprotozoal activity, cytotoxicity in rat L6-cells was determined to assess the selectivity of an inhibitory effect on the parasites rather than mammalian cells.

MATERIALS AND METHODS

General Experimental Procedures. Analytical grade solvents for extraction and HPLC grade solvents for chromatography were purchased from Scharlau (Barcelona, Spain). HPLC grade water was obtained by an EASY-pure II from a Barnstead water purification system (Dubuque, Iowa). Formic acid (98.0−100.0%) was from Sigma-Aldrich (Buchs, Switzerland). Artemisinin was obtained from Sigma Aldrich (Buchs, Switzerland) and melarsoprol (Arsobal) from Sanofi-Aventis, (Geneva, Switzerland). The pyrethroids tetramethrin (**10**), bifenthrin (**11**), τ-fluvalinat (**19**), and flucythrinate (**20**) were purchased from Sigma-Aldrich (Buchs, Switzerland). Dr. Ehrenstorfer GmbH (Augsburg, Germany) provided phenothrin (**6**), allethrin (**7**), resmethrin (**8**), permethrin (**9**), deltamethrin (**12**), cyphenothrin (**13**), λ-cyhalothrin (**14**), cypermethrin (**15**), cyfluthrin (**16**), fenpropathrin (**17**), and fenvalerate (**18**).

Preparative HPLC was done on a LC-8A preparative system consisting of two Model LC-8A pumps, a Model SPD-M10A VP PDA detector, and VP2 software (all from Shimadzu, Tokyo, Japan). Medium pressure liquid chromatography (MPLC) was performed using a Büchi

Sepacore system (Büchi, Flawil, Switzerland), consisting of a control unit C-620, a fraction collector C-660, a UV photometer C-635, and two pump modules C-605, on a prepacked silica gel (40−63 μm) polypropylene cartridge (40 × 150 mm, Büchi). TLC was conducted on precoated Kieselgel 60 F_{254}, 0.25 mm plates (Merck, Darmstadt, Germany). NMR data were acquired at a target temperature of 18 °C on an Avance III 500 MHz spectrometer (Bruker, Fällanden, Switzerland) operating at 500.13 MHz for ^{1}H and 125.77 MHz for ^{13}C. A 1 mm TXI-microprobe with a z-gradient was used for ^{1}H-detected experiments. For processing and evaluation Topspin 2.1 (Bruker) software was used. NMR experiments were done as previously described.[13]

Plant Material. Dried flowers of *Chrysanthemum cinerariifolium* (Trevir.) Vis. (Asteraceae) were purchased from Dixa AG (St. Gallen, Switzerland). A voucher specimen (NL 769) is deposited at Herbarium of the Division of Pharmaceutical Biology, University of Basel, Switzerland.

Extraction and Isolation. One kilogram of finely ground plant material was extracted three times with three liters of *n*-hexane for two hours each, at room temperature. Extracts were combined, and the solvent was evaporated at reduced pressure to yield 16.2 g of crude extract. The pyrethrins were isolated from this extract by preparative chromatography in two steps. The first isolation step consisted of MPLC. A portion (10.9 g) of extract was separated on a silica gel prepacked cartridge (40 × 150 mm) by gradient elution with 0−25% ethyl acetate in *n*-hexane over 4 h. The flow rate was 20 mL/min. Fractions were collected every 60 s and compared by TLC [mobile phase: ethyl acetate/*n*-hexane (25:75 v/v)]. Pyrethrins were detected as dark blue spots after spraying with vanillin sulfuric acid reagent (solvent A, vanillin 1% in ethanol; and solvent B, ethanolic solution of sulfuric acid 10%) and heating at 110 °C.[14] Similar fractions were pooled to give two pyrethrin-enriched fractions 3 (570 mg) and 6 (118 mg). Preparative HPLC was used for the isolation of pyrethrins from these fractions. The column employed was a SunFire RP-18 column (5 μm, 30 mm × 150 mm; Waters, Wexford, Ireland). The mobile system was water (solvent A) and methanol (solvent B) using the following gradient: 50% B to 100% B in 30 min, then 100% B for 5 min. The flow rate was 20 mL/min. Sixty milligrams of the fraction in 300 μL of tetrahydrofuran was injected in each run. The UV absorption was monitored at 230 nm.

From fraction number 3, we isolated pyrethrin I (**4**) (10.4 mg), jasmolin I (**5**) (0.8 mg), and jasmolin II (**2**) (0.7 mg). Fraction 6 afforded pyrethrin II (**1**) (9.4 mg) and cinerin II (**3**) (0.6 mg). Extract, fractions, isolated pyrethrins, as well all the commercial pyrethroids were stored protected from light and oxygen, at 2−8 °C under an argon atmosphere.

The structures of pyrethrins were established by 1D and 2D NMR (COSY, HMBC, HSQC, and NOESY). The data are provided as Supporting Information and are in good accordance with the literature.[3,4,15] Purity of pyrethrins was >95% as determined by the integration of ^{1}H NMR spectra.

Biological Tests. The *n*-hexane extract, pyrethrins, and the synthetic pyrethroids were dissolved in DMSO to obtain a final stock solution concentration of 10 mg/mL. The samples were stored at −20 °C until they were used. Further dilutions were done in media so that the DMSO concentration in the highest test concentration before serial dilution was <1%. The screening of the extract library against *P. falciparum* and *T. brucei rhodesiense* was performed in 96 well plates (Costar, Kennebunk, ME), at concentrations of 4.81 and 0.81 μg/mL.[16] Tests were done in triplicate and repeated twice. IC_{50} values against both parasites as well as rat myoblasts (L6-cells) were determined by serial dilution in duplicate and repeated three times.

Testing against P. falciparum K1 Strain. A modification of the [^{3}H]-hypoxanthine incorporation assay was used to determine intraerythrocytic inhibition of parasite growth. Infected erythrocytes (final parasitemia and hematocrit were 0.3% and 1.25%, respectively) in RPMI 1640 medium were exposed to 2-fold serial drug dilution in 96 well plates (Costar, Kennebunk, ME), which covered a range from 10 μg/mL (19.8 to 33.1 μM) to 0.156 μg/mL (0.31 to 0.52 μM). After 48 h of incubation, 50 μL of [^{3}H]-hypoxanthine (0.5 μCi) in the medium was added, and plates were incubated for an additional 24 h. Parasites were harvested onto glass-fiber filters, and radioactivity was counted using a Betaplate liquid scintillation counter (Wallac, Zürich, Switzerland). The results were recorded as counts per minute (cpm) per well at each drug concentration and expressed as a percentage of untreated controls.[13,16]

Testing against T. brucei rhodesiense STIB 900. Minimum essential medium (MEM) supplemented with 2-mercaptoethanol and 15% heat-inactivated horse serum was used for determining the inhibition of parasite growth. Serial 3-fold drug dilution, which covered a range of 90 μg/mL (178 to 298 μM) to 0.123 μg/mL (0.24 to 0.41 μM), was prepared in 96 well plates. Bloodstream forms of *T. brucei rhodesiense* in 50 μL of medium were added to each well except of the background. The plate was incubated under humidified 5% CO_2 atmosphere at 37 °C for 68 h. Resazurin (Sigma-Aldrich, Zürich, Switzerland) solution (12.5 mg of resazurin dissolved in 100 mL of distilled water; 10 μL) was then added to all wells and the incubation continued for a further 2 to 4 h. The plate was read in a Spectramax Gemini XS micro plate fluorometer (Molecular Devices Cooperation, Sunnyvale, CA) using an excitation wavelength of 536 nm and an emission wavelength of 588 nm. Fluorescence development was measured and expressed as a percentage of the control.[16,17]

Cytotoxicity Test Using L6 Cells. The rat skeletal myoblast cell line (L-6 cells) was used to assess cytotoxicity. The cells were seeded in RPMI 1640 medium supplemented with 1% L-glutamine (200 nM) and 10% fetal bovine serum under humidified 5% CO_2 at 37 °C. Assays were performed in 96 well microtiter plates, with each well receiving 100 mL of culture medium with 4×10^4 cells. After 24 h, the medium was removed from all wells, and serial 3-fold drug dilutions were prepared covering a range from 90 (178.1 to 297.9 μM) to 0.123 μg/mL (0.24 to 0.41 μM). After 68 h of incubation, the plates were inspected under an inverted microscope to ensure the growth of the controls and sterile conditions. Then, 10 μL of resazurin solution (12.5 mg of resazurin dissolved in 100 mL of distilled water) was added to each well, and the plates were incubated for another 2 h. Then, the plates were read with a Spectramax Gemini XS Microplate fluorometer (Molecular Devices Cooperation, Sunnyvale, CA) using an excitation wavelength of 536 nm and an emission wavelength of 588 nm. IC_{50} values were determined using the microplate reader software Softmax Pro (Molecular Devices Cooperation, Sunnyvale, CA).[18]

RESULTS AND DISCUSSION

A medium throughput screen showed that the *n*-hexane extract of *C. cinerariifolium* flowers had significant activity against *P. falciparum* (86% inhibition at a test concentration of 4.8 μg/mL) and against *T. brucei rhodesiense* (99% inhibition at the same concentration). Since highly lipophilic pyrethrins are the characteristic secondary metabolites in an *n*-hexane extract of pyrethrum flowers, we carried out a targeted isolation of pyrethrins. Among the compounds extracted were three esters of pyrethric acid, [pyrethrin II (**1**), jasmolin II (**2**), and cinerin II (**3**)], and two esters of chrysantemic acid, [pyrethrin I (**4**) and jasmolin I (**5**)] (Figure 1). When tested against *P. falciparum*, *T. brucei rhodesiense*, and L-6 cells, most of these exhibited antiprotozoal activity and low cytotoxicity (Table 1). The most active compound in the antiplasmodial assay was **1** with an IC_{50} of 4.0 ± 1.1 μM, followed by **2** and **3** with IC_{50} values of 5.0 ± 0.4 and 5.8 ± 0.4 μM, respectively. Compounds **4** and **5** were somewhat less active (IC_{50} values of 11.7 ± 1.5 and 9.3 ± 1.2 μM, respectively). Accordingly, the three derivatives of pyrethric acid showed the most potent antiplasmodial effect.

Table 1. In Vitro Antiprotozoal Activities of Isolated Natural Pyrethrins 1−5 and Synthetic Pyrethroids 6−20 against *Plasmodium falciparum* and *Trypanosoma brucei rhodesiense*, Cytotoxic Activity in L-6 Cells, and Selectivity Indices (IC_{50} L-6 cells/IC_{50} parasite)[a]

	IC_{50} (μM) ± SEM			selectivity index	
compound	*P. falciparum*	*T.b. rhodesiense*	L-6 cells	*P. falciparum*	*T.b. rhodesiense*
pyrethrin II (**1**)	4.0 ± 1.1	10.6 ± 0.4	95.1 ± 2.5	23.6	9.0
jasmolin II (**2**)	5.0 ± 0.4	12.0 ± 0.2	31.5 ± 2.3	6.3	2.6
cinerin II (**3**)	5.8 ± 0.4	12.2 ± 0.0	28.0 ± 7.8	4.9	2.3
pyrethrin I (**4**)	11.7 ± 1.5	6.9 ± 1.1	146.6 ± 34.5	12.6	21.2
jasmolin I (**5**)	9.3 ± 1.2	30.9 ± 1.4	86.6 ± 12.9	9.3	2.8
phenothrin (**6**)	inactive[b]	36.4 ± 2.4	57.4 ± 3.1		1.6
allethrin (**7**)	18.0 ± 1.5	26.4 ± 3.4	21.2 ± 1.7	1.2	0.8
resmethrin (**8**)	26.1 ± 2.1	25.5 ± 1.1	51.6 ± 1.4	2.0	2.0
permethrin (**9**)	22.4 ± 0.7	24.5 ± 2.3	66.7 ± 2.2	3.0	2.7
tetramethrin (**10**)	inactive[b]	12.9 ± 2.2	15.5 ± 1.32		1.2
bifenthrin (**11**)	8.9 ± 2.0	24.1 ± 2.0	61.1 ± 6.3	6.9	2.5
deltamethrin (**12**)	inactive[b]	51.4 ± 2.1	142.0 ± 10.5		2.8
cyphenothrin (**13**)	inactive[b]	29.8 ± 0.1	93.1 ± 2.8		3.1
λ-cyhalothrin (**14**)	inactive[b]	inactive[c]	181.2 ± 15.9		
cypermethrin (**15**)	inactive[b]	49.9 ± 0.5	150.7 ± 6.7		3.0
cyfluthrin (**16**)	inactive[b]	27.4 ± 2.6	119.1 ± 14.6		4.4
fenpropathrin (**17**)	inactive	26.2 ± 4.4	21.1 ± 1.9		0.8
fenvalerate (**18**)	14.8 ± 0.9	57.8 ± 6.2	111.0 ± 6.4	7.5	1.9
τ-fluvalinate (**19**)	inactive[b]	26.2 ± 2.6	47.7 ± 2.3		1.8
flucythrinate (**20**)	17.6 ± 0.8	33.4 ± 1.9	111.1 ± 5.5	6.3	3.3
artesunate[d]	0.01 ± 0.006	n.d.	n.d.		
chloroquine[d]	0.40 ± 0.252	n.d.	n.d.		
melarsoprol[e]	n.d.	0.01 ± 0.001	n.d.		
podophyllotoxin[f]	n.d.	n.d.	0.02 ± 0.004		

[a] n.d. not determined. SEM: standard error of the mean. Selectivity index: quotient of the activity of the compounds on the parasites and the mammalian cells. [b] No activity observed at the highest test concentration of 10 μg/mL, which corresponds to molar test concentrations of 19.8 to 33.1 μM. [c] No activity observed at the highest test concentration of 90 μg/mL, which corresponds to molar test concentrations of 178 to 298 μM. [d] Reference drug *P. falciparum* assay. [e] Reference drug *T. b. rhodesiense* assay. [f] Reference drug cytotoxicity assay.

The antitrypanosomal activity of the isolated compounds was less pronounced (Table 1). Pyrethrin I (**4**) showed an IC_{50} of 6.9 ± 1.1 μM. The IC_{50} values of compounds **1**, **2**, **3**, and **5** were above 10 μM (10.6 ± 0.4, 12.1 ± 0.2, 12.2 ± 0.02, and 30.9 ± 1.4 μM, respectively).

The compound with the lowest cytotoxicity against L6 cells was **4** followed by **1** (Table 1). With a SI of 23.6, pyrethrin II (**1**) was the most selective compound against *P. falciparum*. The other four pyrethrins showed selectivity indices (SI) between 4.9 and 12.6 (Table 1). Pyrethrin I (**4**) showed the highest SI (21.2) against *T. brucei rhodesiense*, while the other four pyrethrins exhibited SI between 2.3 and 9.0.

We then tested a series of 6 type I (**6**−**11**) and 9 type II pyrethroids (**12**−**20**). Type I pyrethroids were more active against *P. falciparum* than type II compounds but less active than the pyrethrins (**1** − **5**), with the exception of **11**, which showed an IC_{50} of 8.9 ± 2.0 μM. Six (**12**−**16** and **19**) of the nine type II pyrethroids did not show antiplasmodial activity at the highest tested concentration of 10 μg/mL. This corresponds to the molar test concentrations ranging from 19.8 to 33.1 μM for the various substances (Table 1).

Both, type I and type II pyrethroids displayed low activity against *T. brucei rhodesiense* (Table 1). Their IC_{50} values were in the range of 12.9 ± 2.2 μM for **10** (a type I pyrethroid) and 57.8 ± 6.2 μM for **18** (a type II pyrethroid). Selectivity toward the protozoa was low.

In conclusion, pyrethrins were the compounds responsible for the antiplasmodial activity of the lipophilic pyrethrum extract. These compounds had reasonably selective antiplasmodial properties and weaker trypanocidal activity. Among them, pyrethrin II (**1**) was the most active and selective compound. In contrast, all 15 pyrethroids showed a weaker and less selective inhibition on *P. falciparum* and *T. brucei rhodesiense*.

As mentioned above, the main target for pyrethrins and pyrethroids in insects are voltage-gated sodium channels. Neither in *P. falciparum* nor in *T. brucei rhodesiense* has the presence of such channels been reported.[19−21] The antiprotozoal effects reported here may involve some of the other channels or structurally related ones with which pyrethrins and pyrethroids can interact. For instance *T. brucei rhodesiense* has potassium channels,[19] and *P. falciparum* has channels such as aquaporin PfAQP, which could possibly be targets for these compounds.[20,21]

■ ASSOCIATED CONTENT

Supporting Information. ^{1}H NMR spectroscopic data (500 MHz, $CDCl_3$) for compounds (**1**−**5**). This material is available free of charge via the Internet at http://pubs.acs.org.

AUTHOR INFORMATION

Corresponding Author

*Tel: +41 61 267 14 25. Fax: +41 61 267 14 74. E-mail: Michael.Adams@unibas.ch.

Funding Sources

Financial support was provided by the Swiss National Science Foundation (project 31600-113109), the Steinegg-Stiftung, Herisau, and the Fonds zur Förderung von Lehre and Forschung, Basel (to M.H.). Y.H. gratefully acknowledges a Ph.D. stipend from Departamento Administrativo de Ciencia, Tecnología e Innovación de Colombia (COLCIENCIAS) managed by LASPAU.

ABBREVIATIONS USED

GABA, γ-aminobutyric acid; HPLC, high performance liquid chromatography; TLC, thin layer chromatography; NMR, nuclear magnetic resonance; MPLC, medium pressure liquid chromatography; COSY, correlation spectroscopy; HMBC, heteronuclear multiple bond correlation; HSQC, heteronuclear single quantum correlation; NOESY, nuclear Overhauser effect spectroscopy; RPMI 1640, Roswell Park Memorial Institute medium; MEM, minimum essential medium; SI, selectivity index.

REFERENCES

(1) Casida, J. E. Pyrethrum flowers and pyrethroid insecticides. *Environ. Health Perspect.* **1980**, *34*, 189–202.

(2) Casida, J. E.; Quistan, G. B. Golden age of insecticide research: past, present, or future? *Annu Rev. Entomol.* **1998**, *43*, 1–16.

(3) Crombie, L. Chemistry and biosynthesis of natural pyrethrins. *Pestic. Sci.* **1980**, *11*, 102–118.

(4) Rugutt, J. K.; Henry, C. W., III.; Franzblau, S. G.; Warner, I. M. NMR and molecular mechanics study of pyrethrins I and II. *J. Agric. Food Chem.* **1999**, *47*, 3402–3410.

(5) Soderlund, D. M. Toxicology and Mode of Action of Pyrethroid Insecticides. In *Hayes's Handbook of Pesticide Toxicology*, 3rd ed.; Krieger, R. I., Ed.; Elsevier: San Diego, CA, 2010; Vol. 2, pp 1665−1686.

(6) Ranson, H.; N'Guessan, R.; Lines, J.; Moiroux, N.; Nkuni, Z.; Corbel, V. Pyrethroid resistance in African anopheline mosquitoes: what are the implications for malaria control? *Trends Parasitol* **2011**, *27*, 291–292.

(7) Gammon, D. W.; Brown, M. A.; Casida, J. E. Two classes of pyrethroid action in the cockroach. *Pestic. Biochem. Physiol.* **1981**, *15*, 181–191.

(8) Breckenridge, C. B.; Holden, L.; Sturgess, N.; Weiner, M.; Sheets, L.; Sargent, D.; Soderlund, D. M.; Choi, J.; Symington, S.; Clark, J. M.; Burr, S.; Ray, D. Evidence for a separate mechanism of toxicity for the Type I and the Type II pyrethroid insecticides. *NeuroToxicology* **2009**, *30S*, S17–S31.

(9) Bloomquist, J. R. Ion channels as targets for insecticides. *Annu. Rev. Entomol.* **1996**, *41*, 163–90.

(10) Narahashi, T. Nerve membrane Na+ channels as targets of insecticides. *Trends Pharmacol. Sci.* **1992**, *13*, 236–241.

(11) O'Reilly, A. O.; Khambay, B. P. S.; Williamson, M. S.; Field, L. M.; Wallace, B. A.; Davies, T. G. E. Modelling insecticide-binding sites in the voltage-gated sodium channel. *Biochem. J.* **2006**, *396*, 255–263.

(12) Stanberry, L. R.; Bernstein, D. I.; Myers, M. G. Evaluation of the herpes simplex virus antiviral activity of pyrethrins. *Antiviral Res.* **1986**, *6*, 95–102.

(13) Adams, M.; Christen, M.; Plitzko, I.; Zimmermann, S.; Brun, R.; Kaiser, M.; Hamburger, M. Antiplasmodial lanostanes from the *Ganoderma lucidum* mushroom. *J. Nat. Prod.* **2010**, *73*, 897–900.

(14) Kasaj, D.; Rieder, A.; Krenn, L.; Kopp, B. Separation and quantitative analysis of natural pyrethrins by high performance liquid chromatography. *Chromatographia* **1999**, *50*, 607–610.

(15) Bramwell, A. F.; Crombie, L.; Hemesley, P.; Pattenden, G.; Elliott, M.; Janes, N. F. Nuclear magnetic resonance spectra of the natural pyrethrins and related compounds. *Tetrahedron* **1969**, *25*, 1727–1741.

(16) Adams, M.; Zimmermann, S.; Kaiser, M.; Brun, R.; Hamburger, M. A protocol for HPLC-based activity profiling for natural products with activities against tropical parasites. *Nat. Prod. Commun.* **2009**, *4*, 1377–1381.

(17) Räz, B.; Iten, M.; Grether-Bühler, Y.; Kaminsky, R.; Brun, R. The Alamar blue® assay to determine drug sensitivity of African trypanosomes (*T.brucei rhodesiense* and *T.brucei gambiense*) *in vitro*. *Acta Trop.* **1997**, *68*, 139–147.

(18) Kunert, O.; Swamy, R. C.; Kaiser, M.; Presser, A.; Buzzi, S.; Apa Rao, A. V. N.; Schühly, W. Antiplasmodial and leishmanicidal activity of biflavonoids from Indian *Selaginella bryopteris*. *Phytochem. Lett.* **2008**, *1*, 171–174.

(19) Van Der Heyden, N.; Docampo, R. Proton and sodium pumps regulate the plasma membrane potential of different stages of *Trypanosoma cruzi*. *Mol. Biochem. Parasitol.* **2002**, *120*, 127–139.

(20) Ellekvist, P.; Høier Ricke, C.; Litman, T.; Salanti, A.; Colding, H.; Zeuthen, T.; Klaerke, D. A. Molecular cloning of a K^+ channel from the malaria parasite *Plasmodium falciparum*. *Biochem. Biophys. Res. Commun.* **2004**, *318*, 477–484.

(21) Staines, H. M.; Derbyshire, E. T.; Slavic, K.; Tattersall, A.; Vial, H.; Krishna, S. Exploiting the therapeutic potential of *Plasmodium falciparum* solute transporters. *Trends Parasitol.* **2010**, *26*, 284–296.

Supporting information

Antiplasmodial and Antitrypanosomal Activity of Pyrethrins and Pyrethroids

Yoshie Hata,[†,§] Stefanie Zimmermann,[†,‡] Melanie Quitschau[†], Marcel Kaiser,[‡,#] Matthias Hamburger,[†] and Michael Adams, *[,†].

[†] *Department of Pharmaceutical Sciences, University of Basel, Klingelbergstrasse 50, 4056 Basel, Switzerland;* [§]*Departamento de Farmacia, Universidad Nacional de Colombia, Carrera 30 45-03, Bogotá, Colombia;* [‡]*Swiss Tropical and Public Health Institute, Socinstrasse 57, CH-4002 Basel, Switzerland;* [#]*University of Basel, 4056 Basel, Switzerland*

* To whom correspondence should be addressed: Tel: +41 61 267 14 25. Fax: +41 61 267 14 74. E-mail: Michael.Adams@unibas.ch.

Table S1 ^{1}H-NMR spectroscopic data (500 MHz, $CDCl_3$) for compounds (**1**-**5**)

Figure S1 ^{1}H-NMR spectrum in $CDCl_3$ and chemical structure of **1**

Figure S2 ^{1}H-NMR spectrum in $CDCl_3$ and chemical structure of **2**

Figure S3 ^{1}H-NMR spectrum in $CDCl_3$ and chemical structure of **3**

Figure S4 ^{1}H-NMR spectrum in $CDCl_3$ and chemical structure of **4**

Figure S5 ^{1}H-NMR spectrum in $CDCl_3$ and chemical structure of **5**

Table S1. ^{1}H NMR spectroscopic data (500 MHz, $CDCl_3$) for compounds (**1**-**5**)

	1	**2**	**3**	**4**	**5**
	δ_H (*J* in Hz)	**δ_H (*J* in Hz)**	**δ_H (*J* in Hz)**	**δ_H (*J* in Hz)**	**δ_H (*J* in Hz)**
1	1.75, dd (5.3)	1.68, d (5.2)	1.67, d (6.3)	1.37, d (5.4)	1.32, d (5.4)
3	2.20, m*	2.16, m*	2.19, m*	2.04, m*	2.00, dd (6.1, 6.7)
5	1.20, s	1.26, s	1.20, s	1.10, s	1.05, s
6	1.28, s	1.18, s	1.28, s	1.23, s	1.18, s
7	6.43, dd (9.5, 1.2)	6.41, dd (9.4, 1.2)	6.44, dd (9.5, 1.3)	4.88, dd (7.4, 1.2)	4.84, d (7.4)
9	1.92, br s	1.89, s	1.92, d (1.3)	1.67, s	1.63, s
10	-	-	1.70, d (5.2)	1.69, s	1.62, s
11	3.70, s	3.68, s	3.70, s	-	-
1´	5.64, br d (6.2)	5.61, br d (6.5)	5.64, br dd (6.0, 0.6)	5.63, br d (6.2)	5.58, br d (6.0)
5a´	2.20, m*	2.16, m*	2.19, m*	2.19, dd (18.5, 1.9)	2.13, dd (18.7, 1.8)
5b´	2.84, dd (18.6, 6.2)	2.80, dd (18.7 ,6.4)	2.83 dd (18.5, 6.2)	2.62 dd (18.5, 6.3)	2.75, dd (18.7, 6.3)
6´	2.00, s	1.98, s	2.00, s	2.00, s	1.95, s
7´	3.10, d (7.7)	2.93, d (7.2)	2.96, d (7.1)	3.09, d (7.6)	2.89, d (7.2)
8´	5.32, ddd (10.2, 7.3, 7.3)	5.37, m	5.48, m	5.32, ddd (10.4, 7.6, 7.6)	5.33, m
9´	6.01, dd (10.6, 10.6)	5.19, m	5.27, m	6.00, dd (10.8, 10.8)	5.16, m

10´	6.73, ddd (16.5, 10.4, 10.4)	2.10, m	1.70, d (5.07)	6.72, ddd (16.9, 10.4, 10.4)	2.03, m
11	Ha 5.15 d br (10.3);	0.94, t (7.5)	-	5.13, d br (10.7);	0.90, t (7.6)
	Hb 5.21 d br (16.5)			5.19, d br (17.6)	

* Overlapping signals.

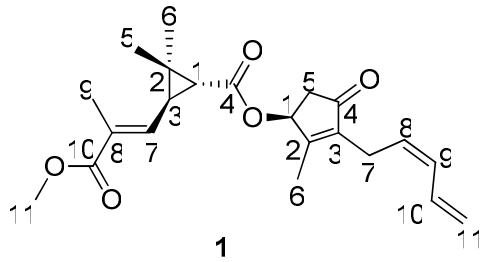

1

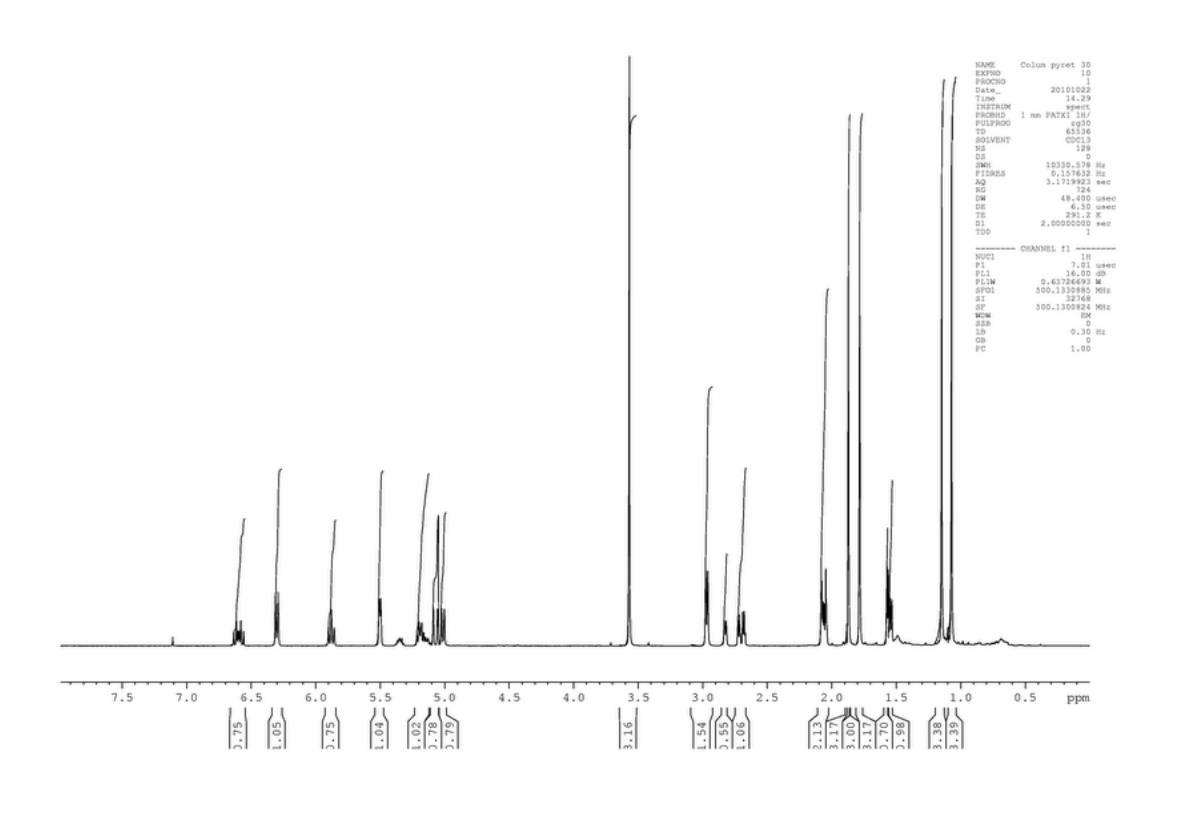

Figure S1 ^{1}H-NMR spectrum in $CDCl_3$ and chemical structure of **1**.

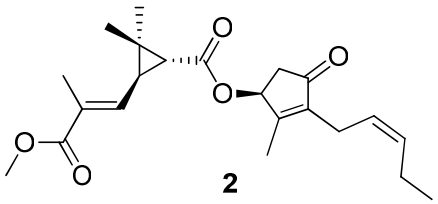

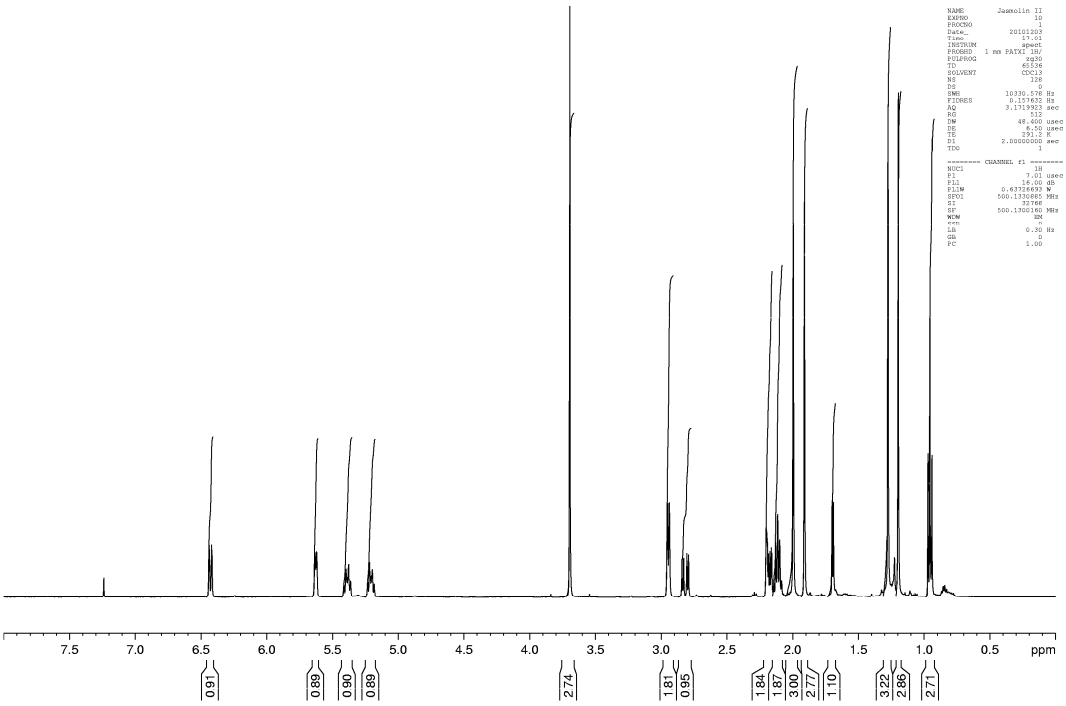

Figure S2 ^{1}H-NMR spectrum in $CDCl_3$ and chemical structure of **2**.

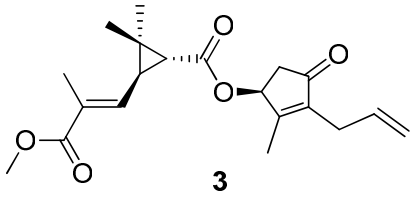

3

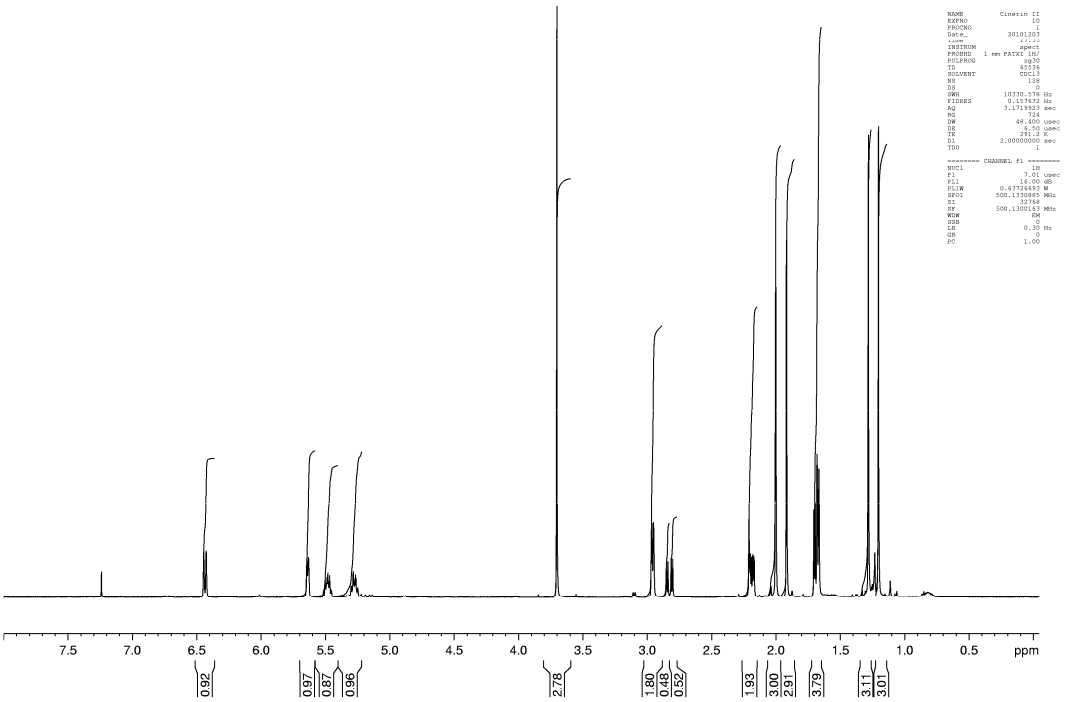

Figure S3 ^{1}H-NMR spectrum in $CDCl_3$ and chemical structure of **3**.

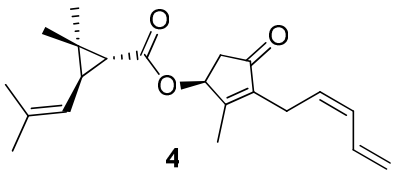

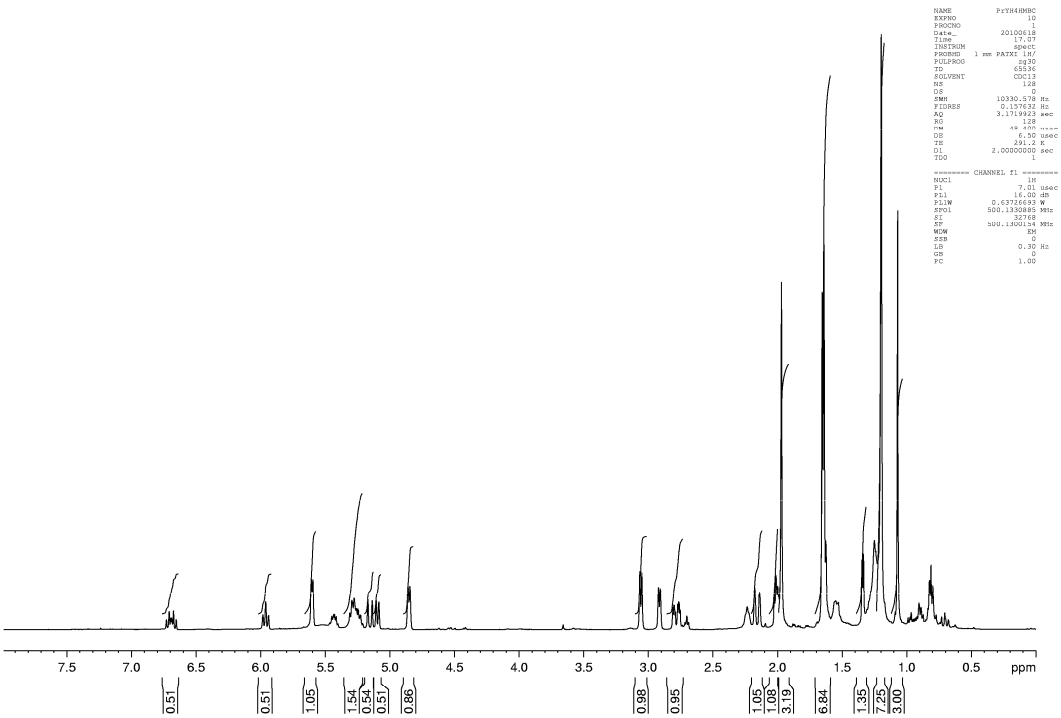

Figure S4 ^{1}H-NMR spectrum in $CDCl_3$ and chemical structure of **4**.

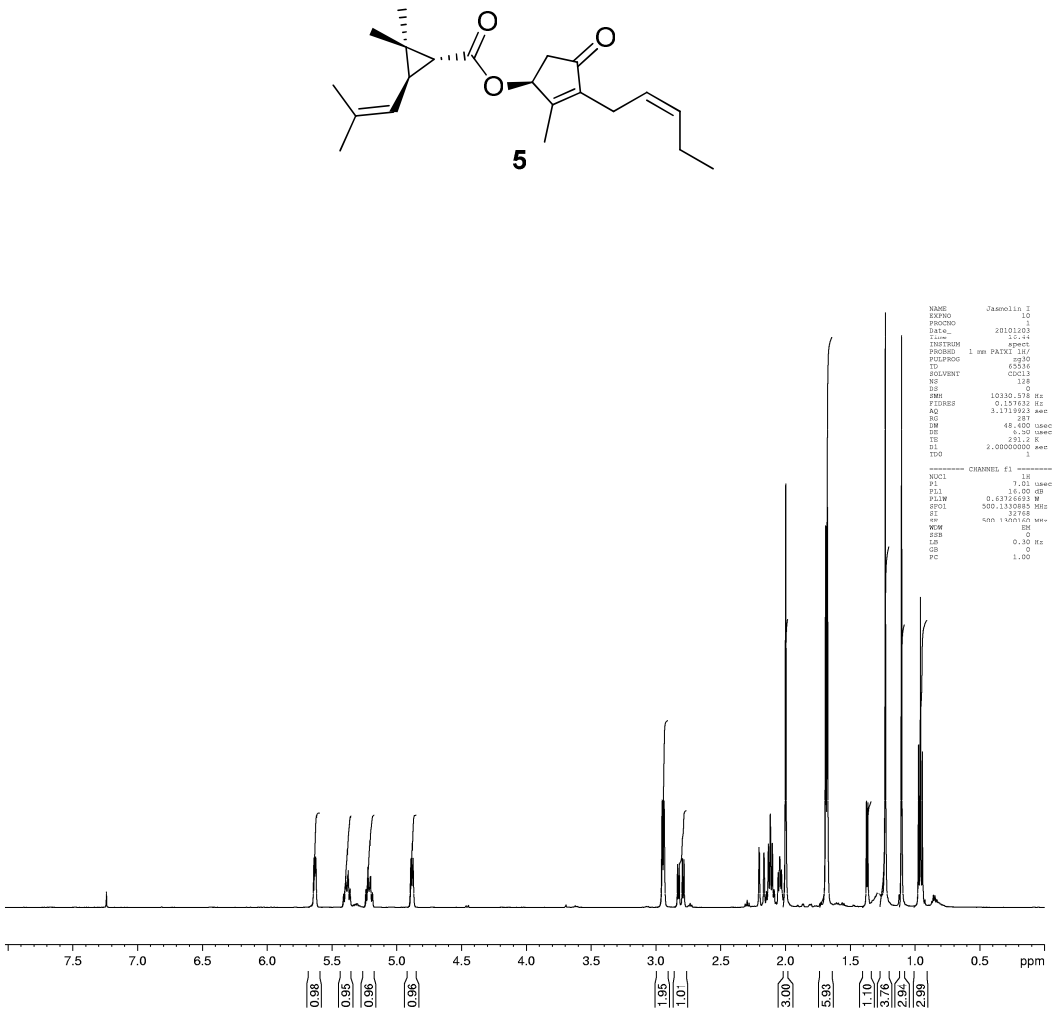

Figure S5 ^{1}H-NMR spectrum in $CDCl_3$ and chemical structure of **5**.

3.7 Antitrypanosomal Sesquiterpene Lactones from *Saussurea costus*

Tasqiah Julianti, **Yoshie Hata**, Stefanie Zimmermann, Marcel Kaiser, Matthias Hamburger, Michael Adams

Fitoterapia, 2011, 82: 955–959. DOI: 10.1016/j.fitote.2011.05.010

As a contribution to the structure activity relationship (SAR) of trypanocidal sesquiterpene lactones from different botanical sources, the activity of the germacrolides costunolide, eupatoriopicrin, and partenolide was compared with the activity of guaianolides dehydrocostuslacone and zaluzanin D, and the eudesmanolides arbusculin B and α-cyclocostunolide. The germacrolides were the most active class of sesquiterpene lactones.

My contributions to this work were: (1) recollection of Eupatorium cannabium; (2) extraction of plant material; (3) isolation of the sesquiterpene lactone eupatoriopicrin; (4) recording and interpretation of analytical data for structure elucidation (HPLC-PDA-ESI, TOF-MS, 1D and 2D NMR); (5) extraction of plant material of Laurus nobilis; (6) isolation of the sesquiterpene lactones costunolide and zaluzanin D; (7) recording and interpretation of analytical data for structure elucidation (HPLC-PDA-ESI, TOF-MS, 1D NMR and 2D NMR; (8) providing the corresponding data for manuscript, figure, table, and supporting information preparation.

Inken Plitzko and Melanie Quitschau supervised structure elucidation. In vitro trypanocidal and cytotoxicity tests were performed by Stefanie Zimmermann in the Swiss TPH. Tasqiah Julianti isolated costunolide, dehydrocostuslacone, and other sesquiterpenlactones from S. costus and wrote the manuscript draft.

Yoshie Hata-Uribe

Fitoterapia 82 (2011) 955–959

Contents lists available at ScienceDirect

Fitoterapia

journal homepage: www.elsevier.com/locate/fitote

Antitrypanosomal sesquiterpene lactones from *Saussurea costus*

Tasqiah Julianti [a,c], Yoshie Hata [a,d], Stefanie Zimmermann [a,b], Marcel Kaiser [b,e], Matthias Hamburger [a], Michael Adams [a,*]

[a] Division of Pharmaceutical Biology, University of Basel, CH-4056 Basel, Switzerland
[b] Department of Medical Parasitology and Infection Biology, Swiss Tropical and Public Health Institute, CH-4002 Basel, Switzerland
[c] Faculty of Pharmacy, Pancasila University, 12640 Jakarta, Indonesia
[d] Department of Pharmacy, National University of Colombia, Carrera 30 45-03, Bogotá, Colombia
[e] University of Basel, CH-4051 Basel, Switzerland

ARTICLE INFO

Article history:
Received 12 April 2011
Accepted in revised form 12 May 2011
Available online 23 May 2011

Keywords:
Saussurea costus
Asteraceae
Sesquiterpene lactones
Trypanosoma brucei rhodesiense
HPLC-based activity profiling

ABSTRACT

In the course of a larger screen of 1800 plant and fungal extracts, the ethyl acetate extract of *Saussurea costus* roots potently inhibited the growth of *Trypanosoma brucei rhodesiense*. Subsequent HPLC based activity profiling led to the identification of the sesquiterpene lactones arbusculin B (**1**), α-cyclocostunolide (**2**), costunolide (**3**), and dehydrocostuslactone (**4**). They were tested for in vitro antitrypanosomal activities and cytotoxicity alongside the structurally related sesquiterpene lactones parthenolide (**5**), zaluzanin D (**6**), and eupatoriopicrin (**7**), and had IC_{50}s between 0.8 and 22 μM. Cytotoxic IC_{50}s were from 1.6 to 19 μM, and selectivity indices from 0.5 to 6.5.

1. Introduction

The fragrant roots of *Saussurea costus* (Falc.) Lipschitz (Asteraceae), synonym: *Saussurea lappa* C.B. Clarke, have been used for thousands of years as medicines, incenses and ointments by many cultures. In India they are called Kur or Kushtha, and in China *Yún mù xiāng* (云木香). In the Ayurveda, Siddha, and Unani medicinal systems *S. costus* roots are used alone or in combination with other drugs to treat asthma, cholera, chronic skin diseases, rheumatism, cough and cold, quartan malaria, leprosy, persistent hiccups, rheumatism, stomach-ache, toothache, and typhoid fever [1,2].

A broad spectrum of biological activities such as anti-inflammatory, anticancer, immunomodulatory, CNS depressant, and antimicrobial properties have been reported for *S. costus* extracts [3–5]. Activities have commonly been related to the presence of sesquiterpene lactones. Furthermore, tannins, steroids, alkaloids, glycosides, terpenoids, flavonoids, peptides, and organic acids have been reported from this plant [3,4].

Our interest in this plant was raised when we performed an antiprotozoal screen of 1800 plant and fungal extracts for effects against the parasites *Trypanosoma brucei rhodesiense*, *Trypanosoma cruzi*, *Plasmodium falciparum* and *Leishmania donovani*, the causal agents of human African trypanosomiasis, Chagas disease, malaria, and leishmaniasis, respectively [6–8]. Amongst the most potent extracts in this screen was an ethyl acetate extract of *S. costus* roots which inhibited *T. b. rhodesiense* by 96% at a test concentration of 4.8 μg/ml.

HPLC based activity profiling was used to identify the active constituents in the extract. In this approach sub-milligramme amounts of extract are separated by analytical scale HPLC and automatically fractionated into 96 well plates. The microfractions obtained are submitted to the bioassay, and the resulting activity profile can be overlaid with the HPLC trace to correlate peaks of activity with peaks in the HPLC chromatogram. On-line spectroscopic data (UV–Vis and MS) collected during separation, combined with database

* Corresponding author at: Institute of Pharmaceutical Sciences, Division of Pharmaceutical Biology University of Basel, CH-4056 Basel, Switzerland. Fax: +41 61 267 1474.
E-mail address: michael.adams@unibas.ch (M. Adams).

0367-326X/$ – see front matter © 2011 Elsevier B.V. All rights reserved.
doi:10.1016/j.fitote.2011.05.010

searches provide structural information on the active principles [6–8].

We here report on the identification and isolation of antitrypanosomal compounds from *S. costus*, and also on the comparative testing of some related sesquiterpene lactones for antiprotozoal and cytotoxic activities. This study was part of a larger screen for new antiprotozoal leads using HPLC based activity profiling which has led to the identification of numerous active compounds [8–11].

2. Materials and methods

2.1. General experimental procedures

Analytical grade solvents for extraction and HPLC-grade eluents for chromatography were purchased from Scharlau (Barcelona, Spain), if not stated otherwise. HPLC-grade water was obtained with an EASY-pure II water purification system (Barnstead; Dubuque, IA, USA). Formic acid was from Sigma-Aldrich (Buchs, Switzerland).

Initial screening of the extract library was done as previously described [6]. HPLC based activity profiling: Separations for microfractionation and for on line data collection were carried out on an Agilent series 1100 system equipped with degasser, binary high pressure mixing pump, column oven and PDA detector (all from Agilent; Waldbronn, Germany). MS spectra were recorded in the range of *m/z* 200–1500 positive and negative mode on an Esquire 3000 Plus ion trap mass spectrometer equipped with an electrospray interface (Bruker Daltonics; Bremen, Germany). Microfractionation was performed with 350 µg of extract in DMSO (10 mg/ml) which were separated on a RP-HPLC SunFire C18 column (3.5 µm, 3×150 mm) (Waters; Wexford, Ireland) with gradient A (water + 0.1% formic acid) and B (acetonitrile + 0.1% formic acid), 10–100% B in 30 min and hold at 100% B for 2 min, at a flow rate of 0.5 ml/min. Hystar 3.2 software (Bruker Daltonics; Bremen, Germany) was used to monitor the HPLC system. An FC 204 fraction collector (Gilson; Middleton, WI, USA) was attached to the HPLC to collect a total of 32 microfractions of 60 s each into 96-deep well plates (Whatman; Florham Park, NJ, USA). The plates were dried in a Genevac EZ-2 Plus™ vacuum centrifuge (Avantec; Ipswich, UK), and microfractions redissolved in 5 µl of DMSO prior to testing for antitrypanosomal activity as described [6].

Semipreparative HPLC for compound isolation was done on an Agilent 1100 series HPLC system consisting of a 1100 series quaternary low-pressure mixing pump with degasser module, column oven, and a 1100 series PDA detector with a 1000 µl loop. A SunFire C18 column (5 µm, 10×150 mm) (Waters) was used. The mobile phase was: A (water) and B (MeOH) with a gradient of 60–100% B in 20 min, followed by flushing 5 min with 100% B, the flow rate was 5 ml/min, and monitored at 220 nm. In each run 15 mg of fraction in 50 µl DMSO was injected.

High resolution HPLC–MS was recorded with an Agilent 1100 series HPLC linked to a micrOTOF-ESI-MS system (Bruker). MS calibration was performed using a reference solution of sodium formate 0.1% in isopropanol–water (1:1) containing 5 mM sodium hydroxide. The typical mass accuracy was ±3 ppm. HyStar 3.0 software (Bruker Daltonics) was used for data acquisition and processing.

NMR experiments were recorded in d_6-DMSO and $CDCl_3$ on a Bruker Avance III spectrometer (Bruker; Fallanden, Switzerland) operating at 500.13 MHz at a target temperature of 18 °C. ^{1}H NMR, COSY, HSQC, and HMBC spectra were measured with a 1 mm TXI probe. The 2D pulse programs were hsqcedetpg, hmbcgplpndqf, and cosygpqf. Spectra processing and analysing was done with Bruker TopSpin 2.1 software.

2.2. Plant material

The dried roots of *S. costus* (MTS 577) were purchased from Peter Weinfurth in 2008 (Bochum, Germany). The leaves of *Laurus nobilis* L. (MTS 693) were purchased from Dixa AG (St. Gallen, Switzerland). The aerial parts of *Eupatorium cannabinum* L. (MTS 771) were harvested near Liestal, Canton Basel Land, Switzerland. The authentication of collected *E. cannabinum* was carried out by Dr. M. Adams. Voucher specimens of all samples are deposited at the Institute of Pharmaceutical Biology, University of Basel, organised under the MTS numbers shown above.

2.3. Extraction and preparative isolation

Dried roots of *S. costus* were finely ground using a ZM1 ultra centrifugal mill (Retsch; Haan, Germany). Maceration of 900 g of the powdered material four times with 4 l of ethyl acetate overnight at room temperature in a glass column 15×26 cm (Pyrex, Ostermundigen, Switzerland) yielded 40 g of a thick brown extract. An aliquot of 30 g of extract was fractionated by open column chromatography (9×59 cm) filled with silica gel (Kieselgel 60™, particle size 40–63 µm) (Merck; Darmstadt, Germany) and isocratic elution with *n*-hexane-ethyl acetate (9:1) at a flow rate of 20 ml/min. Fractions of 500 ml each were collected and monitored with TLC on pre-coated Kieselgel 60 F_{254}, 0.25 mm plates from Merck with a mobile phase of: toluene:ethyl acetate (9:1); detection with vaniline-H_2SO_4. Similar fractions were pooled resulting in 7 fractions. Fraction 5 was obtained as a brown oil (160 mg) and was separated by semi-preparative HPLC as described above to obtain compounds arbusculin B (**1**) (2.5 mg) and α-cyclocostunolide (**2**) (26 mg). Fraction 6 totalling 2.2 g afforded pure costunolide (**3**) (670 mg) and fraction 7 (9.7 g) gave dehydrocostuslactone (**4**) (6.5 g).

Zaluzanin D (**6**) from the ethyl acetate extract of the dried leaves of *Laurus nobilis* L. (Myrtaceae) and eupatoriopicrin (**7**) from the aerial parts of *Eupatorium cannabinum* L. (Asteraceae) were isolated by semipreparative HPLC as described above. Isolated substances **1**–**4**, **6**, and **7** were more than 95% pure according to their ^{1}H NMR spectra. Parthenolide (**5**) was purchased from Alexis Biochemicals (Lausen, Switzerland) with more than 95% pure as stated by the supplier. The compounds **7** were identified by comparison of 1D and 2D ^{1}H NMR, HPLC-HRTOF–MS data with published studies: **1** [12], **2** [13], **3** and **4** [14,15], **6** [16], and **7** [17]. Proton and carbon NMR data of all the isolated compounds are given in the supporting information (Table S1).

2.4. Antitrypanosomal assay

Preparation of *T. b. rhodesiense* STIB 900 stocks and culture media for the bloodstream forms was done according to Baltz et al. [18] with the following modifications: 2-mercaptoethanol 0.2 mM, sodium pyruvate 1 mM, hypoxanthine 0.5 mM, and 15% heat-inactivated horse serum. In vitro screening for antitrypanosomal activity was done with of Alamar Blue® assay [19]. Stock solutions of test compounds and their serial dilutions (5 μl) were transferred into 96 well plates (Costar; Corning Inc., Lowell, MA, USA) containing 50 μl of culture medium per well. Bloodstream forms of STIB 900 in 45 μl of medium were added to each well and the plate was incubated at 37 °C under 5% CO_2 atmosphere for 72 h. Ten microliters of resazurin solution (12.5 mg dissolved in 100 ml distilled water) (Sigma-Aldrich; Zürich, Switzerland) was then added and incubated for further 2–4 h. The fluorescence development was measured in a Spectramax Gemini XS microplate fluorometer (Molecular Devices Corp.; Sunnyvale, CA, USA), operating with an excitation wavelength of 536 nm and an emission wavelength of 588 nm and expressed as percentage of the control. The IC_{50} values were calculated in the graphic programme Softmax Pro (Molecular Devices Corp.). Tests were done at least in three independent experiments in duplicate.

2.5. Cytotoxicity assay

Cytotoxicity was determined using rat skeletal myoblast (L6 cells). The culture medium was RPMI 1640 medium supplemented with L-glutamine 2 mM, HEPES 5.95 g/l, $NaHCO_3$ 2 g/l and 10% foetal bovine serum. Podophyllotoxin (Sigma-Aldrich) was used as the reference drug. The assay was performed following the antitrypanosomal assay protocol [19]. The IC_{50}s were calculated from the sigmoidal growth inhibition curves using Softmax Pro software (Molecular Devices Corp.). Tests were done in three independent experiments in duplicate.

3. Results and discussion

The preliminary screen of our in house extract library showed the ethyl acetate extract of *S. costus* to be highly active against *T. b. rhodesiense* with 96% inhibition at 4.8 μg/ml. This extract was subjected to HPLC based activity profiling to track the activity and identify the active principles. The activity was almost entirely focused in minutes 22 and 23 with 99% to 100% of inhibition. Fig. 1 shows the overlay of the chromatogram (ESI positive MS trace at scan *m/z* 200–1500) with the percent inhibition of these microfractions. Subsequently, compounds **3** and **4** from these two active windows were isolated.

The major compound **3** (t_R 22.4 min) had a molecular formula of $C_{15}H_{20}O_2$ with *m/z* 465.3182 $[2M+H]^+$ (calcd. for $C_{30}H_{41}O_4$ 465.3006) and was identified as costunolide. Compound **4** (t_R 23.0 min) with a molecular formula of $C_{15}H_{18}O_2$ derived from *m/z* 461.2869 $[2M+H]^+$ (calcd. for $C_{30}H_{37}O_4$ 461.2693) was dehydrocostuslactone. In addition, compounds **1** (t_R 24.2 min) and **2** (t_R 25.3 min) were isolated and both had the sum formula $C_{15}H_{20}O_2$ as suggested by the *m/z* 465.3185 $[2M+H]^+$ (calcd. for $C_{30}H_{41}O_4$ 465.3006) and *m/z* 465.3190 $[2M+H]^+$ (calcd. for $C_{30}H_{41}O_4$ 465.3006). They were identified as the known compounds arbusculin B (**1**) and α-cyclocostunolide (**2**) (Fig. 2).

Compounds **2**, **3**, and **4** have been isolated from *S. costus* previously [20]. Whilst compound **1** is reported here for the first time from this plant.

Further possibly active compounds present in the extract in minor concentrations, like the peaks seen in minute 11 and 20, were not isolated. This may be done in further studies.

From *L. nobilis* we isolated the sesquiterpene lactone **6** and from *Eupatorium cannabium* substance **7**. Compound **6** with sum formula of $C_{17}H_{20}O_4$, *m/z* 311.1289 $[M+Na]^+$ (calcd. for $C_{17}H_{20}O_4Na$ 311.1254) was determined as zaluzanin D and compound **7** with molecular formula of $C_{20}H_{26}O_6$, *m/z* 385.1614 $[M+Na]^+$ (calcd. for $C_{20}H_{26}O_6Na$ 385.1622) was characterised as eupatoriopicrin. Substance **5** was from a commercial source. The ^1H and ^{13}C NMR data

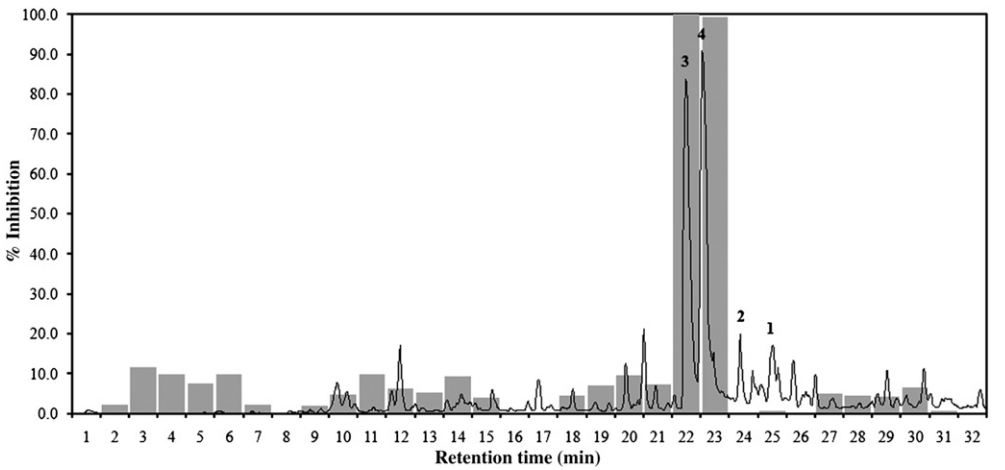

Fig. 1. The antitrypanosomal activity of the 32 one-minute microfractions plotted against the mass trace of the ethyl acetate extract of *Saussurea costus* (ESI-MS positive scan *m/z* 200–1500).

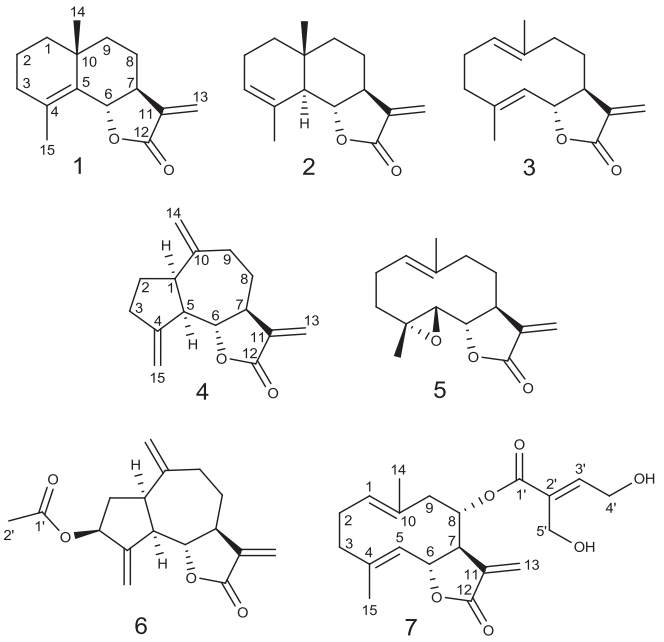

Fig. 2. Chemical structures of seven sesquiterpene lactones isolated from *Saussurea costus*(**1–4**), *Laurus nobilis* (**6**) and *Eupatorium cannabinum* (**7**). Compound **5** was from a commercial source.

for compounds **1–4**, **6**, and **7** are attached as supporting information (Table S1).

Sesquiterpene lactones are classified into several classes based on their carbocyclic skeleton [21]. The compounds in this study are eudesmanolides (6/6 bicyclic), germacranolides (10 member-ring monocyclic), and guaianolides (5/7 bicyclic).

The antitrypanosomal and cytotoxic IC_{50} of the 7 compounds were established (Table 1). The three germacranolides parthenolide (**5**), eupatoriopicrin (**7**), and costunolide (**3**) were the most antitrypanosomally active compounds in this study, followed by the guaianolides dehydrocostuslactone (**4**) and zaluzanin D (**6**), and the eudesmanolides arbusculin B (**1**), and α-cyclocostunolide (**2**). The cytotoxicity of all compounds was within range of IC_{50}s from 1.6 to 19.4 μM and selectivity indices between 0.5 and 6.5.

The three active germacranolides **3**, **5**, and **7** had similar IC_{50} values, suggesting that the presence of the epoxide in **3** or the esterified hydroxyl side chain in **7** did not greatly affect the antitrypanosomal activity. Compounds **3** and **5** were more selective towards *T. b. rhodesiense* than towards mammalian cells (SI: 5.9 and 6.5) whereas **7** was more toxic (SI: 1.3). Amongst the guaianolides, dehydrocostuslactone (**4**) had the threefold activity and twofold toxicity of zaluzanin D (**6**). They both had similar selectivity indices (1.9 and 1.4). The lowest antitrypanosomal activities and selectivities were seen for the two eudesmanolides arbusculin B (**1**) and α-cyclocostunolide (**2**) which were both more active against mammalian cells than against the parasites with selectivity indices of 0.5 and 0.9.

Lirussi et al. [22] report the potent inhibition (IC_{50} = 2.4 μg/ml) of *T. cruzi e*pimastigotes by a methanol extract of *S. costus* roots. Schmidt et al. [23] report parthenolide (**5**) to be highly active against *T. b. rhodesiense* and *T. cruzi*. The study also shows that the tested eudesmanolides tended to have lower antitrypanosomal activities and selectivities than some other types of sesquiterpene lactones. Izumi et al. [24] also previously publish the potent effect of parthenolide (**5**) against *T. cruzi*. The other compounds in this study have so far not been tested for antitrypanosomal effects. We recently reported the potent in vitro and in vivo activity of cynaropicrin, a guaianolide sesquiterpene lactone with a 2-hydroxymethyl-2-propenoyl moiety at C-8, against *T. b. rhodesiense* [9].

Sesquiterpene lactones may exert their various biological activities by the interaction of their α-methylene-γ-butyrolactone moiety with the thiol groups of biomacromolecules through Michael-addition [25].

Table 1
In vitro antitrypanosomal activity and cytotoxicity of sesquiterpene lactones against *T. b. rhodesiense* and cytotoxic effects against L6 cells. Results are expressed as IC_{50} values with the standard deviation (SD) and shown alongside the positive controls.

Compound	*T. b. rhodesiense*	L6 cells	SI
	IC_{50} (μM ± SD)	IC_{50} (μM ± SD)	
1 Arbusculin B	12.0 ± 3.3	6.2 ± 2.3	0.5
2 α-Cyclocostunolide	21.9 ± 1.1	19.4 ± 7.9	0.9
3 Costunolide	1.3 ± 0.4	7.7 ± 1.3	5.9
4 Dehydrocostuslactone	4.4 ± 1.4	8.3 ± 1.9	1.9
5 Parthenolide	0.8 ± 0.5	5.2 ± 0.9	6.5
6 Zaluzanin D	10.8 [a]	15.6 [a]	1.4
7 Eupatoriopicrin	1.2 ± 0.2	1.6 ± 0.08	1.3
Melarsoprol	0.006 ± 0.003		
Podophyllotoxin		0.01 ± 0.002	

[a] IC_{50} value is obtained from a single experiment done in duplicate.

A comprehensive study on 40 sesquiterpene lactones from five sesquiterpene lactone classes confirms the influence of this α-methylene-γ-butyrolactone moiety to their antitrypanosomal and cytotoxic activity. The most potent and selective sesquiterpene lactones reported so far were the pseudoguaianolide helenalin and the xanthanolide 8-epixanthatin-1,5-epoxide. However, a high degree of correlation is also found between such compounds' antiprotozoal activity and mammalian cytotoxicity so that it may be difficult to find a structural explanation for the selectivity observed with some compounds [23]. Cytotoxicity studies of sesquiterpene lactones related to the lactone moiety were shown by Kupchan et al. [26,27].

This study suggests that sesquiterpene lactones may have potential for the development of new leads to treat infection caused by trypanosomes. Further comprehensive structure activity studies to clarify the contribution of sesquiterpene ring systems and/or substitution patterns of sesquiterpene lactones to the overall activity against both *T. b. rhodesiense* and mammalian cell like those reported by Schmidt et al. [23] and especially further in vivo data like Zimmermann et al. [9] are needed.

Acknowledgements

T. Julianti is supported by a fellowship grant from Directorate General of Higher Education, Department of National Education of Indonesia.

Appendix A. Supplementary data

Supplementary data to this article can be found online at doi:10.1016/j.fitote.2011.05.010.

References

[1] Chopra RN, Nayar SL, Chopra IC. Glossary of Indian medicinal plants. CSIR, New Delhi, India: Publication and Information Directorate; 1956.
[2] Dhar GH, Virjee P, Kachroo P, Buth GM. Ethnobotany of Kashmir-I. Sind valley. J Econ Taxon Botany 1984;5:668–75.
[3] Pandey MM, Rastogi S, Rawat AKS. *Saussurea costus*: botanical, chemical and pharmacological review of an Ayurvedic medicinal plant. J Ethnopharmacol 2007;110:379–90.
[4] Parekh J, Chanda S. Antibacterial and phytochemical studies on twelve species of Indian medicinal plants. Afr J Biomed Res 2007;10:175–81.
[5] Yu HH, Lee JS, Lee KH, Kim KY, You YO. *Saussurea lappa* inhibits the growth, acid production, adhesion, and water-insoluble glucan synthesis of *Streptococcus mutans*. J Ethnopharmacol 2007;111:413–7.
[6] Adams M, Zimmermann S, Kaiser M, Brun R, Hamburger M. A protocol for HPLC-based activity profiling for natural products with activities against tropical parasites. Nat Prod Commun 2009;10:1377–81.
[7] Potterat O, Hamburger M. Natural products in drug discovery — concepts and approaches for tracking bioactivity. Curr Org Chem 2006;10:899–920.
[8] Adams M, Plitzko I, Kaiser M, Brun R, Hamburger M. 3-Methoxy carpachromene — a new tetracyclic flavonol from *Pistacia atlantica* with anti plasmodial activity. Phytochem Lett 2009;2:159–62.
[9] Zimmermann S, Adams M, Julianti T, Hata-Uribe Y, Brun R, Hamburger M. HPLC based activity profiling for new antiparasitic leads: in vitro and in vivo antitrypanosomal activity of cynaropicrin. Planta Med 2010;76: WSII_7.
[10] Adams M, Gschwind S, Zimmermann S, Kaiser M, Hamburger M. Renaissance remedies: Antiplasmodial protostane triterpenoids from *Alisma plantago-aquatica* L. (Alismataceae). J. Ethnopharmacol. 2011, doi:10.1016/j.jep.2011.02.026.
[11] Ślusarczyk S, Zimmermann S, Kaiser M, Matkowski A, Hamburger M, Adams M. Antiplasmodial and antitrypanosomal activity of tanshinone type diterpenes from *Salvia miltiorrhiza*. Planta Med. 2011, http://dx.doi.org/10.1055/s-0030-1270933.
[12] Kraut L, Mues R, Sim-Sim M. Sesquiterpene lactones and 3-benzylphtalides from *Frullania muscicola*. Phytochemistry 1994;37:1337–46.
[13] Tomassini TCB, Gilbert B. α-Cyclocostunolide and dihydro-β-cyclocostunolide from *Moquinea velutina*. Phytochemistry 1972;11:1177–9.
[14] Li A, Sun A, Liu R. Preparative isolation and purification of costunolide and dehydrocostuslactone from *Aucklandia lappa* Decne by high-speed counter-current chromatography. J Chromatogr A 2005;1076:193–7.
[15] Ferrari B, Castilho P, Tomi F, Rodrigues AI, Costa MC, Casanova J. Direct identification and quantitative determination of costunolide and dehydrocostuslactone in the fixed oil of *Laurus novocanariensis* by 13C-NMR spectroscopy. Phytochem Anal 2005;16:104–7.
[16] Ando M, Kusaka H, Ohara H, Takase K, Yamaoka H, Yanagi Y. Studies on the syntheses of sesquiterpene lactones. 11.[1] The syntheses of 3-epizaluzanin C, zaluzanin C, zaluzanin D, and related compounds 3α-hydroxyguaia-1(10),4(15),11(13)-trieno-12,6α-lactone and 3α-hydroxyguaia-4(15),9,11(13)-trieno-12,6α-lactone[2]. J Org Chem 1989;54:1952–60.
[17] Jolad SD, Hoffmann JJ, Bates RB, Calders S, McLaughlin SP. Caudatol, a guaianolide from *Pericome caudate*. Phytochemistry 1990;29(9): 3024–8.
[18] Baltz T, Baltz D, Giroud Ch, Crockett J. Cultivation in a semi-defined medium of animal infective forms of *Trypanosoma brucei*, *T. equiperdum*, *T. evansi*, *T. rhodesiense* and *T. gambiense*. EMBO J 1985;4:1273–7.
[19] Räz B, Iten M, Grether-Bühler Y, Kaminsky R, Brun R. The Alamar Blue® assay to determine drug sensitivity of African Trypanosomes (*T. b. rhodesiense* and *T.b. gambiense*) *in vitro*. Acta Trop 1997;68:139–47.
[20] Govindan SV, Bhattacharyya SC. Alantolides and cyclocostunolides from *Saussurea lappa* Clarke (costus root). Indian J Chem 1977;15:956–7.
[21] Seaman FC. Bot Rev 1982;48:121–595.
[22] Lirussi D, Li J, Prieto JM, Gennari M, Buschiazzo H, Rı'os L, Zaidenberg A. Inhibition of *Trypanosoma cruzi* by plant extracts used in Chinese medicine. Fitoterapia 2004;75:718–23.
[23] Schmidt TJ, Nour AMM, Khalid SA, Kaiser M, Brun R. Quantitative structures-antiprotozoal activity relationships of sesquiterpene lactones. Molecules 2009;14:2062–76.
[24] Izumi E, Morello LG, Ueda-Nakamura T, Yamada-Ogatta SF, Filho BPD, Cortez DAG, et al. *Trypanosoma cruzi*: antiprotozoal activity of parthenolide obtained from *Tanacetum parthenium (L.) Schultz Bip.* (Asteraceae, Compositae) against epimastigote and amastigote forms. Exp Parasitol 2008;118:324–30.
[25] Picman AK. Biological activities of sesquiterpene lactones. Biochem Syst Ecol 1986;14:255–81.
[26] Kupchan SM, Fessler DC, Eakin MA, Giacobbe TJ. Reactions of alpha methylene lactone tumor inhibitors with model biological nucleophiles. Science 1970;168:376–8.
[27] Kupchan SM, Eakin MA, Thomas AM. Tumor inhibitors. 69. Structure–cytotoxicity relations among the sesquiterpene lactones. J Med Chem 1971;14(12):1147–52.

Supporting Information

Antitrypanosomal sesquiterpene lactones from *Saussurea costus*

Tasqiah Julianti[a,c], Yoshie Hata[a,d], Stefanie Zimmermann[a,b], Marcel Kaiser[b,e], Matthias Hamburger[a], Michael Adams[a,*]

[a] Division of Pharmaceutical Biology, University of Basel, CH-4056 Basel, Switzerland

[b] Department of Medical Parasitology and Infection Biology, Swiss Tropical and Public Health Institute, CH-4002 Basel, Switzerland

[c] Faculty of Pharmacy, Pancasila University, 12640 Jakarta, Indonesia

[d] Department of Pharmacy, National University of Colombia, Carrera 30 45-03, Bogotá, Colombia

[e] University of Basel, CH-4051 Basel, Switzerland

[*] Corresponding author. Institute of Pharmaceutical Sciences, Division of Pharmaceutical Biology University of Basel, CH-4056 Basel, Switzerland. Tel: +41 61 267 1564. Fax: +41 61 267 1474. E-mail: michael.adams@unibas.ch

S Table 1. ^{13}C (125 Mhz) and ^{1}H (500 MHz) data for compounds **1**-**4** in DMSO-d_6 and compounds **6** and **7** in $CDCl_3$ (δ in ppm and J in Hz). Assignment of ^{13}C shifts was done via HSQC and HMBC correlations.

Position	1		2		3		4		6		7	
	δ_C, mult.	δ_H (J in Hz)	δ_C, mult.	δ_H (J in Hz)	δ_C, mult.	δ_H (J in Hz)	δ_C, mult.	δ_H (J in Hz)	δ_C, mult.	δ_H (J in Hz)	δ_C, mult.	δ_H (J in Hz)
1	41.3, CH_2*	1.58, m; 1.41, m	21.5, CH_2	1.62, m; 1.99, m	126.7, CH	4.82, dd (11.3, 4.3)	47.0, CH	2.95, m	50.3, CH	2.93, m	130.7, CH	4.87, dd (2.8, 11.0)
2	18.8, CH_2*	1.57, m	23.0, CH_2	2.04, m	26.1, CH_2	2.27, m; 2.10, m	30.2, CH_2	1.89, m; 1.82, m	36.0, CH_2	2.43, m; 1.82, m	26.1, CH	2.31, m; 2.20, m
3	31.0, CH_2*	2.00, m; 1.89, m	122.5, CH	5.37, brs	39.3, CH_2	2.25, m; 1.98, m	32.6, CH_2	2.48, m	74.9, CH	5.57, m	39.4, CH_2	2.35, m; 2.07, m
4	139.7, qC		133.2, qC		141.0, qC		152.3, qC		148.9, qC		142.5, qC	
5	130.0, qC		50.7, CH	2.35, brd	127.8, CH	4.77, t (9.7)	52.0, CH	2.86, dd (10.0, 8.8)	44.2, CH	3.01, m	127.2, CH	4.76, d (10.1)
6	83.2, CH	4.61, brd (11.5)	82.0, CH	3.94, t (11.2)	81.7, CH	4.71, t (9.8)	85.0, CH	3.98 t (9.2)	84.5, CH	4.10, dd (9.4, 9.4)	75.4, CH	5.16, dd (9.0, 9.7)
7	50.0, CH	2.55, m	51.0, CH	2.59, m	50.0, CH	2.63, m	44.6, CH	2.97, m	45.1, CH	2.97, m	52.9, CH	2.93, m
8	23.0, CH_2	2.06, m; 1.63, m	39.0, CH_2	1.52, m; 1.39, m	27.7, CH_2	2.12, m; 1.69, m	30.8, CH_2	2.25, m; 1.33, m	30.4, CH_2	2.01, m; 1.44 m	72.3, CH	5.80, d (3.2)
9	40.6, CH_2*	1.50, m; 1.36, m	37.5, CH_2	1.45, m; 1.36, m	40.9, CH_2	2.33, m; 2.08, m	36.2, CH_2	2.43, m; 2.14, m	34.4, CH_2	2.51, m; 2.21, m	44.2, CH_2	2.84, m; 2.32, m
10	37.7, qC		23.3, qC		137.3, qC		150.2, qC		149.0, qC		134.0, qC	
11	127.0, qC		139.8, qC		141.2, qC		140.2, qC		139.8, qC		136.8, qC	
12	170.3, qC		170.7, qC		170.4, qC		169.8, qC		171.0, qC		170.6, qC	
13	118.4, CH_2	6.00, d (3.1); 5.56, d (3.0)	116.5, CH	5.91, d (3.1); 5.48, d (3.1)	119.6, CH_2	6.07, d (3.6) 5.67, d (3.3)	120.1, CH_2	6.09, d (3.6); 5.66, d (3.2)	119.0, CH_2	6.13, d (3.5); 5.59, d (3.2)	120.9, CH_2	6.29, d (3.5); 5.57, d (3.0)
14	27.2, CH_3	1.09, s	17.5, CH_3	0.86, s	16.1, CH_3	1.39, s	112.3, CH_2	4.89, brs; 4.79, brs	112.8, CH_2	4.96, s	17.5, CH_3	1.46, s
15	20.6, CH_3	1.80, s	23.8, CH_3	1.76, s	17.3, CH_3	1.66 s	108.6, CH_2	5.13, brs; 5.03, brs	111.5, CH_2	5.38, m; 5.23,m	19.0, CH_3	1.75, s
1'									170.5, qC		165.9, qC	
2'									19.6, CH_3	2.10, s	131.8, qC	
3'											144.7, CH	6.84, dd (5.7, 5.7)
4'											58.9, CH_2	4.40, d (5.9)
5'											57.3, CH_2	4.33, s

* These signals may be interchangeable.

4. CONCLUSIONS AND OUTLOOK

As a result of a first screening campaign, 10 extracts, which belong to 10 different species and 7 families were chosen based on the following criteria: i) antiprotozoal activity; ii) selectivity; and iii) different genus [1]. Seventeen HPLC-based activity profiles were obtained. However, in most of the cases no activity was observed after micro-fractionation. Only the DCM extract of *Eucomis autumnalis* (flowers/buds) showed activity (90%) against *L. donovani*, but the dereplication of 4'-*O*-methyl-punctatin (homoflavonoid), as a major active compound was performed. Due to these poor results, a second screening was carried out [2]. The extracts of *Abrus precatorius, Clutea pulchella, Drypetes gerrardii,* and *Turraea floribunda* fulfilled the requirements for a follow up by HPLC-based activity profiling. Eighteen HPLC-based activity profiles were obtained by analytical separation of sub-milligram amounts of the extracts. Activity profiles of *A. precatorius, C. pulchella,* and *D. gerrardii* exhibited antiprotozoal inhibition of greater than 50%.

Abruquinone B was dereplicated from the *A. precatorius* HPLC-activity profile. Nevertheless, the chromatogram showed additionally active peaks. Consequently, this extract was prioritized. No records were found for peaks present in the active windows of the HPLC-activity profiles of *D. gerrardii* and *C. pulchella.* Hence, the extracts were also prioritized in the mentioned order.

Preparative isolation of active compounds to perform structure elucidation and *in vitro* test was achieved. Thanks to the combination of chromatographic techniques such as flash chromatography and semi-preparative HPLC chromatography, only a small amount of crude extracts (1.0 g) from *A. precatorius* (Batch I) and *D. gerrardii* was needed to obtain compounds in multi-milligram amounts. Structures were elucidated by HR-ESIMS, and 1D and 2D NMR (^{1}H, ^{13}C, COSY, HMBC, HSQC, and NOESY) spectroscopy by using a 500 MHz spectrometer equipped with 1mm microprobe. When new chiral compounds were found, their absolute configuration was determined by comparison of the electronic circular dichroism (ECD) spectra with calculated ECD.

In addition to South African plants, some European plants such as, *Chrysanthemum cinerariifolium, Laurus nobilis,* and *Eupatorium cannabium* were investigated. Nine compounds were isolated from these plants.

In total, 22 secondary metabolites were isolated. Their *in vitro* antiprotozoal activity and selectivity are listed in Table 6. Following the criteria of activity and selectivity of the Swiss TPH (see Table 5), 15 compounds showed parasite inhibition to some extent, ranging from active to moderately active. The remaining 7 compounds exhibited no activity against the mentioned parasites. The selectivity was calculated by dividing the IC_{50} value for L6 cells by the IC_{50} value in the parasite assay. Both, activity and

selectivity of pure substances, in addition to their structure novelty were criteria to prioritize compounds for large scale isolation to perform primary *in vivo* assays.

Pyrethrin II and Jasmolin II, isolated from *C. cinerariifolium*, showed moderate activity against *P. falciparum,* and low selectivity (IC_{50} 4.0 ± 1.1 μM and 5.0 ± 0.4 μM, SIs of 24 and 6, respectively). Pyrethrins were inactive against *T. b. rhodesiense*. Antiprotozoal properties of pyrethrins were compared with those of pyrethroids. Albeit pyrethrins were more active than pyrethroids (IC_{50} from 8.9 ± 2.0 μM to inactive), neither activity, nor selectivity were sufficient to warrant *in vivo* studies [3].

Sesquiterpene lactones were isolated from *L. nobilis* and *E. cannabinum* to investigate their antiprotozoal properties, and to start a structure-activity relationship study. Two germacrolides, costunolide and eupatoriopicrin, showed higher trypanocidal activity (IC_{50} of 1.3 ± 0.4 μM and 1.2 ± 0.2 μM, respectively) than the guaianolide zaluzanin D (IC_{50} of 10.8 μM) [4]. Other guaianolides, such as cynaropicrin, had shown high trypanocidal activity (IC_{50} of 0.28 ± 0.001 μM) [5]. As a result of further studies performed by our research group, it is now known that an acyl side chain at OH-8, lacking in zaluzanin D and present in cynaropicrin, is essential for such activity [6]. None of the isolated sesquiterpene lactones in this work showed sufficient activity and selectivity to pursue *in vivo* tests.

Abruquinones B and I from *A. precatorius* [7] and the phenanthrenone drypenenone D from *D. gerrardii* [8] fulfilled activity and selectivity requirements to conduct primary *in vivo* tests. Hence, a second batch of each plant was collected to perform large scale isolation since a minimum amount of 25 mg for each pure compound is needed for primary *in vivo* assays.

Phytochemical profiles of batch I and II (second recollection) from *A. precatorius* were compared. Major differences were found in their composition. Abruquinones in batch II were only detected after enrichment by flash chromatography. The isolation of five additional abruquinones was achieved, although in low quantities only. Their trypanocidal activity was assessed *in vitro* (Table 6). All five abruquinones showed remarkable and selective inhibition of *T. b. rhodesiense*. Even though the goal of a large scale isolation of abruquinones from batch II was not achieved, we were able to isolate additional active abruquinones, confirming that this class of compounds shows interesting trypanocidal activity [9]. The inhibition (ranging from 0.28 to 0.007 μM) and selectivity (ranging from 51 to 1379) of active abruquinones were better than inhibition and selectivity of some lead compounds currently under clinical trials for HAT, namely fexinidazole (IC_{50} 0.7 - 3.3 μM, SI >100, Phase II/III) and oxaborole SCYX-7158 (IC_{50} 0.2 – 1.0 μM, SI >100, Phase I) [10, 11]. Thus the *in vivo* assessment of abruquinones is highly recommended.

Table 6. Isolated Compounds, Antiprotozoal Activity and Cytotoxicity in L6-cells

Plant	Compound	*P. falciparum*		*T. b. rhodesiense*		*L. donovani*		Cytotoxicity
		IC_{50} (µM)[a]	SI	IC_{50} (µM)	SI	IC_{50} (µM)	SI	(IC_{50}) (µM)
	Isoflavan quinones							
A. precatorius Batch I	Abruquinone B[d]	4.1 ± 0.4	2.5	0.16 ± 0.06	51	2.9[b]	3.5	10.0 ± 1.3
	Abruquinone I[d]	20.4 ± 1.3	1.1	0.28 ± 0.05	78	3.4	6.5	22.1 ± 3.5
	Abruquinone G	Inactive[c]	-	17.0 ± 4.17	3.0	35	1.5	51.7 ± 11
	Abruquinone H	8.0 ± 1.1	15	12.0 ± 3.83	10	Inactive[b]	-	122 ± 21
	(3*S*)-7,8,3',5'-tetramethoxyisoflavan-1',4'-quinone[d]	8.9 ± 4.2	0.4	0.88 ± 0.14	4.5	5.0	0.8	3.9 ± 0.44
A. precatorius Batch II	Abruquinone K[d]	14.1 ± 0.4	4.1	0.113 ± 0.053	508	Inactive[b]	-	57 ± 4.3
	Abruquinone L[d]	13.4 ± 0.6	0.6	0.020 ± 0.003	374	Inactive[b]	-	7.5 ± 1.2
	Abruquinone A[d]	9.2 ± 1.5	3.7	0.025 ± 0.003	1379	Inactive[b]	-	34.5 ± 16
	Abruquinone D[d]	3.5 ± 0.2	1.4	0.007 ± 0.002	668	Inactive[b]	-	4.8 ± 1.6
	Abruquinone J	84 ± 4.0	1.8	11.2 ± 13.6	13.6	Inactive[b]	-	152 ± 7.8
	Phenanthrenones							
D. gerrardii	Phenanthrenone[d]	0.96 ± 0.25	71	6.0 ± 2.7	11	14.0	4.9	68 ± 4.6
	Phenanthrenone Dimer[d]	2.03 ± 0.15	31	-	-	-	-	64 ± 22
	Terpenes							
D. gerrardii	Putranoside A[d]	Inactive[c]	-	18.0 ± 2.6	3.8	7.8	8.8	68 ± 4.0

Plant	Compound	*P. falciparum*		*T. b. rhodesiense*		*L. donovani*		Cytotoxicity
		IC_{50} (µM)[a]	**SI**	**IC_{50} (µM)**	**SI**	**IC_{50} (µM)**	**SI**	**(IC_{50}) (µM)**
C. cinerariifolium	Pyrethrin II[d]	4.0 ± 1.1	24	10.6 ± 0.4	9.0	-	-	95 ± 2.5
	Jasmolin II[d]	5.0 ± 0.4	6.3	12.1 ± 0.2	2.6	-	-	32 ± 2.3
	Cinerin II	5.8 ± 0.4	4.8	12.2 ± 0.02	2.3	-	-	28 ± 7.8
	Pyrethrin I	11.9 ± 1.5	12.6	6.9 ± 1.1	21	-	-	146 ± 34
	Jasmolin I	9.3 ± 1.2	9.2	30.9 ± 1.4	2.8	-	-	86 ± 12
L. nobilis	Costunolide[d]	-		1.3 ± 0.4	5.9	-		7.7 ± 1.3
	Zaluzanin D	-		10.8*	6.5	-		15.6*
	Spirofolide[d]	-		0.3*	4.3	-		1.3*
E.cannabium	Eupatoriopicrin[d]	-		1.2 ± 0.2	1.3	-		1.6 ± 0.1

[a] Values are expressed as mean ± standard error of the mean. [b] No activity observed at the highest test concentration of 90 µg/mL, which corresponds to molar test concentrations of 269.4 to 220.5 µM. [c] No activity observed at the highest test concentration of 10 µg/mL, which corresponds to molar test concentrations of 24.5 to 1.29 µM. [d] Active compounds against at least one parasite.

No obvious structure activity relationship (SAR) was observed among the ten abruquinones.

Qualitative and quantitative differences in abruquinones content between batch I and II could be due to seasonal effects. Batch I was collected in summer, whereas batch II was collected in autumn. The variation in the content of abruquinone should be taken into account for further material recollection. Additionally, to assure a botanical source of abruquinones, for further phases of discovery, it is necessary to perform studies on the influence of different factors such as, environment and genetics, on the production of abruquinones [12]. Optimization of the extraction method could also be considered. Recently, a method for obtaining abruquinone A from the roots of *A. precatorius* has been patented [13].

Late approaches that endeavour to re-establish natural products in the modern, HTS-based lead discovery paradigm have focused on early compound selection driven by molecular properties associated with lead- and drug likeness [14, 15]. Some descriptors, namely Lipinski's parameters [molecular weight ≤ 500, log P ≤ 5, sum of H-donors/acceptors ≤ 10], rotatable bonds (≤ 10), and polar surface area (PSA) (≤ 60-70 $Å^2$) can predict permeability across biological barriers [16, 17]. In general, abruquinones complied with Lipinski's "rule of 5" requirements, except for abruquinone K, for which the sum of H-donors/acceptors is 12 (Table 7). Accordingly, oral bioavailability of abruquinones can be expected, which is one of the main requirements for an antiprotozoal drug. Abruquinones also fulfil the flexibility criterion (measured as rotatable bonds), but not the PSA requirements. With a PSA higher than 60-70 Å, blood-brain barrier (BBB) permeability might be limited [30]. In drug discovery for HAT, there is a need to find drugs acting against the second stage of the disease, when parasites have already crossed the BBB. Regardless of the high PSA of abruquinones, it is known that some flavonoids are able to reach the brain. One example is kaempferol, a flavonoid which is able to cross the BBB, despite of its high PSA (111.1 Å) [14, 18].

Table 7. Physico-chemical Properties of Most Active and Selective Compounds

Plant	Compounds	H-acceptors	H-donors	MW	CLogP[a]	Rotatable bonds	PSA (Å^2)
	Isoflavan quinones						
A. precatorius Batch I	Abruquinone B[b]	8	0	390.4	-0.67	6	89.5
	Abruquinone I[b]	7	1	346.3	-0.81	5	91.3
A. precatorius Batch II	Abruquinone A[b]	7	0	360.4	-0.55	5	80.3
	Abruquinone D[c]	7	1	346.3	-0.81	4	91.3
	Abruquinone K[c]	8	4	364.4	1.30	4	117.8
	Abruquinone L[c]	7	3	348.4	2.34	4	97.6
	Phenanthrenones						
D. gerarrdii	Phenanthrenone[c]	2	0	252.3	3.96	0	37.3

MW: molecular weight PSA: polar surface area; [a]Values calculated with ChemBioDrawUltra®, [b]Values obtained from SciFinder (calculated with ACD/Labs), [c]Calculated with software Molinspiration Cheminformatics [19].

In addition to molecular parameters, generation of early safety data is crucial to avoid failure in further steps of development [20]. There are a series of proteins involved in development of adverse effects. When the ability of a compound to bind to these proteins is simulated and quantified *in silico,* it is possible to obtain an estimated toxic potential. By using "Virtual ToxLab" technology, binding affinities of the abruquinones toward 16 target proteins were calculated and, hence, an estimated potential of endocrine and/or metabolic disruption, carcinogenicity and cardiotoxicity was obtained. The toxic potential generated must be interpreted as "toxic alerts", i.e. compounds featuring a low toxic potential should not be interpreted as benign, as adverse effects may be mediated through other targets or might trigger undesirable effects under different conditions [21]. Results for abruquinones are shown in Table 8. According to their toxic potential, abruquinones were categorized from low to class II (TP from 0 to IV). Abruquinones which are in class 0, such as abruquinones B, A, and L are unlikely to show adverse effects, triggered by the 16 target proteins tested. Abruquinone I, and D were ranked in class II because both of them showed a high *in silico* binding to glucocorticoid receptor. This might be a potential "off-target" activity of these compounds, which should be further studied, in case the compounds show *in vivo* trypanocidal activity. Importantly, their interactions with the hERG receptor, a potassium ion channel related to cardiotoxicity, were low (ranging from no binding to an affinity of 5.40 μM).

In vitro trypanocidal activity results, together with encouraging drug-like properties, and low to moderate *in silico* predicted toxicity render abruquinones interesting hits to be pursued by medicinal chemists.

In the case of *D. gerrardii*, there were no major differences between the phytochemical profiles of the first and second batch. Thus, obtaining of sufficient amounts of drypetenone D (25 mg) for *in vivo* antimalarial tests was possible. However the compound was inactive when tested in the four-day suppressive test in mice against *P. berghei* (ANKA strain).

The failure in this animal model might be due to either low systemic exposure or/and low specific activity against the parasite. Even though *P. berghei* is the species of choice for *in vivo* screening, some specific genes of this rodent *Plasmodium* may have significantly diverged from the human pathogen. Thus, there is a risk of not identifying compounds selectively inhibiting *P. falciparum*. This is the case of diamidine derivatives, which are known to be efficacious against *P. falciparum* in humans but not against *P. berghei*. To overcome this drawback some authors propose to test failed compounds against *P. berghei* in the *Pf*-huMouse [22]. Nevertheless, ethical and economical considerations must be taken into account.

Drypenenone D fulfils the established drug-likeness criteria (Table 7) and, therefore, oral bioavailability and BBB permeability can be expected. This makes feasible an oral administration, one of the desired characteristics for an ideal antimalarial drug and a potential applicability for the treatment of cerebral malaria [23].

The estimated toxic potential calculated by the "Virtual ToxLab" for drypenenone D was 0.52 (Table 8). This toxic potential value categorized it as a class I compound. Drypenenone D bound to the progesterone receptor with high affinity (IC_{50} of 46.8 nM). This receptor has a fundamental roll during pregnancy. Since antimalarial drugs are expected to be administered in pregnant women, this aspect requires particular attention [23]. However, it is important to note that *in silico* binding affinity to hERG was low (IC_{50} of 40.2 μM).

When applying the Medicines for Malaria Venture (MVV) compound progression criteria for drug discovery pipeline of compounds against malaria [24], drypenenone D fulfills some of the requirements to become a validated hit, such as i) sufficient activity against *P. falciparum* (*in vitro* cell-based assay < 1 μM); ii) sufficient selectivity (SI > 10); iii) drug-like properties; iv) clear identification of the botanical species which contain the active compound. However, it is still necessary to i) establish a possible SAR; ii) predict ADME properties by applying computational models and iii) guarantee a source of plant material to obtain sufficient compound for further steps. *D. gerrardii* is distributed in South Africa, Namibia, Botswana, Lesotho, Swaziland, and Zimbabwe, and occurs also in the tropical region along the eastern African coastline. Abundance of the species must be carefully evaluated, taking into

Table 8. Binding Affinity to the 16 Chosen Targets and Resulting Predicted Toxicity Potential (TP) of the Most Active and Selective Compounds

Plant	Compounds	Binding affinity						TP	TP Class
		N	VL	L	M	H	VH		
	Isoflavan quinones								
A. precatorius Batch I	Abruquinone B[b]	9	0	3	3	1	0	≤ 5	Low
	Abruquinone I[b]	6	0	5	4	1	0	0.63	Class II
	Abruquinone G[b]	13	0	0	1	1	0	0.54	Class I
A. precatorius Batch II	Abruquinone A[b]	9	0	3	4	0	0	0.48	Low
	Abruquinone D[c]	3	0	2	10	1	0	0.59	Class II
	Abruquinone L[c]	10	0	4	2	0	0	≤ 5	Low
	Phenanthrenones								
D. gerarrdii	Phenanthrenone[c]	6	0	3	6	1		0.52	Class I

N: none (IC_{50} > 100 mM), VL: very low (IC_{50} > 1 mM), L: low (IC_{50} > 10 μM), M: medium (IC_{50} > 100 nM), H: high (IC_{50} > 1n M), VH: very high (IC_{50} < 1n M).
TP > 0.8 (extreme, class IV), 0.7 < TP ≤ 0.8 (high, class III), 0.6 < TP ≤ 0.7 (elevated, class II), 0.5 < TP ≤ 0.6 (moderated, class I), TP ≤ 0.5 (low, Class 0).

account that it is necessary to use stems for drypenenone D extraction, as well as the ecological impact of future recollections [25]. So far, there are no reports of any straightforward method of synthesis that allow us to use this alternative.

According to the MMV progression criteria (Table 4) [24], drypenenone D should meet the following criteria to become an early lead compound i) depress parasitemia in a mouse model. So far, this is the main drawback of drypenenone D; ii) not be toxic in mice. Drypenenone D did not show signs of toxicity when tested at 50 mg/Kg in mice; even so, an *in vivo* toxicity test should be conducted; iii) have no known toxicophores/reactive groups. So far, according to the results of the predicted *in silico* toxicity, the toxic potential of the compound is low; iv) have a known mode of action or plans in place to address this; v) be stable in mouse and human plasma; vi) offer initial SAR opportunities for chemical targets with straightforward synthesis.

References

[1] Mokoka, T.A., Zimmermann, S., Julianti, T., Hata, Y., Moodley, N., Cal, M., et al., In vitro screening of traditional South African malaria remedies against *Trypanosoma brucei rhodesiense*, *Trypanosoma cruzi*, *Leishmania donovani*, and *Plasmodium falciparum*, Planta Med. 77 (2011) 1663-7.

[2] Mokoka, T.X., Peter; Zimmermann, Stefanie; Hata, Yoshie; Adams, Michael; Kaiser, Marcel; Moodley, Nivan; Maharaj, Vinesh; Koorbanally, Neil A.; Hamburger, Matthias; Brun, Reto; Fouche, Gerda Antiprotozoal screening of 60 South African plants, and the identification of the antitrypanosomal eudesmanolides schkurin I and II, Planta Med. 79 (2013) 1380.

[3] Hata, Y., Zimmermann, S., Quitschau, M., Kaiser, M., Hamburger, M., Adams, M., Antiplasmodial and antitrypanosomal activity of pyrethrins and pyrethroids, J. Agric. Food Chem. 59 (2011) 9172-6.

[4] Julianti, T., Hata, Y., Zimmermann, S., Kaiser, M., Hamburger, M., Adams, M., Antitrypanosomal sesquiterpene lactones from *Saussurea costus*, Fitoterapia. 82 (2011) 955-9.

[5] Zimmermann, S., Kaiser, M., Brun, R., Hamburger, M., Adams, M., Cynaropicrin: the first plant natural product with in vivo activity against *Trypanosoma brucei*, Planta Med. 78 (2012) 553-6.

[6] Usuki, T., Sato, M., Hara, S., Yoshimoto, Y., Kondo, R., Zimmermann, S., et al., Antitrypanosomal structure-activity-relationship study of synthetic cynaropicrin derivatives, Bioorg. Med. Chem. Lett. 24 (2014) 794-8.

[7] Hata, Y., Raith, M., Ebrahimi, S.N., Zimmermann, S., Mokoka, T., Naidoo, D., et al., Antiprotozoal Isoflavan Quinones from *Abrus precatorius* ssp. *africanus*, Planta Med. 79 (2013) 492-8.

[8] Hata, Y., De Mieri, M., Ebrahimi, S. Mokoka, T. Fouche, G., Maharaj, V., Kaiser, M. Brun, R, Potterat, O. Hamburger, M., Identification of two new phenanthrenones and a saponin as antiprotozoal constituents of *Drypetes gerrardii*, Planta Medica. Ready for Submission.

[9] Hata, Y., Ebrahimi, S.N., De, M.M., Zimmermann, S., Potterat, O., Mokoka, T., et al., Antitrypanosomal isoflavan quinones from *Abrus precatorius*, Fitoterapia. 93 (2014) 81-7.

[10] Maser, P., Wittlin, S., Rottmann, M., Wenzler, T., Kaiser, M., Brun, R., Antiparasitic agents: new drugs on the horizon, Curr. Opin. Pharmacol. 12 (2012) 562-6.

[11] DNDi, R&D Portafolio Patients Needs-Driven Collaborative R&D Model for Neglected Diseases, DNDi, 2013. http://www.dndi.org/images/stories/pdf_portfolios/DNDi_Portfolio2013.pdf

[12] Gutierrez-Gonzalez, J.J., Guttikonda, S.K., Tran, L.-S.P., Aldrich, D.L., Zhong, R., Yu, O., et al., Differential expression of isoflavone biosynthetic genes in soybean during water deficits, Plant Cell Physiol. 51 (2010) 936-48.

[13] Zhang, J., Wan, D., Method for preparation of abruquinone A, Nanjing Biaoke Biotech Co., Ltd., Peop. Rep. China . 2013.

[14] Konczol, A., Muller, J., Foldes, E., Beni, Z., Vegh, K., Kery, A., et al., Applicability of a Blood-Brain Barrier Specific Artificial Membrane Permeability Assay at the Early Stage of Natural Product-Based CNS Drug Discovery, J. Nat. Prod. 76 (2013) 655-63.

[15] Kelder, J., Grootenhuis, P.D.J., Bayada D.M., Delbressine, L.P.C., Ploemen J.P. Polar Molecular Surface as a Dominating Determinant for Oral Absorption and Brain Penetration of Drugs, Pharm. Res. 76 (2013) 655-63.

[16] Lipinski, C.A., Lombardo, F., Dominy, B.W., Feeney, P.J., Experimental and computational approaches to estimate solubility and permeability in drug discovery and development settings, Adv. Drug Delivery Rev. 46 (2001) 3-26.

[17] Pajouhesh, H., Lenz, G.R., Medicinal chemical properties of successful central nervous system drugs, NeuroRx. 2 (2005) 541-53.

[18] Rangel-Ordonez, L., Noeldner, M., Schubert-Zsilavecz, M., Wurglics, M., Plasma levels and distribution of flavonoids in rat brain after single and repeated doses of standardized *Ginkgo biloba* extract EGb 761, Planta Med. 76 (2010) 1683-90.

[19] Cheminformatics, M., Molinspiration, http://molinspiration.com/, Slovak Republic, 2014.

[20] Lipinski, C., Hopkins, A., Navigating chemical space for biology and medicine, Nature. 432 (2004) 855-61.

[21] Vedani, A., Dobler, M., Smiesko, M., VirtualToxLab - a platform for estimating the toxic potential of drugs, chemicals and natural products, Toxicol Appl Pharmacol. 261 (2012) 142-53.

[22] Jimenez-Diaz, M.B., Viera, S., Ibanez, J., Mulet, T., Magan-Marchal, N., Garuti, H., et al., A new *in vivo* screening paradigm to accelerate antimalarial drug discovery, PLoS One. 8 (2013) e66967.

[23] Fidock, D.A., Rosenthal, P.J., Croft, S.L., Brun, R., Nwaka, S., Antimalarial drug discovery: efficacy models for compound screening, Nat. Rev. Drug Discovery. 3 (2004) 509-20.

[24] Medicines for Malaria Venture (MMV), Global Malaria Portafolio, 4Q, 2013, MMV, Geneva, 2013. http://www.mmv.org/research-development/rd-portfolio

[25] Germishuizen, G., A checklist of South African plants: Southern African Botanical Diversity Network Report No. 41, SABONET, Pretoria, 2006.

ACKNOWLEDMENTS

Today a journey comes to an end and a wish becomes true. I thank God for everything I have received. Being in Basel has meaning to me not only walking in the same streets where Paracelsus once walked, but also being in touch with the cutting edge technology in drug discovery, devoted even for the most neglected.

Foremost, I would like to express my most sincere gratitude to Prof. Dr. Matthias Hamburger for accepting me as a PhD student and for all his support and immense knowledge.

Special thanks to the teams of The Council for Scientific and Industrial Research (CSIR) and The Swiss Tropical and Public Health Institute (Swiss TPH) which were involved with this project. Especially to Gerda Fouche (CSIR), Prof. Dr. Reto Brun, and Marcel Kaiser (Swiss TPH) for their excellent work and solicitous help.

I am very grateful to the members of my defense committee for taking the time to read my document and for their valuable inputs. Particularly, Prof. Dr. Irmgard Merfort, my external co-referee and Prof. Dr. Kurt Hersberger, for acting as a moderator.

I am very grateful to Dr. Olivier Potterat for his knowledge, help, and kindness along my PhD.

My gratitude to Prof. Roberto Pinzon and Kurt Hostettmann for introduce me to Prof. Matthias Hamburger.

I would like to thank former postdocs Dr. Inken Plitzko, Dr. Janine Zaugg, Dr. Melanie Raith, and current ones, Dr. Maria De Mieri, Dr. Samad Ebrahimi, and Dr. Eliane Garo for helping me to build my knowledge every day.

Special thanks to:

Manuela Rogalski, she has encouraged me, support me, helped with all the official and administrative issues in German, proof read my documents, including this final one, shared her family and show her country to me.

Diana Rueda, who has become during this time in the sister that I hadn't have before. Thanks for the friendship, fun, embrace, and being my confidant.

Daniela Eingenmann for her friendship, kindness, support, trust, and for proof read this document with patient and dedication.

Dr. Chee Seng Hee for his friendship and kindness for proof-read, the first two chapters of the introduction of this document.

Orlando Fertig for his help and good work. All friends and current and former members of the group, for the good moments, nice work, and support. Dr. Mouhssin Oufir, Christian Abbet, Anja Schramm, Tasqiah Julianti, Teresa Falechini, Evelyn Jähne, Elisabetta Corradi, Alen Bozicevic, Niels Guldbrandsen, Justine Ramseyer, Fahime Moradi, Olga Zabelo, and Petra Weber.

My gratitude is also extended to The National University of Colombia for the “Comision de Estudios”, particularly, to The Faculty of Sciences and The Pharmacy Department for their continuous support. I would like to thank professors Ignacio Mantilla, Jesús Valencia, Julián López, Fabio Aristizabal, and Yolima Baena for their always kind support in all the administrative issues.

Next, I would like to thank Colciencias (Administrative Department of Science, Technology, and Innovation of Colombia) for my grant and Laspau for the administration of this, particularly to Lisa Tapiero.

To professor Lucía Arteaga, for being my mentor. And professors Luis Fernando Ospina, Ahmed Salama, Giovanny Garavito, Mario Guerrero, Noralba Sierra, Maria Teresa Reguero, Afife Mrad de Osorio, Gustavo Buitrago, Lucy Delgado, and Javier Rincon for their knowledge and help along my academic life.

To my uncle and professors Luisa Ponce de Leon, Pilar Luengas, Claudia Mora and Antonio Sanabria, without their trust on me and in this project this would have never be possible. For their caring and love.

To all my friends Rocio Morales, Angela Zambrano, Nadhezda Vergel, María Fernanda Zuluaga, Karen Silva, Juliana Manrique, Angelica Monsalve, Martha Suarez, Claudia Vaca, Esperanza Avella, German Matiz, Luis Franco, Claudia Cordero, Maritza Rojas, and Marcela Aragón, for their patients, love, embracing, caring, advice, and understanding.

And last but not least, my family. My mother, my uncle, and my grandmother (may she rest in peace), for their love, support, and give me all what I needed to be happy and go as far as I have wanted. Additionally, to Consuelo Guerra y Juan Carlos. To them my deepest gratitude.

Curriculum Vitae

Last Name, First Name	**Hata Uribe, Yoshie Adriana**
Address	**Davidsbodenstrasse 38, CH-4056 Basel**
Telephone	**0041 76 7826060**
e-mail	**yoshie.hata-uribe@unibas.ch**

CURRENT POSITION

Ph D Student, Pharmaceutical Biology, University of Basel, Basel, Switzerland

EDUCATION

2009 – present Pharmaceutical Biology, University of Basel, Basel, Switzerland
PhD PHARMACEUTICAL SCIENCES

2006 – 2007 National Pedagogy University, Bogotá, Colombia
TEACHING SPECIALIZATION

2003 - 2005 National University of Colombia, Bogotá, Colombia
MAGISTER IN PHARMACEUTICAL SCIENCES

1993 – 2000 National University of Colombia, Bogotá, Colombia
PHARMACIST

WORK EXPERIENCE

March 2007 – Current	Auxiliary Lecturer and Researcher at Department of Pharmacy, Faculty of Science, National University of Colombia.
January 2004 – December 2006	Lecturer and Assistant Researcher at Department of Pharmacy, Faculty of Science, National University of Colombia.
March 2001 – December 2003	Assistant Researcher at Department of Pharmacy, Faculty of Science, National University of Colombia.
April 2000 – February 2001	Assistant Researcher at Institute of Biotechnology, National University of Colombia.

LANGUAGES

- Spanish: Mother tongue.
- English: Fluent in oral and written communication.
- German: Basics.
- Japanese: Basics.

SKILLS

Pharmacist skilled in natural product isolation, HPLC-UV-MS, NMR spectroscopy, antimalarial *in vitro* (*Plasmodium falciparum*) and *in vivo* (*Plasmodium berghei*) assays, cell culture, *in vivo*-pharmacology (anti-inflammatory rodent models and central nervous system mice models).

PUBLICATIONS

- **Hata Y**., Ebrahimi S., De Mieri M., Zimmermann S., Mokoka T., Naidoo D., Fouche G., Maharaj V., Kaiser M., Brun R., Potterat O., Hamburger M. 2013. **Antitrypanosomal isoflavan quinones from *Abrus precatorius***. Fitoterapia. (ISSN: 0367-326X). DOI: 10.1016/j.fitote.2013.12.015

- Mokoka T., Xolani K.P., Zimmermann S., **Hata Y.**, Moodley N., Adams M., Kaiser M., Maharaj V., Koorbanally N., Hamburger M., Brun R., Fouche G. 2013. **Antiprotozoal screening of 60 South African plants, and the identification of the antitrypanosomal eudesmanolides schkurin I and II**. Planta Medica, 79. 1380-1384. (ISSN: 0032-0943).

- **Hata Y**., Raith M., Ebrahimi S., Zimmermann S., Mokoka T., Naidoo D., Fouche G., Maharaj V., Kaiser M., Brun R., Hamburger M. 2013. **Antiprotozoal isoflavan quinones from *Abrus precatorius ssp. africanus***. Planta Medica, 79. 492-498. (ISSN: 0032-0943).

- **Hata Y**., Zimmermann S., Quitschau M., Kaiser M., Hamburger M., Adams M. 2011. **Antiplasmodial and antitrypanosomal activity of pyrethrins and pyrethroids**. Journal of Agricultural and Food Chemistry, 59. 9172–9176. (ISSN: 0021-8561).

- Mokoka T., Zimmermann S., Tasqiah J., **Hata Y**., Moodley N., Cal M., Adams M., Kaiser M., Brun R., Koorbanally N., Hamburger M. 2011. ***In vitro* screening of traditional South African malaria remedies against *Trypanosoma brucei rhodesiense*, *Trypanosoma cruzi*, *Leishmania donovani*, and *Plasmodium falciparum*.** Planta Medica, 77. 1663-1667. (ISSN: 0032-0943).

- Julianti T., **Hata Y**., Zimmermann S., Kaiser M., Hamburger M., Adams M. 2011. **Antitrypanosomal sesquiterpene lactones from *Saussurea costus***. Fitoterapia, 82. 955-959. (ISSN: 0367-326X).

- Carvajal L., **Hata Y**., Sierra N., Rueda D. 2009. **Preliminary phytochemical analysis of cupatá (*Strychnos schultesiana* krukoff) stems and seeds. (Análisis fitoquímico preliminar de hojas, tallos y semillas de cupatá (*Strychnos schultesiana* Krukoff)**. Revista Colombia Forestal, 12. 161-170. (ISSN: 0120-0739).

- Garavito G., Rincón J., Arteaga L., **Hata Y**., Bourdy G., Jiménez A., Pinzón R., Deharo E. 2006. **Antimalarial activity of some Colombian medicinal plants.** Journal of Ethnopharmacology, 107. 460-462. (ISSN: 0378-8741).

- **Hata Y**. 2004. **Overview of the Colombian potential plants with cosmetic use (Panorama sobre el potencial de las plantas colombianas con aplicación cosmética**). Revista Arte y Ciencia Cosmética, 29. 25-28. (ISSN:0122-8072).

- **Hata Y**., Reguero M.T., Arteaga L., Buitrago G., Álvarez A**.. Analysis of steroidal sapogenins from tubers of Colombian yam "*Dioscorea sp*. (Análisis de las sapogeninas esteroidales de tubérculos de ñame colombiano "*Dioscorea sp*).** Revista Colombiana de Ciencias Químico Farmacéuticas, 32. 149-157. (ISSN: 0034-7418).

CONGRESSES ORAL PRESENTATIONS

- Antiprotozoal isoflavan quinones from Abrus precatorius. Hata Y. et al. 61th International Congress and Annual Meeting of the Society for Medicinal Plant and Natural Product Research (GA), Munster, Germany, September 1st to 5th, 2013.

- Developing of an automatic *Plasmodium falciparum* counting system and applying it to pharmacologically screening of anti-malarial plants (Desarrollo de un conteo automático de *Plasmodium falciparum* y su aplicación al *screening* farmacológico de plantas medicinales). García J.D., Arteaga L., **Hata Y**. *et al*. II National Biotechnology Congress, Bogota, Colombia, Biotechnology Institute, September 1st to September 3rd, 2004.

- Analysis of steroidal sapogenins from tubers of Colombian yam *Dioscorea sp*. from Universidad de Cordoba collection" (Cuantificación de sapogeninas esteroidales de tubérculos de ñame colombiano *Dioscorea sp* obtenidas de la colección de la Universidad de Córdoba). Buitrago G., Reguero R., Arteaga L., Álvarez A., **Hata Y.** VII National Phytochemical Congress, Bogota, Colombia. Pontificia Universidad Javeriana, April 30th to May 3rd, 2002.

CONGRESSES POSTER PRESENTATIONS

- Poster 1: Antiprotozoal compounds from *Drypetes gerrardii*. Hata Y., Ebrahimi S., De Mieri M., Zimmermann S., Mokoka T., Naidoo D., Fouche G., Maharaj V., Kaiser M., Brun R., Potterat O., Hamburger M.

  Annual Research Meeting. University of Basel, Basel, Switzerland, February 10, 2014.

- Poster 2: Antiprotozoal isoflavan quinones from *Abrus precatorius*. Hata Y., Ebrahimi S., Raith M., De Mieri M., Zimmermann S., Mokoka T., Naidoo D., Fouche G., Maharaj V., Kaiser M., Brun R., Hamburger M.

  Swiss Pharma Science Day 2013. University of Bern, Bern, Switzerland, August 28th, 2013.
  Swiss Chemical Society - 2012 Fall Meeting. Lausanne, Switzerland, September 6th, 2013.

- Poster 3: Antiprotozoal isoflavan quinones from *Abrus precatorius ssp. africanus*. Hata Y., Raith M., Ebrahimi S., Zimmermann S., Mokoka T., Naidoo D., Fouche G., Maharaj V., Kaiser M., Brun R., Hamburger M.

  International Congress on Natural Products Research. New York, USA, July 28th to August 1st, 2012.
  Swiss Pharma Science Day 2012. University of Bern, Bern, Switzerland, August 29th, 2012.
  13th International Congress of the Society for Ethnopharmacology. Graz, Austria, September 2nd to 6 th, 2012.
  Swiss Chemical Society - 2012 Fall Meeting. Zürich, Switzerland, September 12th, 2012.
  Annual Research Meeting. University of Basel, Basel, Switzerland, February 14th, 2012.

- Poster 4: Antiplasmodial and antitrypanosomal activity of pyrethrins and pyrethroids. Hata Y., Zimmermann S., Brun R., Kaiser M., Hamburger M., Adams M.

  Pharma Science Day 2011. University of Bern, Bern, Switzerland, September 07th, 2011.
  Annual Research Meeting. University of Basel, Basel, Switzerland, February 2nd, 2011.

- Poster 5: Screening of South African medicinal plants and HPLC based profiling for the identification of leads with antiprotozoal activities. Hata Y., Julianti T., Mokoka T., Moodley N., Zimmermann S., Adams M., Brun R., Kaiser M., Hamburger M.

  58th International Congress and Annual Meeting of the Society for Medicinal Plant and Natural Product Research. Freie Universität, Berlin, Germany, August 29th to September 2nd, 2010.
  Swiss Pharma Science Day 2010. University of Bern, Bern, Switzerland,
  September 8th, 2010.
  11th International Congress of the Society for Ethnopharmacology. Albacete, Spain, September 20th to 24th, 2010.
  Annual Research Meeting. University of Basel, Basel, Switzerland, February, 2010.

- Poster 6: Contribution to the elaboration of a quality control monograph for Abuta grandifolia (Contribución al establecimiento de una monografía para el control de calidad de Abuta grandifolia). Hata Y., Ospina L.F., Luengas P.

X Congreso Colombiano de Fitoquímica, Popayán, Colombia, June 9th to 12th, 2009.

- Poster 7: Anti-protozoal activity of 21 Colombian medicinal plants (Actividad anti-protzoaria de 21 plantas medicinales colombianas). Hata Y., Arteaga L., Calle J., Rincón J., Pinzón R., Ruíz G., Vargas F., Gutiérrez D., Giménez A.

  IX South-American Pharmaceutical Federation Congress, Bogota, Colombia October 29th to November 1st, 2004.

- Poster 8: Standardization of a hemolytic microassay for in vitro anti-complementary activity of plant extracts (Estandarización de un microensayo hemolítico in vitro para la evaluación de la actividad anti-complementaria de extractos vegetales). Arteaga L., Ortiz M., Hata Y.

  VII National Phytochemical Congress, Bogota, Colombia. Pontificia Universidad Javeriana, April 30th to May 3rd, 2002.

- Poster 9: Antimalarial activity of Colombian and Panamanian plants used in folk medicine (Actividad antimalárica de plantas usadas en la medicina folclórica colombiana y panameña). Hata Y., Cifuentes L., Arteaga L., Pinzón S., Vásquez Y., Solís P., Gupta M.

  I Iberoamerican Pharmaceutical Fine Chemical Congress, Salamanca, Spain, Universidad de Salamanca, April 15th to 19th, 2002.